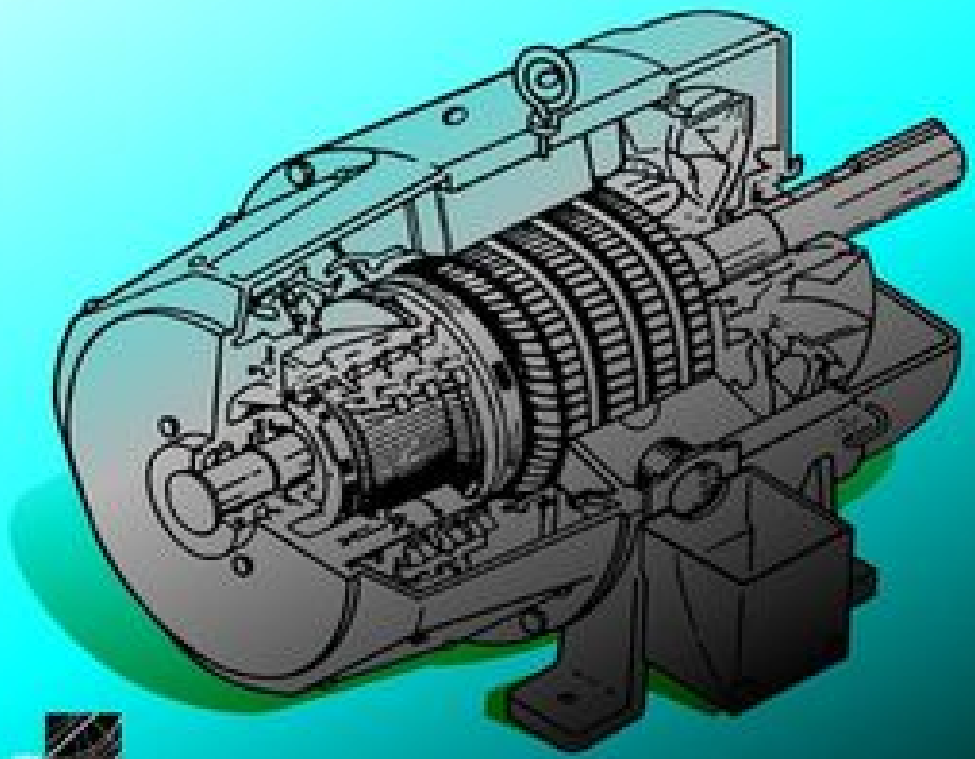
Principles of Electric Machines with Power Electronic Applications

Second Edition

Mohamed E. El-Hawary



IEEE PRESS
Mohamed E. El-Hawary, Series Editor

www.EngineeringEBooksPdf.com

PRINCIPLES OF ELECTRIC MACHINES WITH POWER ELECTRONIC APPLICATIONS

www.EngineeringEBooksPdf.com

PRINCIPLES OF ELECTRIC MACHINES WITH POWER ELECTRONIC APPLICATIONS

Second Edition

MOHAMED E. EL-HAWARY

IEEE Power Engineering Society, *Sponsor*



IEEE Press Power Engineering Series
Mohamed E. El-Hawary, *Series Editor*



IEEE
PRESS



A JOHN WILEY & SONS, INC., PUBLICATION

www.EngineeringEBooksPdf.com

IEEE Press
445 Hoes Lane, P.O. Box 1331
Piscataway, NJ 08855-1331

IEEE Press Editorial Board
Stamatios V. Kartalopoulos, *Editor in Chief*

M. Akay	M. E. El-Hawary	M. Padgett
J. B. Anderson	R. J. Herrick	W. D. Reeve
R. J. Baker	D. Kirk	S. Tewksbury
J. E. Brewer	R. Leonardi	G. Zobrist
	M. S. Newman	

Kenneth Moore, *Director of IEEE Press*
Catherine Faduska, *Senior Acquisitions Editor*
John Griffin, *Acquisitions Editor*
Tony VenGraitis, *Project Editor*

Technical Reviewers
Anjan Bose, Washington State University
Charles Gross, Auburn University

This book is printed on acid-free paper. ♾

Copyright © 2002 by The Institute of Electrical and Electronics Engineers, Inc. All rights reserved.

No part of this publication may be reproduced, stored in a retrieval system or transmitted in any form or by any means, electronic, mechanical, photocopying, recording, scanning or otherwise, except as permitted under Section 107 or 108 of the 1976 United States Copyright Act, without either the prior written permission of the Publisher, or authorization through payment of the appropriate per-copy fee to the Copyright Clearance Center, 222 Rosewood Drive, Danvers, MA 01923, (978) 750-8400, fax (978) 750-4744. Requests to the Publisher for permission should be addressed to the Permissions Department, John Wiley & Sons, Inc., 605 Third Avenue, New York, NY 10158-0012, (212) 850-6011, fax (212) 850-6008. E-Mail: PERMREQ@ WILEY.COM.

For ordering and customer service, call 1-800-CALL WILEY.

Library of Congress Cataloging-in-Publication Data is available.

El-Hawary, Mohamed, E.
Principles of Electric Machines with Power Electronic Applications/
Mohamed, E. El-Hawary.
p. cm.
Includes bibliographical references and index.
ISBN 0-471-20812-4 (cloth: alk. paper)

10 9 8 7 6 5 4 3 2 1

www.EngineeringEBooksPdf.com

CONTENTS

PREFACE ix

Chapter 1 INTRODUCTION 1

1.1 Electric Machines / 1
1.2 Roots in Observation / 2
1.3 Beginnings / 3
1.4 Foundations of Electromagnetism / 5
1.5 The Dawn of Electrodynamics / 7
1.6 Early Electric Generators / 9
1.7 Early Electric Motors / 10
1.8 Alternating Current / 11
1.9 Power Electronics: Scope and A Brief History / 13
1.10 Structure of the Power System / 18
1.11 Outline of the Text / 21

Chapter 2 PRINCIPLES OF ELECTROMAGNETISM AND ELECTROMECHANICAL ENERGY CONVERSION 23

2.1 Introduction / 23
2.2 Magnetic-Field Laws / 24
2.3 Permeability and Magnetic-Field Intensity / 31
2.4 Magnetic Circuits / 35
2.5 Flux Linkages, Induced Voltages, Inductance, and Energy / 50

www.EngineeringEBooksPdf.com

2.6 Hysteresis Loop / 54
2.7 Eddy-Current and Core Losses / 59
2.8 Energy Flow Approach / 60
2.9 Field Energy / 64
2.10 Multiply Excited Systems / 69
2.11 Reluctance Motors / 72
2.12 Doubly Excited Systems / 75
2.13 Salient-Pole Machines / 77
2.14 Round or Smooth Air-Gap Machines / 80
2.15 Machine-Type Classification / 84
2.16 *P*-Pole Machines / 85
Problems / 89

Chapter 3 POWER ELECTRONIC DEVICES AND SYSTEMS 103

3.1 Introduction / 103
3.2 Power Semiconductor Devices / 103
3.3 Control Characteristics of Power Devices / 106
3.4 Power Semiconductor Diodes / 108
3.5 Power Transistors / 115
3.6 The Thyristors / 138
3.7 Power Electronic Systems / 175
3.8 Power Integrated Circuits and Smart Power / 178
Problems / 179

Chapter 4 DIRECT-CURRENT MOTORS 183

4.1 Introduction / 183
4.2 Construction Features / 184
4.3 Circuit Model of dc Generator / 185
4.4 Circuit Model of dc Motors / 187
4.5 dc Series Motors / 190
4.6 dc Shunt Motors / 203
4.7 Compound Motors / 212
4.8 Motor and Load Matching / 224
4.9 Conventional Speed Control of dc Motors / 224
4.10 Reversal of Direction of Rotation / 241
4.11 Starting dc Motors / 241
4.12 Adjustable Speed dc Motor Drives / 251

www.EngineeringEBooksPdf.com

4.13 ac–dc Drives for dc Motors / 255
4.14 dc–dc Drives for dc Motors / 261
Problems / 265

Chapter 5 TRANSFORMERS 273

5.1 Introduction / 273
5.2 Ideal Transformers / 274
5.3 Transformer Models / 278
5.4 Transformer Performance Measures / 286
5.5 Single-Phase Connections / 292
5.6 Three-Winding Transformers / 296
5.7 Three-Phase Systems and Transformer Connections / 300
5.8 Autotransformers / 313
Problems / 316

Chapter 6 INDUCTION MOTORS AND THEIR CONTROL 323

6.1 Introduction / 323
6.2 MMF Waves and the Rotating Magnetic Field / 324
6.3 Slip / 329
6.4 Equivalent Circuits / 331
6.5 Simplified Equivalent Circuits / 334
6.6 Torque Characteristics / 338
6.7 Some Useful Relations / 341
6.8 Internal Mechanical Power / 344
6.9 Effects of Rotor Impedance / 348
6.10 Classification of Induction Motors / 351
6.11 Starting Induction Motors / 354
6.12 Conventional Speed Control of Induction Motors / 362
6.13 Adjustable Speed Drives: General Considerations / 370
6.14 Variable-Voltage–Constant-Frequency Drives / 372
6.15 Variable-Voltage–Variable-Frequency Drives / 376
6.16 dc-Link-Converter Drives / 381
6.17 Voltage-Fed Inverter Drives / 383
6.18 Current-Fed Inverter Drives / 385
6.19 Cycloconverter Drives / 386
6.20 Regulation of Slip Power / 387
Problems / 389

www.EngineeringEBooksPdf.com

Chapter 7 SYNCHRONOUS MACHINES 397

7.1 Introduction / 397
7.2 Round-Rotor Machines: Equivalent Circuit / 401
7.3 Armature Reaction / 406
7.4 Principal Steady-State Characteristics / 410
7.5 Power Angle Characteristics and the Infinite-Bus Concept / 415
7.6 Synchronous-Motor Operation / 423
7.7 Salient-Pole Machines / 430
Problems / 437

Chapter 8 FRACTIONAL-HORSEPOWER ALTERNATING CURRENT MOTORS 443

8.1 Introduction / 443
8.2 Rotating Magnetic Fields in Single-Phase Induction Motors / 443
8.3 Equivalent Circuits for Single-Phase Induction Motors / 448
8.4 Power and Torque Relations / 454
8.5 Starting Single-Phase Induction Motors / 459
Problems / 473

BIBLIOGRAPHY 475

INDEX 477

www.EngineeringEBooksPdf.com

PREFACE

This book offers an introduction to principles of electric machines and the closely related area of power electronics and adjustable speed drives. It is designed for students in electrical and other engineering disciplines, as well as being a useful reference and self-study guide for the professional dealing with this important area. The coverage of the book is intended to enable its use in a number of ways including service courses taught to nonelectrical majors. The organization and details of the material allow a maximum flexibility for the instructor to select topics for inclusion in courses in the modern engineering curriculum.

This book does not require a level of mathematical sophistication beyond that given in undergraduate courses in basic physics and introductory electric circuits. The emphasis in coverage is given to an improved understanding of the operational characteristics of the electric apparatus discussed, on the basis of linear mathematical models. Almost every key concept is illustrated through the use of in-text examples that are worked out in detail to enforce the reader's understanding. Many practical problems in electric machines operation involve the use of known performance variables under a given operational condition to predict the same variables under different operating conditions. These problems can be easily dealt with using the basic performance characteristics to obtain some corollary results that are useful for this purpose. On many occasions, this text takes the time to derive some of these useful relations to allow the student to deal with these common and important problems.

The first chapter provides a historical perspective on the development of electromechanical energy conversion devices and starts by tracing the origins of electricity leading up to the fundamental discoveries of the not too distant past. While this topic is not an integral part of the conventional coverage in texts and courses in this

www.EngineeringEBooksPdf.com

area, this chapter should provide interesting insights into the influence of these developments on present day civilization. It is through an appreciation of the past developments and achievements that we can understand our present and forge ahead with future advances.

Chapter 2 offers some background necessary to comprehend the basics of electric machine operations. The advent of the SCR and subsequent developments in solid state and power electronics technology introduced new elements in the practice of motor speed control. This important area is now of sufficient maturity that it should form an integral part of any comprehensive treatment of electric motors. This text recognizes this need by offering in Chapter 3, a detailed treatment of power electronic devices and systems to allow integration of the discussion with each electric motor with its adjustable speed drive application in the subsequent chapters. Chapters 4 to 8 deal with the conventional topics covered in present courses in electric machines and transformers. Emphasis is given to practical aspects, such as dealing with matching motors to loads, speed control, starting, and in general to the main performance characteristics of the devices discussed.

I have attempted to make this book as self-containing as much as possible. As a result, the reader will find that many background topics such as magnetic circuits, the per unit system and three-phase circuits are included in the text's main body, as opposed to the recent trend towards including many appendices dealing with these topics. In studying and teaching electrical machines, it has been my experience that a problem-solving approach is most effective when exploring this rich area. As a result, the reader will find many problems at the end of each chapter that reinforce the concepts learned in the chapter.

A textbook such as this could not have been written without the continuing input of the many students who have gone through many versions of its material as it was developed. My sincere thanks to the members of the many classes I was privileged to teach this fascinating area. I wish to acknowledge the able work of Elizabeth J. Sanford in putting this manuscript in a better shape than I was able to produce. My continuing association with the IEEE Press and Wiley staff have been valuable through out the many stages of preparing this text. I wish to express my appreciation for their work.

I owe a debt of gratitude to many of my colleagues who reviewed this manuscript and provided many valuable comments that improved this work considerably: It is always a great pleasure to acknowledge with thanks the continuing support of Dalhousie University during the course of preparing this text. As always, my wife, Dr. Ferial El-Hawary's patience and understanding have made this project another joy to look forward to completing.

MOHAMED E. EL-HAWARY

Halifax, Nova Scotia
March 2002

www.EngineeringEBooksPdf.com

PRINCIPLES OF ELECTRIC MACHINES WITH POWER ELECTRONIC APPLICATIONS

www.EngineeringEBooksPdf.com

CHAPTER 1

INTRODUCTION

Electrical engineering is a wide and diversified area of human activity that plays a very important role in today's civilization. If one were to attempt to single out a field of electrical engineering that heralded the dawn of the Electrical Age, the field of electromechanical energy conversion would emerge as a strong contender. It is the main purpose of this chapter to discuss the origins and historical developments that led to present-day electromechanical energy conversion engineering and related areas. The treatment is brief but is intended to provide a historical perspective that highlights advances gained over the years. The brief history is followed by an outline of the text.

1.1 ELECTRIC MACHINES

An electric machine is an electric apparatus with one or more components capable of rotary or linear motion. The operation of the machine depends on electromagnetic induction, which is defined as the production of an electromotive force in an electric circuit by a change in the magnetic flux linking with the circuit.

Electric machines are encountered in almost all areas of activity and, it is worth noting that present high-tech applications such as robotics and computers depend, in no small measure, on advanced, precise, and energy-efficient electric machines operating as motors. Disk and tape drives, printer mechanisms, and manipulator arms rely on the electric motor in their performance.

www.EngineeringEBooksPdf.com

1.2 ROOTS IN OBSERVATION

For many centuries, human beings have observed natural electric and magnetic effects. Atmospheric electrical phenomena such as lightning have been known to the human race since antiquity. Italian sailors navigating the Mediterranean discovered emissions of light from the mastheads of their ships on nights of dry stormy weather. This light is known as the St. Elmo's fire mentioned in the records of the second voyage of Columbus in 1493. Polar lights in the north (*aurora borealis*) and in the south (*aurora australis*) have been observed for many centuries.

Biological electric-field effects displayed by certain creatures of the sea have been observed and reported over 2000 years ago in the writings of Greek philosophers, including Aristotle. A human being could receive a shock by touching the marine creature known as an electric torpedo with a spear. The connection between the torpedo's electric property and that of atmospheric electric effects is recognized in the Arabic name for the torpedo, *ráad*, which is also the word for *thunder*. The electric torpedo was used for medical treatment of headaches at the time of Anthony and Cleopatra.

Lightning, St. Elmo's fire, polar lights, and animal electricity are phenomena that people observe, but in whose generation they do not take an active part. Two other phenomena, however, were observed that do require human action. The property of amber to acquire the power of attracting light objects through friction has been known for at least 2500 years, as evidenced by the writings of Thales, one of the seven wise men of Greece. An ancient reference to the electric property of amber is found in the Middle Eastern romance *The Loves of Majnoon and Leila*. In the text, Majnoon says of his beloved, "She was an amber, and I but a straw; she touched me and I shall ever be attracted to her." The second phenomenon involves the emission of sparks from the human body due to friction. It was known, for example, that Servius Tullius, the sixth King of Rome, gave off sparks as his locks were combed. These are manifestations of static electricity.

The observations of the ancients led to the 1660 invention by Otto Von Guericke of Magdeburg of the first frictional machine. The machine consisted of a sulfur globe mounted on an axis that when rotated against a cloth pressed to its surface emitted sparks and attracted light pieces of straw.

Protection of buildings against damage due to lightning strikes is believed to date back several thousand years. The nature of construction of famous buildings such as the Temple of Juno and Solomon's Temple was such that their roofs were covered by metallic points. The concept of deliberate protection of buildings using lightning conductors was introduced by Benjamin Franklin following the famous (but extremely dangerous) kite experiments in 1750.

Magnetic-field effects appearing in nature have been observed since antiquity. Ancient civilizations made use of magnetism in direction finding as early as 2637 B.C., one of the earlier gadgets being attributed to the time of the Chinese emperor Hoang-Ti. In that invention, a prominent female figure that contained magnetic material was mounted on a chariot and always pointed to the south regardless of the chariot's direction of motion. Chinese south-seeking instruments were again reported 16 centuries later for use as navigational aids on land and sea. By the twelfth century, knowledge of the

www.EngineeringEBooksPdf.com

magnetic compass and its application had spread to many countries. It is well known that Christopher Columbus employed the magnetic compass on his voyages in 1492.

The attraction of iron to lodestone has been known for countless years. Attempts to explain this phenomenon date back to the poetic work of Lucretius in 55 B.C. The early Christian writer Saint Augustine described in his *De Civitate Dei* (A.D. 428) magnetic experiments involving the attraction of a piece of iron lying on a silver dish by a lodestone underneath. The phenomenon of magnetic attraction led to the story of sympathetic needles that prevailed in the sixteenth to eighteenth centuries. William Gilbert of Colchester, physician to Queen Elizabeth I, published a book entitled *De Magnete* dealing with observed phenomena of magnetism and electricity. The publication of the book helped to focus the attention of investigators on new directions that resulted in significant discoveries.

1.3 BEGINNINGS

Further discoveries and applications of electricity resulted from the availability of the frictional machine in the eighteenth century. A notable discovery occurred in 1720, with Stephen Grey announcing the principle of insulation and conduction of electricity. Electric charges were transmitted for hundreds of feet through a hempen cord suspended by silk threads. Transmission of an electric charge for several miles was made possible using metallic wire instead of the hempen cord. Grey's discoveries were a prelude to the discovery of charge storage in a Leyden jar that took place a quarter of a century later.

It has been observed that electrified bodies lost their charge quickly, and it was believed that air abstracted the charge from the conductor. It thus seemed that if an electrified body were surrounded by an insulating material, contact with air, and hence loss of charge, would be reduced. Water appeared to be a convenient recipient of the electric charge and glass seemed to be the most effective insulator. This provided the basis for experiments carried out by many investigators. It is believed that Cunaeus working with Musschenbröek of Leyden on this concept discovered in January 1746 what is now known as the Leyden jar for storing electric charge. Cunaeus held the glass bottle in his right hand; the prime conductor of a powerful frictional machine was connected by a wire to the water inside the bottle. Using his left hand, Cunaeus attempted to disengage the wire from the conductor, believing that enough charge had been accumulated in the water. Needless to say, our friend received quite a convulsive shock, which made him drop the bottle. Musschenbröek repeated the experiment and felt struck in the arms and shoulders and lost his breath. It took him two days to recover, and he stated later that he would not repeat the experiment for the entire kingdom of France.

Improvements on the Leyden experiments followed in many parts of Europe. The object of the experiments was to transmit shock for long distances using chains of Leyden jars. William Watson, a London physician, originated the idea of using two coatings separated by a dielectric to improve the Leyden jar. He also established the idea of positive and negative electrical charges.

www.EngineeringEBooksPdf.com

The discovery of steady electric current is due to the observation of muscle contractions in the legs of dead frogs when in contact with two different metals. In 1678, the Dutch scientist Swammerdam produced convulsions in the muscle of a frog by holding it against a brass ring from which it hung by a silver wire. This experiment clearly resembles that by which Luigi Galvani became famous over 100 years later. The Swiss philosopher Sulzer described an experiment carried out in 1762, in which he placed two pieces of different metals (silver and zinc) above and below his tongue. When the metals were brought in contact, Sulzer reported an itching sensation and a taste of sulfate of iron. Obviously, both Swammerdam and Sulzer had the opportunity to discover galvanism but did not have the good fortune to do so.

Luigi Galvani, born in Bologna in September 1737, was destined to discover the significance of the Swammerdam and Sulzer experiments following his own famous experiments. On November 6, 1780, Galvani was preparing a frog for dissection in the vicinity of an electrical machine and observed that the animal's body suddenly convulsed. After a number of similar experiments, he resolved in 1781 to try the effect of atmospheric electricity. Galvani erected a lightning conductor on the roof of his house and connected it to his laboratory. Nerves of frogs and other animals were connected to the lightning conductor and their muscles were observed to convulse whenever lightning appeared. In 1786, Galvani resumed the experiments with the help of his nephew Camillo Galvani. On September 20, 1786, Camillo had some frogs prepared for the experiments and hung them by an iron hook from the top of an iron rail of the balcony. Soon, he noted convulsions when a frog was pressed against a rail. Luigi Galvani experimented at length and concluded that the convulsions were the result of the simultaneous contact of iron with nerves and muscles. It is interesting to note that Galvani attributed the convulsions to animal electricity, that is, electricity excited by the animal organs themselves.

Alessandro Volta, then a professor of physics at Pavia, was interested in the results of Galvani's experiments. He concluded that the exciting cause of convulsions was nothing but ordinary electricity produced by the contact of two metals. His theory of contact was derived from the Sulzer experiments. In August 1796, Volta took disks, one of copper and the other of zinc, brought them into contact, and suddenly separated them without friction. The usual indications of electricity were found. On June 26, 1800, he made his formal announcement to the Royal Society describing the now-famous voltaic pile. In his setup, Volta placed a disk of silver on a table; on top of it, he placed a disk of zinc, followed by a disk of spongy matter (cardboard) impregnated with a saline solution. The arrangements were repeated thirty to forty times. Shocks and sparks were found to occur, but it was remarkable that the pile recharged itself after a shock has been given. Thus was "born" one of humanity's greatest boons, the electric current.

The thermal effects of electricity were known as early as 1772, when the lightning conductors of St. Paul's Cathedral were observed to become red hot during thunderstorms. The idea of electric conduction through a liquid was established, and decomposition of water into its constituent gases by the use of electricity from a Leyden jar was accomplished by the English physician George Pearson in 1797. Following the invention of the voltaic pile, Nicholson and Carlisle established

www.EngineeringEBooksPdf.com

that water can be decomposed using voltaic current. The similarity between the chemical effects of static and voltaic electricity was thus established.

At the forefront of contributors to the electrochemistry in the nineteenth century is Humphry Davy, who was born in Penzance on December 17, 1778, and became professor of chemistry at the Royal Institution in 1801. His discoveries advanced the understanding and appreciation of the newly found steady electric current. In 1808, Davy made the first public display of the electric arc between two carbon electrodes connected to a voltaic pile. His most brilliant success was the decomposition of fixed alkalies by electricity in 1807.

1.4 FOUNDATIONS OF ELECTROMAGNETISM

The strong resemblance between electricity and magnetism had been observed for many years. These observations were supported by many facts, discovered as early as 1630, when Gassendi observed that lightning imparted magnetism to iron. In 1675, English navigators reported that the compass needles of their ships had their poles weakened and even reversed by lightning strokes. By the middle of the eighteenth century, speculation about the nature of the link between electricity and magnetism was a favorite pursuit.

Franklin noted that electricity is capable of reversing the polarity of magnetic needles. He also showed that the discharge of Leyden jars through a common sewing needle resulted in its magnetization. Many other investigators attempted at the turn of the nineteenth century to establish the connection between electricity and magnetism using the then available voltaic pile. It appears, however, that many of these attempts to demonstrate the effect of the voltaic pile on a magnetic needle were made with the pile open-circuited.

The main breakthrough is credited to a discovery by Hans Christian Oersted (1777–1851), born in Rudköbing on the island of Langeland in the Baltic, and was destined to discover the answer to the mystery of electromagnetism. He was appointed in 1806 to the Chair of Physics at the University of Copenhagen, where it is reported that in a private lecture to advanced students in the winter of 1819–1820, Oersted was demonstrating the then familiar experiment with a magnetic needle in the vicinity of a voltaic pile. Previously, the battery circuit had always been left open, as mentioned earlier. Is it not clear whether in making the demonstration Oersted closed the circuit by a lucky chance or on purpose. In any event, to his delight, he saw the needle move from its position of rest. Oersted pointed to the apparatus with trembling hands and invited his students to repeat the experiment. An account of this significant discovery was published in July 1820.

The enormous effect of Oersted's discovery on the direction of investigations in electricity and magnetism is evidenced by the quantum leap in related reports during that period. Sir Humphry Davy repeated Oersted's experiment and noted that iron filings on a paper near the wire were immediately attracted. Davy also anticipated lines of magnetic force by observing the orientation of steel needles in the neighborhood of the current-carrying conductors. Davy was not alone in immediately taking

www.EngineeringEBooksPdf.com

up Oersted's discoveries; the list includes Ampère and Arago in France, Faraday and Sturgeon in England, Schweigger in Germany, and Joseph Henry in New York.

As stated one of those who followed up on Oersted's discoveries was André Marie Ampère (1775–1836), who was then a professor at the College of France and at the Ecole Polytechnique in Paris. Ampère assumed the first and highest place by his research results, reported on September 18, 1820, to the Academy of Sciences—within two months of Oersted's formal announcement. In his paper Ampère explained the law that determines the position of the magnetic needle relative to the electric current. To illustrate the concept, he proposed a little *bon homme* (good man) swimming in the direction of the current with the positive pole at the feet and the negative at the head. The needle will be aligned at right angles to the current, with the north pole pointing toward the man's left and the south pole pointing toward his right. Ampère established the concept of a complete electric circuit by discussing the effect on the magnetic needles of the current in the battery. He also showed that current-carrying conductors have a magnetic effect on one another.

Yet another important step in the development of electrodynamics was taken during the same period. Johann Schweigger (1779–1857), a German chemist in Halle, announced his famous "multiplier principle" on September 16, 1820. The principle states that a conducting wire twisted upon itself and forming N turns produces a magnetic effect N times greater than a wire with a single turn. Schweigger's discovery resulted in the invention of the galvanometer.

François Arago (1786–1853) was another French physicist who took an interest in Oersted's discovery and in Ampère's theory of magnetism. He placed an ordinary sewing needle in a glass tube and wound a copper wire around the tube. The application of a current through the wire resulted in the magnetization of the needle. Arago's observations bore fruit in the first electromagnet, constructed by William Sturgeon (1783–1850) and displayed in 1825. Sturgeon used a bar of soft iron bent in the form of a horseshoe and coated with insulating varnish. Sixteen turns of bare copper wire were wound around the bar while keeping the turns separate. Upon the application of electric current, the electromagnet lifted a weight of 9 pounds.

The concept of Sturgeon's electromagnet was further improved by Joseph Henry (1797–1878) of New York. Henry brought the turns of wire closer together in a circumferential formation around the rod. To do this, he insulated the wires with silk covering. He was thus able to improve on the lifting power by increasing the number of turns at nearly right angles to the axis of the rod. Henry's first electromagnet was exhibited in June 1828 at the Albany Institute in New York, at which he was a professor. He continued with his experiments, but encountered a problem in his attempts to increase the lifting power by adding more turns, which suggested that turns added beyond a certain point were less effective in improving the lifting power. It is interesting to note that in 1827, Georg Simon Ohm (1789–1854), a professor of physics at Munich, published his now celebrated law. Ohm's law can be used to explain Henry's observation. It is unfortunate, however, that Ohm's law failed to attract attention in that era and was totally unknown to Henry or even to Wheatstone

www.EngineeringEBooksPdf.com

in 1837. Nonetheless, Henry worked out a practical solution, and by doing so discovered some practical implications of Ohm's law.

Henry's solution resulted in two kinds of electromagnets. The first, which he called a quantity magnet, had numerous short coils (low resistance). The second, which he referred to as an intensity magnet, had one very long coil (high resistance). The coils of the quantity magnet were connected (in parallel) to a galvanic cell, which Henry called a quantity battery. To drive a single long coil of the intensity magnet, Henry used a number of galvanic cells (in series), which he called an intensity battery. By so doing, Henry arrived at some very practical corollaries to Ohm's law without even being aware of it. As a professor of natural philosophy at Princeton, Joseph Henry was able in 1833 to demonstrate electromagnets that were capable of lifting up to 3500 pounds.

We have seen that Arago's work inspired the invention of the electromagnet. Another experiment that he carried out provided the inspiration for major breakthroughs by Michael Faraday (1791–1867). In the now-famous Arago's experiment, a copper disk was rotated about an axis. Just above the disk, a magnetic needle was suspended such that its point of suspension was exactly above the center of the disk. A screen of glass separated the needle and disk so that air circulation due to the motion of the disk was not imparted to the needle. The needle deviated from its rest position as the disk rotated, picking up speed until it rotated with the disk.

1.5 THE DAWN OF ELECTRODYNAMICS

Oersted's discovery was followed by a wave of new experiments and discoveries that provided the foundation for linking electricity and magnetism, as we have seen in the preceding section. Up to that point, we know that electrical investigators depended entirely on the voltaic current and the magnetic needle for their work. From our present knowledge, we can claim that the stage was set for the arrival of a person who changed the course of electrical engineering history by discovering a new source of electric current.

Michael Faraday's investigations of electromagnetism came upon the heels of Oersted's discovery in 1820–1821 and resulted in the development of what is now known as electromagnetic rotation. Ten years later, Faraday's interest in the area resulted in the development of electromagnetic induction. Faraday repeated Oersted's experiment and saw the significance of the mutual effect of the current and the magnet. On September 3 and 4, 1821, he set up an experiment whereby a free-moving current-carrying wire was rotated around the pole of a fixed magnet causing a free-moving magnet to rotate around a fixed current-carrying wire. To demonstrate the two effects, Faraday designed a device that he had made for him by an instrument maker. A sketch of this device is shown in Fig. 1.1. Faraday's experimental success demonstrated for the first time the possibility of converting electric current into continuous mechanical motion.

www.EngineeringEBooksPdf.com

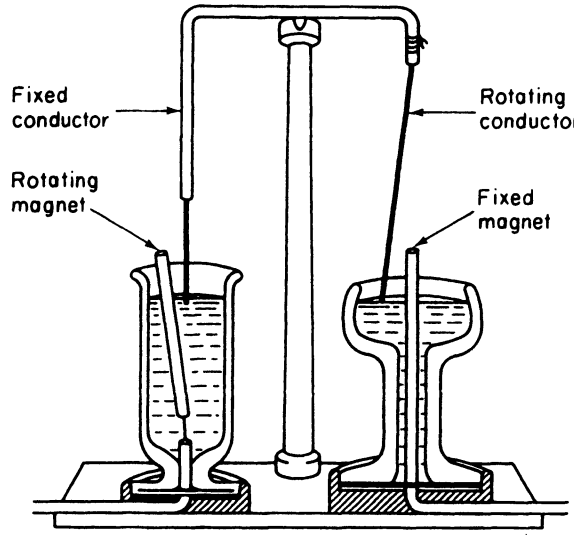


Figure 1.1 Device showing Faraday's electromagentic rotations.

During the period 1821–1831, Faraday continued to be puzzled by one facet of Arago's experiment. Iron was the only substance attracted by a magnet, yet copper appeared to be magnetic when rotated near a pivoted magnet. It was also known that a copper current-carrying wire attracted iron filings. He concluded that he would discover the key by investigating the inductive effects of electric currents. He was rewarded when he found a full explanation of Arago's magnetic phenomenon.

On August 29, 1841, Faraday carried out his famous ring experiment. The experiment involved an iron ring and two coils, *A* and *B*. Coil *A* was made of three sections wound on the left-hand side of the ring. Coil *B* was made of two sections wound on the right-hand side. It is of interest to note that this arrangement constituted the first transformer. The terminals of coil *B* were connected by a long wire passing above a magnetic needle. One section of coil *A* was connected to a battery. On making the connection, Faraday observed the needle move, oscillate, and then settle to its original rest position. When he broke the connection of the *A* coil with the battery, the needle again moved. Faraday repeated the experiment, but with three sections of coil *A* connected to the battery, and observed that the effect on the needle was much stronger than before.

On October 17, 1831, a second major discovery was made. A helix consisting of eight coils of copper wire, connected in parallel to a galvanomenter and wound around a hollow paper cylinder, was used. Faraday thrust the end of a cylindrical bar magnet quickly into the cylinder. There was a sudden deflection of the needle, which then died down. On withdrawing the magnet, the same effect was achieved.

www.EngineeringEBooksPdf.com

Although the transformer experiment and the magnet plunged into a coil were successful in showing the effects of induction, Faraday was still interested in following up on Arago's experiment, and was thus led to his third experiment.

The third experiment was carried out on October 28, 1831, and was modified to its now well-known arrangement on November 4, 1831. A revolving copper plate was mounted on a horizontal brass axle. By means of small magnets fixed to the pole pieces of a powerful magnet, Faraday produced a short gap in which the plate revolved. One contact was made on the disk's periphery and the second one on the axle. This arrangement produced significant currents lasting for as long as the plate was rotated. Faraday's discoveries clearly provide the origins of electrodynamic devices, including the transformer, the alternator, and the direct-current generator.

1.6 EARLY ELECTRIC GENERATORS

The news of Faraday's experiments sparked an unprecedented interest in developing machines that generated electricity from magnetism, as the process was known at the time. In July 1832, an oscillating setup was made by Salvatore dal Negro of Padua in Italy. The arrangements included four coils on a table and four small magnets on a carriage that could be advanced up to the coils and then withdrawn mechanically. Clearly, this setup was not practical, but is served to demonstrate the phenomenon.

The first electromagnetic generator employing rotation was invented by M. H. Pixii of Paris in 1832. In this first generator, a permanent magnet of the horseshoe type was rotated about a vertical axis by means of a hand crank and gearing. Immediately above the magnet were the poles of a wire-wound soft-iron core fixed in a suspending frame. The terminals of the winding were connected to a commutator. The machine produced a rapid succession of sparks when cranked.

An magnetoelectric machine made by Saxton was displayed in June 1833. The machine had a horizontal horseshoe magnet. The armature consisted of a four-armed soft-iron cross. A soft-iron core carrying a coil was attached to each arm. The four-pole armature rotated on a horizontal spindle opposite the end of the magnet. The rotation was provided by a belt from a vertical pulley and hand crank.

By 1850, the development of dynamos depended on their perceived application as a source of electricity for powering lighthouses. The most important designs of that era were due to Frederick Hale Holmes. The first of his designs was a $2\frac{1}{2}$-hp machine. The rotor consisted of six wheels, each carrying six compound permanent magnets, for a total of 36. The frame consisted of five rings, each carrying 24 coils. A direct-current output was obtained through a large commutator.

The success of the trial resulted in Holmes receiving an order for two machines, with the stipulation that the driving speed must not exceed 90 rpm. Holmes complied by modifying the design so that the magnets were stationary. He used 60 magnets that were carried in three vertical planes. Two coil-carrying wheels, each with 80 coils, rotated at 90 rpm. Each of the $2\frac{3}{4}$-hp machines was driven by a steam engine through a belt drive. On December 8, 1858, at South Foreland High Lighthouse, the first electric-powered lighthouse illuminated the sea. An additional Holmes machine

www.EngineeringEBooksPdf.com

was placed in use in 1862 and five years later, two more were ordered. The 1867 design ran at 400 rpm and had fixed magnets and rotating coils.

The idea of replacing permanent magnets by electromagnets in the design of electric machines dates to observations by the Abbés Moigno and Raillard in 1838. Starting with a small machine whose permanent magnet was capable of lifting only a few grams, the electricity generated enabled a larger electromagnet to lift a load of 600 kg. About the same time, Charles G. Page (1812–1868) found that by adding a current-carrying coil around a permanent magnet, the effect of the original magnet was greatly increased.

In February 1867, William Siemens (1823–1883) announced that permanent magnets were not necessary to convert mechanical into electrical energy. Within a few years, he developed a practical machine in which the field magnet was in two parts and the poles faced one another on opposite sides of the armature. The design employed a fundamental invention made in 1856 by Werner Von Siemens (William's brother) in which a cylindrical armature was made to rotate in a closely encircling tunnel in the magnet pole pieces.

An experiment by Henry Wilde involved a small magneto whose electricity output was fed to the field magnet of a second machine. The output of the second machine was led to the field of a third and larger one. Using this cascading approach, Wilde observed the melting of pieces of iron rod. He effected self-excitation in some machines in 1867 by diverting some of the armature current through the field winding. His machines were used in electroplating and as the first electric searchlights on battleships. Within a year, the principles of "shunt" and "series" field windings were well recognized. The machines constructed in this era all suffered from current fluctuations. A solution was proposed by Antonio Pacinotti (1841–1912) in 1860, but unfortunately, this went unnoticed until it was reinvented by Zénobe Théophile Gramme (1826–1901) in 1870.

Improvements to design of dynamos continued, aided by theoretical foundations provided by the publication of James Clerk Maxwell's treatise on electricity and magnetism in 1872. It is worth noting here that Maxwell's work influenced Hopkinson of King's College, Cambridge, who established magnetic flux, and reluctance. These advances had a significant impact on the design of more economical and advanced machines.

1.7 EARLY ELECTRIC MOTORS

The concept of the electric motor emerged at almost the same time as that of the electric generator. Dal Negro demonstrated in 1830 that a rotary motion can be obtained from current supplied by a voltaic battery. The experiment showed that a pivoted magnet could be kept in continuous oscillation by current in an adjacent coil. In 1831, Joseph Henry in the United States discussed the principles of operation of one of the first proposed electromagnetic motors, the operation of which was based on a rocking energized iron bar.

The Vermont inventor Thomas Davenport experimented with some early motor designs, and by 1840 had a workable motor. Simultaneously, Charles Page

www.EngineeringEBooksPdf.com

experimented with an electric motor that emulated beam engines, which were well known at the time. Page replaced the steam cylinder of a beam engine by a solenoid and the piston by an iron core. With the aid of a Congressional grant, he built a double-acting beam-type electric motor with a flywheel and connecting rods.

The fact that a dynamo can be used as well as a motor had been discovered by Heinrich Lenz (1804–1865) as early as 1838. This simple fact went unnoticed until 1860, when Pacinnoti announced a motor concept that created magnetic poles in the armature that were controlled by the commutator such that they did not move with the armature rotation but remained stationary as the iron itself moved.

Thomas Alva Edison (1847–1931) designed a miniature motor for use in his famous electric pen. The pen motor may be claimed as the first electric motor in history to be produced and sold commercially in large quantities. A motor specially designed for traction purposes is due to Immisch (1886). It featured a double horizontal field magnet and a long Gramme armature. In an attempt to reduce magnetic-field distortion and consequent sparking, he employed a particular commutator design. The commutator had two sections side-by-side, with segments staggered to short-circuit the coils as they passed through the neutral positions.

In 1887, Frank Julian Sprague (1857–1934) built a 12-mile street railway in Richmond, Virginia. The Sprague motor design incorporated effective solutions to problems of speed control, housing, suspension, geared drive, and the proper form of trolley contact. The Sprague system can be argued to have innagurated the golden age of electric motors for traction purposes, for railroad electrification grew vigorously beginning in the early 1890s.

1.8 ALTERNATING CURRENT

Alternating current emerged as a challenger to direct current during the last two decades of the nineteenth century. In that period, the field of electrical engineering experienced phenomenal growth following the introduction of the incandescent lamp. Alternating current was used for early arc lamps, as it ensured equal burning of the two carbon electrodes.

Direct current (dc) held the field for a number of years for a number of reasons. One of the strongest arguments is that dc permitted the use of standby batteries, thus ensuring reliability of customer service and providing a nighttime supply when generators were shut down. Efficient and reliable dc motors were developed out of the fundamental work related to the dynamo. However, the scales were tipped in favor of alternating current (ac) with the emergence of two inventions, the transformer and the induction motor. Both devices were developed in the last decade of the nineteenth century.

1.8.1 The Transformer

We have seen that the concept of induction between closely coupled coils has been known since Faraday's famous ring transformer experiments of 1831. The idea was

www.EngineeringEBooksPdf.com

developed further in Henry's experiments (1832), and was closely followed in 1836 by C. G. Page's work on what he termed a "dynamic multiplier." Page correlated the phenomena of self-induction and induction between two discrete conductors. From the prototype of the autotransformer, he evolved a design that featured a separate primary and a secondary.

In 1856, C. F. Varley devised a device in which the advantages of a subdivided iron core to secure minimum eddy-current loss were combined with a simple construction. The core in Varley's construction was a bundle of iron wires. The primary and secondary windings were wound over the center one-third of the core length. The ends of core wires were turned back over the windings to complete the magnetic circuit.

Close to 30 years later, Lucien Gaulard and John D. Gibbs introduced a system of single-phase 2000-V ac distribution. The system's backbone is a transformer with a core of soft-iron wire with a primary of insulated wire coil that is surrounded by six equal coils. The secondaries are brought out to separate terminals on the side, so that six sections can be used if required.

In 1885, George Westinghouse (1846–1914) read of the use of ac in Europe in conjunction with transformers displayed in England by L. Gaulard and J. D. Gibbs. The transformer configuration patented by Gaulard and Gibbs utilized multiple one-to-one turns-ratio transformers with the primary windings connected in series across the high-voltage primary circuit. The secondary circuit then supplied an individual low-voltage secondary. Westinghouse bought the American rights to Gaulard–Gibbs patents and authorized the development of equipment for an experimental power plant at Great Barrington, Massachusetts. Under the direction of William Stanley, the Westinghouse transformers, which were designed in 1886, had the primary windings for the individual units connected in parallel across the high-voltage primary circuit rather than in series. Tests being successful, Westinghouse marketed the first commercial ac system at the end of 1886.

In 1891, W. M. Mordey invented the construction that has been used up to the present. The magnet core was made of soft-iron stampings. Mordey employed the shell-type construction, with the iron sheets assembled around the primary and secondary coils so that the windings were completely surrounded by iron.

The importance of the transformer to the advance of ac stems from the growing demand for electric power. With a large demand in major urban centers, it made obvious sense to produce cheap power at remote centers. The transformer used in a step-up configuration enabled the transmission of power at high voltages with lower transmission losses. Once there, a transformer is used to step-down the voltage so the electric power can be more widely used. Parallel to the development of the transformer were advances in the production of efficient ac motors. We review this presently.

1.8.2 The Induction Motor

In 1879, Walter Bailey demonstrated the possibility of producing a magnetic field that rotated without the aid of mechanical motion.

www.EngineeringEBooksPdf.com

The principles for the design and operation of ac motors were patented by Nikola Tesla (1856–1943) on May 1, 1888. Details were announced on May 16 of the same year. Tesla's paper described three forms of his invention. The common factor between the three forms is the ring-wound stator with four salient poles. The first form had a rotor with four salient poles, forming a reluctance motor that ran at synchronous speed. This form is not self-starting. The second form had a wound rotor and ran at slightly less than synchronous speed. The third form was a synchronous motor, as dc was supplied to the rotor windings. Tesla's motors were designed for two-phase current taken from a dynamo with a drum armature through two coils at right angles connected to two pairs of slip rings instead of the normal commutator.

George Westinghouse bought Tesla's patents and employed him to develop them. The Westinghouse organization produced a practical induction motor in 1892. At the Chicago World Fair in 1893, Westinghouse displayed a 220-V 300-hp two-phase induction motor. The power supply consisted of two single-phase 60-Hz 50-hp alternators on the same engine shaft, but displaced 90 degrees. The motor had 12 poles with a distributed two-phase primary winding of cable threaded through rotor slots.

The Thomson-Houston Company entered the field of designing and producing induction motors, and soon both they and Westinghouse adopted three-phase induction motors for commercial purposes. The invention of the T-connection of two transformers to provide a three-phase supply from two-phase systems is due to C. F. Scott at Westinghouse. The T or Scott connection was a determining factor in the transition from two-phase to three-phase designs.

Single-phase motors require a rotating magnetic field. Tesla invented the split-phase winding to achieve this from a single-phase supply. Two coils displaced by 90 degrees were used, one winding having a much higher resistance than the other, so that the currents were displaced in phase. The high-resistance winding had to be opened when the motor approached full speed. Since 1925, this type of motor has been largely replaced by the capacitor motor.

While these developments were taking place in North America, parallel developments in Britain and on the Continent added to the rapid progress in motor technology. Galileo Ferrari of Turin produced a prototype two-phase induction motor that used high inductance in one coil to produce the necessary phase shift in 1888. W. Langdon Davies produced an experimental single-phase induction motor in 1891, and a more advanced version in 1897. The Davies design featured slotted laminated sheets for stator construction and squirrel-cage conductors in the rotor. At the Frankfurt Exhibition in 1890, a three-phase 100-hp induction motor was displayed.

1.9 POWER ELECTRONICS: SCOPE AND A BRIEF HISTORY

The history of power electronics is much older than many are likely to realize, but the growth and development of this technology have not been smooth and orderly. The episodes that have brought about the most dramatic changes in the field have

www.EngineeringEBooksPdf.com

been largely unanticipated. We begin by looking at the scope of the area, and then we look back briefly at the history of electrical engineering to identify some of the major events that have shaped the growth of power electronics into the major industry it is today.

Power electronics is the technology associated with efficient conversion, control, and conditioning of electric power by static means, from its available input form into the desired electrical output form. This technology involves the efficient use of electrical and electronic components, the application of linear and nonlinear circuit and control theory, the use of skillful design practices, and the development of sophisticated analytical tools toward achieving the following objective:

> The goal of power electronics is to control the flow of energy from an electrical source to an electrical load with high efficiency, high availability, high reliability, small size, light weight, and low cost.

All power electronic systems control and regulate the flow of electric energy between an ac or dc source and one or more electrical loads that need alternating or direct current. The object is to meet the requirements of the load(s), and is achieved by changing the electrical impedance of one or more elements internal to the power converter that is placed between the source and the load(s).

Achieving high reliability requires avoiding the use of parts that have known or unpredictable short life-expectancy limitations such as tubes using heaters and filaments, or certain types of electrolytic capacitors. Avoiding moving parts that require periodic maintenance or replacement is motivated by the requirement that they be readily available. This is true when components are in the path of the main power flow and involved in the regular establishment and interruption of current as an essential part of the power conversion process. In fact, this is the reason for including the word "static" in the definition of power electronics.

Most power electronic circuits can be satisfactorily modeled by an electrical network consisting of controlled sources and lumped purely passive (resistive, capacitive, and inductive) elements in which the current that enters one terminal of any two-terminal element appears instantaneously at the other terminal. For a static power converter to operate efficiently, the variable impedance in the main power path between the source and load should change as rapidly as possible between as high a value and as low a value as possible. In other words, it is desirable that the impedance varies between values that are orders of magnitude apart.

We now turn our attention to the roots of power electronics, which some argue dates back to 1907 when Lee DeForest invented the three-element thermionic vacuum tube. The natural power source for this device is a dc voltage. The nonlinear switching element is resistive and changes from a large value of resistance to a small value under the control of voltage applied to one of its terminals called the grid.

Many authors suggest that the dawn of the power electronics era took place in 1912, five years after DeForest's invention of the vacuum tube. This is when E. F. W. Alexanderson of the General Electric Company applied for a patent on a method for modulating the current from a high-frequency alternator so that it could

www.EngineeringEBooksPdf.com

be used for radio telephony. The Alexanderson patent for the magnetic amplifier is considered to be the first device to meet all the requirements of the definition for power electronics, and most of the goals for power electronic equipment. Being essentially an ac-to-ac power converter, the circuit is a very effective power electronic circuit.

The magnetic amplifier differs from the three-element thermionic vacuum tube in significant ways. The natural power source for the former is a dc voltage, not an ac one, as is the case for magnetic amplifiers. Because vacuum tubes can use batteries for their power source, they are far more attractive than magnetic amplifiers for portable applications. Moreover, magnetic amplifiers are incapable of self-oscillation. By 1916, Alexanderson's magnetic amplifier had been used to modulate as much as 70 kW of power, while DeForest's three-element thermionic vacuum tube was able to handle only a few tens of watts. It was during that year that Alexanderson achieved a major triumph by using magnetic amplifiers to establish the first radio link between the United States and Europe. Although restricted largely to low-power applications, vacuum tubes with truly phenomenal performance soon overshadowed the solid virtues of magnetic amplifiers for most low-power applications and were rapidly developed during the years from 1914 to 1929.

The history of power electronics can be divided into three overlapping periods: those when magnetic amplifiers, gas-tube and vapor-tube controlled rectifiers, and power transistors and semiconductor controlled rectifier were developed. The period between 1928 and 1933 saw the development of gas- and vapor-filled controlled rectifiers, which were designed specifically for higher-power applications. Prominent among the new devices were two controlled rectifiers: the gas-filled thyratron and the mercury-arc ignitron. In both cases, a unidirectional current with a relatively low voltage drop flows after an enabling signal is applied to a third electrode, allowing the gas discharge to start. In the case of the thyratron, the function of the grid is to prevent the initiation of an arc from anode to cathode until after a preselected time in the cycle. In the case of the ignitron, announced in 1933 by Slepian and Ludwig, a pulse of current through the third electrode, called an igniter, initiates a cathode spot on the pool of mercury at the beginning of each conduction period.

During the 1930s, Frank G. Logan, an engineer at Vickers Electric in St. Louis, Missouri, patented nineteen improvements to magnetic amplifiers in which the nonlinear switching effect in the magnetic cores were coordinated with the change in the resistance of the rectifiers between forward conducting and reverse blocking states. The result was a considerably higher power gain with simpler circuit configurations. Such circuits are called self-saturating magnetic amplifiers. As will be seen, these new circuits did not receive much attention in the United States until after World War II.

Numerous applications combined tube controlled rectifiers and magnetic amplifiers. One such application was the stepless variation of theater-stage and auditorium lighting. A few watts expended in the grid circuit of two thyratrons in a push-pull connection provided the variable dc current to control the much larger magnetic-amplifier-output current to lighting loads.

Although there were notable exceptions, throughout the 1930s until the late 1940s the popularity of magnetic amplifiers declined while that of tube controlled rectifiers

www.EngineeringEBooksPdf.com

rose. During that period, the term industrial electronics became popular to describe the high power applications of electronics for purposes other than communication.

By the time of World War II a rotating amplifier called the amplidyne or Rototrol saw a great deal of service. This was a power amplifier that was effectively a combination motor–generator, with no rotating shaft brought to the outside. Because of its nonstatic electromechanical nature, however, such a device does not qualify under the definition of an electronic power conditioner.

Close to the end of World War II, the Allied Forces captured the German heavy cruiser *Prins Eugen*. The Allies discovered that the fire control equipment of the ship's 8-inch guns relied on magnetic amplifiers, which the Germans operated without attention for the life of the vessel. They were also using magnetic amplifiers in a wide range of applications, from stabilizers for range finders and gun mounts to the steering of the buzz bombs and V-2 rockets. The German success had come by taking Logan's circuits of the 1930s and using them with new square-loop magnetic materials such as Orthonol and permalloy, which the Germans had developed along with much improved dry-type copper-oxide and selenium rectifiers. The result was spectacular, and as a result power electronics took a major step forward in the late 1940s, and throughout the 1950s magnetic amplifiers became the equipment of choice for rugged reliable military and industrial control applications.

The introduction of selenium rectifiers in the mid-1940s was heralded as a major advance over the thyratrons, ignitrons, and even copper-oxide devices of the time. However, the selenium era proved to be short-lived. In the late 1940s, a series of important developments initiated the dawn of today's semiconductor era. These involved the invention and development of controllable semiconductor devices. Although point-contact diodes were in use in the 1940s, most important was the invention of the point-contact transistor in 1947, and that of the junction transistor in 1949, both at Bell Laboratories. Supported by countless process innovations, device concepts, and developments in physical understanding, the junction transistor formed the foundation for today's integrated circuits and power electronics businesses.

In 1952, Hall demonstrated the first significant power devices based upon semiconductor technology. The devices were fabricated using germanium mesa alloy junctions that resulted in a rectifier with impressive electrical characteristics for that time, that is, a continuous forward-current capability of 35 A and a reverse blocking voltage of 200 V. Hall also used the recently developed theories of carrier recombination, generation, and current flow to successfully model the electrical characteristics of power rectifiers and transistors.

In the mid-1950s power device characteristics capitalized on the development of single-crystal silicon technology. The larger band gap of silicon rectifiers resulted in higher reverse-voltage capability and higher operating temperatures. By the late 1950s, 500-V rectifiers were available in alloy junctions. The introduction of diffused junctions combined with mesa technology in the late 1950s led in later years to a reverse-blocking capability.

By the mid-1960s, theoretical avalanche breakdown voltages of up to 9000 V had been achieved by optimized contouring of mesa junctions. Increased current-

www.EngineeringEBooksPdf.com

handling capability became a possibility by optimizing device packaging for minimum thermal and mechanical stress on the chip. More recently, 77-mm-diam silicon rectifiers have become available with continuous-current ratings of 5000 A and reverse voltages of 3000 V.

To put this development in perspective, while the first commercially available silicon transistors were announced by Texas Instruments in 1954, almost a decade passed before their practical application to high-power conversion and control was recognized. Emitter current crowding, reliability, and materials processing challenges precluded economic justification. The introduction of the planar process by Fairchild plus the application of photolithography techniques to wafer processing resulted in the birth of the power transistor business in the 1960s. A decade of effort in the industry related to second breakdown, power/speed performance, and unique processes such as epitaxy deposition paid off. By the late 1970s, 200-A 500-V bipolar Darlington transistors with a gain of 50 were available, together with 100-V 10-A transistors that could operate at frequencies up to 1 MHz. Since then, however, the application of MOS technology to power transistors has been a major focus of the industry due to the promise of high-speed and high-input impedance in many low-voltage applications.

Beyond the important developments in material and process technology described earlier, there have been many significant device developments. One of the first of these was the publication of the P-N-P-N transistor switch concept in 1956 by Moll et al. at Bell Labs. Although probably envisioned by Bell for use in signal applications, engineers at General Electric quickly recognized its significance to power conversion and control, and within nine months announced the first commercial silicon-controlled rectifier (SCR) in 1957. This three-terminal power switch was fabricated using a 5-mm^2 alloy-diffused mesa silicon chip and had a continuous-current rating of 25 A and a blocking-voltage capability of 300 V. The shorted emitter concept plus the planar process resulted in planar-diffused SCRs in 1962. These processes resulted in high-voltage blocking capability at junction temperatures of 125 °C and made practical power control and conversion possible.

Since the early 1960s, thyristor producers have capitalized on the process innovations of the signal industry while introducing new devices or structural improvements to existing devices. In 1961 a gate turnoff thyristor (GTO) was introduced that combined the switching properties of a transistor with the low conduction losses of an SCR. In 1964 a bidirectional ac switch (TRIAC) was introduced by General Electric principally for 60-cycle consumer lighting and motor speed control. In 1965, light-triggered thyristors were developed that later found significant application in optoelectronic couplers. In the late 1960s a number of advances were made in the design of thyristor cathode gate structures. Incorporating interdigitated gates made high-power 20-kHz inverters possible. Similarly, the inclusion of pilot gating techniques decreased the gating requirements and improved high-frequency and pulse-duty operation. The reverse conducting thyristor (RCT) and asymetrical SCR were developed in 1970 to provide higher speed capability in those inverter applications where a reverse blocking voltage was not required. In the mid-1970s,

www.EngineeringEBooksPdf.com

thyristor designers were intrigued with electric-field (or voltage) controlled thyristors because they promised higher speed performance. The latter, however, never came to fruition and the application of MOS concepts has proven to offer similar benefits while being easier to manufacture.

The term power electronics came into wide acceptance as the umbrella term to describe the field during the late 1970s, by which time semiconductors had been the almost universal choice to perform the requisite switching-impedance function for a decade and a half.

The most recent trend in power devices has been the utilization of very large-scale integration (VLSI) technology to create a whole new generation of integrated power devices. This started with the power MOS transistor in the late 1970s, and has evolved toward totally new devices such as the MOS-gated thyristor, and, most recently, the insulated gate transistor (IGT) also known as the COMFET. This latter device combines the best features of the MOSFET and the bipolar transistor in a device that conducts more current in a unit area than either. In addition to the new discrete devices, monolithic high-voltage integrated circuits (HVIC) that combine power and signal circuitry on a chip have come on the scene. These devices are a dramatic extension of the trend toward mixed technologies in the IC industry, and for the first time allow the cost efficiencies of integrated circuitry to be applied in the power area. The initial application areas have been in telecommunications, power supplies, displays, and, most recently, power circuits. However, this is just the beginning, and these new HVICs represent a genuine revolution in the power electronics area. The net result could well be a vast extension of electronics into many new application areas in the home industry that have been precluded because of the limited capabilities and high cost of power electronics.

1.10 STRUCTURE OF THE POWER SYSTEM

Since the early days of Central Power Stations, the electric power system has evolved into a myriad of sizes, configurations, and structural components. All interconnected power systems are complex enterprises that share the same basic characteristics in that they consist of three phase ac systems operating with predefined nominal voltage and frequency. Systems can be subdivided into the following major subsystems:

- Generation
- Transmission and subtransmission
- Distribution

1.10.1 Generation Subsystem

The generation subsystem includes generators and transformers. An essential component of power systems is the three-phase synchronous generator or alternator. Synchronous generators have one field produced by the rotor driven at synchronous speed and excited by dc current. Another field is produced in the stator windings by

www.EngineeringEBooksPdf.com

the three-phase armature currents. The dc current for the rotor windings is provided by excitation systems. In older units, the exciters are dc generators mounted on the same shaft, providing excitation through slip rings. Present systems use ac generators with rotating rectifiers, known as *brushless* excitation systems. The excitation system maintains generator voltage and controls the reactive power flow. Because they lack a commutator, these ac generators can generate high power at high voltage, typically 30 kV.

The prime mover is the source of mechanical power supplied to the generator, and may be a hydraulic turbine; steam turbine whose energy comes from the burning of coal, gas, or nuclear fuel; gas turbine; or occasionally internal combustion engines burning oil. Steam turbines operate at relatively high speeds of 3600 or 1800 rpm. They are coupled to cylindrical-rotor, two-pole generators for 3600 rpm and four-pole generators for 1800 rpm operation. Hydraulic turbines, particularly those operating with low pressure, operate at low speed, and usually with salient-type rotor generators with many poles. In a generating plant, several generators are operated in parallel in the power grid to provide the total power needed. They are connected at a common point called a *bus*.

Many alternative energy sources are considered such as employing the untapped energy of the sun and the earth for power generation. Some sources used are solar power, geothermal power, wind power, tidal power, and biomass.

The transformer transfers power with very high efficiency from one level of voltage to another level. Due to its high efficiency, the power transferred to the secondary is almost the same as the primary. Using a step-up transformer reduces losses in the line, which makes the transmission of power over long distances possible.

Insulation requirements and other practical design problems limit the generated voltage to low values, usually 30 kV. Thus, step-up transformers are used for transmission of power. At the receiving end of the transmission lines, step-down transformers are used to reduce the voltage to suitable values for distribution or utilization. The electricity in an electric power system may undergo four or five transformations between generator and consumers.

1.10.2 Transmission and Subtransmission Subsystem

An overhead transmission network transfers electric power from generating units to the distribution system, which ultimately supplies the load. Transmission lines also interconnect neighboring utilities, which allows economic dispatch of power within regions during normal conditions, and the transfer of power between regions during emergencies.

High-voltage transmission lines are terminated in substations called *high-voltage substations*, *receiving substations*, or *primary substations*. The function of some substations is to switch circuits in and out of service; these are referred to as switching stations. At the primary substation, voltage is stepped down to a value more suitable for the next stage toward the load. Very large industrial customers may be served from the transmission system.

www.EngineeringEBooksPdf.com

The portion of the transmission system that connects the high-voltage substations through step-down transformers to the distribution substations is called the subtransmission network. There is no clear distinction between transmission and subtransmission voltage levels. Typically, the subtransmission voltage level ranges from 69 kV to 138 kV. Some large industrial customers may be served from the subtransmission system. Capacitor banks and reactor banks for maintaining the transmission-line voltage are usually installed in the substations.

1.10.3 Distribution Subsystem

The distribution system connects the distribution substations to the consumers' service-entrance equipment. The primary distribution lines operate on voltages from 4 kV to 34.5 kV and supply the load in a well-defined geographical area. Some small industrial customers are served directly by the primary feeders. The secondary distribution network reduces the voltage for utilization by commercial and residential consumers. Lines and cables not exceeding a few hundred feet in length then deliver power to the individual consumers. The secondary distribution serves most of the customers at levels of 240/120 V, single-phase, three-wire; 208Y/120 V, three-phase, four-wire; or 480Y/277 V, three-phase, four-wire. The power for a typical home is derived from a transformer that reduces the primary feeder voltage to 240/120 V using a three-wire line.

Distribution systems involve both *overhead* and *underground* means of power transmission. The growth of underground distribution has been extremely rapid, and as much as 70% of new residential distribution systems are installed underground.

Power systems loads are divided into industrial, commercial, and residential. Industrial loads are composite loads, and induction motors form a high proportion of these loads. These composite loads are functions of voltage and frequency and form a major part of the system load. Commercial and residential loads consist largely of lighting, computing, entertainment, heating, and cooking. These loads are independent of frequency and consume negligibly small reactive power.

For reliable and economical operation of the power system, it is necessary to monitor the entire system in a control center. The modern control center of today is called the *energy control center* (ECC). ECCs are equipped with on-line computers performing all signal processing through the remote acquisition system. Computers work in a hierarchical structure to properly coordinate different functional requirements under normal as well as emergency conditions. Every energy control center contains control consoles, which consist of a visual display unit (VDU), keyboard, and light pen. Computers may give alarms as advance warnings to the operators (dispatchers) when deviation from the normal state occurs. The dispatcher makes decisions and executes them with the aid of a computer. Simulation tools and software packages are implemented for efficient operation and reliable control of the system. In addition, SCADA, an acronym for "supervisory control and data acquisition," systems are auxiliaries to the energy control center.

www.EngineeringEBooksPdf.com

1.11 OUTLINE OF THE TEXT

The importance of the experimental and theoretical foundations of the areas of electrical and electromechanical energy conversion and power electronic engineering is evident from the preceding brief historical review. It is on this basis that Chapter 2 is founded. In Chapter 2, the basic laws, definitions, and relevant phenomena of electromagnetism are discussed. Emphasis is placed on the magnetic circuits of devices treated in this text. Ampère's circuital law is used to establish engineering-oriented procedures for analyzing the electromagnetic behavior of some simple structures. Properties of ferromagnetic materials, including eddy current and hysterisis loss, are discussed in this chapter. Theoretical foundations of electromechanial energy conversion devices are also treated in Chapter 2. The object here is the development of a simple but general approach to the energy conversion process in rotating electric machines. The discussion leads to an appreciation of the differences between the various types of electrical machines.

Chapter 3, which is titled "Power Electronic Devices and Systems," discusses the characteristics and technical performance characteristics of available solid-state power electronics devices. This is followed with a discussion of the various systems based on the availability of devices. Here we discuss ac voltage controllers, controlled rectifiers, choppers, and inverters. It is on the basis of the discussion in this chapter that we introduce aspects of adjustable speed drives along with each motor type discussed in subsequent chapters. In Chapter 4 the dc machine as generator and motor is considered. The discussion of dc generators is brief by necessity, but various connections and performance characteristics are given. The discussion of dc motors is more detailed and incorporates such important issues as matching motor to load, stating, speed control, and applications. Chapter 5 deals with transformers and offers the student an opportunity to appreciate the significance of Faraday's law and principles (discussed in Chapter 2) to the development of this important device. Analysis of the performance of transformers is the central topic of this chapter. The many uses for and connections of transformers are discussed from an application point of view.

Chapter 6 is dedicated to the induction motor, which is the versatile workhorse of today's industrial complex. Our treatment relies on principles discussed in Chapter 2 as well as the treatment of transformers in Chapter 5. Modeling the performance of the induction motor together with important characteristics, is also dealt with. Motor starting and control issues are also discussed in this chapter. In Chapter 7, the synchronous machine is treated from a systems application point of view. Again, performance characteristics for round-rotor and salient-pole machines are dealt with. In addition, the applications of synchronous motors are presented in this chapter.

A number of fractional-horsepower machines are discussed in Chapter 8 to highlight their applications and performance characteristics. An ample number of drill problems at the end of each chapter are designed to follow the natural development of the text material.

www.EngineeringEBooksPdf.com

CHAPTER 2

PRINCIPLES OF ELECTROMAGNETISM AND ELECTROMECHANICAL ENERGY CONVERSION

2.1 INTRODUCTION

The operation of electromechanical energy conversion devices depends on a number of fundamental principles that originate in basic experimental work. In this chapter we discuss some concepts and terminology used in this text to study electric machines.

An electromechanical energy conversion device is essentially a medium of transfer between an input side and an output side, as shown in Fig. 2.1. In the case of an electric motor, the input is electrical energy drawn from the supply source and the output is mechanical energy supplied to the load, which may be a pump, fan, hoist, or any other mechanical load. The electric generator is a device that converts mechanical energy supplied by a prime mover (such as a steam turbine or a hydroturbine) to electrical energy at the output side. Many electromechanical energy conversion devices can act as either generator or motor.

The chapter begins with a brief review of the Lorentz force law, Biot-Savart law, and Ampère's circuital law. Magnetic-circuit concepts are discussed and properties of magnetic materials are covered. Faraday's law, inductance, and energy relations are also treated here.

The remainder of the chapter is devoted to the development of the principal relationships that govern the electromechanical energy conversion process. The relationships sought will be valuable in understanding the operation of electric machines studied in subsequent chapters.

www.EngineeringEBooksPdf.com

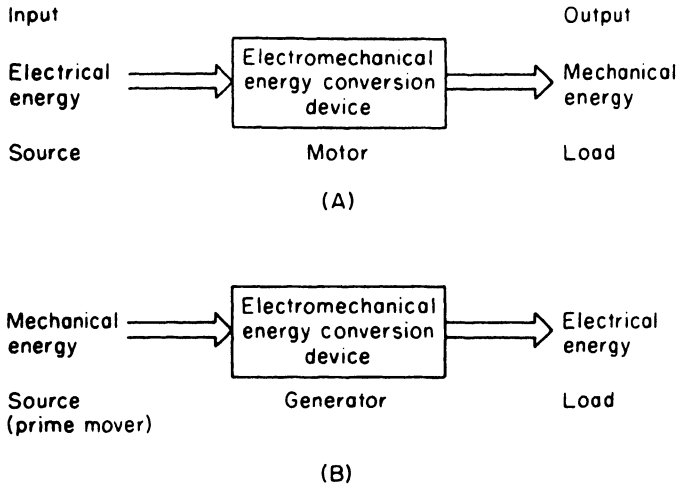


Figure 2.1 Functional block diagram of electromechanical energy conversion devices as (a) motor; (b) generator.

2.2 MAGNETIC-FIELD LAWS

Electric fields are associated with stationary electric charges. If the charges are moving with uniform velocity, a second effect known as magnetism takes place. Thus a magnetic field is associated with moving charges, and as a result, electric currents are sources of magnetic fields.

A magnetic field is identified by a vector **B** called the magnetic flux density. In the SI system of units, the unit of **B** is the tesla (T). The magnetic flux $\Phi = \mathbf{B} \cdot \mathbf{A}$. The unit of magnetic flux Φ in the SI system of units is the weber (Wb). It is clear that

$$1\,\mathrm{T} = 1\,\mathrm{Wb/m^2}$$

The tesla is a large unit and we may use the smaller unit of flux density in the cgs system denoted by the gauss (G), where

$$1\,\mathrm{T} = 10^4\,\mathrm{G}$$

2.2.1 The Cross (Vector) Product

The cross product (sometimes called the vector product) of two vectors **U** and **V** is another vector, **W**. This product is expressed by inserting a cross (an $\times$) between **U** and **V**, thus:

$$\mathbf{W} = \mathbf{U} \times \mathbf{V}$$

www.EngineeringEBooksPdf.com

The cross product **W** has a magnitude that is equal to the product of the magnitudes of **U** and **V** and the sine of the angle θ between **U** and **V**.

$$|\mathbf{W}| = |\mathbf{U} \times \mathbf{V}| = |\mathbf{U}||\mathbf{V}|\sin\theta$$

Geometrically, the magnitude of the cross product is the area of the parallelogram formed with **U** and **V** as adjacent sides. The direction of the cross product **W** is perpendicular to the plane of **U** and **V** and follows the right-hand rule, as shown in Fig. 2.2.

The concept of the cross product of two vectors is useful in formulating magnetic-field laws based on the experimental work of Oersted, Ampère, and Biot-Savart. We start with the Lorentz force law, which deals with the force on a moving charge in a magnetic field.

2.2.2 The Lorentz Force Law

A charged particle q in motion at a velocity **V** in a magnetic field of flux density **B** is found experimentally to experience a force whose magnitude is proportional to the product of the magnitude of the charge q, its velocity, and the flux density **B**, and to the sine of the angle between the vectors **V** and **B**, and is given by a vector in the direction of the $\mathbf{V} \times \mathbf{B}$. Thus we write

$$\mathbf{F} = q\mathbf{V} \times \mathbf{B} \tag{2.1}$$

Equation (2.1) is known as the Lorentz force equation. An interpretation of Eq. (2.1) is given in Fig. 2.3.

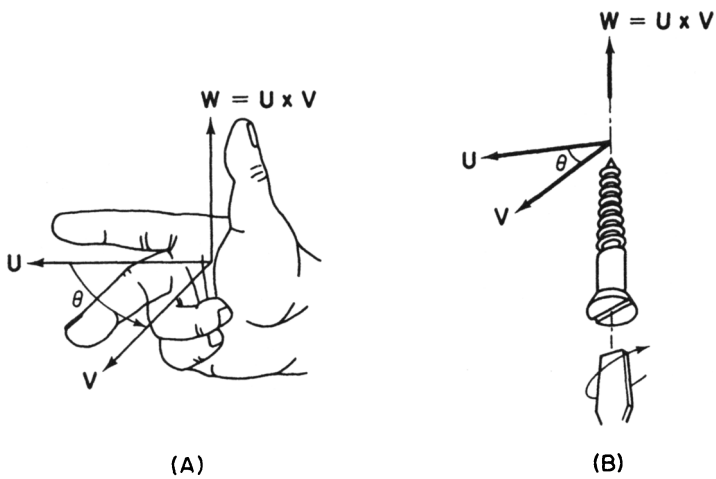


Figure 2.2 Defining the cross product **W** of two vectors **U** and **V**, using (a) the right-hand rule; (b) the right-hand screw rule.

www.EngineeringEBooksPdf.com

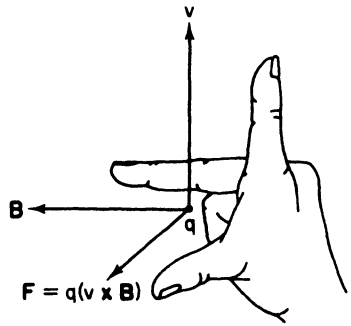


Figure 2.3 Lorentz force law.

On the basis of Eq. (2.1), one can define the tesla as the magnetic flux density that exists when a charge q of 1 coulomb, moving normal to the field at a velocity of 1 m/s, experiences a force of 1 newton.

A distribution of charge experiences a differential force $d\mathbf{F}$ on each moving incremental charge element dq given by

$$d\mathbf{F} = dq(\mathbf{V} \times \mathbf{B})$$

Moving charges over a line constitute a line current, and thus we have

$$d\mathbf{F} = (I\,\mathbf{dl} \times \mathbf{B}) \tag{2.2}$$

Equation (2.2) simply states that a current element I **dl** in a magnetic field **B** will experience a force $d\mathbf{F}$ given by the cross product of I **dl** and **B**. A pictorial presentation of Eq. (2.2) is given in Fig. 2.4.

The differential form (2.2) is of mathematical significance only, as the current element I **dl** cannot exist by itself and must be a part of a complete circuit. The force on an entire loop can be obtained by integrating the current element

$$\mathbf{F} = \oint I\,\mathbf{dl} \times \mathbf{B} \tag{2.3}$$

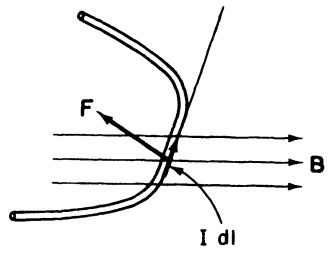


Figure 2.4 The force on the current element I **dl** subject to the magnetic field **B** is perpendicular to the plane of **B** and I **dl** according to Eq. (2.2).

www.EngineeringEBooksPdf.com

Equations (2.2) and (2.3) are fundamental in the analysis and design of electric motors, as will be seen later. Another important law in magnetic-field theory is the Biot-Savart law, which is based on Ampère's work showing that electric currents exert forces on each other and that a magnet could be replaced by an equivalent current.

2.2.3 The Biot-Savart Law

A magnetic field results from the motion of a charged particle q at a velocity $\mathbf{V}$. The flux density $\mathbf{B}$ at a point P, which is at a distance r from q in free space, is given by the Biot-Savart equation:

$$\mathbf{B} = \frac{\mu_0}{4\pi} q \frac{\mathbf{V} \times \mathbf{a}_r}{r^2} \text{ T} \tag{2.4}$$

The constant μ_0 is called the permeability of free space and in SI units is given by

$$\mu_0 = 4\pi \times 10^{-7}$$

The vector $\mathbf{a}_r$ is the unit vector originating at the charge q and directed toward the point P. A distribution of charge causes differential magnetic flux density $d\mathbf{B}$ due to each incremental charge element dq given by

$$d\mathbf{B} = \frac{\mu_0}{4\pi} dq \frac{\mathbf{V} \times \mathbf{a}_r}{r^2}$$

Recall that for line currents

$$(dq)\mathbf{V} = I\mathbf{dl}$$

As a result, we have

$$d\mathbf{B} = \frac{\mu_0}{4\pi} \frac{I\mathbf{dl} \times \mathbf{a}_r}{r^2} \tag{2.5}$$

The interpretation of Eq. (2.5) is shown in Fig. 2.5. The total magnetic field is obtained by integrating the contributions from all the incremental elements:

$$\mathbf{B} = \frac{\mu_0}{4\pi} \oint \frac{I\mathbf{dl} \times \mathbf{a}_r}{r^2} \tag{2.6}$$

As an application of the Biot-Savart law, let us consider the magnetic field of a long straight wire carrying a current I. The current element $I\,\mathbf{dl}$ is shown in Fig. 2.6 directed upward. The point P experiences an incremental magnetic flux density $d\mathbf{B}$

www.EngineeringEBooksPdf.com

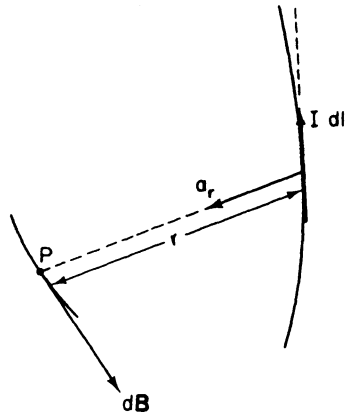


Figure 2.5 Interpreting the Biot-Savart law.

directed into the plane of the paper, as shown. The magnitude of $d\mathbf{B}$ is given by

$$d\mathbf{B} = \frac{\mu_0}{4\pi}\frac{I\mathbf{dl}\sin\theta}{r^2}$$

The total field at P is obtained by integrating over the entire length of the wire. The result is

$$\mathbf{B} = \frac{\mu_0 I}{2\pi R} \tag{2.7}$$

We can thus conclude that the magnetic field is in the form of concentric circles about the wire, with a magnitude that increases in proportion to the current I and decreases as the distance from the wire is increased.

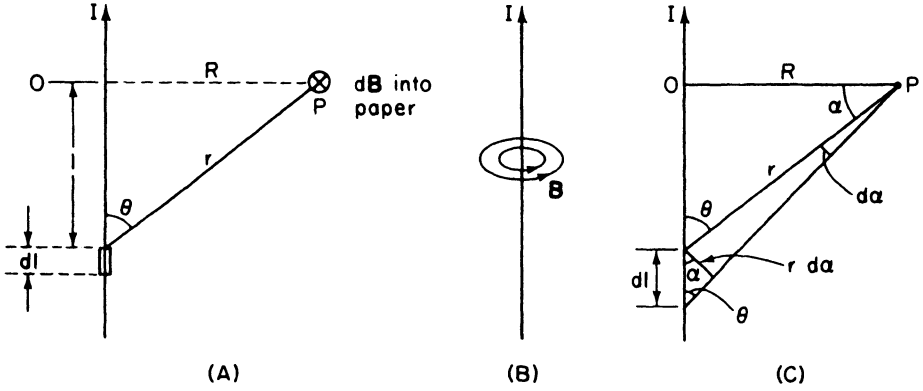


Figure 2.6 Finding the field due to an infinite wire carrying a current I: (a) geometry of wire used to apply Biot-Savart law; (b) showing the magnetic field; (c) elements of geometry to evaluate overall field.

www.EngineeringEBooksPdf.com

The Biot-Savart law provides us with a relation between current and the resulting magnetic flux density **B**. An alternative to this relation is Ampère's circuital law, which we discuss next.

2.2.4 Ampère Circuital Law

Ampère's circuital law states that the line integral of **B** about any closed path in free space is exactly equal to the current enclosed by that path times μ_0:

$$\oint_c \mathbf{B} \cdot \mathbf{dl} = \begin{cases} \mu_0 I & \text{path } c \text{ encloses } I \\ 0 & \text{path } c \text{ does not enclose } I \end{cases} \tag{2.8}$$

It should be noted that the path c can be any arbitrarily shaped closed loop about the net current I.

To illustrate Ampère's circuital law, let us consider the infinite wire carrying a current I, treated earlier using the Biot-Savart law. We have shown that the field is concentric circles about the wire with a flux density magnitude given by Eq. (2.7) as

$$\mathrm{B} = \frac{\mu_0 I}{2\pi R}$$

where R is the shortest distance between P and the wire. As shown in Fig. 2.7(a), the flux density at points on the circle with radius R_1 is constant at

$$\mathbf{B}_1 = \frac{\mu_0 I}{2\pi R_1}$$

We can choose this circle to be the closed path c_1 indicated in Eq. (2.8). The incremental length dl is given by

$$\mathbf{dl} = R_1 d\theta$$

The flux density is in the same direction as dl, and thus we have

$$\mathbf{B}_1 \cdot \mathbf{dl} = \frac{\mu_0 I}{2\pi R_1} R_1 \, d\theta$$

As a result,

$$\oint_{c1} \mathbf{B}_1 \cdot \mathbf{dl} = \int_0^{2\pi} \frac{\mu_0}{2\pi} d\theta = \mu_0 I$$

This confirms the first statement of Ampère's law.

The closed path need not be circular, and to illustrate this, we consider the path c_2 shown in Fig. 2.7(b). Path c_2 consists of the line segment ab and the semicircle bc

www.EngineeringEBooksPdf.com

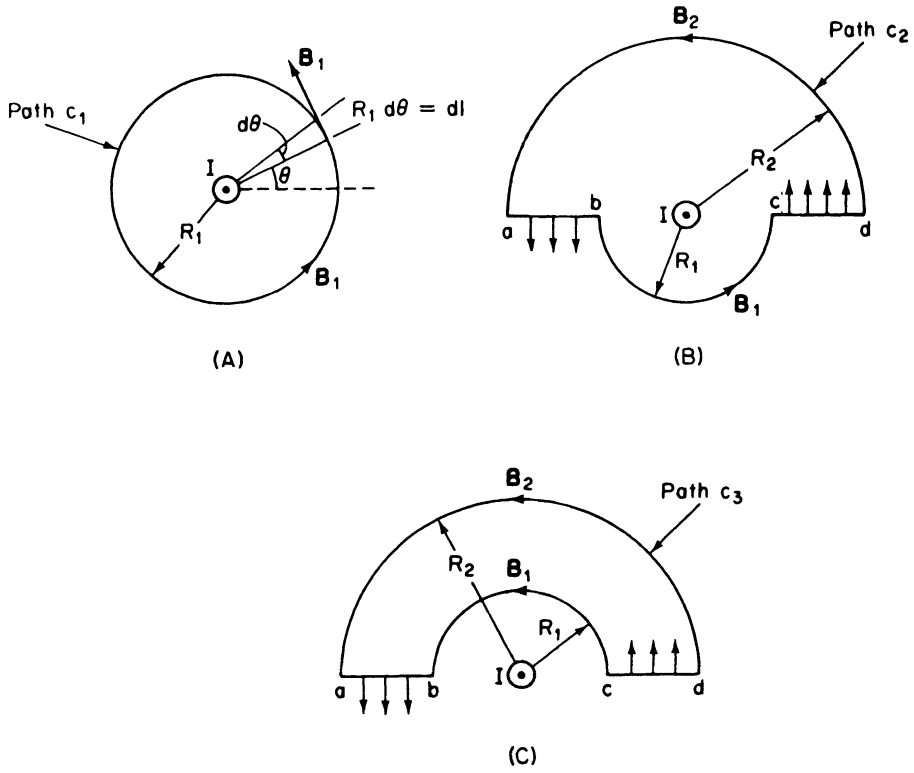


Figure 2.7 Illustrating Ampère's circuital law: (a) path c_1 is a circle enclosing current I; (b) path c_2 is not a circle but encloses current I; (c) path c_3 does not enclose current I.

with radius R_1, the line segment cd, and the semicircle da with radius R_2. The left-hand side of Eq. (2.8) is thus

$$\oint_{c2} \mathbf{B} \cdot \mathbf{dl} = \int_a^b \mathbf{B} \cdot \mathbf{dl} + \int_b^c \mathbf{B} \cdot \mathbf{dl} + \int_c^d \mathbf{B} \cdot \mathbf{dl} + \int_d^a \mathbf{B} \cdot \mathbf{dl}$$

We note that on the line segments ab and dc, the flux is perpendicular to dl and the inner (scalar) product is zero. Thus we have

$$\oint_{c2} \mathbf{B} \cdot \mathbf{dl} = \int_b^c \mathbf{B} \cdot \mathbf{dl} + \int_d^a \mathbf{B} \cdot \mathbf{dl}$$

The first integral is given by

$$\int_b^c \mathbf{B} \cdot \mathbf{dl} = \int_{-\pi}^{0} \frac{\mu_0 I}{2\pi R_1} R_1\, d\theta = \frac{\mu_0 I}{2}$$

www.EngineeringEBooksPdf.com

Similarly, the second integral is

$$\int_d^a \mathbf{B} \cdot \mathbf{dl} = \int_0^{\pi} \frac{\mu_0 I}{2\pi R_2} R_2 \, d\theta = \frac{\mu_0 I}{2}$$

We can therefore conclude that

$$\oint_{c2} \mathbf{B} \cdot \mathbf{dl} = \mu_0 I$$

The closed path c_2 encloses the current I and the statement of Ampère's law is confirmed for this path.

We will consider path c_3 of Fig. 2.7(c), which does not enclose the current I. Ampère's circuital law asserts that the line integral is zero in this case. This is confirmed as follows:

$$\oint_{c3} \mathbf{B} \cdot \mathbf{dl} = \int_a^b \mathbf{B} \cdot \mathbf{dl} + \int_b^c \mathbf{B} \cdot \mathbf{dl} + \int_c^d \mathbf{B} \cdot \mathbf{dl} + \int_d^a \mathbf{B} \cdot \mathbf{dl}$$

Again, the integrands from a to b and c to d are zero since $\mathbf{B}$ and $\mathbf{dl}$ are orthogonal. As a result,

$$\oint_{c3} \mathbf{B} \cdot \mathbf{dl} = \int_b^c \mathbf{B} \cdot \mathbf{dl} + \int_d^a \mathbf{B} \cdot \mathbf{dl}$$

Here we have

$$\int_b^c \mathbf{B} \cdot \mathbf{dl} = \int_{-\pi}^0 \frac{-\mu_0 I}{2\pi R_1} R_1 \, d\theta = \frac{-\mu_0 I}{2}$$
$$\int_d^a \mathbf{B} \cdot \mathbf{dl} = \int_0^{\pi} \frac{\mu_0 I}{2\pi R_2} R_2 \, d\theta = \frac{\mu_0 I}{2}$$

As a result, we conclude that, as expected, we have

$$\oint_{c3} \mathbf{B} \cdot \mathbf{dl} = 0$$

2.3 PERMEABILITY AND MAGNETIC-FIELD INTENSITY

The discussion of Section 2.2 is valid in free space, as we have consistently used the free-space permeability μ_0 in all expressions of magnetic-field laws. To extend these laws to situations where material other than free space is encountered, one must deal

www.EngineeringEBooksPdf.com

with the concept of permeability. The Biot-Savart law given by Eq. (2.5) shows that μ_0 is essentially a ratio of the magnitude of **B** to the current I that produces it. For free space **B** varies linearly with I, and μ_0 is therefore a constant. We can conclude that for materials that exhibit a linear variation of **B** with I, all expressions discussed in Section 2.2 are valid provided that μ_0 is replaced by the permeability corresponding to the material considered.

Material can be classified from a **B**-I-variation point of view into two classes:

1. Nonmagnetic material such as all dielectrics and metals with permeability equal, for all practical purposes, to μ_0.
2. Magnetic material that belongs to the iron group known as ferromagnetic material. For this class, a given current produces a much larger **B** field than in free space. Permeability of ferromagnetic material is much higher than that of free space and is nonlinear, since it varies over a wide range with variations in current.

Ferromagnetic material can be further categorized into two classes:

1. Soft ferromagnetic material for which a linearization of the **B**-I variation in a region is possible.
2. Hard ferromagnetic material for which it is difficult to give a meaning to the term *permeability*. Material in this group is suitable for permanent magnets.

The source of **B** in the case of soft ferromagnetic material can be modeled as being due to the current I. For hard ferromagnetic material, the source of **B** is a combined effect of current I and material magnetization M, which originates entirely in the medium. In order to separate the two sources of the magnetic **B** field, the concept of magnetic-field intensity **H** is introduced.

2.3.1 Magnetic-Field Intensity

The magnetic-field intensity (or strength) denoted by **H** is a vector defined by the relation

$$\mathbf{B} = \mu \mathbf{H} \tag{2.9}$$

For isotropic media (have the same properties in all directions), μ is a scalar, and thus **B** and **H** are in the same direction. On the basis of Eq. (2.9) we can write the statements of the Biot-Savart law given by Eqs. (2.5) and (2.6) as

$$d\mathbf{H} = \frac{1}{4\pi} \frac{I\mathbf{dl} \times \mathbf{a}_r}{r^2} \tag{2.10}$$

$$\mathbf{H} = \frac{1}{4\pi} \oint \frac{I\mathbf{dl} \times \mathbf{a}_r}{r^2} \tag{2.11}$$

www.EngineeringEBooksPdf.com

Moreover, Ampère's circuital law given by Eq. (2.8) is written as

$$\oint \mathbf{H} \cdot \mathbf{dl} = \begin{cases} I & \text{path } c \text{ encloses } I \\ 0 & \text{path } c \text{ does not enclose } I \end{cases} \tag{2.12}$$

Expressions (2.10), (2.11), and (2.12) are independent of the medium and relate the magnetic-field intensity **H** to the current causing it, I.

Equation (2.9) requires further examination, as the permeability μ is not a constant in general, but is dependent on **H** and, strictly speaking, we should state this dependence in the form

$$\mu = \mu(\mathbf{H}) \tag{2.13}$$

For nonmagnetic material, μ is constant at a value equal to $\mu_0 = 4\pi \times 10^{-7}$ for all practical purposes. The **B-H** characteristic of nonmagnetic materials is shown in Fig. 2.8.

The **B-H** characteristics of soft ferromagnetic material, often called the magnetization curve, follow the typical pattern displayed in Fig. 2.9. The permeability of the material in agreement with Eq. (2.9) is given as the ratio of **B** to **H** and is clearly a function of **H**, as indicated by Eq. (2.13):

$$\mu = \frac{\mathbf{B}}{\mathbf{H}} \tag{2.14}$$

The permeability at low values of **H** is called the initial permeability and is much lower than the permeability at higher values of **H**. The maximum value of μ occurs at the knee of the **B-H** characteristic. The permeability of soft ferromagnetic material μ is much larger than μ_0, and it is convenient to define the relative permeability μ_r by

$$\mu_r = \frac{\mu}{\mu_0} \tag{2.15}$$

A typical variation of μ_r with **H** for a ferromagnetic material is shown in Fig. 2.10.

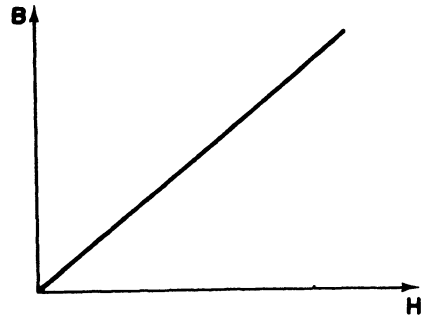


Figure 2.8 B-H characteristic for nonmagnetic material.

www.EngineeringEBooksPdf.com

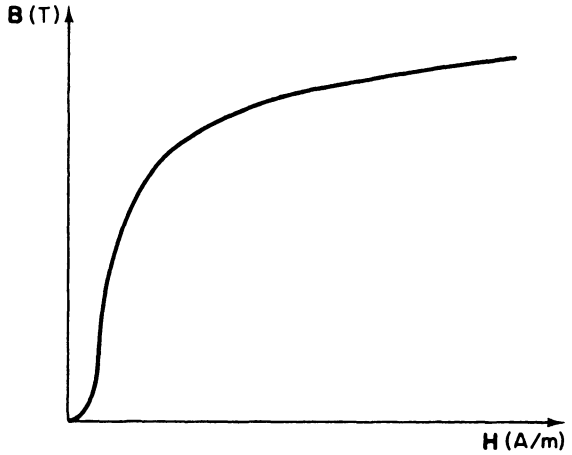


Figure 2.9 B-H characteristic for a typical ferromagnetic material.

For the electromechanical energy conversion devices treated in this text, a linear approximation to the magnetization curve provides satisfactory answers in the normal region of operation. The main idea is illustrated in Fig. 2.11, where a straight line passing through the origin of the **B-H** curve that best fits the data points is drawn and taken to represent the characteristics of the material considered. Within the acceptable range of **H** values, one can then use the following relation to model the ferromagnetic material:

$$\mathbf{B} = \mu_0 \mu_r \mathbf{H} \tag{2.16}$$

It should be noted that μ_r is on the order of thousands for magnetic materials used in electromechanical energy conversion devices (2000 to 80,000, typically). Properties

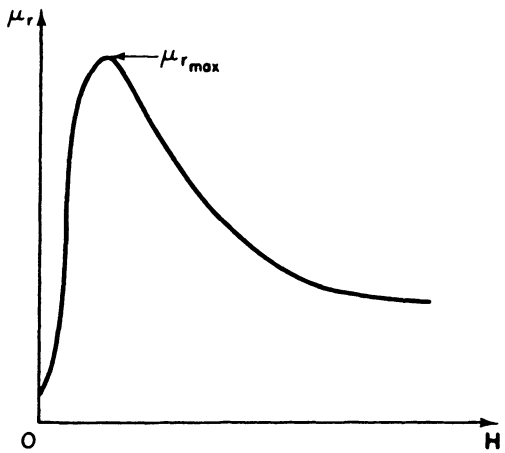


Figure 2.10 Typical variation of μ_r with **H** for a ferromagnetic material.

www.EngineeringEBooksPdf.com

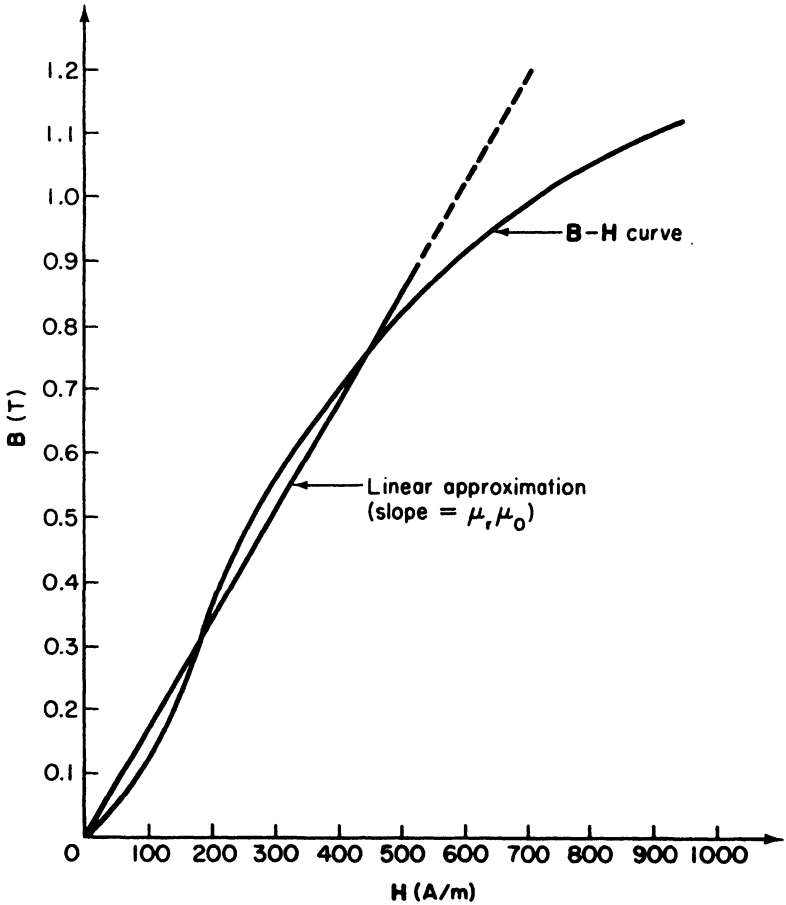


Figure 2.11 Linear approximation of the magnetization curve for a soft ferromagnetic material.

of magnetic materials are discussed further in the following sections. For the present, we assume that μ_r is constant.

2.4 MAGNETIC CIRCUITS

The statement of Ampère's circuital law in Eq. (2.12) is based on the assumption that the path C encloses the current one time. If a path encloses the current N times, the right-hand side of Eq. (2.12) becomes simple NI. Thus, in this case, we write

$$NI = \oint \mathbf{H} \cdot \mathbf{dl} \tag{2.17}$$

www.EngineeringEBooksPdf.com

The left-hand side of Eq. (2.17) is commonly referred to as the magnetomotive force (MMF) $\mathfrak{F}$, and hence we have

$$\mathfrak{F} = NI = \oint \mathbf{H} \cdot \mathbf{dl} \tag{2.18}$$

A magnetic circuit is a structure made for the most part of high-permeability magnetic material. The magnetic flux is confined to paths defined by the structure due to the high permeability of the magnetic material. An elementary example of a magnetic circuit is shown in Fig. 2.12. Here, a toroidal ferromagnetic core carrying an N-turn coil is considered. The torus has a cross-sectional area A, an inner radius a, and an outer radius b. Ampère's circuital law tells us that for a circular path with radius $r < a$, there is no magnetic field, since no current is enclosed by the path.

$$\mathrm{H} = 0 \qquad r < a$$

For a circular path $r \geq b$, we have

$$\oint \mathbf{H} \cdot \mathbf{dl} = N(I - I) = 0$$

Thus we have

$$\mathrm{H} = 0 \qquad r \geq b$$

Inside the torus, the magnetic field is constant on a circular path of radius r, due to symmetry. The field $\mathbf{H}$ is tangential to the circle, and thus

$$\mathbf{H} \cdot \mathbf{dl} = \mathrm{H} r \, d\theta$$

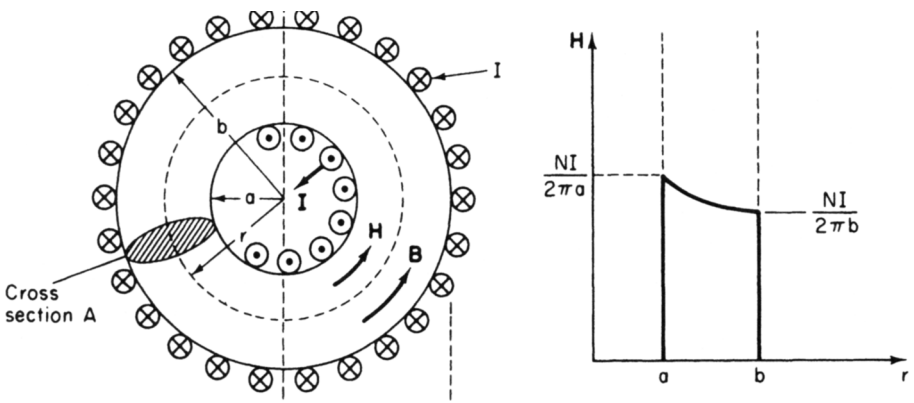


Figure 2.12 Toroidal coil and magnetic-field intensity distribution.

www.EngineeringEBooksPdf.com

As a result, the magnitude of **H** is obtained as

$$\oint \mathbf{H} \cdot \mathbf{dl} = \int_0^{2\pi} \mathrm{H} r \, d\theta = 2\pi r \mathrm{H}$$

We can conclude that

$$2\pi r \mathrm{H} = NI$$

The path clearly encloses the current N times. We can assert that the magnitude of the magnetic-field intensity H inside the structure is given by

$$\mathrm{H} = \frac{NI}{2\pi r} \qquad a < r < b$$

The field inside the toroid varies inversely with the radius r of the path. The magnitude of the flux density B inside the core is obtained by multiplying H by the permeability of the core material:

$$\mathrm{B} = \frac{\mu NI}{2\pi r}$$

The flux Φ is obtained using the expression

$$\Phi = \int \mathbf{B} \cdot \mathbf{dA}$$

As an approximation, we take the flux as the product of B at the average radius r_{av} and the uniform cross-sectional area A. Therefore, we have

$$\Phi = \frac{\mu NIA}{2\pi r_{\mathrm{av}}}$$

where

$$r_{\mathrm{av}} = a + \frac{b-a}{2}$$

As we have already defined the magnetomotive force by $\mathfrak{F} = NI$, we can write

$$\Phi = \mathfrak{F} \frac{\mu A}{2\pi r_{\mathrm{av}}}$$

The length of the circular path at the average radius is given by

$$\mathrm{l}_{\mathrm{av}} = 2\pi r_{\mathrm{av}}$$

www.EngineeringEBooksPdf.com

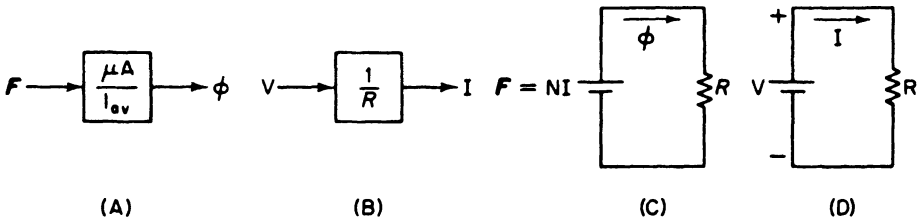


Figure 2.13 Establishing the magnetic-circuit concept.

As a result, we conclude that

$$\Phi = \mathfrak{F}\left[\frac{\mu A}{l_{av}}\right] \tag{2.19}$$

Let us examine Eq. (2.19) from an input–output (cause–effect) point of view. If we consider the magnetomotive force $\mathfrak{F}$ as an input (cause), the flux Φ set up by $\mathfrak{F}$ is an output (effect). This relation is depicted in block diagram form Fig. 2.13(a). Here the output Φ is obtained by multiplying the input $\mathfrak{F}$ by the quantity in brackets in Eq. (2.19). We are already familiar with Ohm's law for dc circuits, as interpreted in Fig. 2.13(b). Inspection of the figure shows us that an analogy between magnetic variables and electric-circuit variables is possible. We can thus establish a correspondence between electric voltage V (electromotive force) and the magnetomotive force $\mathfrak{F}$. Next, we have a correspondence of the electric current I and the flux Φ. As a consequence, we can claim a correspondence between the quantity $\mu A/l_{av}$ and the inverse of the resistance to complete the picture. Indeed, we now define the reluctance of the magnetic circuit denoted by $\mathfrak{R}$ as

$$\mathfrak{R} = \frac{l_{av}}{\mu A} \tag{2.20}$$

As a result, we write Eq. (2.19) as

$$\Phi = \frac{\mathfrak{F}}{\mathfrak{R}} \tag{2.21}$$

The units of reluctance are thus seen to be amperes per weber.

Let us observe that the magnetic reluctance as defined in Eq. (2.20) decreases as the permeability is increased, and in view of Eq. (2.21), a higher value of flux is obtained for the same MMF by using a material of lower reluctance. The advantages of this analogy include the ability to utilize our circuit analysis tools in dealing with magnetic-field problems.

The development of the magnetic circuit concept in this section relies on the analysis of the toroid of Fig. 2.12, where a uniformly wound coil of N turns is the source of MMF. In practice, coils occupying only a portion of the toroid, as shown in

www.EngineeringEBooksPdf.com

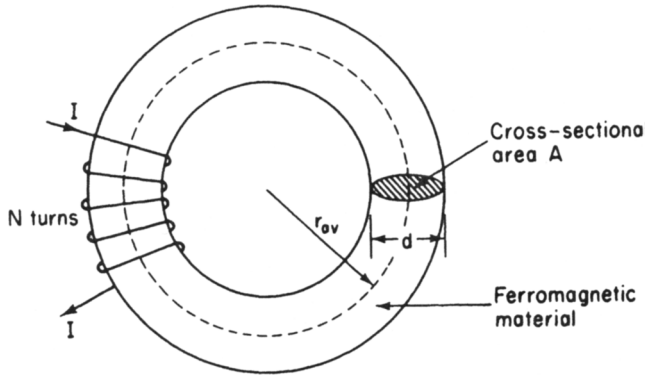


Figure 2.14 Partially wound toroid.

Fig. 2.14, are frequently encountered. Our results are valid from a practical engineering point of view as long as the toroid thickness $(b - a)$ is much smaller than the average length l_m. It should also be noted that analysis results apply to structures that are not circular. It is appropriate now to take a look at a simple example.

Example 2.1 The mean radius of a toroid is 25 cm and its cross-sectional area is 3 cm^2. The toroid is wound with a coil of 600 turns and a direct current of 1.5 A is passed through the coil. Assume that the relative permeability of the toroid is 1500. It is necessary to calculate:

1. The reluctance of the circuit
2. The magnetomotive force $\mathfrak{F}$ and magnetic-field intensity H.
3. The flux and flux density inside the toroid.

Solution

(a) The reluctance is calculated using

$$\mathfrak{R} = \frac{l_{av}}{\mu A}$$

We have

$$l_{av} = 2\pi(0.25)\,\text{m}$$
$$\mu = 1500(4\pi \times 10^{-7})$$
$$A = 3 \times 10^{-4}\,\text{m}^2$$

As a result,

$$\mathfrak{R} = \frac{2\pi(0.25)}{1500(4\pi \times 10^{-7})(3 \times 10^{-4})} = 2.78 \times 10^6\,\text{At/W}$$

www.EngineeringEBooksPdf.com

(b) The magnetomotive force is

$$\mathfrak{F} = NI = 600(1.5) = 900\,\text{At}$$

The magnetic-field intensity is

$$\text{H} = \frac{\mathfrak{F}}{l_{\text{av}}} = \frac{900}{2\pi(0.25)} = 572.96\,\text{At/m}$$

(c) The flux Φ is obtained as

$$\Phi = \frac{\mathfrak{F}}{\mathfrak{R}} = \frac{900}{2.78 \times 10^6}$$
$$= 3.24 \times 10^{-4}\ \text{Wb}$$

The flux density is

$$\text{B} = \frac{\Phi}{A} = \frac{3.24 \times 10^{-4}}{3 \times 10^{-4}} = 1.08\,\text{T}$$

Of course, we could use H directly from part (b) to obtain

$$\text{B} = \mu\text{H} = 1500(4\pi \times 10^{-7})(572.96)$$
$$= 1.08$$

This would provide

$$\Phi = \mathbf{B} \cdot \mathbf{A} = 1.08(3 \times 10^{-4}) = 3.24 \times 10^{-4}\ \text{Wb}$$

Naturally, we obtain the same results.

Assuming uniform fields, the magnetic-circuit concept can be applied to structures composed of different materials, such as that shown in Fig. 2.15. The path of integration in Ampère's law is shown as the closed contour *abcdefgha*. The length of the path *abcde* is denoted by l_1, the length of the path *ef* is denoted by l_2, the length of the path *fgh* is denoted by l_3, and that of *ha* is denoted by l_4. The application of Ampère's law results in

$$\mathfrak{F} = NI = \text{H}_1 l_1 + \text{H}_2 l_2 + \text{H}_3 l_3 + \text{H}_4 l_4$$

The flux Φ is the same everywhere in this single-loop structure, (neglecting leakage), and we thus have the following flux densities:

$$\text{B}_1 = \frac{\Phi}{A_1} \qquad \text{B}_2 = \frac{\Phi}{A_2}$$
$$\text{B}_3 = \frac{\Phi}{A_3} \qquad \text{B}_4 = \frac{\Phi}{A_4}$$

www.EngineeringEBooksPdf.com

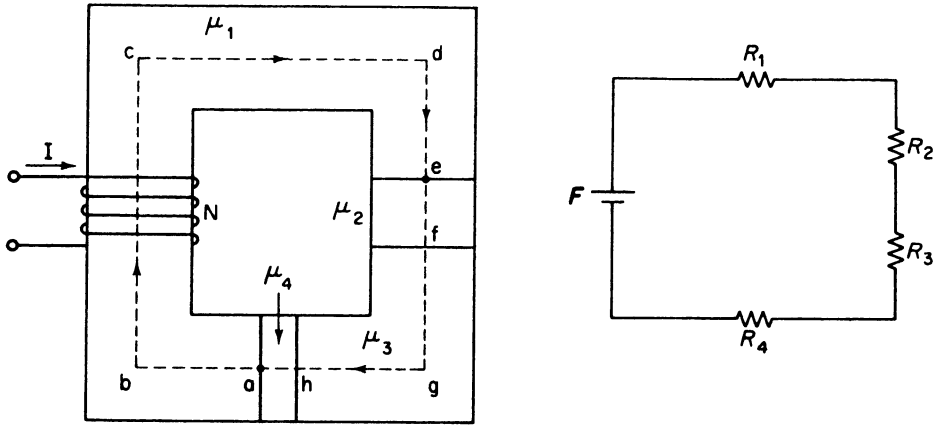


Figure 2.15 Magnetic structure exhibiting reluctances in series.

The areas A_1, A_2, A_3, and A_4 correspond to the sections indicated in the structure. Recall that

$$\mathrm{B}_i = \mu_i \mathrm{H}_i, \qquad i = 1, 2, 3, 4$$

Thus

$$H_i = \frac{\Phi}{\mu_i A_i}$$

As a result, we have

$$\mathfrak{F} = NI = \Phi\left(\frac{l_1}{\mu_1 A_1} + \frac{l_2}{\mu_2 A_2} + \frac{l_3}{\mu_3 A_3} + \frac{l_4}{\mu_4 A_4}\right)$$

Recall the definition of reluctance:

$$\mathfrak{R}_i = \frac{l_i}{\mu_i A_i}$$

We can thus assert that

$$\mathfrak{F} = (\mathfrak{R}_1 + \mathfrak{R}_2 + \mathfrak{R}_3 + \mathfrak{R}_4)\Phi$$

It is clear that the reluctances are in series, as shown in the magnetic equivalent circuit of Fig. 2.15.

The following example deals with a single-loop structure with two materials, the unknown is the MMF, and this problem is the inverse of that given in Example 2.1.

www.EngineeringEBooksPdf.com

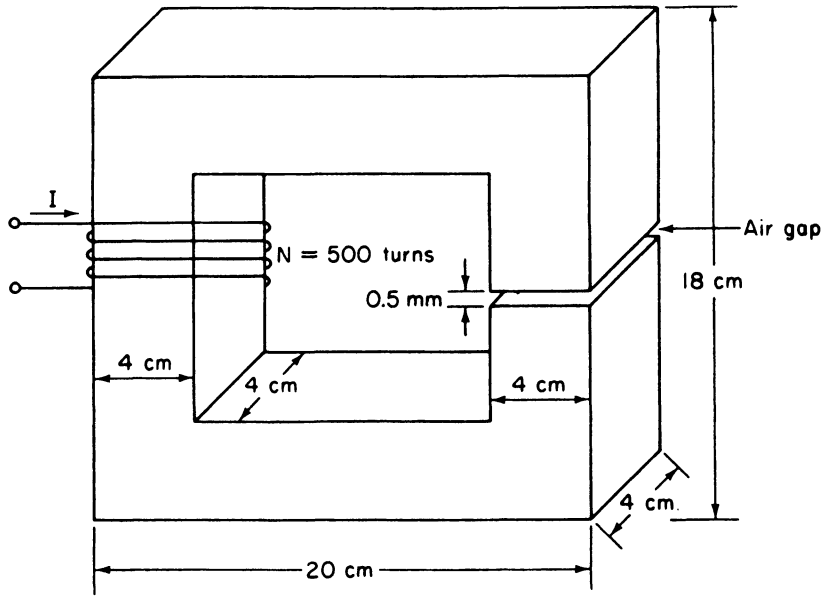


Figure 2.16 Magnetic structure for Example 2.2.

Example 2.2 Consider the magnetic structure shown in Fig. 2.16. Find the current I in the 500-turn winding to set up a flux density of 1 T in the structure. Assume the relative permeability of the structure material to be 3980.

Solution The length of the magnetic-material path is denoted by l_i and is found from the geometry of Fig. 2.16 as

$$l_i = 2(16 + 14) = 60\,\text{cm} = 0.6\,\text{m}$$

The air-gap length is denoted by l_g, and is

$$l_g = 0.5\,\text{mm} = 0.5 \times 10^{-3}\,\text{m}$$

The cross-sectional area of the structure is

$$A_i = A_g = 16 \times 10^{-4}\,\text{m}^2$$

The reluctance of the air gap is thus obtained as

$$\mathfrak{R}_g = \frac{l_g}{\mu_0 A_g} = \frac{0.5 \times 10^{-3}}{(4\pi \times 10^{-7})(16 \times 10^{-4})} = 248.68 \times 10^3$$

www.EngineeringEBooksPdf.com

The reluctance of the iron path is

$$\mathfrak{R}_i = \frac{l_i}{\mu_0 \mu_r A_i} = \frac{0.6}{(4\pi \times 10^{-7})(3980)(16 \times 10^{-4})} = 74.979 \times 10^3$$

Since a flux density of 1 T is required, the flux is

$$\Phi = \mathbf{B} \cdot \mathbf{A} = (1)(16 \times 10^{-4}) = 1.6 \times 10^{-3} \text{ Wb}$$

The MMF required is thus given by

$$\begin{aligned} \mathfrak{F} &= (\mathfrak{R}_g + \mathfrak{R}_i)\Phi \\ &= 1.6 \times 10^{-3}(248.68 \times 10^3 + 74.979 \times 10^3) \\ &= 517.85 \text{ At} \end{aligned}$$

But we need I, so we use

$$I = \frac{\mathfrak{F}}{N} = \frac{517.85}{500} = 1.0357 \text{ A}$$

Our discussion so far has been limited to single-loop structures. In Fig. 2.17, we have a structure with more than one loop. We deduce the equivalent circuit shown in the figure by appealing again to Ampère's circuital law. The contour composed of l_a, l_c, and l_g provides us with

$$\mathfrak{F} = \mathrm{H}_a l_a + \mathrm{H}_c l_c + \mathrm{H}_g l_g$$

Now

$$\mathrm{H}_a = \frac{\Phi}{A_a \mu}$$

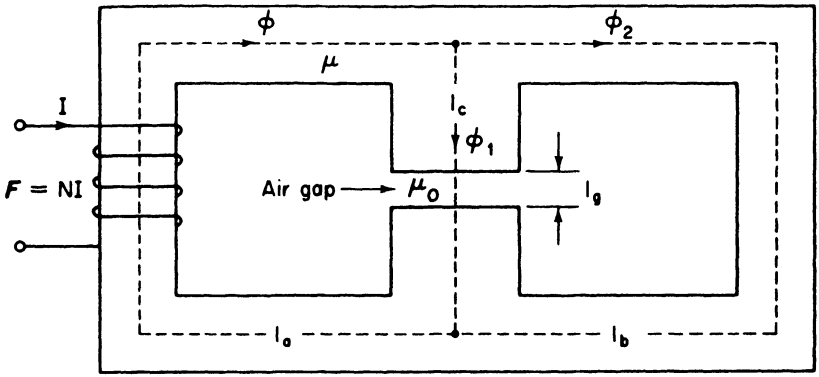
$$\mathrm{H}_c = \frac{\Phi_1}{A_c \mu}$$

$$\mathrm{H}_g = \frac{\Phi_1}{A_g \mu_0}$$

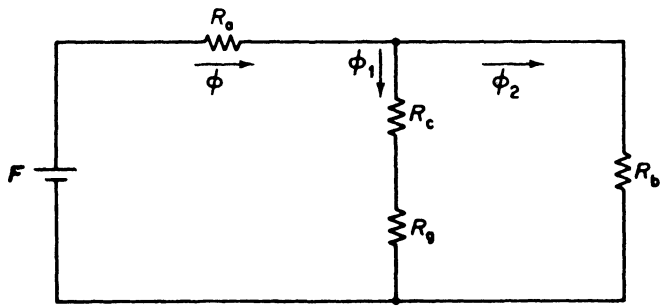
By definition of the reluctances, we obtain the following relation, which is satisfied by the left-hand loop of the equivalent circuit:

$$\mathfrak{F} = \Phi \mathfrak{R}_a + \Phi_1(\mathfrak{R}_c + \mathfrak{R}_g)$$

www.EngineeringEBooksPdf.com



(A)



(B)

Figure 2.17 (a) Multiloop magnetic structure; (b) its equivalent circuit.

where

$$\mathfrak{R}_a = \frac{l_a}{\mu A_a}$$

$$\mathfrak{R}_c = \frac{l_c}{\mu A_c}$$

$$\mathfrak{R}_g = \frac{l_g}{\mu_0 A_g}$$

By continuity of flux, we have

$$\Phi = \Phi_1 + \Phi_2$$

For the contour l_c, l_g, and l_b, we have

$$0 = \mathrm{H}_g l_g + \mathrm{H}_c l_c - \mathrm{H}_b l_b$$

www.EngineeringEBooksPdf.com

Thus we have

$$0 = \Phi_1 \left(\frac{l_g}{\mu_0 A_g} + \frac{l_c}{\mu A_c} \right) - \Phi_2 \left(\frac{l_b}{\mu A_b} \right)$$

As a result,

$$0 = \Phi_1 (\mathfrak{R}_g + \mathfrak{R}_c) - \Phi_2 \mathfrak{R}_b$$

where

$$\mathfrak{R}_b = \frac{l_b}{\mu A_b}$$

The relation just obtained is satisfied by the right-hand loop of the equivalent circuit. It is clear that once we have the equivalent circuit, familiar techniques of circuit analysis can be applied. It is clear that $\mathfrak{R}_b$ is in parallel with the series combination of $\mathfrak{R}_c$ and $\mathfrak{R}_g$.

From a problem-solving point of view, once the geometric dimension and permeability vales are available, two classes of problem arise. In the first, the MMF is given and the flux (or flux densities) values are found in various sections of the structure. The second class involves the inverse problem of finding $\mathfrak{F}$ given a flux (flux density) value in the structure.

Example 2.3 For the magnetic structure of Fig. 2.17, assume that the soft ferromagnetic structure has a constant relative permeability $\mu_r = 4100$. Assume the following dimensions:

$$l_a = l_b = 0.85\,\text{m}$$
$$l_c = 0.36\,\text{m}$$
$$l_g = 0.8\,\text{mm}$$

The structure has a constant cross section of area $A = 8 \times 10^{-3}\,\text{m}^2$. Find the flux density in the air gap for an MMF of 180 At.

Solution We first compute the reluctances involved:

$$\mathfrak{R}_a = \frac{l_a}{\mu_0 \mu_r A} = \frac{0.85}{(4\pi \times 10^{-7})(4100)(8 \times 10^{-3})} = 20.622 \times 10^3$$

Note that

$$\mathfrak{R}_b = \mathfrak{R}_a$$

www.EngineeringEBooksPdf.com

Now

$$\mathfrak{R}_c = \frac{l_c}{\mu_0 \mu_r A} = \frac{0.36}{(4\pi \times 10^{-7})(4100)(8 \times 10^{-3})} = 8.734 \times 10^3$$

$$\mathfrak{R}_g = \frac{l_g}{\mu_0 A} = \frac{0.8 \times 10^{-3}}{(4\pi \times 10^{-3})(8 \times 10^{-3})} = 79.577 \times 10^3$$

We have $\mathfrak{R}_c$ and $\mathfrak{R}_g$ in series, and thus

$$\mathfrak{R}_c + \mathfrak{R}_g = (8.734 + 79.577)10^3 = 88.311 \times 10^3$$

Now $\mathfrak{R}_b$ is in parallel with $(\mathfrak{R}_c + \mathfrak{R}_g)$, and the combination is in series with $\mathfrak{R}_a$. The equivalent reluctance is thus

$$\begin{aligned}\mathfrak{R}_{eq} &= \mathfrak{R}_a + \frac{\mathfrak{R}_b(\mathfrak{R}_c + \mathfrak{R}_g)}{\mathfrak{R}_b + \mathfrak{R}_c + \mathfrak{R}_g} \\ &= \left[20.622 + \frac{20.622(88.311)}{20.622 + 88.311}\right]10^3 \\ &= 37.34 \times 10^3\end{aligned}$$

Since $\mathfrak{F} = 180$, we obtain

$$\Phi = \frac{180}{37.34 \times 10^3} = 4.8205 \times 10^{-3}$$

Now

$$\begin{aligned}\Phi_1 &= \frac{\mathfrak{R}_b}{\mathfrak{R}_b + \mathfrak{R}_c + \mathfrak{R}_g}\Phi \\ &= 4.8205 \times 10^{-3}\left(\frac{20.622}{20.622 + 88.311}\right) \\ &= 912.57 \times 10^{-6}\end{aligned}$$

As a result, the flux density B_1 is

$$B_1 = \frac{\Phi_1}{A} = \frac{912.57 \times 10^{-6}}{8 \times 10^{-3}} = 0.114\,T$$

Magnetic structures may have more than one MMF source. An example structure is shown in Fig. 2.18, where two coils set up the flux in the structure. The concept of

www.EngineeringEBooksPdf.com

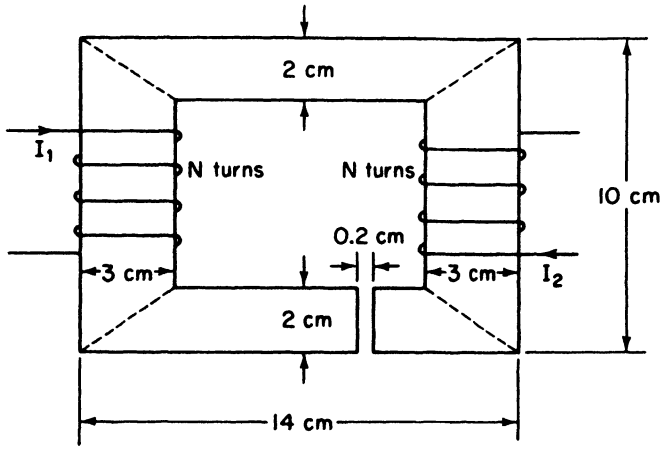


Figure 2.18 Magnetic structure for Example 2.4.

an equivalent magnetic circuit is useful in solving such problems, as indicated in the next example.

Example 2.4 The soft ferromagnetic material of the structure shown in Fig. 2.18 has a relative permeability of 10,000. The thickness of the core is 2 cm. Find the flux in the core given that $N = 400$, $I_1 = 1$ A, and $I_2 = 1.2$ A.

Solution We compute the reluctances in the structure by first finding relevant lengths and areas. It should be noted that the structure is nonuniform. The mean length of the path in the vertical sections is

$$l_1 = 8 \times 10^{-2}\,\text{m}$$

The mean length of the path in the horizontal sections is

$$l_2 = 11 \times 10^{-2}\,\text{m}$$

The air-gap length is

$$l_g = 0.2 \times 10^{-2}\,\text{m}$$

The cross-sectional areas are

$$A_1 = 6 \times 10^{-4}\,\text{m}^2$$

$$A_2 = 4 \times 10^{-4}\,\text{m}^2$$

$$A_g = 4 \times 10^{-4}\,\text{m}^2$$

www.EngineeringEBooksPdf.com

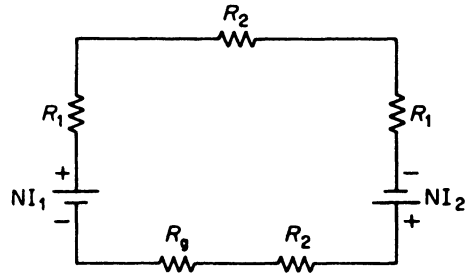


Figure 2.19 Equivalent circuit for structure of Example 2.4.

The reluctance values are therefore given by

$$\mathfrak{R}_1 = \frac{l_1}{\mu A_1} = \frac{8 \times 10^{-2}}{10^4(4\pi \times 10^{-7})(6 \times 10^{-4})} = 10.61 \times 10^3 \text{ A/W}$$

$$\mathfrak{R}_2 = \frac{l_2}{\mu A_2} = \frac{11 \times 10^{-2}}{10^4(4\pi \times 10^{-7})(4 \times 10^{-4})} = 21.884 \times 10^3 \text{ A/W}$$

$$\mathfrak{R}_g = \frac{l_g}{\mu_0 A_g} = \frac{0.2 \times 10^{-2}}{(4\pi \times 10^{-7})(4 \times 10^{-4})} = 3.9789 \times 10^6 \text{ A/W}$$

The equivalent magnetic circuit is shown in Fig. 2.19. As a result, we conclude that

$$\Phi = \frac{N(I_1 + I_2)}{2(\mathfrak{R}_1 + \mathfrak{R}_2) + \mathfrak{R}_g}$$

$$= \frac{400(1 + 1.2)}{[2(10.61 + 21.884) + 3.9789 \times 10^3]10^3}$$

$$= 0.2176 \times 10^{-3} \text{ Wb}$$

It should be noted that the two coils aid in setting up the flux. The polarity of the sources is determined by the right-hand rule.

2.4.1 Effect of Air Gaps

Two points are worth discussing in connection with the presence of air gaps in a magnetic structure. The first has to do with the value of the reluctance of an air gap relative to that of a path in the magnetic material. In Example 2.4 we found that $\mathfrak{R}_g$ is a little over 180 times $\mathfrak{R}_2$. We can conclude that the air-gap reluctance is much higher than the reluctance of a path in iron. This can be seen from

$$\mathfrak{R}_i = \frac{l_i}{\mu_0 \mu_r A}$$

$$\mathfrak{R}_g = \frac{l_g}{\mu_0 A}$$

www.EngineeringEBooksPdf.com

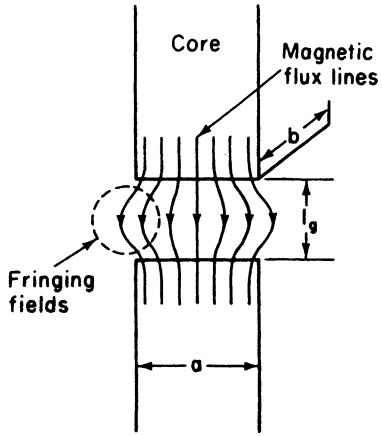


Figure 2.20 Fringing effect in an air gap.

Thus

$$\mathfrak{R}_g = \mathfrak{R}_i \frac{\mu_r}{l_i/l_g}$$

It is clear that if $l_i/l_g \ll \mu_r$, then $\mathfrak{R}_g/\mathfrak{R}_i \gg 1$. In this case, the magnetic path can be approximated by a short circuit (zero reluctance) in the equivalent magnetic circuit.

The second point is that in practice, the magnetic-field lines extend outward somewhat as they cross the air gap, as shown in Fig. 2.20. This phenomenon is called fringing and is accounted for by taking a larger air-gap cross-sectional area. The common practice is to use an air-gap area made by adding the air-gap length to each of the two dimensions making the cross-sectional area. As a result, with reference to Fig. 2.20, accounting for fringing,

$$A_g = (a + l_g)(b + l_g)$$

This approximation is valid for short air gaps. The following example illustrates this point.

Example 2.5 Allow for fringing effects in solving for the required current in the magnetic structure of Example 2.2.

Solution Allowing for fringing, the air-gap area is

$$\begin{aligned} A_g &= (4 + 0.05)(4 + 0.05) = 16.4\,\text{cm}^2 \\ &= 16.4 \times 10^{-4}\ \text{m}^2 \end{aligned}$$

As a result, the reluctance of the air gap is recalculated as

$$\mathfrak{R}_g = \frac{0.5 \times 10^{-3}}{(4\pi \times 10^{-7})(16.403 \times 10^{-4})} = 242.58 \times 10^3$$

www.EngineeringEBooksPdf.com

Note that accounting for fringing reduces the air-gap reluctance. Now, we have from Example 2.2,

$$\Phi = 1.6 \times 10^{-3}$$
$$\mathfrak{R}_i = 74.979 \times 10^3$$

Thus

$$\mathfrak{F} = 1.6 \times 10^{-3}(242.58 + 74.979) \times 10^3$$
$$= 508.09 \text{ At}$$

As a result,

$$I = \frac{508.09}{500} = 1.016 \text{ A}$$

Less current is required in this case than the value obtained when fringing is neglected.

2.5 FLUX LINKAGES, INDUCED VOLTAGES, INDUCTANCE, AND ENERGY

The discussion of the previous sections is limited to situations where the variables of interest, such as current and flux, do not change with time. We now consider the effects of variations of the magnetic system with time. A change in the magnetic field is associated with the establishment of an electric field that is manifested as an induced voltage. This basic fact is due to Faraday's experiments and is expressed by Faraday's law of electromagnetic induction.

Consider a toroidal coil with N turns through which a current i flows, producing a total flux Φ. Each turn encloses or links the total flux and we also note that the total flux links each of the N turns. In this situation we define the flux linkages λ as the product of the number of turns N and the flux Φ linking each turn:

$$\lambda = N\Phi \tag{2.22}$$

In terms of flux linkages, Faraday's law is stated as

$$e = \frac{d\lambda}{dt} = N\frac{d\Phi}{dt} \tag{2.23}$$

The electromotive force (EMF) or induced voltage is thus equal to the rate of change of flux linkages in the structure.

www.EngineeringEBooksPdf.com

The flux linkages λ can be related to the current i in the coil by the definition of inductance L through the relation

$$\lambda = Li \tag{2.24}$$

From this point of view, inductance is the ratio of total flux linkages to the current that they link. Inductance is the passive circuit element that is related to the geometry and material properties of the structure. In the case of the toroid, we have

$$L = \frac{N\Phi}{i} = \frac{NBA}{Hl/N}$$

$$= \frac{N^2 A}{l}\frac{B}{H}$$

For the case of a linear **B-H** curve, we get

$$L = \frac{N^2 A}{l}\mu_0\mu_r \tag{2.25}$$

There is no single definition of inductance that is useful in all cases for which the medium is not linear. The unit of inductance is the henry- or weber-turns per ampere.

The inductance L is related to the reluctance $\mathfrak{R}$ of the magnetic structure of a single-loop structure, since we have

$$L = \frac{N\Phi}{i} = \frac{N\mathfrak{F}}{i\mathfrak{R}}$$

As a result, we get

$$L = \frac{N^2}{\mathfrak{R}} \tag{2.26}$$

Faraday's law (2.23) can be written in the form

$$e = \frac{d}{dt}Li \tag{2.27}$$

In electromechanical energy conversion devices, the reluctance varies with time, and thus L also varies with time. In this case

$$e = L\frac{di}{dt} + i\frac{dL}{dt} \tag{2.28}$$

Note that if L is constant, we get the familiar equation for modeling an inductor in elementary circuit analysis.

www.EngineeringEBooksPdf.com

Power and energy relationships in a magnetic circuit are important in evaluating the performance of the electromechanical energy conversion devices treated in this book. We presently explore some basic relationships, starting with the fundamental definition of power $p(t)$ given by

$$p(t) = e(t)i(t) \tag{2.29}$$

The power into a component (the coil in the case of toroid) is given as the product of the voltage across its terminals $e(t)$ and the current through $i(t)$. Using Faraday's law [Eq. (2.23)], we can write

$$p(t) = i(t)\frac{d\lambda}{dt} \tag{2.30}$$

The units of power are watts (or joules per second).

Let us recall the basic relation stating that power $p(t)$ is the rate of change of energy $W(t)$:

$$p(t) = \frac{dW}{dt} \tag{2.31}$$

Combining Eqs. (2.30) and (2.31), we obtain

$$dW = id\lambda \tag{2.32}$$

Using Eq. (2.22), we can also write the alternative expression

$$dW = Nid\Phi \tag{2.33}$$

Yet another expression of dW can be obtained in terms of $\mathbf{B}$ and $\mathbf{H}$. This is done by recalling that

$$Ni = \mathrm{H}l \qquad \text{and} \qquad \Phi = \mathbf{B}A$$

As a result, we have the expression

$$dW = (lA)\mathbf{H}\, dB \tag{2.34}$$

Equations (2.32) to (2.34) provide us with three related interpretations of the energy taken by the magnetic structure in terms of its properties, as shown in Fig. 2.21. Part (a) depicts Eq. (2.32) assuming that the $\lambda - i$ characteristic is available. In part (b), it is assumed that the $\Phi - \mathfrak{F}$ characteristic is available, and thus Eq. (2.33) is applicable. In part (c), we assume that the **B-H** curve is available and

www.EngineeringEBooksPdf.com

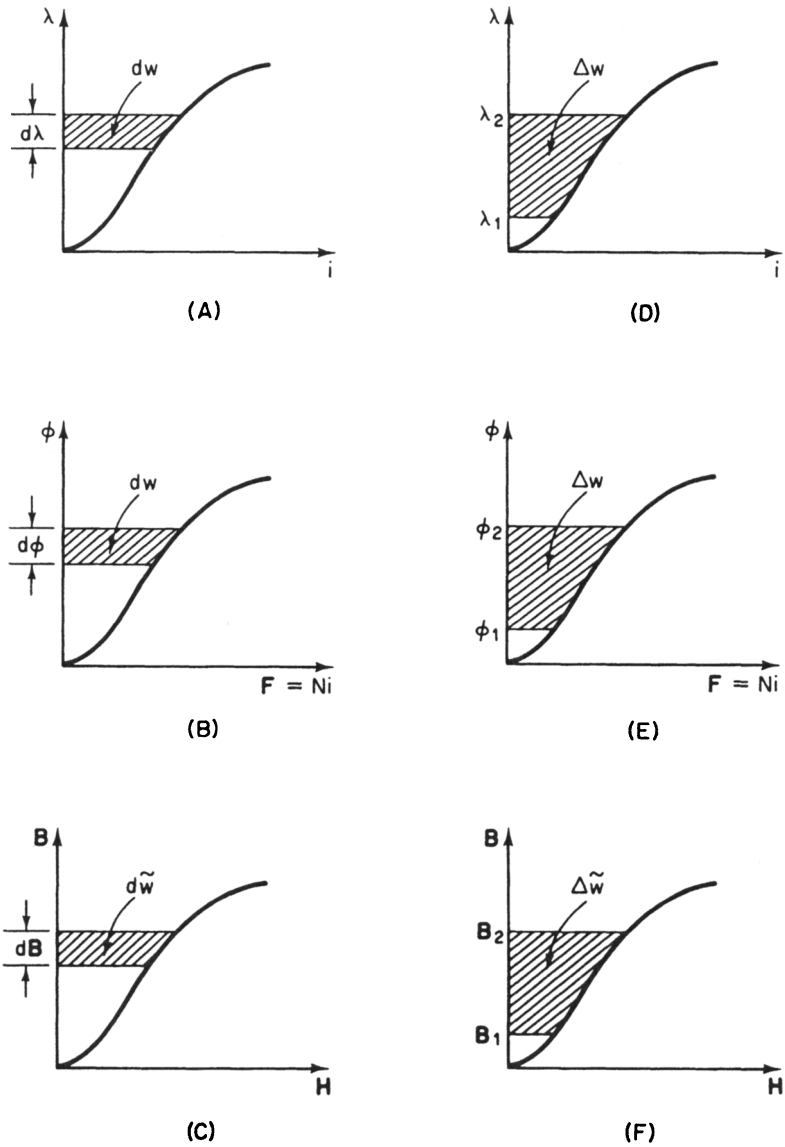


Figure 2.21 Energy in magnetic structures.

that we can thus obtain the incremental energy per unit volume denoted $d\tilde{W}$ as an application of Eq. (2.34).

Consider the case of a magnetic structure that experiences a change in state between the time instants t_1 and t_2. The change in energy into the system is denoted by ΔW and is given by

$$\Delta W = W(t_2) - W(t_1) \tag{2.35}$$

www.EngineeringEBooksPdf.com

Using Eq. (2.32), we get

$$\Delta W = \int_{\lambda_1}^{\lambda_2} i\, d\lambda \tag{2.36}$$

Using Eq. (2.33), we get

$$\Delta W = \int_{\Phi_1}^{\Phi_2} Ni\, d\Phi \tag{2.37}$$

Finally, using Eq. (2.34), we get

$$\Delta W = lA \int_{\mathbf{B}_1}^{\mathbf{B}_2} \mathrm{H}\, d\mathrm{B} \tag{2.38}$$

Equations (2.36) to (2.38) are interpreted in Fig. 2.21(d) to 2.21(f). It is clear that the energy per unit volume expended between t_1 and t_2 is the area between the **B-H** curve and the B axis between B_1 and B_2.

It is important to realize that the energy relations obtained thus far do not require linearity of the characteristics. For a linear structure, we can develop these relations further. Using Eq. (2.24) and substituting into Eq. (2.36), we get

$$\Delta W = \int_{\lambda_1}^{\lambda_2} \frac{\lambda}{L}\, d\lambda$$

Thus

$$\Delta W = \frac{1}{2L}(\lambda_2^2 - \lambda_1^2) \tag{2.39}$$

or

$$\Delta W = (1/2)L(i_2^2 - i_1^2) \tag{2.40}$$

The energy expressions obtained in this section provide us with measures of energy stored in the magnetic field treated. This information is useful in many ways, as will be seen in this text.

2.6 HYSTERESIS LOOP

Ferromagnetic materials are characterized by a **B-H** characteristic that is both nonlinear and multivalued. This is generally referred to as a hysteresis characteristic. To illustrate this phenomenon, we use the sequence of portraits of Fig. 2.22 showing the

www.EngineeringEBooksPdf.com

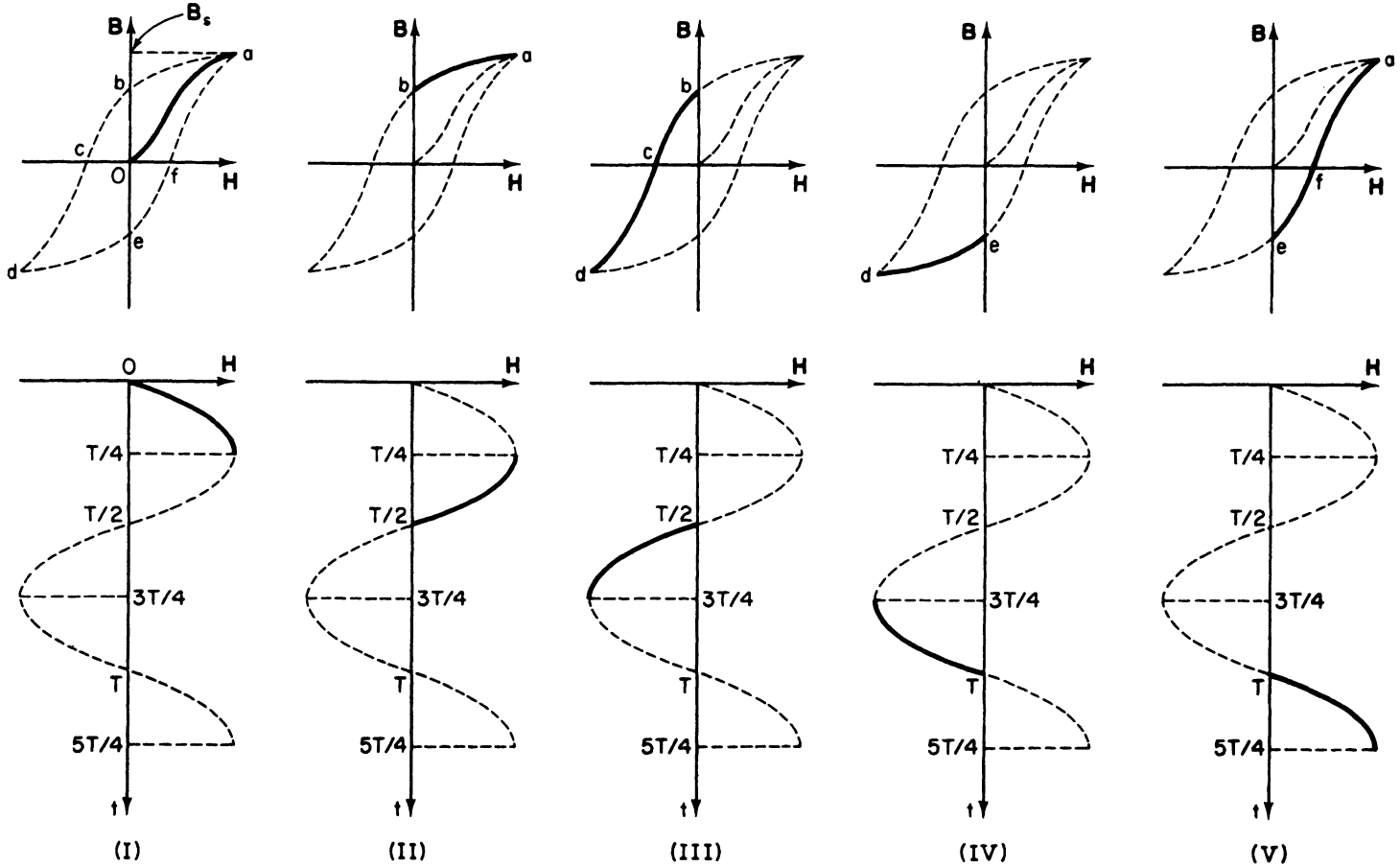


Figure 2.22 Evolution of the hysteresis loop.

www.EngineeringEBooksPdf.com

evolution of a hysteresis loop for a toroid with virgin ferromagnetic core. Assume that the MMF, and hence **H**, is a slowly varying sinusoidal waveform with period T, as shown in the lower portion graphs of Fig. 2.22. We discuss the evolution of the **B-H** hysteresis loop in the following intervals.

Interval I Between $t = 0$ and $T/4$, the magnetic-field intensity H is positive and increasing. The flux density increases along the initial curve (*oa*) up to the saturation value B_s. Increasing H beyond the saturation level does not result in an increase in B.

Interval II Between $t = T/4$ and $T/2$, the magnetic-field intensity is positive but decreasing. The flux density B is observed to decrease along the segment *ab*. Note that *ab* is higher than *oa*, and thus for the same value of H we get different value of B. This is true at *b*, where there is a value for $B = B_r$ that is different from zero even though H is zero at that point in time $t = T/2$. The value of B_r is referred to as the residual field, remanence, or retentivity. If we leave the coil unenergized, the core will still be magnetized.

Interval III Between $t = T/2$ and $3T/4$, the magnetic-field intensity H is reversed and increases in magnitude. B decreases to zero at point *c*. The value of H at which magnetization is zero is called the coercive force H_c. Further decrease in H results in reversal of B up to point *d*, corresponding to $t = 3T/4$.

Interval IV Between $t = 3T/4$ and T, the value of H is negative but increasing. The flux density B is negative and increases from *d* to *e*. The residual field is observed at *e* with $H = 0$.

Interval V Between $t = T$ and $5T/4$, H is increased from 0, and the flux density is negative but increasing up to *f*, where the material is demagnetized. Beyond *f*, we find that B increases up to *a* again.

A typical hysteresis loop is shown in Fig. 2.23. On the same graph, the **B-H** characteristic for nonmagnetic material is shown to show the relative magnitudes involved. It should be noted that for each maximum value of the ac magnetic-field intensity cycle, there is a steady-state loop, as shown in Fig. 2.24. In the figure, the dashed curve connecting the tips of the loops is the dc magnetization curve for the material. The distinction between hard and soft magnetic material on the basis of their hysteresis loops is shown in Fig. 2.25. It is evident from the figure that the coercive force H_c for the soft magnetic material is much lower than that for a hard magnetic material. Table 2.1 lists some typical values for H_c, B_r, and B_s for common magnetic materials.

In Section 2.5, we have shown that the energy supplied by the source per unit volume of the magnetic structure is given by

$$d\tilde{W} = \mathrm{H}d\mathrm{B}$$

and

$$\Delta\tilde{W} = \int_{\mathrm{B}_1}^{\mathrm{B}} \mathrm{H}d\mathrm{B}$$

www.EngineeringEBooksPdf.com

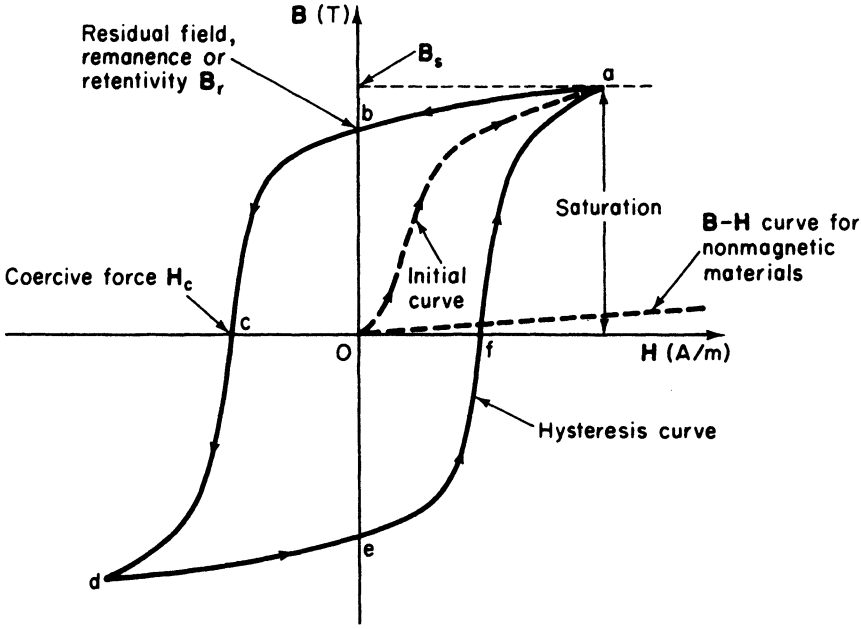


Figure 2.23 Hysteresis loop for a ferromagnetic material.

The energy supplied by the source in moving from *a* to *b* in the graph of Fig. 2.26(a) is negative, since H is positive but B is decreasing. If we continue on from *b* to *d* through *c*, the energy is positive, as H is negative but B is decreasing [see Fig. 2.26(b)].

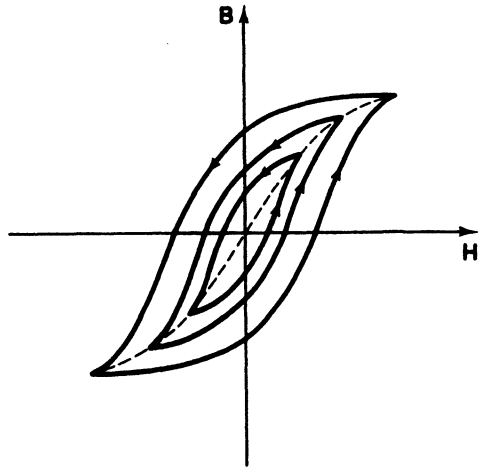


Figure 2.24 Family of hysteresis loops.

www.EngineeringEBooksPdf.com

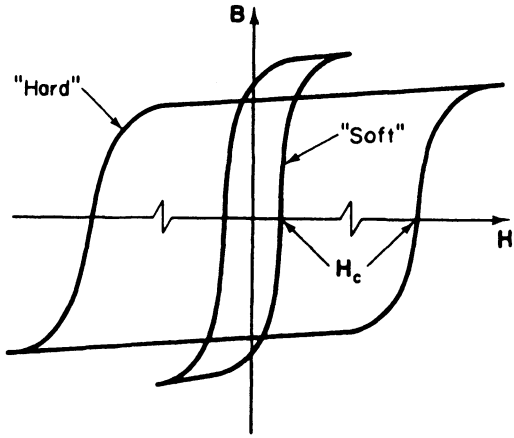


Figure 2.25 Hysteresis loops for soft and hard magnetic materials.

The second half of the loop is treated in Fig. 2.26(b) and is self-explanatory. Superimposing both halves of the loop, we obtain Fig. 2.26(c), which clearly shows that the net energy per unit volume supplied by the source is the area enclosed by the hysteresis loop. This energy is expended in the magnetization–demagnetization process and is dissipated as a heat loss. Note that the loop is described in one cycle, and as a result, the hysteresis loss per second is equal to the product of the loop area and the frequency f of the waveform applied. The area of the loop depends on the maximum flux density, and as a result, we say that the power dissipated through hysteresis P_h is given by

$$P_h = k_h f(\mathrm{B}_m)^n$$

where k_h is a constant, f is the frequency, and B_m is the maximum flux density. The exponent n is determined from experimental results and ranges between 1.5 and 2.5.

TABLE 2.1 Properties of Magnetic Materials and Magnetic Alloys

Material (Composition)	Initial Relative Permeability, μ_i/μ_0	Maximum Relative Permeability, μ_{max}/μ_0	Coercive Force H_c (A/m)	Residual Field B_r (Wb/m^2)	Saturation Field B_s (Wb/m^2)
Commercial iron (0.2 imp)	250	9,000	≃80	0.77	2.15
Silicon-iron (4 Si)	1,500	7,000	20	0.5	1.95
Silicon-iron (3 Si)	7,500	55,000	8	0.95	2.00
Mu metal (5 Cu, 2 Cr, 77 Ni)	20,000	100,000	4	0.23	0.65
78 Permalloy (78.5 Ni)	8,000	100,000	4	0.6	1.08
Supermalloy (79 Ni, 5 Mo)	100,000	1,000,000	0.16	0.5	0.79

www.EngineeringEBooksPdf.com

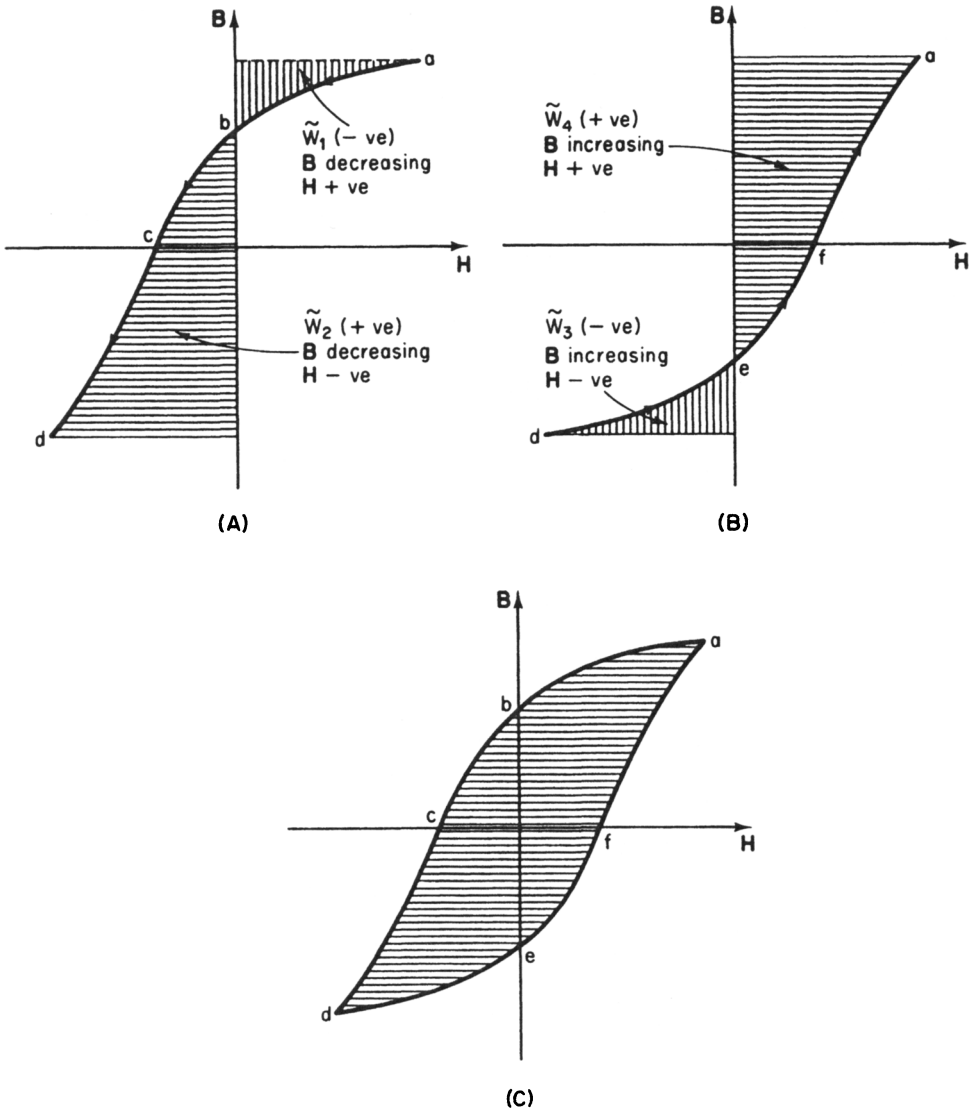


Figure 2.26 Illustrating the concept of energy loss in the hysteresis process.

2.7 EDDY-CURRENT AND CORE LOSSES

In Section 2.6 we saw that if the core is subject to a time-varying magnetic field (sinusoidal input was assumed), energy is extracted from the source in the form of hysteresis losses. There is another loss, called eddy-current loss, mechanism that arises in connection with the application of time-varying magnetic field. A rigorous analysis of the eddy-current phenomenon is a complex process, but the

www.EngineeringEBooksPdf.com

basic model can be explained in simple terms on the basis of Faraday's law, Eq. (2.23).

The change in flux will induce voltages in the core material, which will result in currents circulating in the core. The induced currents tend to establish a flux that opposes the original change imposed by the source. The induced currents, which are essentially the eddy currents, will result in power loss due to heating of the core material. To minimize eddy-current losses, the magnetic core is made of layers of sheet-steel laminations, ideally separated by highly resistive material. It is clear that this effectively results in the actual area of the magnetic material being less than the gross area presented by the stack. To account for this, a stacking factor is employed for practical circuit calculations.

$$\text{Stacking factor} = \frac{\text{Actual magnetic cross-sectional area}}{\text{Gross cross-sectional area}}$$

Typically, lamination thickness ranges from 0.01 mm to 0.35 m, with associated stacking factors ranging between 0.5 and 0.95. The eddy-current power loss per unit volume can be expressed by the empirical formula

$$P_e = K_e(f \mathrm{B}_m t_1)^2 \ \mathrm{W/m^3}$$

This formula shows that the eddy-current power loss per unit volume varies with the square of frequency f, maximum flux density B_m, and the lamination thickness t_1. Of course, K_e is the proportionality constant.

The term *core loss* is used to denote the combination of eddy-current and hysteresis power losses in the material. In practice, manufacturer-supplied data are used to estimate the core loss P_c for given frequencies and flux densities for a particular type of material.

2.8 ENERGY FLOW APPROACH

Let us consider an electromechanical energy conversion device operating as a motor from an energy flow point of view. Our intention is to develop a model of the process that is practical and easy to follow, and therefore takes a macroscopic approach based on the principle of energy conservation. The situation is best illustrated using the diagrams of Fig. 2.27. We assume that an incremental change in electric energy supply, dW_e has taken place. This energy flow into the device can be visualized as made up of three components, as shown in Fig. 2.27(a). Part of the energy will be imparted to the magnetic field of the device and will result in an increase in the energy stored in the field, denoted by dW_f. A second component of energy will be expended as heat losses dW_{loss}. The third and most important component is that output energy is made available to the load (dW_{mech}). The heat losses are due to ohmic (I^2R) losses in the stator (stationary member) and rotor (rotating member),

www.EngineeringEBooksPdf.com

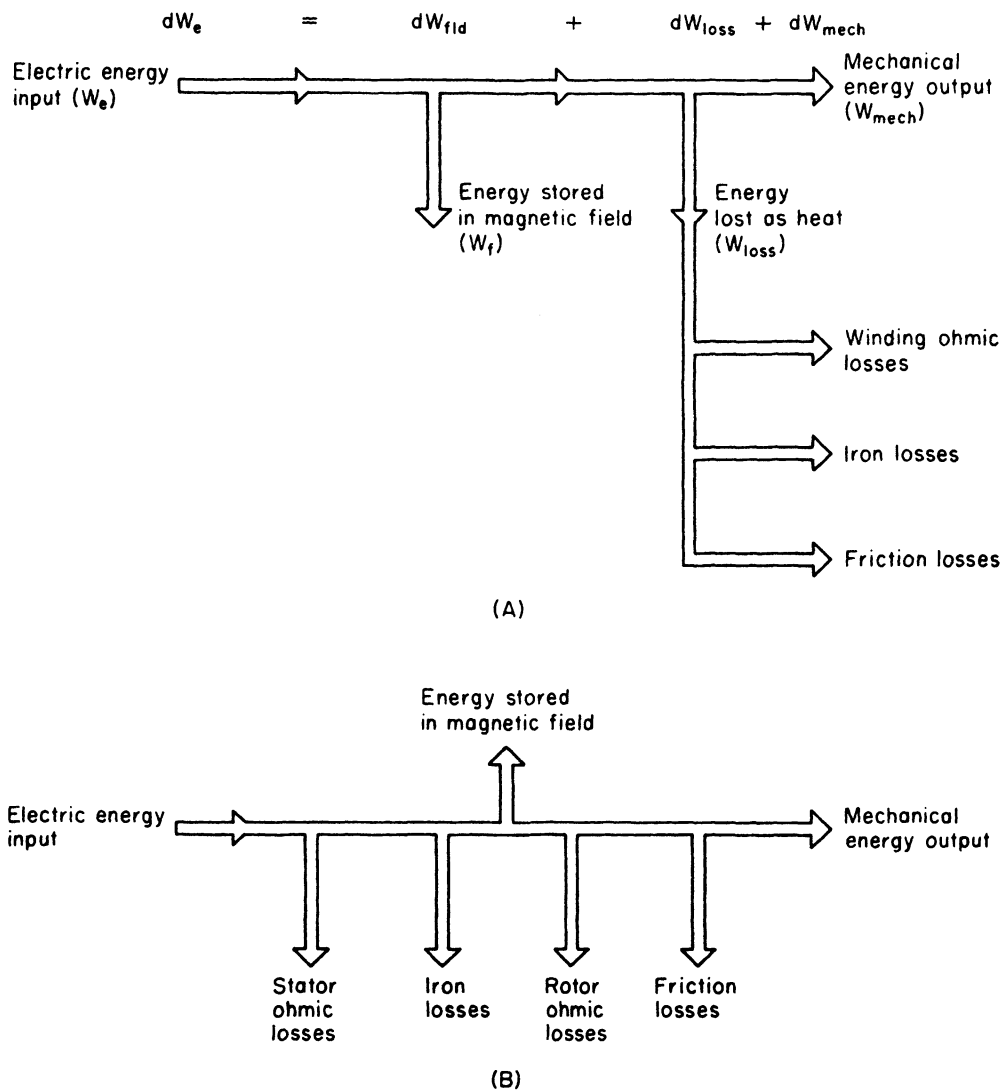


Figure 2.27 Energy flow in an electromechanical energy conversion device: (a) with losses segregated; (b) more realistic representation.

iron or field losses through eddy current and hysteresis, as discussed earlier, and mechanical losses in the form of friction and windage.

In part (b) of the figure, the energy flow is shown in a form that is closer to reality by visualizing Ampère's *bonne homme* making a trip through the machine. Starting in the stator, ohmic losses will be encountered, followed by field losses and a change in the energy stored in the magnetic field. Having crossed the air gap, our friend witnesses ohmic losses taking place in the rotor windings, and in passing to the shaft, bearing frictional losses are also encountered. Finally, a mechanical-energy

www.EngineeringEBooksPdf.com

output is available to the load. It should be emphasized here that the phenomena dealt with here are distributed in nature, and what we are doing is simply developing an understanding in the form of mathematical expressions called models. The trip by our Amperean friend can never take place in real life, but is a helpful means of visualizing the process.

We are now ready to write our energy balance equation based on the foregoing arguments. Here we write

$$dW_e = dW_{\text{fld}} + dW_{\text{loss}} + dW_{\text{mech}} \tag{2.41}$$

To simplify the treatment, let us assume that losses are negligible, as shown in Fig. 2.28.

The electric power input $P_e(t)$ to the device is given in terms of the terminal voltage $e(t)$ and current $i(t)$ by

$$P_e(t) = e(t)i(t) \tag{2.42}$$

The voltage $e(t)$ is related to the flux linkages λ by Faraday's law:

$$e(t) = \frac{d\lambda}{dt} \tag{2.43}$$

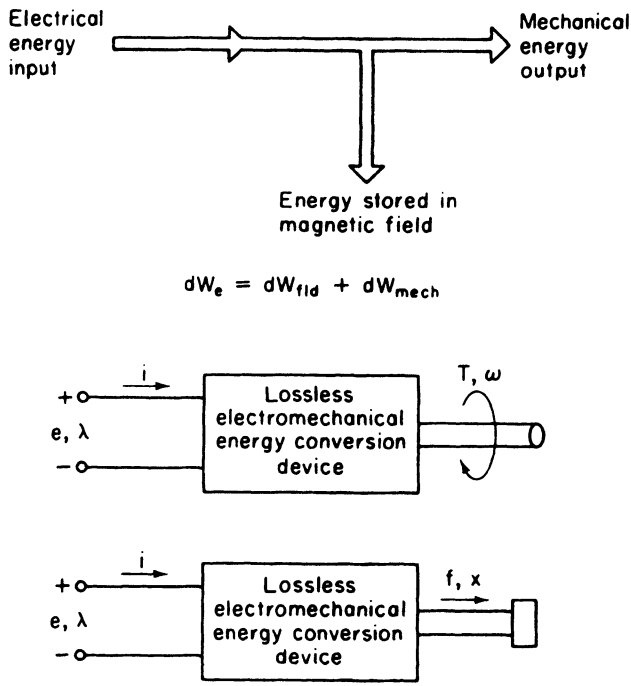


Figure 2.28 Schematic representations of lossless electromechanical energy conversion devices.

www.EngineeringEBooksPdf.com

As a result, we have

$$P_e(t)dt = i(t)\,d\lambda \tag{2.44}$$

We recognize the left-hand side as being the increment in electric energy, dW_e, and we therefore write

$$dW_e = id\lambda \tag{2.45}$$

Assuming a lossless device, we can therefore write an energy balance equation that is a modification of Eq. (2.41):

$$dW_e = dW_{\text{fld}} + dW_{\text{mech}} \tag{2.46}$$

The increment in mechanical output energy can be expressed in the case of a translational (linear motion) increment dx and the associated force exerted by the field F_{fld} as

$$dW_{\text{mech}} = F_{\text{fld}}\,dx \tag{2.47}$$

In the case of rotary motion the force is replaced by torque T_{fld} and the linear increment dx is replaced by the angular increment $d\theta$:

$$dW_{\text{mech}} = T_{\text{fld}}\,d\theta \tag{2.48}$$

As a result, we have for the case of linear motion,

$$dW_{\text{fld}} = id\lambda - F_{\text{fld}}\,dx \tag{2.49}$$

and for rotary motion

$$dW_{\text{fld}} = id\lambda - T_{\text{fld}}\,d\theta \tag{2.50}$$

The foregoing results state that the net change in the field energy is obtained through knowledge of the incremental electric energy input ($id\lambda$) and the mechanical increment of work done.

The field energy is a function of two states of the system. The first is the displacement variable x (or θ for rotary motion) and the second is either the flux linkages λ or the current i. This follows since knowledge of λ completely specifies i through the λ-i characteristic. First let us take the dependence of W_f on λ and x, and write

$$dW_{\text{fld}}(\lambda, x) = \frac{\partial W_f}{\partial \lambda}\,d\lambda + \frac{\partial W_f}{\partial x}\,dx \tag{2.51}$$

The incremental increase in field energy W_f is made up of two components. The first is the product of $d\lambda$ and a (gain factor) coefficient equal to the partial derivative of

www.EngineeringEBooksPdf.com

W_f with respect to λ (x is held constant), and the second component is equal to the product of dx and the partial derivative of W_f with respect to x (λ is held constant). This is a consequence of Taylor's series for a function of two variables. Comparing Eqs. (2.49) and (2.51), we conclude that

$$i = \frac{\partial W_f(\lambda, x)}{\partial \lambda} \tag{2.52}$$

$$F_{\text{fld}} = -\frac{\partial W_f(\lambda, x)}{\partial x} \tag{2.53}$$

This result states that if the energy stored in the field is known as a function of λ and x, then the electric force developed can be obtained by the partial differentiation shown in Eq. (2.53).

For rotary motion, we replace x by θ in the foregoing development to arrive at

$$T_{\text{fld}} = \frac{-\partial W_f(\lambda, x)}{\partial \theta} \tag{2.54}$$

Of course, W_f as a function of λ and θ must be available to obtain the developed torque. Our next task, therefore, is to determine the variations of the field energy with λ and x for linear motion and that with λ and θ for rotary motion.

2.9 FIELD ENERGY

To find the field force we need an expression for the field energy $W_f(\lambda_p, x_p)$ at a given state λ_p and x_p. This can be obtained by integrating the relation of Eq. (2.49), repeated here as

$$dW_f = id\lambda - F_{\text{fld}}\, dx \tag{2.55}$$

from rest ($\lambda = 0$ and $x = 0$) to the given state λ_p and x_p. The path of integration does not have an effect on the final result, as we are dealing with a conservative (no-loss) system. We thus choose the path $0AP$ shown in Fig. 2.29. The segment $0A$ is on the

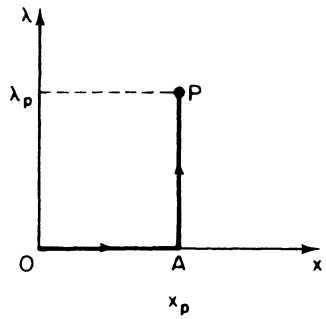


Figure 2.29 Integration of dW_f in the λ-x plane for 0 to P via A.

www.EngineeringEBooksPdf.com

$\lambda = 0$ axis, and thus $d\lambda = 0$ and $F_{\text{fld}} = 0$, since λ is zero. The segment AP is for a constant x value, and hence $dx = 0$. As a result,

$$W_f(\lambda_p, x_p) = \int_0^A dW_f + \int_A^P dW_f$$

But we have $d\lambda$ and $F_{\text{fld}} = 0$ between 0 and A; thus

$$\begin{aligned} W_f(\lambda_p, x_p) &= \int_A^P dW_f \\ &= \int_A^P i\, d\lambda \end{aligned}$$

As a result,

$$W_f(\lambda_p, x_p) = \int_0^{\lambda p} i(\lambda_p, x_p)\, d\lambda \tag{2.56}$$

Equation (2.56) is the desired relationship.

If the λ-i characteristic is linear in i, then

$$\lambda = Li \tag{2.57}$$

Thus Eq. (2.56) reduces to

$$\begin{aligned} W_f(\lambda_p, x_p) &= \int_0^{\lambda p} i(\lambda, x_p)\, d\lambda \\ &= \frac{1}{L}\int_0^{\lambda p} \lambda\, d\lambda \end{aligned}$$

As a result, we conclude that

$$W_f(\lambda_p, x_p) = \frac{\lambda_p^2}{2L} \tag{2.58}$$

Note that L can be a function of x, as is evident from a study of Example 2.6.

Example 2.6 Consider the magnetic circuit shown in Fig. 2.30. Find an expression for the force developed by the field. Suppose that the voltage applied to the coil is

$$e(t) = E_m \cos \omega t$$

Express the developed force as a function of time.

www.EngineeringEBooksPdf.com

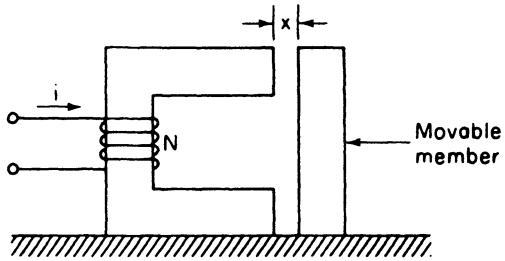


Figure 2.30 Magnetic structure for Example 2.6.

Solution The reluctance of the magnetic structure is

$$\mathfrak{R} = \mathfrak{R}_c + \frac{2x}{\mu_0 A}$$

where $\mathfrak{R}_c$ is the reluctance of the ferromagnetic structure. Thus the inductance is obtained using

$$L = \frac{N^2}{\mathfrak{R}}$$

The energy stored in the field is thus given by Eq. (2.58) as

$$W_f(\lambda, x) = \frac{\lambda^2 \mathfrak{R}}{2N^2} = \frac{\lambda^2}{2N^2}\left(\mathfrak{R}_c + \frac{2x}{\mu_0 A}\right)$$

The force developed is therefore obtained using Eq. (2.53) as

$$\begin{aligned} F_{\text{fld}} &= -\frac{\partial W_f}{\partial x} \\ &= -\frac{\lambda^2}{N^2 \mu_0 A} \end{aligned}$$

Given that the EMF(e) is sinusoidal, then using Faraday's law, we get

$$e(t) = \frac{d\lambda}{dt} = E_m \cos \omega t$$

Thus

$$\int_{\lambda(0)}^{\lambda} d\lambda = \int_0^t E_m \cos \omega t \, dt$$

$$\lambda(t) = \lambda(0) + \frac{E_m}{\omega} \sin \omega t$$

www.EngineeringEBooksPdf.com

As a result,

$$F_{\text{fld}}(t) = \frac{-1}{N^2\mu_0 A}\left[\lambda(0) + \frac{E_m}{\omega}\sin\omega t\right]^2$$

The desired expression for the force developed by the magnetic field is thus obtained. If we assume that the initial flux linkages are zero,

$$\lambda(0) = 0$$

we have

$$F_{\text{fld}} = \frac{-E_m^2}{N^2\mu_0 A\omega^2}\sin^2\omega t$$

Recall the identity

$$\sin^2\theta = \frac{1-\cos 2\theta}{2}$$

As a result, we have

$$F_{\text{fld}} = \frac{-E_m^2}{2N^2\mu_0 A\omega^2}(1-\cos 2\omega t)$$

This result tells us that the force has a sinusoidal component with a frequency that is twice the frequency of the supply.

The force developed by the field is such that it opposes an increase in x (increased reluctance), and can be written as

$$F_{\text{fld}} = -F_0(1-\cos 2\omega t)$$

where

$$F_0 = \frac{E_m^2}{2N^2\mu_0 A\omega^2}$$

The next example is a natural extension of Example 2.6 and introduces dynamics in the development.

Example 2.7 The mass of the movable member of the structure of Example 2.6 is M. Find the current $i(t)$ assuming zero initial velocity.

Solution We can write a dynamic equation for the mass as

$$M\frac{dv}{dt} = F_0(1-\cos 2\omega t)$$

www.EngineeringEBooksPdf.com

Thus

$$Mv(t) = F_0\left(t - \frac{1}{2\omega}\sin 2\omega t\right)$$

This assumes that $v(0) = 0$. The displacement $x(t)$ is now obtained as

$$x(t) = x(0) + \frac{F_0}{M}\int_0^t \left(t - \frac{\sin 2\omega t}{2\omega}\right) dt$$

$$x = (0) + \frac{F_0}{M}\left[\frac{t^2}{2} + \frac{1}{4\omega^2}(\cos 2\omega t - 1)\right]$$

Now we have

$$\lambda = Li$$

where L is the system's equivalent inductance. As a result, substituting for λ and L, we obtain,

$$i(t) = \frac{E_m \sin \omega t[\Re_c + (2x/\mu_0 A)]}{\omega N^2}$$

Note that the expression of x in terms of F_0, M, ω, and t has to be used in conjunction with the last relation.

2.9.1 Coil Voltage

Using Faraday's law, we have

$$e(t) = \frac{d\lambda}{dt} = \frac{d}{dt}(Li)$$

Thus, since L is time dependent, we have

$$e(t) = L\frac{di}{dt} + i\frac{dL}{dt}$$

But

$$\frac{dL}{dt} = \frac{dL}{dx}\left(\frac{dx}{dt}\right) = v\frac{dL}{dx}$$

As a result, we assert that the coil voltage is given by

$$e(t) = L\frac{di}{dt} + iv\frac{dL}{dx} \tag{2.59}$$

where $v = dx/dt$.

www.EngineeringEBooksPdf.com

For the system of Example 2.6

$$L = \frac{N^2}{\mathfrak{R}_c + 2x/\mu_0 A}$$

Thus

$$\frac{dL}{dx} = \frac{-2N^2}{\mu_0 A(\mathfrak{R}_c + 2x/\mu_0 A)^2}$$
$$= \frac{-2L^2}{\mu_0 A N^2}$$

As a result, for the system of Example 2.6 we have

$$e(t) = L\frac{di}{dt} - \frac{2L^2 iv}{\mu_0 A N^2}$$

2.10 MULTIPLY EXCITED SYSTEMS

Systems with more than one exciting winding are referred to as multiply excited systems. We encounter this situation in most rotating electromechanical energy conversion devices. The force (or torque) can be obtained by simple extension of the techniques discussed in the foregoing sections. We will consider a system with three windings, as shown in Fig. 2.31. Of course, our discussion can be simply extended to an arbitrary number of windings, n.

The differential electric-energy input is

$$dW_e = i_1 d\lambda_1 + i_2 d\lambda_2 + i_3 d\lambda_3 \tag{2.60}$$

The mechanical-energy increment is given by

$$dW_{\text{mech}} = F_{\text{fld}} dx$$

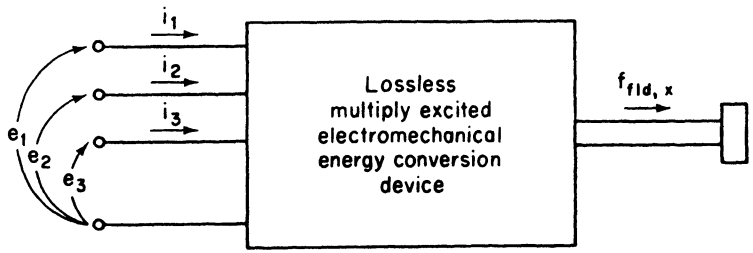


Figure 2.31 Multiply excited lossless electromechanical energy conversion device.

www.EngineeringEBooksPdf.com

Thus the field-energy increment is obtained as

$$\begin{aligned} dW_{\text{fld}} &= dW_e - dW_{\text{mech}} \\ &= i_1 d\lambda_1 + i_2 d\lambda_2 + i_3 d\lambda_3 - F_{\text{fld}} dx \end{aligned} \tag{2.61}$$

If we express W_{fld} in terms of λ_1, λ_2, λ_3, and x, we have

$$dW_f = \frac{\partial W_f}{\partial \lambda_1} d\lambda_1 + \frac{\partial W_f}{\partial \lambda_2} d\lambda_2 + \frac{\partial W_f}{\partial \lambda_3} d\lambda_3 + \frac{\partial W_f}{\partial x} dx \tag{2.62}$$

As a result,

$$F_{\text{fld}} = -\frac{\partial W_f(\lambda_1, \lambda_2, \lambda_3, x)}{\partial x} \tag{2.63}$$

$$i_1 = \frac{\partial W_f(\lambda_1, \lambda_2, \lambda_3, x)}{\partial \lambda_1} \tag{2.64}$$

$$i_2 = \frac{\partial W_f(\lambda_1, \lambda_2, \lambda_3, x)}{\partial \lambda_2} \tag{2.65}$$

$$i_3 = \frac{\partial W_f(\lambda_1, \lambda_2, \lambda_3, x)}{\partial \lambda_3} \tag{2.66}$$

The singly excited case can be seen to be included as a special case of our present result.

If we are dealing with a rotational system, we have

$$T_{\text{fld}} = -\frac{\partial W_f(\lambda_1, \lambda_2, \lambda_3, \theta)}{\partial \theta} \tag{2.67}$$

We will need to find an expression for the field energy at a state corresponding to point P, where $\lambda_1 = \lambda_{1p}$, $\lambda_2 = \lambda_{2p}$, $\lambda_3 = \lambda_{3p}$, and $x = x_p$. Again, since we are dealing with a conservative system (no loss), we can use a simple path of integration *OABCP* as follows:

1. **OA** $\lambda_1 = \lambda_2 = \lambda_3 = 0$ and x varies from 0 to x_p. Thus $d\lambda_1 = d\lambda_2 = d\lambda_3 = 0$ and $F_{\text{fld}} = 0$, and we conclude that

$$\begin{aligned} \int_0^A dW_{\text{fld}} &= \int_0^A (i_1 \, d\lambda_1 + i_2 \, d\lambda_2 + i_3 \, d\lambda_3 - F_{\text{fld}} \, dx) \\ &= 0 \end{aligned} \tag{2.68}$$

2. **AB** $\lambda_1 = 0$, $\lambda_2 = 0$, $x = x_p$, and λ_3 is allowed to vary from 0 to λ_{3p}. Thus $d\lambda_1 = d\lambda_2 = 0$, $dx = 0$, and we have

$$\begin{aligned} \int_A^B dW_{\text{fld}} &= \int_A^B (i_1 \, d\lambda_1 + i_2 \, d\lambda_2 + i_3 \, d\lambda_3 - F_{\text{fld}} \, dx) \\ &= \int_{\lambda_{3=0}}^{\lambda_{3p}} i_{3AB} \, d\lambda_3 \end{aligned} \tag{2.69}$$

www.EngineeringEBooksPdf.com

Here we have

$$i_{3_{AB}} = i_3(\lambda_1 = 0,\ \lambda_2 = 0,\ \lambda_3, x_p) \tag{2.70}$$

That is, λ_1 and λ_2 are held at zero, while x is at x_p and the current is a function of λ_3 only.

3. **BC** $\lambda_1 = 0$, $\lambda_3 = \lambda_{3p}$, $x = x_p$, and λ_2 is varied from zero to λ_{2p}. Here we have $d\lambda_1 = d\lambda_3 = dx = 0$, and we obtain

$$\int_B^C dW_{\text{fld}} = \int_{\lambda_2=0}^{\lambda_{2p}} i_{2_{BC}}\, d\lambda_2 \tag{2.71}$$

where

$$i_{2_{BC}} = i_2(\lambda_1 = 0, \lambda_2, \lambda_3 = \lambda_{3p}, x_p) \tag{2.72}$$

4. **CP** $\lambda_2 = \lambda_{2p}$, $\lambda_3 = \lambda_{3p}$, $x = x_p$, and λ_1 varies from zero to λ_{1p}. We have

$$\int_C^P dW_{\text{fld}} = \int_{\lambda_1=0}^{\lambda_{1p}} i_{1_{CP}}\, d\lambda_1 \tag{2.73}$$

with

$$i_{1_{CP}} = i_1(\lambda_1, \lambda_2 = \lambda_{2p}, \lambda_3 = \lambda_{3p}, x = x_p) \tag{2.74}$$

We can now conclude

$$W_f(\lambda_{1p}, \lambda_{2p}, \lambda_{3p}, x_p) = \int_0^A dW_{\text{fld}} + \int_A^B dW_{\text{fld}} + \int_B^C dW_{\text{fld}} + \int_C^P dW_{\text{fld}}$$

This now can be written as

$$W_f(\lambda_{1p}, \lambda_{2p}, \lambda_{3p}, x_p) = \int_0^{\lambda_{3p}} i_{3_{AB}}\, d\lambda_3 + \int_0^{\lambda_{2p}} i_{2_{BC}}\, d\lambda_2 + \int_0^{\lambda_{1p}} i_{1_{CP}}\, d\lambda_1 \tag{2.75}$$

The energy stored in the field can be obtained using Eq. (2.75). The result is

$$W_f(\lambda_{1p}, \lambda_{2p}, \lambda_{3p}, x_p) = \frac{1}{2}(\Gamma_{11}\lambda_{1p}^2 + \Gamma_{22}\lambda_{2p}^2 + \Gamma_{33}\lambda_{3p}^2) + \Gamma_{12}\lambda_{1p}\lambda_{2p} + \Gamma_{23}\lambda_{2p}\lambda_{3p} + \Gamma_{13}\lambda_{1p}\lambda_{3p} \tag{2.76}$$

where

$$i_1 = \Gamma_{11}\lambda_1 + \Gamma_{12}\lambda_2 + \Gamma_{13}\lambda_3 \tag{2.77}$$

$$i_2 = \Gamma_{12}\lambda_1 + \Gamma_{22}\lambda_2 + \Gamma_{23}\lambda_3 \tag{2.78}$$

$$i_3 = \Gamma_{13}\lambda_1 + \Gamma_{23}\lambda_2 + \Gamma_{33}\lambda_3 \tag{2.79}$$

www.EngineeringEBooksPdf.com

In compact form,

$$\mathbf{I} = \boldsymbol{\Gamma}\boldsymbol{\lambda} \tag{2.80}$$

where the flux linkage vector $\boldsymbol{\lambda}$ is

$$\boldsymbol{\lambda} = \begin{bmatrix} \lambda_1 \\ \lambda_2 \\ \lambda_3 \end{bmatrix} \tag{2.81}$$

The matrix $\boldsymbol{\Gamma}$ is the inverse of $\mathbf{L}$:

$$\boldsymbol{\Gamma} = \mathbf{L}^{-1} \tag{2.82}$$

With elements $\Gamma_{11}, \Gamma_{12}, \ldots,$

$$\boldsymbol{\Gamma} = \begin{bmatrix} \Gamma_{11} & \Gamma_{12} & \Gamma_{13} \\ \Gamma_{12} & \Gamma_{22} & \Gamma_{23} \\ \Gamma_{13} & \Gamma_{23} & \Gamma_{33} \end{bmatrix} \tag{2.83}$$

The stored energy in the field is therefore

$$W_f(\lambda_p, x_p) = \frac{1}{2}\boldsymbol{\lambda}_p^T \boldsymbol{\Gamma} \boldsymbol{\lambda}_p \tag{2.84}$$

We can express the energy stored in the field in terms of currents and inductances by substituting:

$$\boldsymbol{\lambda} = \mathbf{L}\mathbf{I} \tag{2.85}$$

$$W_f(\lambda_p, x_p) = \frac{1}{2}\mathbf{I}_p^T \mathbf{L}^T \mathbf{L} \mathbf{I}_p \tag{2.86}$$

Thus

$$W_f(\lambda_p, x_p) = \frac{1}{2}\mathbf{I}_p^T \mathbf{L}^T \mathbf{I}_p \tag{2.87}$$

2.11 RELUCTANCE MOTORS

The preceding analysis of the electromechanical energy conversion process dealt with devices with single excitation coils. Our examples involved use of a linear motion device to illustrate the concepts discussed. In the preceding development we referred to the case of rotary motion and derived expressions for the torque developed by the electromagnetic field in terms of energy stored.

www.EngineeringEBooksPdf.com

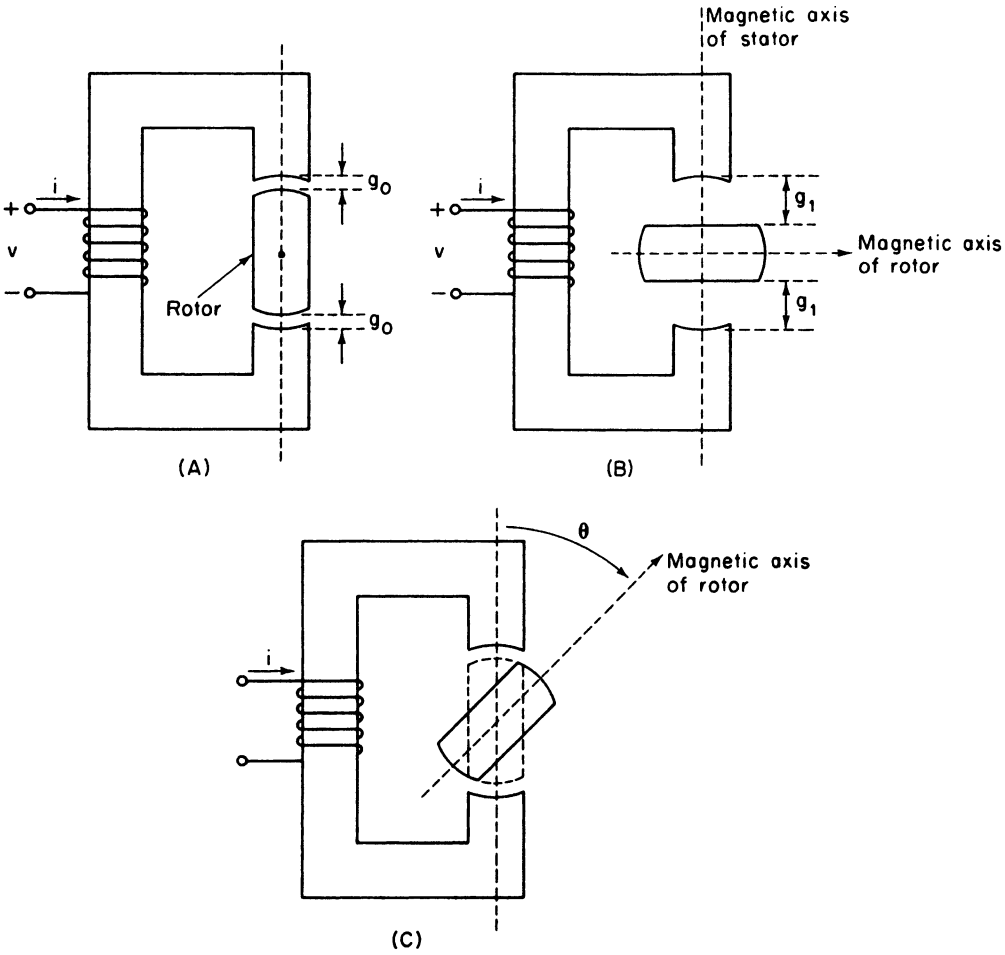


Figure 2.32 Reluctance-type motor.

The present section deals with an important class of singly excited electromechanical energy conversion devices commonly referred to as the reluctance motor. In its simplest form, a reluctance motor consists of a rotor free to rotate on a horizontal axis between the pole pieces of a stationary singly excited magnetic structure, as shown in Fig. 2.32. This type of motor can be found in clocks and phonograph turntables.

It is assumed that when the rotor is in the vertical position, as shown in Fig. 2.32(a), the angle θ between the magnetic axis of the stator and that of the rotor is zero. Let us assume that the permeability of the ferromagnetic path is large enough to enable us to neglect its reluctance relative to that of the air gaps. As a result, for $\theta = 0$ we have

$$\mathfrak{R}_0 = \frac{2g_0}{\mu_0 A_0} \tag{2.88}$$

www.EngineeringEBooksPdf.com

The air-gap length g_0 is indicated in Fig. 2.32(a). The effective air-gap area for $\theta = 0$ is denoted by A_0. The situation for a value of $\theta = \pi/2$ is illustrated in Fig. 2.32(b). The air-gap length is now g_1, and the effective area of the gap is A_1. As a result, for $\theta = \pi/2$ we have

$$\mathfrak{R}_1 = \frac{2g_1}{\mu_0 A_1} \tag{2.89}$$

We now observe that $\mathfrak{R}_1$ is larger than $\mathfrak{R}_0$, since g_1/A_1 is larger than g_0/A_0. Note that although A_1 is larger than A_0, this is more than compensated for by the fact that g_1/g_0 is much larger than A_1/A_0.

At $\theta = \pi$, by symmetry we have that the reluctance is equal to $\mathfrak{R}_0$, and at $\theta = \frac{3}{2}\pi$, its value is $\mathfrak{R}_1$, and for $\theta = 2\pi$, we get back to $\mathfrak{R}_0$. It is thus clear that the reluctance is a function of θ attaining a maximum value of $\mathfrak{R}_1$ at $\theta = \pi/2, 3\pi/2, 5\pi/2, \ldots$ and a minimum value of $\mathfrak{R}_0$ at $\theta = 0,\ \pi,\ 2\pi, \ldots$.

Let us recall that the inductance L is related to the reluctance $\mathfrak{R}$ by

$$L = \frac{N^2}{\mathfrak{R}} \tag{2.90}$$

It is thus clear that L is a function of θ, with maximum values at $\theta = 0,\ \pi,\ 2\pi, \ldots$ and minimum values at $\theta = \pi/2,\ 3\pi/2,\ 5\pi/2, \ldots$ We thus write

$$L(0) = L(\pi) = L_{\max}$$
$$L\left(\frac{\pi}{2}\right) = L\left(\frac{3\pi}{2}\right) = L_{\min}$$

where $L_{\max}$ denotes the maximum values of the inductance and $L_{\min}$ denotes the minimum value of the inductance. The inductance can then be assumed to vary as

$$L = a + b\cos 2\theta \tag{2.91}$$

At $\theta = 0$,

$$L = a + b = L_{\max}$$

At $\theta = \pi/2$,

$$L = a - b = L_{\min}$$

As a result,

$$L = \frac{1}{2}[(L_{\max} + L_{\min}) + (L_{\max} - L_{\min})\cos 2\theta] \tag{2.92}$$

www.EngineeringEBooksPdf.com

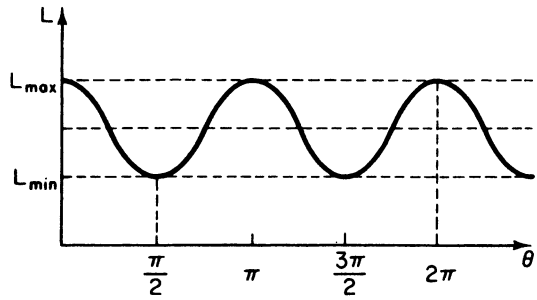


Figure 2.33 Variation of inductance with angular position θ for the electromechanical system of Figure 2.32.

Figure 2.33 shows the variation of L with θ. It should be noted that this sinusoidal variation is an approximation of the actual variation. Design of the pole shapes is based on attempting to achieve this ideal situation.

2.12 DOUBLY EXCITED SYSTEMS

The earlier theoretical discussion provides the basis for treating a multitude of rotating electric machines characterized by more than one exciting winding. As a typical example we take the system shown in Fig. 2.34. Here we have a coil on the stator fed by an electric-energy source 1 and a second coil mounted on the rotor and fed by source 2. This is an example that will prove useful as a prototype of many practical machines.

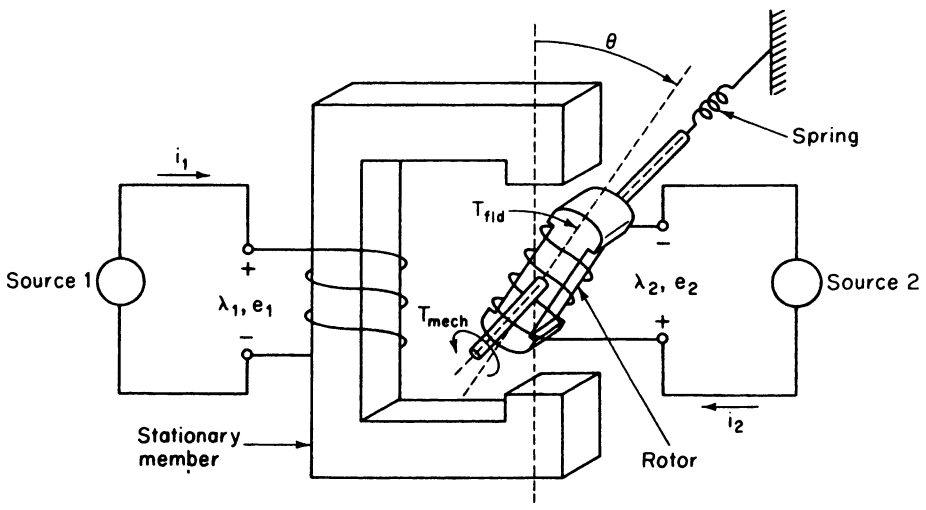


Figure 2.34 Doubly excited electromechanical energy conversion device.

www.EngineeringEBooksPdf.com

For this doubly excited system, we write the relation between flux linkages and currents as

$$\lambda_1 = L_{11}(\theta) i_1 + M(\theta) i_2 \tag{2.93}$$

$$\lambda_2 = M(\theta) i_1 + L_{22}(\theta) i_2 \tag{2.94}$$

The self-inductances L_{11} and L_{22} and the mutual inductance M can be obtained from

$$L_{11}(\theta) = \left.\frac{\lambda_1}{i_1}\right|_{i_2=0} \tag{2.95}$$

$$M(\theta) = \left.\frac{\lambda_1}{i_2}\right|_{i_1=0} = \left.\frac{\lambda_2}{i_1}\right|_{i_2=0} \tag{2.96}$$

$$L_{22}(\theta) = \left.\frac{\lambda_2}{i_2}\right|_{i_1=0} \tag{2.97}$$

We note here that setting $i_2 = 0$ results in a structure excited by the winding on the stator. Therefore, the self-inductance L_{11} is expressed using Eq. (2.92) as

$$L_{11}(\theta) = L_1 + \Delta L_1 \cos 2\theta \tag{2.98}$$

where

$$L_1 = \frac{1}{2}(L_{\max} + L_{\min}) \tag{2.99}$$

$$\Delta L_1 = \frac{1}{2}(L_{\max} - L_{\min}) \tag{2.100}$$

The mutual inductance M is found by evaluating the flux linkages λ_2 of coil 2 due to the current i_1. For $\theta = 0$, the axis of coil 2 is aligned with the stator axis, and as a result the mutual inductance is at a peak M_0. When $\theta = \pi/2$, the coil is perpendicular to the stator axis and zero flux linkages take place. For $\theta = \pi$, the rotor coil is now aligned with the stator flux axis, but in the reverse direction; hence the mutual inductance is at a minimum of $-M_0$. The sinusoidal that fits this behavior is given by

$$M(\theta) = M_0 \cos\theta \tag{2.101}$$

To evaluate the self-inductance of coil 2, we carry out the same reasoning process to arrive at

$$L_{22}(\theta) = L_2 + \Delta L_2 \cos 2\theta \tag{2.102}$$

Note that in many practical applications ΔL_2 is considerably less than L_2, and we can conclude that L_{22} is independent of the rotor position. The torque is then

$$T_{\text{fld}} = -[(i_1^2 \Delta L_1 + i_2^2 \Delta L_2)\sin 2\theta + i_1 i_2 M_0 \sin\theta)] \tag{2.103}$$

www.EngineeringEBooksPdf.com

Let us define

$$T_R = i_1^2 \Delta L_1 + i_2^2 \Delta L_2 \tag{2.104}$$

$$T_M = i_1 i_2 M_0 \tag{2.105}$$

Thus the torque developed by the field is written as

$$T_{\text{fld}} = -(T_M \sin\theta + T_R \sin 2\theta) \tag{2.106}$$

We note that for a round rotor, the reluctance of the air gap is constant, and hence the self-inductances L_{11} and L_{22} are constant, with the result that $\Delta L_1 = \Delta L_2 = 0$. We thus see that for a round rotor $T_R = 0$, and in this case

$$T_{\text{fld}} = -T_M \sin\theta \tag{2.107}$$

For an unsymmetrical rotor the torque is made up of a reluctance torque $T_R \sin 2\theta$ and the primary torque $T_M \sin\theta$.

2.13 SALIENT-POLE MACHINES

The majority of electromechanical energy conversion devices used in present-day applications are in the rotating electric-machinery category with symmetrical stator structure. From a broad geometric configuration point of view, such machines can be classified as being either of the salient-pole type or round-rotor (smooth air gap) classes. We now discuss the salient-pole type, as this class is a simple extension of the discussion of the preceding section.

In a salient-pole machine, one member (the rotor in our discussion) has protruding or salient poles, and thus the air gap between stator and rotor is not uniform, as shown in Fig. 2.35. It is clear that the results of Section 2.12 are applicable here, and we simply modify these results to conform with common machine terminology, shown in Fig. 2.35. Subscript 1 is replaced by s to represent stator quantities, and subscript 2 is replaced by r to represent rotor quantities. Thus we rewrite Eq. (2.93) as

$$\lambda_s = (L_s + \Delta L_s \cos 2\theta) i_s + (M_0 \cos\theta) i_r \tag{2.108}$$

Similarly, Eq. (2.94) is rewritten as

$$\lambda_r = (M_0 \cos\theta) i_s + L_r i_r \tag{2.109}$$

Note that we assume that L_{22} is independent of θ and is represented by L_r. Thus $\Delta L_2 = 0$ under this assumption. The developed torque given by Eq. (2.103) is thus written as

$$T_{\text{fld}} = -i_s i_r M_0 \sin\theta - i_s^2 \Delta L_s \sin 2\theta \tag{2.110}$$

www.EngineeringEBooksPdf.com

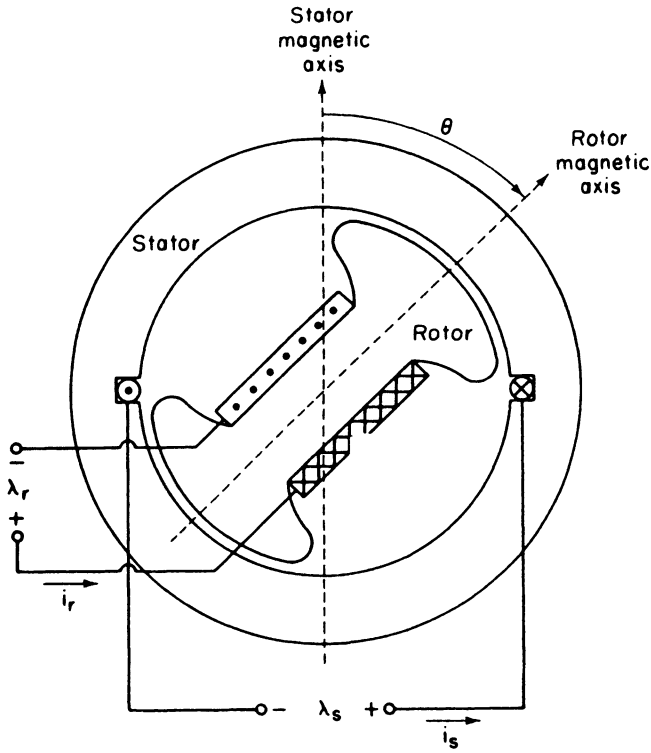


Figure 2.35 Two-pole single-phase salient-pole machine with saliency on the rotor.

We define the primary or main torque T_1 by

$$T_1 = -i_s i_r M_0 \sin\theta \tag{2.111}$$

We also define the reluctance torque T_2 by

$$T_2 = -i_s^2 \Delta L_s \sin 2\theta \tag{2.112}$$

Thus we have

$$T_{\text{fld}} = T_1 + T_2 \tag{2.113}$$

Let us assume that the source currents are sinusoidal.

$$i_s(t) = I_s \sin \omega_s t \tag{2.114}$$

$$i_r(t) = I_r \sin \omega_r t \tag{2.115}$$

Assume also that the rotor is rotating at an angular speed ω_m, and hence

$$\theta(t) = \omega_m t + \theta_0 \tag{2.116}$$

www.EngineeringEBooksPdf.com

We examine the nature of the instantaneous torque developed under these conditions.

The primary or main torque T_1, expressed by Eq. (2.111), reduces to the following form under the assumptions of Eqs. (2.114) to (2.116):

$$T_1 = -\frac{I_s I_r M_0}{4}\{[(\omega_m + \omega_s - \omega_r)t + \theta_0] + \sin[(\omega_m - \omega_s + \omega_r)t + \theta_0] - \sin[(\omega_m + \omega_s + \omega_r)t + \theta_0] - \sin[(\omega_m - \omega_s - \omega_r)t + \theta_0]]\} \tag{2.117}$$

An important characteristic of an electric machine is the average torque developed. Examining Eq. (2.117), we note that T_1 is made of four sinusoidal components, each of zero average value if the coefficient of t is different from zero. It thus follows that as a condition for the nonzero average of T_1, we must satisfy one of the following:

$$\omega_m = \pm\omega_s \pm \omega_r \tag{2.118}$$

For example, when

$$\omega_m = -\omega_s + \omega_r$$

then

$$T_{1_{av}} = -\frac{I_s I_r M_0}{4}\sin\theta_0$$

and when

$$\omega_m = \omega_s + \omega_r$$

$$T_{1_{av}} = \frac{I_s I_r M_0}{4}\sin\theta_0$$

The reluctance torque T_2 of Eq. (2.112) can be written using Eqs. (2.114) to (2.116) as

$$T_2 = -\frac{I_s^2 \Delta L_s}{4}\{2\sin(2\omega_m t + 2\theta_0) - \sin[2(\omega_m + \omega_s)t + 2\theta_0] - \sin[2(\omega_m - \omega_s)t + 2\theta_0]\} \tag{2.119}$$

The reluctance torque will have an average value for

$$\omega_m = \pm\omega_s \tag{2.120}$$

www.EngineeringEBooksPdf.com

When either of the two conditions is satisfied,

$$T_{2_{av}} = \frac{I_s^2 \Delta L_2}{4} \sin 2\theta_0$$

2.14 ROUND OR SMOOTH AIR-GAP MACHINES

The preceding section dealt with a machine with salient poles. Our discussion led to developing conditions for producing a torque with a nonzero average value under sinusoidal excitation to the rotor and stator coils. A round-rotor machine is a special case of salient-pole machine where the air gap between the stator and rotor is (relatively) uniform. The term *smooth air gap* is an idealization of the situation illustrated in Fig. 2.36. It is clear that for the case of a smooth air-gap machine the term ΔL_s is zero, as the reluctance does not vary with the angular displacement θ. Therefore, for the machine of Fig. 2.36, we have

$$\lambda_s = L_s i_s + M_0 \cos\theta i_r \tag{2.121}$$

$$\lambda_r = M_0 \cos\theta i_s + L_r i_r \tag{2.122}$$

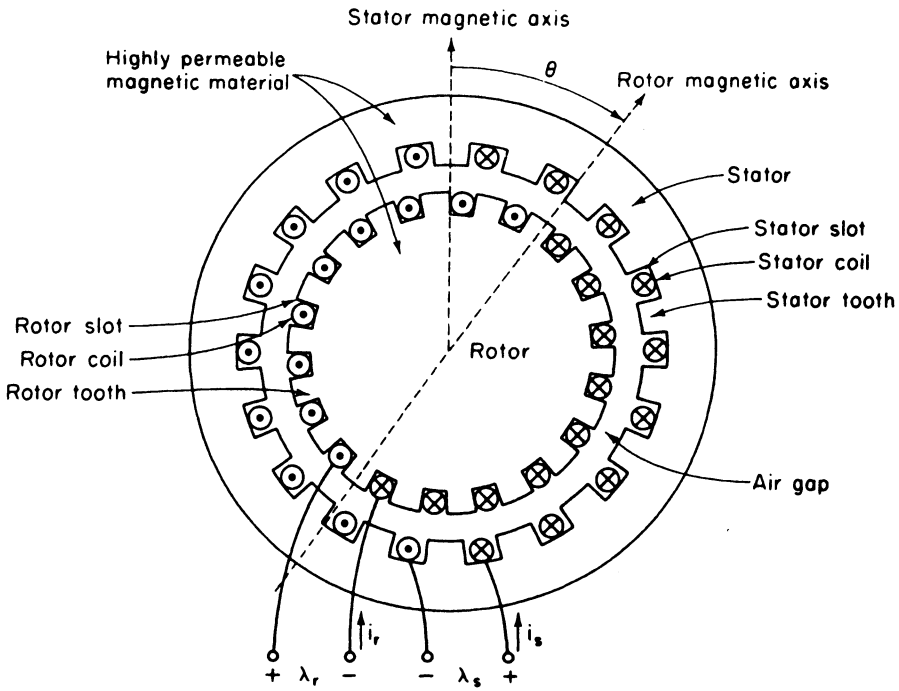


Figure 2.36 Smooth air-gap machine.

www.EngineeringEBooksPdf.com

Under the assumptions of Eqs. (2.114) to (2.116), we obtain

$$T_{\text{fld}} = T_1 \tag{2.123}$$

where T_1 is as defined in Eq. (2.117).

We have concluded that for an average value of T_1 to exist, one of the conditions of Eq. (2.118) must be satisfied:

$$\omega_m = \pm\omega_s \pm \omega_r \tag{2.124}$$

We have seen that for

$$\omega_m = -\omega_s + \omega_r \tag{2.125}$$

then

$$T_{\text{av}} = -\frac{I_s I_r M_0}{4}\sin\theta \tag{2.126}$$

Now substituting Eq. (2.125) in (2.117), we get

$$T_{\text{fld}} = -\frac{I_s I_r M_0}{4}\{\sin\theta_0 + \sin[2(\omega_r - \omega_s)t + \theta_0] - \sin(2\omega_r t + \theta_0) - \sin(-2\omega_s t + \theta_0)\} \tag{2.127}$$

We observe that the first term is a constant, whereas the other three terms are still sinusoidal time functions and each represents an alternating torque. Although these terms are of zero average value, they can cause speed pulsations and vibrations that may be harmful to the machine's operation and life. The alternating torques can be eliminated by adding additional windings to the stator and rotor, as discussed presently.

2.14.1 Two-Phase Machines

Consider the machine of Fig. 2.37, where each of the distributed windings is represented by a single coil. It is clear that this is an extension of the machine of Fig. 2.36 made by adding one additional stator winding (bs) and one additional rotor winding (br) with the relative orientation shown in Fig. 2.36(b). Our analysis of this machine requires first setting up the inductances required. This can be done best using vector terminology. We can write for this four-winding system:

$$\begin{bmatrix} \lambda_{as} \\ \lambda_{ar} \\ \lambda_{bs} \\ \lambda_{br} \end{bmatrix} = \left[\begin{array}{cc|cc} L_s & M_0\cos\theta & 0 & M_0\sin\theta \\ M_0\cos\theta & L_r & -M_0\sin\theta & 0 \\ \hline 0 & M_0\sin\theta & L_s & M_0\cos\theta \\ -M_0\sin\theta & 0 & M_0\cos\theta & L_r \end{array}\right] \begin{bmatrix} i_{as} \\ i_{ar} \\ i_{bs} \\ i_{br} \end{bmatrix} \tag{2.128}$$

www.EngineeringEBooksPdf.com

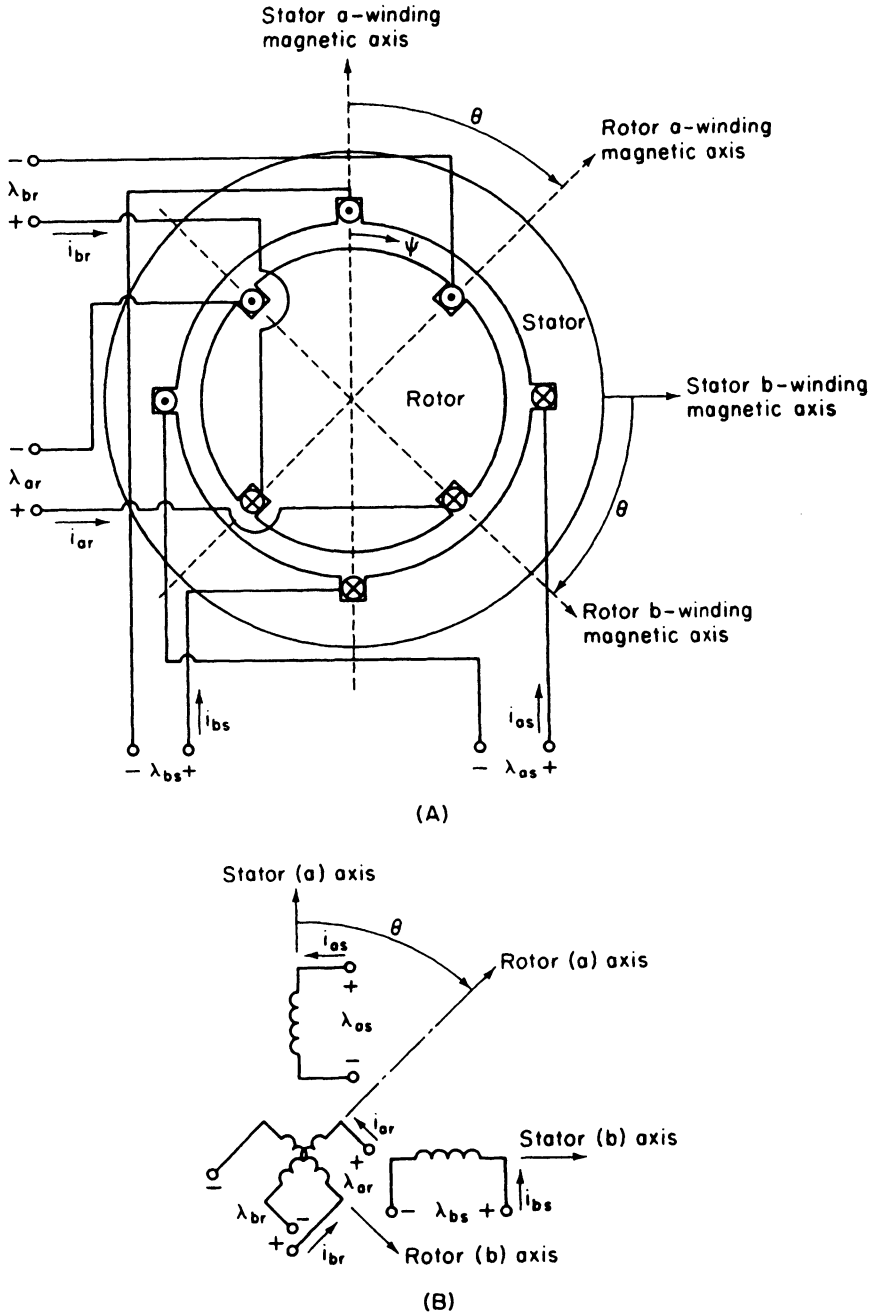


Figure 2.37 Two-phase smooth air-gap machine.

www.EngineeringEBooksPdf.com

or in the notation of Eq. (2.85),

$$\lambda = \mathbf{LI} \tag{2.129}$$

To explain Eq. (2.128), we note first that the upper left-hand corner block of the matrix L represents the self-inductances and mutual inductances involved between the stator and rotor phase a coils, as given in Eqs. (2.121) and (2.122). The lower right-hand corner block corresponds to phase b, and we note that we assume that phase a and phase b coils are similar in this discussion. What remains to be discussed is the upper right corner block (which is seen to be equal to the transponse of the lower left corner block), representing the mutual interaction between phase a and phase b. The mutual terms $L_{(as)(bs)}$ and $L_{(ar)(br)}$ are zero, since phases a and b are at right angles. The term $L_{(as)(br)}$ is equal to $-M_0 \sin\theta$ by the use of projections of flux, and similarly, $L_{(ar)(bs)}$ is equal to $M_0 \sin\theta$.

The field energy is the same as given by Eq. (2.87). The torque is obtained in the usual manner. Let us now assume that the terminal currents are given by the balanced, two-phase current sources

$$i_{as} = I_s \cos\omega_s t \tag{2.130}$$

$$i_{bs} = I_s \sin\omega_s t \tag{2.131}$$

$$i_{ar} = I_r \cos\omega_r t \tag{2.132}$$

$$i_{br} = I_r \sin\omega_r t \tag{2.133}$$

We also assume that

$$\theta(t) = \omega_m t + \theta_0 \tag{2.134}$$

The torque is given by

$$T_{\text{fld}} = M_0[(i_{ar}i_{bs} - i_{br}i_{as})\cos\theta - (i_{ar}i_{as} + i_{br}i_{bs})\sin\theta] \tag{2.135}$$

Substituting Eqs. (2.130) through (2.134) into (2.135), we obtain (after some manipulation)

$$T_{\text{fld}} = -M_0 I_s I_r \sin[(\omega_m - \omega_s - \omega_r)t + \theta_0] \tag{2.136}$$

The condition for nonzero average torque is given by

$$\omega_m = \omega_s - \omega_r \tag{2.137}$$

For this condition, we have

$$T_{\text{fld}} = -M_0 I_s I_r \sin\theta_0 \tag{2.138}$$

The instantaneous torque in this case is constant in spite of the excitation being sinusoidal.

www.EngineeringEBooksPdf.com

2.15 MACHINE-TYPE CLASSIFICATION

The results of the analysis leading to Eq. (2.124) for the machine configuration of Fig. 2.36 and Eq. (2.137) for the machine configuration of Fig. 2.37 provide a basis for defining conventional machine types.

2.15.1 Synchronous Machines

The two-phase machine of Fig. 2.37 is excited by direct current applied to the rotor ($\omega_r = 0$) and balanced two-phase currents of frequency ω_s applied to the stator. Condition (2.127) with $\omega_r = 0$ yields

$$\omega_m = \omega_s \tag{2.139}$$

Thus, to produce a torque with nonzero average value, our machine's rotor should be running at the single value defined by the stator sources. This mode of operation yields a synchronous machine, which is so named because it can convert average power only at one mechanical speed—the synchronous speed, ω_s. The synchronous machine is the main source of electric energy in modern power systems, acting as a generator, and is the subject of Chapter 7.

2.15.2 Induction Machines

In a conventional induction machine, single-frequency alternating currents are fed into the stator circuits and the rotor circuits are all short circuited. The machine in Fig. 2.37 is used again for the analysis. Equations (2.130) and (2.131) still apply and are repeated here:

$$i_{a_s} = I_s \cos \omega_s t \tag{2.140}$$

$$i_{b_s} = I_s \sin \omega_s t \tag{2.141}$$

With the rotor circuits short-circuited,

$$v_{ar} = v_{br} = 0 \tag{2.142}$$

and the rotor is running according to Eq. (2.134):

$$\theta(t) = \omega_m t + \theta_0 \tag{2.143}$$

Conditions (2.142) are written as

$$v_{ar} = R_r i_{ar} + \frac{d\lambda_{ar}}{dt} = 0 \tag{2.144}$$

$$v_{br} = R_r i_{br} + \frac{d\lambda_{br}}{dt} = 0 \tag{2.145}$$

www.EngineeringEBooksPdf.com

Here we assume that each rotor phase has a resistance of $R_r\Omega$. We have, by Eq. (2.128),

$$\lambda_{ar} = M_0 i_{as}\cos\theta + L_r i_{ar} + M_0 i_{bs}\sin\theta \tag{2.146}$$

$$\lambda_{br} = -M_0 i_{as}\sin\theta + M_0 i_{bs}\cos\theta + L_r i_{br} \tag{2.147}$$

As a result, we have

$$0 = R_r i_{ar} + L_r\frac{di_{ar}}{dt} + M_0 I_s\frac{d}{dt}[\cos\omega_s t\cos(\omega_m t + \theta_0) + \sin\omega_s t\sin(\omega_m t + \theta_0)] \tag{2.148}$$

and

$$0 = R_r i_{br} + L_r\frac{di_{br}}{dt} + M_0 I_s\frac{d}{dt}[-\cos\omega_s t\sin(\omega_m t + \theta_0) + \sin\omega_s t\cos(\omega_m t + \theta_0)] \tag{2.149}$$

A few manipulations provide us with

$$M_0 I_s(\omega_s - \omega_m)\sin[(\omega_s - \omega_m)t - \theta_0] = L_r\frac{di_{ar}}{dt} + R_r i_{ar} \tag{2.150}$$

$$-M_0 I_s(\omega_s - \omega_m)\cos[(\omega_s - \omega_m)t - \theta_0] = L_r\frac{di_{br}}{dt} + R_r i_{br} \tag{2.151}$$

The right-hand sides are identical linear first-order differential operators. The left sides are sinusoidal voltages of equal magnitude but are 90 degrees apart in phase. The rotor currents will have a frequency of $(\omega_s - \omega_m)$, which satisfies condition (2.137), and thus an average power and an average torque will be produced by the induction machine.

The induction machine is the subject of detailed study in Chapter 6. For now let us emphasize that currents induced in the rotor have a frequency of $(\omega_s - \omega_m)$ and that average torque can be produced.

2.16 *P*-POLE MACHINES

The configuration of the magnetic field resulting from coil placement in the magnetic structure determines the number of poles in an electric machine. An important point to consider is the convention, adopted for assigning polarities in schematic diagrams, which is discussed presently. Consider the bar magnet of Fig. 2.38(a). The magnetic flux lines are shown as closed loops oriented from the south pole to the north pole within the magnetic material. Fig. 2.38(b) shows a two-pole rotor with a single coil with current flowing in the direction indicated by the dot and cross convention. According to the right-hand rule, the flux lines are directed upward inside

www.EngineeringEBooksPdf.com

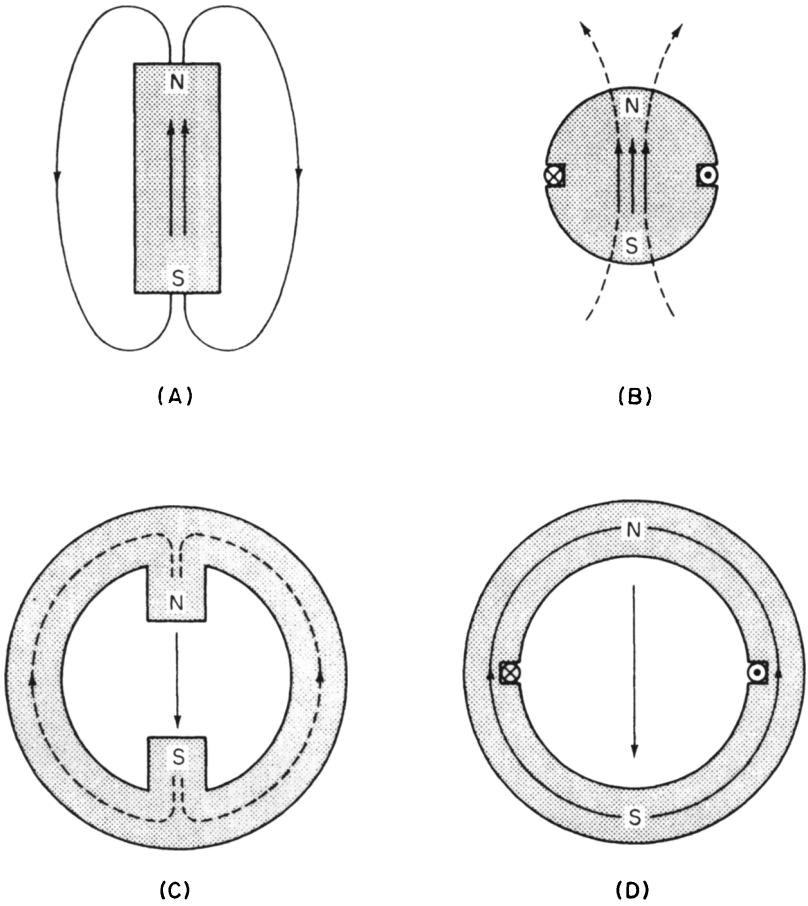


Figure 2.38 Two-pole configurations.

the rotor material, and as a result we assert that the south pole of the electromagnet is on the bottom part and that the north pole is at the top, as shown.

The situation with a two-pole stator is explained in Fig. 2.38(c) and 2.38(d). First consider Fig. 2.38(c), showing a permanent magnet shaped as shown. According to our convention, the flux lines are oriented away from the south pole toward the north pole within the magnetic material (not in air gaps). In Fig. 2.38(d), we have an electromagnet that was made by the insertion of a single coil in slots on the periphery of the stator, as shown. The flux lines are oriented in accordance with the right-hand rule, and we conclude that the north and south pole orientations are as shown in the figure.

Consider now the situation illustrated in Fig. 2.39, where two coils are connected in series and placed on the periphery of the stator in part (a) and on the rotor in part (b). An extension of the prior arguments concerning a two-pole machine results from the combination of the stator and rotor of Fig. 2.39, and is shown in Figure 2.40 to illustrate the orientation of the magnetic axes of rotor and stator.

www.EngineeringEBooksPdf.com

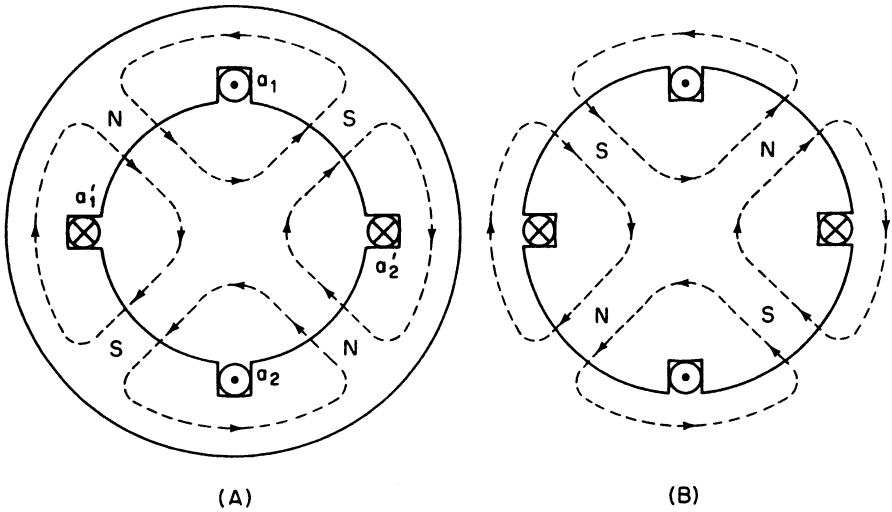


Figure 2.39 Four-pole configurations: (a) stator arrangement; (b) rotor arrangement.

It is clear that any arbitrary even number of poles can be achieved by placing the coils of a given phase in symmetry around the periphery of the stator and rotor of a given machine. The number of poles is simply the number encountered in one round-trip around the periphery of the air gap. It is necessary for successful operation of the machine to have the same number of poles on the stator and rotor.

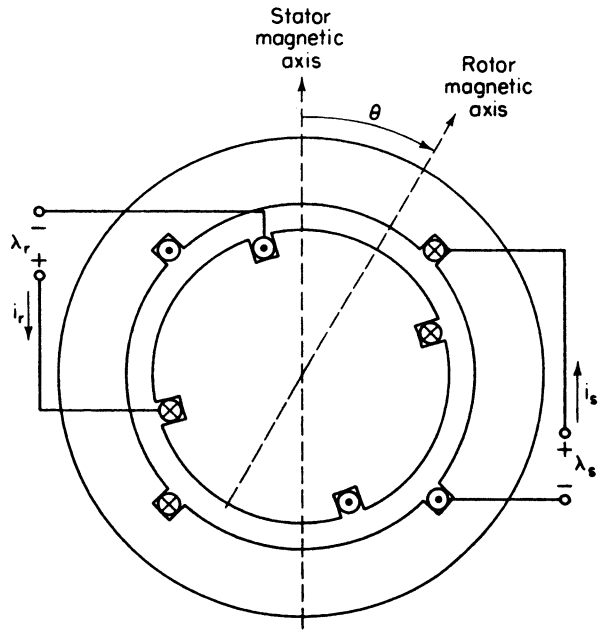


Figure 2.40 Four-pole single-phase machine.

www.EngineeringEBooksPdf.com

Consider the four-pole, single-phase machine of Fig. 2.40. Because of the symmetries involved, the mutual inductance can be seen to be

$$M(\theta) = M_0 \cos 2\theta \tag{2.152}$$

Compared with Eq. (2.101) for a two-pole machine, we can immediately assert that for a P-pole machine,

$$M(\theta) = M_0 \cos \frac{P\theta}{2} \tag{2.153}$$

where P is the number of poles.

We note here that our treatment of the electric machines was focused on two-pole configurations. It is clear that extending our analytic results to a P-pole machine can easily be done by replacing the mechanical angle θ in a relation developed for a two-pole machine by the angle $P\theta/2$, to arrive at the corresponding relation for a P-pole machine. As an example, relations (2.121) and (2.122) for a P-pole machine are written as

$$\lambda_s = L_s i_s + \left(M_0 \cos \frac{P\theta}{2}\right) i_r \tag{2.154}$$

$$\lambda_r = \left(M_0 \cos \frac{P\theta}{2}\right) i_s + L_r i_r \tag{2.155}$$

Similarly, the torque expression [Eq. (2.111)] becomes

$$T_1 = -i_s i_r M_0 \sin \frac{P\theta}{2} \tag{2.156}$$

Note that θ in the preceding expressions is in mechanical degrees.

The torque T_1 under the sinusoidal excitation conditions (2.114) and (2.115) given by Eq. (2.117) is rewritten for a P-pole machine as

$$\begin{aligned} T_1 = -\frac{I_s I_r M_0}{4} \Bigg\{ & \sin\left[\left(\frac{P\omega_m}{2} + \omega_s - \omega_r\right)t + \frac{P\theta_0}{2}\right] \\ & + \sin\left[\left(\frac{P\omega_m}{2} - \omega_s + \omega_r\right)t + \frac{P\theta_0}{2}\right] \\ & - \sin\left[\left(\frac{P\omega_m}{2} + \omega_s + \omega_r\right)t + \frac{P\theta_0}{2}\right] \\ & - \sin\left[\left(\frac{P\omega_m}{2} - \omega_s - \omega_r\right)t + \frac{P\theta_0}{2}\right] \Bigg\} \end{aligned} \tag{2.157}$$

The conditions for average torque production of Eq. (2.118) are written for a P-pole machine as

$$\omega_m = \frac{2}{P}(\pm\omega_s \pm \omega_r) \tag{2.158}$$

www.EngineeringEBooksPdf.com

Thus for given electrical frequencies the mechanical speed is reduced as the number of poles is increased.

A time-saving and intuitively appealing concept in dealing with P-pole machines is that of electrical degrees. Let us define the angle θ_e corresponding to a mechanical angle θ for a P-pole machine as

$$\theta_e = \frac{P}{2}\theta \tag{2.159}$$

With this definition we see that all statements, including θ for a two-pole machine apply to any P-pole machine, with θ taken as an electrical angle.

Consider the first condition of Eq. (2.158) with $\omega_r = 0$ corresponding to synchronous machine operation:

$$\omega_m = \frac{2}{P}\omega_s \tag{2.160}$$

The stator angular speed ω_s is related in hertz to frequency f_s by

$$\omega_s = 2\pi f_s \tag{2.161}$$

The mechanical angular speed ω_m is related to the mechanical speed n in revolutions per minute by

$$\omega_m = \frac{2\pi n}{60} \tag{2.162}$$

Combining Eqs. (2.160) to (2.162), we obtain

$$f_s = \frac{Pn}{120} \tag{2.163}$$

This is an important relation in the analysis of rotating electrical machines.

PROBLEMS

Problem 2.1 A small toroidal coil is shown in Fig. 2.41. Assume that the relative permeability of the core material is 1500 and that the outside radius of the toroid is 0.2 cm. The area of cross section is circular, with diameter 0.05 cm. Find the magnetomotive force required to set up a flux density of 1 millitesla in the core. Find the flux in the core.

Problem 2.2 For the toroidal coil of Problem 2.1, find the flux density in the core for an MMF of 200 At.

www.EngineeringEBooksPdf.com

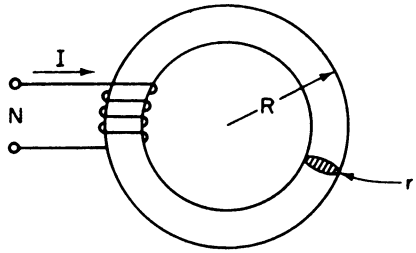


Figure 2.41 Toroid for Problem 2.1.

Problem 2.3 Consider the toroid shown in Fig. 2.42, which is wound with a coil of 200 turns. Assume that the current is 40 A and that the core is nonmagnetic. It is required to calculate:

(a) The reluctance of the circuit.

(b) The flux and flux density inside the core.

Problem 2.4 Consider the magnetic structure shown in Fig. 2.43. Find the current in the 50-turn winding to set up a flux density of 0.8 T in the structure, assuming that the relative permeability of the core material is 2000. Use the concept of reluctance in your solution.

Problem 2.5 For the magnetic structure shown in Fig. 2.44, find the current I required to set up a flux density of 1.5 T in the air gap. Assume that the relative

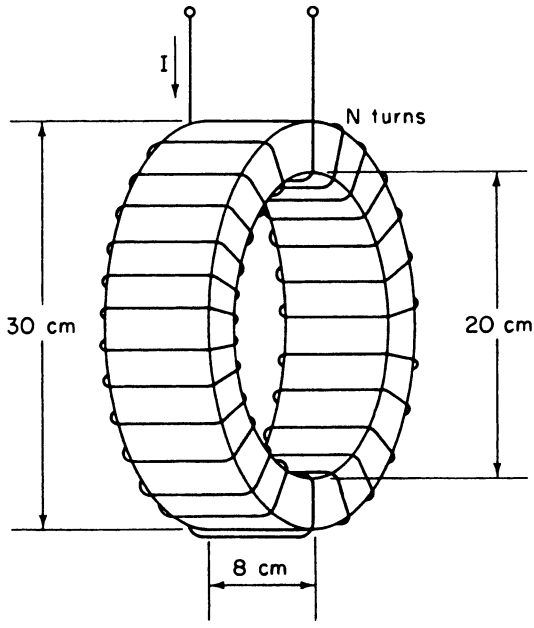


Figure 2.42 Toroid for Problem 2.3.

www.EngineeringEBooksPdf.com

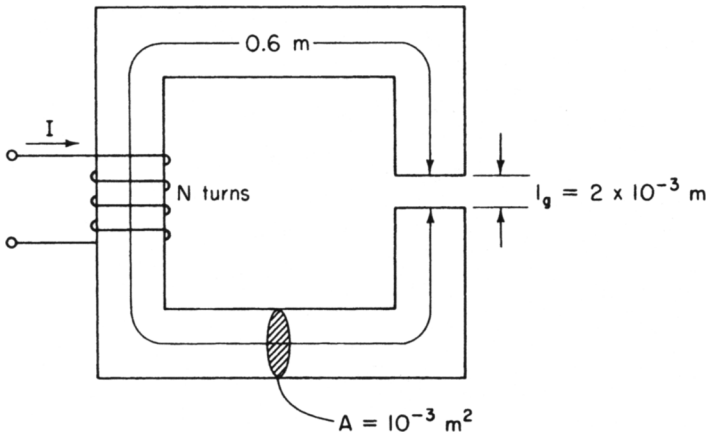


Figure 2.43 Magnetic structure for Problem 2.4.

permeability of the core material is 1800. Use the concepts of magnetic circuit and reluctance in your solution.

Problem 2.6 For the magnetic structure of Problem 2.4, find the flux density in the air gap for a current of 45 A.

Problem 2.7 For the magnetic structure of Problem 2.5, find the flux density in the air gap for a current of 20 A.

Problem 2.8 The material of the magnetic structure of Fig. 2.45 has a relative permeability of 2500. The coil current is 0.1 A and the corresponding flux is 10^{-4} Wb. Find the depth d of the structure.

Problem 2.9 The source MMF in the magnetic structure of Fig. 2.46 is fixed at 200 At. The two rotors are made of a material with relative permeability μ_r, while the core material has a permeability of μ_i. With the rotors absent, the flux is found to be 0.5236×10^{-5} Wb. With the rotors in the circuit, the flux is found to

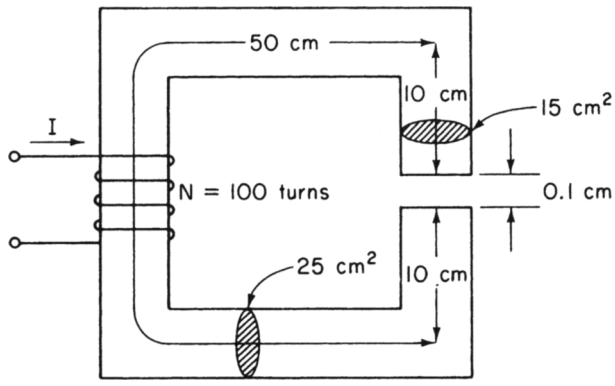


Figure 2.44 Magnetic structure for Problem 2.5.

www.EngineeringEBooksPdf.com

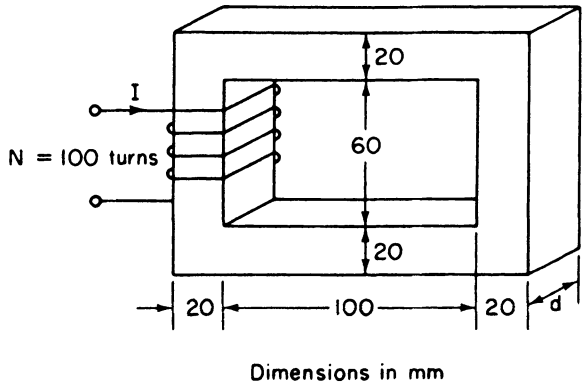


Figure 2.45 Magnetic structure for Problem 2.8.

be 3.122×10^{-5} Wb. Find the relative permeabilities μ_r and μ_i given that the cross section of the structure is uniform with area 4×10^{-4} m^2.

Problem 2.10 The relative permeability of the core of the magnetic structure of Fig. 2.47 is 2000. The MMF is 500 At and the flux is 7×10^{-4} Wb. Find the length l_0.

Problem 2.11 Consider the magnetic structure shown in Fig. 2.48. Draw an equivalent magnetic circuit for the system. Assume that the relative permeability of the core is 2500. Calculate the flux in the right-hand air gap for an MMF in the coil of 800 At.

Problem 2.12 Consider the magnetic structure shown in Fig. 2.49. The flux density in the cast-iron portion is 0.6 T and the flux density in the sheet-steel portion is 1 T. This corresponds to an MMF of 410 At and a flux of 0.35 mWb.

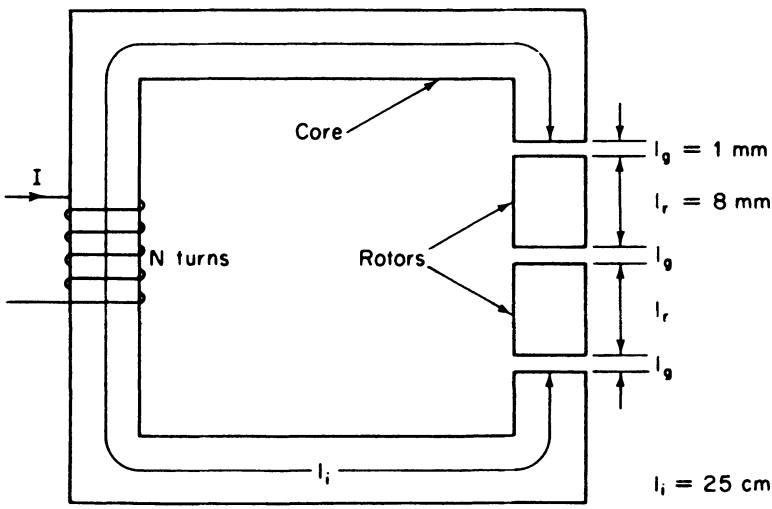


Figure 2.46 Magnetic structure for Problem 2.9.

www.EngineeringEBooksPdf.com

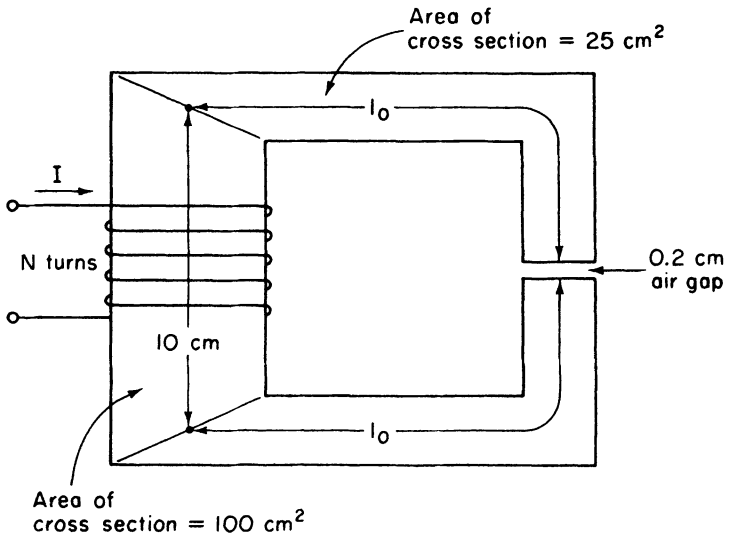


Figure 2.47 Magnetic structure for Problem 2.10.

Assume that the permeability of cast iron is 4×10^{-4} and that the permeability of sheet steel is 4.348×10^{-3}. Find the dimensions w_1, w_2, and d for this structure.

Problem 2.13 For the magnetic structure of Fig. 2.17, assume that the ferromagnetic material has a relative permeability $\mu_r = 3000$. Assume the following dimensions:

$$l_a = 0.9\,\text{m} \qquad l_b = 0.8\,\text{m}$$
$$l_a = 0.3\,\text{m} \qquad l_g = 1\,\text{mm}$$

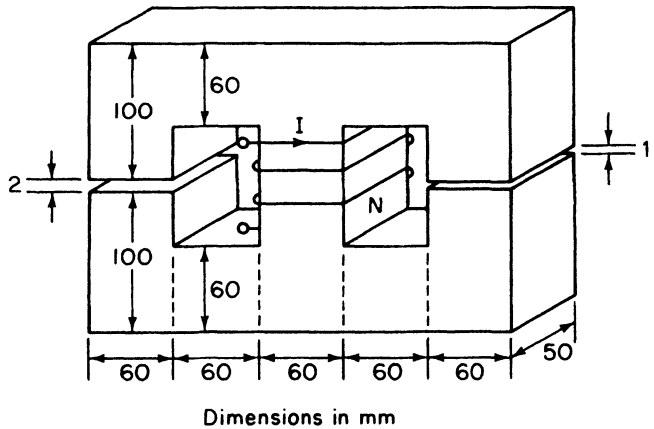


Figure 2.48 Magnetic structure for Problem 2.11.

www.EngineeringEBooksPdf.com

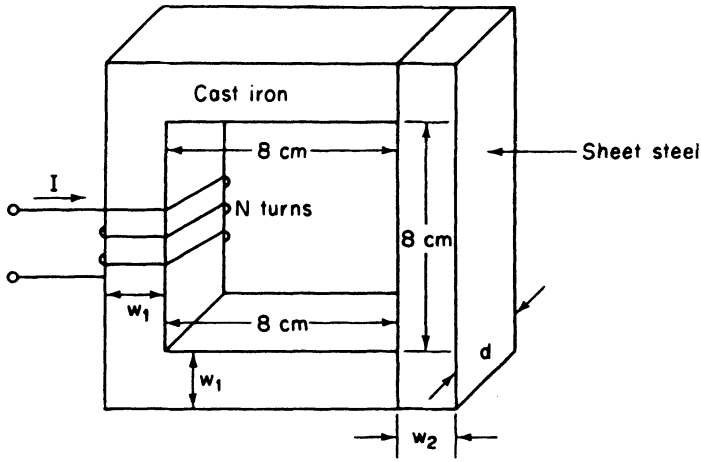


Figure 2.49 Magnetic structure for Problem 2.12.

The structure has a cross-sectional area $A = 6 \times 10^{-3}$ m. Find the flux in the air gap for an MMF of 240 At.

Problem 2.14 The magnetic structure of a synchronous machine is shown in Fig. 2.50. Assume that the rotor and stator iron have relative permeabilities of 3500 and 1800, respectively. The outside and inside diameters of the stator yoke are 1 m and 0.72 m, respectively. The rotor length is 0.7 m and is 0.1 m wide. The air gaps are each 1 cm long. The axial length of the machine is 1 m. Draw an equivalent

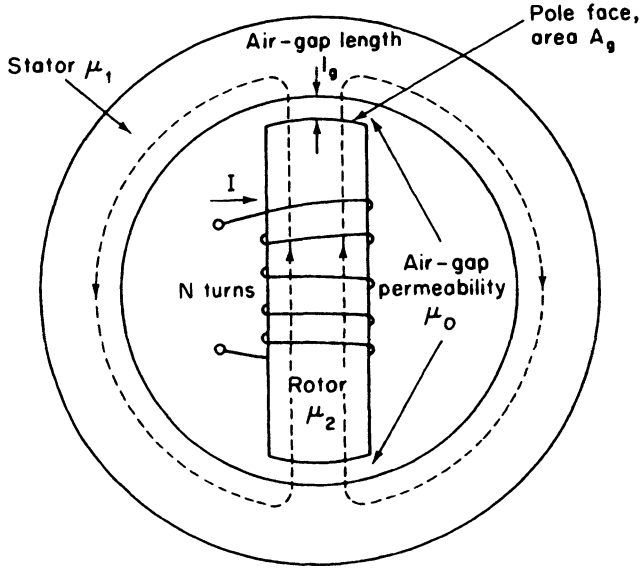


Figure 2.50 Magnetic structure for Problem 2.14.

www.EngineeringEBooksPdf.com

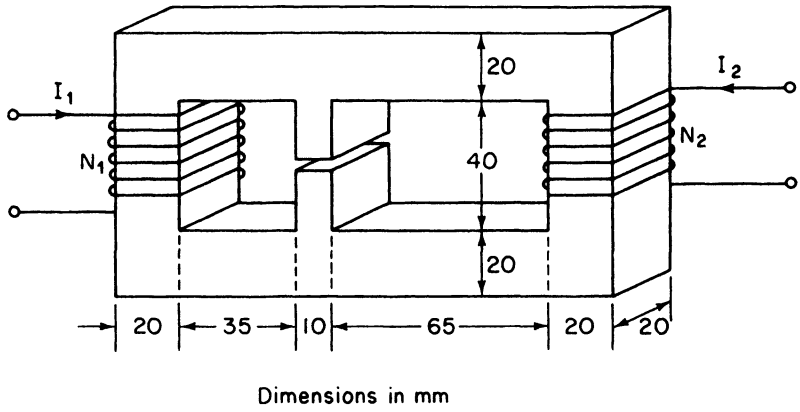


Figure 2.51 Magnetic structure for Problem 2.16.

magnetic circuit of the machine and find the flux density in the air gap for an MMF of 10,000 At.

Problem 2.15 Consider the magnetic structure of Problem 2.13 and assume that the air-gap length is 1.5 mm with all other data unchanged. Find the required MMF to set up a flux of 0.7×10^{-3} Wb in the center section.

Problem 2.16 The magnetic structure of Fig. 2.51 is made of material with relative permeability 2000. The air-gap length is 2 mm. Find the flux in the air gap given that

$$\mathfrak{F}_1 = \mathfrak{F}_2 = 4000 \text{ At}$$

Problem 2.17 For the magnetic structure of Problem 2.16, find $\mathfrak{F}_2$ given that $\mathfrak{F}_1 = 4000$ At, and that the flux in the air gap is 0.5×10^{-3} Wb.

Problem 2.18 Repeat Problem 2.4, accounting for fringing of flux in the air gap using 1.1 as a fringe factor:

$$\text{Fringe factor} = \frac{\text{Cross-sectional area of flux lines}}{\text{Cross section of air gap}}$$

Problem 2.19 Repeat Problem 2.5, accounting for fringing effects assuming that the air gap is square in cross section.

Problem 2.20 Repeat Problem 2.4, assuming that the iron path is cast steel with a magnetization curve as shown in Fig. 2.52.

Problem 2.21 Repeat Problem 2.17 assuming that the magnetization curve of the core is given in Fig. 2.52. Assume that the air-gap flux is 2×10^{-4} Wb and that $\mathfrak{F}_1$ is 1800 At.

Problem 2.22 Find the inductance of the coil of Problem 2.1, assuming that $N = 10$ turns.

www.EngineeringEBooksPdf.com

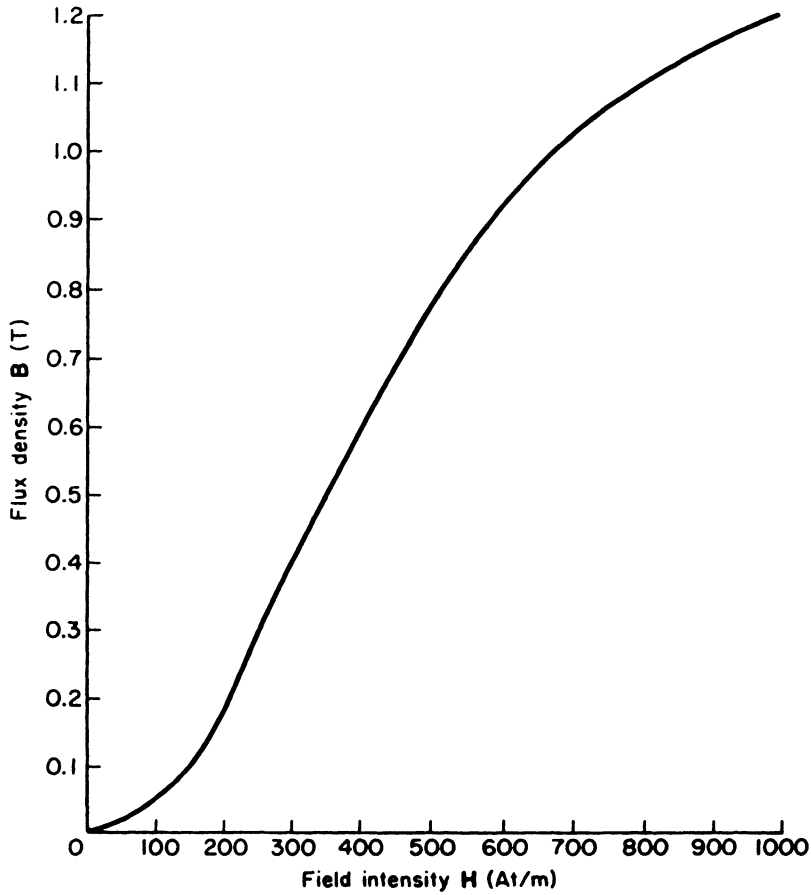


Figure 2.52 Magnetization curve for cast steel.

Problem 2.23 Find the inductance of the coil of Problem 2.4.

Problem 2.24 The flux linkages in a coil are related to the current by the relation

$$\lambda = 1 - 0.5e^{-1.25i}$$

Find the energy stored for a current of 0.8 A.

Problem 2.25 Consider the coil of Problem 2.4. Find the energy stored in the air gap and the magnetic core.

Problem 2.26 The eddy-current and hysteresis losses in a transformer are 500 and 600 W, respectively, when operating from a 60-Hz supply. Find the eddy-current and hysteresis losses when the transformer is operated from a 50-Hz supply with an increase of 10% in flux density. Find the change in core losses.

www.EngineeringEBooksPdf.com

Problem 2.27 The relationship between current, displacement, and flux linkages in a conversative electromechanical device is given by

$$i = \lambda[0.8\lambda + 2.2(x-1)^2]$$

Find expressions for the stored energy and the magnetic-field force in terms of λ and x. Find the force for $x = 0.75$.

Problem 2.28 Repeat Problem 2.27 for the relationship

$$i = \lambda^3 + \lambda(0.1\lambda + x)$$

Problem 2.29 Find an expression for the force exerted by the magnetic field in an electromechanical device with the following nonlinear characteristic:

$$i = I_o \frac{a\lambda + b\lambda^3}{1 + cx}$$

where I_o, a, b, and c are given constants.

Problem 2.30 A plunger-type solenoid is characterized by the relation

$$\lambda = \frac{10i}{1 + 10^4 x/2.54}$$

Find the force exerted by the field for $x = 2.54 \times 10^{-3}$ and $i = 11$ A.

Problem 2.31 An electromagnet used to lift steel slabs is shown in Fig. 2.53. Show that the minimum current required to lift a slab of mass M is given by

$$i = \frac{\mathfrak{R}_c + (2x/\mu_0 A)}{N} \sqrt{\mu_0 MAg}$$

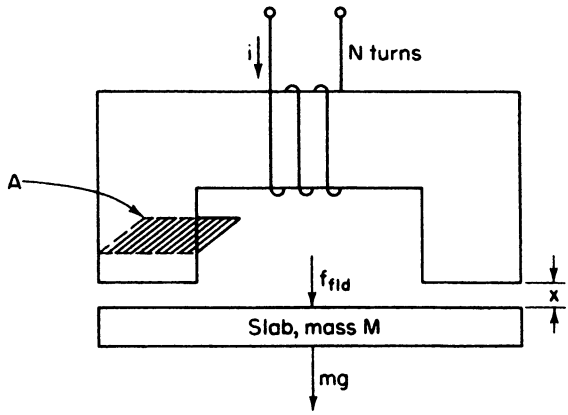


Figure 2.53 Electromagnet for Problem 2.31.

www.EngineeringEBooksPdf.com

In the preceding expression, $\mathfrak{R}_c$ is the reluctance of the magnetic core, A is the cross-sectional area of one air gap, and g is the acceleration of gravity.

Problem 2.32 Find the minimum value of the current i required to lift a slab with $M = 100$ kg using the electromagnet of Problem 2.31, given that

$$A = 16 \times 10^{-4}\,\text{m}^2 \qquad x = 0.15 \times 10^{-2}\,\text{m}$$

$$N = 400\,\text{turns}$$

Neglect the reluctance of the magnetic core.

Problem 2.33 Consider the magnetic structure shown in Fig. 2.54. Show that the dynamics of the system are described by

$$\frac{d\lambda(t)}{dt} = \frac{-(g_1 l_1 + x l_2)\mathrm{R}}{\mu_0 N^2 h l_1 l_2}\lambda(t) + \mathrm{R}I(t)$$

$$\frac{d^2x}{dt^2} = \frac{-\lambda^2}{2\mu_0 M N^2 h l_1} + g$$

where g is the acceleration of gravity. Neglect core reluctance.

Problem 2.34 Assume that the voltage applied to the coil of the magnetic structure shown in Fig. 2.55 is given by

$$e(t) = E_m \cos \omega t$$

Assume that $\lambda(0) = 0$, and find the force exerted on the movable part in terms of the structure geometry, E_m, ω, and time.

Problem 2.35 For the structure of Problem 2.34, assume that $E_m = 10$ V and that the supply frequency is 60 Hz. The coil has 500 turns. The gap length $g = 0.1$ cm,

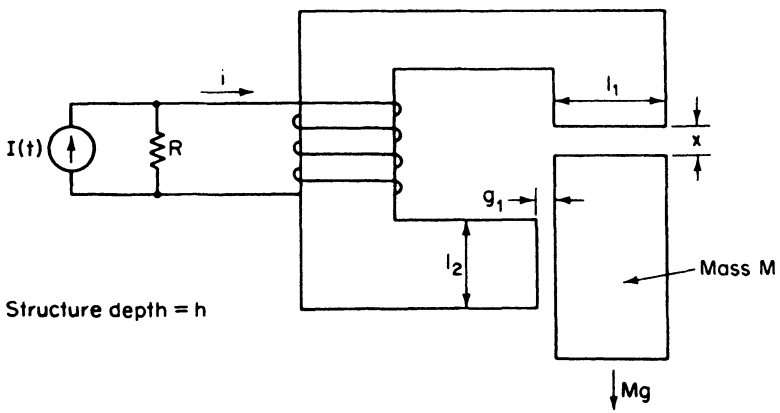


Figure 2.54 Structure for Problem 2.33.

www.EngineeringEBooksPdf.com

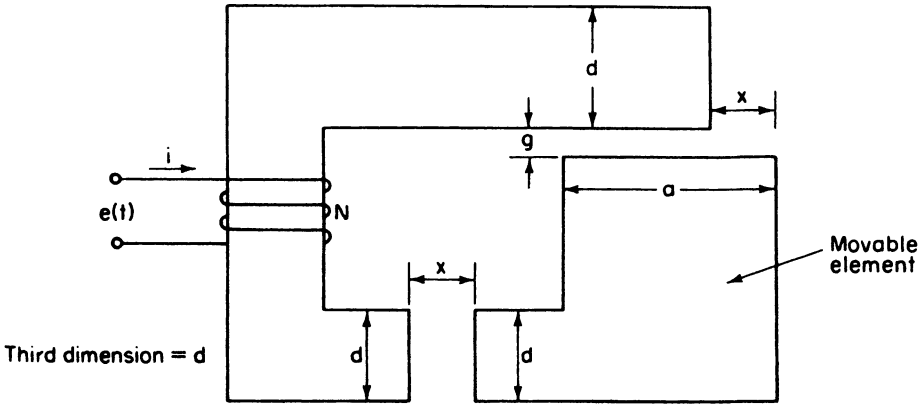


Figure 2.55 Magnetic structure for Problem 2.34.

$d = 10$ cm, and $a = 15$ cm. Find the force in terms of x and time. Calculate the average force in terms of x.

Problem 2.36 The inductance of a coil used with a plunger-type electromechanical device is given by

$$L = \frac{1.6 \times 10^{-5}}{x}$$

where x is the plunger displacement. Assume that the current in the coil is given by

$$i(t) = 5 \sin \omega t$$

where $\omega = 2\pi(60)$. Find the force exerted by the field for $x = 10^{-2}$ m. Assume that x is fixed and find the necessary voltage applied to the coil terminals, given that its resistance is $1\,\Omega$.

Problem 2.37 The reluctance of the magnetic structure for a plunger-type relay is given by

$$\mathfrak{R} = \frac{400}{x(0.02 - x)}$$

Assume that the exciting coil has 1000 turns and that the exciting current is

$$i = 4 \cos t$$

Find the magnetic-field force as a function of time and its average value if the displacement is given by

$$x(t) = 0.01 \cos t$$

www.EngineeringEBooksPdf.com

Problem 2.38 The inductance of the exciting coil of a certain reluctance motor is given by

$$L = \frac{L_0}{1 + a\cos 4\theta}$$

Find an expression for the energy stored in the magnetic field, and hence find an expression for the torque developed in terms of flux linkages and the angular displacement θ and the system parameters. Find the torque developed for $\theta =$ 15 degrees and $i = 10$ A. Assume that $L_0 = 0.05$ H and $a = -0.3$.

Problem 2.39 Repeat Problem 2.38 for the inductance expressed as

$$L = \frac{L_0}{1 + a(\cos 4\theta + \cos 8\theta)}$$

The value of a in this case is -0.25.

Problem 2.40 The reluctance of the magnetic circuit of a reluctance motor is given by

$$\mathfrak{R} = \mathfrak{R}_o(1 + a\cos 4\theta)$$

Let $\mathfrak{R}_o = 2000$ and assume that the number of turns on the exciting coil is 10 turns. Find the developed torque for $i = 10$ A, $\theta = 15$ degrees, assuming that $a = -0.3$.

Problem 2.41 The developed torque for the motor of Problem 2.38 is given by

$$T = -12\lambda^2 \sin 4\theta$$

Assume that

$$\lambda(t) = 0.5\cos \omega t$$

and that

$$\theta(t) = \omega_r t + a$$

Find the instantaneous torque developed and the condition for nonzero average torque.

Problem 2.42 A rotating electromechanical conversion device has a stator and rotor, each with a single coil. The inductances of the device are

$$L_{11} = 0.4\,\text{H} \qquad L_{22} = 2.4\,\text{H}$$
$$L_{12} = 1.25\cos\theta\,\text{H}$$

where the subscript 1 refers to stator and the subscript 2 refers to rotor. The angle θ is the rotor angular displacement from the stator coil axis. Express the torque as a function of currents i_1, i_2, and θ, and compute the torque for $i_1 = 3$ A and $i_2 = 1$ A.

www.EngineeringEBooksPdf.com

Problem 2.43 Assume for the device of Problem 2.42 that

$$L_{11} = 0.4 + 0.1\cos 2\theta$$

All other parameters are unchanged. Find the torque in terms of θ for $i_1 = 3$ A and (a) $i_2 = 0$; (b) $i_2 = 1$ A.

Problem 2.44 Assume for the device of Problem 2.42 that the stator and rotor coils are connected in series, with the current being

$$i(t) = I_m \sin \omega t$$

Find the instantaneous torque and its average value over one cycle of the supply current in terms of I_m and ω.

Problem 2.45 A rotating electromechanical energy conversion device has the following inductances in terms of θ in radians (angle between rotor and stator axes):

$$L_{11} = 0.764\theta$$
$$L_{22} = -0.25 + 1.719\theta$$
$$L_{12} = -0.75 + 1.337\theta$$

Find the torque developed for the following excitations.

(a) $i_1 = 15$ A, $i_2 = 0$.
(b) $i_1 = 0$ A, $i_2 = 15$ A.
(c) $i_1 = 15$ A, $i_2 = 15$ A.
(d) $i_1 = 15$ A, $i_2 = -15$ A.

Problem 2.46 For the machine of Problem 2.42, assume that the rotor-coil terminals are shorted ($e_2 = 0$) and that the stator current is given by

$$i_1(t) = I \sin \omega t$$

Find the torque developed as a function of I, θ, and time.

Problem 2.47 For the device of Problem 2.46, the rotor-coil terminals are connected to a 10-Ω resistor. Find the rotor current in the steady state and the torque developed.

www.EngineeringEBooksPdf.com

CHAPTER 3

POWER ELECTRONIC DEVICES AND SYSTEMS

3.1 INTRODUCTION

The requirements for control of electric power for electric-motor drive systems and industrial control led to the early development of electromechanical systems to obtain a variable dc voltage to control dc-motor drives. The advent of power electronics revolutionized the concept of power control for power conversion and for control of electrical-motor drives. *Power electronics* may be defined as the applications of solid-state electronics for the control and conversion of electric power. It is based primarily on the switching of the power semiconductor devices. With the development of power semiconductor technology, the power-handling capabilities and the switching speed of the power devices have improved tremendously.

Power electronics are used in a great variety of high-power products, including heat controls, light controls, motor controls, power supplies, vehicle propulsion systems, and high-voltage direct-current (HVDC) systems. It is difficult to draw the boundaries for the applications of power electronics; especially with the present trends in the development of power devices and microprocessors, the upper limit is undefined.

3.2 POWER SEMICONDUCTOR DEVICES

The first thyristor, or SCR, was developed in late 1957. Since then, there has been much progress in the power semiconductor devices. Until 1970, the conventional thyristors had been exclusively used for power control in industrial applications.

www.EngineeringEBooksPdf.com

Since 1970, various types of power semiconductor devices were developed and became commercially available. These can be divided broadly into four types: (1) power diodes, (2) thyristors, (3) power bipolar junction transistors (BJTs), and (4) power MOSFETs. The thyristors can be subdivided into seven types: (a) forced-commutated thyristor, (b) line-commutated thyristor, (c) GTO, (d) RCT, (e) static induction thyristor (SITH), (f) gate-assisted turn-off thyristor (GATT), and (g) light-activated silicon-controlled rectifier (LASCR). Static induction transistors (SIT) are also commercially available.

A diode has two terminals: a cathode and an anode. Schottky diodes have low on-state voltage and very small recovery time, typically nanoseconds. The leakage current increases with the voltage rating, and their ratings are limited to 100 V, 300 A. A diode conducts when its anode voltage is higher than that of the cathode, and the forward voltage drop of a power diode is very low, typically 0.5 and 1.2 V. If the cathode voltage is higher than its anode voltage, a diode is said to be in a *blocking mode*. There are three types of power diodes: general purposes, high speed (or fast recovery), and Schottky. General-purpose diodes are available up to 3000 V, 3500 A, and the rating of fast-recovery diodes can go up to 3000 V, 1000 A. The reverse recovery time varies between 0.1 and 5 μs. The fast-recovery diodes are used for high-frequency switching of power converters.

Forward bias is a term describing the application of an external voltage to the anode terminal higher than that at the cathode (i.e., for $v_{AK} > 0$). *Reverse bias* is the term used when $v_{AK} < 0$.

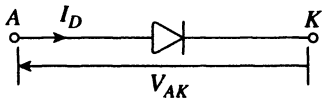
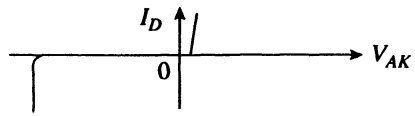
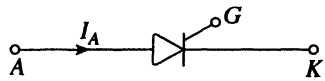
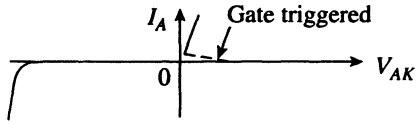
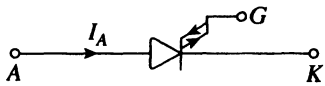
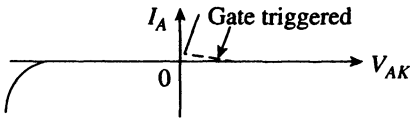
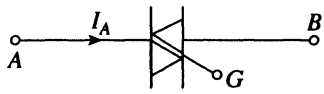
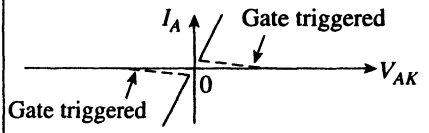
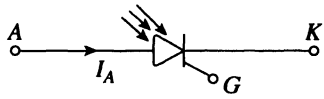
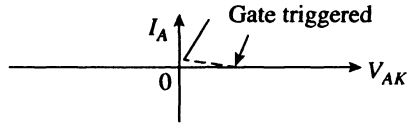
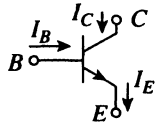
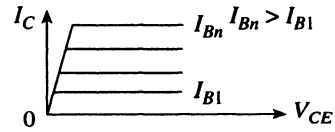
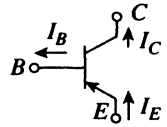
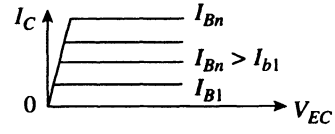
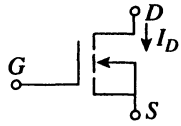
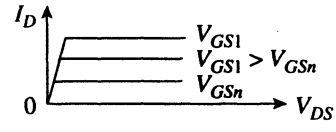
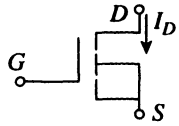
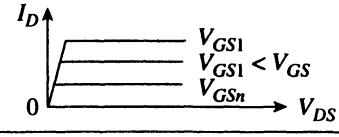
A thyristor has three terminals: an anode, a cathode, and a gate. The thyristor conducts when a small current is passed through the gate terminal to the cathode, provided that the anode terminal is at a higher potential than the cathode. Once a thyristor is conducting, the gate circuit has no control and the thyristor continues to conduct. When a thyristor is in a conduction mode, the forward voltage drop is very small, typically 0.5 V to 2 V. A conducting thyristor can be turned off by making the potential of the anode equal to or less than the cathode potential. The line-commutated thyristors are turned off due to the sinusoidal nature of the input voltage, and forced-commutated thyristors are turned off by an extra circuit called *commutation circuitry.*

Natural or line-commutated thyristors are available with ratings up to 2500 V, 4000 A (and 5000 V, 2500 A). The *turn-off time* is defined as the time interval between the instant when the principal current has decreased to zero after external switching of the principal voltage circuit, and the instant when the thyristor is capable of supporting a specified principal voltage without turning on. The *turn-off time* of high-speed reverse-blocking thyristors have been improved substantially, and it is possible to have 10 to 20 μs in a 1200-V, 2000-A thyristor.

RCTs and GATTS are widely employed in high-speed switching, especially in traction applications. An RCT can be considered to be a thyristor with an inverse-parallel diode. RCTs are available up to 2500 V, 1000 A (and 400 A in reverse conduction), with a switching time of 40 μs. GATTs are available up to 1200 V, 400 A, with a switching speed of 8 μs. LASCRs, which are available up to 6000 V, 1500 A, with a switching speed of 200 to 40 μs, are suitable for high-voltage power systems,

www.EngineeringEBooksPdf.com

TABLE 3.1 Characteristics and Symbols of Some Power Devices

Devices	Symbols	Characteristics
Diode		
Thyristor		
GTO		
TRIAC		
LASCR		
NPN BJT		
PNP BJT		
N-Channel MOSFET		
P-Channel MOSFET		

www.EngineeringEBooksPdf.com

especially in HVDC. For low-power ac applications, TRIACs are widely used in all types of simple heat controls, light controls, motor controls, and ac switches. A TRIAC is similar to two thyristors connected in inverse parallel and having only one gate terminal. The current flow through a TRIAC can be controlled in either direction.

GTOs and SITHs are essentially self-turned-off thyristors, which are turned on by applying a short positive pulse to the gates and are turned off by the application of a short negative pulse to the gate. They do not require commutation circuits. GTOs are very attractive for forced commutation of converters and are available up to 2500 V, within a power range of 1 to 20 MVA. SITHs are applied for medium-power converters with a frequency of several hundred kilohertz and beyond the frequency range of GTOs.

High-power bipolar transistors are employed in power converters at a frequency below 10 kHz and are applied in power ratings up to 100 kW and 1000 V. A bipolar transistor has three terminals: base, emitter, and collector. It is operated as a switch in the common-emitter configuration. As long as the base of an NPN transistor is at a higher potential than the emitter and the base current is sufficiently large to drive the transistor in the saturation region, the transistor remains on, provided that the collector-to-emitter junction is properly biased. The forward drop of a conducting transistor is in the range of 0.5 to 1.5 V. If the base drive voltage is withdrawn, the transistor remains in the nonconduction (or off) mode.

Power MOSFETs are used in high-speed power converters and are available for relatively low power rating in the range of 1000 V, 50 A at a frequency range of several tens of kilohertz. Table 3.1 shows the v-i characteristics and the symbols of some common power semiconductor devices.

Note that thyristor technology is superior to transistors in blocking voltages above 2.5 kV, as they have the best trade-offs between on-state and blocking voltage.

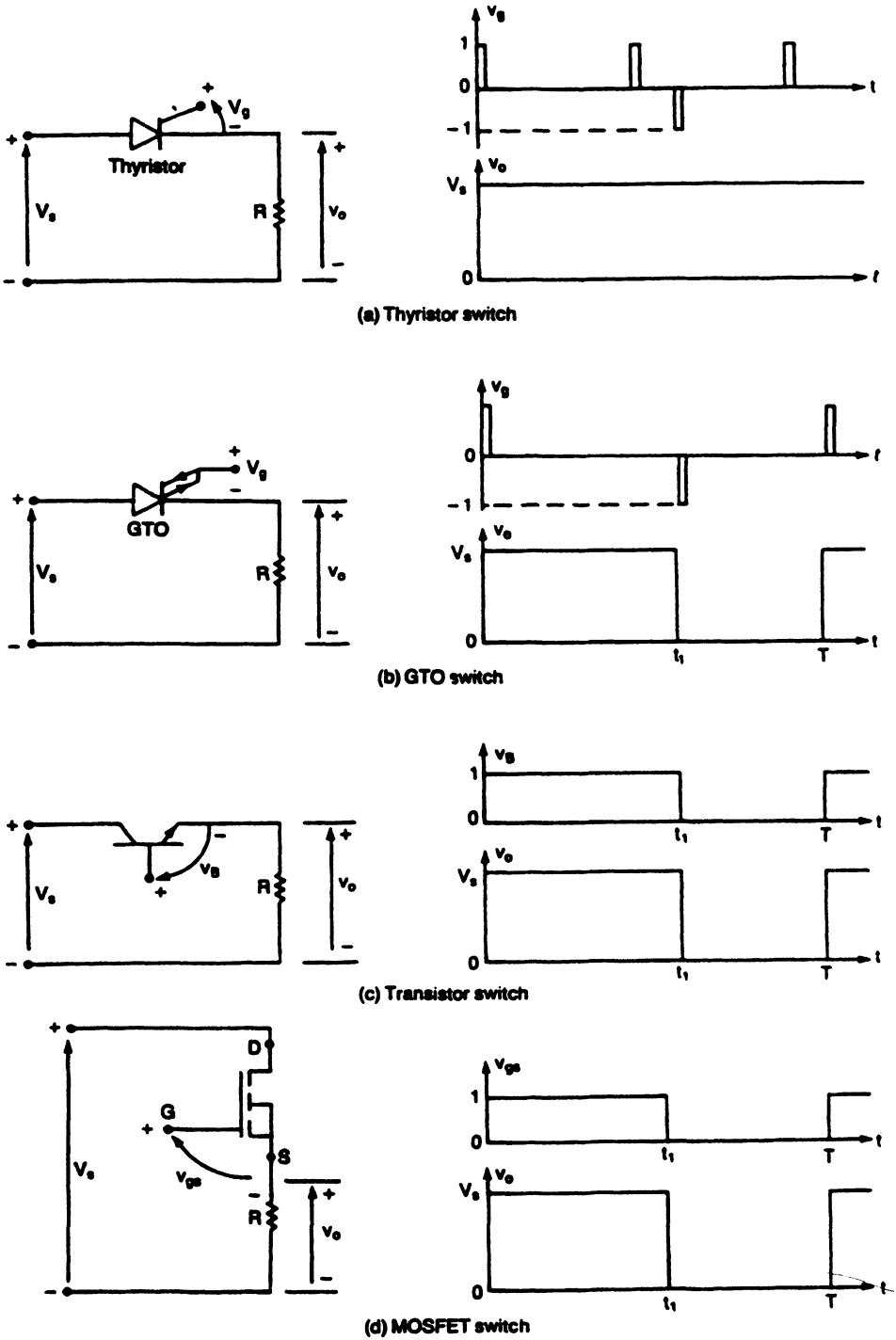
3.3 CONTROL CHARACTERISTICS OF POWER DEVICES

Power semiconductor devices can be operated as switches by applying control signals to the gate terminal of thyristors (and to the base of bipolar transistors). The required output is obtained by varying the conduction time of these switching devices. Figure 3.1 shows the output voltages and control characteristics of common power switching devices. Once a thyristor is conducting, the gate signal of either positive or negative magnitude has no effect on the conduction property, and this is shown in Fig. 3.1(a). When a power semiconductor device is in a normal conduction mode, there is a small voltage drop across the device. In the output voltage waveforms in Fig. 3.1, these voltage drops are considered negligible.

One can classify power semiconductor switching devices on the following basis:

1. Uncontrolled turn-on and -off (e.g., diode)
2. Controlled turn-on and uncontrolled turnoff (e.g., SCR)
3. Controlled turn-on and -off characteristics (e.g., BJT, MOSFET, GTO)

www.EngineeringEBooksPdf.com



(a) Thyristor switch

(b) GTO switch

(c) Transistor switch

(d) MOSFET switch

Figure 3.1 Control characteristics of power switching devices.

www.EngineeringEBooksPdf.com

4. Continuous gate signal requirement (BJT, MOSFET)
5. Pulse gate requirement (e.g., SCR, GTO)
6. Bipolar voltage-withstanding capability (SCR)
7. Unipolar voltage-withstanding capability (BJT, MOSFET, GTO)
8. Bidirectional current capability (TRIAC, RCT)
9. Unidirectional current capability (SCR, GTO, BJT, MOSFET, diode)

3.4 POWER SEMICONDUCTOR DIODES

A diode acts as a switch to perform functions such as freewheeling, charge reversal of capacitor and energy transfer between components in thyristor commutation circuits, energy feedback from the load to the power source, and trapped-energy recovery. The diodes are also used in rectifier circuits. Practical diodes differ from the ideal characteristics and have certain limitations. The power diodes are similar to *pn*-junction signal diodes. However, power diodes have larger power-, voltage-, and current-handling capabilities than that of ordinary signal diodes. The frequency response (or switching speed) is low compared to signal diodes.

3.4.1 Diode Characteristics

A power diode is a two-terminal *pn*-junction device. Figure 3.2 shows a sectional view of a *pn*-junction and diode symbol. When the anode potential is positive with respect to the cathode, the diode is said to be *forward biased* and the diode conducts. There is a relatively small forward voltage drop across a conducting diode, and the magnitude of this drop depends on the manufacturing process and temperature. When the cathode potential is positive with respect to the anode, the diode is said to be *reverse biased*. Under reverse-biased conditions, a small reverse current (also known as leakage current) in the range of micro- or milliampere flows and this leakage current increases slowly in magnitude with the reverse voltage until the avalanche or zener voltage is reached. Figure 3.3 shows the steady-state *v-i* characteristics of a diode.

In a forward-biased junction diode, the current is due to the net effect of majority and minority carriers. Once a diode is in a forward conduction mode and then its forward current is reduced to zero (due to the natural behavior of the diode circuit or by applying a reverse voltage), the diode continues to conduct due to the minority

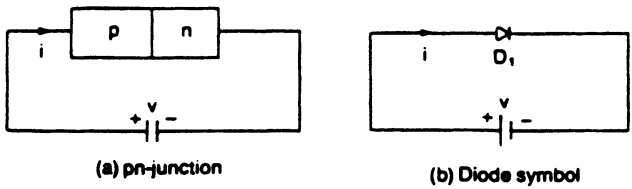


Figure 3.2 *pn*-Junction and diode symbol.

www.EngineeringEBooksPdf.com

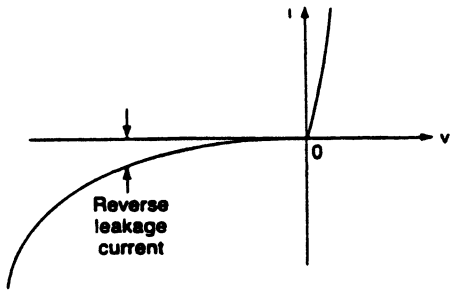


Figure 3.3 v-i Characteristics of diode.

carriers that remain stored in the *pn*-junction and the bulk semiconductor material. The minority carriers require a certain time to recombine with opposite charges and to be neutralized. This time is called the *reverse recovery time* of the diode. Figure 3.4 shows two reverse recovery characteristics of junction diodes. The soft recovery type is more common. The reverse recovery time is denoted as t_{rr} and is measured from the initial zero crossing of the two components, t_a and t_b. Component t_a is due to the charge storage in the depletion region of the junction, and represents the time between the zero crossing and the peak reverse current, I_{RR}. Component t_b is due to the charge storage in the bulk semiconductor material. The ratio t_b/t_a is known as the softness factor (SF). For practical purposes, one needs to consider the total recovery time, t_{rr}, and the value of the peak reverse current, I_{RR}.

The reverse recovery time and the peak reverse current of a diode are functions of the storage charge and the reverse (or reapplied) di/dt. The storage charge depends on the forward diode current, I_F. The peak reverse recovery current, I_{RR}, reverse charge, Q_{RR}, and the softness factor are all of interest in circuit design.

If a diode is reverse biased, a leakage current flows due to the minority carriers. Then applying forward voltage would force the diode to carry current in the forward direction. However, it requires a certain time, known as *forward recovery* (or *turn-on*) *time*, before all the majority carriers over the whole junction can contribute to the current flow. If the rate of rise of the forward current is high and the forward current is concentrated in a small area of the junction, the diode may fail. The forward

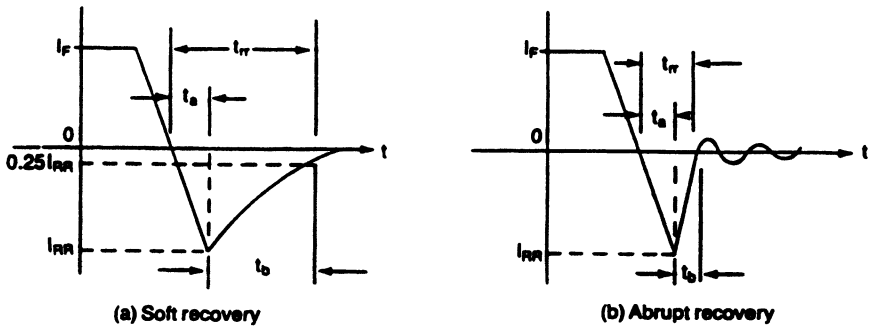


Figure 3.4 Reverse recovery characteristics.

www.EngineeringEBooksPdf.com

recovery time is a limit on the rate of rise of the forward current and the switching speed.

3.4.2 Power Diode Types

An ideal diode should have no reverse recovery time. In many applications, the effects of reverse recovery time are insignificant, and cheap diodes can be used. Depending on the recovery characteristics and manufacturing techniques, power diodes can be classified into three categories. The characteristics and practical limitations of each type restrict their applications.

1. Standard or general-purpose diodes
2. Fast-recovery diodes
3. Schottky diodes

General-purpose Diodes General-purpose rectifier diodes are characterized by relatively high reverse recovery time, typically 25 μs, and are used in low-speed applications, where recovery time is not critical (e.g., diode rectifiers for low frequency up to 1-kHz applications and line-commutated converters). These diodes have current ratings starting at less than 1 A.

Fast-recovery Diodes Fast-recovery diodes have short recovery time, typically less than 5 μs. They are used in chopper and inverter circuits, where the speed of recovery is often important. These diodes have current ratings starting from less than 1 A to hundreds of amperes, with voltage ratings from 50 V to around 3 kV.

Schottky Diodes In a Schottky diode the charge storage problem of a *pn*-junction can be eliminated (or minimized). This is achieved by setting up a "barrier potential" with a contact between a metal and a semiconductor. A layer of metal is deposited on a thin epitaxial layer of n-type silicon. The potential barrier simulates the behavior of a *pn*-junction. However, the rectifying action depends on the majority carriers only, and as a result there is no excess of minority carriers to recombine. The recovery effect is caused only by the self-capacitance of the semiconductor junction.

The recovered charge of a Schottky diode is much lower than that of an equivalent *pn*-junction diode. Since it is due only to the junction capacitance, it is largely independent of the reverse *di/dt*. A Schottky diode has a relatively low forward voltage drop.

The leakage current of a Schottky diode is higher than that of a *pn*-junction diode. A Schottky diode with relatively low conduction voltage has relatively high leakage current, and vice versa. Therefore, its maximum allowable voltage is limited to 100 V. The current rating of Schottky diodes varies from 1 A to 300 A. The Schottky diodes are ideal for high-current and low-voltage dc power supplies. However, they are also used in low-current power supplies to achieve improved efficiency.

www.EngineeringEBooksPdf.com

3.4.3 Performance Parameters of Diodes

The semiconductor diodes are characterized in terms of certain performance parameters. The designer needs to determine the correct semiconductor diode to meet given specifications. These parameters are nonlinear and depend on a number of factors. The manufacturer normally provides characteristic curves for important parameters, in the form of a data sheet.

Maximum Average Forward Current, $I_{F(AV)}$

$I_{F(AV)}$ is the maximum allowable value of average forward current at a specified temperature. These data are normally quoted for a half-sine wave at a case temperature, $T_C = 85°C$.

Maximum rms Forward Current, $I_{F(RMS)}$

$I_{F(RMS)}$ is the maximum permissible root-mean-square (rms) value of forward current. This is related to the heating effect due to i^2R dissipation and is limited due to the thermal stress on the device.

Maximum Peak Repetitive Forward Current, I_{FRM}

I_{FRM} is the maximum peak permissible current that can be applied on a repetitive basis. This is normally specified for a half-sinusoidal waveform.

Maximum Peak One-cycle Nonrepetitive Forward Current, I_{FSM}

I_{FSM} is the maximum peak permissible forward current of half-sine wave with a duration of 10 ms at a specified temperature. A repetition is permissible only after expiration of a minimum interval to reduce the junction temperature to the allowable range. This peak permissible value varies with the number of repetitions.

Maximum Repetitive Peak Reverse Voltage, V_{RRM}

V_{RRM} defines the maximum permissible instantaneous value of repetitive applied reverse voltage that the diode can block. This rating is determined by the *pn*-junction and the case type.

Maximum Peak Nonrepetitive Reverse Voltage, V_{RSM}

V_{RSM} is the maximum instantaneous peak value of applied reverse voltage under transient conditions. V_{RSM} is typically 25% above V_{RRM}.

Forward Voltage Drop, V_F

V_F is the instantaneous value of the forward voltage drop and depends on the junction temperature, T_J. Figure 3.5 shows the variation of instantaneous

www.EngineeringEBooksPdf.com

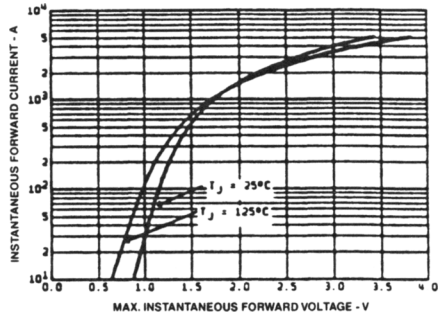


Figure 3.5 Forward characteristics of a power diode.

forward voltage drop with forward current. V_F can be considered as being made up of (1) a value that is independent of the forward current, and (2) a value that is proportional to the instantaneous forward current.

Maximum Peak Forward Voltage, V_{FM}

V_{FM} is the maximum forward voltage drop at a specified forward current and junction temperature.

Threshold Voltage, $V_{(TO)}$

$V_{(TO)}$ is the current-independent portion of the forward voltage drop and depends on the temperature of operation.

Forward Slope Resistance, r_F

r_F is the current-dependent portion of the instantaneous forward voltage drop v_F such that $v_F = V_{(TO)} + ir_F$, where i is the instantaneous diode current.

Maximum Peak Reverse (or Leakage) Current, I_{RRM}

I_{RRM} is the maximum reverse current at the maximum junction temperature and maximum repetitive peak reverse voltage. This current would also cause junction heating, and a low value is desirable.

Reverse Recovery Time, t_{rr}

t_{rr} may be defined as the time interval between the instant the current passes through zero during the changeover from the forward conduction to reverse blocking condition and the moment the reverse current has decayed to 25% of its peak reverse value, i_{RR}. Its value depends on the junction temperature, rate of fall of forward current, and the forward current prior to commutation.

Reverse Recovery Charge, Q_{RR}

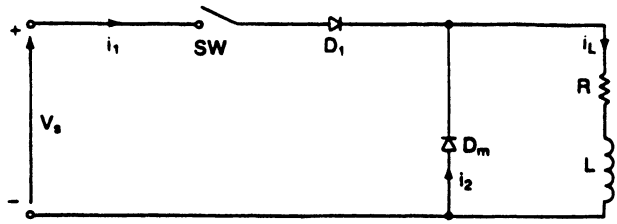
Q_{RR} is the number of charge carriers that flow across the diode in the reverse direction due to change over from the forward conduction to reverse blocking

www.EngineeringEBooksPdf.com

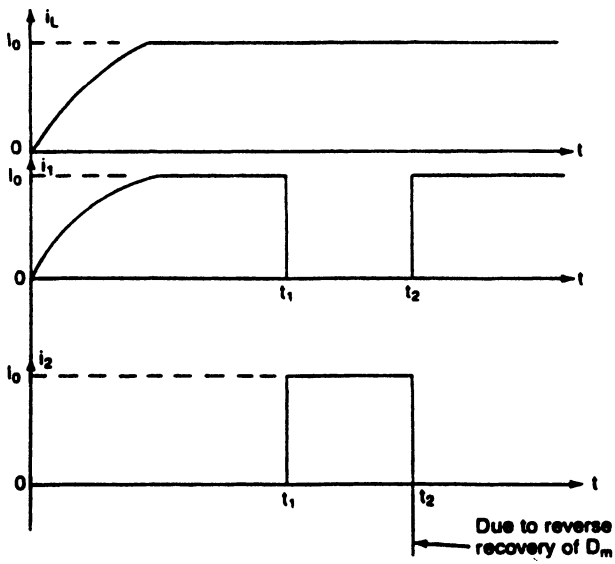
condition. Its value is determined from the area enclosed by the path of the reverse recovery current.

3.4.4 Effects of Forward and Reverse Recovery Time

Consider the circuit shown in Fig. 3.6(a). Assume that the switch, SW, is turned on at $t = 0$ and remains on long enough that a steady-state current of $I_0 = V_s/R$ would flow through the load and the freewheeling diode D_m will be reversed biased. If the switch is turned off at $t = t_1$, diode D_m would conduct and the load current would circulate through D_m. Now, if the switch is turned on again at $t = t_2$, diode D_m would behave as a short circuit. The rate of rise of the forward current of the switch (and diode D_1) and the rate of fall of forward current of diode D_m would be very high, tending to be infinity. The peak reverse current of diode D_m could be very high, and diodes D_1 and D_m may be damaged. Figure 3.6(b) shows the various waveforms for the diode currents. This problem is normally overcome by connecting a *di/dt* limiting inductor, L_s,



(a) Circuit diagram



(b) Waveforms

Figure 3.6 Chopper circuit without *di/dt* limiting inductor.

www.EngineeringEBooksPdf.com

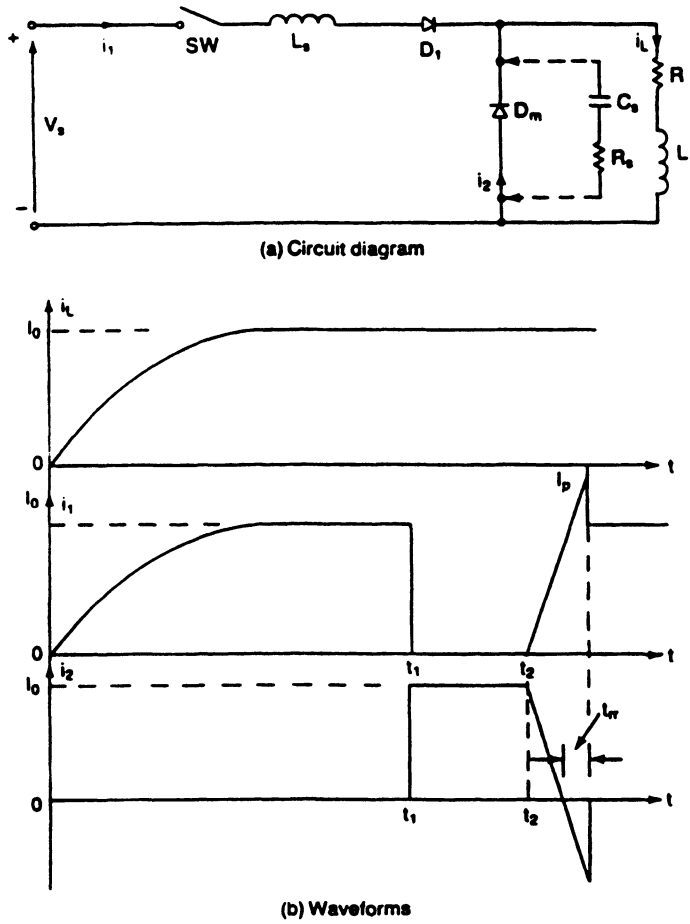


Figure 3.7 Chopper circuit with di/dt limiting inductor.

as shown in Fig. 3.7(a). Practical diodes require a certain turn-on time before the entire area of the junction becomes conductive and the *di/dt* must be kept low to meet the turn-on time limit. This time is sometimes known as forward recovery time, t_{rf}.

The rate of rise of current through diode D_1, which should be the same as the rate of fall of the current through diode D_m, is

$$\frac{di}{dt} = \frac{V_s}{L_s} \tag{3.1}$$

Assume that t_{rr} is the reverse recovery time of D_m, the peak reverse current of D_m is

$$I_{RR} = t_{rr}\frac{di}{dt} = \frac{t_{rr}V_s}{L_s} \tag{3.2}$$

www.EngineeringEBooksPdf.com

and the peak current through the inductor L_s is

$$I_p = I_0 + I_{RR} = I_0 + t_{rr}\frac{t_{rr}V_s}{L_s} \tag{3.3}$$

When the inductor current reaches a value I_p, the diode D_m turns off suddenly (assuming abrupt recovery) and breaks the current flow path. The load current cannot change suddenly from I_0 to I_p due to the highly inductive load. The excess energy stored in L_s would induce a high reverse voltage across D_m, and this may damage the diode D_m. The excess energy stored as a result of the reverse recovery time is found from

$$W_R = \frac{1}{2}L_s[(I_0 + I_{RR})^2 - I_0^2] \tag{3.4}$$

$$W_R = \frac{1}{2}L_s\left[\left(I_0 + \frac{t_{rr}V_s}{L_s}\right)^2 - I_0^2\right] \tag{3.5}$$

The waveforms for the various currents are shown in Fig. 3.7(b). This excess energy can be transferred from the inductor L_s to a capacitor C_s, which is connected across diode D_m. The value of the C_s can be determined from

$$\frac{1}{2}C_sV_c^2 = W_R$$

or

$$C_s = \frac{2W_R}{V_c^2} \tag{3.6}$$

where V_c is the allowable reverse voltage of the diode.

A resistor R_s, which is shown in Fig. 3.7(a) by dashed lines, is connected in series with the capacitor to damp out any transient oscillation. Equation (3.6) is approximate and does not take into account the effects of L_s and R_s during the transients for energy transfer. The effect of t_{rr} is significant for high-frequency sources, but for the case of a normal 60-Hz source, its effect can be considered negligible.

3.5 POWER TRANSISTORS

Power transistors are characterized by controlled turn-on and turn-off characteristics. Transistors, which are used as switching elements, are operated in the saturation region, resulting in a low on-state voltage drop. The switching speed of modern transistors is much higher than that of thyristors. However, their voltage and current

www.EngineeringEBooksPdf.com

ratings are lower than those of thyristors, and transistors are normally used in low- to medium-power applications. Power transistors can be classified as:

1. Biopolar junction transistors (BJTS)
2. Metal-oxide-semiconductor field-effect transistors (MOSFETs)
3. Metal-oxide-semiconductor insulated-gate transistors (MOSIGTs)

BJTs are current-controlled devices and their parameters are sensitive to junction temperature. The phenomenon of secondary breakdown (SB) is a destructive effect caused by the current flow to a small portion of the base, producing localized hot spots. If the energy in these hot spots is sufficient, the excessive localized heating may damage the transistor. Thus secondary breakdown is caused by a localized thermal runway, resulting from high current concentrations. The current concentration may be caused by defects in the transistor structure. The SB occurs at certain combinations of voltage, current, and time. Since time is involved, the secondary breakdown is basically an energy-dependent phenomenon. BJTs suffer from secondary breakdown and require reverse base current during turnoff to reduce storage time. But they have low on-state or saturation voltage.

MOSFETs are voltage-controlled devices that require very low gating power. Their parameters are less sensitive to junction temperature. There is no secondary breakdown problem and no need for negative gate voltage during turnoff. MOSIGTs, which combine the advantages of BJTs and MOSFETs, are voltage-controlled devices and have low on-state voltage similar to BJTs. MOSIGTs have no second breakdown phenomena. A transistor switch is much simpler than a forced-commutated thyristor switch. However, the choice between a BJT and MOSFET in the converter circuits is not obvious.

The characteristics of practical transistors differ from those of ideal devices. The transistors have certain limitations and are restricted to some applications. The characteristics and ratings of each type should be examined to determine its suitability to a particular application.

3.5.1 Bipolar Junction Transistors

A bipolar transistor is formed by adding a second *p*- or *n*-region to a *pn*-junction diode. With two *n*-regions and one *p*-region, two junctions are formed and it is known as a *npn-transistor*, as shown in Fig. 3.8(a). With two *p*-regions and one *n*-region, it is called as a *pnp-transistor*, as shown in Fig. 3.8(b). The three terminals are named *collector*, *emitter*, and *base*. A bipolar transistor has two junctions, collector–base junction (CBJ) and base–emitter junction (BEJ).

Steady-state Characteristics While there are three possible configurations—common-collector, common-base, and common-emitter—the common-emitter configuration, which is shown in Fig. 3.9(a) for an *npn*-transistor, is generally used in switching applications. The typical input characteristics of base current, I_B, versus base–emitter voltage, V_{BE}, are shown in Fig. 3.9(b). Figure 3.9(c) shows the typical

www.EngineeringEBooksPdf.com

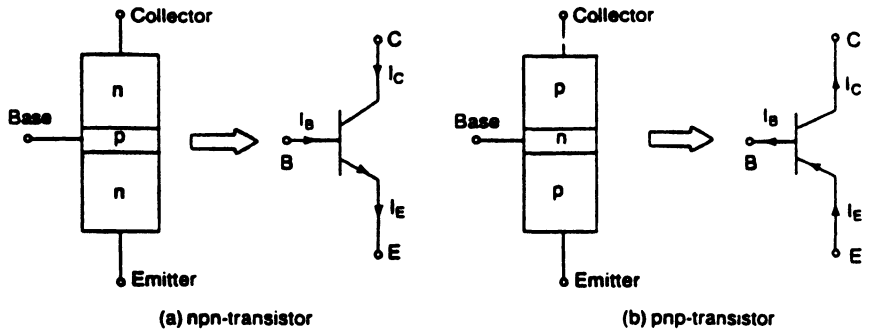


Figure 3.8 Bipolar transistors.

output characteristics of collector current, I_C, versus collector–emitter voltage, V_{CE}. For a *pnp*-transistor, the polarities of all currents and voltages are reversed.

A transistor has three operating regions: cutoff, active, and saturation. In the cutoff region, the transistor is off or the base current is not high enough to turn it on and both junctions are reverse biased. In the active region, the transistor acts as an amplifier, where the collector current is amplified by a gain and the collector–emitter voltage decreases with base current. The CBJ is reverse biased and the BEJ is forward biased. In the saturation region, the base current is sufficiently high so that the

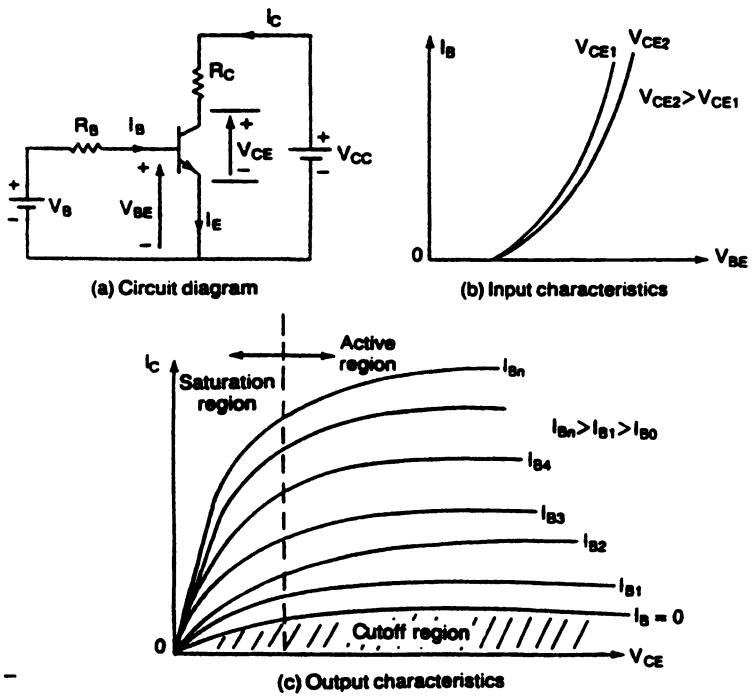


Figure 3.9 Characteristics of *npn*-transistors.

www.EngineeringEBooksPdf.com

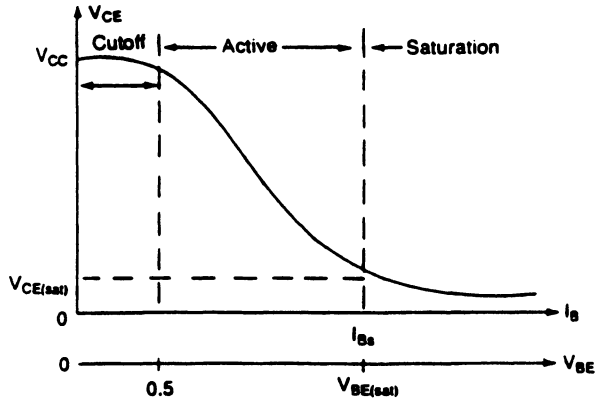


Figure 3.10 Transfer characteristics.

collector–emitter voltage is low and the transistor acts as a switch. Both junctions (CBJ and BEJ) are forward biased. The transfer characteristic, which is a plot of V_{CE} against I_B, is shown in Fig. 3.10.

The model of an *npn*-transistor is shown in Fig. 3.11 under large-signal dc operation. The currents are related by

$$I_E = I_C + I_B \tag{3.7}$$

The base current is effectively the input current, and the collector current is the output current. The ratio of the collector current, I_C, to base current, I_B, is known as the current gain, β:

$$\beta = h_{FE} = \frac{I_c}{I_B} \tag{3.8}$$

The collector current has two components: one due to the base current and other one is the leakage current of the CBJ.

$$I_C = \beta I_B + I_{CEO} \tag{3.9}$$

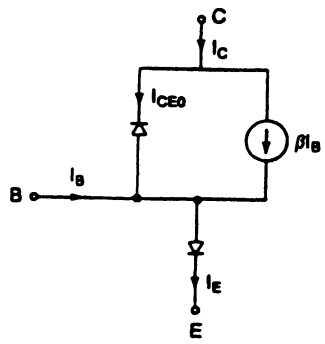


Figure 3.11 Model of *npn*-transistor.

www.EngineeringEBooksPdf.com

where I_{CEO} is the collector-to-emitter leakage current with base open circuit, and can be considered negligible compared to βI_B.

From Eqs. (3.7) and (3.9),

$$I_E = I_B(1+\beta) + I_{CEO} \tag{3.10}$$

$$\cong I_B(1+\beta) \tag{3.10a}$$

$$I_E \approx I_C\left(1+\frac{1}{\beta}\right) = I_C\frac{\beta+1}{\beta} \tag{3.11}$$

The collector current is given by

$$I_C \approx \alpha I_E \tag{3.12}$$

where we define the constant α by

$$\alpha = \frac{\beta}{\beta+1} \tag{3.13}$$

or

$$\beta = \frac{\alpha}{1-\alpha} \tag{3.14}$$

Consider the circuit of Fig. 3.12, where the transistor is operated as a switch.

$$I_B = \frac{V_B - V_{BE}}{R_B} \tag{3.15}$$

$$V_C = V_{CE} = V_{CC} - I_C R_C = V_{CC} - \frac{\beta R_C}{R_B}(V_B - V_{BE}) \tag{3.16}$$

$$V_{CE} = V_{CE} + V_{BE}$$

or

$$V_{CB} = V_{CE} - V_{BE} \tag{3.17}$$

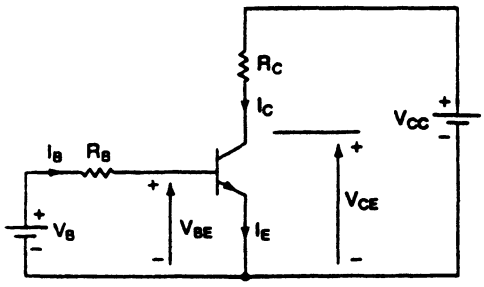


Figure 3.12 Transistor switch.

www.EngineeringEBooksPdf.com

Equation (3.17) demostrates that as long as $V_{CE} \geq V_{BE}$, the CBJ will be reverse biased and the transistor will be in the active region. The maximum collector current in the active region, which can be obtained by setting $V_{CB} = 0$ and $V_{BE} = V_{CE}$, is

$$I_{CM} = \frac{V_{CC} - V_{CE}}{R_C} = \frac{V_{CC} - V_{BE}}{R_C} \tag{3.18}$$

and the corresponding value of base current

$$I_{BM} = \frac{I_{CM}}{\beta} \tag{3.19}$$

If we increase the base current beyond I_{BM}, V_{BE} increases, as will the collector current, and the value of V_{CE} will drop below V_{BE}. This will continue until the CBJ is forward biased with a V_{BC} of about 0.4 to 0.5 V. The transistor then goes into saturation. The transistor saturation can be defined as the point above which any increase in the base current does not increase the collector current significantly.

In the saturation region, the collector current remains almost constant. If the collector–emitter saturation voltage is $V_{CE(\text{sat})}$, the collector current is

$$I_{CS} = \frac{V_{CC} - V_{CE(\text{sat})}}{R_C} \tag{3.20}$$

and the corresponding value of base current is

$$I_{BS} = \frac{I_{CS}}{\beta} \tag{3.21}$$

Normally, the circuit is designed so that I_B is higher than I_{BS}. The ratio of I_B to I_{BS} is called the *overdrive factor* (ODF):

$$\text{ODF} = \frac{I_B}{I_{BS}} \tag{3.22}$$

and the ratio of I_{CS} to I_B is called the *forced* β, β_f where

$$\beta_f = \frac{I_{CS}}{I_B} \tag{3.23}$$

The total power loss in the two junctions is

$$P_T = V_{BE} I_B + V_{CE} I_C \tag{3.24}$$

A high value of overdrive factor will not reduce the collector–emitter voltage significantly. However, V_{BE} will increase due to increased base current, resulting in increased power loss in the BEJ.

www.EngineeringEBooksPdf.com

Example 3.1 The bipolar transistor shown in Fig. 3.12 has β in the range 10 to 60. The load resistance is $R_C = 12$. The dc supply voltage is $V_{CC} = 100$ V and the input voltage to the base circuit is $V_B = 8$ V. Assume that $V_{CE(\text{sat})} = 1.0$ V and $V_{BE(\text{sat})} = 1.5$ V. Find the value of R_B that results in saturation with an overdrive factor of 5, the forced β, and the power loss in the transistor, P_T.

Solution Using Eq. (3.20)

$$I_{CS} = \frac{V_{CC} - V_{CE(\text{sat})}}{R_C} = \frac{100 - 1}{12} = 8.25 \text{ A}$$

From Eq. (3.21)

$$I_{BS} = \frac{I_{CS}}{\beta_{\min}} = \frac{8.25}{10} = 0.825 \text{ A}$$

Equation (3.22) yields the base current for an overdrive factor of 5:

$$I_B = 5 \times 0.825 = 4.125 \text{ A}$$

Equation (3.15) gives the required value of R_B:

$$R_B = \frac{V_B - V_{BE(\text{sat})}}{I_B} = \frac{8 - 1.5}{4.125} = 1.5758\,\Omega$$

From Eq. (3.23)

$$\beta_f = \frac{I_{CS}}{I_B} = \frac{8.25}{4.125} = 2.0$$

Equation (3.24) yields the total power loss as

$$P_T = V_{BE} I_B + V_{CE} I_C = 1.5 \times 4.125 + 1 \times 8.25 = 14.4375 \text{ W}$$

Switching Characteristics A forward-biased *pn*-junction exhibits two parallel capacitances: a depletion-layer capacitance and a diffusion capacitance. Under steady-state conditions, these capacitances do not play any role. However, under transient conditions, they contribute to the turn-on and turn-off behavior of the transistor.

The model of a transistor under transient conditions is shown in Fig. 3.13, where C_{cb} and C_{be} are the effective capacitances of the CBJ and BEJ, respectively. The *transconductance*, g_m, of a BJT is defined as the ratio of I_C to VBE. These capacitances are dependent on the junction voltages and physical construction of the transistor. Condition C_{cb} affects the input capacitance significantly due to the Miller

www.EngineeringEBooksPdf.com

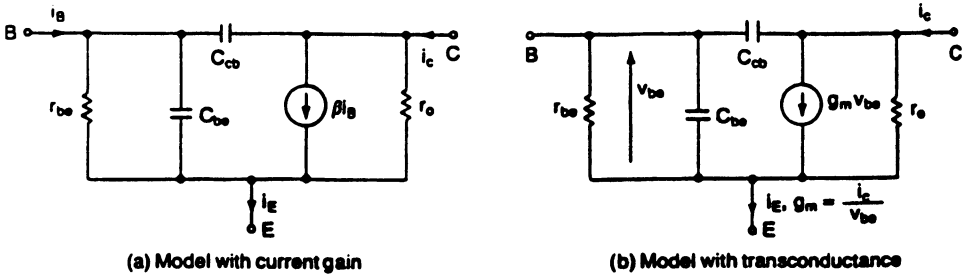


Figure 3.13 Transient model of BJT.

multiplication effect, and r_{CE} and r_{BE} are the resistances of collector to emitter and base to emitter, respectively.

Due to the internal capacitances, the transistor does not turn on instantly. Figure 3.14 illustrates the waveforms and switching times. As the input voltage v_B rises from zero to V_1 and the base current rises to I_{B1}, the collector current does not respond immediately. There is a delay, known as *delay time*, t_d, before any collector current flows. This delay is required to charge up the capacitances of the BEJ to the forward-bias voltage V_{BE} (approximately 0.7 V). After this delay, the collector

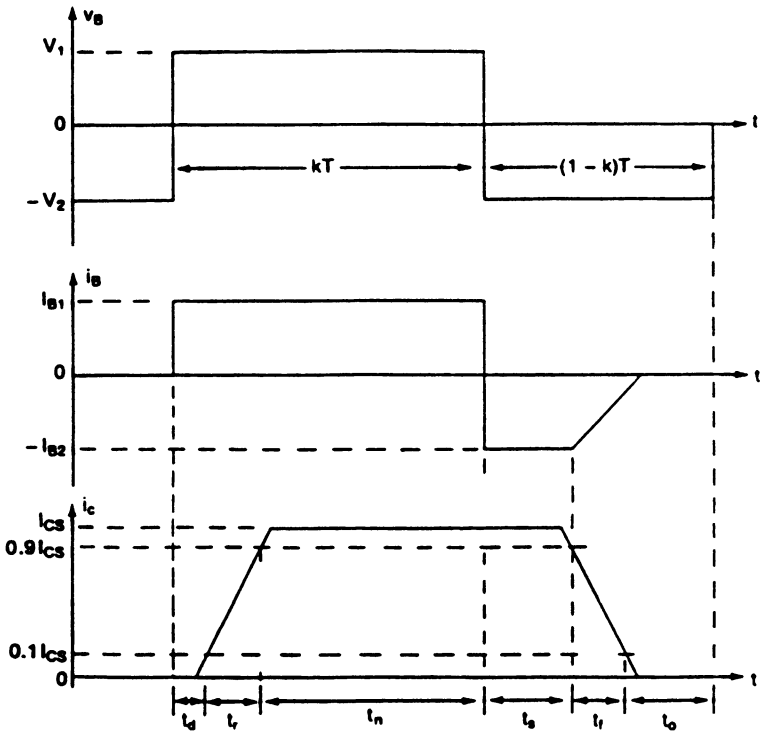


Figure 3.14 Switching times of bipolar transistors.

www.EngineeringEBooksPdf.com

current rises to the steady-state value of I_{CS}. The rise time, t_r, depends on the time constant determined by input capacitances.

The base current is normally more than that required to saturate the transistor. As a result, the excess minority carrier charge is stored in the base region. The higher the ODF, the greater the amount of extra charge stored in the base. This extra charge, which is called the *saturating charge*, is proportional to the excess base drive, I_e:

$$I_e = I_B - \frac{I_{CS}}{\beta} = \text{ODF} \cdot I_{BS} - I_{BS} = I_{BS}(\text{ODF} - 1) \tag{3.25}$$

and the saturating charge is given by

$$Q_s = \tau_s I_e = \tau_s I_{BS}(\text{ODF} - 1) \tag{3.26}$$

where τ_s is known as the storage time constant of the transistor.

When the input voltage is reversed from V_1 to $-V_2$, and the base current is also changed to $-I_{B2}$, the collector current does not change for a time, t_s, called the storage time. Time t_s is required to remove the saturating charge from the base. Since v_{BE} is still positive with approximately 0.7 V, the base current reverses its direction due to the change in the polarity of v_B from V_1 and $-V_2$. The reverse current, $-I_{B2}$, helps to discharge the base and remove the extra charge from the base. Without $-I_{B2}$, the saturating charge has to be removed entirely by recombination and the storage time would be longer.

Once the extra charge is removed, the BEJ capacitance charges to the input voltage, $-V_2$, and the base current falls to zero. The fall time, t_f, depends on the time constant, which is determined by the capacitance of the reverse-biased BEJ.

Figure 3.15(a) shows the extra storage charge in the base of a saturated transistor. During turnoff, this extra charge is removed first in time t_s and the charge profile is changed from a to c, as shown in Fig. 3.15(b). During fall time, the charge profile decreases from profile c until all charges are removed.

The turn-on time, t_{on}, is the sum of delay time, t_d, and the rise time, t_r,

$$t_{on} = t_d + t_r$$

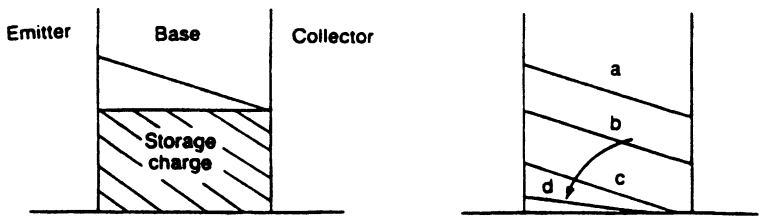


Figure 3.15 Charge storage in saturated bipolar transistors.

www.EngineeringEBooksPdf.com

and the turnoff time, t_{off}, is the sum of storage time, t_s, and fall time, t_f,

$$t_{off} = t_s + t_f$$

Performance Parameters The characteristics of transistors are normally specified by the manufacturer in terms of certain performance parameters for safe operation. The transistor circuits must be designed so that the operating conditions do not exceed their suggested ratings.

dc Gain, h_{FE}

h_{FE} (or β) is the ratio of the collector current, I_C, to base current, I_B, at a specified value of V_{CE}. The gain depends on the temperature. At the rated collector current, the variation in gain with change in temperature is minimum and the circuit should be designed to operate at the rated value. A high gain would reduce the values of forced β and $V_{CE(sat)}$.

Collector–Emitter Saturation Voltage, $V_{CE(sat)}$

A low value of $V_{CE(sat)}$ will reduce the on-state losses. However, $V_{CE(sat)}$ is a function of the collector current, base current, current gain, and junction temperature. The base drive must be sufficient enough to drive the transistor into saturation, but overdrive will decrease the forced β and increase the losses in the base–emitter junction. A small value of forced β (or high value of overdrive factor) decreases the value of $V_{CE(sat)}$. However, a higher junction temperature increases the value of $V_{CE(sat)}$.

Collector–Base Saturation Voltage, $V_{BE(sat)}$

A low value of $V_{BE(sat)}$ will decrease the power loss in the base–emitter junction. Voltage $V_{BE(sat)}$ increases with collector current and forced β. The transconductance ($g_m = I_C/V_{BE}$) of the transistor can be determined from the curves of $V_{BE(sat)}$ versus I_C.

Turn-On Time, t_{on}

The turn-on time can be decreased by increasing the base drive for a fixed value of collector current. Time t_d depends on input capacitances not changing significantly with I_C. However, t_r, increases with the increase in I_C.

Turn-Off Time, t_{off}

The storage time, t_s, which depends on the overdrive factor does not change significantly with I_C. The fall time, t_f, which is a function of capacitance increases with I_C. Time t_s and t_f can be reduced by providing negative base drive during turnoff. It is noted that t_f is less sensitive to negative base drive.

www.EngineeringEBooksPdf.com

Crossover Time, t_c

The crossover time, t_c, is defined as the interval during which the collector voltage, V_{CE}, rises from 10% of its peak off-state value and collector current, I_C, falls to 10% of its on-state value.

Forward-Biased Safe Operating Area

During turn-on and on-state conditions, the average junction temperature and second breakdown limit the power-handling capability of a transistor. The manufacturers usually provide the forward-biased safe operating area (FBSOA) curves under specified test conditions. FBSOA indicates the i_c–v_{CE} limits of the transistor, and for reliable operation, the transistor must not be subjected to greater power dissipation than that shown by the FBSOA curve.

Reverse-Biased Safe Operating Area

During turnoff, a high current and high voltage must be sustained by the transistor, in most cases with the base–emitter junction reverse biased. The collector–emitter voltage must be held to a safe level at or below a specified value of collector current. The manufacturers provide the I_C–V_{CE} limits during reverse-biased turnoff as reverse-biased safe operating area (RBSOA).

Breakdown Voltages

A *breakdown voltage* is defined as the absolute maximum voltage between two terminals with the third terminal open, shorted, or biased in either the forward or reverse direction. At breakdown the voltage remains relatively constant, where the current rises rapidly. The following breakdown voltages are quoted by the manufacturers:

V_{EBO} The maximum voltage between the emitter terminal and base terminal with the collector terminal open circuited.

V_{CEV} *or* V_{CEX} The maximum voltage between the collector terminal and emitter terminal at a specified negative voltage applied between base and emitter.

$V_{CEO(SUS)}$ The maximum sustaining voltage between the collector terminal and emitter terminal with the base open circuited. This rating is specified at the maximum collector current and voltage, appearing simultaneously across the device with a specified value of load inductance.

Let us consider the circuit in Fig. 3.16(a). When the switch SW is closed, the collector current increases, and after a transient, the steady-state collector current is $I_{CS} = (V_{CC} - V_{CE(sat)})/R_C$. For an inductive load, the load line would be the path *ABC* shown in Fig. 3.16(b). If the switch is opened to remove the base current, the collector current will begin to fall and a voltage of $L(di/dt)$ will be induced across the inductor to oppose the current reduction. The transistor will be subjected to a transient voltage. If this voltage reaches the sustaining voltage level, the collector

www.EngineeringEBooksPdf.com

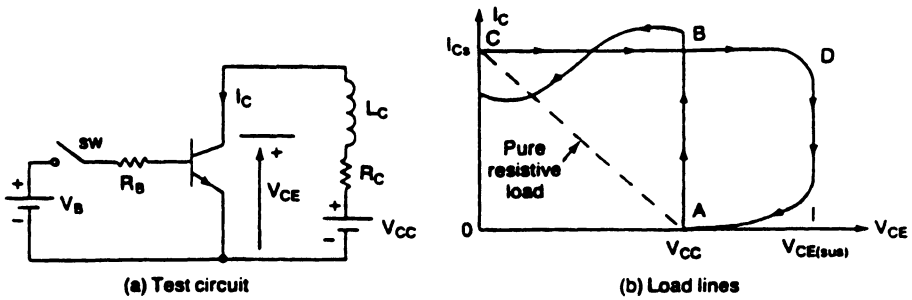


Figure 3.16 Turn-on and turnoff load lines.

voltage remains approximately constant and the collector current will fall. After a short time, the transistor will be in the off-state, and the turnoff line is shown in Fig. 3.16(b) by the path *CDA*.

3.5.2 Power MOSFETS

A BJT is a current-controlled device and requires base current for current flow in the collector. Since the collector current depends on the input (or base) current, the current gain is highly dependent on the junction temperature.

A power MOSFET is a voltage-controlled device and requires only a small input current. The switching speed is very high and the switching times are on the order of nanoseconds. Power MOSFETs are finding increasing applications in low-power high-frequency converters. MOSFETs do not have the problems of second-breakdown phenomena common in BJTs. However, MOSFETs have the problems of electrostatic discharge and require special care in handling. In addition, it is relatively difficult to protect them under short-circuited fault conditions.

MOSFETs are of two types: (1) depletion MOSFETs, and (2) enhancement MOSFETs. An *n*-channel depletion-type MOSFET is formed on a p-type silicon substrate, as shown in Fig. 3.17(a), with two heavily doped n^+ silicon chips for low-resistance connections. The gate is isolated from the channel by a thin oxide layer. The three terminals are called *gate*, *drain*, and *source*. The substrate is normally connected to the source. The gate-to-source voltage, V_{GS}, could be either positive or negative. If V_{GS} is negative, some of the electrons in the *n*-channel area will be repelled and a depletion region will be created below the oxide layer, resulting in a narrower effective channel and high resistance from the drain to source, R_{DS}. If V_{GS} is made negative enough, the channel will be completely depleted, offering a high value of R_{DS}, and there will be no current flow from the drain to source, $I_{DS} = 0$. When this happens, the value of V_{GS} is called *pinch-off voltage*, V_p. On the other hand when V_{GS} is made positive, the channel becomes wider, and I_{DS} increases due to a reduction in R_{DS}. With a *p*-channel depletion-type MOSFET, the polarities of V_{DS}, I_{DS}, and V_{GS} are reversed.

An *n*-channel enhancement-type MOSFET has no channel, as shown in Fig. 3.18. If V_{GS} is positive, an induced voltage will attract the electrons from the *p*-substrate

www.EngineeringEBooksPdf.com

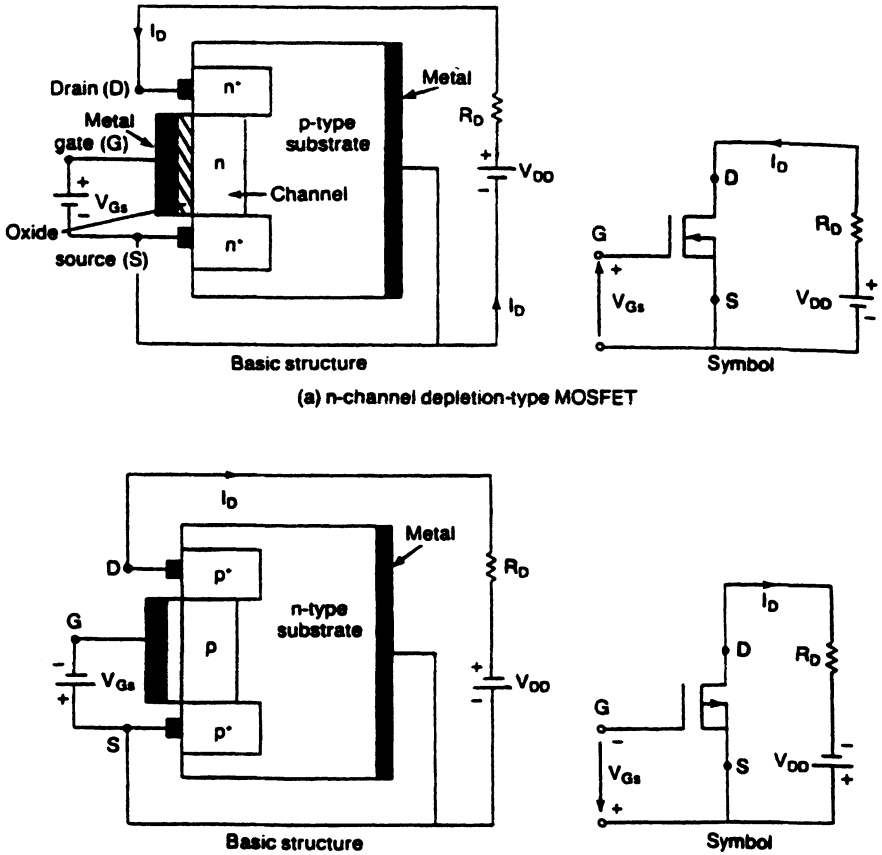


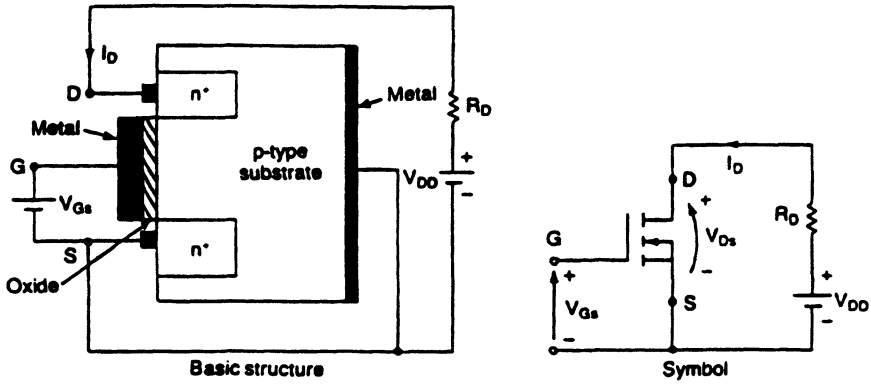
Figure 3.17 Depletion-type MOSFETs.

and accumulate them at the surface beneath the oxide layer. If V_{GS} is greater than or equal to a value known as *threshold voltage*, V_T, a sufficient number of electrons are accumulated to form a virtual n-channel and the current flows from the drain to source. The polarities of V_{DS}, I_{DS}, and V_{GS} are reversed for a p-channel enhancement-type MOSFET.

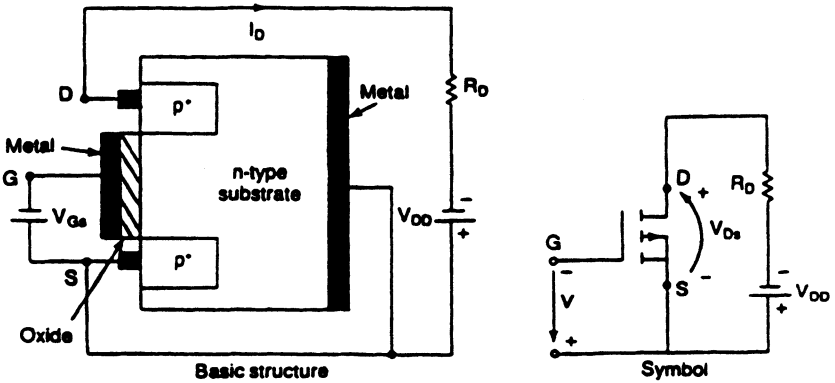
Steady-State Characterisitics The MOSFETs are voltage-controlled devices and have very high input impedance. The gate draws a very small leakage current, of the order of nanoamperes. The current gain is the ratio of drain current, I_D, to input gate current, I_G; it is not an important parameter. The *transconductance*, which is the ratio of drain current to gate voltage, defines the transfer characteristics and is a very important parameter.

The transfer characteristics of n-channel and p-channel MOSFETs are shown in Fig. 3.19. Figure 3.20 shows the output characteristics of an n-channel enhancement MOSFET. There are three regions of operation: (1) cutoff region, where $V_{GS} \leq V_T$;

www.EngineeringEBooksPdf.com



(a) n-channel enhancement-type MOSFET



(b) p-channel enhancement-type MOSFET

Figure 3.18 Enhancement-type MOSFETs.

(2) pinch-off or saturation region, where $V_{DS} \geq V_{GS} - V_T$; and (3) linear region, where $V_{DS} \leq V_{GS} - V_T$. The pinch-off occurs at $V_{DS} = V_{GS} - V_T$. In the linear region, the drain current, I_D, varies in proportion to the drain-source voltage, V_{DS}. Due to high drain current and low drain voltage, the power transistors are operated in the linear region for switching actions. In the saturation region, the drain current remains almost constant for any increase in the value of V_{DS}, and the transistors are used in this region for voltage amplification. It should be noted that saturation has the opposite meaning to that for bipolar transistors.

The steady-state model, which is the same for both depletion-type and enhancement-type MOSFETs, is shown in Fig. 3.21. The transconductance, g_m, is defined as

$$g_m = \left.\frac{I_D}{V_{GS}}\right|_{V_{DS}=\text{constant}} \tag{3.27}$$

www.EngineeringEBooksPdf.com

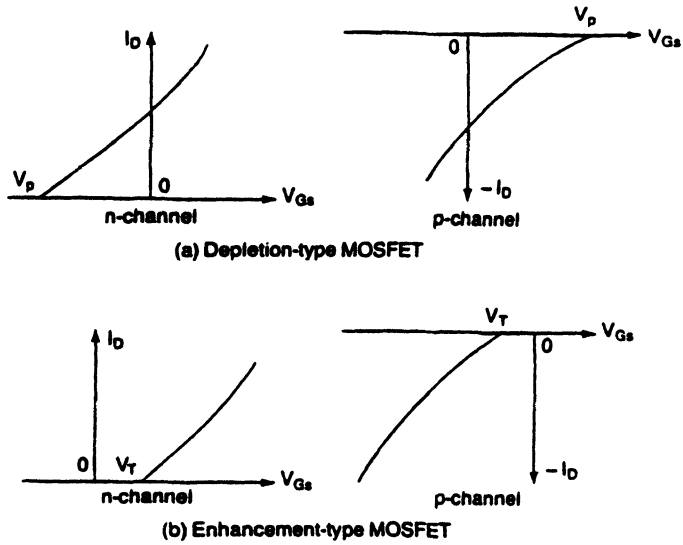


Figure 3.19 Transfer characteristics of MOSFETs.

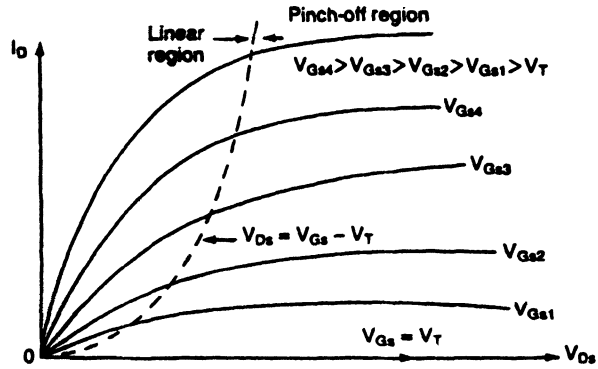


Figure 3.20 Output characteristics of enhancement-type MOSFET.

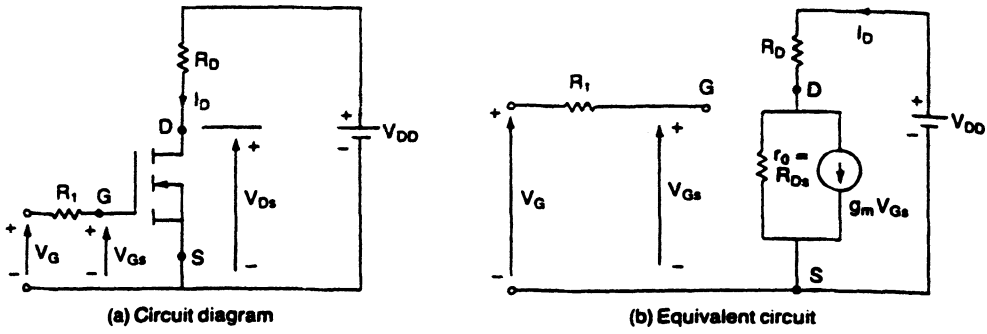


Figure 3.21 Steady-state switching model of MOSFETs.

www.EngineeringEBooksPdf.com

The output resistance, $r_o = R_{DS}$, which is defined as

$$R_{DS} = \frac{\Delta V_{DS}}{\Delta I_D} \tag{3.28}$$

is normally very high in the pinch-off region, typically of the order of megohms and is very small in the linear region, typically of the order of milliohms.

For the depletion-type MOSFETs, the gate (or input) voltage could be either positive or negative. But the enhancement-type MOSFETs respond to a positive gate voltage only. The power MOSFETs are generally of the enhancement type. However, depletion-type MOSFETs would be advantageous and simplify the logic design in some applications that require some form of logic-compatible ac or dc switch that would remain on when the logic supply falls and V_{GS} becomes zero.

Switching Characteristics Without any gate signal, an enhancement-type MOSFET may be considered as two diodes connected back-to-back or as a *npn*-transistor. The gate structure has parasitic capacitances to the source, C_{gs}, and to the drain, C_{gd}. The *npn*-transistor has a reverse-bias junction from the drain to the source and offers a capacitance, C_{ds}. Figure 3.22(a) shows the equivalent circuit of a parasitic bipolar transistor in parallel with a MOSFET. The base–emitter region of an *npn*-transistor is shorted at the ship by metallizing the source terminal, and the resistance from the base to emitter due to bulk resistance of the *n*- and *p*-regions, R_{be}, is small. Hence, a MOSFET may be considered as having an internal diode, and the equivalent circuit is shown in Fig. 3.22(b). The parasitic capacitances depend on their respective voltages.

The switching model of MOSFETs is shown in Fig. 3.23. The typical switching waveforms and times, are shown in Fig. 3.24. The *turn-on delay*, $t_{d(on)}$, is the time that is required to charge the input capacitance to threshold voltage level. The *rise time*, t_r, is the gate charging time from the threshold level to the full-gate voltage, V_{GSP}, which is required to drive the transistor into the linear region. The *turnoff delay time*, $t_{d(off)}$, is the time required for the input capacitance to discharge from the overdrive gate voltage, V_1, to the pinch-off region. Voltage V_{GS} must decrease significantly before V_{DS} begins to rise. The *fall time*, t_f, is the time that is required for the input

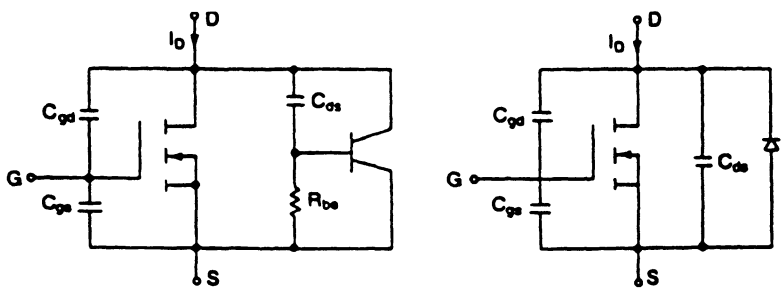


Figure 3.22 Parasitic model of enhancement-type MOSFETs.

www.EngineeringEBooksPdf.com

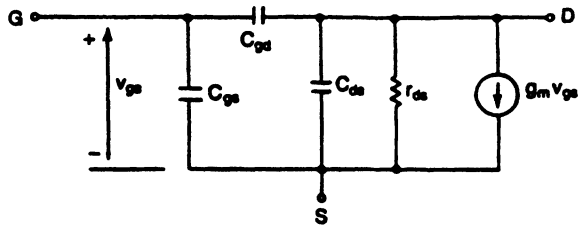


Figure 3.23 Switching model of MOSFETs.

capacitance to discharge from the pinch-off region to threshold voltage. If $V_{GS} \leq V_T$, the transistor turns off.

Performance Parameters The performance parameters of MOSFETs are as follows.

Output Characteristics

The output characteristics are plots of I_D against V_{DS}. For a fixed value of V_{GS}, I_D remains almost constant at the pinch-off region, whereas the output or on-state resistance ($R_{DS} = \Delta V_{DS}/\Delta I_D$) is approximately constant.

Transfer Characteristic

The transfer characteristic is a plot of I_D versus V_{GS} and is temperature dependent.

Transconductance, g_m

Transconductance is a measure of the transfer characteristic and decreases with the junction temperature.

Linear Characteristics

Linear characteristics are the output characteristics at lower values of V_{DS} and are important for switching applications. Since V_{DS} is low in the linear region, they are often identified as saturation characteristics. Saturation signifies the

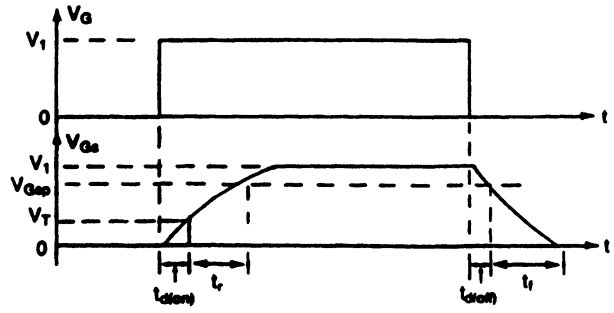


Figure 3.24 Switching waveforms and times.

www.EngineeringEBooksPdf.com

low on-state voltage and high on-state current region of operation similar to BJTs.

On-State Resistance, R_{DS}

R_{DS} represents the power dissipation when the device is conducting. Resistance R_{DS} increases almost linearly with the junction temperature, T_J. The increase in R_{DS} with I_D and V_{GS} is nonlinear. The power dissipation is $P_D = R_{DS}I_D^2 = V_{DS}I_D$. The allowable power dissipation decreases with the case temperature.

Safe Operating Area

The safe operating area (SOA) gives the limit on the maximum value of I_D against the maximum value of V_{DS} during turn-on and turnoff of the device. These are thermal limitations. There is no second breakdown for MOSFETs. But there is a limit on I_D at the lower values of V_{DS} due to the increase in the on-state resistance, R_{DS}. For a shorter on-time, the SOA boundaries extend into higher V_{DS} and I_D. The SOA curve is normally specified at $T_J = 150°C$, but the allowable breakdown voltage limit increases with the junction temperature.

Input and Output Capacitances

The manufacturers specify (1) the effective input capacitance as C_{iss}, (2) effective output capacitance as C_{oss}, and (3) reverse transfer capacitance C_{rss}. These capacitances are dependent on V_{DS}.

Gate Charge, Q_g

During turn-on and turnoff, the input capacitance is charged and discharged. The charge stored on the input capacitance depends on the gate-to-source voltage, V_{GS}. The switching loss due to the gate voltage becomes

$$P_G = Q_g V_{GS} f_s \tag{3.29}$$

where f_s is the switching frequency in hertz.

3.5.3 MOSIGTs

A MOSIGT combines the advantages of BJTs and MOSFETs. A MOSIGT has high input impedance, like MOSFETs, and low on-state conduction losses, like BJTs. But there is no second breakdown problem, like BJTs. By chip design and structure, the equivalent drain-to-source resistance (RDS) is controlled to behave like that of a BJT.

The symbol and circuit of a MOSIGT switch are shown in Fig. 3.25. The three terminals are gate, collector, and emitter instead of gate, drain, and source for a MOSFET. The parameters and symbols of MOSIGT are similar to those of

www.EngineeringEBooksPdf.com

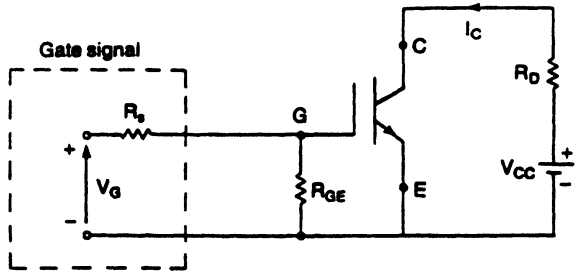


Figure 3.25 Symbol and circuit of a MOSIGT.

MOSFETs, except that the subscripts for source and drain are changed to emitter and collector, respectively.

Output Characteristics

The output characteristics are the plots of collector current, I_C, versus collector–emitter voltage, V_{CE}, for various values of gate–emitter voltage, V_{GE}.

Collector–Emitter Saturation Voltage, $V_{CE(sat)}$

$V_{CE(sat)}$ decreases with increasing value of V_{GE}. It is interesting to note that the temperature coefficient for the variations of $V_{CE(sat)}$ could be either positive or negative, depending on the collector current. A MOSIGT behaves like a BJT at a low I_C value and similar to a MOSFET at a high I_C value. For a fixed value of I_C, $V_{CE(sat)}$ of a MOSIGT is less than V_{DS} of a comparable MOSFET and equal to or greater than $V_{CE(sat)}$ of a comparable BJT.

Transfer Characteristics

The transfer characteristics are plots of I_C versus V_{GE}. They have temperature coefficients that vary with the collector current.

FBSOA

The MOSIGT can conduct continuous current up to the controllable current limit, which is derated due to the temperature limitations. However, there is no second breakdown limit. If the controllable peak current limit is exceeded even for a short time, the device latches on and it cannot be controlled by the gate. In this situation, the device can be turned off by decreasing the load current below the holding current or by reversing the polarity of collector–emitter voltage with an external commutation circuit. The peak collector current, I_{CM}, which increases with the gate–emitter resistance, R_{GE}, is less for inductive load. Induction I_{CM} decreases with the maximum junction temperature, T_J.

www.EngineeringEBooksPdf.com

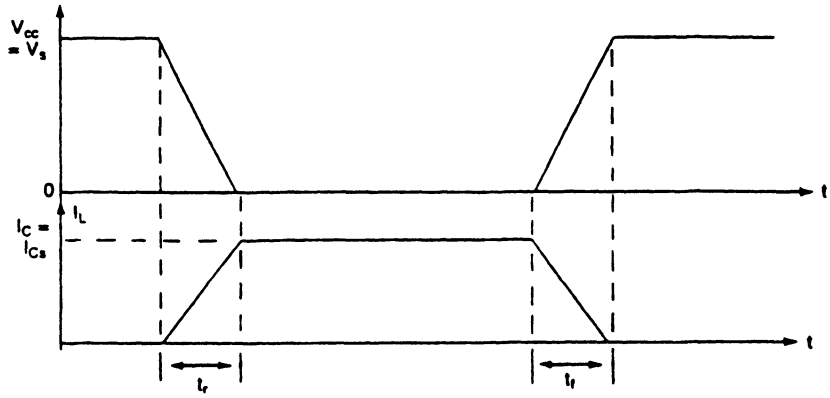


Figure 3.26 Voltage and current waveforms.

Switching Times

The MOSIGT does not require negative gate voltage for reducing turnoff time. However, the turnoff delay time and fall time are functions of R_{GE} and increase with R_{GE}.

3.5.4 *di/dt* and *dv/dt* Limitations

Transistors require certain turn-on and turnoff times. The typical voltage and current waveforms of a BJT switch are shown in Fig. 3.26. During turn-on, the collector current rises and the di/dt is

$$\frac{di}{dt} = \frac{I_L}{t_r} = \frac{I_{cs}}{t_r} \tag{3.30}$$

During turnoff, the collector–emitter voltage must rise in relation to the fall of the collector current, and dv/dt is

$$\frac{dv}{dt} = \frac{V_s}{t_f} = \frac{V_{cc}}{t_f} \tag{3.31}$$

The conditions in Eqs. (3.30) and (3.31) are set by the transistor switching characteristics and must be satisfied during turn-on and turnoff. Protection circuits are normally required to keep the operating *di/dt* and *dv/dt* within the allowable limits of the transistor. A typical transistor switch with *di/dt* and *dv/dt* protections is shown in Fig. 3.27(a), with the operating waveforms in Fig. 3.27(b). The *RC* network across the transistor is known as the *snubber circuit* or *snubber* and limits the *dv/dt*. The inductor L_s, which limits the *di/dt*, is sometimes called a *series snubber*.

Let us assume that under steady-state conditions the load current I_L is freewheeling through diode D_m, which has negligible reverse recovery time. When transistor

www.EngineeringEBooksPdf.com

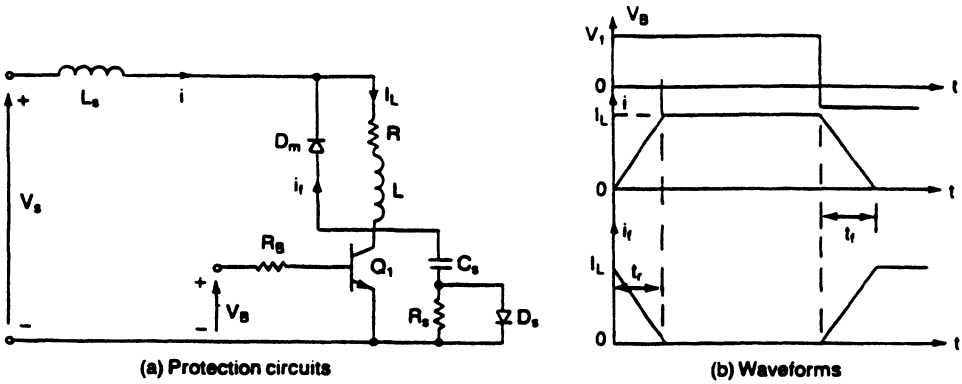


Figure 3.27 Transistor switch with di/dt and dv/dt protections.

Q_1 is turned on, the collector current rises and the current of diode D_m decreases. The equivalent circuit during turn-on is shown in Fig. 3.28(a) and turn-on di/dt is

$$\frac{di}{dt} = \frac{V_s}{L_s} \tag{3.32}$$

Equating Eq. (3.30) to Eq. (3.32) gives the value of L_s,

$$L_s = \frac{V_s t_r}{I_L} \tag{3.33}$$

During turnoff, the capacitor C_s is charged by load current and the equivalent circuit is shown in Fig. 3.28(b). The capacitor voltage will appear across the transistor, and dv/dt is given by

$$\frac{dv}{dt} = \frac{I_L}{C_s} \tag{3.34}$$

Equating Eq. (3.31) to Eq. (3.34) gives the required value of capacitance,

$$C_s = \frac{I_L t_f}{V_s} \tag{3.35}$$

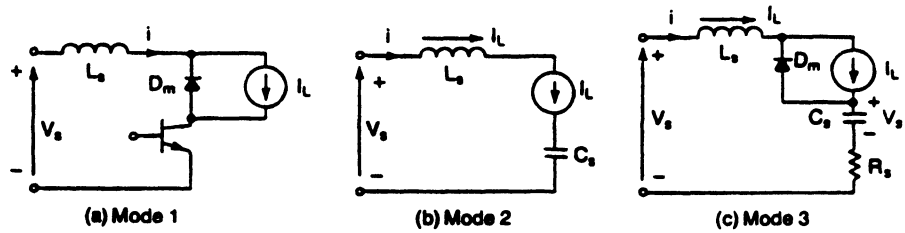


Figure 3.28 Equivalent circuits.

www.EngineeringEBooksPdf.com

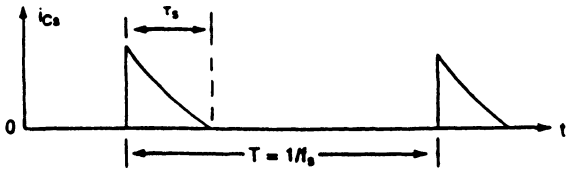


Figure 3.29 Discharge current of snubber capacitor.

Once the capacitor is charged to V_s, the freewheeling diode will turn on. Due to the energy stored in L_s, there will be a damped resonant circuit, as shown in Fig. 3.28(c). The *RLC* circuit is normally made critically damped to avoid oscillations. For unity critical damping, we get

$$R_s = 2\sqrt{\frac{L_s}{C_s}} \tag{3.36}$$

The capacitor C_s has to discharge through the transistor, and this increases the peak current rating of the transistor. The discharge through the transistor can be avoided by placing resistor R_s across C_s instead of placing R_s across D_s.

The discharge current is shown in Fig. 3.29. In choosing the value of R_s, the discharge time, $R_sC_s = \tau_s$ should also be considered. A discharge time of one-third the switching period, T_s, is usually adequate.

$$3R_sC_s = T_s = \frac{1}{f_s} \tag{3.37}$$

or

$$R_s = \frac{1}{3f_sC_s} \tag{3.38}$$

3.5.5 Insulated Gate Bipolar Transistor

An insulated gate bipolar transistor (IGBT) is basically a hybrid MOS-gated turn-on/ -off bipolar transistor that combines the attributes of MOSFET, BJT, and thyristor. Figure 3.30 shows the basic structure of IGBT, which also indicates its equivalent circuit and the device symbol. Its architecture is similar to that of MOSFET, except the n^+ layer at the drain is substituted by a p^+ layer at the collector. The device has the high input impedance of a MOSFET, but BJT-like conduction characteristics. If the gate is positive with respect to the emitter, an *n*-channel is induced in the *p*-region. This forward biases the base–emitter junction of the *pnp*-transistor, turning it on and causing conductivity modulation of the *n*-region, which gives significant improvement of the conduction drop over that of a MOSFET. Because of the parasitic *npn*-transistor, the thyristor-like latching action is prevented by properly controlling the resistivity of the p^+-layer.

www.EngineeringEBooksPdf.com

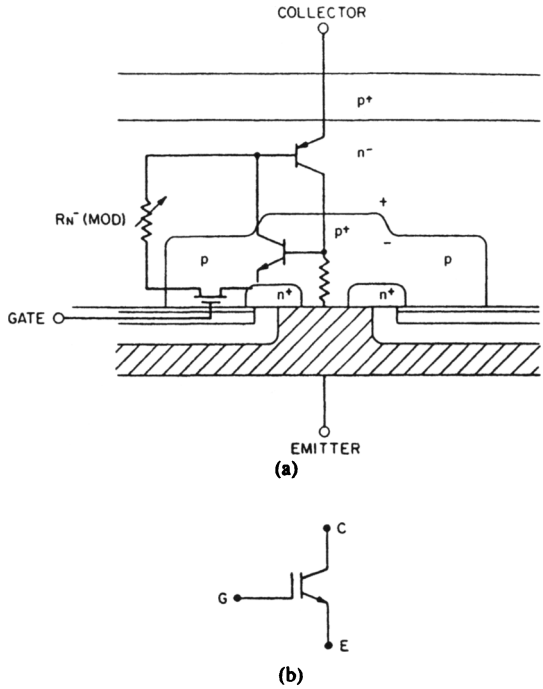


Figure 3.30 Basic structure of IGBT.

The device is normally turned off by zero gate voltage, which removes the conducting channel in the *p*-region. The "tail current" in the modern IGBT is significantly reduced by the proton-irradiated minority carrier lifetime control in the *n*-region, and by adding an extra n^+ buffer layer at the emitter. The device has a higher current density compared to the BJT and MOSFET, and needs 30% of the die size of a MOSFET. Its input capacitance is significantly less than that of the MOSFET. Also, the ratio of gate–collector capacitance to gate–emitter capacitance is lower, giving improved Miller feedback effect during *dv/dt* turn-on and turnoff. The FBSOA and RBSOA of IGBT are thermally limited by the junction temperature, and the device does not show any second-breakdown phenomena. The present IGBTs have a power-handling capability comparable to that of BJT, but can operate at higher switching frequency. Acoustic noise-free ac drives using IGBTs are available in the marketplace. The simplicity of gate drives, ease of protection, power circuit integration capability, snubberless operation, and high switching speed make IGBT converters more attractive than BJT converters.

3.5.6 SIT

The basic structure and device symbol of the SIT are shown in Fig. 3.31. A SIT is a short *n*-channel device where the gate electrodes are embedded within the drain and

www.EngineeringEBooksPdf.com

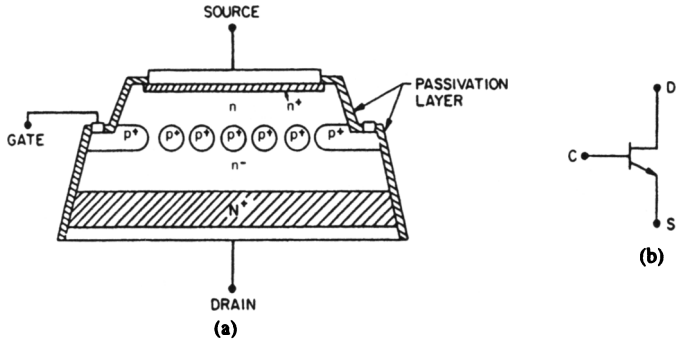


Figure 3.31 (a) Basic structure of SIT and (b) circuit symbol.

source *n*-type epitaxical layers. This device is normally on, but if the gate voltage is negative, the drain current flow will be inhibited.

The SIT is almost identical to junction FET, except that it has lower gate-source channel resistance resulting in lower drop. The reliability, noise, and radiation performance are better than those of MOSFET. A SIT is capable of faster-than-MOSFET switching frequency. SITs have been used in AM/FM transmitters, induction heating, high-voltage lower-current power supplies, linear power amplifiers, and ultrasonic generators.

3.6 THE THYRISTORS

Over 20 power semiconductor devices constructed of alternate layers of *p*- and *n*-type silicon semiconductor material are described by the generic term "thyristor." The term is derived from the words thyratron and transistor; the thyratron is a gas-filled tube that has the same characteristics as a thyristor. The thyristor is the main workhorse in today's power electronics. An important member of the thyristor group is the SCR, which combines the properties of a switch and a diode in one power device. An SCR is a four-layer (*pnpn*) semiconductor device with three terminals and three junctions, as shown in Fig. 3.32. The anode and cathode are power-level terminals, whereas the gate is a control terminal. Basically, it is a trigger-into-conduction

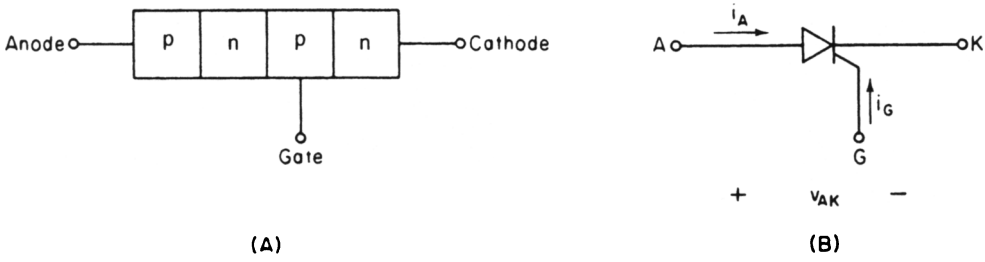


Figure 3.32 SCR: (a) construction; (b) graphic symbol.

www.EngineeringEBooksPdf.com

device that can be turned on by a positive gate current pulse, but once the device is on, a negative gate pulse cannot turn it off.

The thyristor is a two-state device, acting as a high-impedance circuit element in the off state, and presenting a low impedance in the on state. Forward bias is a term describing the application of an external voltage to the anode terminal higher than that at the cathode (i.e., for $v_{AK} > 0$). Reverse bias is the term used when $v_{AK} < 0$. A thyristor is similar to a diode when it is reverse biased, as it does not conduct and remains in the off state for $v_{AK} < 0$. The main difference between a thyristor and a diode is that when the SCR is forward biased, it conducts only if the cathode-to-gate current i_G is given a positive value for a short time. As a result of the positive gate current pulse, the device's resistance decreases to a small value close to zero and the thyristor remains in the on state until the anode current ceases to flow.

With gate current maintained at zero for some time, the thyristor returns to the off state, signified by a high anode-to-cathode resistance. A reverse-biased thyristor can be damaged by the application of a positive gate current pulse. The commutation, or turnoff, is possible by an ac line or load voltage wave, or by an auxiliary transient circuit. A thyristor has a *p-n-p-n* structure, and its triggering action can be explained by the regenerative feedback configuration of the component *pnp*- and *npn*-transistors, which show increasing current gain at higher emitter current. A thyristor can also turn on by excessive anode voltage or its rate of rise (dv/dt), high temperature, or a light shining on the junctions. The device turns on very fast and the time is limited by the rate of rise (di/dt) of anode current. The turnoff process is slow because the minority carriers are to be cleared from the inner junctions by "recovery" and "recombination" processes. The recovery is enhanced by voltage reversal across the device, but the recombination effect is influenced by the lifetime of minority carriers.

Like other power semiconductor devices, a thyristor needs a snubber to (1) protect the device from voltage transients, (2) limit anode di/dt effect, (3) reduce the off state and reapplied anode dv/dt, and (4) reduce switching loss within the device. A thyristor can tolerate a large transient fault current and can be protected by a fast fuse. Within a specified junction temperature limit (125°C), the device can carry larger current on a smaller duty cycle basis that can be further enhanced by improved cooling.

3.6.1 Thyristor Types

Thyristors have been widely used in dc and ac drives, power supplies in electrochemical processes, lighting and heating control, welding control, high-voltage dc (HVDC) conversion, static var compensation, and solid-state circuit breakers. The thyristor must be able to meet the following requirements on its performance characteristics:

1. Higher blocking voltages
2. More current carrying capability
3. Higher di/dt

www.EngineeringEBooksPdf.com

4. Higher dv/dt
5. Shorter turnoff times
6. Lower gate drive
7. Higher operating frequencies

There are many different thyristors that can meet one or more of these requirements but, as always, an improvement in one characteristic is usually only gained at the expense of another. As a result, different thyristors have been optimized for different applications. Commercial thyristors can be classified as:

(a) Phase-control thyristor type
(b) Inverter thyristor type

These can be further classified as:

- Asymmetrical thyristor (ASCR)
- RCT
- Gate-assisted turnoff thyristor
- Light-activated SCR (light-triggered thyristor)

The inverter-grade thyristors have faster turnoff time, but block voltage in the forward direction (asymmetrical blocking) only.

(c) GTO
(d) TRIAC
(e) SITH
(f) FET-controlled thyristors

Phase-Control Thyristors *Phase-control* or *Converter* thyristors generally operate at line frequency, and are turned off by natural commutation and do not have special fast-switching characteristics. Current ratings of phase-control thyristors cover the range from a few amperes to about 5500 A, and voltage ratings from 50 V to around 4000 V. The turnoff time, t_q, is of the order of 50 to 100 μs. This is most suited for low-speed switching applications and is also known as a converter thyristor.

For a 77-mm-diam phase-control thyristor, conduction voltages vary from 1.5 for 600-V rated devices, to 2.3 for 3000-V rated devices, and to 2.6 for 4000-V rated devices. Important design considerations involve ensuring low forward drop, enhancement of the dynamic dv/dt capability, and improvement of the gate sensitivity. The rate of voltage rise reapplied at the end of the turnoff interval (dv/dt effect), in conjunction with the device capacitance, produces a displacement current, which (if sufficiently large) can turn the device on. The use of emitter shorting structures that provide a shunting path for the displacement current has greatly improved dynamic dv/dt capabilities with typical dv/dt ratings of greater than 100 V/μs routinely achieved. High-temperature performance has been improved significantly by

www.EngineeringEBooksPdf.com

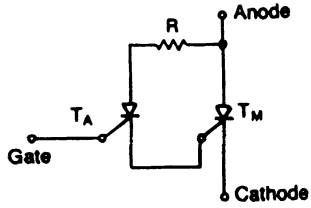


Figure 3.33 Amplifying gate concept.

emitter shorting, since the shorts will also bypass thermally generated currents around the emitter.

In order to simplify the gate-drive requirement and increase sensitivity, the use of an amplifying gate, which was originally developed for fast switching "inverter" thyristors, is widely adopted in phase-control SCR. Here an auxiliary thyristor, T_A, is gated on by a gate signal, and then the amplified output of T_A is applied as a gate signal to the main thyristor, T_M. This is shown in Fig. 3.33. The amplifying gate permits high dynamic characteristics with typical *dv/dt* of 1000 V/μs and *di/dt* of 500 A/μs and simplifies the circuit design by reducing or minimizing *di/dt* limiting inductor and *dv/dt* protection circuits.

Inverter Thyristors Inverter thyristors are also known as fast-switching thyristors. The turnoff time depends on the stored charge at the time of current reversal, the amount of charge removed during the recovery phase, the rate of recombination during the recombination phase, and the amount of charge injected during reapplication of the forward voltage. Short turnoff time is an important application consideration. Fast turnoff is important because it minimizes sizes and weight of commutating and/or reactive circuit components. Fast turnoff time, generally in the range of 5 to 50 μs, depending upon voltage rating, is the feature that distinguishes an inverter thyristor from a standard phase-control type. Maximum average current ratings of 1500 and 1200 A have been achieved with 1200 and 2500 V rated inverter thyristors, respectively. Inverter thyristors are generally used in circuits that operate from dc supplies.

In addition to fast turnoff, fast turn-on time and *di/dt* capability are usually important for inverter thyristors. Achieving this requires proper design of the gate structure aiming to design the device so that no part of the cathode has a potential greater than that of the gate electrode. This requires using a gate electrode with a large perimeter ensuring that the adjacent cathode area is as large as possible. A number of interdigitated designs have been developed to achieve this goal. Perhaps the most effective design in achieving good utilization of the device area is a structure in which both the gate and the cathode have an involute pattern. Modern devices can be designed to have *di/dt* ratings in excess of 100 A/μs. Involute gate structures are widely used in inverter thyristors with 40-mm diam and below. Inverter thyristors have high *dv/dt* of typically 1000 V/μs and *di/dt* of 1000 A/μs. The fast turnoff and high *di/dt* are very important to minimize the size and weight of commutating and/or reactive circuit components. The on-state voltage of a 2200-A 1800-V thyristor is typically 1.7 V.

www.EngineeringEBooksPdf.com

Inverter thyristors with a very limited reverse blocking capability, typically 10 V, and a very fast turnoff time between 3 and 5μs are commonly known as asymmetrical thyristors (ASCRs).

Asymmetrical Thyristors A salient characteristic of ASCRs is that they do not block significant reverse voltage. A typical reverse blocking capability is in the range of 400 to 2000 V. The ASCR is used in voltage-fed inverter circuits requiring antiparallel feedback rectifiers. This keeps the reverse voltage to less than 20 V. The ASCR needs only to block voltage in the forward direction, offering an extra degree of freedom in optimizing turnoff time, turn-on time, and forward voltage drop.

The main difference between an ASCR and the conventional thyristor is the insertion of an n buffer layer between the n base and the p^+ anode. As a result, the ASCR can be made to have faster turn-on without compromising the di/dt capability and turnoff time significantly.

Reverse Conducting Thyristor Many choppers and inverter circuits include an antiparallel diode connected across an SCR to allow reverse current flow due to inductive load and to improve the turnoff requirements of the commutation circuit. This is shown in Fig. 3.34. The diode clamps the reverse blocking voltage of the SCR to 1 or 2 V under steady-state conditions. However, under transient conditions, the reverse voltage may rise to 30 V due to induced voltage in the stray circuit inductance within the device.

The RCT represents the monolithic integration of an asymmetrical thyristor with an antiparallel rectifier. Beyond the obvious advantages of the parts count reduction, the RCT eliminates the inductively induced voltage within the thyristor–diode loop (virtually unavoidable to some extent with separate discrete components) and essentially limits the reverse voltage seen by the thyristor to only the conduction voltage of the diode.

Features such as the asymmetrical structure, lifetime control, high-density cathode shorts, and amplifying gates that are used in ASCR can be effectively implemented in RCT. However, the monolithic incorporation of the antiparallel diode presents a special problem. When the voltage across the device is reversed, the monolithic anitparallel diode becomes forward biased and floods the n-base region with minority carriers. The device will fail to achieve forward blocking unless a long interval of time is provided during which no anode-to-cathode voltage is present. To meet a high commutating dv/dt requirement, the monolithic diode is integrated into the

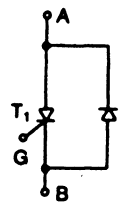


Figure 3.34 Including antiparallel diode to allow reverse current flow.

www.EngineeringEBooksPdf.com

structure at a distance from the main thyristor (a few diffusion lengths), causing it to divert the flow of injected carriers during the supply reversal phase. These methods have proven to be effective and provide a dynamic dv/dt larger than 1000 V/μs.

The range of voltage and current ratings of the RCT is similar to ASCR. The forward blocking voltage varies from 400 V to 2000 V and the current rating goes up to 500 A. The reverse blocking voltage is typically 30 to 40 V. The one drawback of the RCT is that the ratio between the thyristor and diode current carrying capabilities is fixed for a given design. The RCT is therefore, likely to serve specific "dedicated" applications, while the ASCR should find more general usage.

Gate-Assisted Turnoff Thyristor The term gate-assisted turnoff refers to the method for turning off a thyristor with the usual commutation of the anode current, but with the addition of a negative pulse applied to the gate during the time when forward anode voltage is being reapplied. Turnoff time is decreased by the application of the negative gate drive. By using gate-assisted turnoff, the normal trade-off between turnoff loss and conduction loss can be relaxed. Typically, a 50% reduction in turnoff time can be achieved for the same on-state voltage. The gate-assist reverse bias works to reduce the injection efficiency of the cathode junction to assist in breaking the regenerative thyristor action during turnoff.

GATTs are designed with interdigitated cathodes in order to achieve both fast, low-loss turn-on and effective gate-assisted turnoff. Cathode shorts not only improve dv/dt capability, as in standard thyristor design, but actually direct the current paths in such a manner that the effect of the gate-assist bias becomes more reliable and requires lower drive voltage. Overall, the GATT has extended the operating frequency of the thyristor into the 20-kHz range. A turnoff time of less than 4μs has been reported for a 1200-V, 400-A GATT.

Light-Activated Silicon-Controlled Rectifiers (Light-Triggered Thyristors) The turn-on of a thyristor by optical means is an especially attractive approach for devices that are to be used in extremely high-voltage circuits. The area of light-triggered thyristors (a.k.a. LASCRs) has witnessed many developments recently. Direct irradiation of silicon with light creates electron-hole pairs, which, under the influence of an electric field, produce a current that triggers the thyristors. A typical application area is in switches for dc transmission lines operating in the hundreds of kilovolts range, which use series connections of many devices, each of which must be triggered on command. The LASRCs are also used in static reactive power or volt-ampere reactive (VAR) compensation. Optical firing in this application is ideal for providing the electrical isolation between trigger circuits and the thyristor, which floats at a potential as high as hundreds of kilovolts above ground.

The main requirement for an optically triggered thyristor is high sensitivity while maintaining high dv/dt and di/dt capabilities. Because of the small and limited quantity of photon energy available for triggering the thyristor from practical light sources, very high gate sensitivity of the order of 100 times that of the electrically triggered device is needed. However, high gate sensitivity always leads to higher sensitivity to noise or low dv/dt capability. Typical gate regions have areas about

www.EngineeringEBooksPdf.com

10 to 100 times smaller than the gate or pilot thyristor of the corresponding electrically fired device. The main problem dealing with the dv/dt sensitivity trade-off in this manner is the reduction of the di/dt capability of the thyristor. The voltage rating of a LASCR could be as high as 4 kV at 1500 A, with light-triggering power of less than 100 mW. The typical di/dt is 250 A/μs and the dv/dt could be as high 2000 V/μs.

Gate Turn-Off Thyristor A GTO is a thyristor-like *pnpn* device that can be triggered into conduction by a small positive gate current pulse, but also has the capability of being turned off by a negative gate current pulse. This gate turnoff capability is advantageous because it provides increased flexibility in circuit applications, where it becomes possible to control power in dc circuits without the use of elaborate commutation circuitry. However, the turnoff current gain is low (typically 4 or 5). For example, a 4000-V, 3000-A device may need −750-A gate current to turn it off. A GTO is fabricated with a highly sensitive *npn* transistor component and interdigitated gate–cathode boundary, so that negative gate current completely diverts the *pnp* collector current, and thus helps turn off the device. Minority carrier lifetime control and shorted anode construction are frequently used to reduce the turnoff time.

The GTOs have the following advantages over SCRs:

1. Elimination of commutating components in forced commutation, resulting in reduction in cost, weight, and volume
2. Reduction in acoustic and electromagnetic noise due to the elimination of commutation inductors
3. Faster turn-off, permitting high switching frequencies
4. Improved efficiency of converters

In low-power applications, GTOs have the following advantages over bipolar transistors:

1. Higher blocking voltage capability
2. High ratio of peak controllable current to average current
3. High ratio of peak surge current to average current, typically 10 : 1
4. High on-state gain (anode current/gate current), typically 600
5. Pulsed gate signal of short duration

Under surge conditions, a GTO goes into deeper saturation due to regenerative action. On the other hand, a bipolar transistor tends to come out of saturation.

GTOs are available with symmetric or asymmetric voltage-blocking capabilities. A symmetric blocking device cannot have anode shorting, and is therefore somewhat slower. The turn-on behavior of a GTO is almost similar to a thyristor, but its turnoff characteristics are somewhat complex. Figure 3.35 shows the device symbol and the turnoff characteristics. During the steep fall time of the anode current, even a very small leakage inductance in the snubber will create an anode spike voltage that will

www.EngineeringEBooksPdf.com

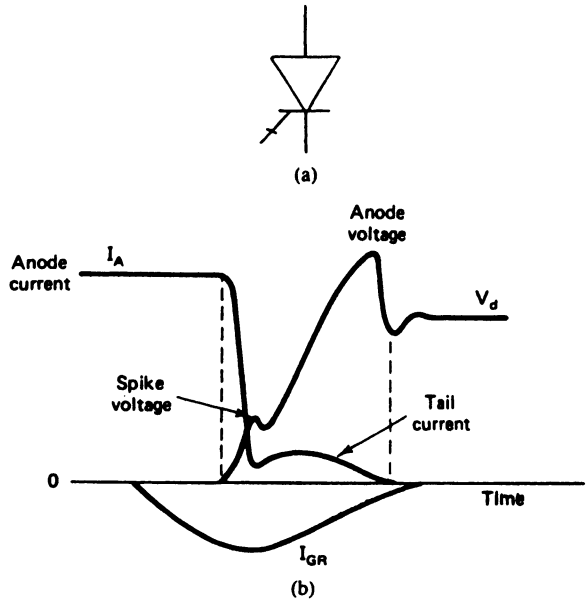


Figure 3.35 Device symbol and turnoff characteristics of GTO.

tend to cause a second breakdown failure. Besides, a large anode tail current during device voltage buildup causes excessive power dissipation. Therefore, GTO circuits should be designed with large snubbers to avoid these problems. Because of high snubber loss, the switching frequency is usually restricted to 1 or 2 kHz. Recently, regenerative snubbers have been suggested to improve the converter efficiency.

A GTO has low gain during turnoff, typically 6, and requires a relatively high negative current pulse to turn off. It has higher on-state voltage than that of SCRs. The on-state voltage of a typical 550-A, 1200-V GTO is typically 3.4 V.

GTOs are used in dc and ac machine drives, uninterruptible power supply systems (UPS), static var compensators, induction heating, and photovoltaic and fuel-cell converters from a few hundred kilowatts to several megawatts, and this boundary is continuously increasing. Additional applications lie in the higher voltage end (>1200 V) where bipolar transistors and power MOSFETs are unable to compete effectively. The GTO with the highest voltage-current ratings is a 2500-V rated device with a 1000-A turnoff capability.

Bidirectional Triode Thyristors A TRIAC has a complex multiple-junction structure, but functionally it is an integrated pair of phase-controlled thyristors connected in antiparallel. A TRIAC can conduct in both directions and is normally used in ac phase control (e.g., ac voltage controllers). It can be considered as two SCRs connected in antiparallel with a common gate connection, as shown in Fig. 3.36(a). The *v-i* characteristics are shown in Fig. 3.36(c). Since a TRIAC is a bidirectional device, its terminals cannot be designated as anode and cathode. If terminal MT_2 is positive with respect to terminal MT_1, the TRIAC can be turned on

www.EngineeringEBooksPdf.com

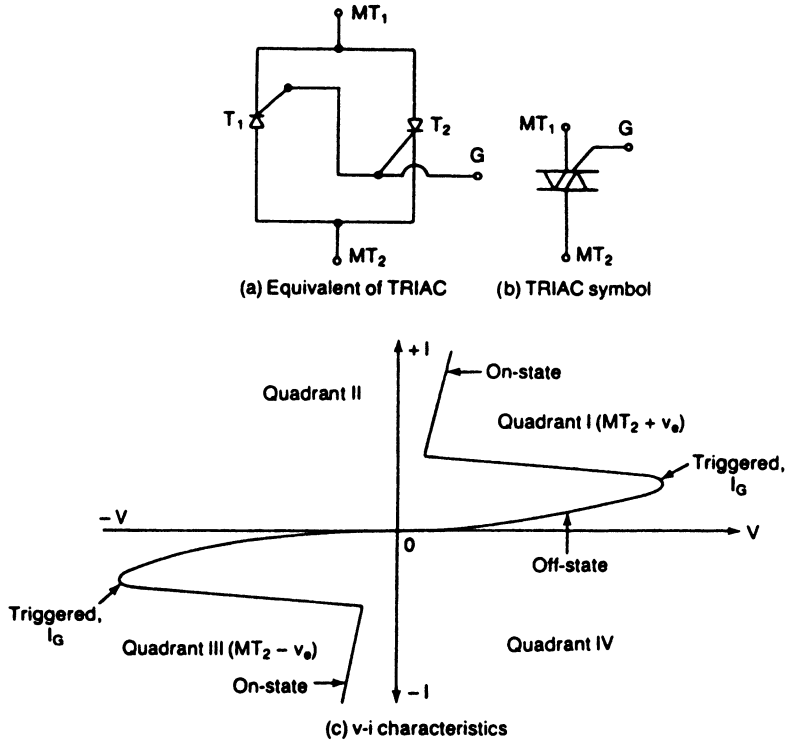


Figure 3.36 TRIAC circuit.

by applying a positive gate signal between gate G and terminal MT_1. If terminal MT_2 is negative with respect to terminal MT_1, it is turned on by applying a negative gate signal between gate G and terminal MT_1. It is not necessary to have both polarities of gate signals, and a TRIAC can be turned on with either a positive or negative gate signal. In practice, the sensitivities vary from one quadrant to another, and the TRIACs are normally operated in quadrant I (positive gate voltage and gate current) or quadrant III (negative gate voltage and gate current).

A TRIAC is more economical than a pair of thyristors in antiparallel, and its control is simpler, but the integrated construction has limitations of poor reapplied dv/dt, poor gate-current sensitivity for firing, and longer turnoff time. TRIACs are popularly used in 60-Hz phase-control resistive loads, such as heating and lighting control and in solid-state ac relays.

Static Induction Thyristors A SITH, or SI-thyristor, is a self-controlled GTO-like on–off device. The basic structure and device symbol of a SITH are shown in Fig. 3.37. A SITH is normally turned on by applying a positive gate voltage like normal thyristors, and is turned off by application of negative voltage to its gate. It is a normally on device, with the n-region saturated with a minority carrier. If the gate is reverse biased with respect to the cathode, a depletion layer will block the anode

www.EngineeringEBooksPdf.com

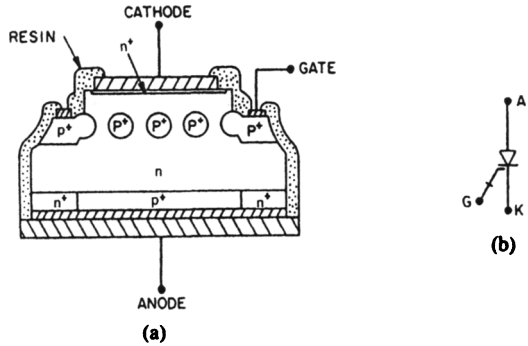


Figure 3.37 Structure and a symbol of SITH.

current flow. The device does not have reverse-blocking capability, due to the emitter shorting that is needed for high-speed operation. The characteristics of SITH are similar to those of a MOSFET, while its turnoff behavior is similar to that of GTO, that is, the negative gate current is large, and the anode circuit shows a tail current. The general comparison with GTO can be summarized as follows:

- Unlike GTO, it is a normally on device
- The conduction drop is slightly higher
- The turnoff current gain is lower (below 3) compared to 4 to 5 for GTO
- Both devices show a long tail current
- The switching frequency is higher
- The *dv/dt* and *di/dt* ratings are higher
- The SOA is improved

SITH has low on-state resistance or voltage drop, and it can be made with higher voltage and current ratings. SITH has fast switching speeds and high *dv/dt* and *di/dt* capabilities. The switching time is of the order of 1 to 6 μs. The voltage rating can go up to 2500 V and the current rating is limited to 500 A. This device is extremely process sensitive, and small perturbations in the manufacturing process would produce major changes in the device characteristics.

FET-Controlled Thyristors A FET-controlled thyristors (FET-CTH) device combines a MOSFET and a thyristor in parallel, as shown in Fig. 3.38. If a sufficient voltage is applied to the gate of the MOSFET, typically 3 V, a triggering current for the thyristor is generated internally. It has high switching speed, high *di/dt*, and high *dv/dt*.

This device can be turned on like conventional thyristors, but it cannot be turned off by gate control. This would find applications where optical firing is to be used for providing electrical isolation between the input or control signal and the switching device of the power converter.

www.EngineeringEBooksPdf.com

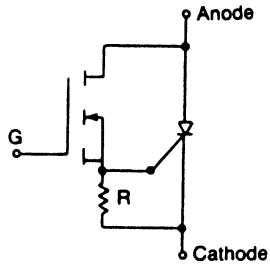


Figure 3.38 FET-CTH.

Thyristors are characterized by certain performance parameters, and the manufacturers specify these parameters in the data sheet for thyristors. Although there are various types of thyristors, the parameters are similar, except for the gate characteristics. The characteristic parameters of a diode are applicable to thyristors, except for the gate characteristics.

3.6.2 SCR Performance Characteristics

The performance characteristics of the SCR are described in terms of the plot of the anode current i_A versus the anode-to-cathode voltage v_{AK}. First-quadrant performance in the i_A–v_{AK} plane corresponds to forward bias. The effect of the magnitude of v_{AK} on the state of the SCR with zero gate current is examined first.

As discussed earlier, with zero gate current the SCR does not conduct for low values of v_{AK}. As the voltage across the SCR is increased, conduction occurs at a voltage level known as the forward breakover voltage, V_{FBO}. At that point the SCR conducts and the voltage between its terminals drops. The anode current increases to a value limited only by the impedance of the external load circuit. The i_A–v_{AK} characteristic for an SCR without gate current is shown in Fig. 3.39. The SCR is not designed for turn-on by forward breakover voltage.

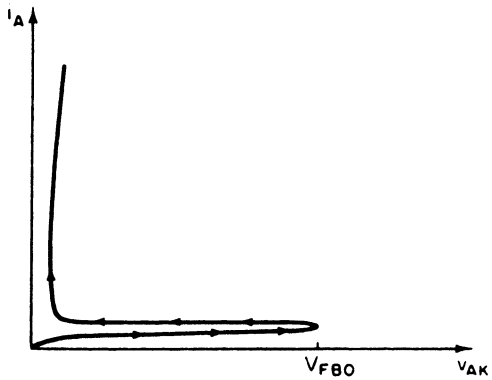


Figure 3.39 SCR performance characteristic with zero gate current.

www.EngineeringEBooksPdf.com

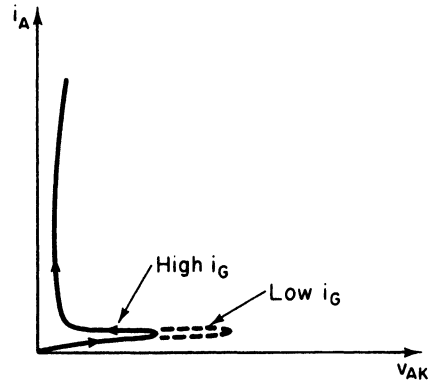


Figure 3.40 SCR performance characteristic with applied gate current.

With an applied gate current, conduction does not start unless the anode-to-cathode voltage is at a certain level, as indicated in Fig. 3.40. The higher the value of the gate current, the lower the anode-to-cathode voltage required for turn-on. The voltage scale in the diagram is much amplified to show the phenomenon clearly. When the SCR is subject to negative v_{AK}, it is said to be reverse biased. In this case leakage current is small for negative voltages up to V_{RB}, the repetitive peak reverse voltage. At V_{RB} the SCR switches to the on-state with negative anode current. Operating in the reverse mode is in the third quadrant of the i_A–v_{AK} plane, but should be avoided. Figure 3.41 shows the i_A–v_{AK} characteristic for a reverse-blocking thyristor. Note that in the figure V_{RBT}, the nonrepetitive peak reverse voltage is slightly lower than V_{RB}.

3.6.3 The SCR: Model, Turn-On, and Dynamic Characteristics

The present section offers a brief discussion of the pertinent characteristics and ratings of the SCR. A first step is to consider a circuit model for this device.

Two-Transistor Model The four-layer (*pnpn*) structure of Fig. 3.42(a) can be represented as two complementary three-layer structures, as shown in Fig. 3.42(b). The first structure is modeled as a *pnp*-transistor T_1, and the second is an *npn*-transistor T_2, as shown n Fig. 3.42(c). The base of T_1 is the collector of T_2, whereas

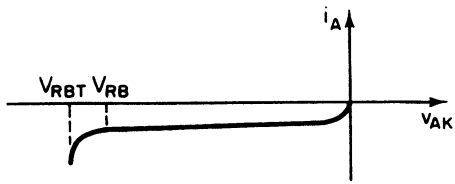


Figure 3.41 SCR characteristic in the reverse-blocking mode.

www.EngineeringEBooksPdf.com

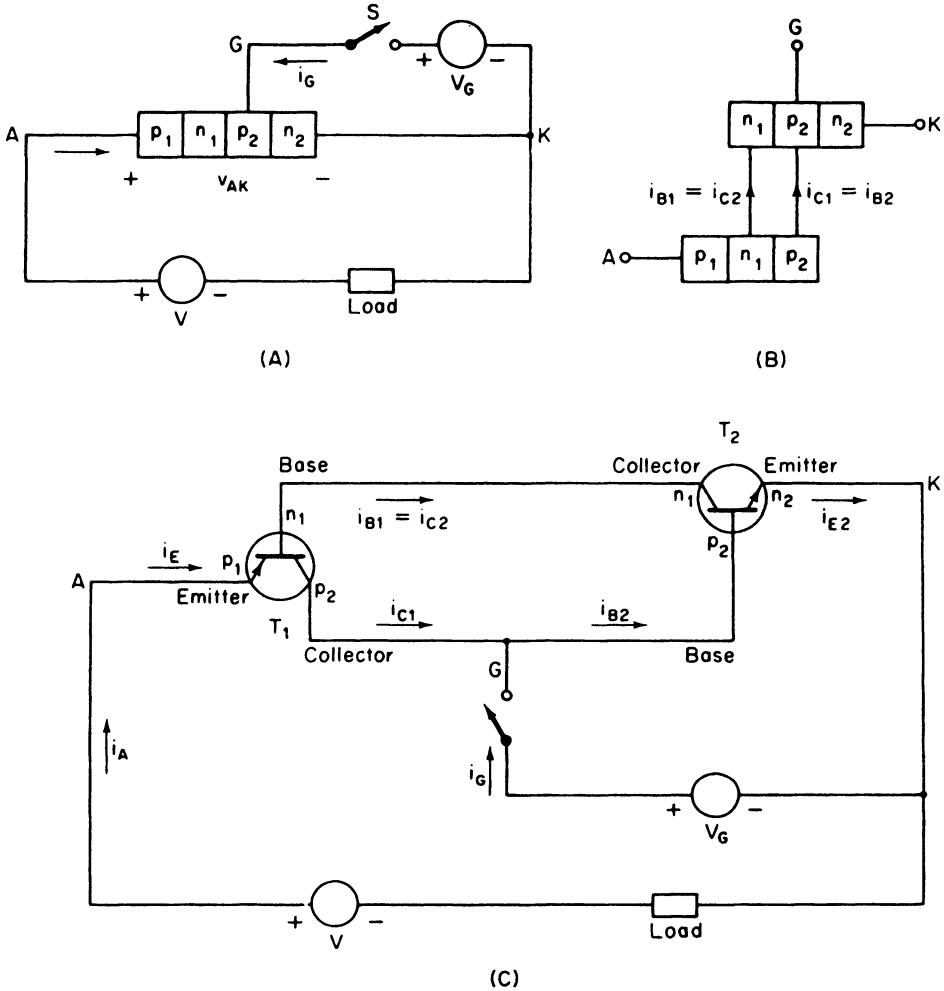


Figure 3.42 Two-transistor model of SCR: (a) original structure; (b) two-structure model; (c) equivalent circuit.

the collector of T_1 is the base of T_2. A gate voltage source V_G is connected through a switch to the gate terminal. The circuit of Fig. 3.42(c) is the two-transistor model of the SCR.

Assuming that the gate current is zero $i_G = 0$, then

$$i_A = i_{E_1} = i_{E_2} \tag{3.39}$$

From the circuit, we have

$$i_{B_1} = i_{C_2} \tag{3.40}$$

$$i_{C_1} = i_{B_2} \tag{3.41}$$

www.EngineeringEBooksPdf.com

From Kirchhoff's current law, neglecting leakage,

$$i_E = i_B + i_C$$

The current transfer ratio β of the transistor is defined by

$$\beta = \frac{i_C}{i_B}$$

As a result we conclude by eliminating i_B that

$$i_C = \frac{\beta}{1+\beta} i_E$$

The preceding relation applies for transistors 1 and 2 in the model of the thyristor. Thus we have

$$i_{C_1} = \frac{\beta_1}{1+\beta_1} i_{E_1} \tag{3.42}$$

$$i_{C_2} = \frac{\beta_2}{1+\beta_2} i_{E_2} \tag{3.43}$$

The anode current i_A is equal to the emitter current i_{E_1}. This is the sum of the base current i_{B_1} and collector current i_{C_1}, as well as the leakage current i_{C_0} crossing the common junction, n_1–p_2:

$$i_A = i_{C_1} + i_{C_2} + i_{C_0}$$

Substituting for i_{C_1} and i_{C_2} in terms of i_{E_1} and i_{E_2}, we obtain

$$i_A = \frac{\beta_1}{1+\beta_1} i_{E_1} + \frac{\beta_2}{1+\beta_2} i_{E_2} + i_{C_0}$$

Note that since $i_A = i_{E_1} = i_{E_2}$, we write

$$i_A \left(1 - \frac{\beta_1}{1+\beta_1} - \frac{\beta_2}{1+\beta_2}\right) = i_{C_0}$$

A few simplification steps result in

$$i_A = \frac{(1+\beta_1)(1+\beta_2)}{1-\beta_1\beta_2} i_{C_0} \tag{3.44}$$

The leakage current i_{C_0} is sufficiently small under normal conditions so that it can be neglected. The anode current is very small for $\beta_1\beta_2 \ll 1$, and this corresponds to the

www.EngineeringEBooksPdf.com

off state (or forward blocking). The product $\beta_1\beta_2$ can approach unity under certain conditions corresponding to the turn-on state, where the anode current will be large. SCR turn-on can be due to a number of causes, as discussed next.

SCR Turn-On The turning on of the SCR is associated with an increase in the emitter current. Factors that cause an increase in emitter current are as follows.

1. **Injection of Gate Current** The closing of the switch connecting the gate voltage source to the SCR for a short duration allows the flow of current i_G, which increases the base current i_{B_2}. This results in an increase in i_{C_2} and β_2, and thus i_{C_1} and β_1 increase. The product $\beta_1\beta_2$ is thus increased to close to unity. As a consequence, the anode current i_A is increased to an amount that is limited only by the impedance of the external load circuit.

   Injection of a short gate-current pulse is the means normally used for SCR turn-on. The effect of the magnitude of grid current i_G on conduction is discussed together with the SCR characteristics.
2. **Optical Turn-On** A beam of light directed at an unshielded junction of the SCR can produce sufficient energy to initiate turn-on. In a light-activated SCR this is the normal means for device turn-on.
3. **Thermal Turn-On** An increase in the SCR's temperature results in an increase in the leakage current i_{C_0}. Collector currents and hence the product $\beta_1\beta_2$ increase and turn-on is initiated.
4. **Breakover Voltage Turn-On** With an increase in the forward anode–cathode voltage above a certain value, V_{FB_0}, the forward breakover voltage-causes a sufficient increase in the product $\beta_1\beta_2$, and hence causes SCR turn-on without an applied gate current.
5. **Rate of Change of Voltage** The n_1-p_2 junction acts as a capacitor, and thus a large rate of change of voltage can produce sufficient charging current to initiate SCR turn-on.
6. **Radiation** When permitted to strike an SCR, radiation such as X rays and gamma rays cause a thyristor turn-on.

The initiation of an SCR turn-on results in a dynamic process that involves a number of important parameters which are discussed next.

SCR Dynamic Characteristics At the instant of gate-current application, there is no significant increase in anode current. This lasts for an interval of time referred to as the *delay time* t_d. This is defined either in terms of anode current rise or in terms of anode-to-cathode voltage drop. The time elapsed from initiation of gate current until the anode current reaches 10% of its final value is defined as the delay time, t_d. The corresponding definition in terms of anode-to-cathode voltage measures, t_d is the time elapsed between the instant of gate-current initiation to the instant at which the value of v_{AK} is 90% of V_{FB}, the repetitive forward-blocking voltage. Here V_{FB} is defined as the maximum instantaneous value of forward voltage that occurs across the thyristor, including all repetitive voltages.

www.EngineeringEBooksPdf.com

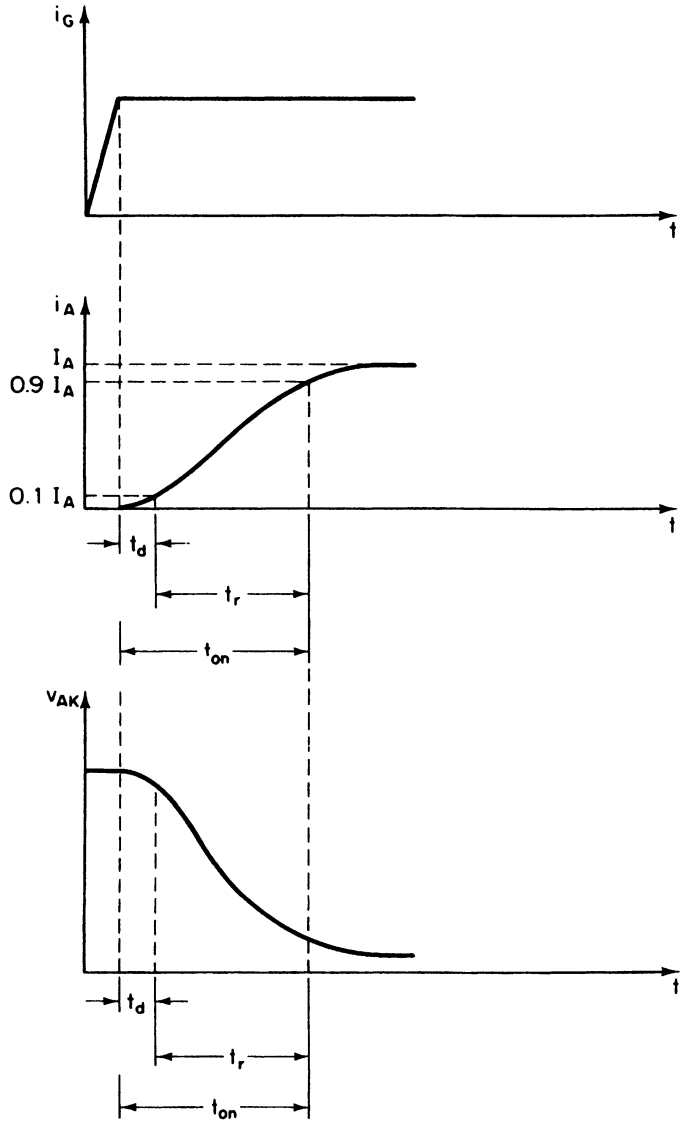


Figure 3.43 Turn-on dynamics.

The *rise time* t_r is the time interval between the instant at which v_{AK} is 90% to the instant when it is 10% of its final value. The turn-on time t_{on} is equal to $(t_d + t_r)$. The time variations of v_{AK}, i_A, and i_G are shown in Fig. 3.43, where definitions of t_d, t_r, and t_{on} are clearly marked.

At the time of application of a gate-current pulse to the SCR, conduction commences in a relatively small area in the neighborhood of the gate. In many designs, the area of conduction increases at the rate of about 1 cm each 10^{-4} s. The rate of increase of anode current with respect to time in circuits with relatively low

www.EngineeringEBooksPdf.com

inductance to resistance ratio can be higher than the rate of spread of the conduction area. As a result, high power density areas develop that are associated with local hot spots within the device. The hot spots can lead to permanent damage to the SCR.

Rates of change of currents in an SCR are important. The term *rate of change of anode currents* refers in practice to the critical rate of rise of the on-state current. The maximum allowable rate of increase of anode current is commonly referred to as *di/dt*. To avoid *di/dt* failures two obvious solutions are available. In the first, a high value of gate current, of the order of three to five times I_{gt}, is applied. The second is directed at improved geometric designs of the cathode to ensure a large initial conduction area.

3.6.4 The SCR: Ratings and Parameters

A number of additional specification parameters and ratings of the SCR are discussed. One of the most important aspects is that corresponding to heat dissipation in an SCR.

Junction Temperature and Power Dissipation The operating junction temperature range in thyristor devices depends on the type and design of the unit. The lower temperature limit corresponds to thermal stress due to the difference in the thermal expansion characteristics of materials used in fabricating the device. The upper operating temperature limit is due to the dependence of the breakdown voltage and turnoff time on temperature. A storage temperature that is related to the stability of the junction coating compounds is also specified.

The rated maximum operating junction temperature is used to determine the steady state, transient, and recurrent overload capability of the device for a given heatsink system and maximum ambient temperature. Conversely, for a given loading, the required heatsink system can be determined using the thermal-impedance approach. It should be noted that the device may actually operate beyond the specified maximum operating junction temperature for transient periods and still be applied within its rating.

The forward-current rating is a function of the maximum junction temperature, total device losses, and its thermal impedance. For a given junction temperature the on-state forward voltage drop V_F varies with the peak forward current i_F, as shown in the typical characteristic shown in Fig. 3.44. The device's power dissipation versus average forward current $I_{F(AV)}$ for the same device for different conduction angles is shown in Fig. 3.45. Points on the characteristic are obtained from the given V_F-i_F characteristic and the assumed anode current waveform. Power is simply the product of current and voltage. The dependence of power dissipation on waveform is verified by comparing Figs. 3.45 and 3.46, with the latter showing the characteristic for a square waveform.

The power dissipation in the junction region is due to a number of components. These are turn-on, switching, conduction, turnoff, blocking, and triggering. For the normal duty cycle in the range 50 to 400 Hz and low (*di/dt*) current waveforms, on-state conduction losses are major components of junction heating.

www.EngineeringEBooksPdf.com

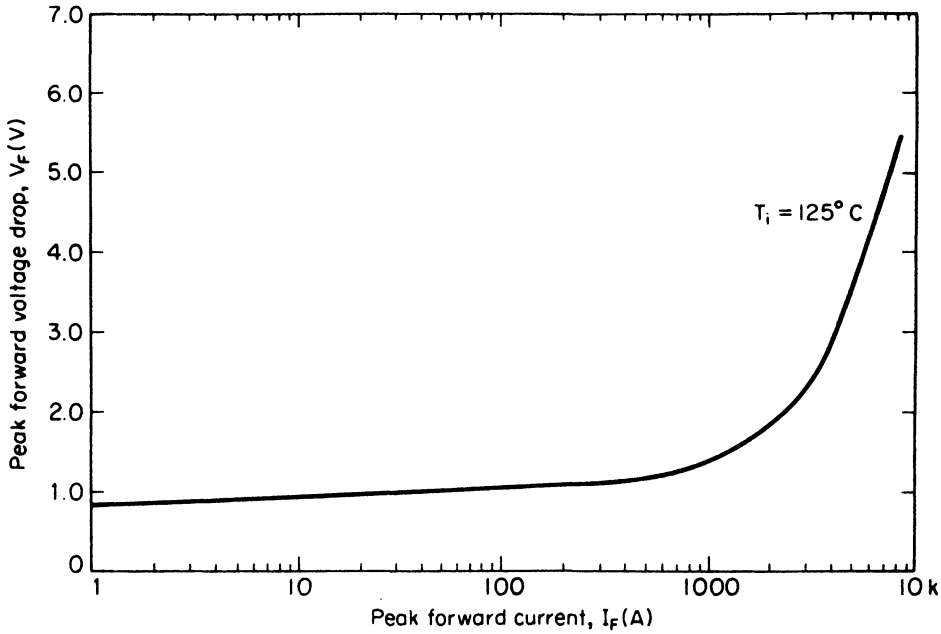


Figure 3.44 Forward voltage versus forward current characteristic for Westinghouse Type 282 SCR.

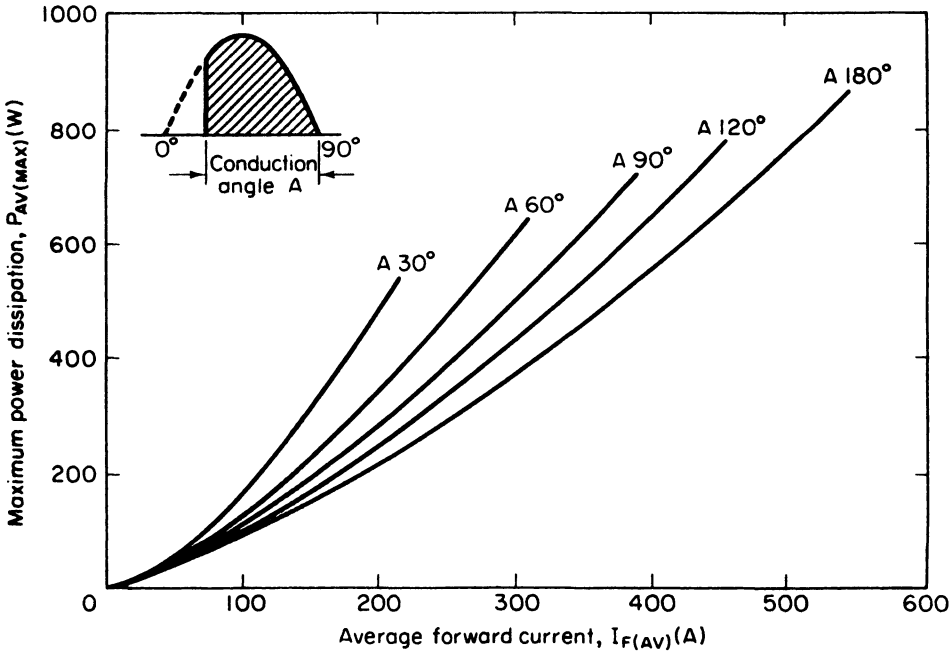


Figure 3.45 Power dissipation versus forward current, half-wave sinusoid.

www.EngineeringEBooksPdf.com

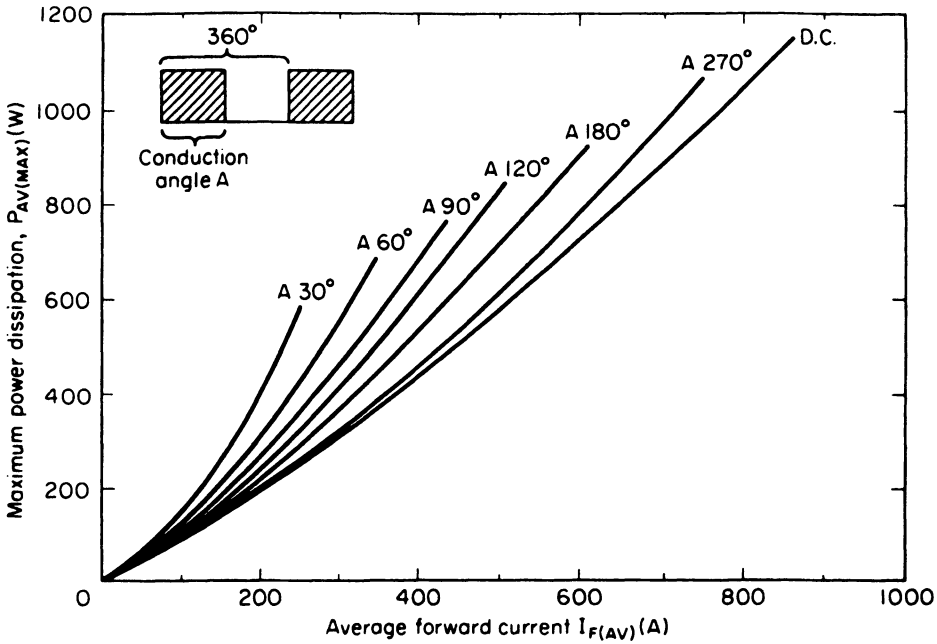


Figure 3.46 Power dissipation versus forward current, rectangular wave.

Recurrent and Nonrecurrent SCR Current Ratings A major requirement in SCR applications is that the junction temperature must not exceed its maximum allowed value. When this requirement is met, the device can be applied on a recurrent (repetitive) basis for normal operating conditions. The design of the circuit is thus based on the available recurrent SCR current ratings.

The SCR may be subject to some abnormal overload conditions, such as surges during its operating life. Protective circuits are designed to intervene when this occurs. The SCR is provided with an overcurrent capability allowing for coordination with protective circuits. This capability is due to a second group of SCR current ratings, which are termed *nonrecurrent current ratings*, and allow the maximum allowable junction temperature to be exceeded for a brief time. Nonrecurrent ratings are understood to apply to load conditions that will not occur for more than a limited number of times in the life of the SCR. The Joint-Electron Device Engineering Council (JEDEC) defines this number to be not less than 100. Nonrecurrent current ratings apply only when the overload is not repeated before the junction temperature has returned to its maximum rated value or less. The length of the interval between surges does not change the rating.

Recurrent Current Ratings There are two ratings for the SCR in terms of current for normal recurrent operation. The first is based on the average forward current, while the second is in terms of rms current rating.

www.EngineeringEBooksPdf.com

1. **Average Current Rating (recurrent)** Manufacturer-supplied data provide the average current ratings for a given SCR corresponding to the applied recurrent waveform and conduction angles. The variation of maximum case temperature with average anode current provides guidelines for the circuit designer in choosing the required system configuration.
2. **RMS Current Rating (recurrent)** Waveforms encountered in SCR applications are characterized by form factors larger than 1 (form factor = rms value/average value). The rms value of the current exceeds the average value considerably. For a fixed average current, the rms value of the current increases as the delay angle increases (conduction angle decrease). It should be recalled that heat generation is a function of the rms value of the current. Thus the rating curves are cut off at a value of average current corresponding to the limiting value of rms current for the circuit.

Nonrecurrent Current Ratings We stated earlier that nonrecurrent ratings are intended for abnormal conditions that may take place during the operation of the SCR. Presently, we discuss two nonrecurrent current ratings commonly used.

1. **I^2t Rating** During overloads, line faults, and short circuits, the SCR must withstand conditions leading to high junction temperatures. The I^2t rating is used for protective circuit coordination and is intended for emergency operation for less than one half-cycle. The current I is the rms value of the fault current, and t is the time in seconds.
2. **Surge Current Rating** The surge current rating is based on peak current values and 180-degree conduction, and defines a particular capability used under fault conditions. This is a nonrepetitive rating, and the SCR is designed to withstand a maximum of 100 surges during its lifetime. The surge current rating is commonly denoted by I_{FM}.

Critical Rate of Rise of Forward Voltage The application of a fast-rising forward-voltage wavefront results in the flow of current through the junctions. The steeper the wavefront, the higher the likelihood for the device to turn on below its forward-voltage rating. The resulting current is due to the charging effect and is a function of the junction temperature, the blocking voltage, and the rate dv/dt. Causes of high rate of rise of forward voltage include ac switching transients and surges and high-frequency inverter and cycloconverter applications.

The standard dv/dt definition relates to either of the waveforms shown in Fig. 3.47. For the exponential wave, the slope dv/dt is obtained for the intersection at $t = \tau$, where τ is the time constant of the exponential waveform. Note that

$$\tau = \frac{0.632V_{FB}}{dv/dt}$$

The static dv/dt capability for a typical SCR is shown in Fig. 3.48. The characteristic can be seen to depend on the bias voltage and the magnitude of voltage step. It should be noted that reverse biasing increases the dv/dt withstanding capability.

www.EngineeringEBooksPdf.com

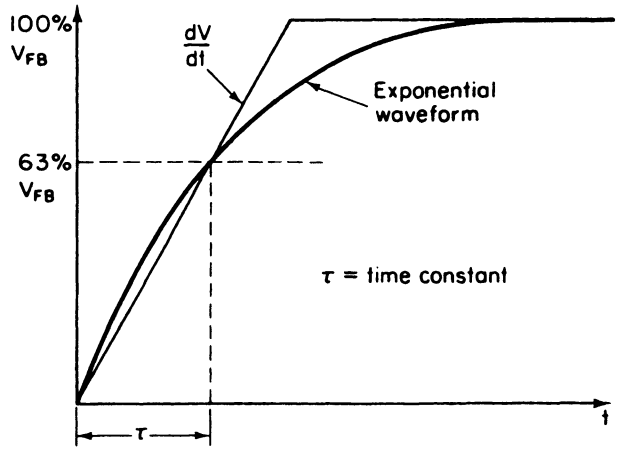


Figure 3.47 Standard waveforms for dv/dt definition.

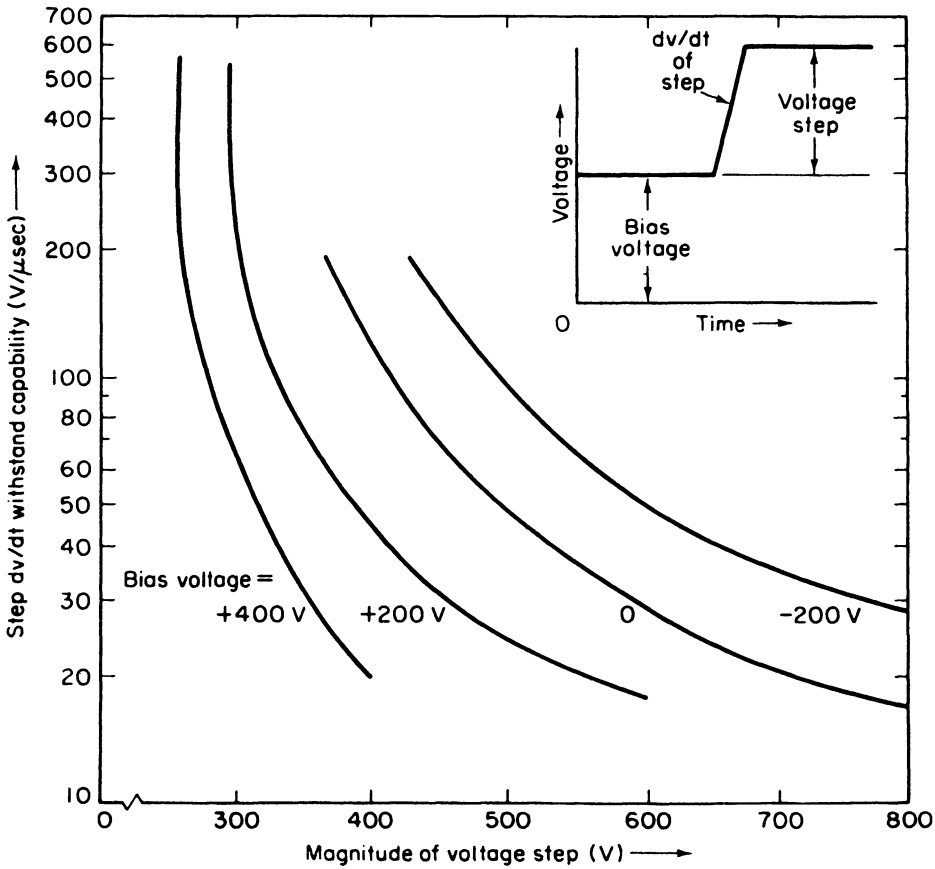


Figure 3.48 Typical dv/dt withstanding capability of SCR.

www.EngineeringEBooksPdf.com

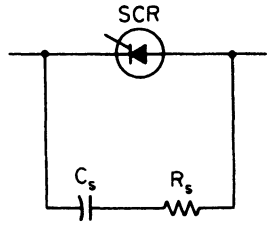


Figure 3.49 *dv/dt* suppression, *RC* snubber network.

An inductor may be used to reduce the value of *dv/dt* at switching. This is impractical, however, and the use of snubber circuits is recommended. In its simplest form, a snubber is a series combination of a capacitor C_s and a resistance R_s connected across the SCR, as shown in Fig. 3.49. During the negative half-cycle of the source voltage, the capacitor C_s will be charged in a positive direction up to the instant of SCR turn-on. At that instant there will be a step increase in current as a result of discharging C_s, and the resulting *di/dt* will be high but limited by R_s.

3.6.5 The SCR: Turnoff and Commutation

When the SCR is conducting, each of the three junctions is forward biased and the base regions are saturated. Conduction is maintained without a gate signal. To achieve turnoff, the load current must be diverted or brought to zero for a specific length of time to allow recombination of charge carriers. Once recombination takes place, the device regains its forward-blocking capability. Normally, the anode-to-cathode voltage is reduced until the holding current can no longer be supported to achieve turnoff.

The process of turnoff is known as *commutation*. In ac applications the required conditions for turnoff can be satisfied. For dc applications, it is necessary to introduce a reverse bias by external means to reduce the anode current. The process is then called *forced commutation*.

The time interval, t_{off}, that must elapse after the forward current has ceased before forward voltage can again be applied without turn-on is called *turnoff time*. Typical turnoff times are specified by the manufacturer. To measure the required interval, the device is operated with current and voltage waveforms, as shown in Fig. 3.50. The interval between t_2 and t_7 is then decreased until the SCR can just support reapplied forward voltage.

The waveforms of Fig. 3.50 correspond to the conventional rating procedure where a current pulse of sufficient width is applied to ensure that the total cathode region is in conduction prior to the turnoff cycle. A second procedure is termed *concurrent testing* and involves a narrow current pulse, as shown in Fig. 3.51. In this case forward losses enter into the rating.

In Fig. 3.50 the anode current is I_F in the interval t_0 to t_1 and the corresponding anode voltage is V_F. At the time instant t_1, the anode current is reduced at the rate di_R/dt, becomes zero at t_2, and continues decreasing up to t_3, where it attains its peak value I_R, called *reverse recovery current*. The anode voltage is positive up to t_3. At t_3,

www.EngineeringEBooksPdf.com

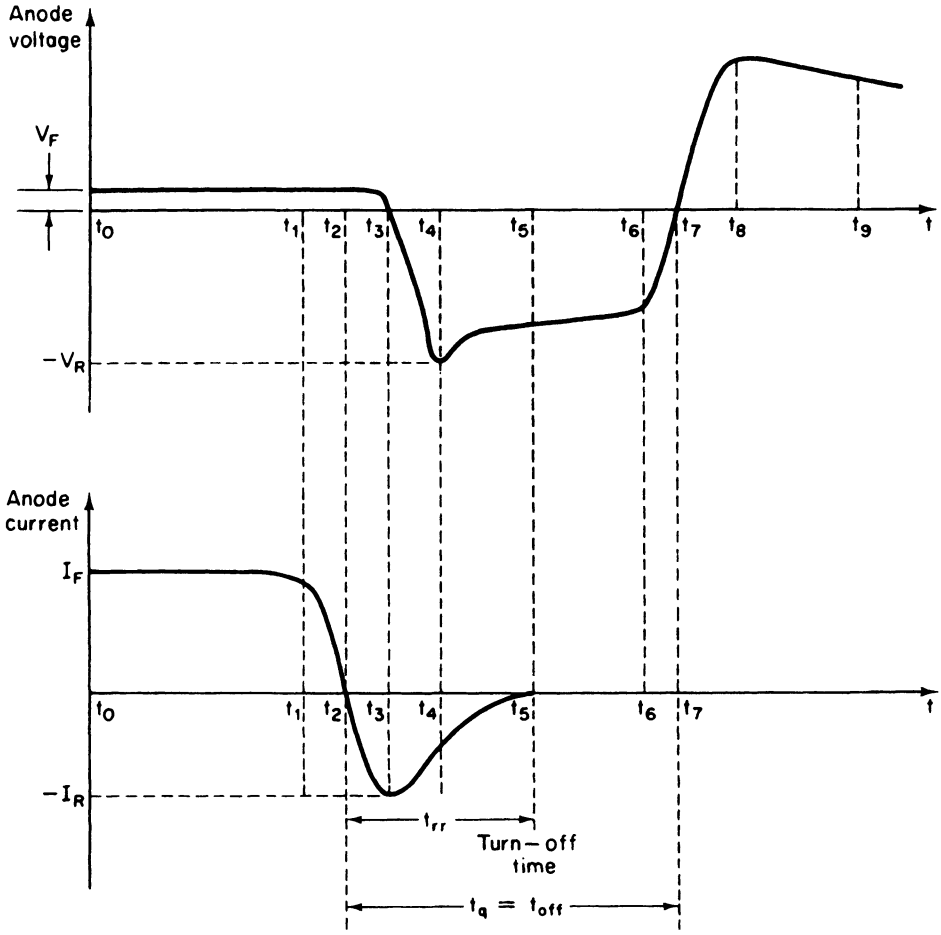


Figure 3.50 Voltage and current waveforms for conventional rating turnoff.

the anode voltage becomes reverse biased and decreases to a peak ($-V_R$) at t_4. Between t_3 and t_5 the negative anode current is decreasing to zero at t_5. The interval t_2 to t_5 is called the *reverse recovery time*, t_{rr}. The reappearance of a forward voltage at t_7 should not cause a turn-on without a gate signal.

The turnoff time interval t_{off} is not a constant for a given device. The following factors affect the length t_{off}:

1. **Junction Temperature** The required turnoff time increases as the junction temperature increases.
2. **Forward-Current Magnitude** The value of t_{off} increases with an increase in the magnitude of the peak forward current.
3. **Rate of Decay of Forward Current (t_1 *to* t_2)** An increase in di_R/dt increases t_{off}.

www.EngineeringEBooksPdf.com

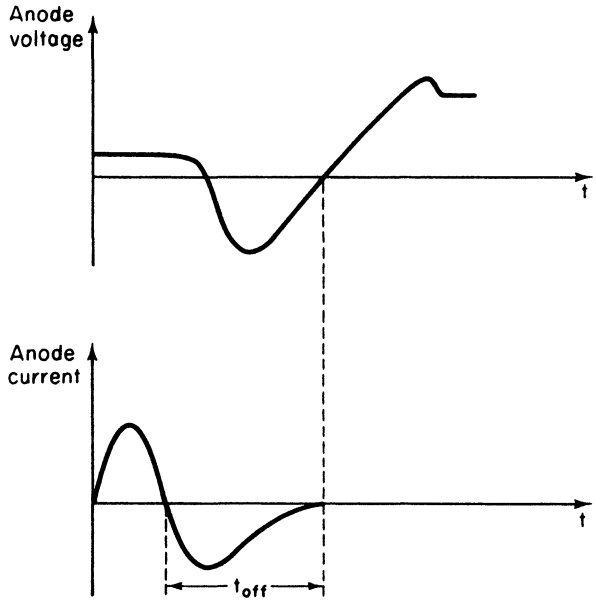


Figure 3.51 Voltage and current waveforms for concurrent rating turnoff.

4. **Peak Reverse Current (t_3)** A decrease in I_R increases t_{off}.
5. **Reverse Voltage (t_4 *to* t_6)** A decrease in this parameter will increase t_{off}.
6. An increase in the rate of reapplication of forward blocking voltage will increase t_{off}.
7. An increase in forward blocking voltage will increase t_{off}.

Reapplied dv/dt The specification of the reapplied *dv/dt* is part of the SCR's turnoff specification. It is defined as the maximum allowable rate of reapplication of off-state blocking voltage, while the device is regaining its rated off-state blocking voltage, following the device's turnoff time, t_q, under the given circuit and temperature conditions.

There are many methods for producing commutation in power electronic systems. The chief methods are discussed briefly next.

Method A: Line Commutation This commutation method applies to circuits with an alternating voltage source in series with the SCR and load, such as that shown in Fig. 3.52. Load current will flow in the circuit during the positive half-cycle. The current in the circuit is zero at an instant, following which the forward voltage on the SCR will be negative. With zero gate signal, the thyristor will turn off, provided the duration of the half-cycle is longer than the turn-off time of the device. Figure 3.53 shows the waveforms involved.

Method B: Series Capacitor Commutation The simplest form of this commutation method involves inserting a capacitor *C* in series with the inductive load (*RL*), as

www.EngineeringEBooksPdf.com

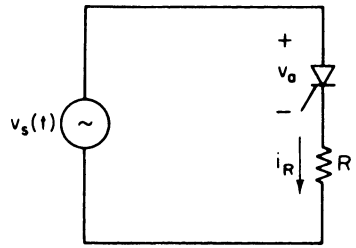


Figure 3.52 Circuit to illustrate ac line commutation.

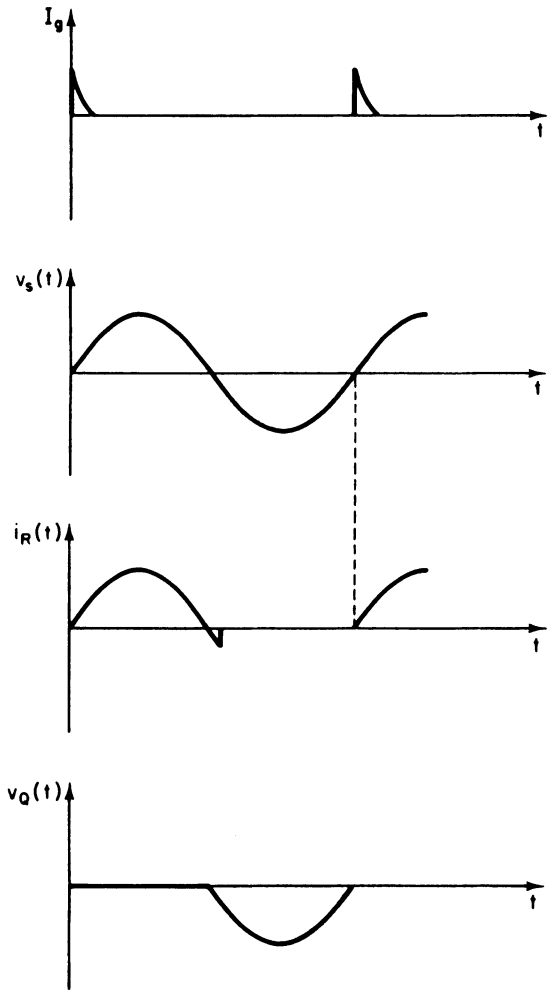


Figure 3.53 Waveforms for ac line commutation.

www.EngineeringEBooksPdf.com

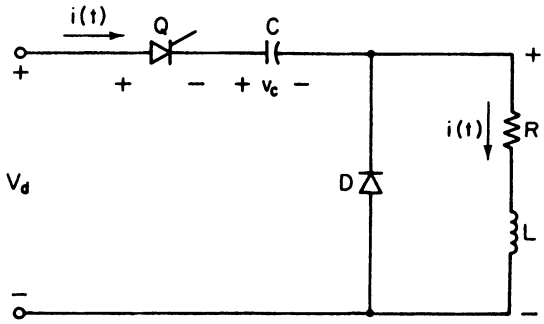


Figure 3.54 Basic circuit for series capacitor series commutation.

shown in Fig. 3.54. The freewheeling diode D is used to provide a means for dissipating the energy stored in L at the time of switching.

Application of Kirchhoff's voltage law around the loop results in

$$L\frac{di}{dt} + \frac{1}{C}\int_0^t i\,dt + v_c(0) + Ri = V_d \tag{3.45}$$

Note that the thyristor is assumed to conduct, and thus $v_{AK} = 0$. The initial voltage across the capacitor is denoted by $v_c(0)$. The preceding equation is differentiated to yield

$$\frac{d^2i}{dt^2} + \frac{R}{L}\frac{di}{dt} + \frac{l}{LC}i = 0$$

In dealing with second-order systems such as the present circuit, it is customary to formulate the solution in terms of a canonical (standard) form by defining the resonant frequency ω_n and damping ratio ξ by

$$\omega_n = \frac{1}{\sqrt{LC}} \tag{3.46}$$

$$2\xi\omega_n = \frac{R}{L} \tag{3.47}$$

$$\sigma = \xi\,\omega_n \tag{3.48}$$

$$\omega_d = \omega_n\sqrt{1 - \xi^2} \tag{3.49}$$

The radian frequency ω_d is termed the damped natural frequency or the ringing radian frequency. It is assumed here that $\xi < 1$, or that the circuit is underdamped. As a result, the current $i(t)$ is given by

$$i(t) = e^{-\sigma t}(A\,e^{j\omega_d t} + Be^{-j\omega_d t})$$

www.EngineeringEBooksPdf.com

Using Euler's equation, we obtain

$$i(t) = e^{-\sigma t}[(A + B)\cos\omega_d t + j(A - B)\sin\omega_d t]$$

The constants A and B are determined form the initial conditions $i(0) = 0$ and

$$v_L(0) + v_c(0) = V_d$$

As a result, we get

$$i(t) = \frac{V_d - v_c(0)}{\omega_d L} e^{-\sigma t}\sin\omega_d t \tag{3.50}$$

The current in the circuit is a decaying sinusoid, as shown in Fig. 3.55.

The capacitor voltage $v_c(t)$ can be obtained as

$$v_c(t) = V_d - \frac{V_d - v_c(0)}{\omega_d} e^{-\sigma t}(\sigma\sin\omega_d t + \omega_d\cos\omega_d t) \tag{3.51}$$

The current $i(t)$ in the circuit becomes zero at the instant t_1 given by

$$\omega_d t_1 = \pi \tag{3.52}$$

At that instant the thyristor is turned off. The voltage across the capacitor at that instant is given by

$$v_c(t_1) = V_d + [V_d - v_c(0)]e^{-\sigma\pi/\omega_d}$$

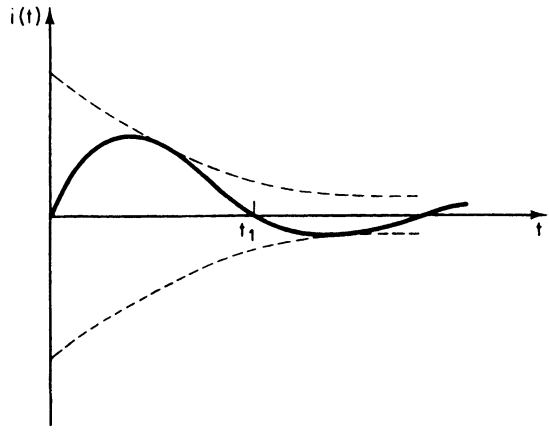


Figure 3.55 Current in *RLC* circuit.

www.EngineeringEBooksPdf.com

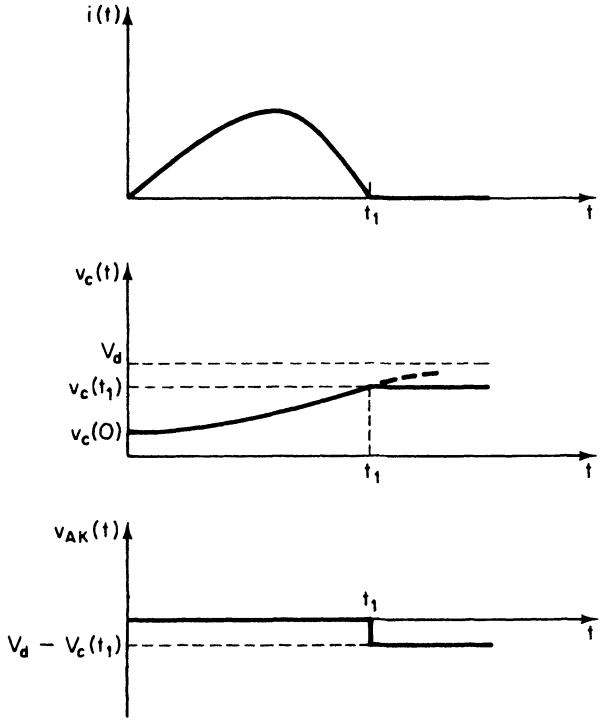


Figure 3.56 Current and voltage waveforms for circuit of Fig. 3.54.

Since the current $i(t_1)$ is zero, and in accordance with Kirchhoff's voltage law, the voltage across the thyristor is obtained as

$$\begin{aligned} v_{AK}(t_1) &= V_d - v_c(t_1) \\ &= [v_c(0) - V_d]e^{-\sigma\pi/\omega_d} \end{aligned} \tag{3.53}$$

Note that since $v_c(0) < V_d$, the voltage v_{AK} is negative. The variation of $i(t)$, $v_c(t)$, and $v_{AK}(t)$ with time for this circuit is shown in Fig. 3.56.

It is thus possible to turn off the thyristor as the current goes through zero in a finite time. The negative value of v_{AK} following turnoff indicates that some method of discharging the capacitor must be used before the thyristor can conduct again.

Example 3.2 For the circuit of Fig. 3.57, assume that $V = 100$ V and that the load parameters are

$$R = 4\,\Omega \qquad L = 20\,\text{mH}$$

Assume that the load is commutated at $t_1 = 0.01$ s using series capacitor commutation. Find the value of the required capacitance.

www.EngineeringEBooksPdf.com

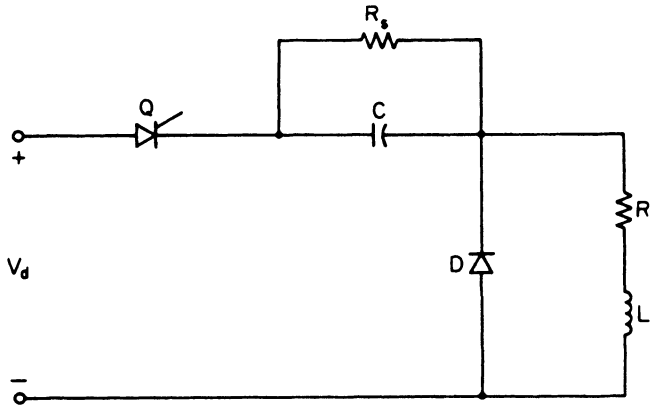


Figure 3.57 Series capacitor commutation with shunt resistor for capacitor discharge.

Solution Combining Eqs. (3.52), (3.49), and (3,47), we have

$$\frac{2\xi}{\sqrt{1-\xi^2}} = \frac{4(0.01)}{20 \times 10^{-3}\pi}$$

As a result

$$\xi = 0.3033$$

Using Eq. (3.47)

$$\omega_n = \frac{R}{2L\xi} = \frac{4}{(40 \times 10^{-3})(0.3033)} = 329.691$$

From Eq. (3.46) the required value is

$$C = \frac{1}{\omega_n^2 L} = \frac{1}{(329.691)^2(20 \times 10^{-3})} = 460\,\mu\text{F}$$

One possible way of discharging the capacitor is to employ a resistor in parallel with the capacitor, as shown in Fig. 3.57. The time constant of the R_sC combination determines the minimum time to elapse before a gate pulse is applied to the thyristor to commence conduction.

An improved scheme of discharging the capacitor is shown in Fig. 3.58. In this case, an inductor L_s in series with a thyristor Q_2 is connected in parallel with the capacitor. While Q_1 is conducting, thyristor Q_2 is off and the capacitor is charged.

www.EngineeringEBooksPdf.com

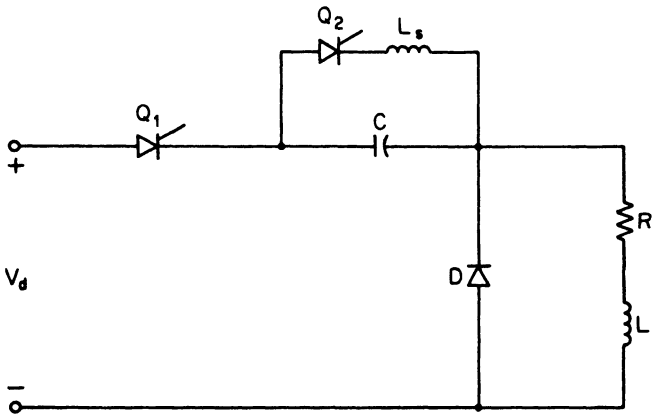


Figure 3.58 Series-capacitor commutation with capacitor discharge through inductor L_s and thyristor Q_2.

Thyristor Q_2 is turned on later than the turnoff time of Q_1, allowing the capacitor to discharge through the inductor L_s and the thyristor Q_2.

The principle of load commutation employing a series capacitor is used in series inverters for high output frequency in the range 200 Hz to 100 kHz. Figure 3.59 shows a basic series inverter circuit. Note that thyristor Q_2 is placed in parallel with the load and series capacitor. The thyristors are turned on alternately by short pulses of gate currents i_{G_1} and i_{G_2} applied at intervals matching the required load frequency. It should be noted that in this circuit the source may be short-circuited through Q_1 and Q_2. This occurs when Q_1 has not had enough time to turn off, and simultaneously Q_2 is turned on by the high dv/dt resulting from the capacitor discharge. It is for this reason that Q_1 and Q_2 are provided with protective elements. The protection is in the form of snubber r_1c_1 and inductor L_1 for thyristor Q_1 and similarly for Q_2, as shown in Fig. 3.60.

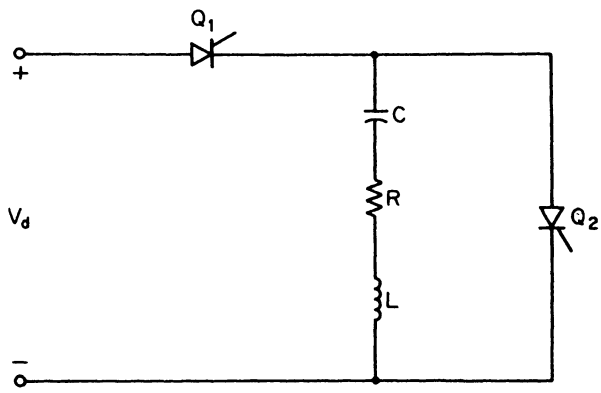


Figure 3.59 Basic series inverter circuit.

www.EngineeringEBooksPdf.com

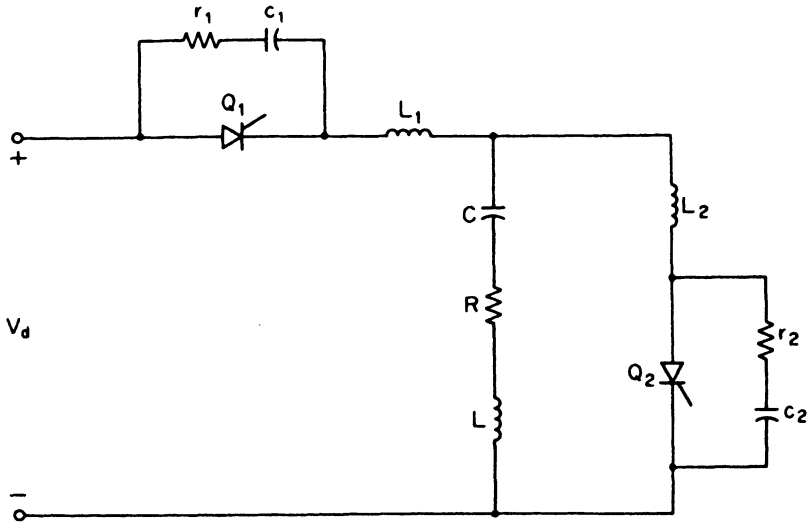


Figure 3.60 Series inverter circuit with protective snubbers and inductors.

Method C: Parallel-Capacitor Commutation The basic concept in parallel-capacitor commutation is to switch a precharged capacitor across the thyristor at the beginning of commutation. The application of a reverse bias across the thyristor causes turnoff. As shown in Fig. 3.61, the capacitor is switched across the thyristor by applying a gate pulse i_{G_2} to the second thyristor Q_2, causing it to conduct, and therefore creating the extinction loop made of C, Q_2, and Q_1.

Initially Q_1 is conducting and the load current flows through the loop made by the source, thyristor Q_1, and load R_L. The capacitor is initially charged to a voltage $(-V_{c_0})$ by external means and Q_2 is not conducting. At the time Q_2 is fired (through

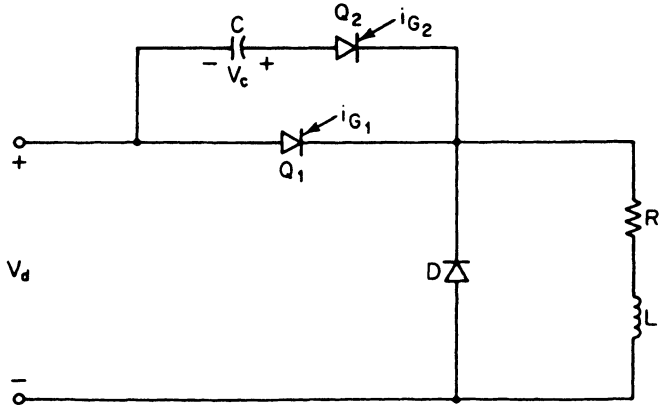


Figure 3.61 Basic concept of parallel-capacitor commutation.

www.EngineeringEBooksPdf.com

the application of gate pulse i_{G_2}), the load current I_L is diverted from Q_1 to the branch Q_2-C. We thus have

$$I_L = C\frac{dv_c}{dt}$$

Assuming I_L to be constant in the interval of interest, we conclude that

$$\begin{aligned} v_c(t) &= v_c(0) + \frac{I_L t}{C} \\ &= -V_{c_0} + \frac{I_L t}{C} \end{aligned}$$

Thus the capacitor voltage rises linearly from $(-V_{c_0})$ to positive values. The capacitor voltage becomes zero at t_0, obtained from

$$0 = -V_{c_0} + \frac{I_L t_0}{C}$$

Thus

$$t_0 = \frac{CV_{c_0}}{I_L} \tag{3.54}$$

The time t_0 is known as the available turnoff time.

Example 3.3 For the parallel capacitor commutation circuit shown in Fig. 3.61, assume that $V = 100$ V, $R = 4\ \Omega$, and $L = 20$ mH. Assume that the load is commutated at $t_1 = 0.01$ when the load current is $i_L(t_1) = 21.617$ A.

Find the available turnoff time for the following combinations:

(a) $C = 10 \times 10^{-3}$ F and $V_{C_0} = 10$ V
(b) $C = 200 \times 10^{-6}$ F and $V_{C_0} = 50$ V

Assume that the commutation commences at $t = 0.01$ s.

Solution Using Eq. (3.54), we have

$$t_0 = \frac{CV_{c_0}}{21.617}$$

For the combination of (a), we get

$$t_0 = 4.626 \times 10^{-3}\ \text{s}$$

For the combination of (b), we get

$$t_0 = 0.462 \times 10^{-3}\ \text{s}$$

www.EngineeringEBooksPdf.com

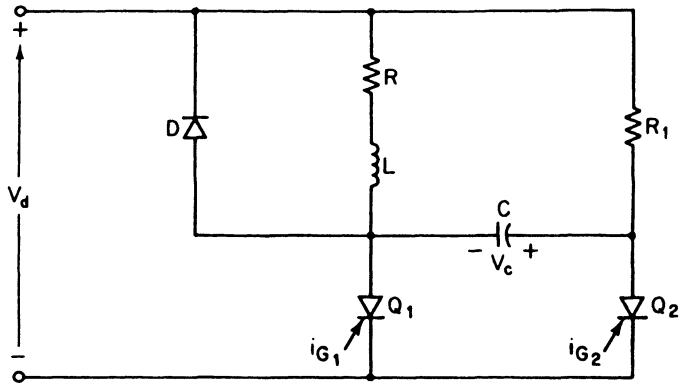


Figure 3.62 Basic parallel-capacitor commutation circuit.

The circuit of Fig. 3.62 is a practical implementation of the concept of parallel-capacitor commutation. When Q_1 is conducting, capacitor C will charge to potential V_{c0} through R_1. As a result of triggering Q_2, a reverse-bias voltage will be applied across Q_1, causing turnoff in a manner similar to that in the circuit of Fig. 3.61. Note that for the circuit shown in Fig. 3.62, the capacitor charging current does not flow through the load. The initial capacitor voltage value in this configuration is limited to the source voltage. This is disadvantageous in high-frequency and high-current applications, as this voltage value may not be enough to achieve turnoff of Q_1.

In the circuit shown in Fig. 3.63, the resistor R_1 of Fig. 3.62 is replaced by the series combination of an inductor L_1 and auxiliary thyristor Q_3. This modification results in resonant charging of the capacitor. The main thyristor Q_1 is turned on and the auxiliary thyristor Q_3 is turned on simultaneously. As a result, C is charged with the polarity indicated through the loop L_1, Q_3, C, Q_1, and the source. The capacitor potential V_c is higher than the source voltage V_d. It should be noted that this arrangement requires a higher rating for Q_1, as it will have to support both load

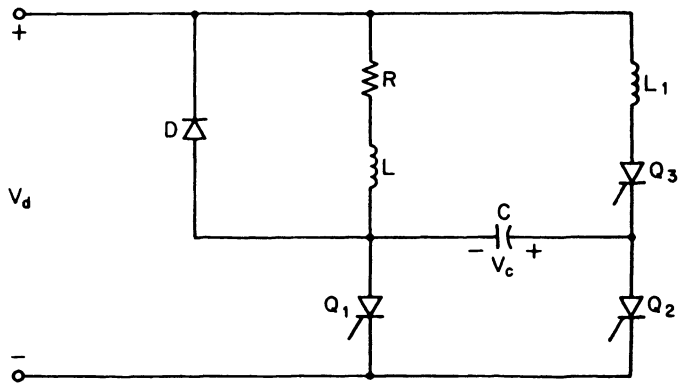


Figure 3.63 Parallel-capacitor commutation circuit using *LC* charging.

www.EngineeringEBooksPdf.com

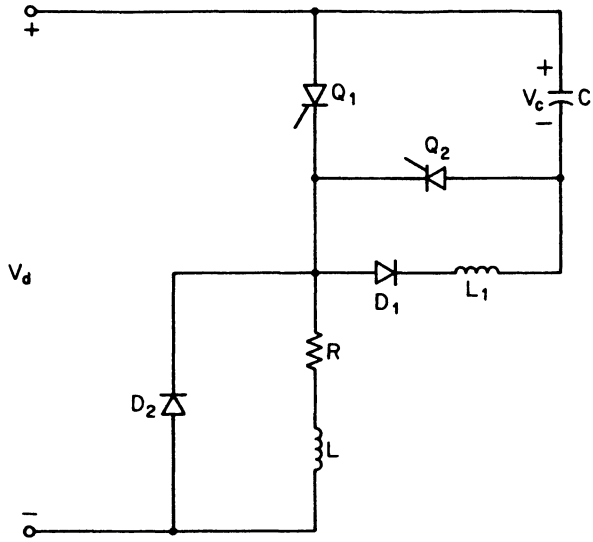


Figure 3.64 Parallel-capacitor commutation circuit with capacitor charging flowing into the load (in-line chopper switch).

current and the capacitor charging current. The possibility that Q_2 and Q_3 can be on simultaneously due to a fault condition can lead to loss of devices.

To overcome the difficulties encountered with the preceding circuit, an alternative circuit (in-line chopper switch) is used, as shown in Fig. 3.64. The operation of the circuit is as follows. First Q_2 must be triggered to charge the capacitor in the polarity shown. As soon as C is charged, Q_2 will turn off due to lack of current. When Q_1 is triggered, the current flows into two paths: the load current flows in RL; the commutating current flows through Q_1, D_1, L_1, and C, and the charge on C is reversed and held with the hold-off diode D_1. At any desired time Q_2 can be triggered, which then places C across Q_1 via Q_2, and Q_1 is thus turned off.

Method D: Parallel LC Commutation In parallel LC commutation, a reverse voltage is applied to the load-carrying thyristor Q_1 from the overshoot of a series LC resonant circuit connected across the SCR, as shown in Fig. 3.65. The series-capacitor approach relies on the load circuit forming part of the tuned path. This provides a limited control range and results in reduced effectiveness of the commutation circuit due to variations in the load impedance. The parallel LC commutation concept avoids these limitations.

Before the gate pulse is applied to Q_1, the capacitor C charges up to the polarity indicated. When Q_1 is triggered, current flows into two paths. The load current I_L flows through the load; a pulse of current flows through the resonant LC circuit and charges C up in the reverse polarity. The resonant circuit current will reverse and attempt to flow through Q_1 in opposition to the load current. The thyristor Q_1

www.EngineeringEBooksPdf.com

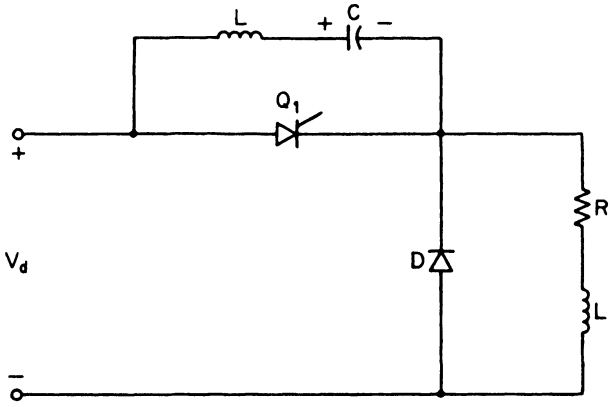


Figure 3.65 Parallel capacitor–inductor or *LC* free-running commutation circuit.

will turn off when the reverse resonant circuit current is greater than the load current. Note that a nonlinear inductor may be used in place of L. As soon as Q_1 is turned off, C will recharge with its original polarity through L and the load.

The Morgan Circuit The Morgan circuit is an improved version of the parallel capacitor–inductor circuit, and employs a saturable reactor, as shown in Fig. 3.66. From the previous cycle of operation, the capacitor is charged in the polarity shown. The reactor core is in positive saturation at this time. The polarity of a positively saturated core is shown in the circuit. The triggering of Q_1 and subsequent conduction closes the loop Q_1L_2C. The following sequence of events takes place:

1. As a result of the polarity of voltage applied to the reactor, it is pulled out of saturation. The unsaturated reactor presents a high inductance to the circuit. The capacitor then discharges into L_2.

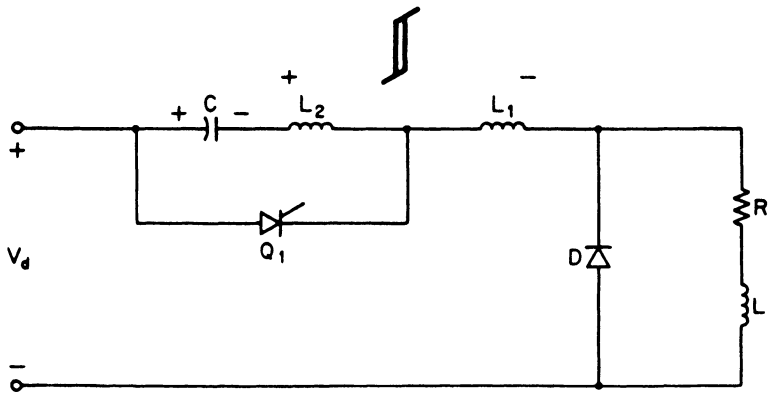


Figure 3.66 Morgan circuit.

www.EngineeringEBooksPdf.com

2. As soon as full-load current flows, the capacitor current decreases and the voltage induced across L_2 reverses polarity. The reactor core then goes into negative saturation and the inductance of L_2 changes from the high value to the low saturated value.
3. The resonant charging of C now proceeds more rapidly to a peak value. This is followed by a decrease in current and the voltage across L_2 reverses. The reversal of voltage pulls the reactor from saturation. The inductance of L_2 rises to the high value, and the recharging of C proceeds again.
4. The voltage across the inductor is held for a period of time and positive saturation occurs.
5. The capacitor is switched directly across Q_1 via the saturated inductance of L_2. If the reverse current exceeds the load current, Q_1 will be turned off. The remaining charge in C is then dissipated in the load, and then C is charged up and ready for the next cycle.

The Jones Circuit The Jones commutation circuit is used extensively in electric vehicle control schemes. The circuit is shown in Fig. 3.67 and does not require that the capacitor be charged before commutation can be achieved.

Let us assume that C is not charged initially. When Q_1 is triggered, the load current flows through Q_1, L_1, and load. As a result of the close coupling between L_1 and L_2, an induced voltage appears in L_2. The capacitor is therefore charged to the polarity indicated in the figure. The charge on C is trapped by the diode D_1. When Q_2 is triggered, turnoff of Q_1 commences and C gets charged in a polarity opposite to that indicated in the figure. At the next time Q_1 is triggered, C discharges through Q_1, L_2 with a reverse polarity and is now ready for the next commutation. The value of the voltage on C depends on whether the voltage induced in L_2 is greater than the reversal of positive charge built up while Q_2 was conducting. It is emphasized here that the periods of conduction of Q_1 guarantee the charging of C for commutation requirements.

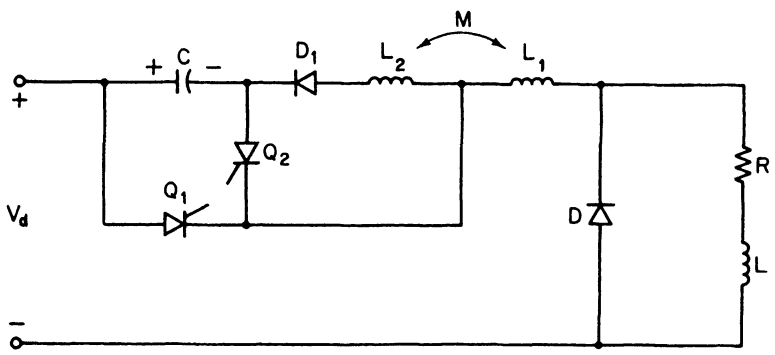


Figure 3.67 Jones circuit.

www.EngineeringEBooksPdf.com

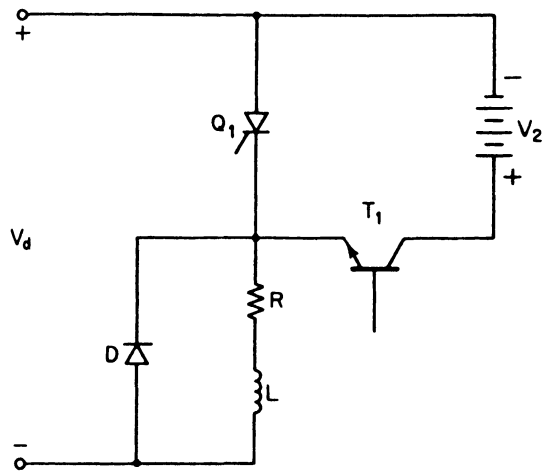


Figure 3.68 Auxiliary transistor, external pulse commutation circuit.

Method E: External Pulse Commutation In this commutation circuit, the commutation energy is obtained from an external source in the form of a pulse. The duration of the commutation pulse must be greater than the turnoff time of the device. The simplest circuit is shown in Fig. 3.68 and employs an auxiliary voltage source V_2 with the polarity shown. At the desired instant of commutation a current pulse is applied to the auxiliary transistor T_1. As a result, V_2 is connected across Q_1, turning it off. The base drive pulse is maintained until complete turnoff has been achieved.

Another example of this class is shown in Fig. 3.69. Here the external pulse generator energy is injected in series with Q_1 through a pulse transformer. The transformer is designed so that no saturation takes place under loading conditions. The voltage drop across the transformer is negligible. When Q_1 is triggered, current flows through the load and pulse transformer. To turn Q_1 off, a positive pulse is applied to the cathode of Q_1 from the generator through the transformer. Capacitor C is

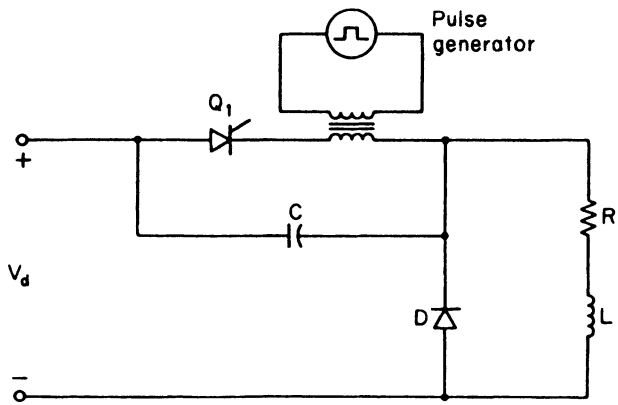


Figure 3.69 External pulse commutation circuit.

www.EngineeringEBooksPdf.com

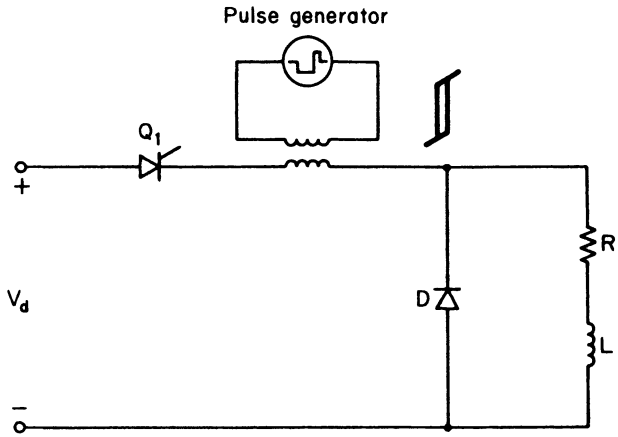


Figure 3.70 External pulse commutation circuit.

charged only to about 1 V and can be considered a short circuit for the duration of commutation.

Another variant of pulse commutation circuits is shown in Fig. 3.70. When Q_1 is turned on, the pulse transformer saturates and offers a low impedance in the load current path. In preparation for turnoff, the pulse transformer is desaturated by the application of a negative pulse. This temporarily increases the voltage across the load and the current through it. As soon as the transformer is desaturated, a pulse in the reverse polarity is applied to turnoff the thyristor. The pulse should be held for the required turnoff time.

3.7 POWER ELECTRONIC SYSTEMS

Solid-state power components are able to control the switching of voltages and currents of high power levels. These components are used in power electronic systems that perform specific energy conversion functions based on this switching ability. Power electronic systems are made by suitable interconnections of thyristor devices and other components into a static energy converter. The term static is used to emphasize the fact that there are no moving parts in these systems. The function of a static energy converter is to convert energy at its input side from an available form (ac or dc) into another form at the output side (again, ac or dc). In this section we introduce a number of these systems in terms of their functions, classification, and the associated terminology.

3.7.1 ac Voltage Controllers

Given a power source with a fixed ac voltage level at the input side, an ac voltage controller converts the energy into ac, but with a different value of the rms voltage at

www.EngineeringEBooksPdf.com

the output side, which is connected to the load. The variable-voltage ac output is used to control lighting, heating, and induction heating equipment as well as fractional-horsepower and three-phase induction motors.

Voltage control is achieved using one of two major techniques:

1. **On–Off Control** The ac source is connected to the load for a number of cycles and then disconnects it for a similar interval. The procedure is termed pulse-burst modulation, where a fixed time period T is defined corresponding to a number of cycles of the ac source frequency. The period T is divided into an on-interval T_{ON} and an off-interval T_{OFF}. The duration T_{ON} is determined to correspond to speed requirements in the controlled device. The concept of on–off control is illustrated in Fig. 3.71(a).
2. **Phase Control** This technique uses the switching characteristics of the SCR to connect the ac source to the load for only a portion of each cycle. The delay angle α is the control parameter in this case.

3.7.2 Controlled Rectifiers

A controlled rectifier is used to vary the average value of the direct voltage applied to the load circuit. The input is a constant-voltage ac power source. The thyristors are

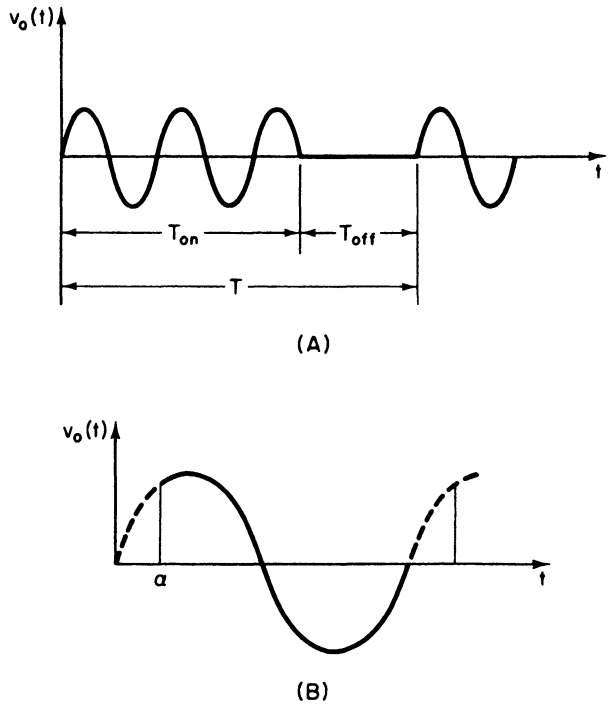


Figure 3.71 Principles of ac voltage control: (a) on–off, or pulse-burst modulation; (b) phase control.

www.EngineeringEBooksPdf.com

phase controlled in this application. Controlled rectifier systems are widely used in dc-motor speed-control schemes.

Controlled rectifiers are classified either according to the number of phases of the ac source or according to the number of pulses of current through the load circuit during one cycle of the source voltage. Available configurations vary form the simple single-phase half-wave rectifier (one pulse converter) to the more involved three-phase full-wave converter. An increase in the number of phases of ac power supply results in less fluctuations (power ripple) in the output side.

The term *controlled rectifier* is used whenever gate control is employed by the use of thyristors. An uncontrolled rectifier is a device that uses power diodes in its function. A controlled rectifier is called a *full converter* or *two-quandrant converter* if all its active components are thyristors, since in this case the inverse process, called *synchronous inversion*, is possible. Synchronous inversion is the term used when the converter delivers ac from a dc input. Many dc-motor-control applications require four-quadrant operation, that is, both polarities of dc voltage and current. A four-quadrant converter is obtained by placing two two-quadrant converters in a back-to-back arrangement called the dual converter.

3.7.3 Choppers (dc-to-dc Converters)

The dc-to-dc converter or chopper is a power electronic system that converts power from a constant dc voltage source to direct voltage with a variable average value. The main function of a chopper is to alternately switch the source dc voltage on and off in one of the following ways:

1. **Pulse-width Modulation (PWM)** In this case, using terms shown in Fig. 3.72, the period T is maintained constant while T_{ON} or T_{OFF} are varied.
2. **Frequency Modulation** Here T_{ON} is held constant while T_{OFF} is varied, and hence T is varied.
3. **Combined Modulation** In this arrangement both T_{ON} and T_{OFF} are varied and T is varied as well. This is a combination of the PWM and FM techniques.

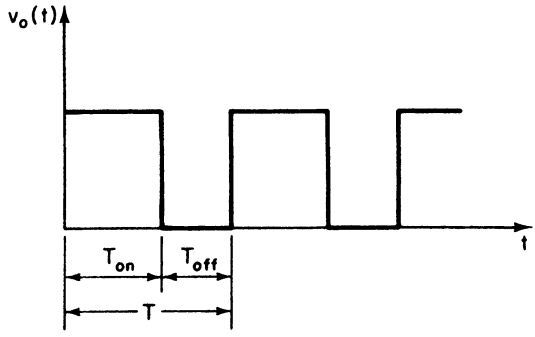


Figure 3.72 The principle of chopper operation.

www.EngineeringEBooksPdf.com

3.7.4 Inverters

The term *inverter* is used to describe a power electronic system with fixed dc input and fixed- or variable-frequency ac voltage (single-phase or three-phase) output. Control of the output voltage is achieved by either controlling the dc voltage input to the inverter or by controlling the voltage within the inverter.

Controlling the dc voltage input is done through the use of a chopper. If the source voltage is ac, we can use a phase-controlled converter or an uncontrolled rectifier with a variable dc voltage output. This latter requirement is obtained either using an autotransformer to supply the rectifier or by cascading the rectifier to a chopper.

Controlling the voltage within the inverter involves PWM, either by controlling the width of the output pulse or by rapidly switching the output of the inverter on and off a number of times during each half-cycle to produce a train of constant-amplitude pulses.

3.7.5 ac-to-ac Converters

This application area requires converting a fixed ac power source of a given frequency and voltage into different frequency and voltage ac outputs. The most obvious means of achieving this involves an intermediate dc link. In this case, the given ac is converted to dc through rectification, which is followed by inversion to the desired ac voltage and frequency. A more efficient system is termed the *cycloconverter*, and is a frequency changer that produces a low output frequency (less than one-third of the input frequency) in one stage. It is noted that the dc-link-converter concept is applicable for all applications, in contrast to the output frequency limitations of a cycloconverter.

3.8 POWER INTEGRATED CIRCUITS AND SMART POWER

The term power integrated circuit (PIC) is used to refer to an IC that combines both logic-level control and protection features with power-handling capability on the same chip. Loosely speaking, a PIC is referred to as *smart power*. The motivation for power circuit integration is cost reduction and improved reliability. A PIC is often differentiated from a HVIC, where the voltage is high but the current is small. The on-chip power dissipation of an HVIC may be low enough to allow placing silicon chips in standard packages. In any case, the same fabrication process may result in ICs with low and high output current, making them HVICs or PICs, depending on the application.

In the operation of any PIC, the internal heat generated is critical to both device performance and the chip's operating temperature. A device's usefulness is an exponential function of junction temperature; the life span decreases by about a factor of 2 for every 10°C increase in temperature. Adequate chip cooling or heatsinks must be employed to safeguard against device failure due to junction temperature rise. Control circuits can monitor the chip temperature and regulate it by reducing operating currents or shutdown.

www.EngineeringEBooksPdf.com

The emergence of smart-power technology in the 1990s is attributed to the ability to develop integrated gate drive circuits for power MOSFETs and IGBTs with their voltage-controlled characteristics, and hence simplified control circuits. The control circuit must be capable of performing level shifting to high voltages. The development of integrated control circuits also motivated incorporating protective circuits on the chips. Moreover, the need to interface with microprocessors led to the incorporation of logic circuits to provide encode/decode capabilities.

Smart-power technology involves interfacing digital-control logic and power load. In its simplest form it may consist of a level shifting and drive circuit that converts the logic-level signals from a microprocessor to voltage and current levels of such magnitude as to allow energizing a load.

Three fundamental functions involved in smart-power technology involve power control, sensing/protection, and interfacing. Power control is done by power devices and their drive circuits. The latter must be designed to operate at up to 30 volts to furnish sufficient voltage to the gates of the former. The drive circuits must also be able to perform level shifting to high voltages. The regulation of power flow is done by a variety of power devices.

The second element of smart power is sensing and protection. This involves detecting overcurrents, overvoltages, excessive temperature rise, no-load, and/or undervoltage conditions. The protection of the integrated circuit is achieved by using a feedback loop containing high-frequency bipolar transistors. This portion requires implementing high-performance analog circuits.

The interface function is accomplished using CMOS-technology logic circuits, which perform the encode/decode operations. The chip must be able to respond to signals received from a microprocessor and must also be able to send messages regarding operating status and information related to load monitoring.

The main issue in smart-power integrated circuits is the isolation between low- and high-voltage/power devices. Many technical solutions have been proposed, but the cross talk between power and low-voltage devices is a problem for realizing PICs. Concepts such as traditional *pn*-junction isolation, high resistivity subtrate, and dielectric isolation were found useful in resolving the problem to some extent. Silicon-on-insulator (SOI) technology offers superior dielectric isolation (DI) and results in a smaller chip area, and allows the integration of multiple power devices by decreasing parasitic capacitance and leakage currents. The disadvantage of this technology is high prices. An intermediate solution employs dielectric for horizontal isolation and *pn*-junctions for vertical isolation. This lower-cost architecture offers a good compromise.

PROBLEMS

Problem 3.1 The beta (β) of the biopolar transistor in Fig. 3.12 varies from 8 to 40. The load resistance is $R_c = 10\,\Omega$, the dc supply voltage is $V_{CC} = 100$ V, and the input voltage to the base circuit is $V_B = 8$ V. If $V_{CE(\text{sat})} = 2.5$ V and $V_{BE(\text{sat})} = 1.75$ V, find (a) the value of R_B that will result in saturation with an overdrive factor of 20; (b) the forced β; and (c) the power loss in the transistor, P_T.

www.EngineeringEBooksPdf.com

Problem 3.2 The beta (β) of the biopolar transistor in Fig. 3.12 varies from 12 to 75. The load resistance is $R_C = 2\,\Omega$, the dc supply voltage is $V_{CC} = 40$ V, and the input voltage to the base circuit is $V_B = 6$ V. If $V_{CE(sat)} = 1.2$ V, $V_{BE(sat)} = 1.6$ V, and $R_B = 0.7\,\Omega$, determine (a) the ODF; (b) the forced β; and (c) the power loss in the transistor, P_T.

Problem 3.3 The beta (β) of the bipolar transistor in Fig. 3.12 is 12. The load resistance is $R_C = 5\,\Omega$. If $V_{CE(sat)} = 2.5$ V and the base current $I_B = 5$ A, find the dc supply voltage V_{CC} and the forced β assuming an overdrive factor of 20.

Problem 3.4 Consider the bipolar transistor of Fig. 3.12, the dc supply voltage is $V_{CC} = 120$ V, and the input voltage to the base circuit is $V_B = 10$ V. If $V_{CE(sat)} = 3$ V, R_C when $R_B = 0.3$ results in saturation with an overdrive factor of 18. Find the value of the forced β.

Problem 3.5 The input voltage to the base circuit of the bipolar transistor of Fig. 3.12 is $V_B = 12$ V. The value of the dc supply voltage is $V_{CC} = 100$ V, while $V_{BE(sat)} = 2$ V and $V_{CE(sat)} = 2.8$ V. Assume that the ratio $R_C/R_B = 15$ and that the overdrive factor for this condition is 18. Find the value of beta (β) of the bipolar transistor.

Problem 3.6 A bipolar transistor is operated as a chopper switch at a frequency of $f_s = 10$ kHz. The circuit arrangement is shown in Fig. 3.26(a). The dc input voltage of the chopper is $V_S = 220$ V and the load current is $I_L = 120$ A. The switching times are $t_r = 1$ μs and $t_f = 3$ μs. Determine the values of L_s, C_s, R_s for critically damped condition, R_s if the discharge time is limited to one-third of the switching period, R_s if peak discharge current is limited to 5% of load current. Assume $V_{CE(sat)} = 0$.

Problem 3.7 A MOSFET is operated as a chopper switch at a frequency of $f_s = 40$ kHz. The circuit arrangement is shown in Fig. 3.26(a). The dc input voltage of the chopper is $V_s = 30$ V and the load current is $I_L = 40$ A. The switching times are $t_r = 60$ ns and $t_f = 25$ ns. Determine the values of L_s, C_s, R_s for critically damped condition, R_s if the discharge time is limited to one-third of switching period, R_s if peak discharge current is limited to 5% of load current. Assume $V_{CE(sat)} = 0$.

Problem 3.8 Show for the series-capacitor commutation method that the capacitance value is related to L, R, and the commutation time by

$$C = \frac{4Lt_1^2}{4\pi^2L^2 + R^2t_1^2}$$

Use this formula to verify the results of Example 3.3.

Problem 3.9 Consider a load whose parameters are

$$R = 80\ \Omega \qquad L = 10\,\text{mH}$$

Find the value of the capacitance, C, required to commutate the load at $t_1 = 125$ s using series capacitance commutation.

www.EngineeringEBooksPdf.com

Problem 3.10 Consider a load whose parameters are

$$R = 1\,\Omega \qquad L = 0.03\,\text{H}$$

Find the value of the capacitance C required to commutate the load at $t_1 = 30 \times 10^{-3}$ s.

Problem 3.11 Assume that a 400-μF capacitor is used for the series-capacitor commutation circuit of Example 3.3. Find the value of t_1 (use the formula derived in Problem 3.8) to show that

$$t_1 = \frac{2\pi L}{\sqrt{4L/C - R^2}}$$

Problem 3.12 Assume that a 0.2-μF capacitor is used for series-capacitor commutation of the circuit of Problem 3.9. Find the value of t_1 (use the formula given in statement of Problem 3.1).

Problem 3.13 Repeat Problem 3.12 for the circuit of Problem 3.10 with $C = 2 \times 10^{-3}$ F.

Problem 3.14 Parallel-capacitor commutation is used for the load of Problem 3.9, with $C = 0.2 \times 10^{-6}$. Find the required capacitor voltage for an available turnoff time of 125 s. Repeat for $C = 1$ μF.

Problem 3.15 Parallel-capacitor commutation is used for the load of Problem 3.10, with $C = 4 \times 10^{-3}$ F and $V_{C_0} = 50$ V. Find the available turnoff time. Suppose that the turnoff time is to be 30 ms. What value of capacitance is required for $V_{C_0} = 50$ V?

www.EngineeringEBooksPdf.com

CHAPTER 4

DIRECT-CURRENT MOTORS

4.1 INTRODUCTION

From a historical point of view, the dc machine was the earliest electromechanical energy conversion device and heralded the dawn of the electrical age. The famous copper-disk experiments of Faraday led to further inventions that contributed to the evolution of the dc machine into first electric-energy source used for illumination purposes.

The most distinctive feature of the dc machine is its versatility. The machine is reversible, so it can operate either as a generator converting mechanical energy into electrical energy in the form of direct current and voltage, or as a motor converting electrical energy into useful mechanical work. Dc generators are not in widespread use at present because ac generation, transmission, and distribution are more advantageous from an economic point of view. Dc generators can be used in situations where electric-energy consumption takes place very close to the generation site, and where output voltages are required to follow closely prespecified patterns. The latter application area can also be met by solid-state-controlled rectification devices.

The operating characteristics of dc motors offer distinct advantages that make them attractive for many industrial applications. A wide variety of speed–torque characteristics can be obtained as a result of the various combinations of separately excited, series, shunt, and compound-field winding connections. Wide ranges of speed and precise control can be obtained easily using systems of dc machines.

This chapter treats dc motors from an application point of view, and therefore emphasis is given more to operating characteristics than to design details and procedures.

www.EngineeringEBooksPdf.com

4.2 CONSTRUCTION FEATURES

A dc machine is a rotating electromechanical energy conversion device that has a stator with salient poles that are excited by one or more field windings. The armature winding of a dc machine is on the rotor, with current conducted from or to it by means of carbon brushes in contact with copper commutator segments. A cutaway view of a dc motor is shown in Fig. 4.1, and a schematic representation of a two-pole dc machine is given in Fig. 4.2.

The armature windings consist of many coil sides placed on the rotor with the conductors parallel to the shaft. The field windings are fed with dc, and as a result the air-gap flux is almost constant under each of the salient poles. The rotor is turned

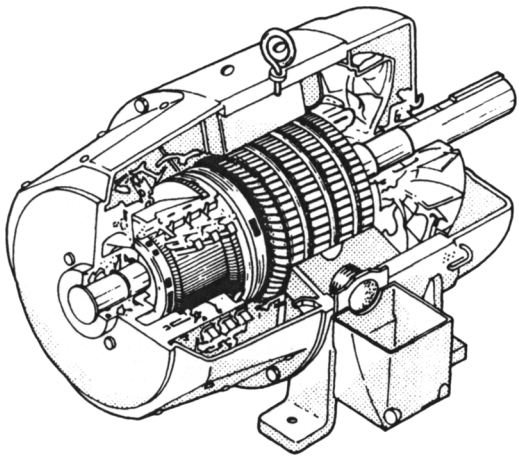


Figure 4.1 A dc motor. (Courtesy of General Electric Company.)

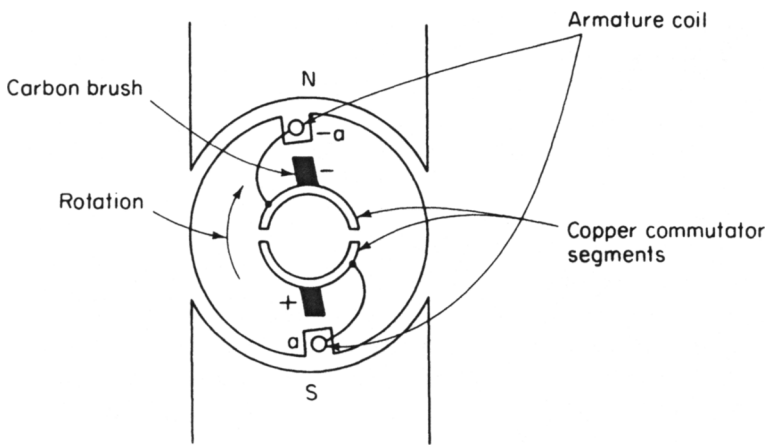


Figure 4.2 Schematic representation of a dc machine.

www.EngineeringEBooksPdf.com

at a constant speed, and as a result, induced voltages appear in the armature coils. The induced voltages are alternating and must be rectified to produce dc.

Rectification is traditionally carried out using a commutator, which is a cylinder mounted on the rotor and formed of copper segments insulated from each other and from the rotor shaft. Commutator segments are in contact with stationary carbon brushes. For the configuration of Figure 4.2, the commutator connects the coil side, which is under the south pole to the positive brush and that which is under the north pole to the negative brush at all times. The commutator is essentially a mechanical full-wave rectifier.

The magnetic field established by the dc in the field winding is stationary with respect to the stator. The armature currents create a stationary magnetic-flux distribution whose axis is at right angles to that of the field flux. The interaction of the two flux distributions creates the torque in the dc machine.

4.3 CIRCUIT MODEL OF dc GENERATOR

In a dc generator the armature conductors rotate at a constant speed n rpm relative to the field flux. The flux linkages λ can be written

$$\lambda(t) = -N\phi \cos \omega t$$

where N is the number of coil turns, ϕ is the flux per pole, and ω is the angular velocity in electrical radians per second. The induced voltage $e(t)$ is given by Faraday's law as

$$e(t) = \frac{d\lambda}{dt} = N\omega\phi \sin \omega t$$

Due to the commutator action, the induced voltage is rectified with an average value given by

$$E_{av} = \frac{1}{\pi}\int_0^{\pi} e(t)\, d\omega t$$

As a result,

$$E_{av} = \frac{2N\phi\omega}{\pi}$$

The average voltage equation can be rearranged to yield a practical formula by using the speed in rpm instead of ω and expressing N in terms of the number of armature conductors. First recall that

$$\omega = \frac{\omega_m P}{2} = \frac{2\pi n}{60}\frac{P}{2}$$

www.EngineeringEBooksPdf.com

Also, if Z is the number of armature conductors and a is the number of parallel paths, we have the numbers of coils in a parallel path given by

$$N = \frac{Z}{2a}$$

We therefore have

$$E_g = \frac{ZnP\phi}{60a} \tag{4.1}$$

Equation (4.1) is a practical formula that relates the generated voltage, E_g, to the speed of rotation, n, in rpm, flux per pole, ϕ, number of armature conductors, Z, number of poles, P, and number of armature parallel paths, a. From an analysis point of view for a given generator, Z, P, and a are constants and we therefore write

$$E_g = K_g \phi \omega \tag{4.2}$$

It is clear that the armature-generated voltage depends on the flux and rotational speed. The flux, in turn, varies with the field current I_f according to the magnetization curve pertinent to the machine. In general, the curve is not linear, especially in the saturation region, as discussed earlier. Analysis of dc machines, including saturation effects can be done effectively by using approximate straight-line segments. For most practical application purposes, a simple straight-line approximation of the magnetization curve provides reasonable procedures and results. We therefore rewrite Eq. (4.2) as

$$E_g = K\omega I_f \tag{4.3}$$

where I_f is the field current.

4.3.1 Armature-Circuit Model

The armature of a dc generator is modeled by a simple circuit consisting of an ideal voltage source, E_g, in series with the armature resistance, R_a, for steady-state analysis purposes. For transient-analysis studies, appropriate representations of the winding inductances are necessary. The armature circuit model described earlier is shown in Fig. 4.3 and is simply the familiar Thévenin equivalent of the machine looking into the armature terminals.

The terminal voltage of the armature is denoted by V_a, as shown in Fig. 4.3, and the armature current is I_a. We thus write for the generator case

$$V_a = E_g - I_a R_a \tag{4.4}$$

www.EngineeringEBooksPdf.com

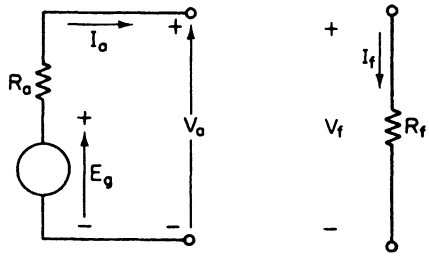


Figure 4.3 Armature-circuit and field-circuit models for a dc generator.

From an electric power point of view, we can rewrite Eq. (4.4) as

$$V_a I_a = E_g I_a - I_a^2 R_a$$

or

$$P_a = P_{\text{in}} - I_a^2 R_a \tag{4.5}$$

Thus the output power of the armature $P_a = V_a I_a$ is the net of the input power $P_{\text{in}} = E_g I_a$ and the armature-circuit ohmic losses $I_a^2 R_a$. Note that this representation does not account for additional losses, such as rotational, eddy-current, and hysteresis losses.

4.3.2 Field-Circuit Model

The field windings are represented simply by a resistance R_f, as shown in Figure 4.3. Note that the source of the field excitation voltage is left unspecified, for there are various ways of obtaining this voltage, as discussed next.

4.4 CIRCUIT MODEL OF dc MOTORS

A dc machine is reversible in the sense that it can be operated either as a generator or as a motor. From an analytical point of view, the models adopted for the generator case are equally applicable to the motor case. We note that electric power is supplied to the motor and the output is mechanical power represented by a torque (T) in the armature and a shaft rotational speed. It is therefore clear than the power flow in a dc motor is the reverse of that in a dc generator. The difference, then, from a model point of view, is the form of the basic armature–voltage relationship. The armature-developed voltage, denoted by E_g for the generator case, is referred to as the *back* EMF, E_c.

4.4.1 Armature-Circuit Model

The armature circuit of a dc motor is represented by the model of Fig. 4.4. The voltage applied to the armature is denoted by V_a and the counter (back) EMF is

www.EngineeringEBooksPdf.com

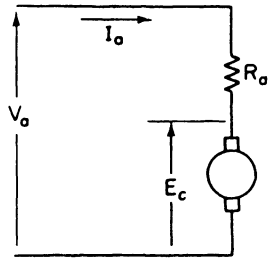


Figure 4.4 Armature-circuit model for a dc motor.

denoted by E_c. The resistance of the armature windings is denoted by R_a. The armature current I_a can be obtained from the basic voltage relationship

$$V_a = E_c + R_a I_a \tag{4.6}$$

The back EMF, E_c, varies with the field flux, ϕ_f, and armature speed, ω, according to

$$E_c = K_1 \phi_f \omega \tag{4.7}$$

The constant of proportionality, K_1, is a machine parameter that depends on the number of conductors in the armature, the number of poles, and the number of winding connections.

It is clear that at standstill, the motor speed, ω, is zero, and thus at starting, the motor's back EMF, E_c, is zero. It is then evident that the armature current at starting will be of a large value unless a reduced value of V_a is applied to the armature at that time. Special attention should be paid to this aspect, discussed later.

The power input to the armature circuit is given by

$$P_{a_i} = V_a I_a \tag{4.8}$$

This power supplies the armature power losses and the armature power, P_a. Thus

$$P_{a_i} = I_a^2 R_a + P_a \tag{4.9}$$

The developed armature power P_a is given by

$$P_a = E_c I_a \tag{4.10}$$

The net output power P_o is obtained by subtracting the motor's rotational losses P_{rot} from P_a:

$$P_o = P_a - P_{rot} \tag{4.11}$$

The net output power P_o is the available shaft power.

The output torque in newton-meters is obtained from the relation

$$T_o = \frac{P_o}{\omega} \tag{4.12}$$

www.EngineeringEBooksPdf.com

where ω is the armature speed in radians per seconds. An example is in order at this time.

Example 4.1 A voltage of 230 V applied to the armature of a dc motor results in a full-load armature current of 205 A. Assume that the armature resistance is 0.2 Ω. Find the back EMF E_c, the net output power, and the torque, assuming that the rotational losses are 1445 W at a full-load speed of 1750 rpm.

Solution The armature voltage and current are specified as

$$V_a = 230\,\text{V}$$
$$I_a = 205\,\text{A}$$

The back EMF is obtained as

$$\begin{aligned} E_c &= V_a - I_a R_a \\ &= 230 - 205(0.2) \\ &= 189\,\text{V} \end{aligned}$$

The power developed by the armature is thus

$$\begin{aligned} P_a &= E_c I_a \\ &= 189(205) = 38{,}745\,\text{W} \end{aligned}$$

The net output power is thus obtained by subtracting the rotational losses from the armature developed power:

$$\begin{aligned} P_\text{o} &= P_a - P_\text{rot} \\ &= 38{,}745 - 1445 \\ &= 37{,}300\,\text{W} \end{aligned}$$

The net output torque is now calculated as

$$\begin{aligned} T_\text{o} &= \frac{P_\text{o}}{\omega} \\ &= \frac{37{,}300}{\frac{2\pi}{60}(1750)} \\ &= 203.536\,\text{N} \cdot \text{m} \end{aligned}$$

4.4.2 Field-Circuit Model

A full analysis of the performance of a dc motor requires knowledge of the field-circuit connection. We note here that the back EMF depends on the field flux, ϕ_f,

www.EngineeringEBooksPdf.com

as indicated in Eq. (4.7). The field flux varies with the field current in a manner similar to the saturation characteristic of the magnetic material of the machine. It is common practice to assume that the machine is operated such that the field flux is proportional to the field current. In this case we have

$$\phi_f = K_2 I_f \tag{4.13}$$

The field current is denoted by I_f. As a result, we have

$$E_c = K_1 K_2 I_f \omega \tag{4.14}$$

The field-circuit windings are modeled by a resistance R_f.

A complete circuit model of a dc motor is shown in Fig. 4.5. The dc source voltage is denoted by V_t and its current is denoted by I_L. The field circuit is placed between the source and the armature circuit. In a series motor, the field circuit is connected in series with the armature, as shown in Fig. 4.6(a). In a shunt motor, the field circuit is connected in parallel (shunt) with the armature circuit, as shown in Fig. 4.6(b). Combinations of the two connections result in compound motors.

4.5 dc SERIES MOTORS

As mentioned earlier, in a dc series motor the field windings are connected in series with the armature windings. The resistance of the field is denoted by R_s, as shown in the schematic diagram of Fig. 4.7. It is clear that the armature current, field current, and line current are the same. The terminal voltage, V_t, is equal to the sum of the armature voltage and the voltage drop across the series field resistance

$$I_L = I_f = I_a \tag{4.15}$$

$$V_t = V_a + I_a R_s \tag{4.16}$$

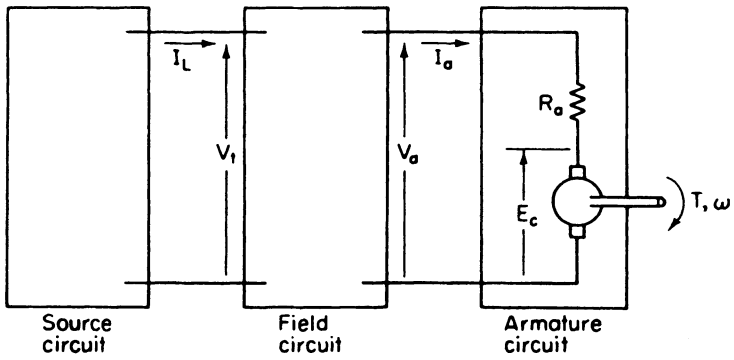


Figure 4.5 Functional block diagram of a dc motor.

www.EngineeringEBooksPdf.com

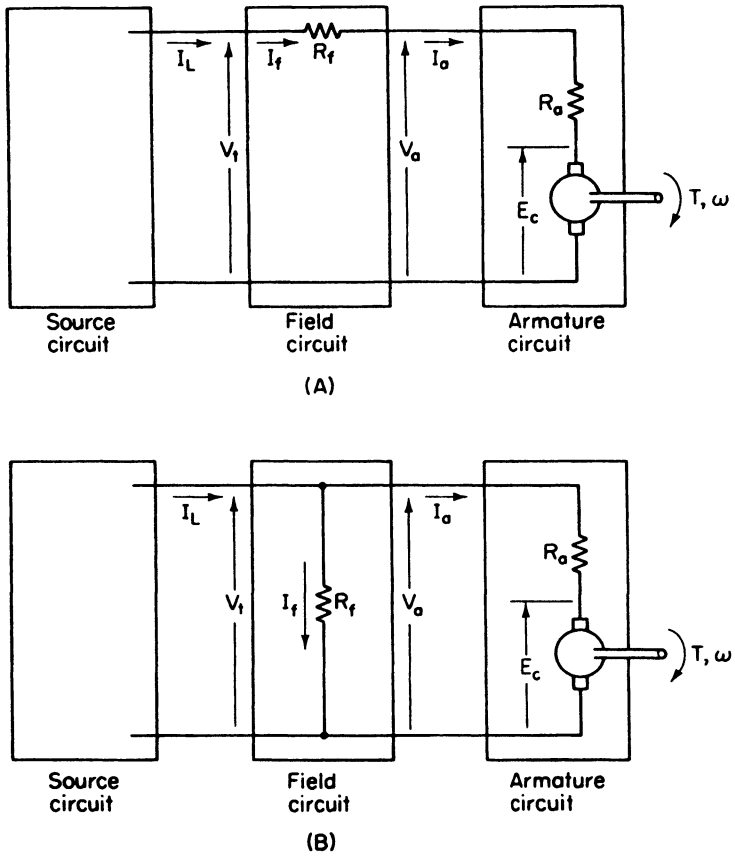


Figure 4.6 Circuit representations of dc: (a) series motor; (b) shunt motor.

As a result, we can write

$$V_t = E_c + I_a(R_a + R_s) \tag{4.17}$$

Equation (4.14) can be written as

$$E_c = K_1 K_2 I_a \omega \tag{4.18}$$

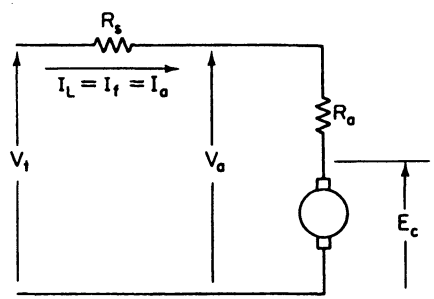


Figure 4.7 Schematic diagram of a dc series motor.

www.EngineeringEBooksPdf.com

We are now in a position to derive performance analysis equations for the dc series motor.

Basic performance characteristics of a dc motor involve the variations of output variables such as armature-developed power, P_a, torque, T, and speed, ω, with the armature current, I_a. In practice, it is also desired to obtain performance characteristics displaying the variation of armature current, I_a, torque, T, and speed, ω, versus output power, P_o. These practical characteristics are first obtained as variations with armature-developed power, P_a, and are then corrected for rotational losses to obtain the required characteristics in terms of, P_o. Important economic performance characteristics of a motor are naturally the variation of power losses efficiency with loading. These characteristics can be obtained using our basis relations discussed earlier.

4.5.1 P_a-I_a Characteristic

The armature-developed power (internal power) is given by Eq. (4.10) as

$$P_a = E_c I_a \tag{4.19}$$

Substituting for E_c from Eq. (4.12), we obtain

$$P_a = [V_t - I_a(R_a + R_s)]I_a \tag{4.20}$$

It is clear that for a specified terminal voltage and machine parameters, the power developed by the armature follows a parabolic (second-order) variation with the armature current. In fact, for a given armature power, P_a, there are two solutions of Eq. (4.20) for I_a, obtained from the following modified form of Eq. (4.20):

$$(R_a + R_s)I_a^2 - V_t I_a + P_a = 0$$

The solutions for I_a are given by

$$I_a = \frac{V_t \pm \sqrt{V_t^2 - 4P_a(R_a + R_s)}}{2(R_a + R_s)} \tag{4.21}$$

From Eq. (4.21) it is clear that there is a value of P_a for which there is only one solution for I_a. This condition requires that the quantity under the square-root sign be zero, which results in

$$P_{a_m} = \frac{V_t^2}{4(R_a + R_s)} \tag{4.22}$$

with the corresponding armature current given by

$$I_{a_m} = \frac{V_t}{2(R_a + R_s)} \tag{4.23}$$

www.EngineeringEBooksPdf.com

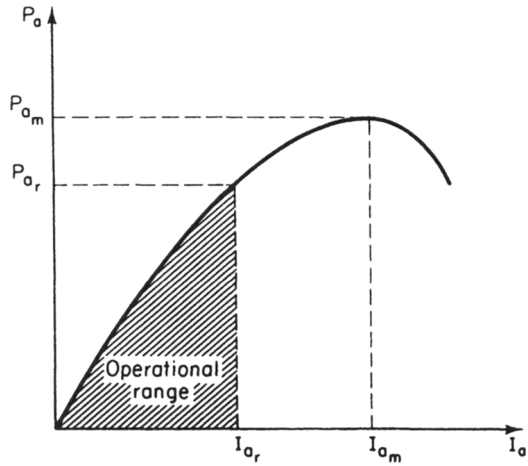


Figure 4.8 Variation of armature-developed power with armature current in a dc series motor.

Note that the subscript m refers to the fact that this power value is the maximum attainable by the motor. To verify this statement, we differentiate Eq. (4.20) with respect to I_a and set the result to zero, to obtain

$$\frac{\partial P_a}{\partial I_a} = V_t - 2(R_a + R_s)I_a = 0 \tag{4.24}$$

Clearly, this leads to Eq. (4.23). A typical sketch of the variation of P_a with I_a for a dc series motor is shown in Fig. 4.8.

The operational range of the motor is well below that corresponding to maximum developed armature power. In this range we take the negative sign in Eq. (4.21), with the result that

$$I_a = \frac{V_t - \sqrt{V_t^2 - 4P_a(R_a + R_s)}}{2(R_a + R_s)} \tag{4.25}$$

An approximation for the value of I_a is obtained by neglecting the armature and series field resistances, to yield

$$I_a \cong \frac{P_a}{V_t} \tag{4.26}$$

The approximate expression yields a lower value for I_a than the more detailed expression of Eq. (4.25). The error, however, is small for lower values of P_a. An example is appropriate at this time.

Example 4.2 The combined armature and series field resistance of a 10-hp 240-V dc series motor is 0.6 Ω. Neglecting rotational losses, it is required to calculate:

www.EngineeringEBooksPdf.com

(a) Armature current at full rated load

(b) The value of maximum developed armature power and the corresponding armature current

(c) The armature current at half-rated load using Eqs. (4.25) and (4.26)

Solution

(a) At full-rated load, neglecting rotational losses, the armature developed power is

$$P_a = 10 \times 746 = 7460\,\text{W}$$

The armature current is obtained as

$$I_a = \frac{240 - \sqrt{(240)^2 - 4(7460)(0.6)}}{2(0.6)}$$
$$= 33.968\,\text{A}$$

Note that the second solution for I_a is 366.032 A if we take the positive signs in Eq. (4.21). The approximate solution of Eq. (4.26) is 31.083 A with an error of 2.885 A.

(b) For maximum armature power we have

$$I_{a_m} = \frac{240}{2(0.6)} = 200\,\text{A}$$

The value of P_a at this current is obtained using Eq. (4.22) as

$$P_{a_m} = \frac{(240)^2}{4(0.6)} = 24{,}000\,\text{W}$$

(c) At half-rated load we have

$$P_a = 5 \times 746 = 3730\,\text{W}$$

The corresponding armature current is

$$I_a = \frac{240 - \sqrt{(240)^2 - 4(3730)(0.6)}}{2(0.6)}$$
$$= 16.198\,\text{A}$$

The approximate equation [Eq. (4.43)] yields

$$I_a \cong \frac{3730}{240} = 15.542\,\text{A}$$

The error in this case is 0.656 A.

www.EngineeringEBooksPdf.com

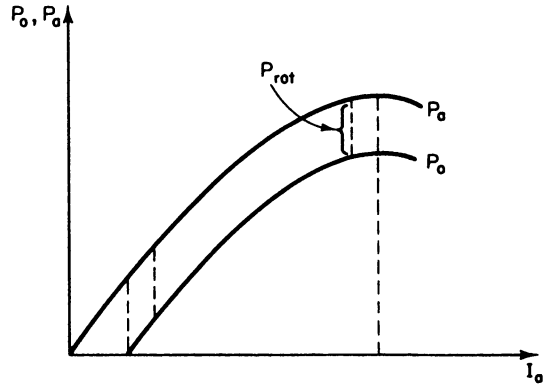


Figure 4.9 Obtaining the variation of output power with armature current for a dc series motor.

The output (or shaft) power of the motor is obtained by subtracting the rotational power losses form the armature-developed power. The resulting characteristic is shown in Fig. 4.9.

4.5.2 Torque and Speed Characteristics

The armature-developed torque (internal torque) is obtained using the basic relation

$$T_a = \frac{P_a}{\omega} \tag{4.27}$$

Using Eqs. (4.18) and (4.19), we conclude that

$$T_a = K_1 K_2 I_a^2 \tag{4.28}$$

Thus, ideally, the torque varies as the square of armature current, as shown in Fig. 4.10.

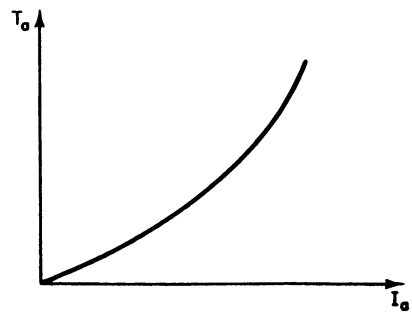


Figure 4.10 Variation of armature-developed torque with armature current for a dc series motor.

www.EngineeringEBooksPdf.com

The motor speed in radians per second is obtained in terms of armature current by combining Eqs. (4.17) and (4.18) to eliminate E_c to obtain

$$V_t = K_1 K_2 I_a \omega + I_a(R_a + R_s)$$

As a result,

$$\omega = \frac{V_t}{K_1 K_2 I_a} - \frac{R_a + R_s}{K_1 K_2} \tag{4.29}$$

Equation (4.29) tells us that for small values of armature current, the motor speed is high. Thus at no load on the motor a runaway condition (extremely high speed) exists. A series motor is used only in applications where a load is always connected to the shaft. Examples include hoists and cranes as well as railway motors. A centrifugal switch must be used to protect a series motor against runaway. A typical characteristic of speed versus armature current for a dc series motor is shown in Fig. 4.11.

The armature current in terms of armature speed is obtained from Eq. (4.29) as

$$I_a = \frac{V_t}{K_1 K_2 \omega + (R_a + R_s)} \tag{4.30}$$

Substituting Eq. (4.30) in (4.28), we obtain

$$T_a = \frac{K_1 K_2 V_t^2}{[K_1 K_2 \omega + (R_a + R_s)]^2} \tag{4.31}$$

Equation (4.31) provides us with the torque–speed characteristic of a dc series motor shown in Fig. 4.12.

Example 4.3 A 600-V, 150-hp dc series motor operates at its full-rated load at 600 rpm. The armature resistance is 0.12 Ω and the series field resistance is

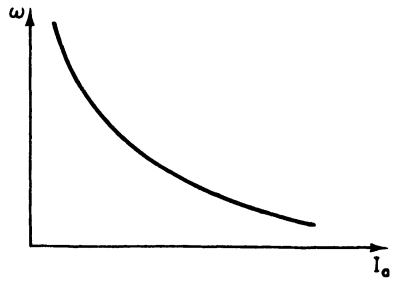


Figure 4.11 Variation of speed with armature current for a dc series motor.

www.EngineeringEBooksPdf.com

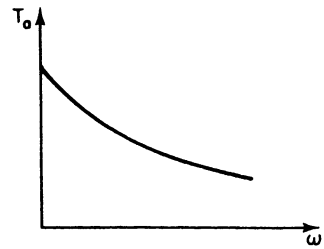


Figure 4.12 Torque speed characteristic of a dc series motor.

0.04 Ω. The motor draws 200 A at full load.

(a) Find the armature back EMF at full load
(b) Find the armature-developed power and internal-developed torque
(c) Assume that a change in load results in the line current dropping to 150 A. Find the new speed in rpm and the new developed torque

Solution

(a) The armature back EMF is obtained from

$$\begin{aligned} E_{c_1} &= V_t - I_{a_1}(R_a + R_s) \\ &= 600 - 200(0.12 + 0.04) \\ &= 568\ \text{V} \end{aligned}$$

(b) The power developed by the armature is

$$\begin{aligned} P_{a_1} &= E_{c_1} I_{a_1} \\ &= 568(200) = 113.6 \times 10^3\ \text{W} \end{aligned}$$

As a result, we calculate the internal developed torque as

$$T_{a_1} = \frac{P_{a_1}}{\omega_1} = \frac{113.6 \times 10^3}{(2\pi/60)(600)} = 1808\ \text{N} \cdot \text{m}$$

(c) For the new line current, we can calculate a new value for the back EMF:

$$E_{c_2} = 600 - 150(0.16) = 576\ \text{V}$$

From Eq. (4.18) we have

$$\begin{aligned} E_{c_1} &= K_1 K_2 I_{a_1} \omega_1 \\ E_{c_2} &= K_1 K_2 I_{a_2} \omega_1 \end{aligned}$$

As a result,

$$\frac{\omega_2}{\omega_1} = \frac{I_{a_1}}{I_{a_2}} \frac{E_{c_2}}{E_{c_1}}$$

www.EngineeringEBooksPdf.com

Thus

$$\omega_2 = \frac{200}{150}\left(\frac{576}{568}\right)\omega_1$$

or

$$n_2 = \frac{200}{150}\left(\frac{576}{568}\right)(600)$$
$$= 811.268 \text{ r/min}$$

In a similar manner, from Eq. (4.28), we can write

$$\frac{T_2}{T_1} = \left(\frac{I_2}{I_1}\right)^2$$

Thus

$$T_2 = 1808\left(\frac{150}{200}\right)^2 = 1017 \text{ N} \cdot \text{m}$$

4.5.3 Starting

It is clear that at standstill, the motor speed and hence the armature back EMF, E_c, are zero. The application of rated voltage to the armature circuit will result in a high value of current. This can be seen from Eq. (4.17) with $E_c = 0$, giving

$$I_{a_{st}} = \frac{V_t}{R_a + R_s} \tag{4.32}$$

To limit the value of starting current one of two means must be used, the most logical being applying a reduced value of voltage through a variable dc supply, the other being the conventional method of inserting a starter resistor R_{st} that limits the value of I_a at starting to an acceptable level. This resistance is commonly a variable resistance that is gradually reduced to zero as the motor picks up speed. If the starting resistor is left in the armature circuit as the motor picks up speed, an inferior performance will result. It should be realized that dc series motors are characterized by a high value of starting torque, as can be seen from Eq. (4.31). An example is in order here.

Example 4.4 The series motor of Example 4.3 is required to be started using a starting resistor R_{st} such that the starting current is limited to 150% of rated value:

(a) Find the required value of R_{st} and the starting torque
(b) If the starting resistor is left in the armature circuit and the motor line current drops to its rated value of 200 A, find the armature back EMF and the speed of the motor

www.EngineeringEBooksPdf.com

Solution

(a) At starting $E_c = 0$:

$$V_t = I_a(R_a + R_s + R_{st})$$
$$600 = 300(0.16 + R_{st})$$

Thus

$$R_{st} = 1.84\,\Omega$$

We know from Example 4.3 that for an armature current of 200 A, the corresponding torque is 1808 N·m. Thus for a starting current of 300 A, we have

$$T_{st} = T_{fld}\left(\frac{I_{st}}{I_{fld}}\right)^2$$
$$= 1808\left(\frac{300}{200}\right)^2 = 4068\ \text{N}\cdot\text{m}$$

(b) With the starting resistor left in the armature circuit, we have

$$E_c = V_t - I_a(R_a + R_s + R_{st})$$
$$= 600 - 200(2)$$

Thus

$$E_c = 200\,\text{V}$$

We now have

$$\frac{E_{c_2}}{E_{c_1}} = \frac{n_2}{n_1}$$

or

$$\frac{200}{568} = \frac{n_2}{600}$$

As a result,

$$n_2 = 211.268\ \text{rpm}$$

4.5.4 Power Loss and Efficiency

The input power to a dc series motor is given by

$$P_{in} = V_t I_a \tag{4.33}$$

www.EngineeringEBooksPdf.com

The power losses in the motor include losses in the armature and series field resistances as well as the rotational losses, which are considered constant P_{rot}. Thus

$$P_l = I_a^2(R_a + R_s) + P_{\text{rot}} \tag{4.34}$$

The output power is, therefore, given by substituting into

$$P_{\text{o}} = P_{\text{in}} - P_l \tag{4.35}$$

The efficiency of the motor is given by

$$\eta = \frac{P_{\text{o}}}{P_{\text{in}}} \tag{4.36}$$

It is clear that the efficiency varies with the armature current, and hence with the motor load.

The efficiency increases as the armature current is increased up to the point of maximum efficiency, and then drops as the armature current is increased further. To obtain the value of armature current corresponding to maximum efficiency, we set to zero the derivative of the efficiency with respect to armature current:

$$\frac{\partial \eta}{\partial I_a} = 0$$

As a result, we have

$$P_{\text{in}} \frac{\partial P_{\text{o}}}{\partial I_a} - P_{\text{o}} \frac{\partial P_{\text{in}}}{\partial I_a} = 0 \tag{4.37}$$

Using Eq. (4.35), we get

$$P_{\text{in}} \frac{\partial P_l}{\partial I_a} = P_l \frac{\partial P_{\text{in}}}{\partial I_a} \tag{4.38}$$

The required derivatives are

$$\frac{\partial P_l}{\partial I_a} = 2I_a(R_a + R_s)$$

$$\frac{\partial P_{\text{in}}}{\partial I_a} = V_t$$

Thus the condition for maximum efficiency is

$$2V_t I_a^2(R_a + R_s) = V_t[I_a^2(R_a + R_s) + P_{\text{rot}}]$$

www.EngineeringEBooksPdf.com

Simplifying, we get

$$P_{\text{rot}} = I_a^2(R_a + R_s) \tag{4.39}$$

The efficiency is a maximum when the fixed losses represented by the rotational losses in this case is equal to the I^2R losses. Thus

$$I_{a_{\max}} = \sqrt{\frac{P_{\text{rot}}}{R_a + R_s}} \tag{4.40}$$

The maximum value of the efficiency is given by

$$\eta_{\max} = \frac{P_{\text{in}_m} - 2P_{\text{rot}}}{P_{\text{in}_m}} \tag{4.41}$$

The formula for maximum efficiency can also be written

$$\eta_{\max} = 1 - \frac{2[P_{\text{rot}}(R_a + R_s)]^{1/2}}{V_t} \tag{4.42}$$

From the preceding development, we can conclude that the maximum efficiency is a function of rotational losses, armature and series field resistances, and terminal voltage. As can reasonably be anticipated, the maximum efficiency of the motor is increased by an increase in the terminal voltage and by reducing the armature and series field resistances.

Example 4.5 Consider the dc series motor of Example 4.3. The full-load output is 150 hp with full-load current given by 200 A.

(a) Find the rotational losses
(b) Find the armature current and power output at maximum efficiency as well as the value of maximum efficiency
(c) Find the full-load efficiency

Assume the rotational losses are fixed.

Solution

(a) The output power at full load is

$$P_o = 150 \times 746 = 111.9 \times 10^3 \text{ W}$$

From Example 4.3, the armature developed power at full load

$$P_a = 113.6 \times 10^3 \text{ W}$$

As a result,

$$P_{\text{rot}} = P_a - P_o$$
$$= 1.7 \times 10^3 \text{ W}$$

www.EngineeringEBooksPdf.com

(b) For maximum efficiency, the armature current is obtained by

$$I_a = \sqrt{\frac{1.7 \times 10^3}{0.16}} = 103.1 \text{ A}$$

The back EMF for this current is

$$\begin{aligned} E_c &= 600 - 103.1(0.16) \\ &= 583.5 \text{ V} \end{aligned}$$

The power developed by the armature is thus

$$P_a = 583.5 \times 103.1 = 60.16 \times 10^3 \text{ W}$$

As a result,

$$\begin{aligned} P_o &= 60.16 \times 10^3 - 1.7 \times 10^3 \\ &= 58.46 \times 10^3 \text{ W} \end{aligned}$$

The corresponding input power is

$$\begin{aligned} P_{in} &= 600 \times 103.1 \\ &= 61.86 \times 10^3 \text{ W} \end{aligned}$$

As a result, the maximum efficiency is

$$\eta_{max} = \frac{58.46 \times 10^3}{61.86 \times 10^3} = 0.945$$

(c) The full-load input power is

$$P_{in} = 600 \times 200 = 120 \times 10^3 \text{ W}$$

The output power at full load is

$$P_o = 150 \times 746 = 111.9 \times 10^3 \text{ W}$$

Thus the full-load efficiency is

$$\eta = \frac{111.9 \times 10^3}{120 \times 10^3} = 0.9325$$

Note that at full load, the motor is operating beyond the point of maximum efficiency.

www.EngineeringEBooksPdf.com

4.6 dc SHUNT MOTORS

In a dc shunt motor, the field winding is connected in parallel with the armature circuit. The resistance of the field is denoted by R_f, as shown in the schematic diagram of Fig. 4.13. The terminal voltage V_t is identical with both field voltage V_f and armature voltage V_a:

$$V_t = V_f = V_a \tag{4.43}$$

The line current I_L is the sum of armature and field currents:

$$I_L = I_a + I_f \tag{4.44}$$

The field current I_f is given by

$$I_f = \frac{V_t}{R_f} \tag{4.45}$$

As a result, we can write

$$V_t = E_c + I_a R_a \tag{4.46}$$

Equation (4.31) can be written as

$$E_c = K_1 K_2 \frac{V_t}{R_f} \omega \tag{4.47}$$

Let us define

$$K_{sh} = K_1 K_2 \frac{V_t}{R_f} \tag{4.48}$$

Thus we have

$$E_c = K_{sh} \omega \tag{4.49}$$

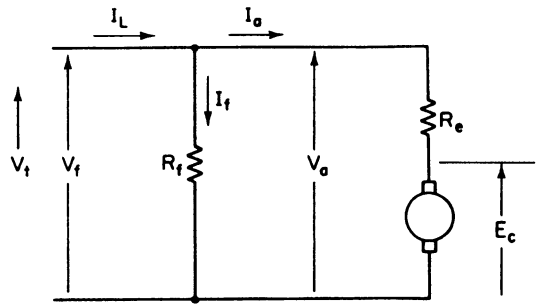


Figure 4.13 Schematic diagram of a dc shunt motor.

www.EngineeringEBooksPdf.com

For a fixed terminal voltage and field resistance, the back EMF is proportional to the armature speed ω. We will now consider performance-analysis equations along the same lines adopted in the analysis of a dc series motor.

4.6.1 P_a-I_a Characteristics

The armature-developed power is

$$P_a = E_c I_a$$

Using Eq. (4.46), we get

$$P_a = (V_t - I_a R_a) I_a \tag{4.50}$$

Note that Eq. (4.50) is of the same form as that of Eq. (4.20) with $R_s = 0$. We can thus conclude that for a given armature power there are two values of I_a:

$$I_a = \frac{V_t \pm \sqrt{V_t^2 - 4P_a R_a}}{2R_a} \tag{4.51}$$

The maximum value of armature-developed power is

$$P_{a_m} = \frac{V_t^2}{4R_a} \tag{4.52}$$

With the corresponding armature current

$$I_{a_m} = \frac{V_t}{2R_a} \tag{4.53}$$

A typical sketch of the variation of P_a with I_a for a dc shunt motor is shown in Fig. 4.14.

Again, in the range of operation, we take the negative sign in applying Eq. (4.50), to obtain

$$I_a = \frac{V_t - \sqrt{V_t^2 - 4P_a R_a}}{2R_a} \tag{4.54}$$

An approximation to I_a is obtained by neglecting $I_a R_a$ in Eq. (4.50), to obtain

$$I_a \cong \frac{P_a}{V_t} \tag{4.55}$$

Thus we can conclude that the armature current varies approximately in proportion to the armature-developed power.

www.EngineeringEBooksPdf.com

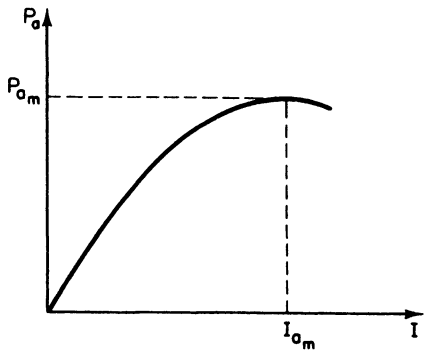


Figure 4.14 Variation of armature-developed power with armature current for a dc shunt motor.

4.6.2 Torque and Speed Characteristics

The armature-developed torque is obtained using

$$T_a = \frac{P_a}{\omega}$$

From Eq. (4.49), we conclude that

$$T_a = K_{sh} I_a \tag{4.56}$$

It is clear that the internal-developed torque is proportional to the armature current in a dc shunt motor, as shown in Fig. 4.15.

The motor speed can be obtained in terms of armature current by substituting Eq. (4.49) in (4.46), to obtain

$$\omega = \frac{V_t - I_a R_a}{K_{sh}} \tag{4.57}$$

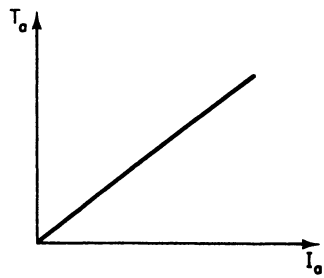


Figure 4.15 Variation of internal torque with armature current in a dc shunt motor.

www.EngineeringEBooksPdf.com

At no load, the armature current is zero and thus

$$\omega_0 = \frac{V_t}{K_{sh}} \tag{4.58}$$

Thus

$$\omega = \omega_0 - \frac{R_a}{K_{sh}} I_a \tag{4.59}$$

The coefficient R_a/K_{sh} is usually too small, and thus a dc shunt motor can be assumed to be a constant-speed motor for all practical purposes. The variation of ω with I_a is shown in Fig. 4.16.

The torque–speed variation is obtained from Eqs. (4.56) and (4.57) as

$$T_a = \frac{K_{sh}}{R_a}(V_t - K_{sh}\omega)$$

Using Eq. (4.58), we get

$$T_a = \frac{K_{sh}^2}{R_a}(\omega_0 - \omega) \tag{4.60}$$

where ω_0 is the speed at no load. The inverse relation specifying the speed in terms of torque is given by

$$\omega = \frac{V_t}{K_{sh}} - \frac{T_a R_a}{K_{sh}^2}$$

or

$$\omega = \omega_0 - \frac{T_a R_a}{K_{sh}^2} \tag{4.61}$$

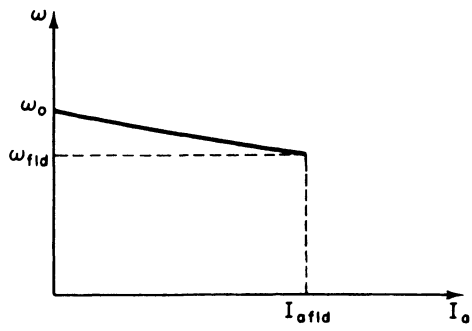


Figure 4.16 Variation of speed with armature current for a dc shunt motor.

www.EngineeringEBooksPdf.com

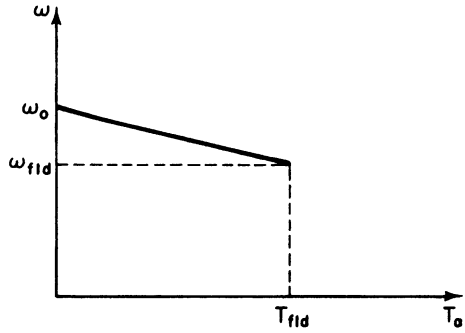


Figure 4.17 Speed–torque characteristic for a dc shunt motor.

The speed–torque characteristic of a dc shunt motor is shown in Fig. 4.17 and is simply the result of a scaling of Fig. 4.16, since torque is proportional to armature current in this case.

Example 4.6 The armature resistance of a 10-hp, 230-V dc shunt motor is 0.3 Ω. The field resistance is 160 Ω. The motor draws a line current of 3.938 A on no load at a speed of 1200 rpm. At full load, the armature current is 40 A.

(a) Find the armature current at no load
(b) Find the power developed by the armature on no load
(c) Find the full-load efficiency of the motor
(d) Find the full-load speed of the motor

Solution

(a) The field current is obtained as

$$I_f = \frac{230}{160} = 1.438\,\text{A}$$

Thus the armature current is obtained at

$$I_a = I_L - I_f = 3.938 - 1.438 = 2.5\ \text{A}$$

(b) The back EMF on no load is calculated as

$$\begin{aligned} E_c &= V_t - I_a R_a \\ &= 230 - 2.5(0.3) = 229.25\ \text{V} \end{aligned}$$

Thus we obtain the no-load armature power as

$$\begin{aligned} P_{\text{no load}} &= E_c I_a \\ &= 229.25(2.5) = 572.125\,\text{W} \end{aligned}$$

www.EngineeringEBooksPdf.com

(c) At full load, we have

$$E_c = 230 - 40(0.3) = 218 \text{ V}$$

The armature power is thus calculated as

$$P_a = E_c I_a = 218(40) = 8720 \text{ W}$$

The net power output is obtained by subtracting the no-load power (rotational losses) from part (b) from the armature power:

$$P_o = 8720 - 573.125 = 8146.875 \text{ W}$$

The power input is found as

$$\begin{aligned} P_{\text{in}} &= V_t I_L \\ &= 230(41.438) = 9530.625 \text{ W} \end{aligned}$$

As a result, we calculate the efficiency:

$$\begin{aligned} \eta &= \frac{8146.875}{9530.625} \\ &= 0.855 \end{aligned}$$

(d) From part (c), the full-load back EMF is given by

$$E_{c_2} = 218 \text{ V}$$

The no-load back EMF from part (b) is

$$E_{c_1} = 229.25 \text{ V}$$

Thus we can find the full-load speed as

$$\begin{aligned} n_{fld} &= n_{\text{no load}} \frac{E_{c_2}}{E_{c_1}} \\ &= 1200\left(\frac{218}{229.25}\right) = 1141.112 \text{ rpm} \end{aligned}$$

4.6.3 Power Loss and Efficiency

The power input to the motor is given by

$$P_{\text{in}} = V_t I_L$$

www.EngineeringEBooksPdf.com

Recall that the line current is the sum of field current, I_f, and armature current, I_a:

$$I_L = I_a + I_f$$

Thus

$$P_{\text{in}} = V_t I_a + P_f \tag{4.62}$$

where P_f is the power loss in the shunt-field circuit resistance defined by

$$P_f = \frac{V_t^2}{R_f} = V_t I_f \tag{4.63}$$

The power input to the armature is $V_t I_a$ and supplies the armature power loss and the rotational losses with a net mechanical power output given by

$$P_{\text{o}} = V_t I_a - I_a^2 R_a - P_{\text{rot}} \tag{4.64}$$

The motor's efficiency is thus obtained as

$$\eta = \frac{P_{\text{o}}}{P_{\text{in}}}$$

Clearly, the motor's efficiency depends on the armature current.

The point at which maximum efficiency occurs is obtained by setting the derivative of η with respect to current to zero. As a result, we obtain

$$P_{\text{in}} \frac{\partial P_{\text{o}}}{\partial I_a} - P_{\text{o}} \frac{\partial P_{\text{in}}}{\partial I_a} = 0$$

Performing the required operations, we obtain

$$\frac{\partial P_{\text{o}}}{\partial I_a} = V_t - 2I_a R_a$$
$$\frac{\partial P_{\text{in}}}{\partial I_a} = V_t$$

We can thus obtain the condition for maximum efficiency:

$$(V_t I_a + P_f)(V_t - 2I_a R_a) - (V_t I_a - I_a^2 R_a - P_{\text{rot}})V_t = 0$$

Simplifying, we get

$$R_a I_a^2 + 2I_a I_f R_a - (P_{\text{rot}} + P_f) = 0 \tag{4.65}$$

www.EngineeringEBooksPdf.com

The solution to the foregoing quadratic equation in I_a yields the desired value at which maximum efficiency occurs.

A practical approximation to the preceding formula results if we consider that the product $I_f R_a$ is usually small, and as a result

$$R_a I_{a_{max}}^2 \cong P_{rot} + P_f \tag{4.66}$$

This result is similar to that obtained for the dc series motor, where it was concluded that for maximum efficiency, the fixed losses are equal to the armature losses.

Example 4.7 A 230-V, 25-hp dc shunt motor draws an armature current of 90 A at full rated load. Assume that the armature resistance is 0.2 Ω and that the shunt field resistance is 216 Ω. Find the rotational losses at full load and the motor efficiency in this case.

Solution At a full rated armature current of 90 A, the power developed by the armature is given by

$$\begin{aligned} P_a &= (V_t - I_a R_a) I_a \\ &= [230 - 90(0.2)](90) = 19{,}080 \text{ W} \end{aligned}$$

The output power at full load is

$$P_o = 25 \times 746 = 18{,}650 \text{ W}$$

As a result, the rotational losses are obtained from

$$\begin{aligned} P_{rot} &= P_a - P_o \\ &= 19{,}080 - 18{,}650 = 430 \text{ W} \end{aligned}$$

The line current is given by

$$\begin{aligned} I_L &= I_a + \frac{V_t}{R_f} \\ &= 90 + \frac{230}{216} = 91.065 \end{aligned}$$

The input power is thus

$$\begin{aligned} P_{in} &= V_t I_L = 230(91.065) \\ &= 20{,}944.91 \text{ W} \end{aligned}$$

The efficiency can thus be computed as

$$\eta = \frac{P_o}{P_{in}} = \frac{18{,}650}{20{,}944.91} = 0.89$$

www.EngineeringEBooksPdf.com

Example 4.8 The rotational losses for a 230-V, 25-hp dc shunt motor are found to be 430 W. The armature resistance is 0.2 Ω and the shunt-field resistance is 216 Ω. Obtain the armature current corresponding to maximum efficiency using both the exact and approximate expressions. Calculate the output power in both cases and the corresponding maximum efficiency.

Solution The exact formula is given by Eq. (4.65) as

$$R_a I_a^2 + 2I_a I_f R_a - (P_{\text{rot}} + P_f) = 0$$

We have

$$R_a = 0.2\ \Omega$$
$$I_f = \frac{230}{216} = 1.065\ \text{A}$$
$$P_f = \frac{(230)^2}{216} = 244.907\ \text{W}$$
$$P_{\text{rot}} = 430\ \text{W}$$

Thus we have

$$0.2I_a^2 + 2I_a(1.065)(0.2) - (430 + 244.907) = 0$$

Alternatively,

$$I_a^2 + 2.13I_a - 3374.537 = 0$$

The solution for I_a is obtained as

$$I_a = \frac{-2.13 \pm 116.201}{2}$$

We take

$$I_{a_{\max \eta_1}} = 57.036\,\text{A}$$

The output power is given by Eq. (4.64) as

$$\begin{aligned} P_{\text{o}} &= V_t I_a - I_a^2 R_a - P_{\text{rot}} \\ &= 230(57.036) - (57.036)^2(0.2) - 430 \\ &= 12{,}037.66\,\text{W} \end{aligned}$$

www.EngineeringEBooksPdf.com

The input power is given by Eq. (4.62) as

$$\begin{aligned} P_{\text{in}} &= V_t I_a + P_f \\ &= 230(57.036) + 244.907 = 13{,}363.187 \text{ W} \end{aligned}$$

As a result, the maximum efficiency on the basis of the exact calculation is

$$\eta_{\max_1} = \frac{12{,}037.66}{13{,}363.187} = 0.901$$

The approximate formula [Eq. (4.66)] provides the value of armature current for maximum efficiency as

$$\begin{aligned} I_{a_{\max \eta_2}} &= \sqrt{\frac{P_{\text{rot}} + P_f}{R_a}} \\ &= 58.091 \text{ A} \end{aligned}$$

The output power is calculated as

$$\begin{aligned} P_{\text{o}} &= V_t I_a - I_a^2 R_a - P_{\text{rot}} \\ &= 230(58.091) - (58.091)^2(0.2) - 430 \\ &= 12{,}256.017 \text{ W} \end{aligned}$$

The input power is calculated as

$$\begin{aligned} P_{\text{in}} &= V_t I_a + P_f \\ &= 230(58.09) + 244.907 \\ &= 13{,}605.837 \text{ W} \end{aligned}$$

The corresponding maximum efficiency is

$$\eta_{\max_2} = \frac{12{,}256.017}{13{,}605.837} = 0.901$$

The final answers are the same to the assumed accuracy.

4.7 COMPOUND MOTORS

In a dc compound motor both shunt- and series-field windings are employed. The resulting field is a combination of the contributions of the two windings. The shunt-field contribution exeeds that of the series field. When the series field aids

www.EngineeringEBooksPdf.com

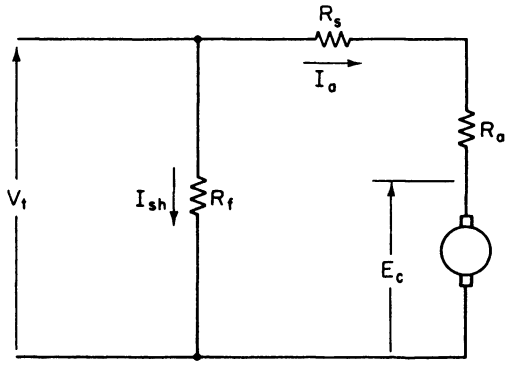


Figure 4.18 Schematic of a dc compound motor.

the shunt field, the compounding is *cumulative*. When the series field opposes the shunt field, the compounding is *differential*. Note also that the series field may be connected in series with the armature in the long-shunt case, or in series with the line in the short-shunt case. Our analysis assumes that a long-shunt connection is employed, as shown in Fig. 4.18.

The field flux ϕ_f in a *cumulative* compound machine is given by

$$\phi_f = K_3 I_{\text{sh}} + K_4 I_a \tag{4.67}$$

The constants K_2 and K_4 pertain to the shunt- and series-field parameters, assuming that the motor operates in the linear region of its magnetization characteristic. For a *differential* compound motor, we have

$$\phi_f = K_3 I_{\text{sh}} - K_4 I_a \tag{4.68}$$

We observe that the first term in both Eqs. (4.67) and (4.68) is essentially constant, while the second term varies linearly with the armature current and hence with the load on the motor.

From the circuit model of Fig. 4.18, we conclude that

$$V_t = E_c + I_a(R_s + R_a) \tag{4.69}$$

$$I_{\text{sh}} = \frac{V_t}{R_f} \tag{4.70}$$

The power developed by the armature is given by

$$P_a = E_c I_a \tag{4.71}$$

The developed torque is given by

$$T_a = \frac{P_a}{\omega} \tag{4.72}$$

www.EngineeringEBooksPdf.com

Recalling that the back EMF is given by

$$E_c = K_1 \phi_f \omega \tag{4.73}$$

we conclude from Eqs. (4.67) and (4.68) that

$$E_c = K_1 (K_3 I_{sh} \pm K_4 I_a) \omega \tag{4.74}$$

The plus sign pertains to a cumulative compound motor and the minus sign pertains to a differential compound motor. We now have the ingredients necessary for performance analysis of a compound motor.

The variation of P_a with I_a is easily obtained from Eqs. (4.69) and (4.71) as

$$P_a = [V_t - I_a(R_s + R_a)]I_a \tag{4.75}$$

This is of the same form as for the series- and shunt ($R_s = 0$) -motor cases, with identical conclusions as to the maximum value of the armature-developed power and linear variation of P_a with I_a for small-resistance voltage drops.

Using Eqs. (4.71) to (4.73), we have

$$T_a = K_1 \phi_f I_a \tag{4.76}$$

Substituting for ϕ_f from Eq. (4.67) or (4.68), we conclude that the armature-developed (internal) torque is given by

$$T_a = K_1 (K_3 I_{sh} \pm K_4 I_a) I_a \tag{4.77}$$

Equation (4.77) shows us that the torque developed by a compound motor exhibits a characteristic that combines both a shunt-motor and a series-motor characteristic, as shown in Fig. 4.19. For a cumulative compound motor the torque will be higher than that from a shunt motor with the same armature current. For a differential compound motor, the developed torque is lower than that for a shunt motor with the same armature current.

The motor speed ω can be expressed in terms of armature current using Eqs. (4.74) and (4.69) as

$$\omega = \frac{V_t - I_a(R_s + R_a)}{K_1 (K_3 I_{sh} \pm K_4 I_a)} \tag{4.78}$$

For a cumulative compound motor (with plus sign), as the motor load is increased, I_a increases and the numerator of Eq. (4.78) decreases while the denominator increases. Thus the drop in speed of a cumulative compound motor is at a faster rate than the speed of the shunt motor, as shown in Fig. 4.20.

www.EngineeringEBooksPdf.com

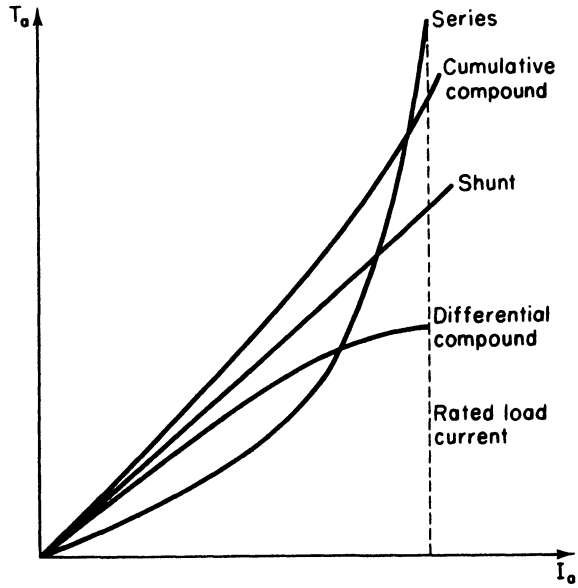


Figure 4.19 Comparison of developed torque versus armature current for dc motor connections.

A differential compound connection is rarely used in practice, as this connection is *inherently unstable*, as is shown presently. Let us rewrite Eq. (4.78) for a differential connection:

$$\omega = \frac{V_t - I_a(R_s + R_a)}{K_1(K_3 I_{sh} - K_4 I_a)} \tag{4.79}$$

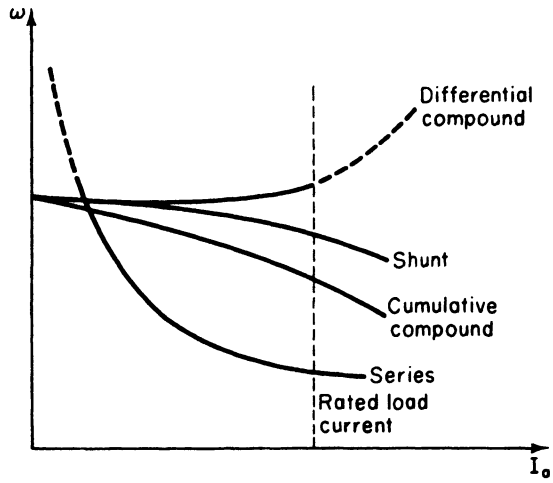


Figure 4.20 Comparison of speed versus armature current characteristics for dc motor connections.

www.EngineeringEBooksPdf.com

The denominator will decrease as I_a (motor load) is increased. The speed will increase and a runaway condition can exist if $(K_3 I_{sh} - K_4 I_a)$ approaches zero.

Some useful relationships can be derived from the torque and speed equations [Eqs. (4.77) and (4.78)]. Let us rewrite Eq. (4.77) for a cumulative motor as

$$T_a = K_1 K_3 I_{sh}(1 + \beta I_a) I_a \tag{4.80}$$

where

$$\beta = \frac{K_4}{K_3 I_{sh}} \tag{4.81}$$

If the motor develops a torque T_{a1} for an armature current I_{a1} and a torque T_{a2} for an armature current I_{a2}, Eq. (4.80) leads to

$$\frac{T_{a_1}}{T_{a_2}} = \frac{(1 + \beta I_{a_1}) I_{a_1}}{(1 + \beta I_{a_2}) I_{a_2}} \tag{4.82}$$

Similarly, we write Eq. (4.78) as

$$\omega = \frac{V_t - I_a(R_s + R_a)}{K_1 K_3 I_{sh}(1 + \beta I_a)} \tag{4.83}$$

From Eq. (4.83) we can conclude that

$$\frac{\omega_1}{\omega_2} = \frac{V_t - I_{a_1}(R_s + R_a)}{V_t - I_{a_2}(R_s + R_a)} \frac{(1 + \beta I_{a_2})}{(1 + \beta I_{a1})} \tag{4.84}$$

In eq. (4.84), ω_1 is the speed corresponding to armature current, I_{a1}, and ω_2 is the speed corresponding to armature current, I_{a2}.

The preceding relations are based on the assumption that β of Eq. (4.81) is available. The value of β can be obtained using the following procedure. Assume that the motor is run as a shunt motor with a torque T_{sh} corresponding to an armature current I_a. In this case we have

$$T_{sh} = K_1 K_3 I_{sh} I_a \tag{4.85}$$

The motor is then connected as a cumulative compound connection and the armature current is adjusted to the same value I_a obtained with shunt operation. The corresponding torque is T_c and given by

$$T_c = K_1 K_3 I_{sh}(1 + \beta I_a) I_a \tag{4.86}$$

Equations (4.85) and (4.86) yield

$$\frac{T_c}{T_{sh}} = 1 + \beta I_a \tag{4.87}$$

www.EngineeringEBooksPdf.com

Thus β is found as

$$\beta = \frac{1}{I_a}\left(\frac{T_c}{T_{sh}} - 1\right) \tag{4.88}$$

An example is appropriate at this junction.

Example 4.9 A cumulative compound motor is operated as a shunt motor and develops a torque of 2000 N·m when the armature current is 140 A. When reconnected as a cumulative compound motor at the same current, it develops a torque of 2400 N·m. Find the torque when the compound motor load is increased such that the armature current is increased by 10%.

Solution We use Eq. (4.88) to obtain

$$\beta I_{a_1} = \frac{2400}{2000} - 1 = 0.2$$

We now have

$$I_{a_2} = I_{a_1}(1.1)$$

As a result, we use Eq. (4.82) to obtain

$$\frac{T_{a_1}}{T_{a_2}} = \frac{(1 + 0.2)140}{[1 + 1.1(0.2)](1.1 \times 140)}$$
$$= \frac{1.2}{1.1(1.22)} = 0.8942$$

But

$$T_{a_1} = 2400\,\text{N} \cdot \text{m}$$

Thus

$$T_{a_2} = \frac{2400}{0.8942} = 2684\ \text{N} \cdot \text{m}$$

Clearly, the developed torque increases with an increase in armature current. The following example deals with the speed variations for the motor considered in this example.

Example 4.10 Assume that the combined armature and series field resistance of the motor of Example 4.9 is 0.16 Ω. Assume that the terminal voltage is 600 V.

www.EngineeringEBooksPdf.com

Let the motor speed be 1200 rpm when operating as a cumulative compound motor with an armature current of 140 A. Find the speed corresponding to an armature current of 110% of 140 A.

Solution A direct application of Eq. (4.84) is all that we need:

$$\frac{\omega_1}{\omega_2} = \frac{600 - 0.16(140)}{600 - 0.16(140 \times 1.1)} \left[\frac{1 + 0.2(1.1)}{1 + 0.2}\right]$$
$$= 1.004$$

With

$$n_1 = 1200 \text{ rpm}$$

then

$$n_2 = \frac{n_1}{1.004} = 1195.346 \text{ rpm}$$

Clearly, the motor speed drops with an increase in armature current.

4.7.1 Torque–Speed Characteristic

The torque–speed characteristic for a compound motor is slightly more involved than that of the series and shunt cases. The torque developed can be written on the basis of Eq. (4.77) as

$$T_a = T_{\text{sh}} + T_s$$

where

$$T_{\text{sh}} = K_1 K_3 I_{\text{sh}} I_a$$
$$T_s = K_1 K_4 I_a^2$$

The armature current can be obtained from Eq. (4.78) as a function of ω as

$$I_a = \frac{V_t - K_1 K_3 I_{\text{sh}} \omega}{R_a + R_s + K_1 K_4 \omega} \tag{4.89}$$

As a result, we conclude that

$$T_a = K_1 \left[K_3 I_{\text{sh}} \frac{V_t - K_1 K_3 I_{\text{sh}} \omega}{R_a + R_s + K_1 K_4 \omega} + K_4 \frac{(V_t - K_1 K_3 I_{\text{sh}} \omega)^2}{(R_a + R_s + K_1 K_4 \omega)^2}\right] \tag{4.90}$$

www.EngineeringEBooksPdf.com

The torque is clearly composed of two components T_{sh} and T_s related to shunt- and series-field contributions. It must be observed, however, that T_{sh} contains a component due to the series-field effect and similarly for T_s.

4.8 MOTOR AND LOAD MATCHING

The torque–speed characteristic of a dc motor depends on the motor connection. For a series motor we concluded in Eq. (4.31) that

$$T_a = \frac{K_1 K_2 V_t^2}{[K_1 K_2 \omega + (R_a + R_s)]^2} \tag{4.91}$$

The constant K_1K_2 is obtained from the defining relation for back EMF given by

$$E_c = K_1 K_2 I_a \omega \tag{4.92}$$

For a shunt motor we have, by Eq. (4.60),

$$T_a = \frac{K_{sh}^2}{R_a}(\omega_0 - \omega) \tag{4.93}$$

where

$$\omega_0 = \frac{V_t}{K_{sh}} \tag{4.94}$$

The constant K_{sh} can be obtained on the basis of

$$E_c = K_{sh}\omega \tag{4.95}$$

The cumulative compound motor torque–speed characteristic is given by

$$T_a = K_1 \left[K_3 I_{sh} \frac{V_t - K_1 K_3 I_{sh}\omega}{R_a + R_s + K_1 K_4 \omega} + K_4 \frac{(V_t - K_1 K_3 I_{sh}\omega)^2}{(R_a + R_s + K_1 K_4 \omega)^2} \right] \tag{4.96}$$

where the constants are defined by the back EMF relation

$$E_c = K_1(K_3 I_{sh} + K_4 I_a)\omega \tag{4.97}$$

Mechanical loads driven by motors have their own torque–speed characteristics, depending on the application. The load torque–speed characteristic is determined experimentally and can be classified as follows:

1. Constant torque load as in extruder drives
2. Torque that increases linearly with speed

www.EngineeringEBooksPdf.com

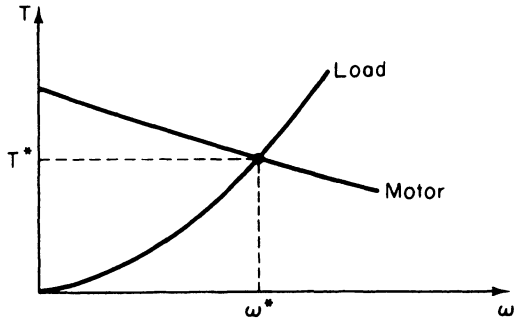


Figure 4.21 Matching motor and load torque–speed characteristics.

3. Constant power load, as in reeling drives
4. Torque varying as speed squared, as in fan drives

In general, the load torque–speed characteristic is written as

$$T_l = f_l(\omega) \tag{4.98}$$

The intersection of the two torque–speed characteristics for motor and load provide us with the values of torque and the corresponding speed for operation, as shown in Fig. 4.21. Examples should clarify these points.

Example 4.11 The combined armature and series-field resistance of a dc series motor is 0.15 Ω. The motor operates from a 250-V supply, drawing an armature current of 85 A at a speed of 62.83 rad/s. Establish the torque–speed characteristic of the motor. Find the torque and speed when driving a constant power load with the characteristic

$$T_l = \frac{21.334 \times 10^3}{\omega}$$

Solution We note at the outset that we can solve the problem by assuming that armature-developed power is 21.334×10^3 W and apply techniques already known to us. We opt, however, for the following solution procedure.

We have

$$V_t = 250\,\text{V} \qquad I_a = 85\,\text{A} \quad \text{at } 62.83\,\text{rad/s}$$

Thus

$$E_c = 250 - (85)(0.15) = 237.25\,\text{V}$$

$$K_1 K_2 = \frac{237.25}{85(62.83)} = 44.424 \times 10^{-3}$$

www.EngineeringEBooksPdf.com

As a result,

$$T_a = \frac{2.7765 \times 10^3}{(44.424 \times 10^{-3}\omega + 0.15)^2}$$

To match the load, we require that

$$\frac{2.7765 \times 10^3}{(44.424 \times 10^{-3}\omega + 0.15)^2} = \frac{21.334 \times 10^3}{\omega}$$

Thus

$$1.9735 \times 10^{-3}\omega^2 - 116.82 \times 10^{-3}\omega + 22.5 \times 10^{-3} = 0$$

The solution for ω is

$$\omega^* = 59.00 \text{ rad/s}$$

The corresponding torque is

$$T^* = 361.59 \text{ N} \cdot \text{m}$$

Example 4.12 A 120-V dc shunt motor has an armature resistance of 0.1 Ω and develops a torque of 111.16 N·m when running at 1100 rpm. Neglecting rotational losses, it is required to:

(a) Establish the torque–speed characteristic of this motor
(b) Find the developed torque at a speed of 1150 rpm
(c) Find the motor speed when the developed torque is 30 N·m
(d) Find the motor speed when it drives a load with the following torque–speed characteristic:

$$T_l = 6.2778\sqrt{\omega}$$

(e) Calculate the torque, armature-developed power, and armature current for the conditions of part (d)
(f) Assuming that the field resistance is 120 Ω, find the line current and the power input for the load conditions of part (d)

Solution

(a) We have

$$V_t = 120 \text{ V} \qquad T = 111.16 \text{ N} \cdot \text{m} \quad \text{at 1100 rpm}$$
$$R_a = 0.1 \text{ Ω}$$

www.EngineeringEBooksPdf.com

The power developed by the armature can be calculated as

$$P_a = 111.16\left(\frac{2\pi}{60}1100\right) = 12.805 \times 10^3\,\text{W}$$

But

$$P_a = (V_t - I_a R_a)I_a$$

Thus

$$12.805 \times 10^3 = (120 - 0.1I_a)I_a$$

As a result,

$$0.1I_a^2 - 120I_a + 12.805 \times 10^3 = 0$$

$$I_a = 118.39\,\text{A}$$

$$E_c = 120 - 0.1(118.39) = 108.16\,\text{V}$$

$$K_{\text{sh}} = \frac{E_c}{\omega} = \frac{108.16}{(2\pi/60)(1100)} = 938.97 \times 10^{-3}$$

$$\omega_0 = \frac{V_t}{K_{\text{sh}}} = 127.8\ \text{rad/s}$$

$$\frac{K_{\text{sh}}^2}{R_a} = 8.8166$$

We can conclude that

$$T_a = 8.8166(127.8 - \omega)$$

(b) For $n = 1150$ rpm, we get

$$T_a = 8.8166\left[127.8 - \frac{2\pi}{60}(1150)\right] = 64.998\,\text{N} \cdot \text{m}$$

(c) For $T_a = 30\ \text{N} \cdot \text{m}$,

$$30 = 8.8166(127.8 - \omega)$$

As a result,

$$\omega = 124.4\ \text{rad/s}$$

www.EngineeringEBooksPdf.com

(d) For a load with the torque–speed characteristic

$$T_l = 6.2778\sqrt{\omega}$$

to match, we have

$$6.2778\sqrt{\omega} = 8.8166(127.8 - \omega)$$

Thus

$$0.507 \times 10^{-3}\omega = (127.8 - \omega)^2$$

or

$$\omega^2 - 256.11\omega + 16.333 \times 10^3 = 0$$

The solution is

$$\omega = 119.95 \text{ rad/s}$$

(e) The torque is obtained from

$$T_l = 6.2778\sqrt{119.98} = 68.764 \text{ N} \cdot \text{m}$$

The armature-developed power is

$$P_a = T_l\omega = 8.2503 \times 10^3 \text{ W}$$

Thus we use

$$P_a = (V_t - I_a R_a)I_a$$

To obtain I_a:

$$8.2503 \times 10^3 = (120 - 0.1I_a)I_a$$

or

$$0.1I_a^2 - 120I_a + 8.250 \times 10^3 = 0$$

As a result,

$$I_a = 73.22 \text{ A}$$

www.EngineeringEBooksPdf.com

(f) The field current is calculated as

$$I_f = \frac{120}{120} = 1 \text{ A}$$

Thus

$$\begin{aligned} I_L &= I_a + I_f \\ &= 74.22 \text{ A} \end{aligned}$$

The power input is

$$\begin{aligned} P_{\text{in}} &= V_t I_L \\ &= 120(74.22) \\ &= 8.9064 \times 10^3 \text{ W} \end{aligned}$$

4.9 CONVENTIONAL SPEED CONTROL OF dc MOTORS

There are many applications where the speed of a dc motor is required to vary within a prescribed range for a given load. A number of methods are available for controlling the speed of a dc motor. The general idea stems from the basic relations

$$E_c = V_a - I_a R_a \tag{4.99}$$

$$E_c = K_1 \phi_f \omega \tag{4.100}$$

As a result, we can see that the angular speed is given by

$$\omega = \frac{V_a - I_a R_a}{K_1 \phi_f} \tag{4.101}$$

It is clear that a change in the applied armature voltage will result in a change in speed. Two major means are available to achieve these changes. The first involves use of an adjustable voltage source, while the next employs variable resistors to affect the required changes. Next, we discuss some of the options, starting with the dc series motor.

4.9.1 Series Motor Speed Control

The methods used to control the speed of a dc series motor include: (1) series resistance voltage control, (2) armature shunt resistance current control, (3) series and shunt armature resistance control, (4) shunt diverter in parallel with the series field, and (5) line-voltage control. We discuss each of these methods in turn.

www.EngineeringEBooksPdf.com

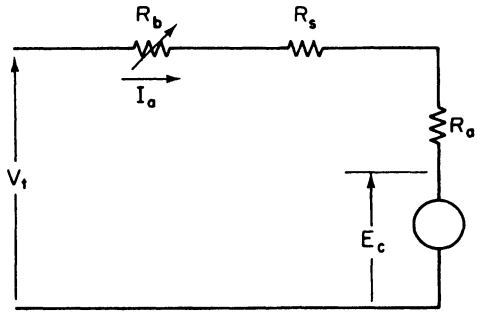


Figure 4.22 dc series motor speed control by series resistance.

Series Resistance Voltage Control The simplest means for adjusting the speed of a dc series motor is to insert a variable resistance R_b in series with the armature and series-field circuit, as shown in Fig. 4.22. The effect of the additional resistance can be seen from the torque–speed relation

$$T_a = \frac{K_1 K_2 V_t^2}{[K_1 K_2 \omega_A + (R_a + R_s)]^2} \tag{4.102}$$

With resistance R_b, we get

$$T_a = \frac{K_1 K_2 V_t^2}{[K_1 K_2 \omega_B + (R_a + R_s + R_b)]^2} \tag{4.103}$$

It is clear that the torque–speed characteristic is shifted to a lower position by increasing R_b. Stated differently, for the same torque, we have

$$K_1 K_2 \omega_A + (R_a + R_s) = K_1 K_2 \omega_B + (R_a + R_s + R_b)$$

Thus

$$\omega_B = \omega_A - \frac{R_b}{K_1 K_2} \tag{4.104}$$

The angular speed ω_B is less than ω_A, corresponding to no additional resistances, as shown in Fig 4.23.

Example 4.13 A dc series motor is rated at 250 V and has a combined armature and series-field resistance of 0.15 Ω. The constant $K_1 K_2$ is found to be

$$K_1 K_2 = 44.424 \times 10^{-3} \text{ V/A} \cdot \text{rads/s}$$

www.EngineeringEBooksPdf.com

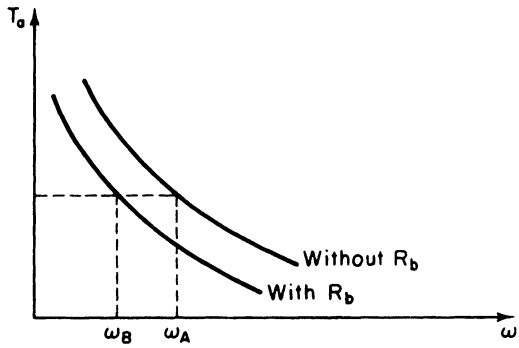


Figure 4.23 Effect of series resistance on torque–speed characteristic of series motor.

The motor drives a load with characteristic

$$T_l = \frac{21.334 \times 10^3}{\omega}$$

It is desired to drive the load at 55 rad/s. Find the required value of a series resistance, R_b, to achieve this requirement.

Solution The motor torque with R_b inserted in series with the field is

$$T_a = \frac{44.424 \times 10^{-3}(250)^2}{(0.15 + R_b + 44.424 \times 10^{-3}\omega)^2}$$

With $\omega = 55$ rad/s, the load torque is

$$T_l = \frac{21.334 \times 10^3}{55} = 387.89 \text{ N} \cdot \text{m}$$

To match the load, we have

$$387.89 = \frac{2.7765 \times 10^3}{(R_b + 2.5933)^2}$$

Thus we get

$$R_b = 0.0821\ \Omega$$

Armature Shunt Resistance Current Control In this method a shunt resistance, R_c, is placed in parallel with the armature circuit, as shown in Fig. 4.24. The line current passes through the series-field winding. The armature current, I_a, is less than the series-field current due to the presence of R_c.

www.EngineeringEBooksPdf.com

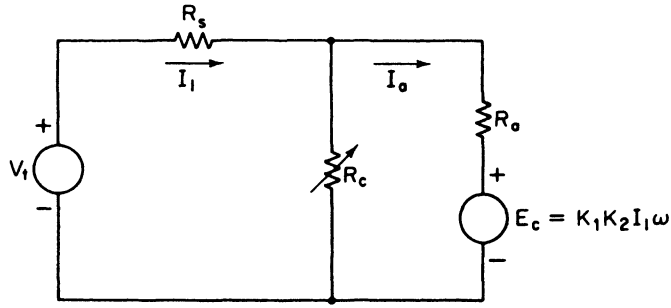


Figure 4.24 Armature shunt resistance current control equivalent circuit.

The armature's developed torque is given by

$$T_a = \frac{E_c I_a}{\omega} \tag{4.105}$$

The back EMF is given by

$$E_c = K_1 \phi_f \omega = K_1 K_2 I_l \omega \tag{4.106}$$

Note that the field flux is proportional to the current I_l passing through the series-field resistance. As a result, the torque is given by

$$T_a = K_1 K_2 I_l I_a \tag{4.107}$$

We can obtain I_l and I_a using the following two loop equations obtained form the circuit of Fig. 4.24

$$V_t = I_l R_s + I_a R_a + K_1 K_2 \omega I_l \tag{4.108}$$

$$V_t = I_l R_s + (I_l - I_a) R_c \tag{4.109}$$

Solving the two equations, we get

$$I_a = \frac{V_t(R_c - K_1 K_2 \omega)}{\Delta} \tag{4.110}$$

$$I_l = \frac{V_t(R_a + R_c)}{\Delta} \tag{4.111}$$

where

$$\Delta = R_a(R_s + R_c) + R_c(R_s + K_1 K_2 \omega) \tag{4.112}$$

As a result, the torque is given by the compact form

$$T_a = \frac{K_1 K_2 V_t^2}{\Delta^2}(R_a + R_c)(R_c - K_1 K_2 \omega) \tag{4.113}$$

www.EngineeringEBooksPdf.com

The torque can be written as

$$T_a = \frac{K_1 K_2 V_t^2 (R_c - K_1 K_2 \omega)}{(R_a + R_c)\{R_s + [R_c/(R_a + R_c)](R_a + K_1 K_2 \omega)\}^2} \tag{4.114}$$

This form allows us to explore some cases of interest. First, without R_c, we should expect the familiar series motor torque–speed formula. With the R_c open circuit, we have R_c approaching infinity. The resulting expression is

$$\lim_{R_c \to \infty} T_a = \lim_{R_c \to \infty} \frac{K_1 K_2 V_t^2 (1 - K_1 K_2 \omega / R_c)}{(1 + R_a/R_c)\{R_s + [1/(1 + R_a/R_c)](R_a + K_1 K_2 \omega)\}^2}$$

$$= \frac{K_1 K_2 V_t^2}{(R_s + R_a + K_1 K_2 \omega)^2} \tag{4.115}$$

This is exactly the result for a dc series motor. The second case of interest is for $R_c = 0$. The result is

$$\lim_{R_c \to 0} T_a = \frac{-(K_1 K_2)^2 V_t^2 \omega}{R_a R_s^2}$$

This result leads us to conclude that the direction of rotation may be reversed for small values of R_c. This is not surprising, since for $R_c = 0$, as can be seen from the equivalent circuit,

$$I_l|_{R_c = 0} = \frac{V_t}{R_s} \tag{4.116}$$

$$I_a|_{R_c = 0} = \frac{-E_c}{R_a} = -\frac{K_1 K_2 I_l \omega}{R_a} = -\frac{K_1 K_2 V_t \omega}{R_a R_s} \tag{4.117}$$

If the armature and series-field resistances are neglected, the torque is approximately given by

$$T_a \cong \frac{V_t^2}{K_1 K_2} \left(\frac{1}{\omega^2} - \frac{K_1 K_2}{\omega R_c} \right) \tag{4.118}$$

It is clear that reducing R_c reduces the torque for a constant speed. Conversely, with a constant torque, a reduction in R_c reduces the speed ω. These effects are shown in Fig. 4.25.

Example 4.14 Assume that the speed of the series motor of Example 4.13 is controlled to the same specifications, but now we use an armature shunt resistance control scheme. Find the required value of R_c, given that $R_a = 0.1\,\Omega$.

www.EngineeringEBooksPdf.com

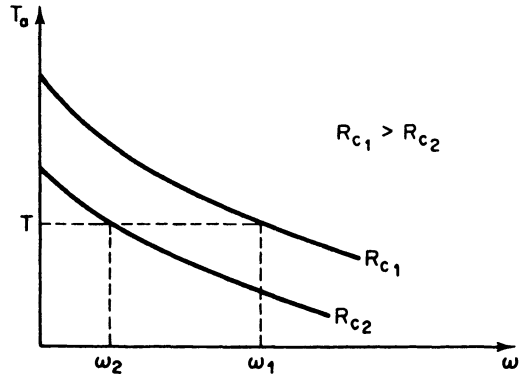


Figure 4.25 Effect of armature shunt resistance R_c on torque–speed characteristic of dc series motor.

Solution Our specifications call for

$$T_l = 387.89 \text{ N} \cdot \text{m}$$
$$\omega = 55 \text{ rad/s}$$

We are given that

$$R_a = 0.1\,\Omega$$

Thus

$$R_s = 0.05\,\Omega$$

We use the torque expression

$$T_a = \frac{K_1 K_2 V_t^2 (R_c - K_1 K_2 \omega)}{(R_a + R_c)\{R_s + [R_c/(R_a + R_c)](R_a + K_1 K_2 \omega)\}^2}$$

We thus have

$$387.89 = \frac{2.7765 \times 10^3 (R_c - 2.4433)}{(0.1 + R_c)\{0.5 + [R_c/(0.1 + R_c)](2.5433)\}^2}$$

After a few manipulations, we obtain

$$R_c^2 - 38.799 R_c - 4.0393 = 0$$

The required answer is obtained as

$$R_c = 38.903\,\Omega$$

www.EngineeringEBooksPdf.com

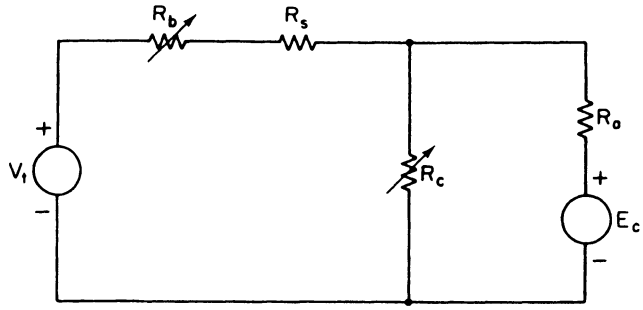


Figure 4.26 Series and shunt armature resistance control of a dc series motor.

Series and Shunt Armature Resistance Control In this method a combination of methods 1 and 2 is employed. As shown in Fig. 4.26, a resistance R_b is placed in series with the series-field winding, while a shunt resistance R_c is placed in parallel with the armature circuit.

It is clear that the torque–speed relation for this case can be obtained form the previous analysis simply by replacing R_s by $(R_s + R_b)$. The result is

$$T_a = \frac{K_1 K_2 V_t^2 (R_c - K_1 K_2 \omega)}{(R_a + R_c)\{R_s + R_b + [R_c/(R_a + R_c)](R_a + K_1 K_2 \omega)\}^2} \tag{4.119}$$

For a constant torque, increasing R_b reduces the speed, while decreasing R_c reduces the speed.

Example 4.15 For the motor of Example 4.13, suppose that a resistance $R_c = 50\,\Omega$ is available. It is now decided to use series and shunt armature resistance control to achieve the required specifications. Find the value of the required R_b.

Solution With $R_c = 50\ \Omega$, our torque equation becomes

$$387.89 = \frac{2.7765 \times 10^3 (50 - 2.4433)}{(50.1)[0.05 + R_b + (50/50.1)(2.5433)]^2}$$

We solve for R_b to obtain

$$R_b = 18.419 \times 10^{-3}\,\Omega$$

Shunt Diverter In this method a diverter resistance R_d is placed in shunt with the series-field winding, as shown in Fig. 4.27. The line current is equal to the armature current in this case, but the field current is less.

www.EngineeringEBooksPdf.com

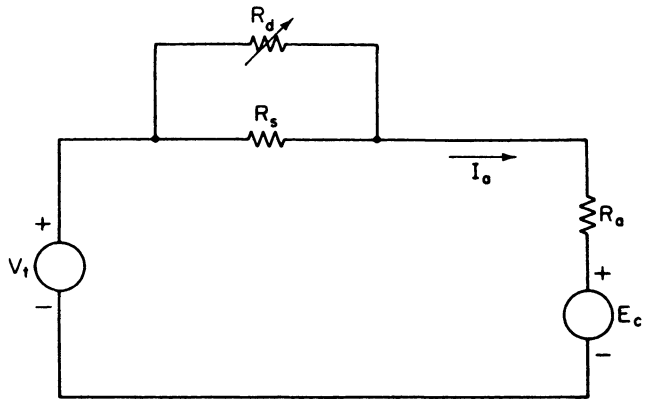


Figure 4.27 Shunt-diverter speed control of dc series motor.

The developed torque is given by

$$T_a = K_1 K_2 I_s I_a \tag{4.120}$$

But from the circuit, we have

$$I_s = \frac{R_d}{R_s + R_d} I_a \tag{4.121}$$

Thus

$$T_a = K_1 K_2 \frac{R_d}{R_s + R_d} I_a^2 \tag{4.122}$$

From the circuit we can show that

$$V_t = E_c + I_a \left(R_a + \frac{R_d R_s}{R_d + R_s} \right) \tag{4.123}$$

But

$$E_c = K_1 K_2 I_a \frac{R_d}{R_d + R_s} \omega \tag{4.124}$$

Therefore,

$$I_a = \frac{V_t}{R_a + [R_d R_s/(R_d + R_s)] + [K_1 K_2 R_d \omega/(R_d + R_s)]} \tag{4.125}$$

www.EngineeringEBooksPdf.com

As a result, we conclude that

$$T_a = \frac{K_1 K_2 \alpha V_t^2}{[R_a + \alpha(R_s + K_1 K_2 \omega)]^2} \tag{4.126}$$

where

$$\alpha = \frac{R_d}{R_s + R_d} \tag{4.127}$$

If we assume that R_a and R_s are negligible, we can write

$$T_a \cong \frac{V_t^2}{\alpha K_1 K_2 \omega^2} \tag{4.128}$$

Since $\alpha < 1$, we realize that for the same speed, the torque is increased by use of the diverter.

Example 4.16 Assume that a diverter is used with the motor of Example 4.13, such that $\alpha = 0.9$. For the speed of 55 rad/s, find the resulting torque.

Solution The torque developed is obtained as

$$T_a = \frac{2.7765 \times 10^3 (0.9)}{[0.1 + 0.9(0.05 + 2.5433)]^2}$$

As a result, we conclude that

$$T_a = 421.8 \text{ N} \cdot \text{m}$$

Note that this torque is higher than that without the diverter.

Line-Voltage Control The torque–speed characteristic can be changed simply by adjusting the supply voltage V_t. This can be facilitated by using solid-state drives, as discussed later.

4.9.2 Shunt-Motor Speed Control

Many methods exist to control the speed of a dc shunt motor. Among them, we have (1) field resistance control, (2) shunt-field and series armature resistance control, (3) series and shunt armature resistance control, and (4) line-voltage control. Each of these methods is discussed in turn.

Field Resistance Control In this method a variable resistance R_e is inserted in series with the field winding. The effect of an increasing R_e is to decrease the current in the field. Figure 4.28 shows the shunt motor's equivalent circuit in this case. The

www.EngineeringEBooksPdf.com

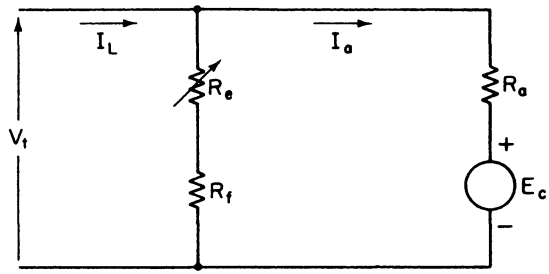


Figure 4.28 Field resistance control for a shunt dc motor.

following analysis provides us with the torque–speed characteristic with R_e included.

The back EMF is given by

$$E_c = K_1 K_2 \frac{V_t}{R_e + R_f} \omega \tag{4.129}$$

Recall that without R_e, the constant K_{sh} was defined as

$$K_{sh} = K_1 K_2 \frac{V_t}{R_f} \tag{4.130}$$

As a result, we write

$$E_c = K_{sh} \frac{R_f}{R_e + R_f} \omega \tag{4.131}$$

The developed torque is thus

$$T_a = K_{sh} \frac{R_f}{R_e + R_f} I_a \tag{4.132}$$

The armature current is obtained from

$$E_c = V_t - I_a R_a$$

Thus

$$I_a = \frac{V_t - (K_{sh} R_f \omega / R_e + R_f)}{R_a}$$

The torque–speed relation can thus be obtained as

$$\omega = \omega_0 \left(1 + \frac{R_e}{R_f}\right) - \left(1 + \frac{R_e}{R_f}\right)^2 \frac{R_a}{K_{sh}^2} T_a \tag{4.133}$$

www.EngineeringEBooksPdf.com

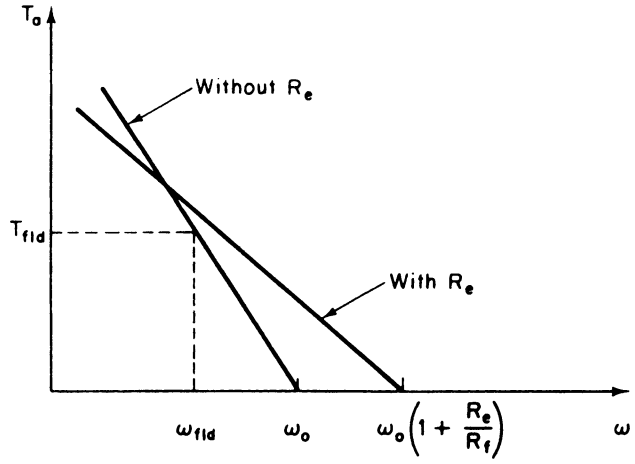


Figure 4.29 Torque–speed characteristic of a dc shunt motor with field resistance control.

where

$$\omega_0 = \frac{V_t}{K_{sh}} \tag{4.134}$$

The result of the foregoing development is that the torque–speed characteristic is still a straight line, as shown in Fig. 4.29. The effect of the additional field resistance R_e is to increase the speed at zero torque and increase the magnitude of the slope of the line.

Example 4.17 The armature resistance of a dc shunt motor is 0.1 Ω and its shunt-field resistance is 120 Ω. The value of ω_0 is 127.8 rad/s and the constant K_{sh} is 0.93897. The motor torque is 65 N·m. Find the value of R_e for the motor to run at 1100 rpm carrying this load.

Solution We use

$$\omega = \omega_0 x - x^2\left(\frac{R_a}{K_{sh}^2}T_a\right)$$

where

$$x = 1 + \frac{R_e}{R_f}$$

Thus

$$\frac{2\pi(1100)}{60} = 127.8x - \frac{0.1(65)}{(0.93897)^2}x^2$$

www.EngineeringEBooksPdf.com

As a result,

$$x = 16.381 \quad \text{or} \quad 0.954$$

We take

$$x = 1 + \frac{R_e}{R_f} = 16.381$$

Thus

$$\frac{R_e}{R_f} = 15.381$$

As a result,

$$R_e = 15.381(120) = 1.846 \times 10^3\ \Omega$$

Shunt-Field and Series Armature Resistance Control As indicated in Fig. 4.30, a variable resistance R_b is inserted in series with the armature circuit in addition to the resistance R_e inserted in series with the field winding. The torque-speed relation is given by

$$\omega = \omega_0\left(1 + \frac{R_e}{R_f}\right) - \left(1 + \frac{R_e}{R_f}\right)^2 \frac{R_a + R_b}{K_{sh}^2} T_a \tag{4.135}$$

This is the same expression as that obtained for case 1, but with R_a replaced by $(R_b + R_a)$. The effect of additional R_b is to reduce the speed, as shown in Fig. 4.31.

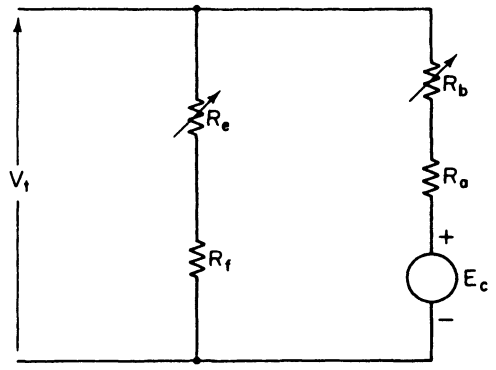


Figure 4.30 Shunt-field and series armature resistance control of a dc shunt motor.

www.EngineeringEBooksPdf.com

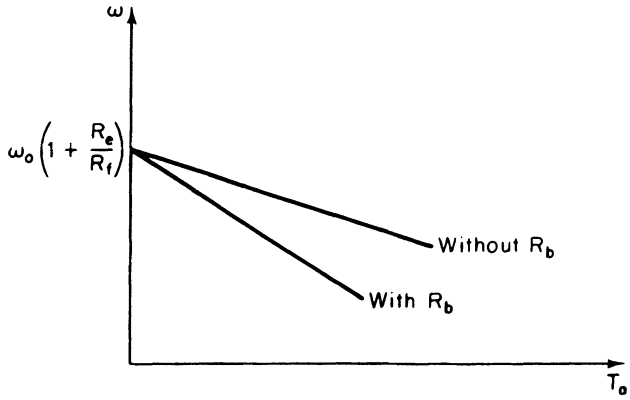


Figure 4.31 Speed–torque characteristic for shunt-field and series armature resistance control.

Example 4.18 For the motor of Example 4.17, suppose that $R_e = 1.5 \times 10^3\,\Omega$. Now we want to achieve the same results, but with shunt-field and series armature resistance control. Find the required value of R_b.

Solution We use

$$\omega = \omega_0\left(1+\frac{R_e}{R_f}\right) - \left(1+\frac{R_e}{R_f}\right)^2 \frac{R_a + R_b}{K_{\text{sh}}^2} T_a$$

Thus

$$115.19 = 127.8\left(1+\frac{1500}{120}\right) - \left(1+\frac{1500}{120}\right)^2 \frac{(R_a + R_b)65}{(0.93897)^2}$$

As a result,

$$R_a + R_b = 0.11983$$

The required value of R_b is then

$$R_b \cong 0.02\,\Omega$$

Series and Shunt Armature Resistance Control As shown in Fig. 4.32, the armature circuit is shunted by the resistance R_c in addition to the resistance R_b inserted in series with the armature. The back EMF E_c is given by

$$E_c = K_{\text{sh}}\omega \tag{4.136}$$

www.EngineeringEBooksPdf.com

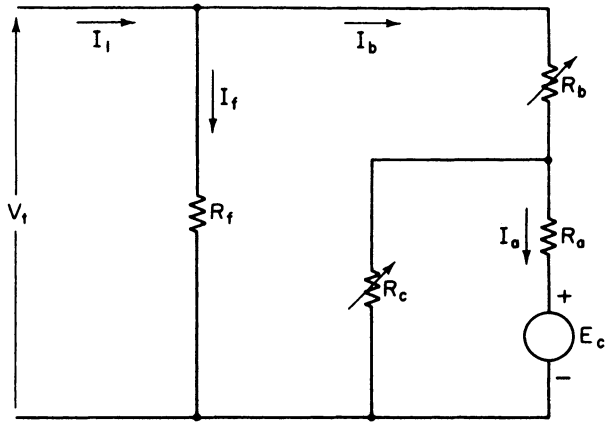


Figure 4.32 Series and shunt armature resistance speed control of a dc shunt motor.

The torque developed by the armature is therefore given by

$$T_a = K_{sh} I_a \tag{4.137}$$

The armature current I_a is obtained by solving the following two loop equations:

$$V_t - E_c = R_a I_a + R_b I_b \tag{4.138}$$

$$V_t = -R_c I_a + (R_b + R_c) I_b \tag{4.139}$$

The solution for I_a is

$$I_a = \frac{R_c V_t - (R_b + R_c) E_c}{R_a (R_b + R_c) + R_b R_c} \tag{4.140}$$

As a result, we have

$$T_a = \frac{K_{sh}}{R_a (R_b + R_c) + R_b R_c} [R_c V_t - K_{sh} \omega (R_b + R_c)] \tag{4.141}$$

This can be rearranged to

$$\omega = \omega_0 \frac{1}{1 + R_b / R_c} - \frac{R_a + [R_b R_c / (R_b + R_c)]}{K_{sh}^2} T_a \tag{4.142}$$

where

$$\omega_0 = \frac{V_t}{K_{sh}} \tag{4.143}$$

Clearly, increasing R_b and R_c reduces the motor speed.

www.EngineeringEBooksPdf.com

Example 4.19 For the motor of Example 4.17, assume that series and shunt armature resistance control is used with $R_b = 0.03\,\Omega$. Find the value of R_c to obtain a torque of 65 N·m at a speed of 1100 rpm.

Solution Let

$$y = \frac{1}{1 + (R_b/R_c)}$$

Thus

$$\omega = \omega_0 y - \frac{R_a + R_b y}{K_{sh}^2} T_a$$

As a result,

$$115.19 = 127.8y - \frac{(0.1 + 0.3y)65}{(0.93897)^2}$$

The solution for y is

$$y = 0.97591$$

Thus

$$R_c = 1.2152\,\Omega$$

Line-Voltage Control In this case, solid-state drives are used to provide adjustable voltage levels for the armature circuit as well as the field circuit, if desired.

4.9.3 Compound-Motor Speed Control

The mechanisms for speed control of a compound dc motor are similar in basic concept to those employed with a shunt motor. The following methods are discussed briefly: (1) shunt-field resistance control, (2) shunt-field and series armature resistance control, (3) series and shunt armature resistance control, and (4) line-voltage control.

Shunt-Field Series Resistance Control A variable resistance R_e is inserted in series with the shunt-field winding, as shown in the circuit of Fig. 4.33. It is clear that for this case

$$I_{sh} = \frac{V_t}{R_f + R_e} \tag{4.144}$$

www.EngineeringEBooksPdf.com

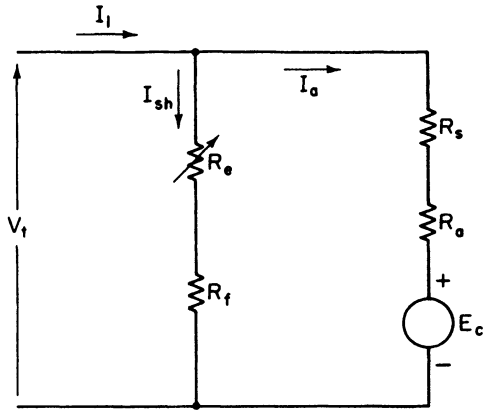


Figure 4.33 Compound-motor speed control through a series resistance in shunt field.

Increasing R_e decreases I_{sh}, and hence the field flux,

$$\phi_f = K_3 I_{sh} + K_4 I_a \tag{4.145}$$

The compound motor's torque–speed relation still applies:

$$T_a = K_1 \left[K_3 I_{sh} \frac{V_t - K_1 K_3 I_{sh} \omega}{R_a + R_s + K_1 K_4 \omega} + K_4 \frac{(V_t - K_1 K_3 I_{sh} \omega)^2}{(R_a + R_s + K_1 K_4 \omega)^2} \right] \tag{4.146}$$

Shunt-Field and Series Armature Resistance Control This arrangement is shown in Fig. 4.34. As was done in the case of a shunt motor, in addition to the series

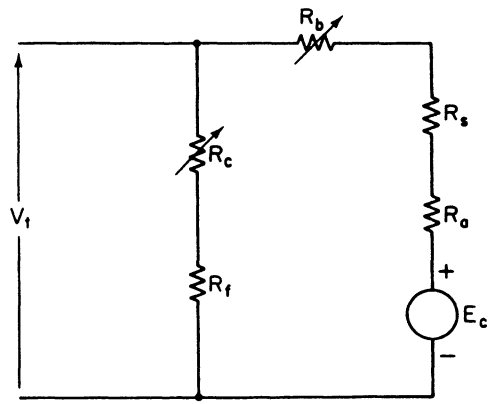


Figure 4.34 Shunt-field and series armature resistance control of a compound motor.

www.EngineeringEBooksPdf.com

resistance in the shunt-field circuit denoted by R_e, we also include the variable resistance, R_b, in series with the armature circuit. It is clear that

$$I_{sh} = \frac{V_t}{R_e + R_f} \tag{4.147}$$

The torque–speed characteristic are modified by replacing $R_s + R_a$ by $R_s + R_a + R_b$ in the expression derived for the straight circuit. As a result, we write

$$T_a = K_1 \left[K_3 I_{sh} \frac{V_t - K_1 K_3 I_{sh} \omega}{R_a + R_s + R_b + K_1 K_4 \omega} + K_4 \frac{(V_t - K_1 K_3 I_{sh} \omega)^2}{(R_a + R_s + R_b + K_1 K_4 \omega)^2} \right] \tag{4.148}$$

Series and Shunt Armature Resistance Control In this case we include R_b and R_c, as shown in Fig. 4.35. We note the similarity of this circuit to the corresponding circuit in use with the shunt motor. We can therefore assert that

$$I_a = \frac{R_c V_t - (R_b + R_s + R_c) E_c}{R_a (R_b + R_s + R_c) + (R_b + R_s) R_c} \tag{4.149}$$

This is obtained by replacing R_b in Eq. (4.140) by $(R_s + R_b)$. We also have that

$$E_c = K_1 (K_3 I_{sh} + K_4 I_b) \omega \tag{4.150}$$

The current I_b is given by

$$I_b = I_a [1 + (R_a / R_c)] + E_c / R_c \tag{4.151}$$

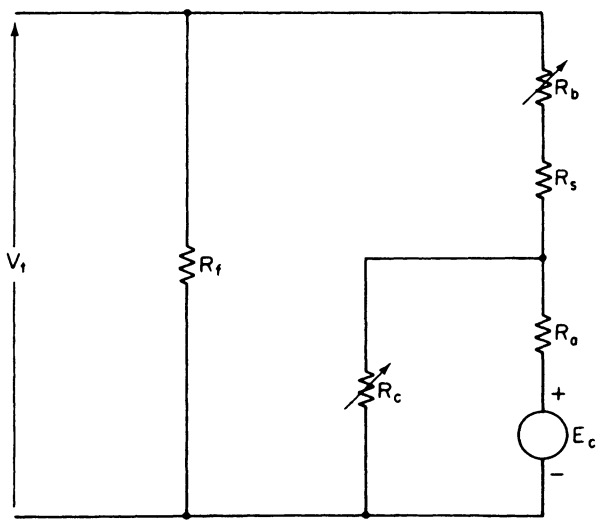


Figure 4.35 Series and shunt armature resistance control of a dc compound motor.

www.EngineeringEBooksPdf.com

Clearly, we have

$$I_{sh} = \frac{V_t}{R_f} \tag{4.152}$$

The torque is given by

$$T_a = K_1(K_3 I_{sh} + K_4 I_b) I_a \tag{4.153}$$

The torque–speed characteristic can thus be obtained by substituting for I_a and I_b in Eq. (4.153).

Line-Voltage Control This is similar in principle to the shunt-motor case, with adjustable voltage being applied to the shunt field as well as the series field and armature circuits.

4.10 REVERSAL OF DIRECTION OF ROTATION

The requirement of reversing the direction of rotation of a dc motor is met by reversing the direction of the armature current with respect to the direction of the magnetic field, or vice versa. Reversal of both circuits will produce the same direction of rotation. As a general rule, it is preferred to reverse the armature current rather than field current, since the field windings are highly inductive, making it necessary to avoid switching before the field stored energy has been fully dissipated.

The mechanism for reversing a dc motor is shown in Fig. 4.36, where reversal of the direction of rotation is achieved through the reversal of the polarity of the voltage applied to the armature circuit using a switch.

Note that in the figure, the block labeled "field circuit" serves as a general-purpose convention where the appropriate circuit (series, shunt, or compound) for field excitation is placed.

It is one of the advantages of dc motors that they can operate in a number of modes according to the four-quadrant operation scheme shown in Fig. 4.37. A summary of the prevailing conditions in the four modes is given in Table 4.1.

4.11 STARTING dc MOTORS

The armature of a dc motor is designed to have a low resistance to minimize the losses and hence improve efficiency. At starting, the speed of the motor is zero, and thus the back EMF, E_c, is zero. The armature current at starting will therefore be high, as can be seen from

$$I_{a_{st}} = \frac{V_a}{R_A}$$

The supply voltage to the dc motor is fixed in many installations and mechanisms for reducing the voltage applied to the armature at starting must be sought. If a variable

www.EngineeringEBooksPdf.com

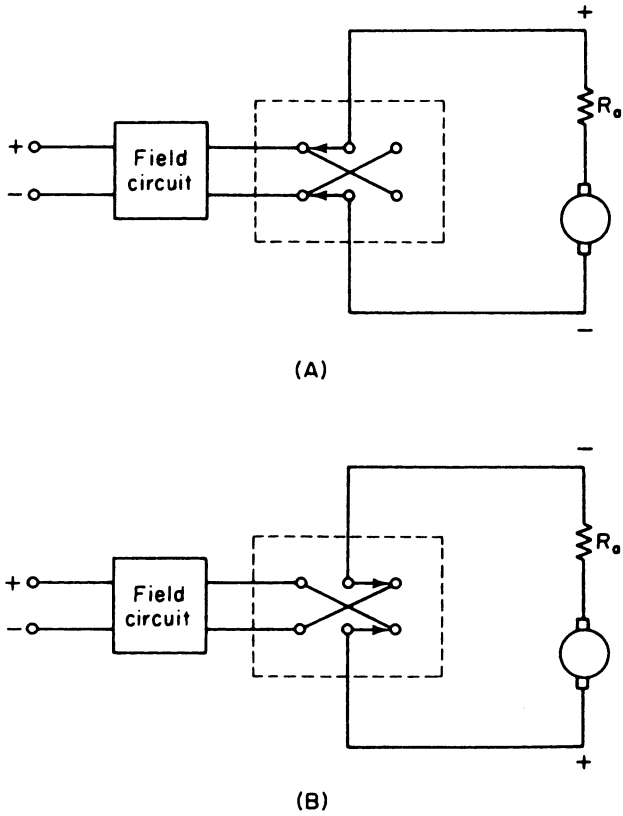


Figure 4.36 Reversal of rotation direction of a dc motor: (a) forward; (b) backward.

dc supply is available, the motor is started at a low voltage, which is then gradually increased as the motor picks up speed. The conventional method for starting, however, involves inserting a large resistance value in the armature circuit at starting and gradually reducing its value as the motor picks up speed.

An interesting design problem is to find the values of the resistance sections to limit the current to acceptable values as the motor is started. Consider the manual starting arrangement shown in Fig. 4.38. The starter is arranged in resistance sections, r_1, r_2, r_3,..., r_{n-1}, with the nth section being the resistance of the armature and series-field resistance. The total resistance available in the circuit at starting ($t = 0$) is denoted by R_1 and is given by

$$R_1 = r_1 + r_2 + r_3 + \cdots + r_n$$

At $t = 0$, the motor is at standstill, and there is no back EMF to oppose the applied voltage V_t. The armature current at $t = 0$ will therefore be given by

$$i_a(0) = \frac{V_t}{R_1}$$

www.EngineeringEBooksPdf.com

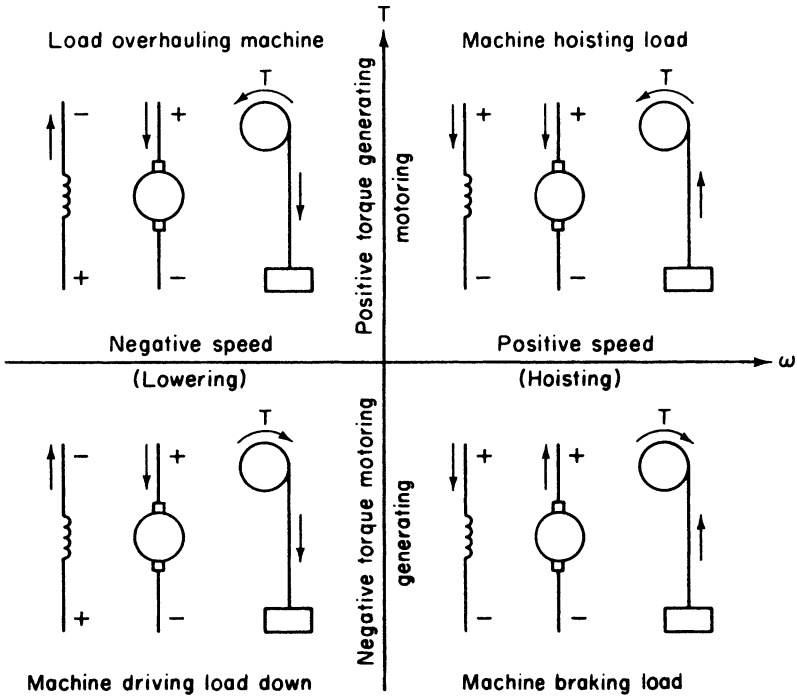


Figure 4.37 Four-quadrant operation of dc machine.

This current value will be assumed to be the maximum allowable, I_{max}. As a result,

$$I_{max} = \frac{V_t}{R_1} \tag{4.154}$$

Immediately following the switching, the rotating motor develops a back EMF that opposes the applied voltage. At $t = t_1^-$, the back EMF is assumed to have reached a value of E_{1_f} while the circuit resistance is still R_1. The armature current

TABLE 4.1 Summary of Four-Quadrant Operation of dc Motor

	Quadrant			
	First	Second	Third	Fourth
Mode Action	Hoisting Motoring	Overhauling Generating	Down drive Motoring	Braking Generating
$(V_t - E_c)$ and I_a	+	−	+	−
P_a	+	−	+	−
T	+	+	−	−
ω	+	−	−	+

www.EngineeringEBooksPdf.com

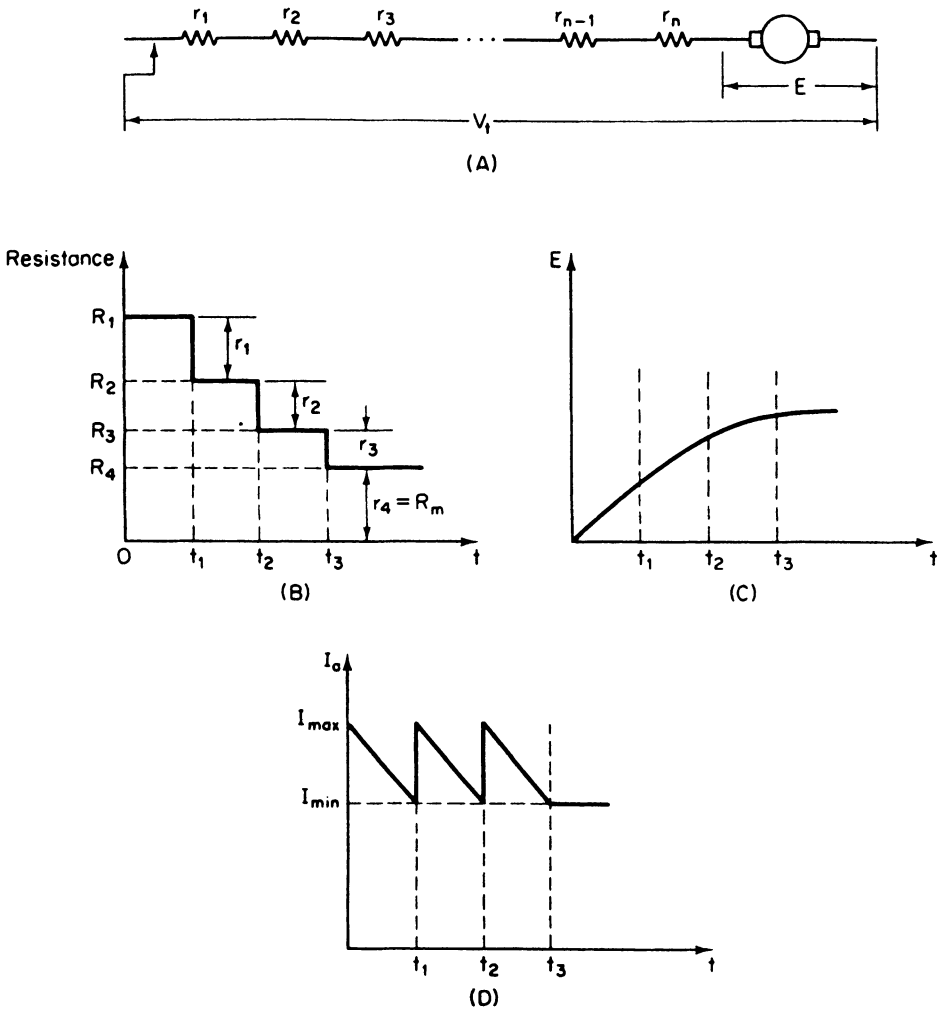


Figure 4.38 dc series motor starter: (a) schematic; (b) resistance-time diagram; (c) EMF buildup; (d) armature current-time diagram.

at that instant is

$$i_a(t_1^-) = \frac{V_t - E_{1_f}}{R_1}$$

This current is smaller than $i_a(0)$, as shown in Fig. 4.38. The value of armature current at t_1^- is assumed to be the specified minimum

$$I_{\min} = i_a(t_1^-) = \frac{V_t - E_{1_f}}{R_1}$$

www.EngineeringEBooksPdf.com

It is now possible to remove one section, r_1, from the circuit by notching up one step. The resistance available is now R_2:

$$R_2 = R_1 - r_1$$

At $t = t_1^+$, the back EMF is E_{2_i} with the subscript 2 referring to the second time interval, and the subscript i referring to initiating the interval. The armature current will rise to the value

$$i_a(t_1^+) = \frac{V_t - E_{2_i}}{R_2}$$

This again will be deemed to be the maximum allowable:

$$I_{\max} = \frac{V_t - E_{2_i}}{R_2}$$

The back EMF will increase in the time interval t_1 to t_2^- with an increase in motor speed. As a result, at t_2^- the current drops to

$$I_{\min} = i_a(t_2^-) = \frac{V_t - E_{2_f}}{R_2}$$

At t_2^+, section r_2 is removed, and the process is continued.

We can now consider the problem of designing resistance steps for a dc motor starter. At the instant, t_k, we have immediately before notching up

$$I_{\min} = \frac{V_t - E_{k_f}}{R_k} \tag{4.155}$$

After notching up, we have

$$I_{\max} = \frac{V_t - E_{(k+1)_i}}{R_{(k+1)}} \tag{4.156}$$

Recall that the back EMF is proportional to the product of speed and flux, and since we cannot expect a change in speed instantaneously, we can conclude that

$$\frac{E_{(k+1)_i}}{E_{k_f}} = \frac{\phi_{\max}}{\phi_{\min}}$$

Let us assume that

$$\frac{\phi_{\max}}{\phi_{\min}} = a$$

www.EngineeringEBooksPdf.com

Thus

$$\frac{E_{(k+1)_i}}{E_{k_f}} = a \tag{4.157}$$

We also define the ratio of maximum and minimum current as K:

$$K = \frac{I_{\max}}{I_{\min}} \tag{4.158}$$

Using Eq. (4.154) eq. (4.155) can be written as

$$E_{k_f} = I_{\max} R_1 - I_{\min} R_k \tag{4.159}$$

Equation (4.156) can be written as

$$E_{(k+1)_i} = I_{\max} R_1 - I_{\max} R_{k+1}$$

Using Eq. (4.157), we have

$$aE_{k_f} = I_{\max}(R_1 - R_{k+1}) \tag{4.160}$$

Eliminating E_{k_f} between Eqs. (4.159) and (4.160) and using (4.158), we obtain

$$a\left(R_1 - \frac{R_k}{K}\right) = R_1 - R_{k+1}$$

Thus by a slight rearrangement, we get

$$R_{k+1} = R_1(1 - a) + R_k \frac{a}{K} \tag{4.161}$$

Replacing $(k + 1)$ by (k) and (k) by $(k - 1)$ in the preceding equation, we get

$$R_k = R_1(1 - a) + R_{k-1} \frac{a}{K} \tag{4.162}$$

The resistance of the kth section, r_k, is given by

$$r_k = R_k - R_{k+1}$$

Using Eqs. (4.161) and (4.162), we get

$$\begin{aligned} r_k &= \frac{a}{K}(R_{k-1} - R_k) \\ &= \frac{a}{K} r_{k-1} \end{aligned}$$

www.EngineeringEBooksPdf.com

Define

$$b = \frac{a}{K} \tag{4.163}$$

As a result,

$$r_k = br_{k-1} \tag{4.164}$$

The resistance sections therefore form a geometric progression with ratio b.

The total resistance R_1 at starting is given by

$$R_1 = r_1 + r_2 + \cdots + r_{n-1} + r_n$$

Using Eq. (4.163), we get

$$R_1 = r_1(1 + b + b^2 + \cdots + b^{n-2}) + r_n$$

Performing the required summation, we obtain

$$R_1 = r_1 \frac{1 - b^{n-1}}{1 - b} + r_n \tag{4.165}$$

Recall that

$$r_1 = R_1 - R_2 \tag{4.166}$$

Using Eqs. (4.161) and (4.163) in (4.166), we get

$$r_1 = R_1 - R_1(1 - a) - bR_1$$

Thus

$$r_1 = (a - b)R_1 \tag{4.167}$$

Using Eq. (4.163) in (4.167), we get

$$r_1 = b(K - 1)R_1 \tag{4.168}$$

Substituting Eq. (4.168) in (4.165), we get

$$R_1 = b(K - 1)\frac{1 - b^{n-1}}{1 - b}R_1 + r_n \tag{4.169}$$

Dividing by R_1 and recalling that

$$r_n = R_m = R_a + R_s$$

www.EngineeringEBooksPdf.com

we obtain, after some rearranging,

$$b^{n-1} = 1 - \frac{1-b}{b(K-1)}\left(1 - \frac{R_m}{R_1}\right)$$

Taking logarithms of both sides, we conclude that

$$n = 1 + \frac{\log\{1 - [(1-b)/b(K-1)](1 - R_m/R_1)}{\log b} \tag{4.170}$$

Equation (4.170) specifies the required number of sections n.

Example 4.20 A starter for a 220-V dc series motor is required such that the maximum current be 270 A and the minimum current is not be less than 162 A. The armature and series field resistances add up to 0.12 Ω. The magnetization characteristic of the motor is as follows:

Motor Current (A)	162	180	198	216	234	252	270
EMF at 750 rpm	193	200	206	211.2	215.8	220	224

Find the required number of resistance steps, n.

Solution With the given information, we have

$$I_{max} = 270\text{ A}$$
$$I_{min} = 163\text{ A}$$

Thus

$$K = \frac{I_{max}}{I_{min}} = \frac{270}{162} = 1.66667$$

From the magnetization characteristic

$$E_{max} = 224$$
$$E_{min} = 193$$

Thus

$$a = \frac{E_{max}}{E_{min}} = \frac{224}{193} = 1.16062$$

We can now find b:

$$b = \frac{a}{K} = \frac{1.16062}{1.66667} = 0.696373$$

www.EngineeringEBooksPdf.com

The resistance R_1 is obtained from

$$R_1 = \frac{V_t}{I_{\max}} = \frac{220}{270} = 0.814815\,\Omega$$

We also have

$$R_m = 0.12\,\Omega$$

All the necessary ingredients of Eq. (4.170) are now available and we thus have

$$n = 1 + \frac{\log\{1 - [(1 - 0.696)/0.696(1.667 - 1)](1 - 0.12/0.8148)\}}{\log 0.696373}$$
$$= 3.2543$$

We note that n is noninteger. We therefore take the closest integer of higher value than the calculated value. Thus we take

$$n = 4$$

Equation (4.169) will not be satisfied with the adjustment of n to the next larger integer unless a change is made in one of the other parameters. Two possible remedies are to increase $I_{\min}$ or decrease $I_{\max}$. The object is to satisfy Eq. (4.169) rewritten as

$$1 - \frac{R_m}{R_1} = b(K - 1)\frac{1 - b^{n-1}}{1 - b} \tag{4.171}$$

Note that if $I_{\max}$ is left unchanged, the left-hand side of (4.171) is also unchanged. A change in $I_{\min}$ will change the values of K, a, and b. A simple procedure to find the required value of $I_{\min}$ requires a plot of y versus $I_{\min}$ where

$$y = b(K - 1)\frac{1 - b^{n-1}}{1 - b}$$

The intersection of the characteristic with the constant y_0 line provides the required value of $I_{\min}$. Here y_0 is given by

$$y_0 = 1 - \frac{R_m}{R_1}$$

We can now continue with our example to find the required value of $I_{\min}$ for the choice $n = 4$.

Example 4.20 (Continued) The task here is to find $I_{\min}$. We start by noting that

$$y_0 = 1 - \frac{R_m}{R_1} = 1 - \frac{0.12}{0.8148} = 0.8527$$

www.EngineeringEBooksPdf.com

Since we had $I_{min} = 162$ A already, we move up to the next point on the magnetization characteristic. Thus take

$$I_{min} = 180\,\text{A}$$
$$E_{min} = 200\,\text{V}$$

Thus

$$K = \frac{270}{180} = 1.5$$
$$a = \frac{224}{200} = 1.12$$
$$b = \frac{a}{K} = 0.74667$$

We now calculate

$$y = b(K-1)\frac{1-b^3}{1-b}$$
$$= 0.86023$$

The process is repeated for $I_{min} = 198$ A to obtain

$$y = 0.70558$$

In Fig. 4.39 we plot the two points in the $y - I_{min}$ plane. A simple linear approximation to solve for I^*_{min} requires solving

$$\frac{198 - I^*_{min}}{I^*_{min} - 180} = \frac{0.8527 - 0.70}{0.86 - 0.8527}$$

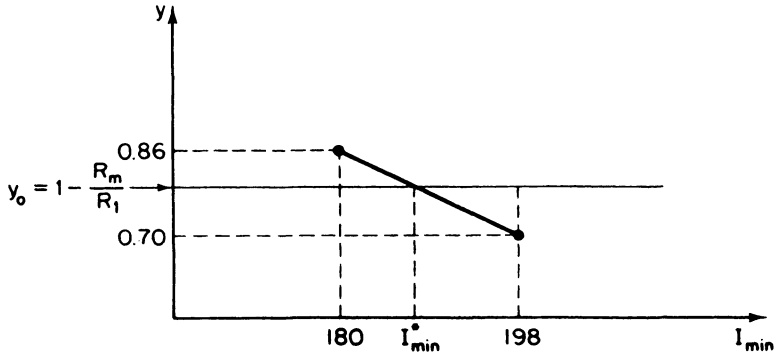


Figure 4.39 Finding I^*_{min}.

www.EngineeringEBooksPdf.com

As a result, we conclude that

$$I^*_{\text{min}} = 180.8\,\text{A}$$

Having obtained the proper values of n and I_{min}, we can now conclude our design example by finding the resistance steps.

Example 4.20 (Conclusion) For $I_{\text{min}} = 180.8\,\text{A}$, we obtain

$$K = \frac{270}{180.8} = 1.4934$$

$$a = \frac{224}{200.3} = 1.1183$$

$$b = \frac{1.1183}{1.4934} = 0.7488$$

Now we have

$$R_1 = 0.8148\,\Omega$$

$$r_1 = b(K-1)R_1 = 0.7488(1.4934-1)(0.8148) = 0.301\,\Omega$$

$$r_2 = br_1 = 0.22544\,\Omega$$

$$r_3 = br_2 = 0.16882\,\Omega$$

This concludes the starter design.

4.12 ADJUSTABLE-SPEED dc MOTOR DRIVES

Historically, the demand for variable-speed motor drives for industrial applications has been met by dc motors with a fixed field flux and a variable armature voltage for speed control. The variable dc voltage was obtained from a motor-generator set arranged in a Ward–Leonard system introduced in the 1890s. In this arrangement the generator-field flux is adjusted to obtain the desired variable dc voltage to provide a wide range of motor speeds. This system gained wide acceptance, and commercially available packaged drives were common beginning immediately before World War II. There are many disadvantages to the Ward–Leonard approach, including low overall efficiency, bulk and size restrictions, and the undesirable requirements for periodic maintenance, inspection, and replacement of generator parts. The advent of the SCR and the associated developments of power electronic systems provided an attractive alternative to the Ward–Leonard approach.

A separately excited dc motor is a doubly fed device that can be controlled through its armature circuit and/or its field circuit. Depending on the available power source, control is obtained using controlled rectifiers in an ac–dc drive, as shown in Fig. 4.40(a), or using choppers in a dc–dc drive as shown in Fig. 4.40(b). Note that in ac–dc drives a single-phase ac supply can be used in low-horsepower applications.

www.EngineeringEBooksPdf.com

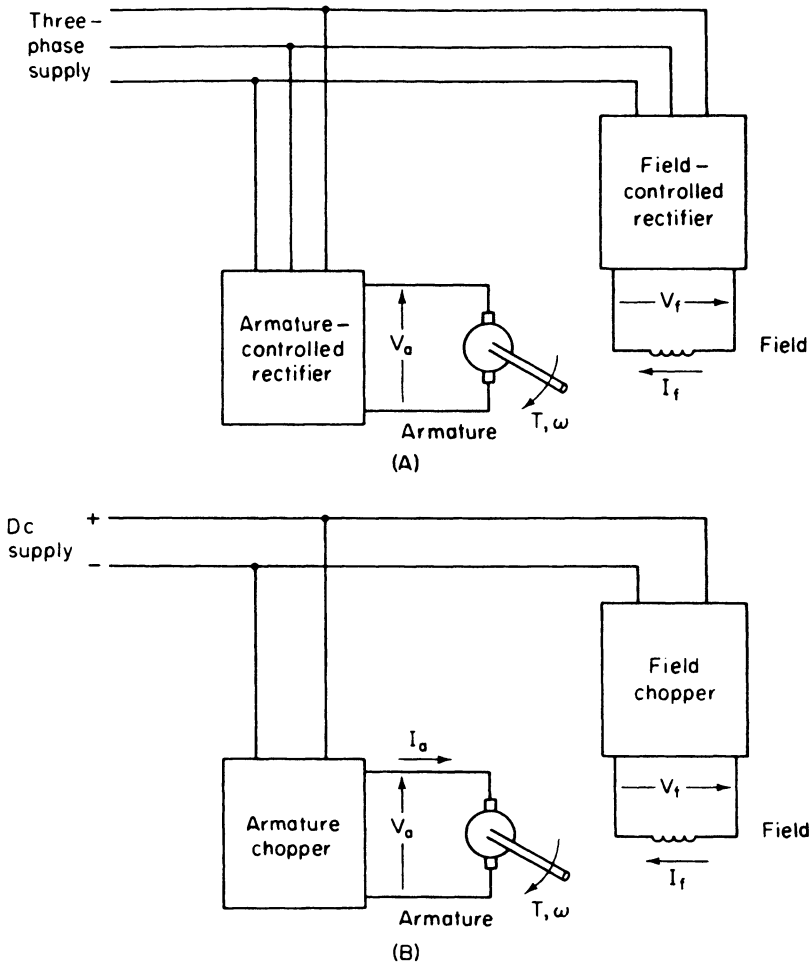


Figure 4.40 Separately excited dc motor adjustable-speed drives: (a) ac–dc drive; (b) dc–dc drive.

The strategy adopted in practice for control of dc motors is to divide the speed range of interest into two regions, with the motor's rated (base) speed separating the two regions (Fig. 4.41). In the first region, the field excitation is fixed at its rated value, and speed adjustments are made via firing-angle control of the motor's armature power circuit. This region is called the *constant-torque* or *armature voltage control region*. Above base speed, field weakening is employed, and this is called the *field control of constant-horsepower region*. Normally, the latter region extends to twice the base speed.

Region I In this region the output torque is required to be maintained constant over the speed range from zero to base motor speed ω_b. The base motor speed is

www.EngineeringEBooksPdf.com

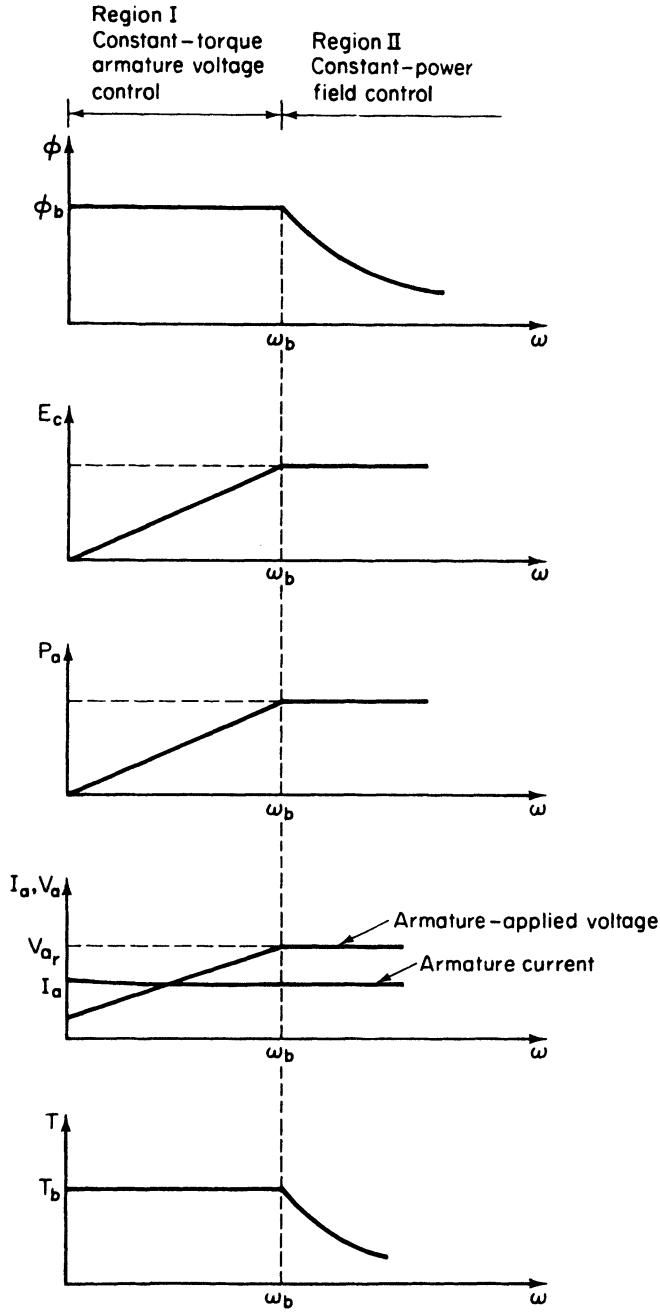


Figure 4.41 Regions of speed control in a separately excited dc motor.

www.EngineeringEBooksPdf.com

determined by the full-rated armature voltage and full-rated field flux. The field flux is kept constant at its rated value throughout this region. In meeting the constant-torque requirement under these conditions, the armature current should therefore be maintained constant. This follows since by Eqs. (4.10) and (4.12), we have

$$T_0 = K_1 \phi_f I_a \tag{4.172}$$

The armature current is related to the applied armature terminal voltage V_a and the motor's back EMF by Eq. (4.6) as

$$I_a = \frac{V_a - E_c}{R_a} \tag{4.173}$$

Note that the back EMF E_c varies in proportion to the speed according to Eq. (4.17), given by

$$E_c = K_1 \phi_f \omega \tag{4.174}$$

It is therefore clear that the armature terminal voltage varies with the motor speed according to

$$V_a = K_1 \phi_f \omega + \frac{T_0}{K_1 \phi_f} R_a \tag{4.175}$$

The power output is obtained using Eq. (4.10) as

$$P_a = E_c I_a = K_1 \phi_f I_a \omega \tag{4.176}$$

Thus the power output in region I increases in proportion to the motor speed. The torque output is constant at the rated value given by

$$T_o = K_1 \phi_f I_a \tag{4.177}$$

Region II For the region where motor speed exceeds the base speed ω_b, armature voltage control cannot be used, since full-rated voltage is applied to the armature terminals. Here the armature voltage V_a is maintained at its rated value V_{a_r}, and the field control is applied. In this region, the horsepower output is maintained constant by weakening the field through reducing the voltage applied to the field. To maintain a constant-power output, we require that the product of field flux and speed be kept constant at

$$\phi_f \omega = \frac{P_a}{K_1 I_a} = \text{constant} \tag{4.178}$$

www.EngineeringEBooksPdf.com

As a result, the field is weakened as the required speed increases. Note that the back EMF remains at its rated value, and hence the armature current remains constant in this region.

4.13 ac–dc DRIVES FOR dc MOTORS

Controlled rectifiers are used to provide the variable dc voltage to the armature and field circuits in a dc motor. In this section we will focus our attention on the separately excited motor. An important factor to consider is the ripple content in the dc output of the rectifier. In a single-phase half-wave rectifier circuit, one pulse of current is produced every supply cycle, and this provides an output that is rich in harmonics, resulting in excessive heating and torque pulsations. For 60-Hz operation there are 60 pulses per second, as opposed to 120 pulses per second for the single-phase full-wave rectifier case. Single-phase sources are used primarily for motors with horsepower output of 5 hp or less, for their simplicity and economy that offsets the poor wave shape.

For larger-horsepower applications the three-phase full-wave bridge configuration is used, and this has 360 pulses per second, which improves the harmonics content. It is often found necessary to employ two parallel phase-shifted three-phase full-wave controlled rectifier circuits to provide lower ripple.

4.13.1 Armature Voltage Control using Controlled Rectifiers

When the available supply is ac, controlled rectifier circuits are employed to provide control of the voltage applied to the armature circuit. Control is achieved by adjusting the thyristor's firing angles.

Single-Phase ac Supply In this case a full-wave bridge rectifier circuit or one with a center-tapped secondary is used. In the circuit of Fig. 4.42, we show instantaneous values of the variables involved, with the motor's back EMF, E_c, assumed constant. The back EMF actually depends on the motor's speed, which is time varying. A practical approximation is obtained. Our object is to obtain an equivalent circuit, as shown in Fig. 4.42(b), that represents the average performance of the system over one cycle of the source voltage.

The average voltage applied to the motor's armature circuit is a function of the firing angle α of the thyristors. The average current into the load circuit (motor's armature current) is given by

$$I_{o_{av}} = \frac{1}{2\pi R}\{V_m[\cos\alpha - \cos(\alpha + \gamma)] - \gamma E_c\} \tag{4.179}$$

The conduction angle γ determines the mode of operation and is obtained using information available about the load circuit. Let us assume that the armature circuit

www.EngineeringEBooksPdf.com

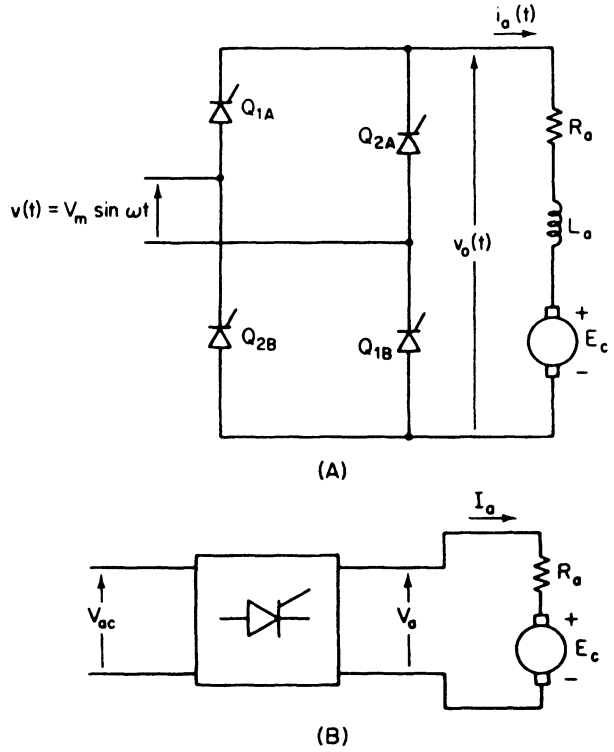


Figure 4.42 A dc-motor armature voltage control using single-phase full-wave controlled rectifier: (a) circuit details; (b) equivalent-circuit model of average performance.

inductance is chosen large enough to result in continuous operation, and therefore we take $\gamma = \pi$. In this case, Eq. (4.179) yields

$$I_{o_{av}} = \frac{V_m \cos\alpha}{\pi R} - \frac{E_c}{2R} \tag{4.180}$$

This is the average value of the armature circuit current over one cycle of the supply frequency if a single-phase half-wave controlled rectifier is used for armature voltage control.

In the more practical case, where a single-phase full-wave controlled rectifier bridge is used, there are two load current pulses in one cycle of the supply frequency. We can therefore conclude that the average value of the motor's armature current over one cycle of the source voltage waveform is obtained by multiplying the right-hand side of Eq. (4.180) by 2 to obtain

$$I_a = \frac{2V_m \cos\alpha}{\pi R} - \frac{E_c}{R} \tag{4.181}$$

www.EngineeringEBooksPdf.com

As a result, we have

$$E_c = \frac{2V_m \cos\alpha}{\pi} - I_a R_a \tag{4.182}$$

In terms of the dc motor's equivalent circuit sown in Fig. 4.42, we have

$$V_a = \frac{2V_m \cos\alpha}{\pi} \tag{4.183}$$

Alternatively, with the rms value of the supply voltage V, we have

$$V_a = \frac{2\sqrt{2}V}{\pi} \cos\alpha \tag{4.184}$$

Three-Phase ac Supply When the available ac supply is a three-phase source, a full-wave controlled rectifier circuit is employed. In this case the average armature applied voltage is given as

$$V_a = \frac{3V_m}{\pi} \cos\alpha \tag{4.185}$$

In terms of the effective value of the line-to-line voltage V_{LL}, we have

$$V_a = \frac{3\sqrt{2}}{\pi} V_{LL} \cos\alpha \tag{4.186}$$

Example 4.21 A 230-V three-phase supply is available to drive a separately excited dc motor through a three-phase full-wave bridge rectifier circuit connected to the armature terminals. The armature resistance is 0.2 Ω, and the motor draws a current of 205 A when running at 1750 rpm with an armature voltage of 230 V dc.

(a) Find the firing angle α under the specified conditions
(b) Find the firing angle α required for the motor to run at 875 rpm
(c) Find the motor's speed for a firing angle of 75 degrees
(d) Find the motor's speed for a firing angle of zero

Solution

(a) We apply Eq. (4.186):

$$230 = \frac{3\sqrt{2}}{\pi} (230) \cos\alpha$$

As a result,

$$\alpha = 42.2°$$

www.EngineeringEBooksPdf.com

(b) For a speed of 1750 rpm, we have

$$E_{c_1} = V_{a_1} - I_a R_a = 230 - 205(0.2) = 189\,\text{V}$$

For a speed of 875 rpm, we require

$$E_{c_2} = E_{c_1}\frac{\omega_2}{\omega_1} = \frac{189}{2} = 94.5\ \text{V}$$

As a result,

$$V_{a_2} = E_{c_2} + I_a R_a = 94.5 + 205(0.2) = 135.5\,\text{V}$$

We can now obtain the required firing angle:

$$V_{a_2} = 135.5 = \frac{3\sqrt{2}}{\pi}(230)\cos\alpha_2$$

$$\alpha_2 = 64.14°$$

(c) With $\alpha_3 = 75$ degrees, we obtain

$$V_{a_3} = \frac{3\sqrt{2}}{\pi}(230)\cos 75° = 80.39\,\text{V}$$

Thus

$$E_{c_3} = V_{a_3} - I_a R_a$$

$$= 80.39 - 205(0.2) = 39.39\,\text{V}$$

$$n_3 = n_1\frac{E_{c_3}}{E_{c_1}} = (1750)\frac{39.39}{189} = 364.74\ \text{rpm}$$

(d) With $\alpha_4 = 0$ degrees, we have

$$V_{a_4} = \frac{3\sqrt{2}}{\pi}(230) = 310.61\,\text{V}$$

As a result,

$$E_{c_4} = 310.61 - 41 = 269.61\,\text{V}$$

$$n_4 = 1750\left(\frac{269.61}{189}\right) = 2496.4\,\text{rpm}$$

www.EngineeringEBooksPdf.com

4.13.2 Field Control using Controlled Rectifiers

With an ac supply available, controlled rectifiers are used to provide a variable-voltage dc supply to the field circuit. The load on the rectifier is an *RL* circuit, and the rectifier is assumed to operate continuously with $\gamma = \pi$. For a single-phase controlled half-wave rectifier, we have,

$$I_f = \frac{V_m}{\pi R_f} \cos\alpha \tag{4.187}$$

For a single-phase full-wave controlled rectifier supplying the field circuit, we obtain

$$I_f = \frac{2V_m}{\pi R_f} \cos\alpha \tag{4.188}$$

When a three-phase full-wave controlled rectifier is employed, then we have the average field voltage given in terms of the maximum value of the line-to-line voltage by

$$V_f = \frac{3V_m}{\pi} \cos\alpha \tag{4.189}$$

Therefore, the average field current is given by

$$I_f = \frac{3V_m}{\pi R_f} \cos\alpha \tag{4.190}$$

It is clear that the average field current is a function of the firing angle α, and, in general, we write

$$I_f = I_{f_b} \cos\alpha \tag{4.191}$$

The base field current I_{f_b} corresponds to rated field flux, and is given in terms of the effective value of the ac voltage for the single-phase full-wave rectifier by

$$I_{f_b} = \frac{2\sqrt{2}}{\pi R_f} V \tag{4.192}$$

For a three-phase full-wave rectifier, we have

$$I_{f_b} = \frac{3\sqrt{2}}{\pi R_f} V_{LL} \tag{4.193}$$

where V_{LL} is the rms value of the ac line-to-line voltage.

www.EngineeringEBooksPdf.com

4.13.3 Speed–Firing-Angle Relations

From the analysis of the preceding subsections we can develop the relation between motor speed and controlled rectifier firing angles α_a for the armature circuit in region I and α_f for the field in region II.

Region I It is convenient to write Eqs. (4.184) and (4.186) as

$$V_a = K_a \cos \alpha_a \tag{4.194}$$

Where the constant K_a is defined by

$$K_a = \frac{2\sqrt{2}}{\pi} V$$

For a single-phase full-wave rectifier bridge, and

$$K_a = \frac{3\sqrt{2}}{\pi} V_{LL}$$

for a three-phase full-wave rectifier bridge. Combining Eqs. (4.173) to (4.175), and (4.194), we conclude that

$$\omega = \frac{1}{K_1 \phi_f} \left(K_a \cos \alpha_a - \frac{T_o R_a}{K_1 \phi_f} \right) \tag{4.195}$$

It is clear that an increase in α_a is associated with a decrease in speed in the constant-torque region.

Region II From Eqs. (4.191), (4.10), and (4.178), we can write

$$\omega = \frac{P_a}{K_1 K_2 I_a I_{f_b}} \frac{1}{\cos \alpha_f} \tag{4.196}$$

It is clear that an increase in α_f increases ω in the constant-horsepower region.

Example 4.22 For the motor of Example 4.21, assume that the speed corresponding to $\alpha = 0$ is the base speed. Find the firing angle of the field rectifier circuit corresponding to a speed of 3000 rpm. What would be the firing angle for a speed that is twice base speed?

Solution Operation in region II should satisfy Eq. (4.178), requiring that

$$I_{f_b} \omega_b = I_f \omega$$

www.EngineeringEBooksPdf.com

Invoking Eq. (4.191), we have

$$I_{f_b}\omega_b = I_{f_b}\omega\cos\alpha$$

Thus

$$\cos\alpha = \frac{\omega_b}{\omega} = \frac{2496.38}{3000}$$
$$\alpha = \cos^{-1} 0.83 = 33.7°$$

For $\omega = 2\omega_b$,

$$\cos\alpha = 0.5$$

As a result,

$$\alpha = 60°$$

4.14 dc–dc DRIVES FOR dc MOTORS

A dc supply is used to power motors for rapid transit, electric, railroad trains, battery-operated vehicles, and electric forklift trucks. Dc-to-dc drives employing chopper control offer an attractive alternative to resistance-control schemes that prevailed in this application area. The use of semiconductor power control avoids the excessive heat generated in resistive speed control. This is an important consideration, especially in underground applications such as transportation in tunnels and mining operations.

As discussed in Chapter 3, dc-to-dc converters (choppers) provide a variable direct voltage by varying the duration of thyristor on-time t_{on} in relation to the chopping frequency T in the time-ratio-control (TRC) scheme. Choppers are widely employed to control separately excited and series dc motors in traction applications. A typical one-quadrant chopper scheme for armature control of a separately excited dc motor is shown in Fig. 4.43, with an input LC filter and a smoothing reactor inserted in the circuit to reduce the possible wide variations in supply and motor currents.

4.14.1 One-Quadrant Chopper Control

In Section 4.3 we found that the current waveform for a load consisting of a dc motor's armature can be either continuous or discontinuous. The criterion that determines the mode of operation is the value of the critical on-time t^*_{on} given by

$$t^*_{on} = \tau\, ln\left[1 + \frac{E_c}{V_i}(e^{T/\tau} - 1)\right] \tag{4.197}$$

www.EngineeringEBooksPdf.com

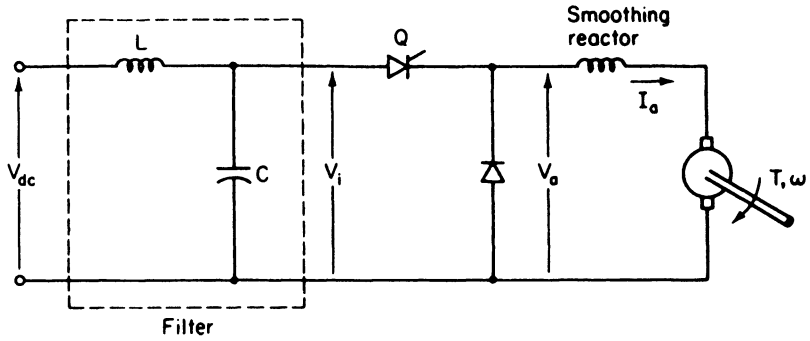


Figure 4.43 One-quadrant chopper armature voltage-control circuit.

We recall Eq. (4.174) showing that E_c varies with the speed ω, and conclude that the mode of operation depends on speed. Clearly, for $\omega = 0$, the critical on-time is zero and any value of thyristor on-time results in continuous operation of the chopper. For speeds other than zero, definite values of t_{on}^* exist, and if $t_{on} \geq t_{on}^*$, the output current is continuous, and conversely if $t_{on} < t_{on}^*$, the output current is discontinuous.

The discontinuous current operation mode involves an interval of time between t_x and T when the instantaneous output current is zero for constant V_i. Here the value of t_x is given by

$$t_x = \tau \ln\left[1 + \frac{V_i}{E_c}(e^{t_{on}/\tau} - 1)\right] \tag{4.198}$$

In this case the average of the output current is given by

$$I_a = \left(\frac{t_{on}}{T} V_i - \frac{t_x}{T} E_c\right) \frac{1}{R_a} \tag{4.199}$$

In region I, the average output torque is given by Eq. (4.177) as

$$T_0 = K_1 \phi_f I_a \tag{4.200}$$

The field flux is held constant in this region. We also have, by Eq. (4.174),

$$E_c = K_1 \phi_f \omega \tag{4.201}$$

As a result, we conclude that by combining Eqs. (4.199) and (4.201), the motor's speed is given by

$$\omega = \frac{t_{on}}{t_x} \frac{V_i}{K_1 \phi_f} - \frac{R_a}{(K_1 \phi_f)^2} \frac{T}{t_x} T_0 \tag{4.202}$$

www.EngineeringEBooksPdf.com

In the continuous mode of operation, with $t_{on} > t_{on}^*$, we have $t_x = T$. As a result Eq. (4.202) reduces to

$$\omega = \frac{(t_{on}/T)V_i - (R_a/K_1\phi_f)T_o}{K_1\phi_f)} \tag{4.203}$$

This completes our analysis of armature voltage control using one-quadrant choppers.

In region II, with one-quadrant chopper control of the field circuit, our analysis results are obtained by setting $E_c = 0$, since the field-circuit model consists of a series RL combination. From Eq. (4.197), we note that with $E_c = 0$, the field current is continuous for any t_{on}. Therefore, the field-circuit average current is

$$I_f = \frac{t_{on}}{T}\frac{V_{fi}}{R_f} \tag{4.204}$$

From Eqs. (4.178), (4.10), and (4.204), we get the desired expression for the average motor speed in region II as

$$\omega = \frac{P_a}{K_1K_2I_aI_{f_b}}\frac{T}{t_{on}} \tag{4.205}$$

where the base field current I_{f_b} is defined by Eq. (4.204) for $t_{on} = T$ as

$$I_{f_b} = \frac{V_{fi}}{R_f} \tag{4.206}$$

The dc voltage supply to the field circuit is denoted by V_{fi} in the preceding expressions,

Example 4.23 The armature voltage of a separately excited dc motor is controlled by a one-quadrant chopper with chopping frequency of 200 pulses per second from a 300 V dc source. The motor runs at a speed of 800 rpm when the chopper's time ratio is 0.8. Assume that the armature circuit resistance and inductance are 0.08 Ω and 15 mH, respectively, and that the motor develops a torque of 2.72 N·m per ampere of armature current.

Find the mode of operation of the chopper, the output torque, and horsepower under the specified conditions.

Solution From the problem specifications at 800 rpm, using Eq. (4.201), we get,

$$E_c = (2.72)\frac{2\pi}{60}(800) = 227.9 \text{ V}$$

www.EngineeringEBooksPdf.com

The armature circuit time constant is obtained as

$$\tau = \frac{L_a}{R_a} = \frac{15 \times 10^{-3}}{0.08} = 187.5 \times 10^{-3}\,\text{s}$$

The chopping period is given by

$$T = \frac{1}{200} = 5 \times 10^{-3}\text{s}$$

We obtain the critical on-time using Eq. (4.197) as

$$t_{\text{on}}^{*} = 187.5 \times 10^{-3}\, ln\left[1 + \frac{227.9}{300}(e^{5/187.5} - 1)\right]$$
$$= 3.8 \times 10^{-3}\text{s}$$

We know that $t_{\text{on}} = 0.8 \times 5 \times 10^{-3} = 4 \times 10^{-3}$. As a result, we conclude that the chopper output current is continuous.

To obtain the torque output, we use Eq. (4.203) rearranged as

$$T_{\text{o}} = \frac{K_1\phi_f}{R_a}\left(\frac{t_{\text{on}}}{T}V_i - K_1\phi_f\omega\right)$$

Thus we obtain

$$T_{\text{o}} = \frac{2.72}{0.08}[0.8(300) - 227.9]$$
$$= 411.4\,\text{N} \cdot \text{m}$$

The power output is obtained as

$$P_{\text{o}} = (411.4)\frac{2\pi}{60}(800) = 34.5 \times 10^3\,\text{W}$$
$$= 46.2\,\text{hp}$$

To illustrate the principle of field control, we have the following example.

Example 4.24 Assume for the motor of Example 4.23 that field chopper control is employed to run the motor at a speed of 1500 rpm while delivering the same power output as obtained at 800 rpm and drawing the same armature current.

Solution Although we can use Eq. (4.205), we use basic formulas instead,

$$E_c = \frac{P_a}{I_a} = \frac{34.5 \times 10^3}{151.3} = 227.9\,\text{V}$$

www.EngineeringEBooksPdf.com

This is the same back EMF. Recall that

$$E_c = K_1 \phi_f \omega$$

Thus the required field flux is obtained as

$$\phi_{f_n} = \phi_{f_0} \frac{\omega_0}{\omega_n} = \frac{8}{15} \phi_{f_0}$$

where the subscript n denotes the present case, and the subscript 0 denotes the field flux for Example 4.23. Assume that ϕ_{f_0} corresponds to full applied field flux; then

$$\frac{\phi_{f_0}}{\phi_{f_n}} = \frac{V_i}{V_o} = \frac{15}{8}$$

The required chopped output voltage is V_o. Now we have

$$\frac{V_o}{V_i} = \frac{t_{on}}{T}$$

Thus

$$\frac{t_{on}}{T} = \frac{8}{15}$$

Assuming that $T = 5 \times 10^{-3}$ s, we get

$$t_{on} = 2.67 \times 10^{-3} \text{ s}$$

PROBLEMS

Problem 4.1 A 240-V dc motor has an armature resistance of 0.4 Ω. The armature current is 40 A at a steady speed of 1200 rpm.

(a) Find the armature's back EMF.
(b) Find the internal power of the armature and the developed torque.
(c) Find the speed of the motor if the field flux is reduced to 75% of its value.
(d) Find the torque of the motor if the field flux is reduced to 80% of its value, corresponding to the conditions of part (b).

Problem 4.2 A 600-V 150-hp 600 rpm dc series motor has an armature and series-field resistance of 0.16 Ω. The full-load current is 210 A.

(a) Find the back EMF at full load.
(b) Find the armature-developed power and torque at full load.
(c) Compute the efficiency of the motor, neglecting rotational losses.

www.EngineeringEBooksPdf.com

Problem 4.3 A 230-V dc series motor has a line current of 80 A and a rated speed of 750 rpm. The armature circuit and series-field resistances are 0.14 Ω and 0.11 Ω, respectively. Calculate:

(a) The speed when the line current drops to 40 A.
(b) The no-load speed for a line current of 2 A.
(c) The speed at 150% rated load when the line current is 120 A and the series field flux is 125% of the full-load flux due to saturation.

Problem 4.4 The power developed by the armature of a 230-V dc series motor at a speed of 750 rpm is 16,800 W. The combined armature and field resistance is 0.25 Ω. Find the armature current and back EMF under these conditions. If the line current is reduced to half of its previous value, find the new motor speed assuming that the field flux is proportional to the field current.

Problem 4.5 A 250-V 25-hp dc series motor takes a current of 85 A when its speed is 62.83 rad/s. The armature circuit resistance is 0.1 Ω and the series field resistance is 0.05 Ω.

(a) Find the speed when the line current is 100 A.
(b) Find the torque at a speed of 100 rad/s.

Problem 4.6 A 20-hp 1150-rpm 230-V dc shunt motor has an armature resistance of 0.188 Ω and a shunt-field resistance of 144 Ω. Compute:

(a) The line current if the motor is connected directly across the 230-V supply without a starting resistance.
(b) The resistance of a starting resistor that limits starting current to 150% of the full-rated current of 74.6 A.
(c) Full-load back EMF.

Problem 4.7 The armature resistance of a 100-hp 600-V shunt motor is 0.1 Ω. The shunt-field resistance is 600 Ω. The motor draws a line current of 11 A on no-load at a speed of 1200 rpm. At full load, the line current is 138.148 A.

(a) Find the armature current and armature-developed power on no-load.
(b) Find the full-load speed and efficiency of the motor.

Problem 4.8 A 20-hp 230-V 1150-rpm dc shunt motor has an armature resistance of 0.3 Ω. The armature current is 36.7 A for a given load. As the mechanical load is increased, the field flux is increased by 15% with a corresponding increase in armature current to 75 A. Find:

(a) The armature back EMF at the 36.7-A load.
(b) The armature back EMF and speed at the 75-A load.
(c) The armature power developed at both loads.

www.EngineeringEBooksPdf.com

Problem 4.9 A 10-hp 230-V dc shunt motor has an armature circuit resistance of 0.03 Ω. The armature current is 36.7 A at a speed of 1150 rpm. An additional resistance of 1 Ω is inserted in series with the armature, while the shunt-field resistance of 128 Ω and torque output remain unchanged.

(a) Find the resulting change in line current.
(b) Find the speed at which the motor will run.

Problem 4.10 The rotational losses of a 50-hp 230-V dc shunt motor at full-rated load are given by 1445 W. Assume that the armature resistance is 0.2 Ω and that the full-load speed is 1750 rpm. Find the armature current at rated load.

Problem 4.11 A 1000-hp 500-V dc shunt motor has an armature resistance of 0.07 Ω. At full-load power, the armature current is 1550 A at 750 rpm. Calculate the full-load rotational losses. Find the output power and motor speed if the armature current is 1200 A.

Problem 4.12 A 230-V 25-hp dc shunt motor has an armature resistance of 0.2 Ω. Find the maximum horsepower developed by the armature and the corresponding armature current. Find the full-load armature current. Neglect rotational losses.

Problem 4.13 The following data are available for a dc series motor:

$$V_t = 240\,\text{V} \qquad E_c = 217.2\,\text{V} \quad \text{at 600 rpm}$$
$$R_a + R_s = 0.6$$

Find the torque and speed of the motor when driving a load with the following torque–speed characteristic:

$$T_l = 3.9536\omega$$

where T_l is in N·m and ω is in rad/s.

Problem 4.14 Repeat Problem 4.13 for a load with the following torque–speed characteristic:

$$T_l = 182.27 \times 10^{-3}\,\omega^2$$

Problem 4.15 A 600-V dc series motor has a combined armature and series-field resistance of 0.16 Ω. The motor draws an armature current of 210 A when running at 600 rpm. Establish the torque–speed characteristic of the motor. The motor drives a load with the characteristic

$$T_l = A\omega^2$$

The speed is found to be 600 rpm. Find the constant A.

www.EngineeringEBooksPdf.com

Problem 4.16 A 230-V dc series motor has a combined armature and series-field resistance of 0.25 Ω. The armature current is 80 A at 750 rpm. Find the torque–speed characteristic of the motor. The motor drives a load with the following characteristic:

$$T_l = 100e^{a\omega}$$

Find a, given that the motor's speed is 725 rpm when driving this load.

Problem 4.17 The armature resistance of a dc shunt motor is 0.05 Ω. The armature current is found to be 180.5 A at a sped of 1300 rpm. Assume that the motor is operating off a 230-V supply. Find the torque and speed when the motor drives a load with the following torque–speed characteristic:

$$T_l = 638.25 \times 10^{-3}\omega$$

where T_l is in N·m and ω is in rad/s.

Problem 4.18 Repeat Problem 4.17 for a load characteristic given by

$$T_l = 78.69\sqrt{\omega}$$

Problem 4.19 The armature resistance of a dc shunt motor is 0.3 Ω. The motor operates from a 230-V mains and draws an armature current of 36.7 A at 1150 rpm. Establish the torque-speed characteristic of the motor. Find the torque and speed of the motor when it drives a load with the characteristic

$$T_l = 0.5\omega$$

Problem 4.20 A 600-V dc shunt motor has a resistance of the armature circuit of 0.1 Ω. The motor draws an armature current of 137.148 A at 1174.28 rpm. Establish the torque–speed characteristic of the motor. The motor is driving a load with the following characteristic

$$T_l = A\sqrt{\omega}$$

Find A assuming that the motor's speed is 122 rad/s when driving this load.

Problem 4.21 The power delivered by a 230-V dc shunt motor is 20 hp at 1150 rpm. The armature resistance is 0.188 Ω. Establish the torque–speed characteristic of the motor. Assume that the motor is driving a load with the torque–speed characteristic

$$T_l = a + 0.2\omega$$

Find a such that the motor runs at a speed of 125 rad/s when driving this load.

Problem 4.22 For the motor of Problem 4.2, find the additional series resistance required to produce full-load torque at a speed of 580 rpm.

www.EngineeringEBooksPdf.com

Problem 4.23 For the motor of Problem 4.13, find the additional series resistance required to carry the load at a speed of 48 rad/s.

Problem 4.24 Repeat Problem 4.22 using armature shunt resistance control, assuming that armature resistance is 0.1 Ω.

Problem 4.25 Repeat Problem 4.23 using armature shunt resistance control, assuming that the armature resistance is 0.4 Ω.

Problem 4.26 For the motor of Problems 4.22 and 4.24, assume that $R_c = 150\,\Omega$ is available. Find the required value of R_b in a series shunt resistance control scheme to achieve the required specifications.

Problem 4.27 For the motor of Problems 4.23 and 4.25, assume that $R_c = 50\,\Omega$ is available. Find the required value of R_b in a series shunt resistance control scheme to achieve the required specifications.

Problem 4.28 Assume that a shunt diverter with $\alpha = 0.9$ is used for the motor of Problem 4.2. Find the resulting torque at a speed of 580 rpm. Assume that $R_a = 0.1\,\Omega$.

Problem 4.29 Assume that a shunt diverter with $\alpha = 0.85$ is used for the motor of Problem 4.3. Find the resulting torque at 48 rad/s, assuming that the armature resistance is 0.4 Ω.

Problem 4.30 Consider the shunt motor of Problem 4.6. Find the full-load torque. Assume that field resistance control is used with $R_e = 10\,\Omega$. Find the speed in rpm for the same torque as in the full-load case.

Problem 4.31 Assume for the motor of Problem 4.30 that an armature resistance $R_b = 0.05\,\Omega$ is used in addition to the extra field resistance of 10 Ω. Find the resulting speed in rpm for the same torque.

Problem 4.32 For the motor of Problem 4.30, series and shunt armature resistance control is used with $R_b = 0.05\ \Omega$ and $R_c = 2\ \Omega$. Find the speed in rpm for full-load torque, as obtained in Problem 4.30.

Problem 4.33 Find R_e for the motor of Problem 4.30 such that the motor carries full-load torque at a speed of 1200 rpm.

Problem 4.34 Find R_b for the motor of Problem 4.31 such that the speed is 1180 rpm for the same torque.

Problem 4.35 Assume that the motor of Problem 4.32 is controlled with the same values of R_c and R_b. Find the load torque if the speed is 1080 rpm.

Problem 4.36 A 240-V dc motor has a combined armature and series-field resistance of 0.6 Ω and a shunt-field resistance of 180 Ω. The motor is operated as a series motor with the armature current being 40 A at a speed of 595 rpm. When operated as a compound motor, the line current is found to be 42 A. Assuming that the flux is increased by 50% due to compounding, find the speed of the motor when

www.EngineeringEBooksPdf.com

running as a compound motor. Evaluate the constants K_1K_4 and K_1K_3, and determine the torque developed for the given conditions using Eq. (4.77).

Problem 4.37 For the motor of Problem 4.36, assume that shunt-field resistance control with $R_e = 20\,\Omega$ is used. Find the torque for the speed given in Problem 4.36.

Problem 4.38 For the motor of Problem 4.37, assume that the additional series armature resistance of $0.05\,\Omega$ is used in conjunction with R_e. Find the new value of the torque for the same speed.

Problem 4.39 For the motor of Problem 4.37, assume that series and shunt resistance control is used with $R_c = 100\,\Omega$ and $R_b = 0.05\,\Omega$. Assume that $R_s = 0.4\,\Omega$ and $R_a = 0.02\,\Omega$. Find the armature current and the torque for the speed of 41.462 rad/s.

Problem 4.40 For the motor of Problem 4.37, find the additional shunt-field resistance, R_e, required to drive a load with torque of 215 N·m at the same specified speed.

Problem 4.41 For the motor of Problem 4.38, find R_b such that a load torque of 210 N·m is carried at the same specified speed.

Problem 4.42 For the motor of Example 4.20, find the required number of starter steps to obtain

$$I_{max} = 198\,A \qquad I_{min} = 100\,A$$

Problem 4.43 A 220-V three-phase supply is available to drive a separately excited dc motor through a three-phase full-wave bridge rectifier circuit connected to the armature terminals. The armature resistance is $0.15\,\Omega$ and the motor draws a current of 190 A when running at 1600 rpm with an armature voltage of 200 V dc.

(a) Find the firing angle α under the specified conditions.
(b) Find the firing angle α required for the motor to run at 1800 rpm.
(c) Find the motor's speed for a firing angle of 60 degrees.

Problem 4.44 A 230-V three-phase supply is available to drive a separately excited dc motor through a three-phase full-wave bridge rectifier circuit connected to the armature terminals. The armature resistance is $0.18\,\Omega$ and the motor draws a current of 200 A when running at 1800 rpm with an armature voltage of 240 V dc.

(a) Find the firing angle α under the specified conditions.
(b) Find the firing angle α required for the motor to run at 1200 rpm.
(c) Find the motor's speed for a firing angle of 75 degrees.

www.EngineeringEBooksPdf.com

Problem 4.45 A 220-V three-phase supply is available to drive a separately excited dc motor through a three-phase full-wave bridge rectifier circuit connected to the armature terminals. The armature resistance is $0.12\,\Omega$, and the motor draws a current of 180 A when running at 1500 rpm with an armature voltage of 180 V dc.

(a) Find the firing angle α under the specified conditions.
(b) Find the firing angle α required for the motor to run at 875 rpm.
(c) Find the motor's speed for a firing angle of 80 degrees.

Problem 4.46 A separately excited dc motor is supplied by a three-phase full-wave bridge rectifier circuit whose line-to-line voltage is 220 V. The motor's armature resistance is $0.15\,\Omega$. The motor supplies a load at a speed of 800 rpm with an output torque of 300 N·m. The armature current is 90 A under these conditions. Find the firing angle of the rectifier bridge. If the firing angle is adjusted to 30 degrees, find the motor's speed.

Problem 4.47 A separately excited dc motor is supplied by a three-phase full-wave bridge rectifier circuit whose line-to-line voltage is 230 V. The motor's armature resistance is $0.08\,\Omega$. The motor supplies a load at a speed of 1000 rpm with an output torque of 220 N·m. The armature current is 130 A under these conditions. Find the firing angle of the rectifier bridge. If the firing angle is adjusted to 40 degrees, find the motor's speed.

Problem 4.48 A separately excited dc motor is supplied by a three-phase full-wave bridge rectifier circuit whose line-to-line voltage is 120 V. The motor's armature resistance is $0.05\,\Omega$. The motor supplies a load at a speed of 600 rpm with an output torque of 140 N·m. The armature current is 60 A under these conditions. Find the firing angle of the rectifier bridge. If the firing angle is adjusted to 30 degrees, find the motor's speed.

Problem 4.49 For the motor of Problem 4.43, assume that the speed corresponding to $\alpha = 0$ is the base speed. Find the firing angle of the field rectifier circuit corresponding to a speed of 2800 rpm.

Problem 4.50 For the motor of Problem 4.44, assume that the speed corresponding to $\alpha = 0$ is the base speed. Find the firing angle of the field rectifier circuit corresponding to a speed of 2800 rpm.

Problem 4.51 For the motor of Problem 4.45, assume that the speed corresponding to $\alpha = 0$ is the base speed. Find the firing angle of the field rectifier circuit corresponding to a speed of 3000 rpm.

Problem 4.52 Find the required chopper on-time for the motor of Example 4.23 to deliver a torque of 4000 N·m at a speed of 600 rpm. Repeat for a speed of 900 rpm. Verify that the chopper operates in the continuous current mode in both cases.

www.EngineeringEBooksPdf.com

Problem 4.53 The armature resistance of a separately excited dc motor is 0.5 Ω and its inductance is 7 mH. The motor develops a torque of 1.34 N·m per ampere of armature current and is controlled by a one-quadrant chopper with chopping period of 5×10^{-3} s and an on-time of 4×10^{-3} s. Assume that the dc supply is 220 V. Find the average armature current, torque, and power output.

Problem 4.54 For the motor of Problem 4.53, find the required chopper on-time at a speed of 1000 rpm while delivering the same torque.

www.EngineeringEBooksPdf.com

CHAPTER 5

TRANSFORMERS

5.1 INTRODUCTION

The transformer is a valuable electric power apparatus, for it enables us to utilize different voltage levels across the power system for the most economical value. Generation of power at the synchronous machine level is normally at a relatively low voltage, which is most desirable economically. Stepping up this generated voltage to high voltage, or extra-high voltage, is done through power transformers to suit the power transmission requirements to minimize losses and increase the transmission capacity of the lines. This transmission voltage level is then stepped down in many stages for distribution and utilization purposes. Transformers are used at all levels of the system. An electronic device designed to operate on normal household voltage and frequency has a transformer to supply suitable voltage for the various components of the device. Audio-frequency (up to 20 kHz) transformers are used for impedance matching at the input or output of audio-frequency amplifiers or between amplifiers. Control-type transformers are used to provide desired modifications to the magnitude and phase of voltages at various points in the electric system. Instrument-type transformers are used to interface the high-energy side of a system to instruments and devices that monitor the state of the system.

Transformer action requires a varying flux to link the two windings. This will be more effective if an iron core is used because an iron core confines the flux to a definite path linking both windings. A magnetic material such as iron undergoes a loss of energy due to the application of alternating voltage to its magnetic induction–magnetizing-force (B-H) loop. The losses consist of two parts. The first is the eddy-current loss, and the second is the hysteresis loss. Eddy-current loss is basically an I^2R loss due to the induced currents in the magnetic material. To reduce these

www.EngineeringEBooksPdf.com

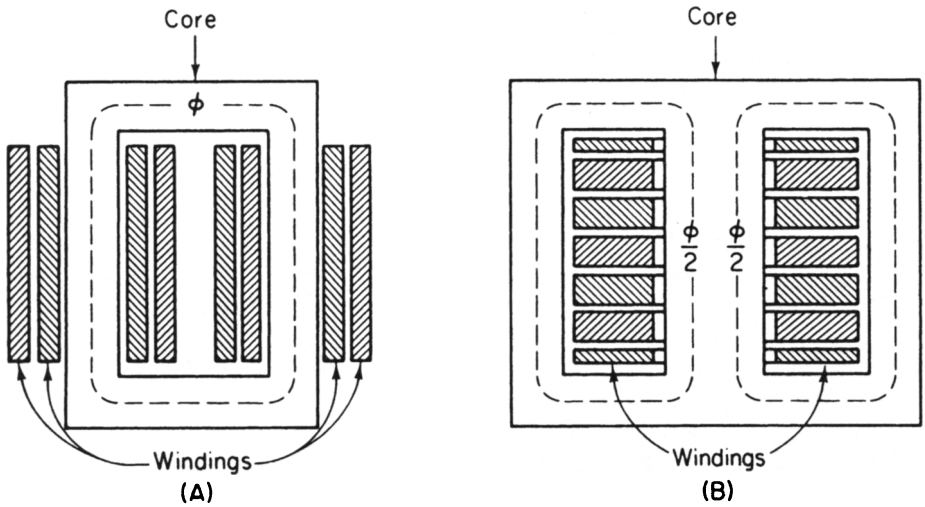


Figure 5.1 (a) Core-type, and (b) shell-type transformer construction.

losses, the magnetic circuit is usually made of a stack of thin laminations. For high-frequency applications, the core is made of fine-particle magnetic material. Hysteresis loss is caused by the energy used in orienting the magnetic domains of the material along the field. The loss depends on the material used.

Two types of construction are used, as shown in Fig. 5.1. The first is the core type, which is a single ring encircled by one or more groups of windings. The mean length of the magnetic circuit for this type is long, whereas the mean length of windings is short. The reverse is true for the shell type, where the magnetic circuit encloses the windings.

The present discussion is mainly oriented toward power system transformers operating at power frequency (50 or 60 Hz) levels. In this case, capacitive effects are negligible. For high-frequency applications, the effects of capacitance must be included. To understand transformer operation, we first study the ideal transformer. Although we will never encounter an ideal transformer in real life, the concept is extremely useful in modeling and analysis studies.

5.2 IDEAL TRANSFORMERS

A transformer consists of two or more windings, as shown in Fig. 5.2, linked by a mutual field. The primary winding is connected to an alternating voltage source, which results in an alternating flux whose magnitude depends on the voltage, frequency, and number of turns of the primary winding. The alternating flux links the secondary winding and induces a voltage in it with a value that depends on the number of turns of the secondary winding. If the primary voltage is v_1, the core flux ϕ is established such that the counter EMF, e_1, equals the impressed voltage

www.EngineeringEBooksPdf.com

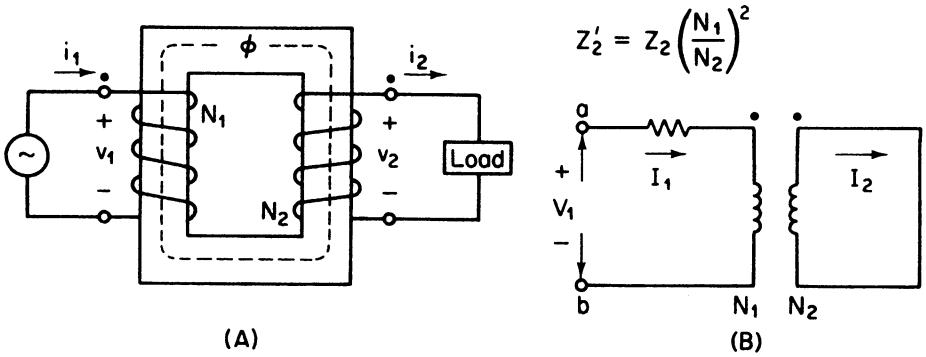


Figure 5.2 Ideal transformer and a load impedance.

(neglecting winding resistance). Thus

$$v_1 = e_1 = N_1 \frac{d\phi}{dt} \tag{5.1}$$

Here N_1 denotes the number of turns of the primary winding. The EMF, e_2, is induced in the secondary by the alternating core flux:

$$v_2 = e_2 = N_2 \frac{d\phi}{dt} \tag{5.2}$$

Taking the ratio of Eq. (5.1) to Eq. (5.2), we see that

$$\frac{v_1}{v_2} = \frac{N_1}{N_2} \tag{5.3}$$

Neglecting losses, the instantaneous power is equal on both sides of the transformer:

$$v_1 i_1 = v_2 i_2 \tag{5.4}$$

Combining Eqs. (5.3) and (5.4), we get

$$\frac{i_1}{i_2} = \frac{N_2}{N_1} \tag{5.5}$$

Thus, in an ideal transformer, the current ratio is the inverse of the voltage ratio. We can conclude that almost any desired voltage ratio of transformation can be obtained by adjusting the number of turns of the transformer.

Transformers can be broadly classified as either step-up or step-down types. In a step-up transformer, the ratio N_1/N_2 is less than 1, and hence v_2 is higher than v_1. A step-down transformer will have a ratio (N_1/N_2) higher than 1, and in this case, v_2 is lower than v_1.

www.EngineeringEBooksPdf.com

Let us assume that the flux is given by the sinusoidal waveform

$$\phi(t) = \phi_m \sin \omega t \tag{5.6}$$

As a result of Eq. (5.1), we see that

$$e_1(t) = N_1 \phi_m \omega \cos \omega t$$

Since $\omega = 2\pi f$, with f being the supply frequency, we see that

$$e_1(t) = 2\pi N_1 \phi_m f \sin(\omega t + 90 \text{ deg})$$

The primary EMF $e_1(t)$ is written as

$$e_1(t) = \sqrt{2} E_1 \sin(\omega t + 90 \text{ deg}) \tag{5.7}$$

where E_1 is the effective (or rms) value of the primary EMF. It is thus clear that

$$E_1 = \frac{2\pi}{\sqrt{2}} N_1 \phi_m f$$

or

$$E_1 = 4.44 N_1 \phi_m f \tag{5.8}$$

The voltage is thus proportional to the number of turns, flux magnitude, and frequency. It should also be noted that according to Eqs. (5.6) and (5.7), the voltage phasor E_1 leads the flux phasor by 90 deg.

Consider an ideal transformer (with negligible winding resistances and leakage reactances and no exciting losses) connected to a load, as shown in Fig. 5.2. Clearly Eqs. (5.1) and (5.5) apply. The dot markings indicate terminals of corresponding polarity in the sense that both windings encircle the core in the same direction if we begin at the dots. Thus comparing the voltages of the two windings shows that the voltages from a dot-marked terminal to an unmarked terminal will be of the same polarity for the primary and secondary windings (i.e., v_1 and v_2 are in phase). From Eqs. (5.3) and (5.5), we can write for sinusoidal steady-state operation

$$\frac{V_1}{I_1} = \left(\frac{N_1}{N_2}\right)^2 \frac{V_2}{I_2} \tag{5.9}$$

But the load impedance Z_2 is

$$\frac{V_2}{I_2} = Z_2 \tag{5.10}$$

www.EngineeringEBooksPdf.com

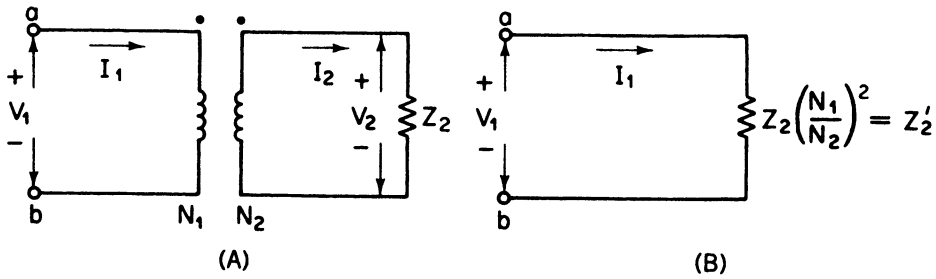


Figure 5.3 Equivalent representations of impedance loads on the secondary of an ideal transformer.

Thus

$$\frac{V_1}{I_1} = \left(\frac{N_1}{N_2}\right)^2 Z_2 \tag{5.11}$$

The result is that as far as its effect is concerned, Z_2 can be replaced by an equivalent impedance Z_2' in the primary circuit. Thus

$$Z_2' = \left(\frac{N_1}{N_2}\right)^2 Z_2 \tag{5.12}$$

The equivalence is shown in Fig. 5.3.

The impedance Z_2' is simply the load impedance, Z_2, referred to the primary side. From Eq. (5.12) it is clear that impedance ratios vary as the square of the turns ratio. An example is appropriate at this point.

Example 5.1 A 440/110-V single-phase 5-kVA 60-Hz transformer delivers a secondary current of 40 A at 0.8 power factor (PF) leading at rated secondary voltage. Assume that the transformer is ideal.

(a) Find the primary voltage and current.
(b) Find the load impedance.
(c) Find the impedance of the load referred to the primary side.

Solution From the specifications available we have

$$V_2 = 110\angle 0$$
$$I_2 = 40\angle \cos^{-1} 0.8$$
$$= 40\angle 36.87 \text{ deg}$$

(a) The transformer ratio is

$$\frac{V_1}{V_2} = \frac{N_1}{N_2} = \frac{440}{110} = 4$$

www.EngineeringEBooksPdf.com

Thus

$$V_1 = 440\,\text{V}$$
$$I_2 = \frac{N_2}{N_1} I_2 = \frac{1}{4}(40\angle 36.87\ \text{deg})$$
$$= 10\angle 36.87\ \text{deg A}$$

(b) The load impedance is

$$Z_2 = \frac{V_2}{I_2} = \frac{110\angle 0}{40\angle 36.87\ \text{deg}} = 2.75\angle -36.97\ \text{deg}\,\Omega$$

(c) The impedance of the load referred to the primary side is

$$Z_2' = \left(\frac{N_1}{N_2}\right)^2 Z_2$$
$$= (4)^2(2.75\angle -36.87\ \text{deg})$$
$$= 44\angle -36.87\ \text{deg}$$

Note that we can get this value by simply using the basic definition of impedance:

$$Z_2' = \frac{V_1}{I_1} = \frac{440}{10\angle 36.87\ \text{deg}} = 44\angle -36.87\ \text{deg}\ \Omega$$

With this background on the performance of an ideal transformer, we can now proceed to deal with a more realistic view of the transformer.

5.3 TRANSFORMER MODELS

The ideal transformer is a very simple mathematical model that accounts only for the voltage, current, and impedance transformations in a transformer. We now discuss more realistic models of a transformer in the form of equivalent circuits.

Let us start by assuming that the primary winding is connected to a source with voltage $v_1(t)$ and that the current in the primary winding is $i_1(t)$. We will assume that the resistance of the primary winding is R_1, and as a result, a net voltage $\bar{v}_1(t)$ is produced, as shown in Fig. 5.4:

$$v_1(t) = \bar{v}_1(t) + R_1 i_1(t) \tag{5.13}$$

According to Faraday's law, we have

$$\bar{v}_1(t) = N_1 \frac{d\phi_1}{dt} \tag{5.14}$$

www.EngineeringEBooksPdf.com

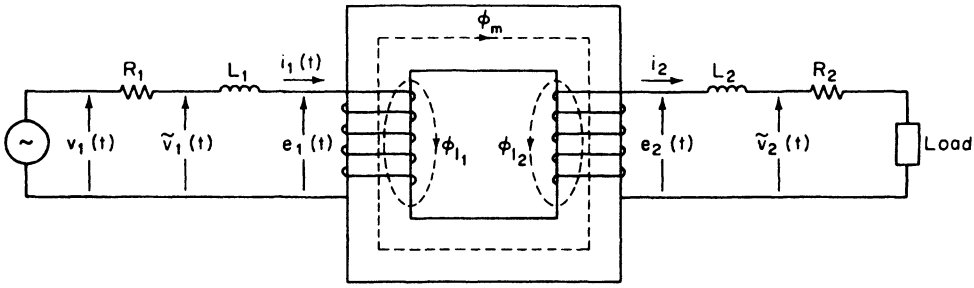


Figure 5.4 Modeling a transformer.

The flux ϕ_1 links the primary winding. If the permeability of the core is infinite, that is, it has zero reluctance, then the flow of ϕ_1 should be confined to the iron path. To account for this less than ideal situation, we assume that a portion of ϕ_1 (however small) is leaked, ϕ_{l_1}. The remainder, denoted by ϕ_m, is the flux in the core structure and links both primary and secondary windings:

$$\phi_1 = \phi_{l_1} + \phi_m \tag{5.15}$$

An equivalent magnetic circuit of the transformer is shown in Fig. 5.5.

As a result of Eq. (5.15), we can combine Eqs. (5.13) and (5.14) to obtain

$$v_1(t) = R_1 i_1(t) + N_1 \frac{d\phi_{l_1}}{dt} + N_1 \frac{d\phi_m}{dt} \tag{5.16}$$

The leakage inductance of the primary winding is now defined by

$$L_1 \frac{di_1}{dt} = N_1 \frac{d\phi_{l_1}}{dt} \tag{5.17}$$

We also define the EMF induced in the primary e_1 as

$$e_1 = N_1 \frac{d\phi_m}{dt} \tag{5.18}$$

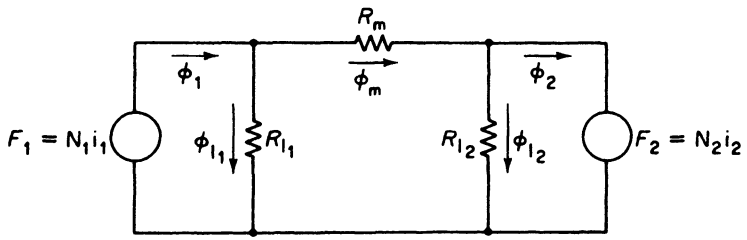


Figure 5.5 Equivalent magnetic circuit of a transformer.

www.EngineeringEBooksPdf.com

As a result, Kirchhoff's voltage law for the primary loop given by Eq. (5.16) reduces to

$$v_1(t) = R_1 i_1(t) + L_1 \frac{di_1}{dt} + e_1(t) \tag{5.19}$$

Let us take a look at the equivalent magnetic circuit of Fig. 5.5. It is clear that the flux ϕ_m is set up as a result of the difference for $\Im_1$ and $\Im_2$. Thus we have

$$\phi_m \Re_m = N_1 i_1 - N_2 i_2 \tag{5.20}$$

The preceding expression assumes a linear B-H characteristic. Alternatively, we define an exciting current, i_ϕ, that is required of the primary to set up the flux ϕ_m:

$$N_1 i_\phi = N_1 i_1 - N_2 i_2 \tag{5.21}$$

Note that by doing this we are no longer bound by the linearity assumption. From the preceding, we can write the primary current as the sum:

$$i_1 = i_\phi + \frac{N_2}{N_1} i_2 \tag{5.22}$$

At this point we assume that the source voltage, $v_1(t)$ is sinusoidal and that the core material is represented by a hysteresis loop to model the relation between ϕ_m and the exciting current i_ϕ. Assuming that $\phi_m(t)$ is sinusoidal, the construction of Fig. 5.6 reveals that the resulting $i_\phi(t)$ is not sinusoidal, but is periodic. The implications of this discovery are that i_1 and e_1 are not sinusoidal, which creates a paradox. To get around this difficulty, we recall that a periodic function can be resolved using Fourier series into the sum of sinusoids with frequencies that are integer multiples of the main function frequency. Essentially what we are saying is that

$$i_\phi = i_{\phi_1} + i_{\phi_3} + \cdots \tag{5.23}$$

The current i_{ϕ_1} is sinusoidal with a frequency equal to that of the source. The current i_{ϕ_3} is a third-harmonic current with a frequency that is three times the source frequency, and so on. Figure 5.7 illustrates this concept. Note that, in practice, the third harmonic of the exciting current is of a much smaller magnitude than the fundamental's i_{ϕ_1}. By assuming that i_{ϕ_3} is negligible, we get around the difficulty of the distortion in i_ϕ.

Let us proceed with the development of the transformer model, assuming that the exciting current $i_\phi(t)$ is sinusoidal as indicated by the first harmonic i_{ϕ_1}. Comparing the $i_m(t)$ and $i_{\phi_1}(t)$ waveforms, we discover that there is a phase shift between the two waves. Note that if the λ–i or ϕ–i characteristic were linear, we would expect no phase shift between ϕ and i, and thus we have an inductance to model the exciting

www.EngineeringEBooksPdf.com

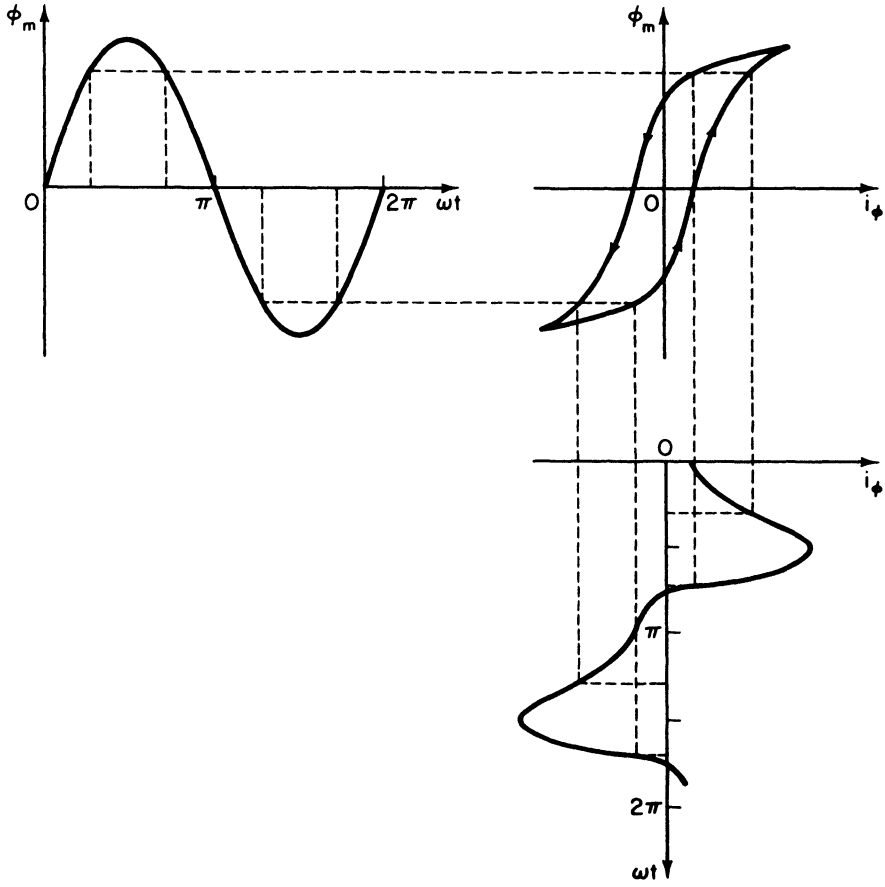


Figure 5.6 Developing the exciting current waveform from a sinusoidal flux waveform.

current process. The phasor diagram of Fig. 5.8 shows that to account for the phase shift, we can resolve i_ϕ into two components $i_m(t)$ and $i_c(t)$. The current i_m is referred to as the magnetizing current and is in phase with the flux. The current $i_c(t)$ represents the component that goes to cover the core losses and is in phase with the voltage E_1. The exciting current phenomenon discussed here can be modeled by a parallel combination of a resistor whose conductance is G_c and an inductor whose susceptance (inverse of reactance) is B_m.

The voltage e_1 is transformed into e_2 through the action of an ideal transformer of turns ratio N_1/N_2, and the current in the secondary winding is i_2. Through an argument similar to that used with the primary winding, we can conclude that a leakage inductance L_2 appears on the secondary side, as does a resistance R_2 representing the ohmic voltage drop in the secondary winding. This concludes the process of modeling a realistic transformer and we can therefore reason that the equivalent circuit of Fig. 5.9 is a realistic representation of a practical transformer under steady-state sinusoidal operating conditions.

www.EngineeringEBooksPdf.com

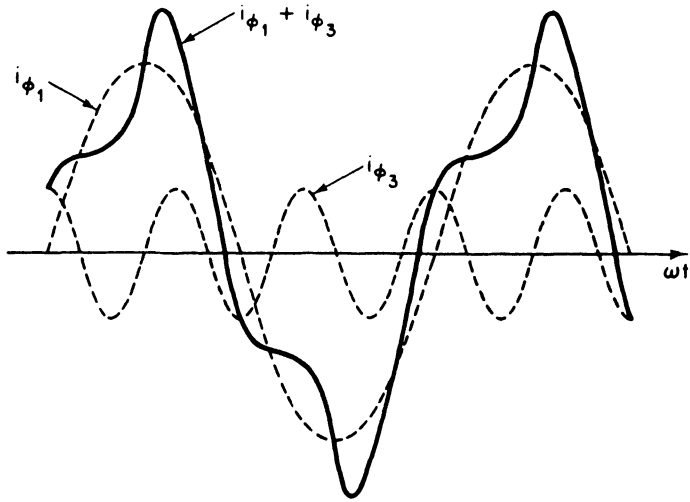


Figure 5.7 Interpreting Eq. (5.23).

The equivalent circuit of Fig. 5.9(a) can be reduced to that of Fig. 5.9(b) by simply referring the secondary side to the primary side using the following:

$$V_2' = \frac{N_1}{N_2} V_2 \tag{5.24}$$

$$I_2' = \frac{N_2}{N_1} I_2 \tag{5.25}$$

$$R_2' = R_2 \left(\frac{N_1}{N_2}\right)^2 \tag{5.26}$$

$$X_2' = X_2 \left(\frac{N_1}{N_2}\right)^2 \tag{5.27}$$

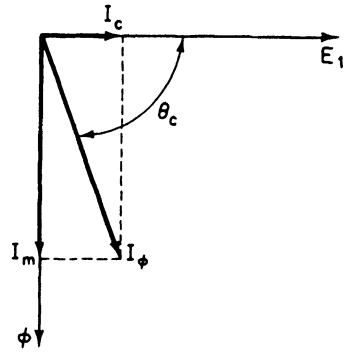


Figure 5.8 Phasor representation of exciting current.

www.EngineeringEBooksPdf.com

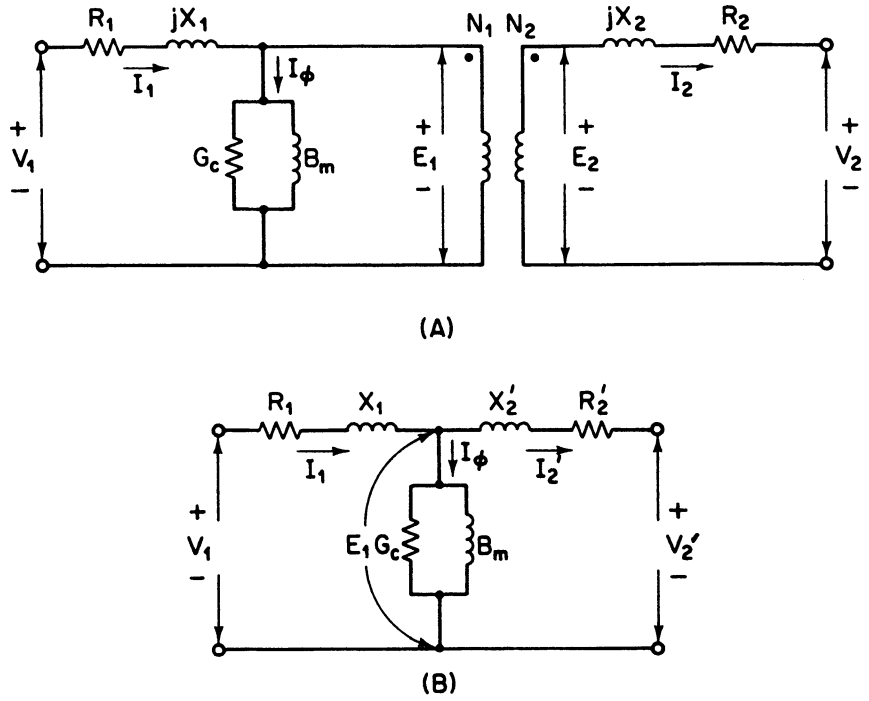


Figure 5.9 Equivalent circuits of transformer.

Although the equivalent circuit just illustrated is simply a T-network, it is customary to use approximate circuits such as shown in Fig. 5.10. In the first two circuits, we move the shunt branch either to the secondary or primary sides to form inverted L-circuits. Further simplifications are shown with the shunt branches neglected [Fig. 5.10(c)], and finally with the resistances neglected [Fig. 5.10(d)]. These last two circuits are of sufficient accuracy in most power system applications. In Fig. 5.10 note that

$$R_{eq} = R_1 + R_2' \tag{5.28}$$

$$X_{eq} = X_1 + X_2' \tag{5.29}$$

A practical example will illustrate the principles and orders of approximations involved.

Example 5.2 A 100-kVA 400/2000-V single-phase transformer has the following parameters:

$$R_1 = 0.01\ \Omega \qquad R_2 = 0.25\ \Omega$$

$$X_1 = 0.03\ \Omega \qquad X_2 = 0.75\ \Omega$$

$$G_c = 2.2\ \text{mS} \qquad B_m = -6.7\ \text{mS}$$

www.EngineeringEBooksPdf.com

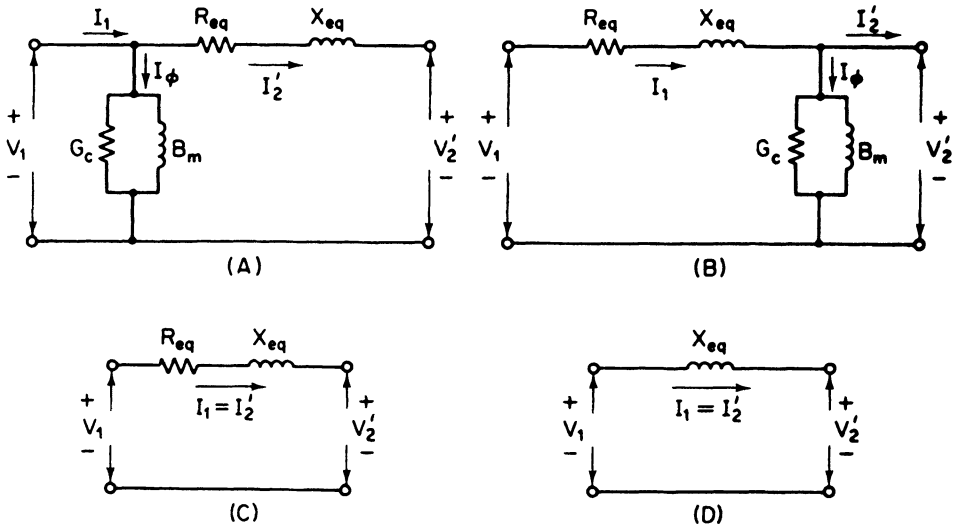


Figure 5.10 Approximate equivalent circuits for the transformer, all referred to primary side.

Note that G_c and B_m are given in terms of primary reference. The transformer supplies a load of 90 kVA at 2000 V and 0.8 PF lagging. Calculate the primary voltage and current using the equivalent circuits shown in Fig. 5.10. Use the equivalent circuit of Fig. 5.9(b) to establish the orders of approximation involved.

Solution Let us refer all the date to the primary (400-V) side:

$$R_1 = 0.01\ \Omega \qquad X_1 = 0.03\ \Omega$$

$$R_2' = 0.25\left(\frac{400}{2000}\right)^2 \qquad X_2' = 0.75\left(\frac{400}{2000}\right)^2$$

$$= 0.01\ \Omega \qquad = 0.03\ \Omega$$

Thus

$$R_{eq} = R_1 + R_2' \qquad X_{eq} = X_1 + X_2'$$

$$= 0.02\ \Omega \qquad = 0.06\ \Omega$$

The voltage $V_2 = 2000$ V; thus

$$V_2' = 2000\left(\frac{400}{2000}\right) = 400\ \text{V}$$

The current I_2' is thus

$$|I_2'| = \frac{90 \times 10^3}{400} = 225\ \text{A}$$

www.EngineeringEBooksPdf.com

The PF of 0.8 lagging implies that

$$I_2' = 225\angle -36.87 \text{ deg A}$$

For ease of computation, we start with the simplest circuit of Fig. 5.10(d). Let us denote the primary voltage calculated through this circuit by V_{1_d}. It is clear that

$$\begin{aligned} V_{1_d} &= V_2' + jI_2'(X_{eq}) \\ &= 400\angle 0 + j(0.06\angle -36.87 \text{ deg})(225) \\ &= 408.243\angle 1.516 \text{ deg V} \\ I_{1_d} &= 225\angle -36.87 \text{ deg A} \end{aligned}$$

Comparing circuits (c) and (d) in Fig. 5.10, we deduce that

$$V_{1_c} = V_2' + I_2'(R_{eq} + jX_{eq}) = V_{1_d} + I_2'(R_{eq})$$

Thus

$$\begin{aligned} V_{1_c} &= 408.243\angle 1.516 \text{ deg} + (225\angle -36.87 \text{ deg})(0.02) \\ &= 411.7797\angle 1.127 \text{ deg V} \\ I_{1_c} &= I_2' = 225\angle -36.87 \text{ deg A} \end{aligned}$$

Let us consider circuit (a) in Fig. 5.10, where we see that

$$V_{1_a} = V_{1_c} = 411.7797\angle 1.127 \text{ deg}$$

But

$$\begin{aligned} I_{1_a} &= I_2' + (G_c + jB_m)V_{1_a} \\ &= 225\angle -36.87 \text{ deg} + (411.7797\angle 1.127 \text{ deg})\ (2.2 - j5.7)10^{-3} \\ &= 227.418\angle -37.277 \text{ deg A} \end{aligned}$$

Circuit (b) in Fig. 5.10 is a bit different since we start with V_2' impressed on the shunt branch. Thus

$$\begin{aligned} I_{1_b} &= I_2' + (G_c + jB_m)V_2' \\ &= 225\angle -36.87 \text{ deg} + (2.2 - j6.7)10^{-3}(400) \\ &= 227.3177\angle -37.277 \text{ deg} \end{aligned}$$

Now

$$\begin{aligned} V_{1_b} &= V_2' + I_{1_b}(R_{eq} + jX_{eq}) \\ &= 400\angle 0 + (227.3177\angle -37.277 \text{ deg})(0.02 + j0.06) \\ &= 411.958\angle 1.12652 \text{ deg} \end{aligned}$$

www.EngineeringEBooksPdf.com

The exact equivalent circuit of Fig. 5.9(b) is now considered. We first calculate E_1:

$$\begin{aligned} E_1 &= V_2' + I_2'(R_2' + jX_2') \\ &= 400\angle 0 + (225\angle -36.87 \text{ deg})(0.01 + j0.03) \\ &= 405.87\angle 0.57174 \text{ deg} \end{aligned}$$

Next, we calculate I_1 as

$$\begin{aligned} I_1 &= I_2' + E_1(G_c + jB_m) \\ &= (225\angle -36.87 \text{ deg}) + (405.87\angle 0.57174 \text{ deg})(2.2 - j6.7)10^{-3} \\ &= 227.37\angle -37.277 \text{ deg} \end{aligned}$$

As a result, we obtain the primary voltage as

$$\begin{aligned} V_1 &= E_1 + I_1(R_1 + jX_1) \\ &= 405.87\angle 0.57174 \text{ deg} + (227.37\angle -37.277 \text{ deg})(0.01 + j0.03) \\ &= 411.87\angle 1.127 \text{ deg V} \end{aligned}$$

The computed values of primary voltage and current from the exact equivalent circuit are used as a benchmark to evaluate the approximate circuits. We start by the simplest form of Fig. 5.10(d). The error in voltage magnitude computation is 3.627 V, or 0.88%, while the error in voltage phase angle is -0.389 deg, or -34%. In the current magnitude, we encounter a 1.04% error, while for the current phase angle, the error is -1.09%.

Including the resistance in the form of Fig. 5.10(c) results in a considerable improvement in the error in voltage magnitude and phase angle. The errors in current are the same as those for circuit (d) in Fig. 5.10. Circuit (b) in Fig. 5.10 has improved current errors and reasonably close voltage errors.

Depending on the purpose of the study, one of the simplified circuits can provide satisfactory results. Of course, one would expect circuit (c) in Fig. 5.10 to be a favorite in large-scale system applications.

5.4 TRANSFORMER PERFORMANCE MEASURES

The selection of a proper transformer for a given application involves evaluating certain important performance measures. Two important measures are the voltage regulation and efficiency of the device.

The voltage regulation is a measure of the variation in the secondary voltage when the load is varied from zero to rated value at a constant power factor. The percentage voltage regulation (PVR) is thus given by

$$\text{PVR} = 100\frac{|V_{2(\text{no-load})}| - |V_{2\text{rated}}|}{|V_{2\text{rated}}|} \tag{5.30}$$

www.EngineeringEBooksPdf.com

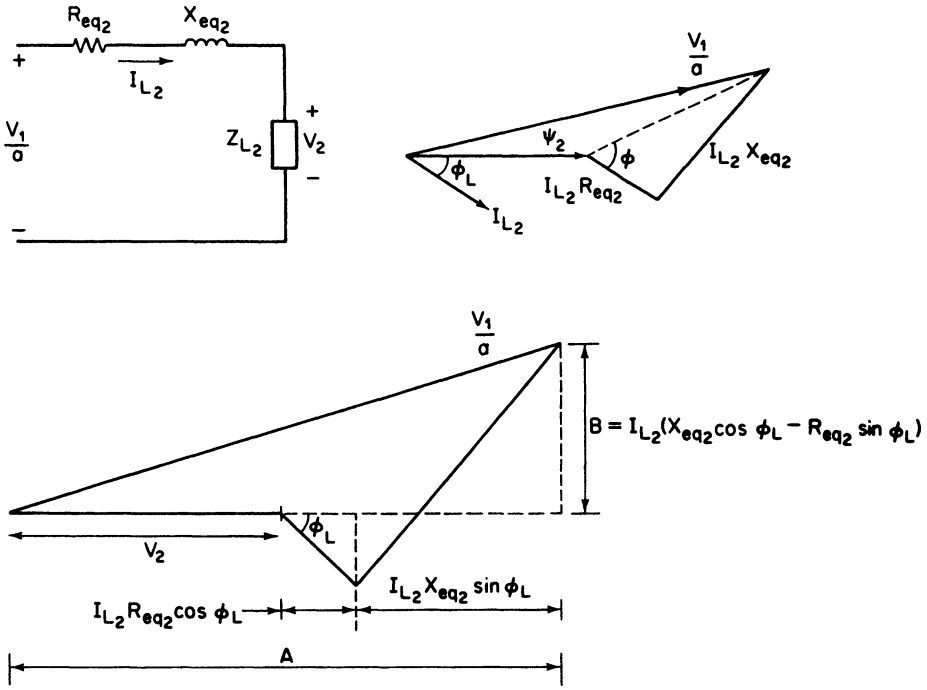


Figure 5.11 Transformer approximate equivalent circuit and associated phasor diagrams for voltage-regulation derivation.

If we neglect the exciting current and refer the equivalent circuit to the secondary side, by inspection of Fig. 5.11, we have

$$\text{PVR} = 100\frac{|V_2/a| - |V_2|}{|V_2|}$$

where a is the transformer ratio. Thus

$$a = \frac{N_1}{N_2}$$

From the phasor diagram of Fig. 5.11, we have

$$\left|\frac{V_1}{a}\right| = \sqrt{A^2 + B^2} = A\left(1 + \frac{B^2}{A^2}\right)^{1/2}$$

We use the following approximation:

$$\frac{V_1}{a} = A\left(1 + \frac{B^2}{2A^2} + \cdots\right) \cong A + \frac{B^2}{2A}$$

www.EngineeringEBooksPdf.com

Hence the percentage voltage regulation is

$$\text{PVR} = \left(\frac{A - V_2 + B^2/2A}{V_2}\right)100 \cong \left(\frac{A - V_2 + B^2/2V_2}{V_2}\right)100$$

In terms of transformer constants, we get

$$\text{PVR} \cong 100\left\{\frac{I_{L_2}(R_{eq_2}\cos\phi_L + X_{eq_2}\sin\phi_L)}{V_2} + \frac{1}{2}\left[\frac{I_{L_2}(X_{eq_2}\cos\phi_L - R_{eq_2}\sin\phi_L)}{V_2}\right]^2\right\} \tag{5.31}$$

The efficiency of the transformer is the ratio of output (secondary) power to the input (primary) power. Formally, the efficiency is η:

$$\eta = \frac{P_2}{P_1} \tag{5.32}$$

If we deal with the transformer as referred to the secondary side, we have

$$P_2 = |V_2||I_L|\cos\phi_L \tag{5.33}$$

where I_L is the load current. The input power P_1 is the sum of the output power and power loss in the transformer. Thus

$$P_1 = P_2 + P_l \tag{5.34}$$

The power loss in the transformer is made of two parts: the I^2R loss and the core loss P_c. Thus

$$P_l = P_c + |I_L|^2(R_{eq}) \tag{5.35}$$

As a result, the efficiency is given by

$$\eta = \frac{|V_2||I_L|\cos\phi_L}{|V_2||I_L|\cos\phi_L + P_c + |I_L|^2(R_{eq})} \tag{5.36}$$

The efficiency of a transformer varies with the load current I_L. It attains a maximum when

$$\frac{\partial\eta}{\partial I_L} = 0 \tag{5.37}$$

www.EngineeringEBooksPdf.com

Using Eq. (5.32), the derivative is

$$\frac{\partial \eta}{\partial I_L} = \frac{P_1(\partial P_2/\partial |I_L|) - P_2(\partial P_1/\partial |I_L|)}{P_1^2} \tag{5.38}$$

Thus the condition for maximum power is

$$\frac{P_1}{P_2} = \frac{\partial P_1/\partial |I_L|}{\partial P_2/\partial |I_L|} \tag{5.39}$$

Using Eqs. (5.33) to (5.35), we get

$$\frac{P_1}{P_2} = \frac{|V_2|\cos\phi_L + 2|I_L|R_{eq}}{|V_2|\cos\phi_L} \tag{5.40}$$

This reduces to

$$P_1 = P_2 + 2|I_L|^2 R_{eq} \tag{5.41}$$

Thus, for maximum efficiency, we have

$$P_1 = P_c + |I_L|^2 R_{eq} \tag{5.42}$$

As a result, the maximum efficiency occurs for

$$P_c = |I_L|^2 R_{eq} \tag{5.43}$$

That is, when the I^2R losses equal the core losses, maximum efficiency is attained.

The following example utilizes results of Example 5.2 to illustrate the computations involved.

Example 5.3 Find the percentage voltage regulation and efficiency of the transformer of Example 5.2.

Solution Let us refer quantities to the secondary side:

$$V_2 = 2000\ \text{V}$$

$$I_{L_2} = \frac{90 \times 10^3}{2000} = 45\ \text{A}$$

$$R_{eq_2} = 0.02(5)^2 = 0.5\ \Omega$$

$$X_{eq_2} = 0.06(5)^2 = 1.5\ \Omega$$

www.EngineeringEBooksPdf.com

Thus, substituting in Eq. (5.31), we get

$$\text{PVR} = 100\left\{\frac{45[0.5(0.8) + 1.5(0.6)]}{2000} + \frac{1}{2}\left[\frac{45[1.5(0.8) - 0.5(0.6)]}{2000}\right]^2\right\}$$
$$= 2.9455\%$$

Let us compare this with the results of applying Eq. (5.30) with no approximations but for those of circuit (c) in Fig. 5.10. Here we have

$$V_1 = 411.7797$$
$$V_2' = 400\,\text{V}$$

Referred to the secondary, we have

$$V_1' = 411.7797(5)$$

On no-load, the current is zero, and hence

$$V_{2(\text{no-load})} = V_1'$$

The rated secondary voltage is

$$V_{2\text{rated}} = 2000$$

As a result,

$$\text{PVR} = \frac{411.7797 - 400}{400}$$
$$= 2.9449\%$$

To calculate the efficiency, we apply the basic definition, for which we need P_1 and P_2. We use the exact circuit results, for which

$$P_2 = V_2 I_2 \cos\phi_2$$
$$= 400(225)(0.8) = 72{,}000\,\text{W}$$
$$P_1 = V_1 I_1 \cos\phi_1$$

The angle ϕ_1 is that between the voltage, V_1, and current, I_1, and is given by

$$\phi_1 = 1.127 - (-37.277)$$
$$= 38.404$$

www.EngineeringEBooksPdf.com

We also have

$$V_1 = 411.87\,\text{V}$$
$$I_1 = 227.37\,\text{A}$$

As a result,

$$P_1 = 411.87(227.37)\cos 38.404$$
$$= 73{,}386\,\text{W}$$

The efficiency is now found as

$$\eta = \frac{72{,}000}{73{,}386} = 0.9811$$

Example 5.4 Find the maximum efficiency of the transformer of Example 5.2 under the same PF and voltage conditions.

Solution First we need the core losses. These are obtained from the exact equivalent circuit as

$$P_c = |E_1|^2(G_c)$$
$$= (405.87)^2(2.2 \times 10^{-3})$$
$$= 362.41\,\text{W}$$

For maximum efficiency,

$$P_c = I_L^2(R_{\text{eq}})$$

Referred to the primary, we thus have

$$362.41 = I_L^2(0.02)$$

Thus for maximum efficiency, we get

$$I_L = 134.61\,\text{A}$$

As a result,

$$\eta_{\max} = \frac{V_2'|I_L|\cos\phi_L}{V_2'|I_L|\cos\phi_L + 2P_c}$$
$$= \frac{400(134.61)(0.8)}{400(134.61)(0.8) + 2(362.41)}$$
$$= 0.98345$$

www.EngineeringEBooksPdf.com

5.5 SINGLE-PHASE CONNECTIONS

Single-phase transformers can be connected in a variety of ways. To start with, consider two single-phase transformers A and B. They can be connected in four different combinations, provided that the polarities are observed.

5.5.1 Series–Series Connections

The primaries of the two transformers are connected in series, as are the secondaries. The connection is shown in Fig. 5.12. The voltage V_1 is the sum of the voltages V_{1_A} and V_{1_B}, and similarly, V_2 is the sum of the secondary voltages V_{2_A} and V_{2_B}. The primary current of the combination passes through the primaries of transformers A and B, and similarly, the secondary current of the combination passes through the secondaries of both transformers. It is clear that the allowed currents should not exceed the rated current of either transformer. This results in a derating of the combination as shown in the following example.

Example 5.5 Assume that transformer A is rated at 1000 VA and transformer B is rated at 600 VA. Both transformers have a voltage ratio of 240/120. It is clear that the rated currents on the primary side are

$$I_{1_{A_r}} = \frac{1000}{420} = 4.167 \text{ A}$$

$$I_{1_{B_r}} = \frac{600}{240} = 2.5 \text{ A}$$

The allowable current for the primaries connected in series is the lowest of the two rated currents,

$$I_1 = 2.5 \text{ A}$$

On the secondary side, we should have

$$I_2 = 5 \text{ A}$$

The series combination has a voltage ratio of 480/240 V. The volt-ampere rating is now given by

$$\text{VA} = 480 \times 2.5 = 1200 \text{ VA}$$

5.5.2 Series–Parallel Connections

The primaries of transformers A and B are connected in series, while their secondaries are connected in parallel, as shown in Fig. 5.13(a).

www.EngineeringEBooksPdf.com

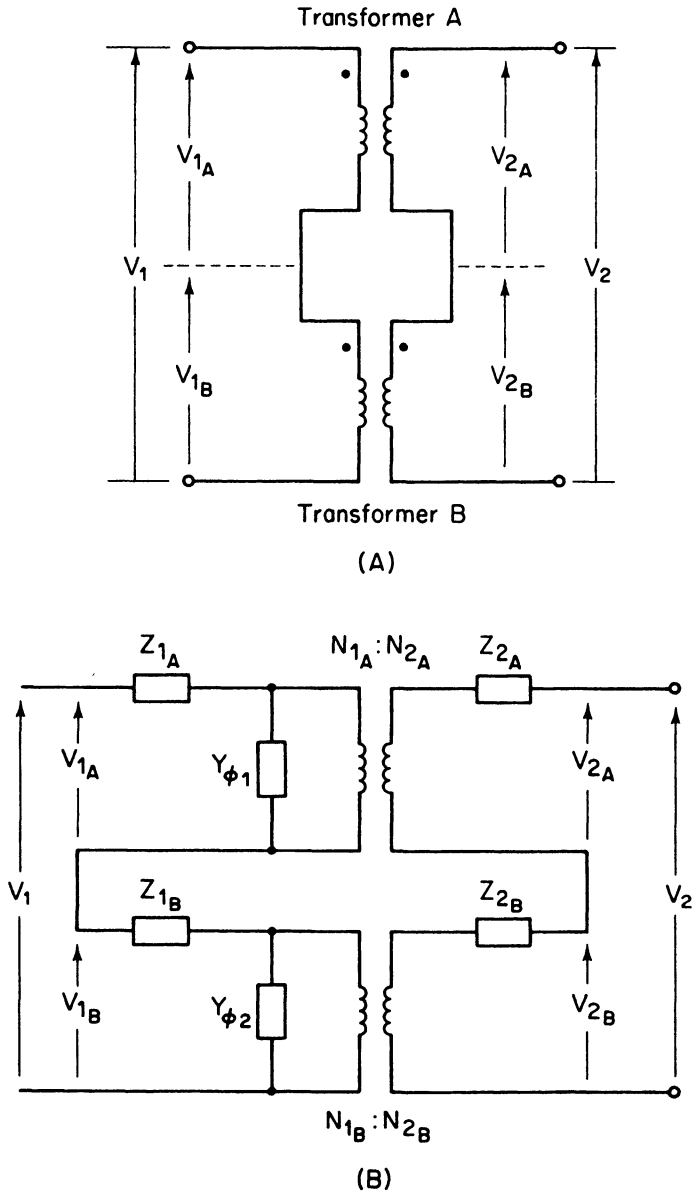
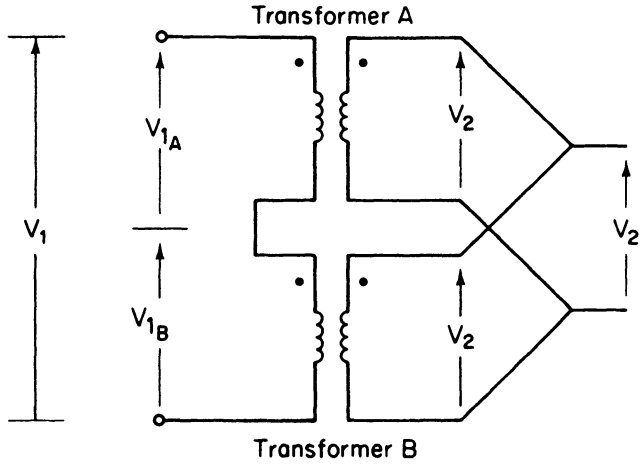


Figure 5.12 Connection diagram for two transformers with primaries connected in series and secondary connected in series.

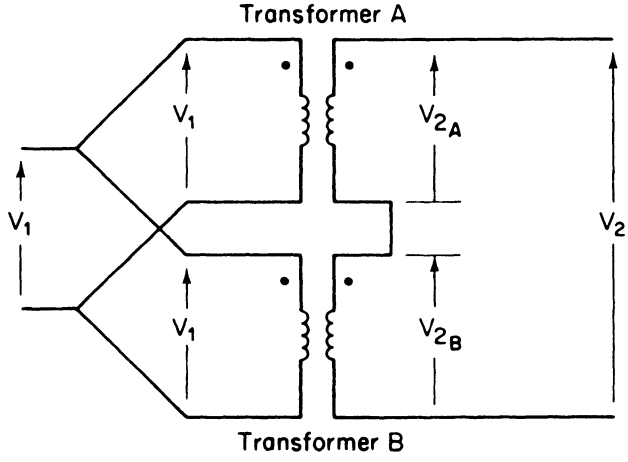
5.5.3 Parallel–Series Connections

The primaries of transformers *A* and *B* are connected in parallel, and their secondaries are connected in series, as shown in Fig. 5.13(b). Note that when windings are connected in parallel, those having the same voltage and polarity are paralleled.

www.EngineeringEBooksPdf.com



(A)



(B)

Figure 5.13 (a) Series–parallel, and (b) parallel–series connections for single-phase transformers.

When connected in series, windings of opposite polarity are joined in one junction. Coils of unequal voltage ratings can be series-connected, either aiding or opposing.

5.5.4 Parallel Connections

Figure 5.14 shows two transformers *A* and *B* connected in parallel, with their approximate equivalent circuit indicated as well. Assume that Z_A is the ohmic equivalent

www.EngineeringEBooksPdf.com

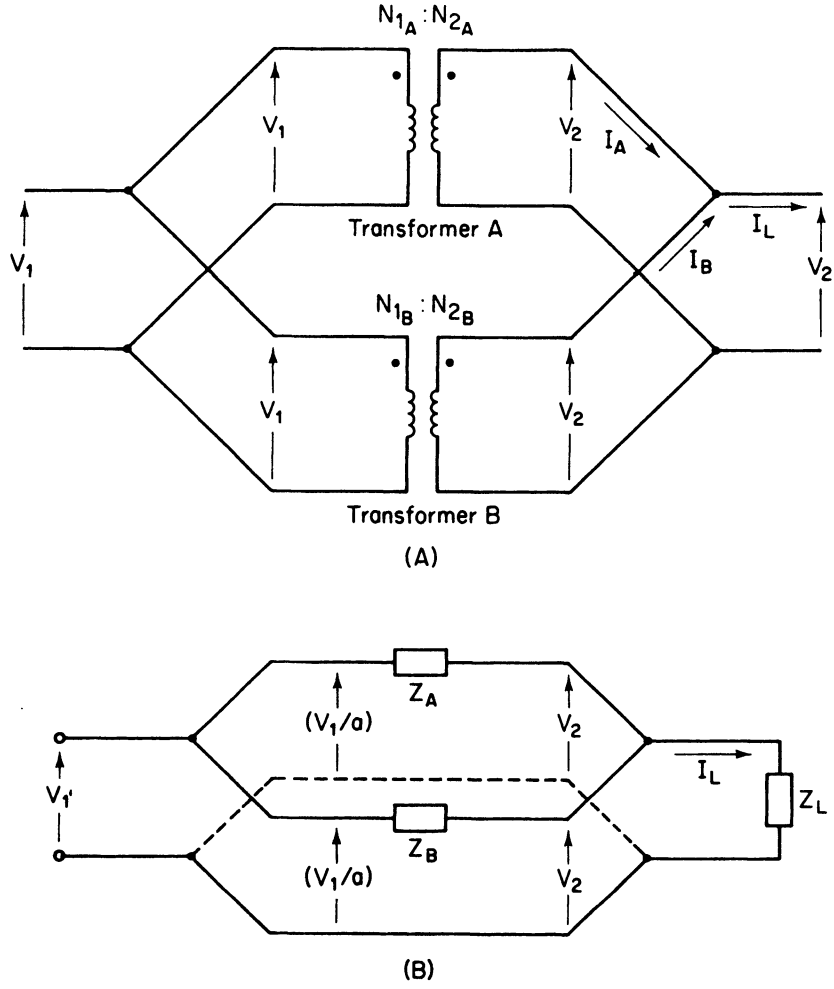


Figure 5.14 Parallel-connected single-phase transformers: (a) connection diagram; (b) equivalent circuit.

impedance of transformer A referred to its secondary side. Similarly, Z_B is the ohmic equivalent impedance of transformer B referred to its secondary side, and Z_L is the load impedance. Impedance V_A is the primary voltage on both transformer primaries. The turns ratio for each of the transformers should be identical for the parallel combination to make sense

$$a = \frac{N_{1_A}}{N_{2_A}} = \frac{N_{1_B}}{N_{2_B}}$$

The current delivered by transformer A is I_A. Thus

$$I_A = \frac{\Delta V}{Z_A} \tag{5.44}$$

www.EngineeringEBooksPdf.com

Similarly,

$$I_B = \frac{\Delta V}{Z_B} \tag{5.45}$$

where

$$\Delta V = \frac{V_1}{a} - V_2 \tag{5.46}$$

The load current is

$$I_L = I_A + I_B \tag{5.47}$$

Thus using Eqs. (5.44) to (5.47), we get

$$I_L = \frac{\Delta V}{Z_{eq}} \tag{5.48}$$

where Z_{eq} is the parallel combination of Z_A and Z_B given by

$$\frac{1}{Z_{eq}} = \frac{1}{Z_A} + \frac{1}{Z_B} \tag{5.49}$$

Now

$$\Delta V = \frac{V_1}{a} - I_L Z_L \tag{5.50}$$

Thus using Eq. (5.50) in Eq. (5.48), we conclude that

$$I_L = \frac{V_1/a}{Z_L + Z_{eq}} \tag{5.51}$$

This result is expected, as Z_A and Z_B in parallel are in series with Z_L across the voltage (V_1/a). The current division between the two transformers is obtained from

$$I_A = \frac{I_L Z_{eq}}{Z_A} = \frac{\Delta V}{Z_A} \tag{5.52}$$

$$I_B = \frac{I_L Z_{eq}}{Z_B} = \frac{\Delta V}{Z_B} \tag{5.53}$$

5.6 THREE-WINDING TRANSFORMERS

The three-winding transformer is used in many parts of the power system for the economy achieved when using three windings on the one core. Figure 5.15 shows

www.EngineeringEBooksPdf.com

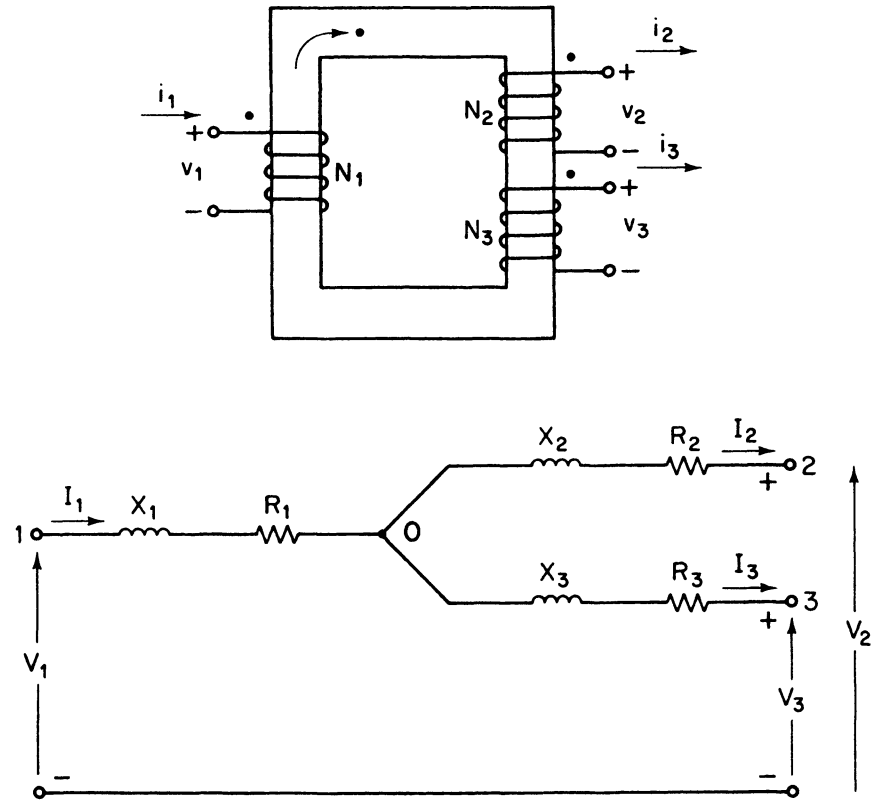


Figure 5.15 Three-winding transformer and its practical equivalent circuit.

a three-winding transformer with a practical equivalent circuit. The impedances Z_1, Z_2, and Z_3 are calculated from the three impedances obtained by considering each pair of windings separately with

$$Z_1 = \frac{Z_{12} + Z_{13} - Z_{23}}{2} \tag{5.54}$$

$$Z_2 = \frac{Z_{12} + Z_{23} - Z_{13}}{2} \tag{5.55}$$

$$Z_3 = \frac{Z_{13} + Z_{23} - Z_{12}}{2} \tag{5.56}$$

The I^2R loss for a three-winding transformer can be obtained from analysis of the equivalent circuit shown.

Example 5.6 Consider a three-winding transformer with the particulars shown in the equivalent circuit referred to the primary side given in Fig. 5.16. Assuming that

www.EngineeringEBooksPdf.com

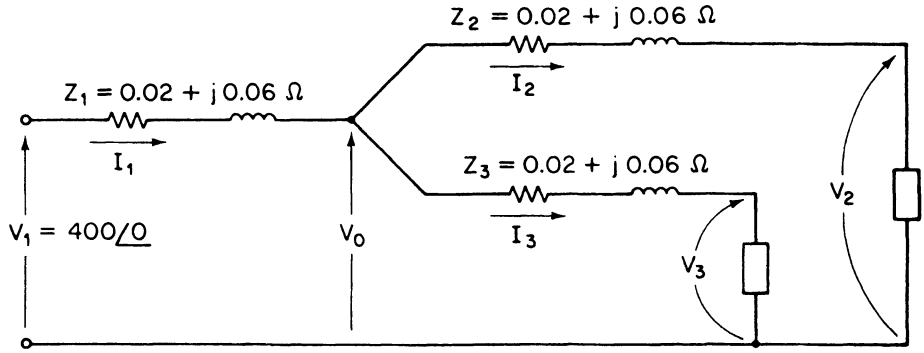


Figure 5.16 Circuit for Example 5.6.

V_1 is the reference, calculate the following:

(a) The secondary and tertiary voltages referred to the primary side.
(b) The apparent powers and power factors at the primary, secondary, and tertiary terminals.
(c) The transformer efficiency.

Assume that

$$I_2 = 50\angle -30 \text{ deg}$$
$$I_3 = 50\angle -35 \text{ deg}$$

Solution

(a) The primary current is

$$I_1 = I_2 + I_3$$
$$= 99.9048\angle -32.5 \text{ deg}$$

Now the voltage at point 0 is

$$V_0 = V_1 - I_1 Z_1$$
$$= 400 - (99.9048\angle -32.5 \text{ deg})(0.02 + j0.06)$$
$$= 395.114\angle -0.577 \text{ deg V}$$

The secondary voltage is obtained referred to the primary as

$$V_2 = V_0 - I_2 Z_2$$
$$= 395.114\angle -0.577 \text{ deg} - (50\angle -30 \text{ deg})(0.02 + j0.06)$$
$$= 392.775\angle -0.887 \text{ deg V}$$

www.EngineeringEBooksPdf.com

The tertiary voltage is obtained referred to the primary as

$$\begin{aligned} V_3 &= V_0 - I_3 Z_3 \\ &= 395.114\angle -0.577 \text{ deg} - (50\angle -35 \text{ deg})(0.02 + j0.06) \\ &= 392.598\angle -0.856 \text{ deg V} \end{aligned}$$

(b) The apparent power into the load connected to the secondary winding is thus

$$\begin{aligned} S_2 &= V_2 I_2^* \\ &= 19{,}638.75\angle 29.113 \text{ deg VA} \end{aligned}$$

As a result,

$$\text{PF}_2 = \cos(29.113 \text{ deg}) = 0.87366$$

Similarly, for the tertiary winding, we get

$$\begin{aligned} S_3 &= V_3 I_3^* \\ &= 19{,}629.9\angle 34.144 \text{ deg VA} \end{aligned}$$

As a result,

$$\text{PF}_3 = \cos(34.144 \text{ deg}) = 0.8276$$

The apparent power at the primary side is

$$\begin{aligned} S_1 &= V_1 I_1^* \\ &= 39{,}961.9\angle 32.5 \text{ deg VA} \end{aligned}$$

As a result,

$$\text{PF}_1 = \cos(32.5 \text{ deg}) = 0.84339$$

(c) The active powers are

$$\begin{aligned} P_2 &= 19{,}638.75 \cos 29.113 \text{ deg} \\ &= 17{,}157.6 \text{ W} \\ P_3 &= 19{,}629.9 \cos 34.144 \text{ deg} \\ &= 16{,}246.28 \text{ W} \\ P_1 &= 39{,}961.92 \cos 32.5 \text{ deg} \\ &= 33{,}703.54 \text{ W} \end{aligned}$$

www.EngineeringEBooksPdf.com

The efficiency is therefore

$$\eta = \frac{P_2 + P_3}{P_1}$$
$$= 0.991$$

5.7 THREE-PHASE SYSTEMS AND TRANSFORMER CONNECTIONS

The major potion of all the electric power currently used is generated, transmitted, and distributed using balanced three-phase voltage systems. A balanced three-phase voltage system is composed of three single-phase voltages having the same magnitude and frequency, but time-displaced from one another by 120 deg. Figure 5.17(a) is a schematic representation where the three single-phase voltage sources appear in a Y-connection; a Δ-configuration is also possible. Also, a phasor diagram showing each of the phase voltages is given in Fig. 5.17(b). As the phasors revolve at the angular frequency with respect to the reference line in the counterclockwise (positive) direction, the positive maximum value first occurs for phase *a* and then in succession for phases *b* and *c*. Stated in a different way, to an observer in the phasor space, the voltage of phase *a* arrives first, followed by that of *b* and then that of *c*. For this reason, the three-phase voltage of Fig. 5.17 is said to have the phase sequence *abc* (*order* or *phase sequence* or *rotation* are all synonymous terms). This is important for certain applications. For example, in three-phase induction motors, the phase sequence determines whether the motor turns clockwise or counterclockwise.

Balanced three-phase systems can be studied using techniques developed for single-phase circuits. The arrangement of the three single-phase voltages into a Y- or a Δ-configuration requires some modifications in dealing with the overall system.

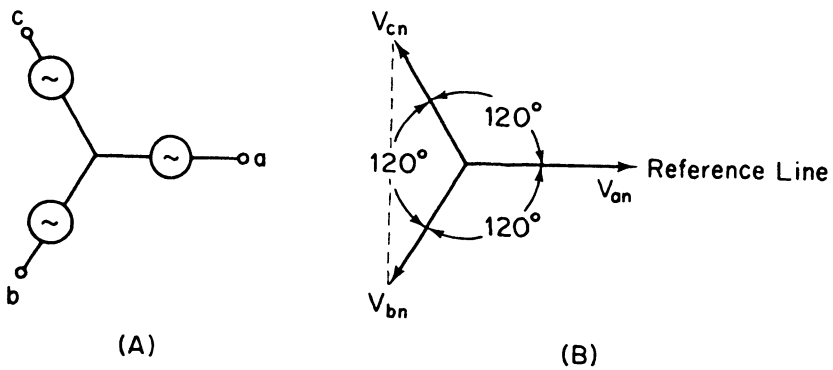


Figure 5.17 Y-Connected three-phase system and the corresponding phasor diagram.

www.EngineeringEBooksPdf.com

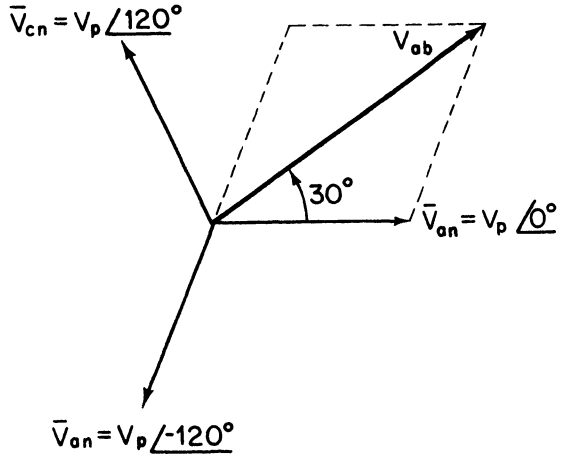


Figure 5.18 Illustrating the phase and magnitude relations between the phase and line voltage of a Y-connection.

5.7.1 Y-Connection

With reference to Fig. 5.17, the common terminal n is called the *neutral* or *star* (Y) point. The voltages appearing between any two of the line terminals a, b, and c have different relationships in magnitude and phase to the voltages appearing between any one line terminal and the neutral point, n. The set of voltages V_{ab}, V_{bc}, and V_{ca} are called the *line voltages*, and the set of voltages V_{an}, V_{bn}, and V_{cn} are referred to as the *phase voltages*. Analysis of phasor diagrams provides the required relationships.

The effective values of the phase voltages are shown in Fig. 5.18 as V_{an}, V_{bn}, and V_{cn}. Each has the same magnitude, and each is displaced 120 deg from the other two phasors. To obtain the magnitude and phase angle of the line voltage from a to b (i.e., V_{ab}), we apply Kirchhoff's voltage law:

$$V_{ab} = V_{an} + V_{nb} \tag{5.57}$$

This equation states that the voltage existing form a to b is equal to the voltage from a to n (i.e., V_{an}) plus the voltage from n to b. Thus Eq. (5.57) can be rewritten as

$$V_{ab} = V_{an} - V_{bn} \tag{5.58}$$

Since for a balanced system, each phase voltage has the same magnitude, let us set

$$|V_{an}| = |V_{bn}| = |V_{cn}| = V_p \tag{5.59}$$

www.EngineeringEBooksPdf.com

where V_p denotes the effective magnitude of the phase voltage. Accordingly, we can write

$$V_{an} = V_p \angle 0 \tag{5.60}$$
$$V_{bn} = V_p \angle -120 \text{ deg} \tag{5.61}$$
$$V_{cn} = V_p \angle -240 \text{ deg} = V_p \angle 120 \text{ deg} \tag{5.62}$$

Substituting Eqs. (5.60) and (5.61) in Eq. (5.58) yields

$$V_{ab} = V_p(1 - 1\angle -120 \text{ deg})$$

or

$$V_{ab} = \sqrt{3} V_p \angle 30 \text{ deg} \tag{5.63}$$

Similarly, we obtain

$$V_{bc} = \sqrt{3} V_p \angle -90 \text{ deg} \tag{5.64}$$
$$V_{ca} = \sqrt{3} V_p \angle 150 \text{ deg} \tag{5.65}$$

The expressions just obtained for the line voltages show that they constitute a balanced three-phase voltage system whose magnitudes are $\sqrt{3}$ times the phase voltages. Thus we write

$$V_L = \sqrt{3} V_p \tag{5.66}$$

A current flowing out of a line terminal a (or b or c) is the same as that flowing through the phase source voltage appearing between terminals n and a (or n and b, or n and c). We can thus conclude that for a Y-connected three-phase source, the line current equals the phase current. Thus

$$I_L = I_p \tag{5.67}$$

where I_L denotes the effective value of the line current and I_p denotes the effective value for the phase current.

5.7.2 Δ-Connections

Now we consider the case when the three single-phase sources are rearranged to form a three-phase Δ-connection, as shown in Fig. 5.19. It is clear from inspection of the circuit shown that the line and phase voltages have the same magnitude:

$$|V_L| = |V_p| \tag{5.68}$$

www.EngineeringEBooksPdf.com

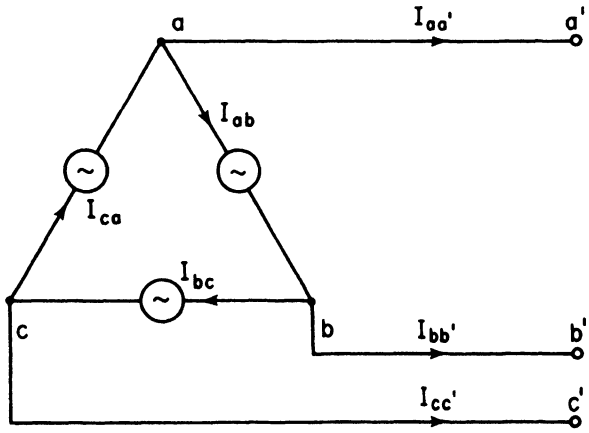


Figure 5.19 Δ-Connected three-phase source.

The phase and line currents, however, are not identical, and the relationship between them can be obtained using Kirchhoff's current law at one of the line terminals.

In a manner similar to that adopted for the Y-connected source, let us consider the phasor diagram shown in Fig. 5.20. Assume the phase currents to be

$$I_{ab} = I_p \angle 0 \tag{5.69}$$

$$I_{bc} = I_p \angle -120 \text{ deg} \tag{5.70}$$

$$I_{ca} = I_p \angle 120 \text{ deg} \tag{5.71}$$

The current that flows in the line joining a to a' is denoted $I_{aa'}$ and is given by

$$I_{aa'} = I_{ca} - I_{ab}$$

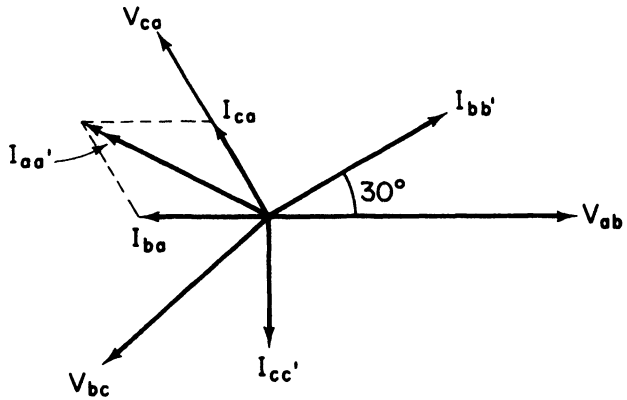


Figure 5.20 Illustrating the relation between phase and line currents in Δ-connection.

www.EngineeringEBooksPdf.com

As a result, we have

$$I_{aa'} = I_p(1\angle 120 \text{ deg} - 1\angle 0)$$

which simplifies to

$$I_{aa'} = \sqrt{3}I_p\angle 150 \text{ deg} \tag{5.72}$$

Similarly,

$$I_{bb'} = \sqrt{3}I_p\angle 30 \text{ deg} \tag{5.73}$$

$$I_{cc'} = \sqrt{3}I_p\angle -90 \text{ deg} \tag{5.74}$$

Note that a set of balanced three-phase currents yields a corresponding set of balanced line currents that are $\sqrt{3}$ times the phase values:

$$I_L = \sqrt{3}I_p \tag{5.75}$$

where I_L denotes the magnitude of any of the three line currents.

5.7.3 Power Relationships

Assume that the three-phase generator is supplying a balanced load with three sinusoidal phase voltages:

$$v_a(t) = \sqrt{2}V_p \sin \omega t$$

$$v_b(t) = \sqrt{2}V_p \sin(\omega t - 120 \text{ deg})$$

$$v_c(t) = \sqrt{2}V_p \sin(\omega t + 120 \text{ deg})$$

with the currents given by

$$i_a(t) = \sqrt{2}I_p \sin(\omega t - \phi)$$

$$i_b(t) = \sqrt{2}I_p \sin(\omega t - 120 \text{ deg} - \phi)$$

$$i_c(t) = \sqrt{2}I_p \sin(\omega t + 120 \text{ deg} - \phi)$$

where ϕ is the phase angle between the current and voltage in each phase. The total power in the load is

$$P_{3\phi}(t) = v_a(t)i_a(t) + v_b(t)i_b(t) + v_c(t)i_c(t)$$

This reduces to

$$P_{3\phi}(t) = 3V_pI_p \cos\phi$$

www.EngineeringEBooksPdf.com

When referring to the voltage level of a three-phase system, one invariably understands the line voltages. From the preceding discussion, the relationship between the line and phase voltages in a Y-connected system is

$$|V_L| = \sqrt{3}|V| \tag{5.76}$$

The power equation thus reads in terms of line quantities:

$$P_{3\phi} = \sqrt{3}|V_L||I_L|\cos\phi \tag{5.77}$$

We note that the total instantaneous power is constant, having a magnitude of three times the real power per phase. We may be tempted to assume that the reactive power is of no importance in a three-phase system since the Q terms cancel out. However, this situation is analogous to the summation of balanced three-phase currents and voltages that also cancel out. Although the sum cancels out, these quantities are still very much in evidence in each phase. We thus extend the concept of complex or apparent power (S) to three-phase systems by defining

$$S_{3\phi} = 3V_pI_p^* \tag{5.78}$$

where the active power and reactive power are obtained form

$$S_{3\phi} = P_{3\phi} + jQ_{3\phi} \tag{5.79}$$

as

$$P_{3\phi} = 3|V_p||I_p|\cos\phi \tag{5.80}$$

$$Q_{3\phi} = 3|V_p||I_p|\sin\phi \tag{5.81}$$

In terms of line values, we can assert that

$$S_{3\phi} = \sqrt{3}V_LI_L^* \tag{5.82}$$

and

$$P_{3\phi} = \sqrt{3}|V_L||I_L|\cos\phi \tag{5.83}$$

$$Q_{3\phi} = \sqrt{3}|V_L||I_L|\sin\phi \tag{5.84}$$

In specifying rated values for power system apparatus and equipment such as generators, transformers, circuit breakers, and so on, we use the magnitude of the apparent power, $S_{3\phi}$, as well as line voltage for specification values.

www.EngineeringEBooksPdf.com

5.7.4 Three-Phase Transformer Connections

For three-phase system applications, it is possible to install three-phase transformer units or banks made of three single-phase transformers connected in the desired three-phase configurations. The latter arrangement is advantageous from a reliability standpoint, since it is then possible to install a single standby single-phase transformer instead of a three-phase unit. This provides a considerable cost saving. We have seen that there are two possible three-phase connections: the Y-connection and the Δ-connection. We thus see that three-phase transformers can be connected in four different ways. In the Y/Y-connection, both primary and secondary windings are connected in Y. In addition, we have Δ/Δ-, Y/Δ-, or Δ/Y-connections. The Y-connected windings may or may not be grounded.

The Y/Δ-configuration is used for stepping down from a high voltage to a medium or low voltage. This configuration provides a neutral grounding on the high-voltage side. Conversely, the Δ/Y-configuration is used in stepping up to a high voltage. The Δ/Δ-connection enables one to remove one transformer for maintenance while the other two continue to function as a three-phase bank (with reduced rating) in an open-delta or V-connection. The difficulties arising from the harmonic contents of the exciting current associated with the Y/Y-connection make it seldom used.

In Fig. 5.21, the four common three-phase transformer connections are shown along with the voltage and current relations associated with the transformation. It is important to realize that the line-to-ground voltages on the Δ side lead the corresponding Y-side values by 30 deg, and that the line currents on the Δ side also lead the currents on the Y side by 30 deg. The proof of this statement is given now.

Consider the Y/Δ three-phase transformer shown in Fig. 5.22. The secondary voltage E_s is given in terms of the line-to-ground voltages by

$$E_s = V_{an} - V_{cn}$$

Assuming phase sequence *a-b-c*, taking V_{an} as the reference, we have

$$V_{cn} = V_{an} \angle 120 \text{ deg}$$

As a result,

$$E_s = (1 - 1\angle 120 \text{ deg}) V_{an}$$

or

$$E_s = \sqrt{3} V_{an} \angle -30 \text{ deg} \tag{5.85}$$

This last result can be verified either analytically or by reference to the phasor diagram in Fig. 5.22. Assuming that each winding of the primary has N_1 turns and that each secondary winding has a number of turns N_2, we have

$$E_p = \frac{N_1}{N_2} E_s$$

www.EngineeringEBooksPdf.com

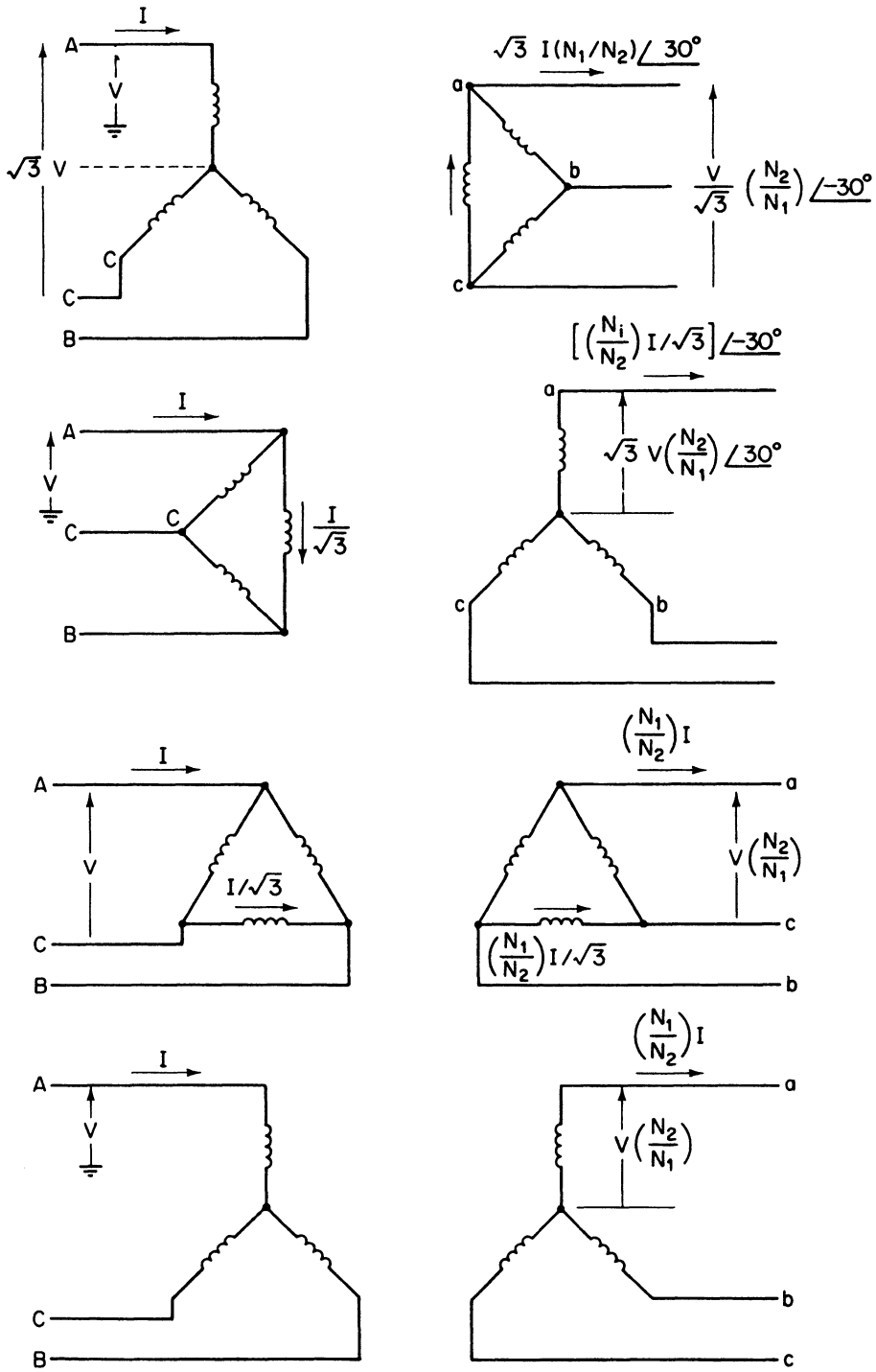


Figure 5.21 Three-phase transformer connections.

www.EngineeringEBooksPdf.com

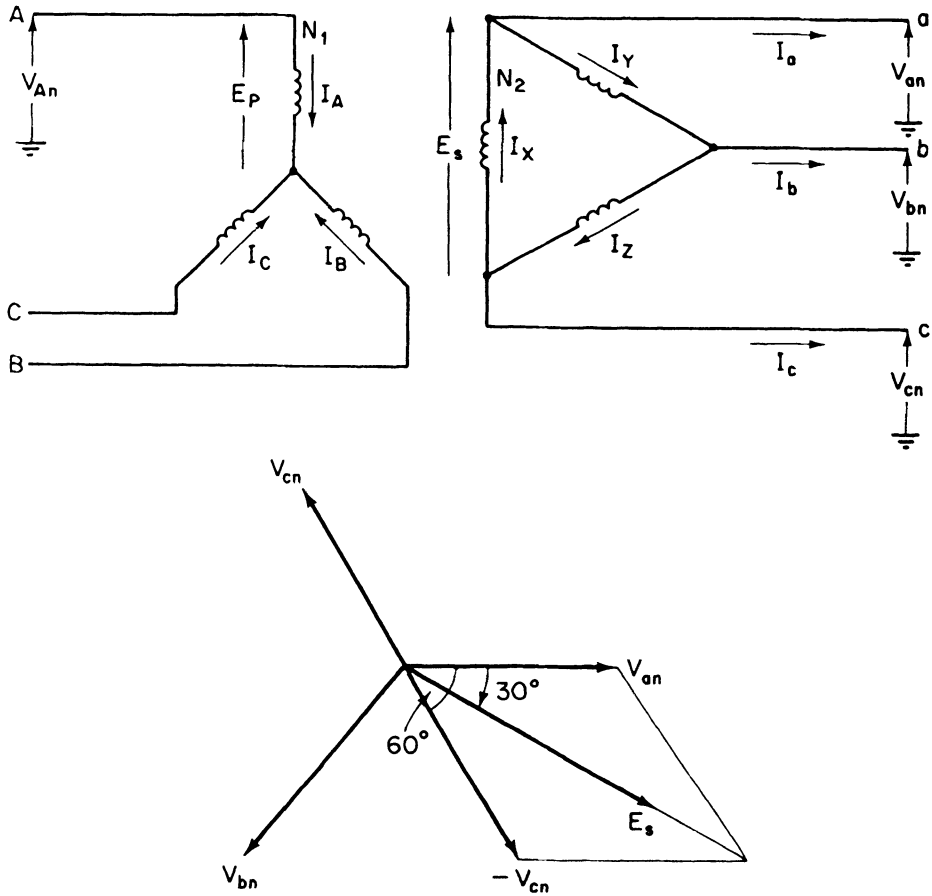


Figure 5.22 Y/Δ-transformer and a phasor diagram.

or

$$E_p = \frac{N_1}{N_2}\sqrt{3}V_{an}\angle -30 \text{ deg}$$

But the line-to-ground voltage on the Y side is

$$V_{An} = E_p$$

Thus we have

$$V_{An} = \frac{N_1}{N_2}\sqrt{3}V_{an}\angle -30 \text{ deg} \tag{5.86}$$

We can conclude that the Δ-side line-to-ground secondary voltage V_{an} leads the Y-side line-to-ground primary voltage V_{an} by 30 deg.

www.EngineeringEBooksPdf.com

Turning our attention now to the current relations, we start by

$$I_x = \frac{N_1}{N_2} I_A$$

$$I_y = \frac{N_1}{N_2} I_B = \frac{N_1}{N_2} I_A \angle -120 \text{ deg}$$

But

$$\begin{aligned} I_a &= I_x - I_y \\ &= \frac{N_1}{N_2} I_A (1 - 1\angle -120 \text{ deg}) \end{aligned}$$

This reduces to

$$I_a = \frac{N_1}{N_2} \sqrt{3} I_A \angle 30 \text{ deg} \tag{5.87}$$

Thus the secondary line current leads the primary current by 30 deg.

Example 5.7 A three-phase bank of three single-phase transformers steps up the three-phase generator voltage of 13.8 kV (line to line) to a transmission voltage of 138 kV (line to line). The generator rating is 41.5 MVA. Specify the voltage, current, and kVA ratings of each transformer for the following connections.

(a) Low-voltage windings Δ, high-voltage windings Y.
(b) Low-voltage windings Y, high-voltage windings Δ.
(c) Low-voltage windings Y, high-voltage windings Y.
(d) Low-voltage windings Δ, high-voltage windings Δ.

Solution The low voltage is given by

$$V_1 = 13.8 \text{ kV} \qquad \text{(line to line)}$$

The high voltage is given by

$$V_2 = 138 \text{ kV} \qquad \text{(line to line)}$$

The apparent power is

$$|S| = 41.5 \text{ MVA}$$

(a) Consider the situation with the low-voltage windings connected in Δ, as shown in Fig. 5.23. Each winding is subject to the full line-to-line voltage, Thus

$$E_p = 13.8 \text{ kV}$$

www.EngineeringEBooksPdf.com

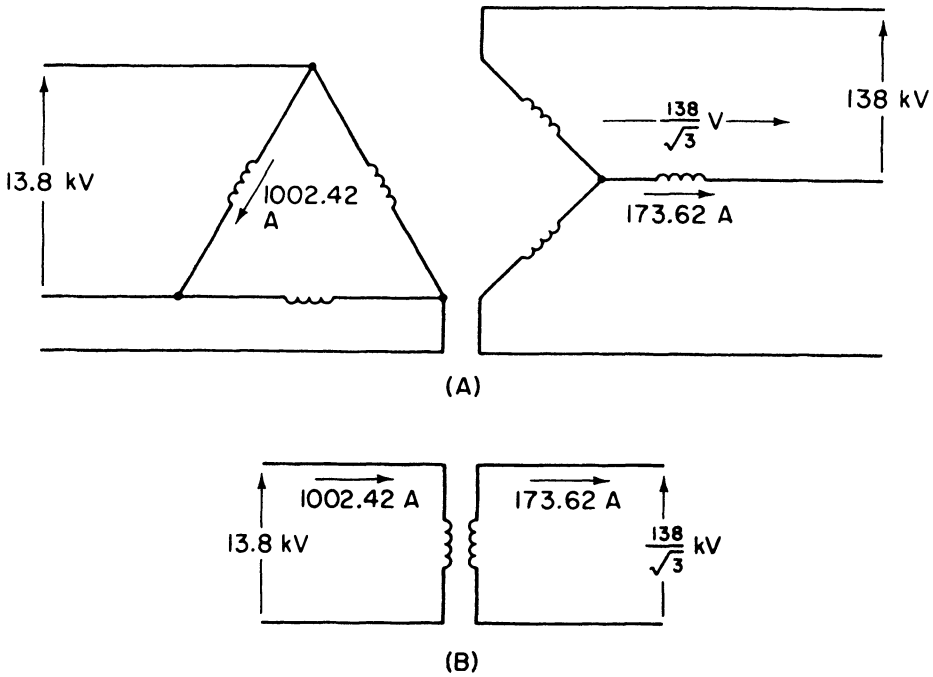


Figure 5.23 (a) Δ/Y-Transformer with variables indicated; (b) single transformer loading.

The power per winding is $|S|/3$; thus the current in each winding is

$$I_p = \frac{41.5 \times 10^6}{3(13.8 \times 10^3)} = 1002.42\,\text{A}$$

With the secondary connected in Y, the voltage on each winding is the line-to-ground value

$$E_s = \frac{138}{\sqrt{3}} = 79.67\,\text{kV}$$

The current in each winding is obtained as

$$I_s = \frac{41.5 \times 10^6}{3(79.67 \times 10^3)} = 173.62\,\text{A}$$

The kVA rating of each transformer is thus

$$|S_1| = E_p I_p = E_s I_s = 13.83\,\text{MVA}$$

www.EngineeringEBooksPdf.com

(b) When the low-voltage windings are connected in Y, the voltage on each winding is the line-to-ground value

$$E_p = \frac{13.8}{\sqrt{3}} = 7.97\,\text{kV}$$

The current is

$$I_p = \frac{41.5 \times 10^6}{3(7.97)(10^3)} = 1736.23\,\text{A}$$

With the secondary windings connected in Δ, the voltage on each winding is

$$E_s = 138\,\text{kV}$$

The current is calculated as

$$I_s = \frac{41.5 \times 10^6}{3(138 \times 10^3)} = 100.24\,\text{A}$$

The kVA rating of each transformer is therefore

$$|S_1| = E_p I_p = E_s I_s = 13.83\,\text{MVA}$$

The arrangement is shown in Fig. 5.24.

(c) With low-voltage windings connected in Y, from the solution to part (b), we have

$$E_p = 7.97\,\text{kV}$$
$$I_p = 1736.23\,\text{A}$$

With high-voltage windings connected in Y, from the solution to part (a) we have

$$E_s = 79.67\,\text{kV}$$
$$I_s = 173.62\,\text{A}$$

This arrangement is shown in Fig. 5.25.

(d) With low-voltage windings connected in Δ, from the solution to part (a), we get

$$E_p = 13.8\,\text{kV}$$
$$I_p = 1002.42\,\text{A}$$

www.EngineeringEBooksPdf.com

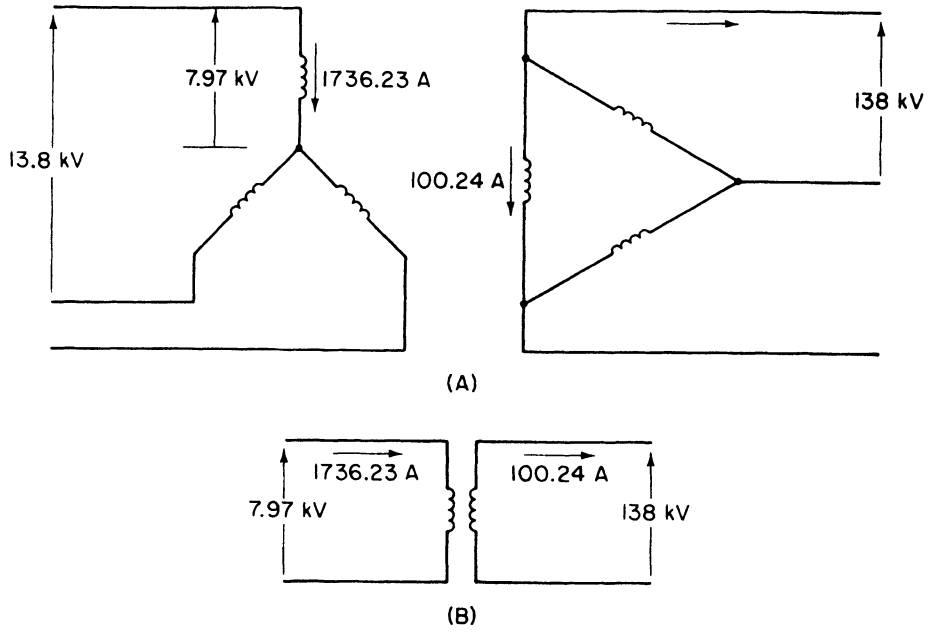


Figure 5.24 (a) Y/Δ-Transformer with variables indicated for Example 5.7; (b) single transformer loading.

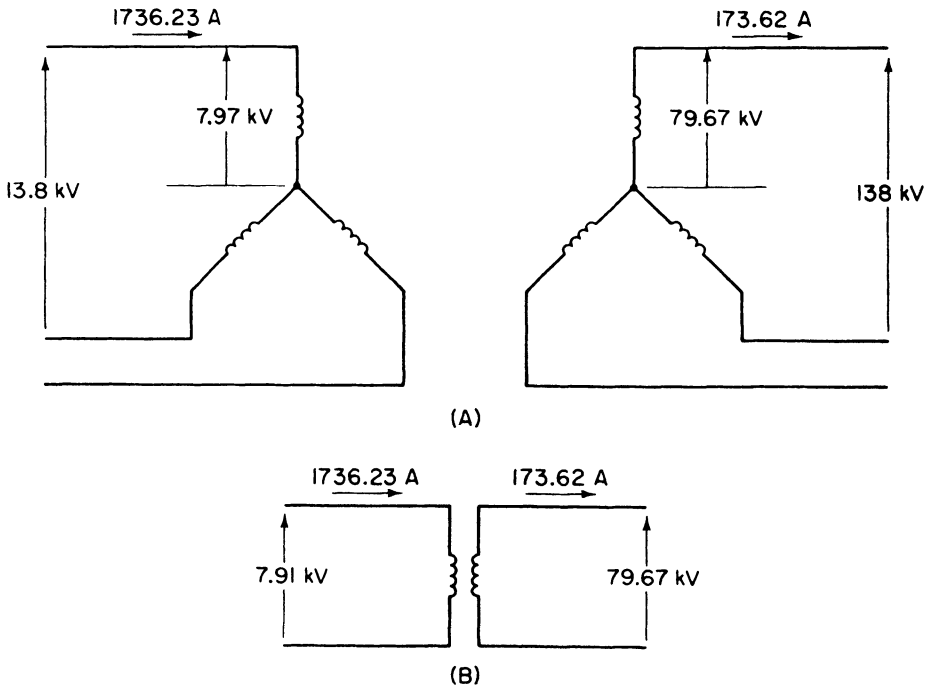


Figure 5.25 Y/Y-Transformer with variables indicated for Example 5.7.

www.EngineeringEBooksPdf.com

TABLE 5.1 Comparison of Single-Transformer Ratings for Different Three-Phase Connections

	Δ/Y	Y/Δ	Y/Y	Δ/Δ
E_p (kV)	13.8	7.97	7.97	13.8
I_p (A)	1002.42	1736.23	1736.23	1002.42
E_s (kV)	79.67	138	79.67	138
I_s (A)	173.62	100.24	173.62	100.24

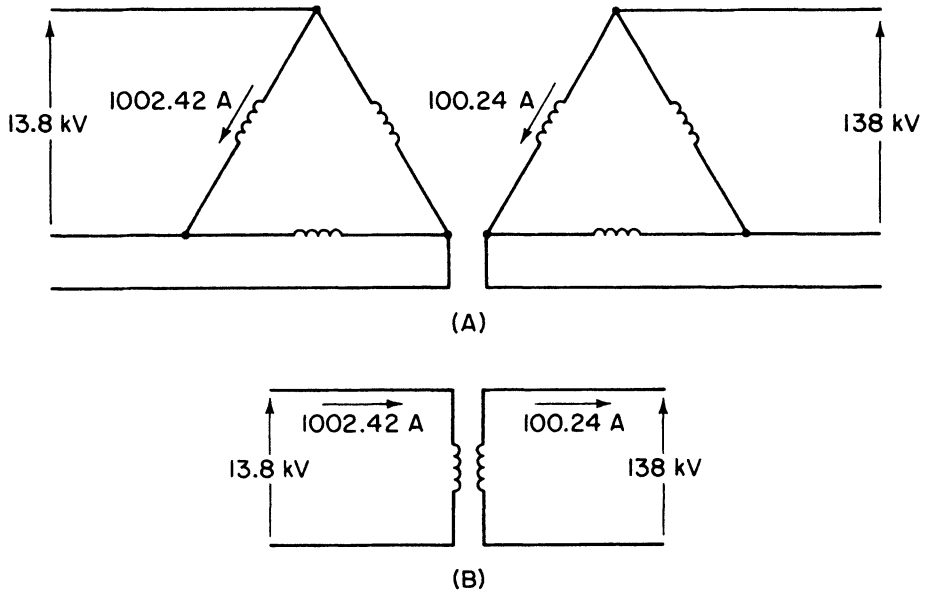


Figure 5.26 (a) Δ/Δ-Transformer with variables indicated for Example 5.7; (b) single transformer loading.

With high-voltage windings connected in Δ, from the solution to part (b), we get

$$E_s = 138\,\text{kV}$$
$$I_s = 100.24\,\text{A}$$

The situation is shown in Fig. 5.26. Table 5.1 summarizes the voltage and current ratings for the single-phase transformers associated with each transformer connection.

5.8 AUTOTRANSFORMERS

The basic idea of the autotransformer is to permit the interconnection of the windings electrically. Figure 5.27 shows a two-winding transformer connected in an

www.EngineeringEBooksPdf.com

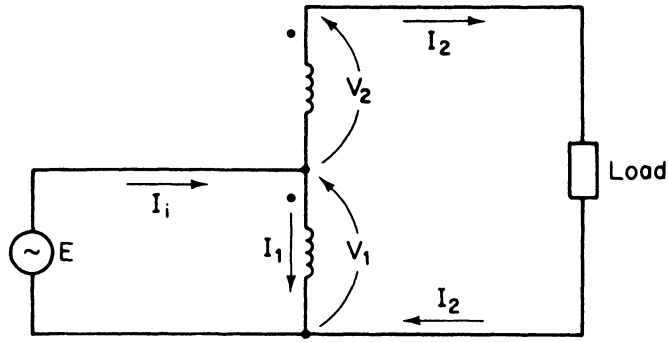


Figure 5.27 Step-up autotransformer.

autotransformer step-up configuration. We will assume the same voltage per turn; that is

$$\frac{V_1}{N_1} = \frac{V_2}{N_2} \tag{5.88}$$

The rating of the transformer when connected in a two-winding configuration is

$$S_{\text{rated}} = V_1 I_1 = V_2 I_2 \tag{5.89}$$

In the configuration chosen, the apparent power into the load is

$$\begin{aligned} S_0 &= (V_1 + V_2) I_2 \\ &= V_2 I_2 \left(1 + \frac{N_1}{N_2}\right) \end{aligned} \tag{5.90}$$

The apparent input power is

$$\begin{aligned} S_i &= V_1 (I_1 + I_2) \\ &= V_1 I_1 \left(1 + \frac{N_1}{N_2}\right) \end{aligned} \tag{5.91}$$

Thus the rating of the autotransformer is higher than the original rating of the two-winding configuration. Note that each winding passes the same current in both configurations, and as a result, the losses remain the same. Due to the increased power rating, the efficiency is thus improved.

Autotransformers are generally used when the ratio is 3 : 1 or less. Two disadvantages are the lack of electric isolation between primary and secondary and the increased short-circuit current over that for the corresponding two-winding configuration.

Example 5.8 A 30-kVA 2.4/0.6-kV transformer is connected as a step-up autotransformer from a 2.4-kV supply. Calculate the currents in each part of the transformer and the load rating. Neglect losses.

www.EngineeringEBooksPdf.com

Solution With reference to Fig. 5.27, the primary rated winding rated current is

$$I_1 = \frac{30}{2.4} = 12.5\,\text{A}$$

The secondary rated current is

$$I_2 = \frac{30}{0.6} = 50\,\text{A}$$

Thus the load current is

$$I_L = 50\,\text{A}$$

The load voltage is

$$V_L = V_1 + V_2 = 3\ \text{kV}$$

As a result, the load rating is

$$S_L = V_L I_L = 150\ \text{kVA}$$

Note that

$$\begin{aligned} I_i &= I_1 + I_2 \\ &= 62.5\,\text{A} \\ V_i &= V_1 = 2.4\ \text{kV} \end{aligned}$$

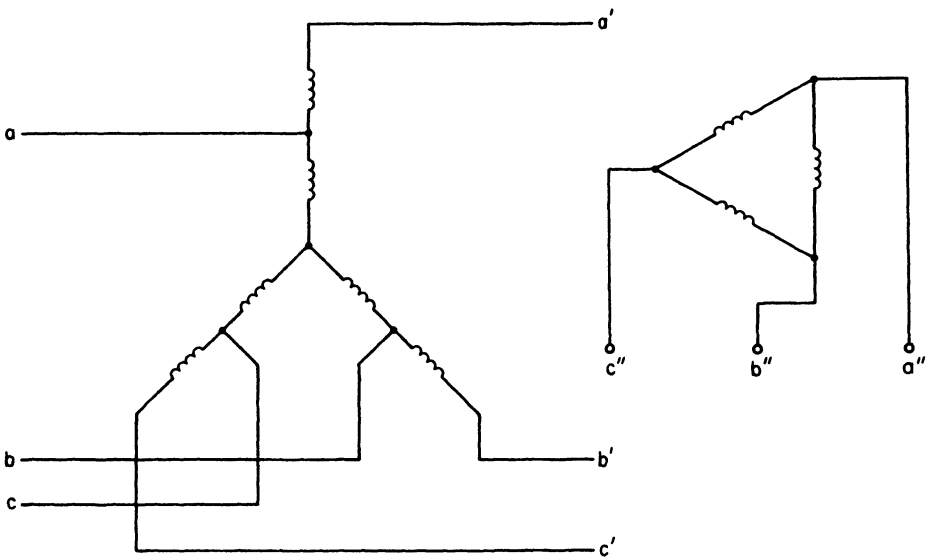


Figure 5.28 Schematic diagram of a three-winding autotransformer.

www.EngineeringEBooksPdf.com

Thus

$$S_i = 2.4(62.5) = 150 \text{ kVA}$$

Three-phase autotransformers are usually Y/Y-connected with the neutral grounded. A third (tertiary) Δ-connected set of windings is included to carry the third harmonic component of the exciting current. A schematic diagram of a three-phase autotransformer with a Δ tertiary is shown in Fig. 5.28.

PROBLEMS

Problem 5.1 A single-phase transformer has a turns ratio of 4 : 1. The transformer can be considered ideal. A load impedance of $10\angle 30$ deg is connected across the secondary terminals, and the secondary voltage is 120 V and is taken as the reference. Find the current in the primary and secondary windings, the primary voltage, and the load impedance referred to the primary.

Problem 5.2 A 50-kVA, 400/2000-V, single-phase transformer delivers a load of 40 kVA at 2000 V and 0.8 PF lagging. Assume that the transformer is ideal.

(a) Find the load impedance.
(b) Find the load impedance referred to the primary side.

Problem 5.3 The load connected to the secondary of an ideal single-phase transformer is 10 kVA and its impedance is $Z_2 = 2\angle -32$. The load impedance referred to the primary is $32\angle -32$ deg. Find the turns ratio, the primary and secondary current, and the voltage.

Problem 5.4 A single-phase 10 : 1 ideal transformer has a primary voltage of 39.8 kV and a primary apparent power of 1000 kVA at 0.8 PF lagging. Find the load impedance connected to the secondary winding.

Problem 5.5 Calculate the turn ratio, voltage, and volt-ampere ratings of an ideal transformer so that maximum power is transferred to a resistive load of 1 Ω from a source with internal voltage of 250 and series reactance of 36 Ω.

Problem 5.6 Having designed the transformer of Problem 5.5, it was decided that the source's internal resistance of 4 Ω should be included in the design. Instead of changing the transformer, a capacitor with reactance X_c is inserted in series with the source to maintain maximum power transfer to the load. Calculate the required reactance.

Problem 5.7 Consider the circuit shown in Fig. 5.29 and assume that both transformers are ideal. Impedance values are given on the basis of the voltage level in the corresponding portion of the circuit. Obtain an equivalent representation of the circuit referred to the 33-kV side and hence find V_1 and I_1, taking the load voltage as reference:

www.EngineeringEBooksPdf.com

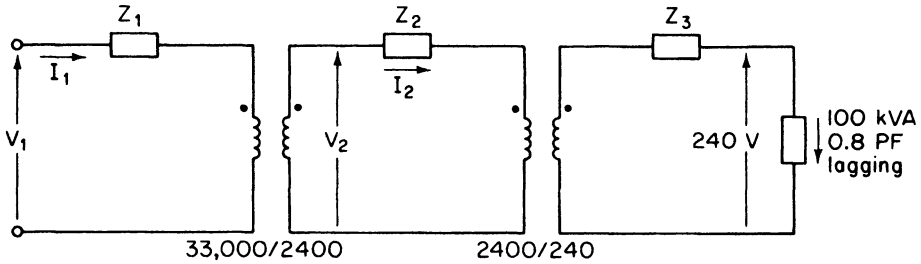


Figure 5.29 Circuit for Problem 5.7.

$$Z_1 = 10.5 + j35\ \Omega$$
$$Z_2 = 0.5 + j0.64\ \Omega$$
$$Z_3 = (4 + j6)10^{-3}\ \Omega$$

Problem 5.8 Consider the circuit of Problem 5.7. Find the current I_2 and voltage V_2 by referring the circuit to the 2400-V side.

Problem 5.9 Find the current I and the source voltage V_1 in the circuit shown in Fig. 5.30.

Problem 5.10 Find the current I in the circuit shown in Fig. 5.31, given that

$$V_1 = 13.8 \qquad V_2 = 13.8\angle 15 \text{ deg}$$
$$Z_1 = Z_4 = 0.01 + j0.03$$
$$Z_2 = Z_3 = 1 + j3$$
$$Z_L = 0.06 + j0.08$$

Problem 5.11 A 10-kVA, 480/120-V, single-phase transformer has the following parameters:

$$R_1 = 0.6\ \Omega \qquad X_1 = 1\ \Omega$$
$$R_2 = 37.5 \times 10^{-3}\ \Omega \qquad X_2 = 62.5 \times 10^{-3}\ \Omega$$
$$G_c = 0.333 \times 10^{-3}\ \text{S} \qquad B_m = 2 \times 10^{-3}\ \text{S}$$

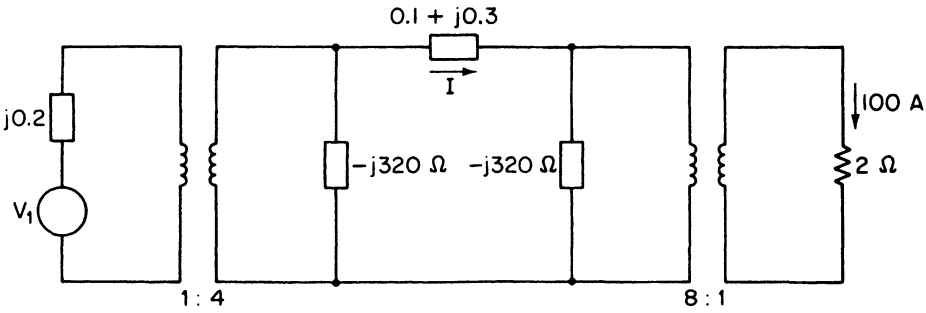


Figure 5.30 Circuit for Problem 5.9.

www.EngineeringEBooksPdf.com

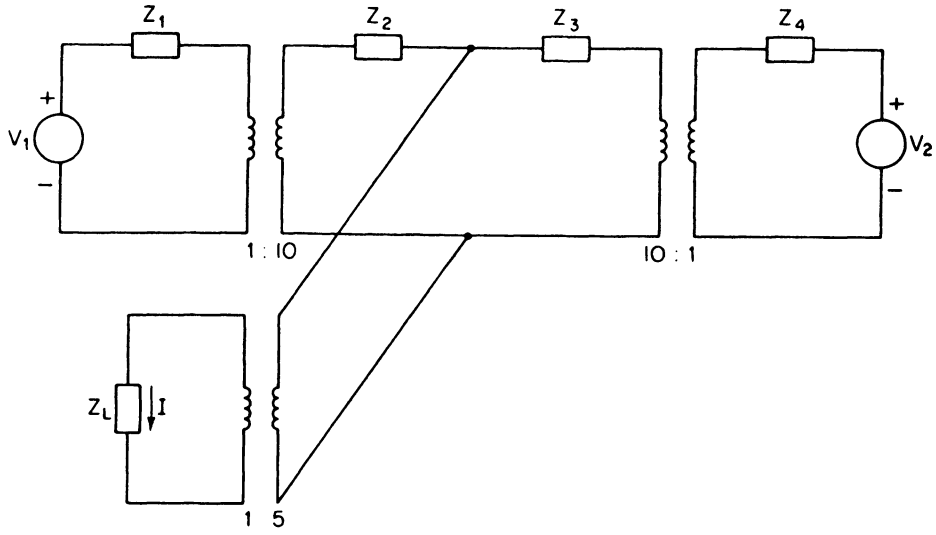


Figure 5.31 Circuit for Problem 5.10.

Use the equivalent circuit of Fig. 5.9(b) to calculate the voltage and current at the primary terminals for a load of 10 kVA at 120 V and a power factor of 0.85 lagging.

Problem 5.12 Calculate the power losses in the secondary winding, the primary winding, and in the core as well as the efficiency of the transformer of Problem 5.11.

Problem 5.13 Repeat Problem 5.11 using the equivalent circuit of Fig. 5.10(a) and find the PF at the primary and the efficiency of the transformer.

Problem 5.14 A 50-kVA 400/2000-V single-phase transformer has the following parameters:

$$R_1 = 0.02\,\Omega \qquad R_2 = 0.5\,\Omega$$
$$X_1 = 0.06\,\Omega \qquad X_2 = 1.5\,\Omega$$
$$G_c = 2\,\text{mS} \qquad B_m = -6\,\text{mS}$$

Note that G_c and B_m are given in terms of primary reference. The transformer supplies a load of 40 kVA at 2000 V and 0.8 PF lagging. Calculate the primary voltage and current using the equivalent circuits shown in Figs. 5.9 and 5.10.

Problem 5.15 Find the voltage regulation and efficiency for the transformer of Problem 5.14.

Problem 5.16 Find the maximum efficiency of the transformer of Problem 5.14 under the same conditions.

Problem 5.17 The equivalent impedance referred to the primary of a 2300/230-V 500-kVA, single-phase transformer is

$$Z = 0.2 + j0.6\ \Omega$$

www.EngineeringEBooksPdf.com

Calculate the PVR when the transformer delivers rated capacity at 0.8 PF lagging at rated secondary voltage. Find the efficiency of the transformer at this condition given that core losses at the rated voltage are 2 kW.

Problem 5.18 A 500/100-V two-winding transformer is rated at 5 kVA. The following information is available:

(a) The maximum efficiency of the transformer occurs when the output of the transformer is 3 kVA.
(b) The transformer draws a current of 3 A, and the power is 100 W when a 100-V supply is impressed on the low-voltage winding with the high-voltage winding open-circuit.

Find the rated efficiency of the transformer at 0.8 PF lagging.

Problem 5.19 A 50-kVA 400/2000-V single-phase transformer has the following equivalent-circuit parameters referred to the primary:

$$Z_{eq} = 0.04 + j0.12\ \Omega$$

Assume that the transformer supplies a load of 40 kVA at 2000 V and 0.8 PF lagging. Calculate the primary voltage of the transformer and its efficiency.

Problem 5.20 The load at the end of a feeder is 100 A at 0.85 PF and 132 V. The feeder's impedance is

$$Z_3 = 0.003 + j0.01\ \Omega$$

Power is supplied to the feeder by a 10:1 transformer whose impedance referred to the primary is

$$Z_2 = 4 + j8\ \Omega$$

High-voltage power is provided to the transformer through a radial link with series impedance:

$$Z_3 = 1 + j4.8\ \Omega$$

Find the voltage, current, and power factor at the sending end of the link. Calculate the efficiency of the system.

Problem 5.21 The no-load input power to a 50-kVA, 2300/230-V, single-phase transformer is 200 VA at 0.15 PF at rated voltage. The voltage drops due to resistance and leakage reactance are 0.012 and 0.018 times rated voltage when the transformer operates at rated load. Calculate the input power and power factor when the load is 30 kW at 0.8 PF lagging at rated voltage.

www.EngineeringEBooksPdf.com

Problem 5.22 Two 230/115-V transformers are available. The rating of transformer A is 5 kVA, while that of transformer B is 4 kVA. Find the rating of the combination in the following configurations:

(a) Primaries connected in series aiding and secondaries connected in series aiding.
(b) Primaries connected in series aiding and secondaries connected in parallel.

Problem 5.23 A 5-kVA 230/115-V transformer is connected in a parallel–series configuration with a 3-kVA 230/23-V transformer. Find the rating of the combination.

Problem 5.24 Two 2300/230-V transformers are connected in parallel to supply a load of 500 kVA at 0.8 PF lagging. Find the power supplied by each transformer, given that

$$Z_A = 0.1 + j0.2$$
$$Z_B = 0.12 + j0.2$$

Impedances are given on the basis of the 2300-V side.

Problem 5.25 Two 2300/230-V transformers are connected in parallel. The following is the apparent power loading of each:

$$S_A = 300 \times 10^3 \angle 40 \text{ deg}$$
$$S_B = 200 \times 10^3 \angle 35 \text{ deg}$$

Assume that the series reactance of each transformer is 0.1 Ω. Find the series resistance of each transformer.

Problem 5.26 Repeat Example 5.6 for

$$I_2 = 40\angle -30 \text{ deg}$$
$$I_3 = 40\angle -35 \text{ deg}$$

Problem 5.27 Consider the three-winding transformers of Example 5.6. Given that $V_1 = 400, S_1 = 32,000\angle 32.5$ deg, and $V_2 = 394\angle -0.7$ deg, find the efficiency of the transformer.

Problem 5.28 A Y-connected balanced three-phase load consisting of three impedances of $10\angle 30$ deg each is supplied with balanced line-to-neutral voltages:

$$V_{an} = 220\angle 0 \text{ V}$$
$$V_{bn} = 220\angle 240 \text{ deg V}$$
$$V_{cn} = 220\angle 120 \text{ deg V}$$

www.EngineeringEBooksPdf.com

(a) Calculate the phasor currents in each line.
(b) Calculate the line-to-line phasor voltages.
(c) Calculate the total active and reactive power supplied to the load.

Problem 5.29 Repeat Problem 5.28 if the same three impedances were connected in a Δ-connection.

Problem 5.30 Find the phase currents I_A, I_B, and I_C as well as the neutral current I_n for a three-phase network with an unbalanced load:

$$Z_A = 1 + j3$$
$$Z_B = 1 + j3$$
$$Z_C = 0.8 + j2.4\ \Omega$$

Assume that the applied three-phase voltage is balanced with a magnitude of 100 V. Calculate the apparent power consumed by the load.

Problem 5.31 A 60-hp three-phase 400-V induction motor operates at 0.75 PF lagging. Find the active, reactive, and apparent power consumed per phase. Find the values of R and jX if the motor is modeled as a balanced three-phase impedance $Z = R + jX$ connected in a Y-connection.

Problem 5.32 A three-phase bank of three single-phase transformers steps up the three-phase generator voltage of 13.8 kV (line to line) to a transmission voltage of 138 kV (line to line). The generator rating is 83 MVA. Specify the voltage, current, and kVA ratings of each transformer for the following connections:

(a) Low-voltage windings Δ, high-voltage windings Y.
(b) Low-voltage windings Y, high-voltage windings Δ.
(c) Low-voltage windings Y, high-voltage windings Y.
(d) Low-voltage windings Δ, high voltage windings Δ.

Problem 5.33 The equivalent impedance referred to the secondary of a 13.8/138-kV 83-MVA three-phase Δ/Y-connected transformer is

$$Z = 2 + j13.86\ \Omega$$

Calculate the percentage voltage regulation when the transformer delivers rated capacity at 0.8 PF lagging at rated secondary voltage. Find the efficiency of the transformer at the condition given that core losses at rated voltages are 76.5 kW.

Problem 5.34 The load at the end of a high-voltage three-phase line is 30 MVA at 0.85 PF and 11 kV (line to line). Power is transmitted from the remote source through a step-up 11-kV/110-kV transformer T1 feeding the high-voltage line TL. At the end of the line is a step-down 110-kV/11-kV transformer T2. The equivalent

www.EngineeringEBooksPdf.com

circuit parameters of the individual components are

$$Z_{T1} = 1.45 + j26.6\ \Omega$$
$$Z_{TL} = 10.2 + j34\ \Omega$$
$$Z_{T2} = 6.8 + j106\ \Omega$$

Find the sending end voltage and the transmission efficiency of the system. Assume that impedance values are given on the basis of 110 kV.

Problem 5.35 Three identical 500-kVA 2300/230-V single-phase transformers are Δ/Y-connected. Each transformer has the following equivalent impedance referred to the high-voltage side:

$$Z = 0.2 + j0.6\ \Omega$$

Each transformer delivers its rated VA at 0.8 PF at its rated secondary voltage to a three-phase load. Find the primary line-to-line voltage.

Problem 5.36 A 50-kVA 2.4/0.6-kV transformer is connected as a step-up autotransformer from a 2.4-kV supply. Calculate the currents in each part of the transformer and the load rating. Neglect losses.

Problem 5.37 A step-up autotransformer is configured using a 2.4/0.6-kV single-phase transformer to supply a load of 180 kVA. Find the volt-ampere rating of the single-phase transformer, the primary winding current, and the input current.

www.EngineeringEBooksPdf.com

CHAPTER 6

INDUCTION MOTORS AND THEIR CONTROL

6.1 INTRODUCTION

An induction machine (Fig. 6.1) is one in which alternating currents are supplied directly to stator windings and by transformer action (induction) to the rotor. The flow of power from stator to rotor is associated with a change of frequency, and the output is the mechanical power transmitted to the load connected to the motor shaft. The induction motor is the most widely used motor in industrial and commercial utilization of electric energy. Reasons for the popularity of induction motors include simplicity, reliability, and low cost, combined with reasonable overload capacity, minimal service requirements, and good efficiency. The rotor of an induction motor may be one of two types. In the wound-rotor motor, distributed windings are employed with terminals connected to insulated slip rings mounted on the motor shaft. The second type is called the squirrel-cage rotor, where the windings are simply conducting bars embedded in the rotor and short-circuited at each end by conducting end rings. The rotor terminals are thus inaccessible in a squirrel-cage construction, whereas for the wound-rotor construction the rotor terminals are made available through carbon brushes bearing on the slip rings.

The stator of a three-phase induction motor carries three sets of windings that are displaced by 120 deg in space to constitute a three-phase winding set. The application of a three-phase voltage to the stator winding results in the appearance of a rotating magnetic field, as we discover in the next section. It is clear that induced currents in the rotor (due to the rotating field) interact with the field to produce a torque that rotates the rotor in the direction of the rotating field.

www.EngineeringEBooksPdf.com

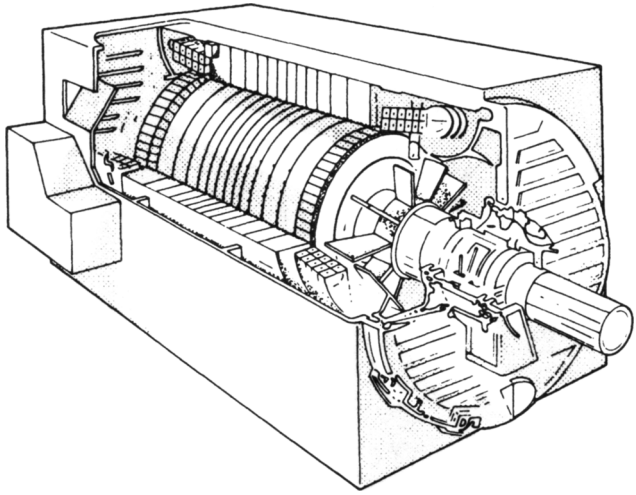


Figure 6.1 Cutaway of a three-phase cage-type induction motor.

6.2 MMF WAVES AND THE ROTATING MAGNETIC FIELD

Consider the N-turn coil that spans 180 electrical degrees shown in Fig. 6.2. This coil is referred to as a full-pitch coil (as opposed to fractional-pitch coils spanning less than 180 electrical degrees) and is embedded in the stator slots as shown. We assume that the permeability of the stator and rotor iron paths is much greater than that of the air, and therefore that all the reluctance of the magnetic circuit is in the two air gaps. The magnetic-field intensity H in the air gap at angle θ is the same in magnitude as that at $\theta+\pi$ due to symmetry, but the fields are in the opposite direction. The MMF around any closed path in the vicinity of the coil side is Ni. The MMF is uniformly distributed around the sides, and hence we can conclude that the MMF is constant at $Ni/2$ between the sides ($\theta = -\pi/2$ to $+\pi/2$) and abruptly changes to $-Ni/2$, as shown in Fig. 6.2. In part (a) of the figure the physical arrangement is shown, and in part (b) the rotor and stator are laid flat so that the corresponding waveforms can be shown in part (c) in relation to the physical position on the periphery.

The MMF waveform of the concentrated full-pitch coil is rectangular, as shown in Fig. 6.2(c), and one needs to resolve it into a sum of sinusoidals. There are two reasons for this. The first is that electrical engineers prefer to use sinusoids due to the wealth of available techniques that enable convenient analysis of such waveforms. The second is that in the design of ac machines, the windings are distributed such that a close approximation to a sinusoid is obtained. In resolving a periodic waveform into a sum of sinusoids, one uses the celebrated Fourier series, which for our present purposes states that the rectangular waveform can be written

$$F_\theta = \frac{4Ni}{2\pi}\left[\cos\theta + \frac{1}{3}\cos 3\theta + \cdots\right]$$
$$F_1 = \frac{4}{\pi}\frac{Ni}{2}\cos\theta \tag{6.1}$$

www.EngineeringEBooksPdf.com

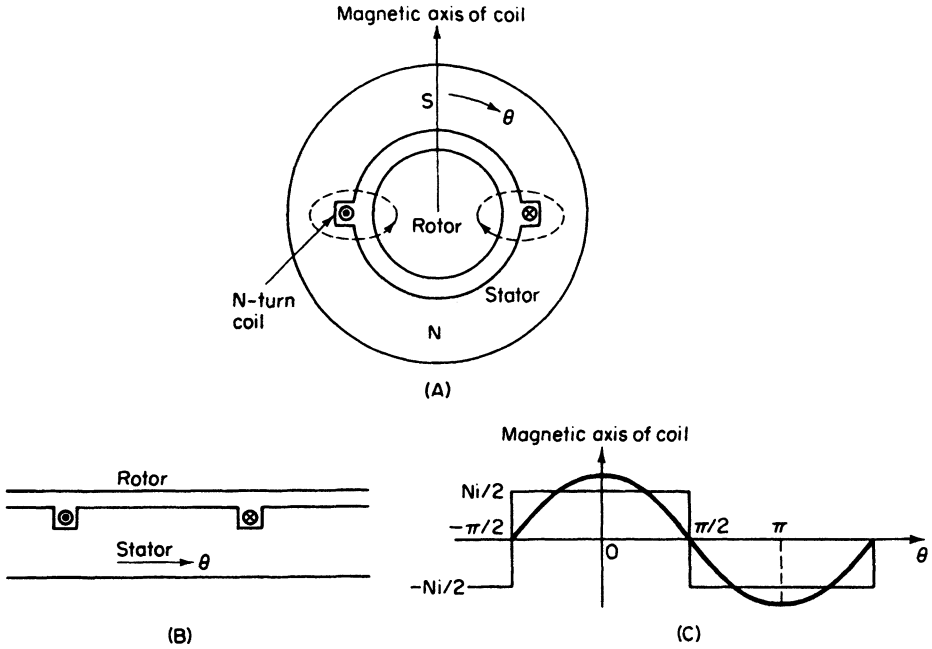


Figure 6.2 MMF of a concentrated full-pitch coil: (a) physical arrangement; (b) rotor and stator laid flat; (c) MMF waves.

If the remaining harmonics are negligible, we see that the MMF of the coil is approximated by a sinusoidal space waveform.

6.2.1 Distributed Windings

Windings that are spread over a number of slots around the air gap are referred to as distributed windings and are shown in Fig. 6.3. Phase a is shown in detail in the figure, and we assume a two-pole three-phase ac configuration. The empty slots are occupied by phases b and c. We deal with phase a only, whose winding is arranged in two layers such that each coil of n_c turns has one side in the top of a slot and the other coil side in the bottom of a slot pole pitch (180 electrical degrees) away. The coil current is i_c.

The MMF wave is a series of steps each of height $2n_c i_c$ equal to the ampere conductors in the slot. The fundamental component of the Fourier series expansion of the MMF wave is shown by the sinusoid in the figure. Note that this arrangement provides a closer approximation to a sinusoidal distribution. The fundamental component is given by

$$F_{a_1} = Ki_a \cos\theta \tag{6.2}$$

www.EngineeringEBooksPdf.com

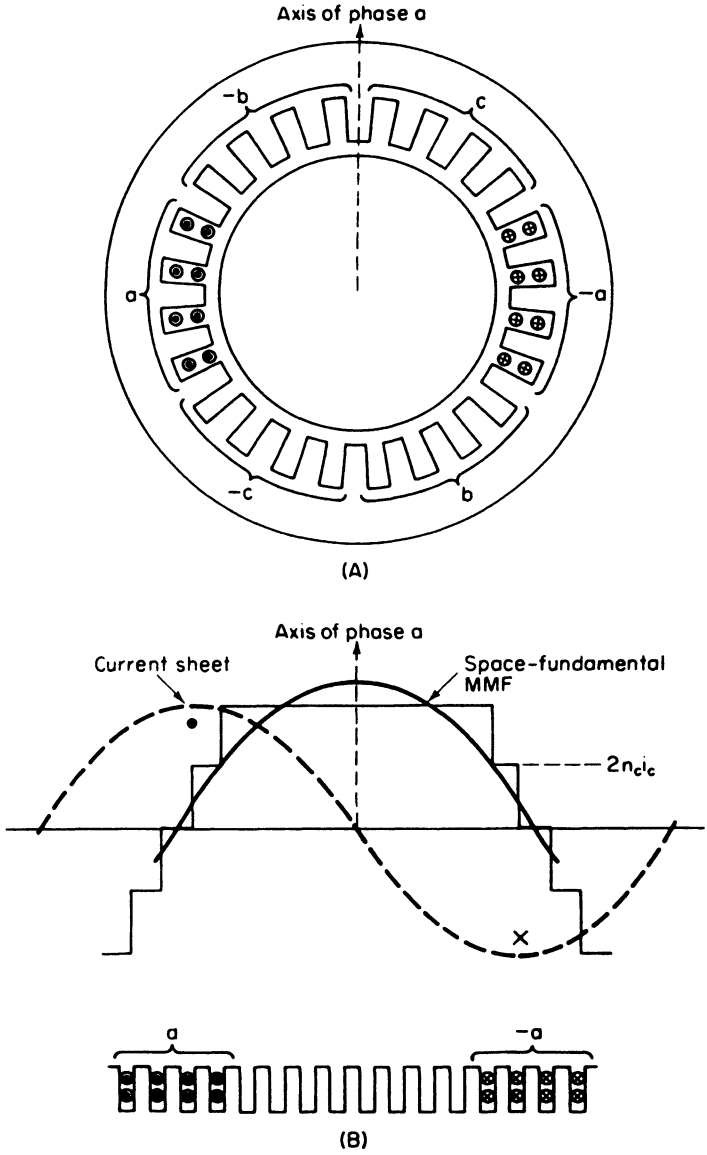


Figure 6.3 MMF wave for one phase (full-pitch coil).

where

$$K = \frac{4}{\pi} k_w \frac{N_{ph}}{P} \tag{6.3}$$

The factor k_w accounts for the distribution of the winding, N_{ph} is the number of turns per phase; and P is the number of poles. It is assumed that the coils are series connected, and thus $i_c = i_a$.

www.EngineeringEBooksPdf.com

The MMF is a standing wave with a sinusoidal spatial distribution around the periphery. Assume that the current i_a is sinusoidal such that

$$i_a(t) = I_m \cos \omega t \tag{6.4}$$

Thus we have

$$F_{a_1}(t) = KI_m \cos\theta \cos \omega t \tag{6.5}$$

The preceding relation can be written as

$$F_{a_1}(t) = A_{a(p)} \cos\theta \tag{6.6}$$

where $A_{a(p)}$ is the amplitude of the MMF component wave at time t,

$$A_{a(p)} = F_{\max} \cos \omega t \tag{6.7}$$

with

$$F_{\max} = KI_m \tag{6.8}$$

6.2.2 Rotating Magnetic Fields

An understanding of the nature of the magnetic field produced by a polyphase winding is necessary for the analysis of polyphase ac machines. We consider a two-pole three-phase machine. The windings of the individual phases are displaced by 120 electrical degrees in space. This is shown in Fig. 6.4. The magnetomotive forces developed in the air gap due to currents in the windings will also be displaced 120 electrical degrees in space. Assuming sinusoidal, balanced three-phase operation, the phase currents are displaced by 120 electrical degrees in time. The instantaneous

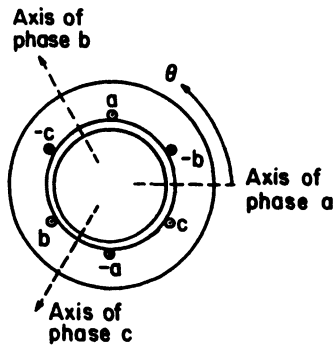


Figure 6.4 Simplified two-pole three-phase stator winding.

www.EngineeringEBooksPdf.com

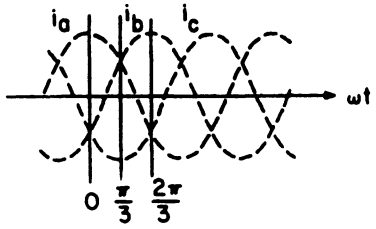


Figure 6.5 Instantaneous three-phase currents.

values of the currents are

$$i_a = I_m \cos \omega t \tag{6.9}$$

$$i_b = I_m \cos (\omega t - 120 \text{ deg}) \tag{6.10}$$

$$i_c = I_m \cos (\omega t - 240 \text{ deg}) \tag{6.11}$$

where I_m is the maximum value of the current and the time origin is arbitrarily taken as the instant when the phase a current is *a* positive maximum. The phase sequence is assumed to be *abc*. The instantaneous currents are shown in Fig. 6.5. As a result, we have

$$A_{a(p)} = F_{\max} \cos \omega t \tag{6.12}$$

$$A_{b(p)} = F_{\max} \cos (\omega t - 120 \text{ deg}) \tag{6.13}$$

$$A_{c(p)} = F_{\max} \cos (\omega t - 240 \text{ deg}) \tag{6.14}$$

where $A_{a(p)}$ is the amplitude of the MMF component wave at time t.

At time t, all three phases contribute to the air-gap MMF at a point P (whose spatial angle is θ). We thus have the resultant MMF given by

$$A_p = A_{a(p)} \cos + A_{a(p)} \cos (\theta - 120 \text{ deg}) + A_{c(p)} \cos (\theta - 240 \text{ deg}) \tag{6.15}$$

Using Eqs. (6.12) to (6.14), we have

$$\begin{aligned} A_p = F_{\max} [&\cos \theta \cos \omega t + \cos (\theta - 120 \text{ deg}) \cos (\omega t - 120 \text{ deg}) \\ &+ \cos (\theta - 240 \text{ deg}) \cos (\omega t - 240 \text{ deg})] \end{aligned} \tag{6.16}$$

Equation (6.16) can be simplified using the following trigonometric identity:

$$\cos \alpha \cos \beta = \frac{1}{2} [\cos (\alpha - \beta) + \cos (\alpha + \beta)]$$

www.EngineeringEBooksPdf.com

As a result, we have

$$A_p = \frac{1}{2}[\cos(\theta - \omega t) + \cos(\theta + \omega t) + \cos(\theta - \omega t) + \cos(\theta + \omega t - 240 \text{ deg}) + \cos(\theta - \omega t) + \cos(\theta + \omega t - 480 \text{ deg})]F_{\max}$$

The three cosine terms involving $(\theta + \omega t)$, $(\theta + \omega t - 240 \text{ deg})$, and $(\theta + \omega t - 480 \text{ deg})$ are three equal sinusoidal waves displaced in phase by 120 degrees with a zero sum. Therefore,

$$A_p = \frac{3}{2}[F_{\max}\cos(\theta - \omega t)] \tag{6.17}$$

The wave of Eq. (6.17) depends on the spatial position θ as well as time. The angle ωt provides rotation of the entire wave around the air gap at the constant angular velocity ω. At time t_1 the wave is sinusoid with its positive peak displaced ωt_1 from the point P (at θ); at a later instant (t_2), the wave has its positive peak displaced ωt_2 from the same point. We thus see that a polyphase winding excited by balanced polyphase currents produces the same effect as a permanent magnet rotating within the stator.

6.3 SLIP

When the stator is supplied by a balanced three-phase source, it will produce a magnetic field that rotates at synchronous speed as determined by the number of poles and applied frequency f_s:

$$n_s = \frac{120 f_s}{P} \text{ rpm} \tag{6.18}$$

The rotor runs at a steady speed n_r rpm in the same direction as the rotating stator field. The speed n_r is very close to n_s when the motor is running light and decreases as the mechanical load is increased. The difference $(n_s - n_r)$ is termed the *slip* and is commonly defined as a per unit value s. Thus

$$s = \frac{n_s - n_r}{n_s} \tag{6.19}$$

As a result of the relative motion between stator and rotor, induced voltages will appear in the rotor with a frequency f_r, called the slip frequency. Thus

$$f_r = s f_s \tag{6.20}$$

www.EngineeringEBooksPdf.com

From the preceding we can conclude that the induction motor is simply a transformer with a secondary frequency f_r.

Example 6.1 Determine the number of poles, the slip, and the frequency of the rotor currents at rated load for three-phase 5-hp induction motors rated at:

(a) 220 V, 50 Hz, 1440 rpm.
(b) 120 V, 400 Hz, 3800 rpm.

Solution Using n_r, the rotor speed given, we use Eq. (6.18) to obtain P.
(a) We have

$$P = \frac{120 \times 50}{1440} = 4.17$$

But P should be an even number. Therefore, take $P = 4$. Hence the synchronous speed is

$$n_s = \frac{120f}{P} = \frac{120 \times 50}{4} = 1500 \text{ rpm}$$

The slip is thus given by

$$s = \frac{n_s - n_r}{n_s} = \frac{1500 - 1440}{1500} = 0.04$$

The rotor frequency is calculated as

$$f_r = sf_s = 0.04 \times 50 = 2 \text{ Hz}$$

(b) We have

$$P = \frac{120 \times 400}{3800} = 12.63$$

Take $P = 12$, to obtain

$$n_s = \frac{120 \times 400}{12} = 4000 \text{ rpm}$$
$$s = \frac{4000 - 3800}{4000} = 0.05$$
$$f_r = 0.05 \times 400 = 20 \text{ Hz}$$

The analysis of the performance of a three-phase induction motor can be greatly facilitated through the use of equivalent circuits, which is the subject of the next section.

www.EngineeringEBooksPdf.com

6.4 EQUIVALENT CIRCUITS

An equivalent circuit of the three-phase induction motor can be developed on the basis of the foregoing considerations and the transformer models treated in Chapter 5. Looking into the stator terminals, we find that the applied voltage V_s will supply the resistive drop I_sR_1 as well as the inductive voltage jI_sX_1 and the counter EMF, E_1, where I_s is the stator current and R_1 and X_1 are the effective stator resistance and inductive reactance, respectively. In a manner similar to that employed for the analysis of the transformer, we model the magnetizing circuit by the shunt conductance G_c and inductive susceptance $-jB_m$.

The induced voltage in the rotor circuit E_2 is referred to the stator side using the ratio of the number of stator conductors, N_s, to the number of rotor conductors to obtain

$$E_{2s} = \frac{N_s}{N_r} E_2 \tag{6.21}$$

The rotor's induced voltage referred to the stator, E_{2s}, is related to the stator EMF by

$$E_{2s} = sE_1 \tag{6.22}$$

The inclusion of s in the preceding equation is necessary to account for the relative motion between stator and rotor. The rotor current referred to the stator side is denoted by I_r. The induced EMF E_{2s} supplies the resistive voltage component I_rR_2 and inductive component $jI_r(sX_2)$. The rotor resistance is R_2, and the rotor inductive reactance is X_2 on the basis of the stator frequency and voltage. Thus

$$E_{2s} = I_rR_2 + jI_r(sX_2)$$

or

$$sE_1 = I_rR_2 + jI_r(sX_2) \tag{6.23}$$

From the preceding we conclude that

$$\frac{E_1}{I_r} = \frac{R_2}{s} + jX_2 \tag{6.24}$$

The complete equivalent circuit of the induction motor is shown in Fig. 6.6. The rotor circuit impedance referred to the stator side is a series combination of the resistance (R_2/s) and the rotor reactance. Both R_2 and X_2 are referred to the stator side.

6.4.1 Power Considerations

If we consider the active power flow into the induction machine, we find that the input power P_s supplies the stator I^2R losses as well as the core losses. The remaining

www.EngineeringEBooksPdf.com

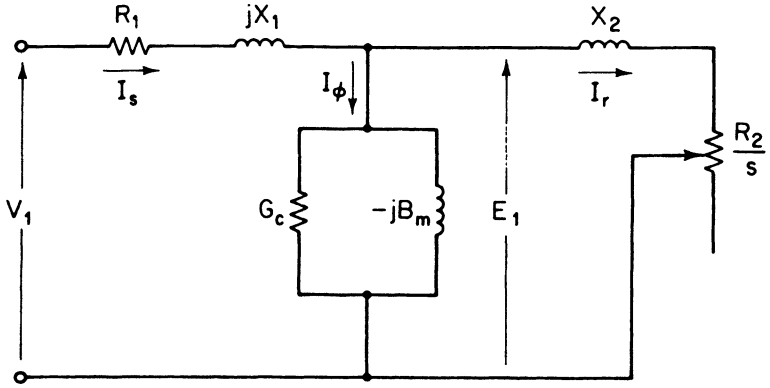


Figure 6.6 Equivalent circuit for a three-phase induction motor.

power denoted by the air-gap power is expended as rotor I^2R losses, with the remainder being the mechanical power delivered to the motor shaft. We can express the air-gap power as

$$P_g = 3I_r^2 \frac{R_2}{s} \tag{6.25}$$

The rotor I^2R losses are given by

$$P_{1r} = 3I_r^2 R_2 \tag{6.26}$$

As a result, the mechanical power output (neglecting mechanical losses) is

$$\begin{aligned} P_r &= P_g - P_{1r} \\ &= 3I_r^2 \frac{1-s}{s} R_2 \end{aligned} \tag{6.27}$$

Formula (6.27) suggests a splitting of R_2/s into the sum of R_2 representing the rotor resistance and a resistance R_e:

$$R_e = \frac{1-s}{s} R_2 \tag{6.28}$$

which is the equivalent resistance of the mechanical load. As a result, it is customary to modify the equivalent circuit to the form shown in Fig. 6.7.

6.4.2 Efficiency

The input power to the motor P_s is given by

$$P_s = 3V_1 I_s \cos\phi_s \tag{6.29}$$

www.EngineeringEBooksPdf.com

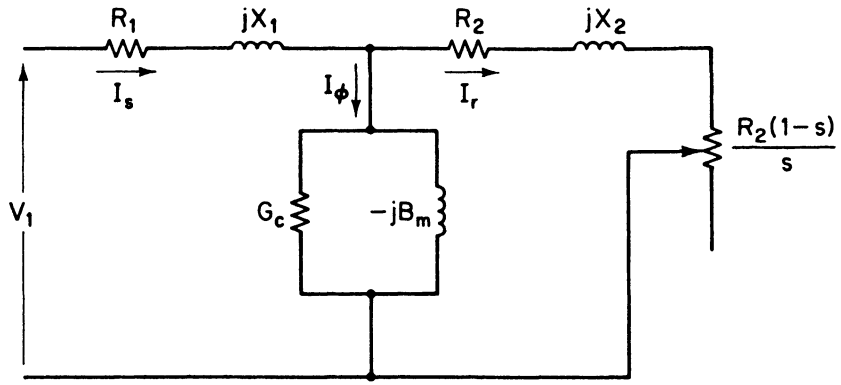


Figure 6.7 Modified equivalent circuit of the induction motor.

where V_1 is the phase voltage and $\cos \phi_s$ is the motor power factor. The efficiency of the motor is given by

$$\eta = \frac{P_o}{P_s} \tag{6.30}$$

The output power is equal to the rotor-developed mechanical power minus the mechanical losses due to friction P_f.

$$P_o = P_r - P_f \tag{6.31}$$

6.4.3 Torque

The torque T developed by the motor is related to P_r by

$$T = \frac{P_r}{\omega_r} \tag{6.32}$$

with ω_r being the angular speed of the rotor. Thus

$$\omega_r = \omega_s(1 - s) \tag{6.33}$$

The angular synchronous speed ω_s is given by

$$\omega_s = \frac{2\pi n_s}{60} \tag{6.34}$$

As a result, the torque is given by

$$T = \frac{3I_r^2 R_2}{s\omega_s} \tag{6.35}$$

The torque is slip dependent. An example is appropriate now.

www.EngineeringEBooksPdf.com

Example 6.2 The power input to a three-phase 220-V 60-Hz three-phase induction motor at full load is 20,800 W. The corresponding line current is 64 A, and the speed is 830 rpm at that load. The motor is rated at 25 hp and has a no-load speed of 895 rpm. Calculate the slip, power factor, torque, and efficiency at full load.

Solution To find the number of poles, we use

$$n_s \cong 895 = \frac{120f}{P} = \frac{120(60)}{P}$$

Thus $P \cong 8.044$. Only even integers are allowed; thus $P = 8$ and

$$n_s = \frac{120(60)}{8} = 900 \text{ rpm}$$

Thus at full load

$$s = \frac{900 - 830}{900} = 0.0778$$

The power factor is obtained from

$$\cos\phi = \frac{P_s}{\sqrt{3}V_1 I_L} = \frac{20,800}{220\sqrt{3}(64)} = 0.853$$

The output power at full load is

$$P_o = 25 \times 746 \text{ W}$$

Thus the torque is calculated as

$$T = \frac{25 \times 746}{(2\pi/60)(830)} = 214.57 \text{ N} \cdot \text{m}$$

The efficiency is

$$\eta = \frac{25 \times 746}{20,800} = 0.8966$$

6.5 SIMPLIFIED EQUIVALENT CIRCUITS

It is customary to utilize a simplified equivalent circuit for the induction motor in which the shunt branch is moved to the voltage-source side. This situation is shown

www.EngineeringEBooksPdf.com

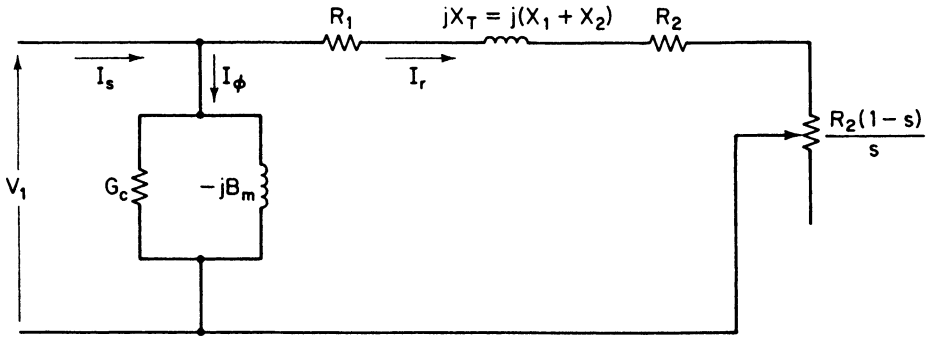


Figure 6.8 Approximate equivalent circuit of induction motor.

in Fig. 6.8. The stator resistance and shunt branch can be neglected in many instances. A total reactance X_T is defined as the sum of X_1 and X_2, as shown.

On the basis of the approximate equivalent circuit, we can find the rotor current as

$$I_r = \frac{V_1}{R_1 + R_2/s + jX_T} \tag{6.36}$$

At starting, we have $\omega_r = 0$; thus $s = 1$. The rotor starting current is hence given by

$$I_{r_{st}} = \frac{V_1}{(R_1 + R_2) + jX_T} \tag{6.37}$$

It is clear that the motor starting current is much higher than the normal (or full-load) current. Depending on the motor type, the starting current can be as high as six to seven times the normal current. We now consider two examples.

Example 6.3 A 50-hp 440-V three-phase 60-Hz six-pole Y-connected induction motor has the following parameters per phase:

$$R_2 = 0.12\ \Omega$$
$$R_1 = 0.1\ \Omega$$
$$G_c = 6.2 \times 10^{-3}\ \text{S}$$
$$X_T = 0.75\ \Omega$$
$$B_m = 0.07\ \text{S}$$

The rotational losses are equal to the stator hysteresis and eddy-current losses. For a slip of 3%, find the following:

(a) The line current and power factor.
(b) The horsepower output.

www.EngineeringEBooksPdf.com

(c) The starting torque

Solution

(a) Using the equivalent circuit of Fig. 6.8, we obtain the current I_r using Eq. (6.36) as

$$I_r = \frac{440/\sqrt{3}}{(0.1 + 0.12/0.03) + j0.75}$$
$$= 60.948\angle -10.366 \text{ deg}$$

The no-load current is

$$I_\phi = \frac{400}{\sqrt{3}}(6.2 \times 10^{-3} - j0.07)$$
$$= 1.575 - j17.78$$

Thus the stator current is

$$I_s = I_r + I_\phi$$
$$= 67.9137\angle -25.0446 \text{ deg}$$

Thus

$$\phi_s = 25.0 \text{ deg}$$
$$\cos\phi_s = 0.906 \text{ lagging}$$

(b) The air-gap power is given by

$$P_g = 3I_r^2 \frac{R_2}{s}$$
$$= 3(60.948)^2\left(\frac{0.12}{0.03}\right) = 44.576 \times 10^3 \text{ W}$$

The mechanical shaft power is

$$P_m = (1 - s)P_g = 43.239 \times 10^3 \text{ W}$$

The core losses are

$$P_c = 3\left(\frac{400}{\sqrt{3}}\right)^2 (6.2 \times 10^{-3}) = 1200 \text{ W}$$

www.EngineeringEBooksPdf.com

Thus

$$P_{rl} = 1200 \text{ W}$$
$$P_o = P_m - P_{rl}$$
$$= 42.038 \times 10^3 \text{ W}$$
$$= 56.35 \text{ hp}$$

(c) At starting $s = 1$,

$$I_r = \frac{440/\sqrt{3}}{(0.1 + 0.12) + j0.75} = 325.02\angle -73.652 \text{ deg}$$
$$P_g = 3(325.02)^2(0.12) = 38.029 \text{ kW}$$
$$\omega_s = \frac{2\pi(60)}{3} = 40\pi$$

As a result, we conclude that

$$T = \frac{P_g}{\omega_s} = 302.63 \text{ N} \cdot \text{m}$$

Example 6.4 The rotor resistance and reactance at standstill of a three-phase four-pole 110-V induction motor are 0.18 Ω and 0.75 Ω, respectively. Find the rotor current at starting as well as when the speed is 1720 rpm. Assume that the frequency is 60 Hz. Calculate the equivalent resistance of the load.

Solution

$$R_2 = 0.18\,\Omega \qquad X_2 = 0.75\,\Omega$$
$$n_s = \frac{120f}{P} = \frac{120 \times 60}{4} = 1800 \text{ rpm}$$
$$s = \frac{1800 - 1720}{1800} = 0.0444$$

At standstill, $s = 1$,

$$I_r = \frac{V}{\sqrt{R_2^2 + X_2^2}} = \frac{110/\sqrt{3}}{\sqrt{(0.18)^2 + (0.75)^2}} = 82.34 \text{ A}$$

For a speed of 1720 rpm, we get

$$I_r = \frac{V}{\sqrt{(R_2/s)^2 + X_2^2}} = 15.419 \text{ A}$$

www.EngineeringEBooksPdf.com

The equivalent resistance of the load is

$$R_L = R_2 \frac{1-s}{s}$$
$$= 3.87\,\Omega$$

6.6 TORQUE CHARACTERISTICS

The torque developed by the motor can be derived in terms of the motor parameters and slip using the expressions given earlier.

$$T = \frac{3|V_1|^2}{\omega_s} \frac{R_2/s}{(R_1 + R_2/s)^2 + X_T^2} \tag{6.38}$$

The maximum torque occurs for

$$\frac{\partial T}{\partial (R_2/s)} = 0 \tag{6.39}$$

The result is

$$R_1^2 + X_T^2 = \left(\frac{R_2}{s}\right)^2 \tag{6.40}$$

Thus we obtain the slip at which maximum torque occurs as

$$s_{\max T} = \frac{R_2}{\sqrt{R_1^2 + X_T^2}} \tag{6.41}$$

The value of maximum torque is

$$T_{\max} = \frac{3|V_1|^2}{2\omega_s\left(R_1 + \sqrt{R_1^2 + X_T^2}\right)} \tag{6.42}$$

If we neglect the resistance of the stator,

$$s_{\max T} = \frac{R_2}{X_T} \tag{6.43}$$

and

$$T_{\max} = \frac{3|V_1|^2}{2\omega_s X_T} \tag{6.44}$$

www.EngineeringEBooksPdf.com

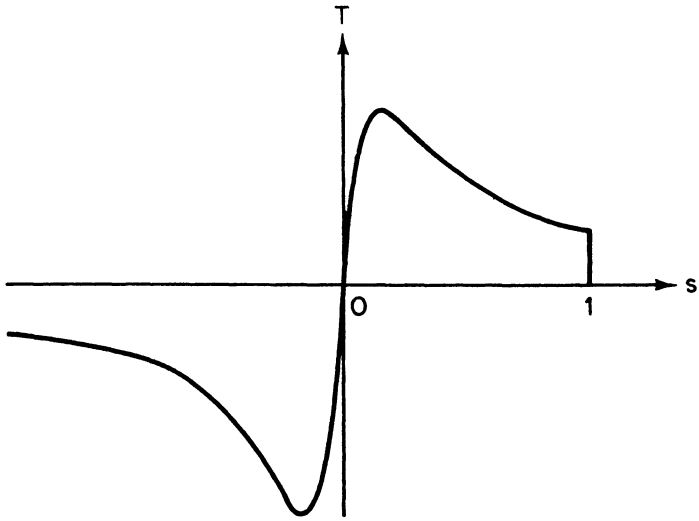


Figure 6.9 Torque–slip characteristics for induction motor.

The maximum torque does not depend on the rotor resistance. The torque–slip variations are shown in Fig. 6.9.

We now present an example.

Example 6.5 The rotor resistance and reactance of a squirrel-cage induction-motor at standstill are 0.12 Ω per phase and 0.7 Ω per phase, respectively. Assuming a transformer ratio of unity, from the eight-pole stator having a phase voltage of 254 at 60 Hz to the rotor secondary, calculate the following:

(a) Rotor starting current per phase.
(b) The value of slip-producing maximum torque.

Solution

(a) At starting $s = 1$; as a result,

$$I_r = \frac{254}{0.12 + j0.7} = 357.64\angle -80.27 \text{ deg A}$$

(b)

$$s_{\max T} = \frac{R_2}{X_T} = \frac{0.12}{0.7} = 0.17143$$

Example 6.6 The maximum torque of a 220-V three-phase four-pole 60-Hz induction motor is 180 N·m, at a slip of 0.15. If the motor is operated on a 50-Hz 220-V supply, find the value of the maximum torque, slip, and speed at which this occurs. Neglect stator impedance.

www.EngineeringEBooksPdf.com

Solution We have

$$T_{\max} = \frac{3|V|^2}{2\omega_s X_T}$$

In terms of frequency, we have

$$T_{\max} = \frac{3|V|^2}{(2\pi/60)(120f/P)(2\pi f L_T)}$$

Thus

$$T_{\max} = \frac{3|V|^2 P}{8\pi^2 f^2 L_T}$$

The number of poles does not change and the inductance L_T is assumed unchanged. As a result,

$$\frac{T_{\max 2}}{T_{\max 1}} = \frac{|V_2|^2 f_1^2}{|V_1|^2 f_2^2}$$

We thus obtain

$$T_{\max 2} = 180\left[\frac{200(60)}{220(50)}\right]^2$$
$$= 214.21 \text{ N} \cdot \text{m}$$

The slip at maximum torque is

$$S_{\max_T} = \frac{R_2}{X_T} = \frac{R_2}{2\pi f L_T}$$

Thus

$$\frac{s_2}{s_1} = \frac{f_1}{f_2}$$
$$s_2 = 0.15\left(\frac{60}{50}\right) = 0.18$$

The slip at maximum torque for 50 Hz is 18%. The synchronous speed in this case is

$$n_s = \frac{120(50)}{4} = 1500 \text{ rpm}$$

www.EngineeringEBooksPdf.com

Thus the speed at maximum torque is

$$n_r = 1500(1 - 0.18) = 1230\,\text{rpm}$$

This is lower than that for maximum torque at 60 Hz:

$$n_r = 1800(1 - 0.15) = 1530\,\text{rpm}$$

6.7 SOME USEFUL RELATIONS

In many electric-machine problems, knowledge of variables such as current and torque under a certain operating condition can be used to obtain the corresponding values under another operating condition. To start, we consider the torque equation

$$T = \frac{3I_r^2 R_2}{s\omega_s}$$

For operating condition 1, we have

$$T_1 = \frac{3I_1^2 R_2}{s_1\omega_s}$$

For a different operating condition, we have

$$T_2 = \frac{3I_2^2 R_2}{s_2\omega_s}$$

As a result

$$\frac{T_1}{T_2} = \frac{s_2}{s_1}\left(\frac{I_1}{I_2}\right)^2 \tag{6.45}$$

If, for example, condition 1 is starting the motor ($s = 1$) and condition 2 is full-load operation, s_f, then

$$\frac{T_{st}}{T_f} = s_f\left(\frac{I_{st}}{I_f}\right)^2 \tag{6.46}$$

Now consider the rotor-current equation written for condition *1* as

$$I_1^2 = \frac{V^2}{(R_2/s_1)^2 + X_T^2}$$

www.EngineeringEBooksPdf.com

For condition 2, we have

$$I_2^2 = \frac{V^2}{(R_2/s_2)^2 + X_T^2}$$

Thus

$$\left(\frac{I_1}{I_2}\right)^2 = \frac{(R_2/s_2)^2 + X_T^2}{(R_2/s_1)^2 + X_T^2}$$

Recall that

$$\frac{R_2}{X_T} = s_{\max T}$$

As a result,

$$\left(\frac{I_1}{I_2}\right)^2 = \frac{1 + (s_{\max T}/s_2)^2}{1 + (s_{\max T}/s_1)^2} \tag{6.47}$$

Let condition 1 be starting the motor and condition 2 be that for full load; then

$$\left(\frac{I_{st}}{I_f}\right)^2 = \frac{1 + (s_{\max T}/s_f)^2}{1 + s_{\max T}^2}$$

Similarly,

$$\left(\frac{I_{\max T}}{I_f}\right)^2 = \frac{1 + (s_{\max T}/s_f)^2}{2}$$

We can combine Eqs. (6.45) and (6.47) to get

$$\frac{T_1}{T_2} = \frac{s_2}{s_1}\frac{1 + (s_{\max T}/s_2)^2}{1 + (s_{\max T}/s_1)^2} \tag{6.48}$$

From the preceding relation, we can conclude first that

$$\frac{T}{T_{\max}} = \frac{2ss_{\max T}}{s_{\max T}^2 + s^2} \tag{6.49}$$

This provides a relation between torque at slip s and the maximum torque in terms of slip. We can further write

$$\frac{T_{st}}{T_{\max}} = \frac{2s_{\max T}}{1 + s_{\max T}^2} \tag{6.50}$$

www.EngineeringEBooksPdf.com

Finally,

$$\frac{T_{st}}{T_{max}} = s_f \frac{1 + (s_{max_T}/s_f)^2}{1 + s_{max_T}^2} \tag{6.51}$$

The following example illustrates the concepts of operating conditions comparison.

Example 6.7 The full-load slip of a squirrel-cage induction motor is 0.05, and the starting current is four times the full-load current. Neglecting the stator core and copper losses as well as the rotational losses, obtain:

(a) The ratio of starting torque to the full-load torque.
(b) The ratio of maximum to full-load torque and the corresponding slip.

Solution

(a) We have

$$s_{fld} = 0.05 \qquad I_{st} = 4I_{fld}$$

Using Eq. (6.46), and neglecting stator resistance, we have

$$\frac{T_{st}}{T_{fld}} = \left(\frac{I_{st}}{I_{fld}}\right)^2 s_{fld}$$

Thus

$$\frac{T_{st}}{T_{fld}} = (4)^2(0.05) = 0.8$$

(b) We have

$$I_{fld}^2 = \frac{V_1^2}{(R_2/s)^2 + X_T^2}$$

$$I_{st}^2 = \frac{V_1^2}{R_2^2 + X_T^2}$$

Thus we get

$$\left(\frac{I_{st}}{I_{fld}}\right)^2 = \frac{(R_2/0.05)^2 + X_T^2}{R_2^2 + X_T^2} = (4)^2$$

Thus we have

$$400R_2^2 + X_T^2 = 16R_2^2 + 16X_T^2$$

$$384R_2^2 = 15X_T^2$$

www.EngineeringEBooksPdf.com

As a result,

$$s_{\max_T} = \frac{R_2}{X_T} = \sqrt{\frac{15}{384}} = 0.19764$$

We now have

$$T_{\text{fld}} = \frac{3|V_1|^2(R_2/s)}{(R_2/s)^2 + X_T^2}$$

Substituting

$$R_2 = X_T s_{\max_T}$$

we get

$$T_{\text{fld}} = \frac{3|V_1|^2(s_{\max_T}/s)}{X_T[1 + (s_{\max_T}/s)^2]}$$

As a result, we use Eq. (6.44) to get

$$\begin{aligned}\frac{T_{\max}}{T_{\text{fld}}} &= \frac{s_{\text{fld}}}{s_{\max_T}} \frac{(s_{\max}/s_{\text{fld}})^2 + 1}{2} \\ &= \frac{0.05}{0.19764} \frac{(0.19764/0.05)^2 + 1}{2} \\ &= 2.1\end{aligned}$$

6.8 INTERNAL MECHANICAL POWER

The internal mechanical power developed by an induction motor can be analyzed in a manner similar to the torque. The internal mechanical power is given by

$$P_m = 3I_r^2 R_2 \frac{1 - s}{s} \tag{6.52}$$

Substituting for the rotor current, we obtain

$$P_m = 3V_1^2 \frac{R_2(1 - s)/s}{(R_1 + R_2/s)^2 + X_T^2} \tag{6.53}$$

Let

$$a = \frac{R_2}{s} \tag{6.54}$$

www.EngineeringEBooksPdf.com

Thus

$$P_m = 3V_1^2 \frac{a - R_2}{(R_1 + a)^2 + X_T^2} \tag{6.55}$$

The maximum internal mechanical power is obtained by setting $\partial P_m / \partial a = 0$, to obtain

$$(R_1 + a)^2 + X_T^2 + 2(R_1 + a)(R_2 - a) = 0$$

This reduces to

$$a^2 - 2aR_2 - [X_T^2 + R_1(R_1 + 2R_2)] = 0 \tag{6.56}$$

Define a new reactance:

$$\tilde{X}_T^2 = X_T^2 + R_1(R_1 + 2R_2) \tag{6.57}$$

Clearly, if stator resistance is negligible, then $\tilde{X}_T$ and X_T are equal. As a result, the condition for maximum power is

$$a^2 - 2aR_2 - \tilde{X}_T^2 = 0$$

Thus the required value of a is

$$a = R_2 + \sqrt{R_2^2 + \tilde{X}_T^2} \tag{6.58}$$

As a result, the slip at maximum power is obtained as

$$s_{\max P} = \frac{R_2}{R_2 + Z_B} \tag{6.59}$$

where Z_B is the blocked rotor impedance defined by

$$Z_B = \sqrt{R_2^2 + \tilde{X}_T^2} \tag{6.60}$$

The maximum internal power is now found to be

$$P_{m_{\max}} = \frac{3V_1^2}{2(R_1 + a)} \tag{6.61}$$

or

$$P_{m_{\max}} = \frac{3V_1^2}{2(R_1 + R_2 + Z_B)} \tag{6.61}$$

www.EngineeringEBooksPdf.com

where

$$Z_B = \sqrt{R_1^2 + X_T^2 + R_2(R_2 + 2R_1)} \tag{6.62}$$

The slip at which maximum internal power is developed is less than the slip for maximum torque. This follows, since

$$s_{\max T} = \frac{R_2}{\sqrt{R_1^2 + X_T^2}} \tag{6.63}$$

As a result,

$$\frac{s_{\max T}}{s_{\max P}} = \frac{R_2 + Z_B}{\sqrt{R_1^2 + X_T^2}} \tag{6.64}$$

This ratio is greater than 1 since Z_B is greater than $\sqrt{R_1^2 + X_T^2}$.

In most applications it is convenient to neglect the stator resistance R_1. This yields simpler expressions. In this case we have

$$Z_B = \sqrt{R_2^2 + X_T^2} \tag{6.65}$$

$$s_{\max P} = \frac{R_2}{R_2 + Z_B} \tag{6.66}$$

$$P_{m_{\max}} = \frac{3V_1^2}{2(R_2 + Z_B)} \tag{6.67}$$

The relation of slip at maximum torque to that at maximum power reduces to

$$\frac{s_{\max T}}{s_{\max P}} = \frac{R_2 + \sqrt{R_2^2 + X_T^2}}{X_T} \tag{6.68}$$

Thus we have the desired result

$$\frac{1}{s_{\max P}} = 1 + \sqrt{\left(\frac{1}{s_{\max T}}\right)^2 + 1} \tag{6.69}$$

Example 6.8 An eight-pole 60-Hz induction motor has rotor resistance and reactance at standstill of 0.1 Ω and 0.8 Ω per phase, respectively. Assume that the voltage per phase is 120 V and neglect stator and core effects. Find the slip at maximum power, the maximum power developed, and the torque at maximum power. Compare the maximum torque to that obtained for maximum power.

www.EngineeringEBooksPdf.com

Solution We have $R_2 = 0.1$ and $X_T = X_2 = 0.8$. Thus

$$Z_B = \sqrt{(0.1)^2 + (0.8)^2} = 0.8062$$

The slip for maximum power is

$$s_{\max_P} = \frac{0.1}{0.1 + 0.8062} = 0.1103$$

The maximum power is now obtained as

$$P_{m_{\max}} = \frac{3(120)^2}{2(0.1 + 0.8062)} = 23{,}835.12 \text{ W}$$

The corresponding torque is obtained using

$$T = \frac{P}{\omega_s(1 - s)}$$

Now

$$n_s = \frac{120(60)}{8} = 900 \text{ rpm}$$

Thus

$$T = \frac{23{,}835.12}{(2\pi/60)(900)(1 - 0.1103)}$$
$$= 284.2667 \text{ N} \cdot \text{m}$$

The slip for maximum torque is obtained as

$$s_{\max_T} = \frac{R_2}{X_T} = \frac{0.1}{0.8} = 0.125$$

The corresponding rotor current is obtained from

$$I_r = \frac{120}{\sqrt{(0.1/0.125)^2 + (0.8)^2}} = 106.066 \text{ A}$$

The mechanical power is obtained for maximum torque as

$$P_m = 3I_r^2 R_2 \frac{1 - s}{s}$$
$$= 3(106.066)^2 \left(\frac{0.1}{0.125}\right)(1 - 0.125)$$
$$= 23{,}625 \text{ W}$$

www.EngineeringEBooksPdf.com

This is clearly lower than the maximum power. The maximum torque is now obtained as

$$T_{\max} = \frac{P_m}{\omega_s(1 - s_{\max T})}$$
$$= \frac{23,625}{(2\pi/60)(900)(1 - 0.125)} = 286.479 \text{ N} \cdot \text{m}$$

This is higher than the torque at maximum power.

6.9 EFFECTS OF ROTOR IMPEDANCE

Speed control of induction motors of the wound-rotor type can be achieved by inserting additional rotor resistance (R_a). In addition to this, torque control at a given speed can be achieved using this method. Let

$$K = \frac{3V^2}{\omega_s} \tag{6.70}$$

$$a_1 = \frac{R_2}{s_1} \tag{6.71}$$

$$a_2 = \frac{R_1 + R_a}{s_2} \tag{6.72}$$

$$\alpha = \frac{T_2}{T_1} \tag{6.73}$$

where the subscript 1 refers to operating conditions without additional rotor resistance and the subscript 2 refers to conditions with the additional rotor resistance. Neglect stator resistance in the present analysis and we have

$$T = \frac{3V^2(R_2/s)}{\omega_s[(R_2/s)^2 + X_T^2]} \tag{6.73}$$

or

$$T = K\frac{a}{a^2 + X_T^2} \tag{6.74}$$

Introducing a resistance in the rotor winding will change a. Let the original torque be T_1. Thus

$$T_1 = K\frac{a_1}{a_1^2 + X_T^2} \tag{6.75}$$

www.EngineeringEBooksPdf.com

Let the new torque with additional resistance be T_2. Thus

$$T_2 = K\frac{a_2}{a_2^2 + X_T^2} \tag{6.76}$$

By the definition of the torque ratio, α, we get

$$\alpha = \frac{a_1^2 + X_T^2}{a_2^2 + X_T^2}\frac{a_2}{a_1} \tag{6.77}$$

Equation (6.77) provides us with the means to derive the value of additional resistance, R_a, required to obtain the same torque ($T_1 = T_2$) at two different values of slip (or rotor speed). To do this we set $\alpha = 1$, to obtain

$$a_2(a_1^2 + X_T^2) = a_1(a_2^2 + X_T^2)$$

or

$$(a_2 - a_1)(X_T^2 - a_1 a_2) = 0 \tag{6.78}$$

Thus for $T_1 = T_2$, we get $a_1 = a_2$, or

$$\frac{R_2}{s_1} = \frac{R_2 + R_a}{s_2}$$

or

$$R_a = R_2\left(\frac{s_2}{s_1} - 1\right) \tag{6.79}$$

Let us note here that for equal torque, the rotor-circuit currents are the same, since

$$I_r = \frac{V}{\sqrt{(R_2/s)^2 + X_T^2}} = \frac{V}{\sqrt{a^2 + X_T^2}} \tag{6.80}$$

$$\left(\frac{I_{r_1}}{I_{r_2}}\right)^2 = \frac{a_2^2 + X_T^2}{a_1^2 + X_T^2} = 1 \qquad \text{for} \qquad T_1 = T_2 \tag{6.81}$$

Example 6.9 The rotor resistance and reactance of a wound-rotor induction motor at standstill are 0.1 Ω per phase and 0.8 Ω per phase, respectively. Assuming a transformer ratio of unity, from the eight-pole stator having phase voltage of 120 V at 60 Hz to the rotor secondary, find the additional rotor resistance required to produce maximum torque at:

(a) Starting $s = 1$.
(b) A speed of 450 rpm.

www.EngineeringEBooksPdf.com

Solution Given that

$$R_2 = 0.1\ \Omega$$
$$X_2 = 0.8\ \Omega$$

we get for maximum torque operation (condition 1),

$$s_1 = s_{\max T} = \frac{R_2}{X_2} = 0.125$$

(a) The second condition of operation is that at starting,

$$s_2 = s_{st} = 1$$

Thus we use

$$R_a = R_2\left(\frac{s_2}{s_1} - 1\right)$$

to get

$$R_a = 0.1[(0.125)^{-1} - 1]$$
$$= 0.7\ \Omega$$

(b) The synchronous speed is

$$n_s = \frac{120f}{P}$$
$$= \frac{120(60)}{8} = 900\,\text{rpm}$$

For $n_r = 450$ rpm, we have

$$s_2 = \frac{900 - 450}{900} = 0.5$$

As a result, we calculate

$$R_a = 0.1\left(\frac{0.5}{0.125} - 1\right)$$
$$= 0.3\ \Omega$$

The slip at maximum torque is proportional to the rotor resistance, whereas the maximum torque is independent of the rotor resistance. This can be verified

www.EngineeringEBooksPdf.com

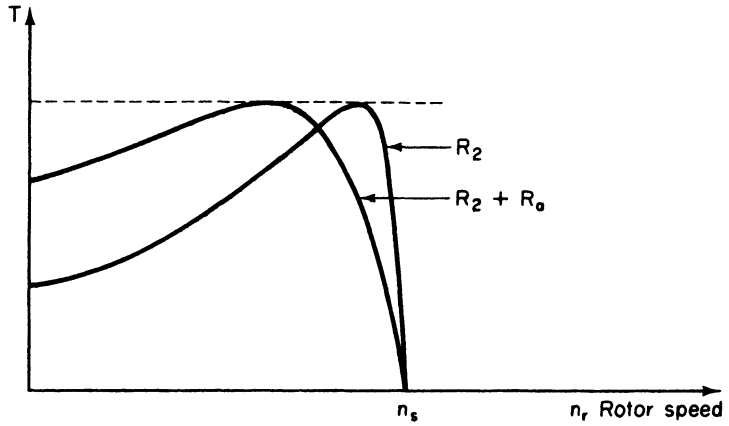


Figure 6.10 Effect of rotor resistance on torque–speed characteristics of a three-phase induction motor.

by reference to Eqs. (6.43) and (6.44). As a result, we assert that an additional resistance inserted in the rotor circuit will increase the slip at maximum torque (lower rotor speed); the maximum torque is unchanged, however. The torque–slip characteristics of a three-phase induction motor with varying rotor resistance are shown in Fig. 6.10.

6.10 CLASSIFICATION OF INDUCTION MOTORS

Integral-horsepower three-phase squirrel-cage motors are available from manufacturers' stock in a range of standard ratings up to 200 hp at standard frequencies, voltages, and speeds. (Larger motors are regarded as special-purpose motors.) Several standard designs are available to meet various starting and running requirements. Representative torque–speed characteristics of four designs are shown in Fig. 6.11. These curves are typical of 1800-rpm (synchronous-speed) motors with ratings from 7.5 hp to 200 hp.

To help industry select appropriate motors for varying applications in the integral-horsepower range, the National Electrical Manufacturers Association (NEMA) in the United States and the International Electrotechnical Commission (IEC) in Europe have defined a series of standard designs with different torque–speed curves. These standard designs are referred to as *design classes*, and an individual motor may be referred to as a design class X motor. Figure 6.11 shows typical torque–speed curves for the four standard NEMA design classes. The characteristic features of each standard design class are given below.

Design Class A Design class A motors are the standard motor design, with a normal starting torque, a normal starting current, and low slip. The full-load slip of design A motors must be less than 5%, and must be less than that of a design B motor

www.EngineeringEBooksPdf.com

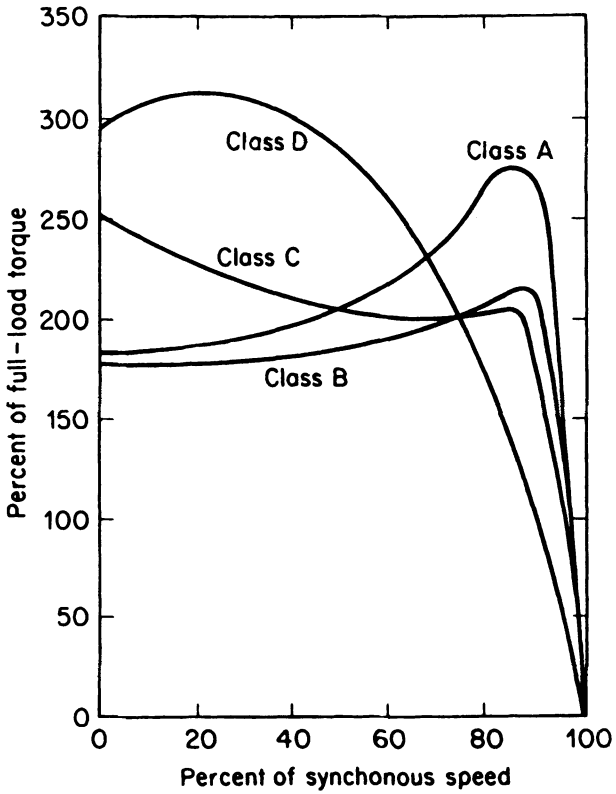


Figure 6.11 Typical torque–speed curves for 1800-rpm general-purpose induction motors.

of equivalent rating. The pullout torque is 200 to 300% of the full-load torque and occurs at a low slip (less than 20%). The starting torque of this design is at least the rated torque for larger motors, and is 200% or more of the rated torque for smaller motors. The problem with this class is its very high starting current, typically 500 to 800% of rated current. In sizes above 7.5 hp, reduced voltage starting is used to avoid voltage dip problems in the power system. In the past, design class A motors were the standard design for most applications below 7.5 hp and above 200 hp, but they largely have been replaced by design class B motors recently. Typical applications for these motors are driving fans, blowers, pumps, lathes, and other machine tools.

Design Class B Design class B motors have a normal starting torque, a lower starting current, and low slip. This motor produces about the same starting torque as the class A motor with about 25% less current. The pullout torque is greater than or equal to 200% of the rated load torque, but less than that of the class A design because of the increased rotor reactance. Rotor slip is still relatively low (less than 5%) at full load. Applications are similar to those for design A, but design B is preferred because of its lower starting-current requirements. Design class B motors have largely replaced design class A motors in recent installations.

www.EngineeringEBooksPdf.com

Design Class C Design class C motors have a high starting torque with low starting currents and low slip (less than 5%) at full load. The pullout torque is slightly lower than that for class A motors, while the starting torque is up to 250% of the full-load torque. These motors are built from double-cage rotors, so they are more expensive than motors in classes A and B. They are used for high-starting-torque loads, such as loaded pumps, compressors, and conveyors.

Design Class D Design class D rotors have a very high starting torque (275% or more of the rated torque) and a low starting current. They also have a high slip at full load. They are essentially ordinary class A induction motors, but with the rotor bars made smaller and with a higher-resistance material. The high rotor resistance shifts the peak torque to a very low speed. It is possible for the highest torque to occur at zero speed (100% slip). Full-load slip for these motors is quite high because of the high rotor resistance. It is typically 7 to 11%, but may go as high as 17% or more. These motors are used in applications requiring the acceleration of extremely high-inertia-type loads, especially the large flywheels used in punch presses or shears.

In addition to these four design classes, NEMA used to recognize design classes E and F, which were called *soft-start* induction motors. These designs were distinguished by having very low starting currents and were used for low-starting-torque loads in situations where starting currents were a problem. These designs are now obsolete.

Continual improvements in the quality of the steels, casting techniques, the insulation, and the construction features used in induction motors, resulted in a smaller motor for a given power output, yielding considerable savings in construction costs. In fact, a 100-hp motor of today's design is the same physical size as a 7.5-hp motor of 1897.

Improvements in induction-motor design were not associated with improvements in operating efficiency. More effort was given to reducing the initial cost of the machines than to increasing their efficiency. The reason is that electricity was so inexpensive, making the capital cost of a motor the principal criterion used by end users in its selection.

The lifetime operating cost of machines has recently become more important, while the initial installation cost has become relatively less important. Therefore, both manufacturers and users have placed new emphasis on motor efficiency.

High-efficiency induction motors are forming an ever-increasing share of the market. To improve the efficiency of these motors compared to the traditional standard-efficiency designs, the following techniques are used:

1. To reduce copper losses in the stator windings more copper is used.
2. The rotor and stator core length is increased to reduce the magnetic flux density in the air gap, to reduce the magnetic saturation. This decreases core losses.
3. More steel is used in the stator, allowing greater heat transfer out of the motor and reducing its operating temperature. The rotor's fan is then redesigned to reduce windage losses.

www.EngineeringEBooksPdf.com

4. The steel used in the stator is a special high-grade electrical steel that allows low hysteresis losses.
5. The steel is made of laminations that are very close together, and the steel has a very high internal resistivity. Both effects tend to reduce the eddy-current losses.
6. The rotor is carefully machined to produce a uniform air gap, reducing stray load losses.

6.11 STARTING INDUCTION MOTORS

In Section 6.7 we saw that the ratio of current at starting to that at full load can be obtained from

$$\left(\frac{I_{st}}{I_f}\right)^2 = \frac{1 + (s_{max_T}/s_f)^2}{1 + s^2_{msc_T}}$$

It is clear that the rotor current at starting is much higher than that at full load. Although induction motor designs provide for a rugged construction that can withstand large starting currents, it is undesirable to start induction motors with full applied voltage. One reason for this is simply the current overloading of the source circuit, which may not be able to withstand the current inrush. A second reason is that the large drop in voltage (due to feeder impedence) may result in voltage dip (a reduced voltage) supply at the stator terminals that does not result in sufficient starting torque. The motor may not start at all.

For squirrel-cage induction motors, the starting current can vary widely depending primarily on the motor's rated power and on the effective rotor resistance at starting. To estimate the rotor current at starting conditions, all squirrel-cage motors now have a starting *code letter* (not to be confused with their *design class* letter) on their nameplates. The code letter sets limits on the amount of current the motor can draw at starting. These limits are expressed in terms of the apparent starting power of the motor as a function of its horsepower rating. Table 6.1 contains the starting kVA per horsepower for each code letter.

To determine the starting current for an induction motor, read the rated voltage, horsepower, and code letter from its nameplate. Then the starting reactive power for the motor will be

$$S_{start} = (\text{Rated horsepower})(\text{Code letter factor})$$

and the starting current can be found from

$$I_L = \frac{S_{start}}{\sqrt{3}V_T}$$

www.EngineeringEBooksPdf.com

TABLE 6.1 NEMA Code Letters,[a] Indicating the Starting Kilovoltamperes per Horsepower of Rating for a Motor

Nominal Code Letter	Locked Rotor, kVA/hp	Nominal Code Letter	Locked Rotor, kVA/hp
A	0–3.15	L	9.00–10.00
B	2.16–3.55	M	10.00–11.20.
C	3.55–4.00	N	11.20–12.50
D	4.00–4.50	P	12.50–14.00
E	4.50–5.00	R	14.00–16.00
F	5.00–5.60	S	16.00–18.00
G	5.60–6.30	T	18.00–20.00
H	6.30–7.10	U	20.00–22.40
J	7.10–8.00	V	22.40 and up
K	8.00–9.00		

[a] Each code letter extends up to, but does not include, the lower bound of the next higher class.
Source: Reproduced by permission from *Motors and Generators*, NEMA Publication MG-1, copyright 1987 by NEMA.

Methods for reducing the starting current in an induction motor can be classified into two categories: methods that apply reduced voltage to the stator at starting, and those that increase the resistance of the rotor circuit at starting and decrease it as the motor speed in increased.

6.11.1 Reduced-Voltage Starting

For low-rotor-resistance squirrel-cage motors, a three-phase autotransformer is employed. At starting a low value of voltage is applied to the stator, which is then restored to full voltage when the rotor speed is within 25% of full-load value. In Fig. 6.12 contacts *a* and *c* are closed at starting, and are subsequently open while contacts *b* are closed.

An alternative method is the Y/Δ switching technique, which requires that both ends of each phase of the stator windings be accessible. At standstill the stator is connected in Y, and as full speed is approached, a switch is activated to connect the stator in a Δ-connection. The effect of Y/Δ switching is equivalent to an autotransformer starter with a ratio of $1/\sqrt{3}$.

6.11.2 Variable-Resistance Starting

The basic principle involved in variable-resistance starting is to cause the rotor resistance at standstill to be several times as much as its value when the motor is running at full speed. There are two basic methods to achieve this:

1. *External-Resistance Starting* This method is used for the wound-rotor induction motor, where a three-phase bank of resistors is connected to the

www.EngineeringEBooksPdf.com

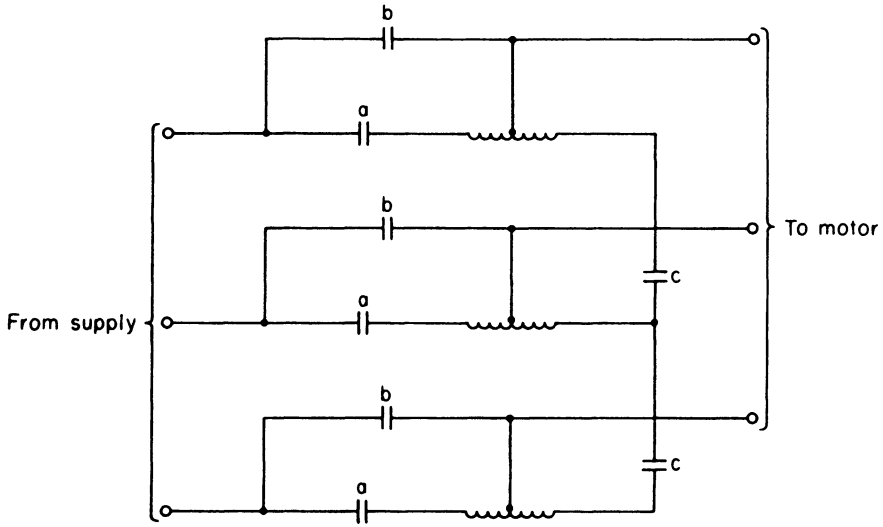


Figure 6.12 Autotransformer starting.

rotor slip rings at starting. As a result, a reduced starting current is obtained simultaneously with an increased starting torque. It is clear that high starting torques can be achieved simply by inserting additional rotor resistance of value corresponding to the maximum torque production at starting. One advantage of this method is that energy lost as heat is dissipated through the environment, not within the motor itself.

2. *Deep-Bar and Double-Squirrel-Cage Rotors* The main idea is that the frequency of induced voltages in the rotor is equal to the product of slip and synchronous frequency. At standstill, the slip is unity, and 60-Hz frequency currents flow in the rotor circuit, while at full speed, a rotor frequency of 2 to 3 Hz is common. It is therefore clear that if the rotor circuit is arranged such that a higher effective resistance is offered by the rotor at starting, and a lower value of effective resistance is obtained at running, the desired effect is obtained.

For the latter, two methods are available: (1) deep-bar rotors, and (2) double-cage rotors. In the deep-bar-rotor design, the rotor conductors are formed of deep, narrow bars that can be considered to be a large number of layers of differential depth. The leakage inductance of the bottom layer is greater than that for the top layer. The current in the low-reactance upper layer will be greater than that in the high-reactance bottom layers when alternating currents are considered. As a result, the effective resistance of the rotor at stator frequency is much higher than its value for lower frequencies. As speed increases, the rotor frequency decreases, and therefore the rotor effective resistance decreases.

In the double-cage arrangement the squirrel cage winding is made of layers of bars short-circuited by end rings. The low bars have a larger cross section than

www.EngineeringEBooksPdf.com

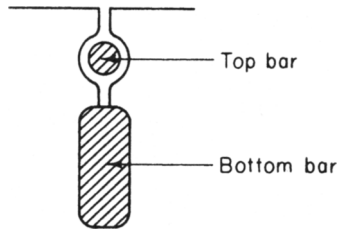


Figure 6.13 Double-cage arrangement.

the upper bars, as shown in Fig. 6.13, and consequently have lower resistance. The inductance of the lower bars is greater than that of the upper ones. At standstill, the current in the rotor is concentrated mainly in the upper bars because the lower bars have a high reactance. Thus at starting the rotor offers high impedance corresponding to the high-resistance upper layer. At low rotor frequencies, with low slip, the impedance is negligible and the rotor resistance approaches that of the two layers in parallel.

Example 6.10 A 230-V three-phase four-pole 60-Hz double-cage motor has the following parameters:

Upper cage: $R_u = 2.4\ \Omega, X_u = 1\ \Omega$
Lower cage: $R_l = 0.24\ \Omega, X_l = 4.20\ \Omega$

Assume that mutual reactance between the cages is negligible. It is required to find:

(a) The currents in the upper and lower cages at starting and at a full-load slip of 0.04.
(b) The torques developed by the upper and lower cages at starting and at a full-load slip of 0.04.

Solution

(a) The approximate equivalent circuit of the motor, neglecting stator circuit and no-load variables, is shown in Fig. 6.14. The impedance of the upper cage is

$$Z_u = \frac{2.4}{s} + j1$$

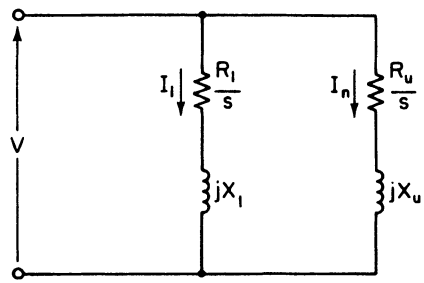


Figure 6.14 Equivalent circuit of a double-cage motor.

www.EngineeringEBooksPdf.com

The impedance of the lower cage is

$$Z_l = \frac{0.24}{s} + j4.2$$

At starting, $s = 1$

$$Z_u = 2.4 + j1 = 2.6\angle 22.62 \text{ deg}\,\Omega$$
$$Z_l = 0.24 + j4.2 = 4.2069\angle 86.73 \text{ deg}\,\Omega$$

Thus at starting

$$I_u = \frac{230\angle -22.62 \text{ deg}}{\sqrt{3}(2.6)} = 51.073\angle -22.62 \text{ deg A}$$
$$I_l = \frac{230\angle -86.73 \text{ deg}}{\sqrt{3}(4.2069)} = 31.565\angle -86.73 \text{ deg A}$$

Note that at starting the current in the upper cage is larger than that in the lower cage. The motor starting current is

$$I_{st} = I_u + I_l = 70.8\angle -46.26 \text{ deg}$$

(b) The torques are obtained using

$$T = \frac{3I^2R}{s\omega_s}$$

The motor has four poles, thus

$$\omega_s = \frac{2\pi}{60}\left(\frac{120 \times 60}{4}\right) = 60\pi$$

At starting,

$$T_u = \frac{3(51.073)^2(2.4)}{60\pi} = 99.637 \text{ N} \cdot \text{m}$$
$$T_l = \frac{3(31.565)^2(0.24)}{60\pi} = 3.8058 \text{ N} \cdot \text{m}$$

The total starting torque is

$$T_{st} = T_u + T_l = 103.44 \text{ N} \cdot \text{m}$$

The ratio of upper to lower cage torques at starting is 26.18.

www.EngineeringEBooksPdf.com

At full load, $s = 0.04$,

$$Z_u = 60 + j1 = 60.008\angle 0.955 \text{ deg } \Omega$$
$$Z_l = 6 + j4.2 = 7.3239\angle 34.992 \text{ deg } \Omega$$

Thus the cage currents are

$$I_u = \frac{230}{\sqrt{3}Z_u} = 2.2129\angle -0.9555 \text{ deg}$$
$$I_l = \frac{230}{\sqrt{3}Z_l} = 18.731\angle -34.992 \text{ deg}$$

The current in the upper cage is much less than that in the lower cage at full load. The torques are obtained as

$$T_u = \frac{3(2.213)^2(2.4)}{0.04(60\pi)} = 4.6762 \text{ N} \cdot \text{m}$$
$$T_l = \frac{3(18.131)^2(0.24)}{0.04(60\pi)} = 31.392 \text{ N} \cdot \text{m}$$

The motor full-load torque is therefore

$$T_{\text{fld}} = 36.068 \text{ N} \cdot \text{m}$$

The major portion of the torque is due to the lower cage on full load.

6.11.3 Induction-Motor Starting Circuits

A typical full-voltage or across-the-line magnetic induction motor starter circuit is shown in Fig. 6.15, and the symbols used are explained in Fig. 6.16. As shown in Fig. 6.15, when the start button is pressed, the relay (or *contactor*) coil M is energized, causing the normally open contacts M_1, M_2, and M_3 to close. When these contacts close, power is applied to the induction motor, and the motor starts. Contact M_4 also closes, which shorts out the starting switch, allowing the operator to release it without removing power from the M relay. When the stop button is pressed, the M relay is deenergized, and the M contacts open, stopping the motor.

A magnetic motor starter circuit such as this includes the following protective features:

1. Short-circuit protection
2. Overload protection
3. Undervoltage protection

www.EngineeringEBooksPdf.com

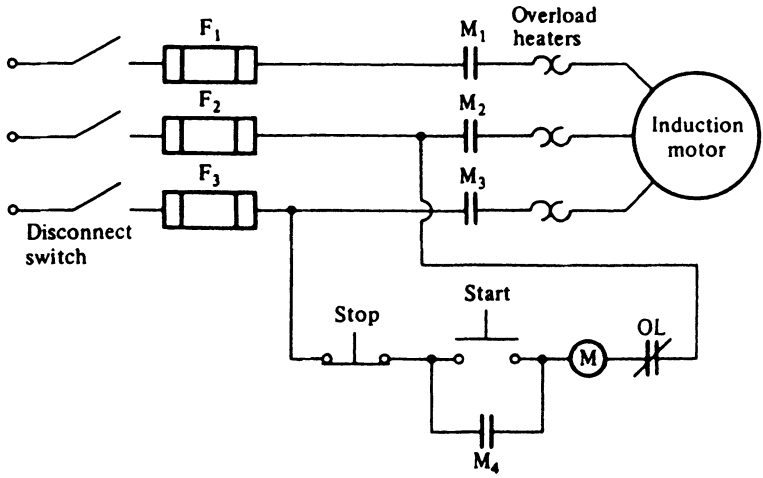


Figure 6.15 A typical across-the-line starter for an induction motor.

Short-circuit protection for the motor is provided by fuses F_1, F_2, and F_3. If a sudden short circuit develops within the motor and causes a current flow many times larger than the rated current, these fuses will blow, disconnecting the motor from the power supply and preventing heat damage to it. However, these fuses must not open during normal motor starting, so they are designed to require currents

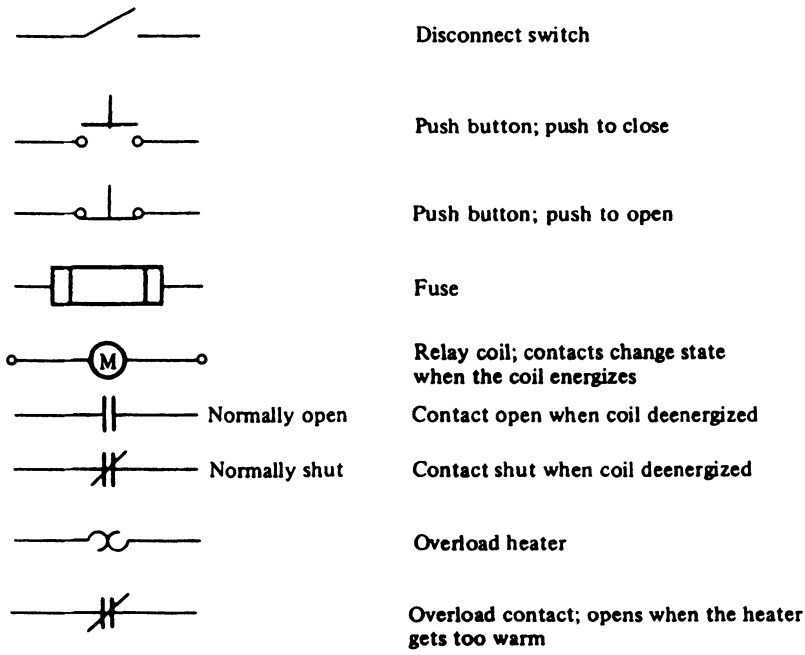


Figure 6.16 Typical components found in induction-motor control circuits.

www.EngineeringEBooksPdf.com

many times greater than the full-load current before they open the circuit. This means that short circuits through a high resistance and/or excessive motor loads will not be cleared by the fuses.

Overload protection is provided by the devices labeled OL. These devices consist of two parts, an overload heater element and overload contacts. Under normal conditions, the overload contacts are closed. However, when the temperature of the heater elements rises far enough, the OL contacts open, deenergizing the M relay, which in turn opens the normally open M contacts and removes power from the motor.

When the motor is overloaded, it may be damaged by the excessive heating caused by high current. This takes time, however, and an induction motor will not normally be hurt by brief periods of high currents (such as starting currents). Only if the high current is sustained will damage occur. The overload heater elements also depend on heat for their operation, so they will not be affected by brief periods of

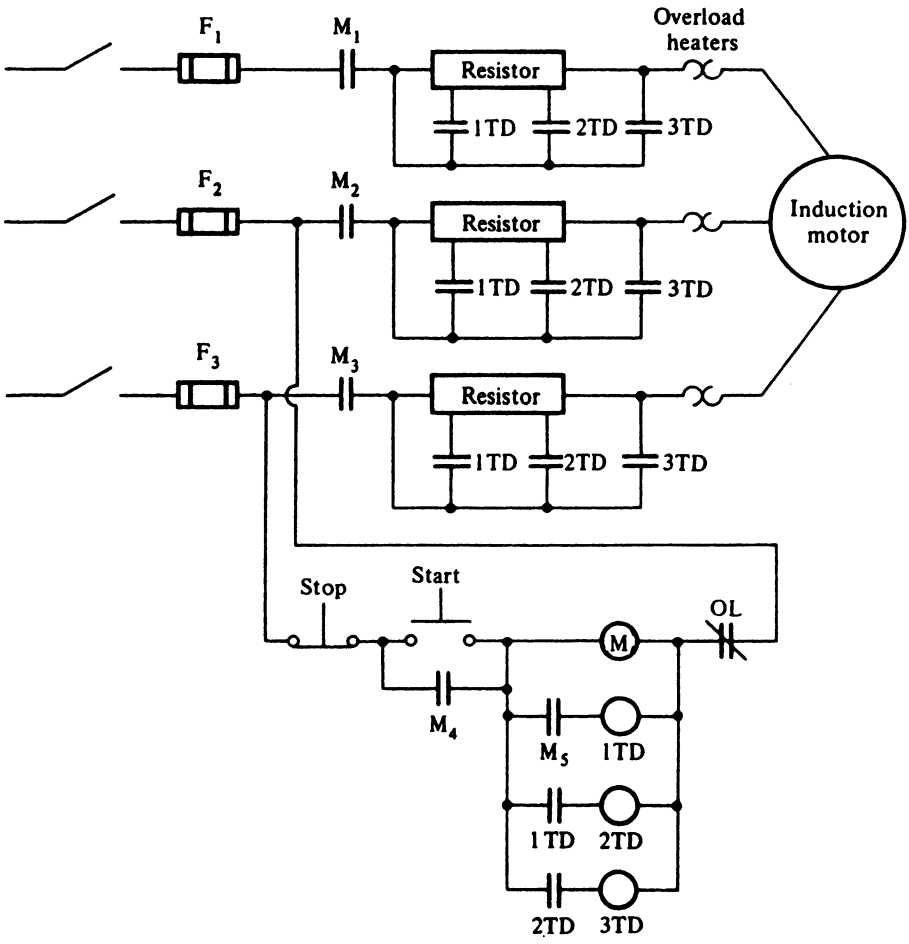


Figure 6.17 A three-step resistive starter for an induction motor.

www.EngineeringEBooksPdf.com

high current during starting, and yet they will operate during long periods of high current, removing power from the motor before it can be damaged.

Undervoltage protection is provided by the controller as well. Note that the control power for the M relay comes from directly across the lines to the motor. If the voltage applied to the motor falls too much, the voltage applied to the M relay will also fall and the relay will deenergize. The M contacts then open, removing power from the motor terminals.

An induction-motor starting circuit with resistors to reduce the starting current flow is shown in Fig. 6.17. This circuit is similar to the previous one, except that there are additional components present to control removal of the starting resistor. Relays 1TD, 2TD, and 3TD in Fig. 6.17 are so-called on-time delay relays, meaning that when they are energized there is a set time delay before their contacts shut.

When the start button is pushed in this circuit, the M relay energizes and power is applied to the motor as before. Since the 1TD, 2TD, and 3TD contacts are all open, the full starting resistor is in series with the motor, reducing the starting current.

When the M contacts close, the 1TD relay is energized. However, there is a finite delay before the 1TD contacts close. During that time, the motor partially speeds up, and the starting current drops off slightly. Subsequently, the 1TD contacts close, cutting out part of the starting resistance and simultaneously energizing the 2TD relay. After another delay, the 2TD contacts close, cutting out the second part of the resistor and energizing the 3TD relay. Finally, the 3TD contacts close, and the entire starting resistor is out of the circuit.

6.12 CONVENTIONAL SPEED CONTROL OF INDUCTION MOTORS

The speed of a three-phase induction motor driving a given load is determined by matching the torque–speed characteristics of the motor and load, as shown in Fig. 6.18. The operating point is the intersection of the two characteristics and is fixed for a given load and motor parameters.

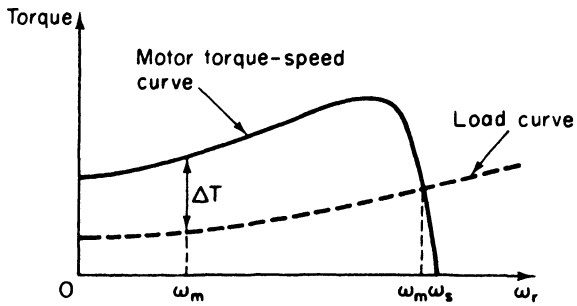


Figure 6.18 Induction-motor torque–speed curve and curve of load torque.

www.EngineeringEBooksPdf.com

Until the emergence of modern solid-state drives, induction motors were not favored for considerable speed control applications. For design classes A, B, and C, the normal operating slip range of a typical induction motor is restricted to less than 5%. Even if the slip could be increased, the motor efficiency would drop significantly because of the corresponding increase in rotor-copper losses.

If it is desired to change motor speed while carrying the same load, then a change in the torque-speed characteristic of the motor is needed. There are two major options for doing this: (1) changing the synchronous speed n_s, and (2) changing the slip at which the operating point takes place. For each option, we have a number of possible methods, which are now discussed.

6.12.1 Changing Synchronous Speed

It is clear from Eq. (6.38) that changing ω_s results in a change in the torque–speed characteristics. Recall that

$$n_s = \frac{120f}{P}$$

We can conclude that a change in n_s can be obtained either through a change in the number of stator poles or by a change in supply frequency. We thus have two categories.

1. *Speed Control by Pole Changing* There are three major approaches to changing the number of poles in an induction motor

(a) The method of consequent poles
(b) Multiple stator windings
(c) Pole-amplitude modulation (PAM)

The method of consequent poles is one of the earliest speed-control methods. It allows us to change n_s in discrete steps. A two-pole stator set of windings is changed to a four-pole configuration by a simple switching operation, as shown in Fig. 6.19. Of course, this can be done for any number of poles for a ratio of 2 : 1. This mechanism is simple to implement in squirrel-cage rotor motors, but for the wound-rotor type, we must also rearrange the rotor windings.

A traditional approach to overcome the limitations of the consequent pole method employs multiple stator windings with different numbers of poles and to energize only one set at a time. This method increases the cost and weight of the motor and is therefore used only when absolutely necessary. Combining the method of consequent poles with multiple stator windings, allows us to build a four-speed induction motor. For example, with separate four- and six-pole windings, we can produce a 60-Hz motor that has synchronous speeds of 600, 900, 1200, and 1800 rpm.

The PAM method achieves multiple sets of poles in a single stator winding, where the resulting number of poles can be in ratios other than 2 : 1. Switching the number

www.EngineeringEBooksPdf.com

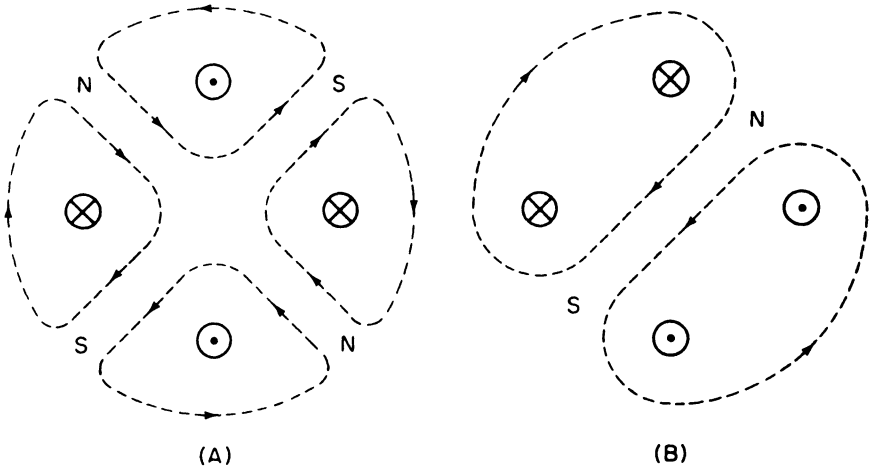


Figure 6.19 Illustrating four-pole-to-two-pole switching: (a) four-pole mode; (b) two-pole mode.

of poles in a winding is achieved by changing the connections at six terminals, in the same manner as in the method of consequent poles. To create an induction motor with two close speeds, PAM windings are preferred over multiple-stator windings because they cost about 75% of two complete separate windings.

In PAM, the spatial distribution of the magnetomotive-force waves in the machine stator are multiplied together, with the resulting output consisting of components with frequencies equal to the sum and the difference of two original frequencies. If the winding of a machine normally having P poles is modulated by making N switches in the connections on the phase groups in a given phase, then two magnetomotive-force waves will be produced in the stator winding, one of them having $P + N$ poles and the other having $P - N$ poles. If one of these waveforms can be selected over the other, then the motor will have that number of poles on its stator, and the same number of poles will, of course, be induced in the squirrel-cage rotor.

Example pole ratios available with the PAM technique and the resulting synchronous speed ratios for 60-Hz operation are as follows:

$$\text{Pole ratio} = 4/6 \rightarrow 1800/1200$$
$$\text{Pole ratio} = 6/8 \rightarrow 1200/900$$
$$\text{Pole ratio} = 8/10 \rightarrow 900/720$$

From a mathematical point of view, we express the magnetomotive force produced by a conventional P-pole winding in terms of time and position as

$$F = F_M \sin\left(\frac{P}{2}\theta - \omega t\right) \tag{6.82}$$

www.EngineeringEBooksPdf.com

If Q is the desired final number of poles on the machine, then $P-Q$ is the *difference* between the original number of poles and the desired number of poles. Now, modulate the original spatial waveform by switching connections at P-Q uniformly spaced points in each phase. The resulting mangetomotive-force waveform is

$$F = F_M \sin\left(\frac{P}{2}\theta - \omega t\right) \sin\left(\frac{P}{2} - \frac{Q}{2}\right)\theta \tag{6.83}$$

Now, use the trignometric identity

$$\sin\alpha \sin\beta = \frac{1}{2}\cos(\alpha - \beta) - \frac{1}{2}\cos(\alpha + \beta)$$

so the magnetomotive-force expression reduces to

$$F = \frac{F_M}{2}\cos\left(-\frac{Q}{2}\theta + \omega t\right) - \frac{F_M}{2}\cos\left[\left(P - \frac{Q}{2}\right)\theta - \omega t\right] \tag{6.84}$$

This magnetomotive force can be expressed as

$$F = \frac{F_M}{2}\cos\left(\frac{Q}{2}\theta - \omega t\right) - \frac{F_M}{2}\cos\left[\left(P - \frac{Q}{2}\right)\theta - \omega t\right] \tag{6.85}$$

Note that there are two different spatial distributions of poles present in the resulting magnetomotive force. If Q is the desired number of poles in the motor, then we need to reject the other distribution. This is accomplished by a proper choice of the distribution and chording of the stator windings.

This analysis is approximate, because we assume the modulating spatial wave is sinusoidal when it is a square wave. Square-wave modulation introduces more spatial harmonics into the mangetomotive force distribution, which may be reduced by the proper choice of winding chording.

In practice, the choice of spatial modulating frequency, winding chording, winding distribution, and other factors required to achieve a given speed ratio is an art based on the experience of the designer.

2. *Speed Control by Changing Line Frequency* Changing the electrical frequency applied to the stator of an induction motor causes the rate of rotation of its magnetic field n_s, to change in direct proportion to the change in electrical frequency, and the no-load point on the torque–speed characteristic curve will change with it. The synchronous speed of the motor at rated conditions is known as the *base speed*. By using variable frequency control, it is possible to adjust the speed of the motor either above or below base speed. A properly designed variable-frequency induction-motor drive can be *very* flexible. It can control the speed of an induction motor over a range from as little as 5% of base speed up to about twice

www.EngineeringEBooksPdf.com

base speed. However, it is important to maintain certain voltage and torque limits on the motor to ensure safe operation as the frequency is varied.

When running at speeds below the base speed of the motor, it is necessary to reduce the terminal voltage applied to the stator for proper operation. The terminal voltage applied to the stator should be decreased linearly with decreasing stator frequency. This is called *derating*, and is needed so the iron core of the motor does not saturate and cause excessive magnetization currents to flow in the machine. As with any transformer, the flux in the core of an induction motor can be found from Faraday's law of sinusoidal operation as

$$\Phi = \frac{V_m}{\omega N} \cos \omega t$$

If the electrical frequency ω is reduced by a factor α, then the flux in the core will increase by a factor $1/\alpha$, and the magnetization current of the motor will increase.

In the unsaturated region of the motor's magnetization curve, the increase in magnetization current will also be about $1/\alpha$. In the saturated region of the motor's magnetization curve, however, an increase in flux $1/\alpha$ requires a much larger increase in the magnetization current. Induction motors are normally designed to operate near the saturation point on their magnetization curves, so the increase in flux due to a decrease in frequency will cause excessive magnetization currents to flow in the motor. To avoid excessive magnetization currents, it is customary to decrease the applied stator voltage in direct proportion to the decrease in frequency whenever the frequency falls below the rated frequency of the motor.

When the voltage applied to an induction motor is varied linearly with frequency below the base speed, the flux in the motor will remain approximately constant. Therefore, the maximum motor torque remains fairly high. However, the maximum power rating of the motor must be decreased linearly with the decrease in frequency to protect the stator circuit from overheating. The power supplied to a three-phase induction motor is

$$P = \sqrt{3} V_L I_L \cos \Phi$$

If the voltage V_L is decreased, then the maximum power P must also be decreased, or else the current flowing in the motor will increase, and the motor will overheat.

Figure 6.20 shows a family of induction-motor torque–speed characteristic curves for speeds below base speed, assuming that the magnitude of the stator voltage varies linearly with frequency.

When the electrical frequency applied to the motor exceeds the rated frequency of the motor, the stator voltage is held constant at the rated value. Although saturation considerations would permit the voltage to be raised above the rated value under these conditions, it is limited to the rated voltage to protect the winding insulation of the motor. With high electrical frequency above base speed, the resulting flux in the machine decreases and the maximum torque decreases with it. Figure 6.21 shows a family of induction-motor torque–speed characteristic curves for speeds above base speed, assuming that the stator voltage is held constant.

www.EngineeringEBooksPdf.com

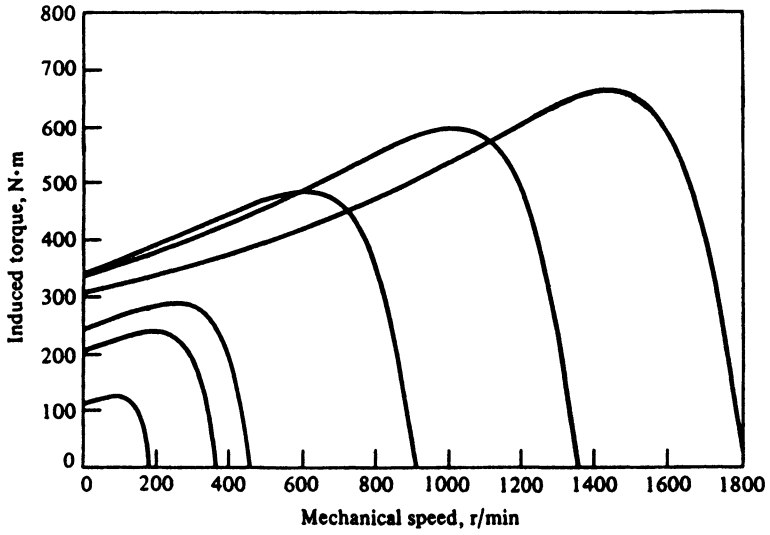


Figure 6.20 Family of torque–speed characteristic curves for speeds below base speed.

If the stator voltage is varied linearly with frequency below base speed and is held constant at rated value above base speed, then the resulting family of torque–speed characteristics is as shown in Fig. 6.22.

The principal disadvantage of electrical-frequency control as a method of speed changing was that it requires a dedicated generator, or mechanical frequency changer.

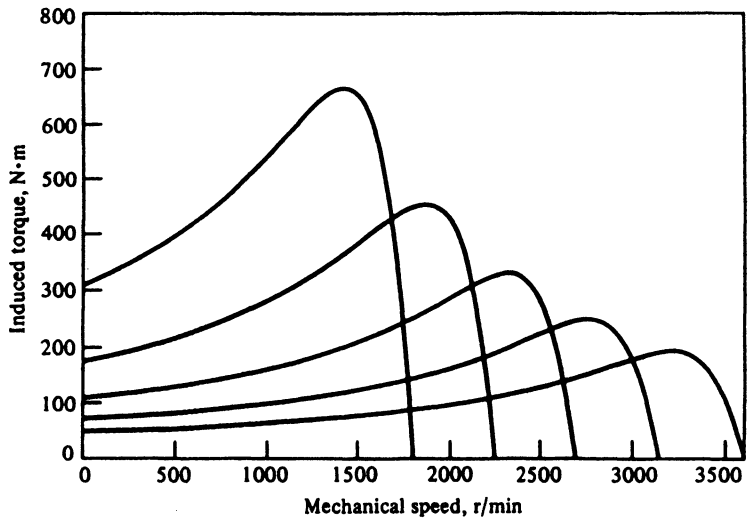


Figure 6.21 Family of torque–speed characteristic curves for speeds above base speed, holding the line voltage constant.

www.EngineeringEBooksPdf.com

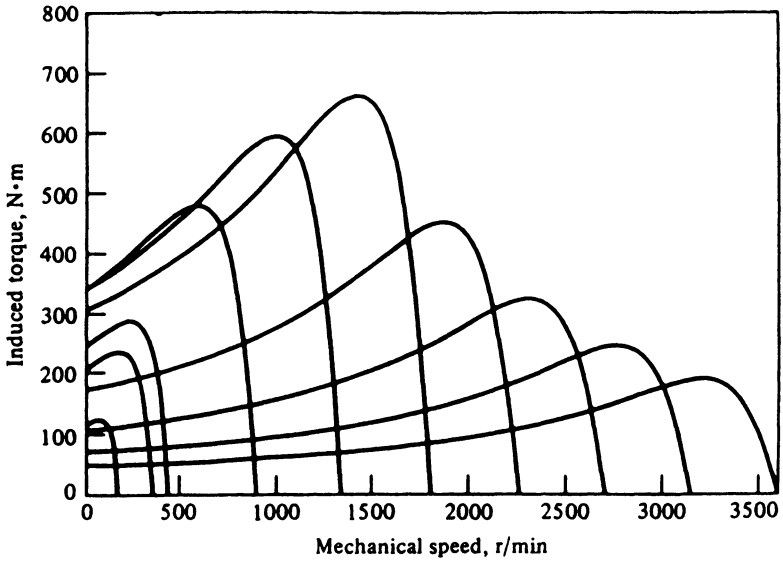


Figure 6.22 Torque–speed characteristic curves for all frequencies.

The development of modern solid-state variable-frequency motor drives has overcome this limitation, and it is now the method of choice for induction-motor speed control. Note that this method can be used with *any* induction motor, unlike the pole-changing technique, which requires a motor with special stator windings.

We now turn our attention to the second major category of speed-control techniques.

6.12.2 Changing Slip

Changing the slip is a major category that involves changing the torque–speed characteristics. Means for achieving this include:

(a) *Line-Voltage Control* The torque developed varies with the square of the applied voltage. As shown in Fig. 6.23, the speed can be varied simply by changing the voltage applied to the stator. This method is common for squirrel-cage motors.

(b) *Rotor-Resistance Control* This is suitable for the wound-rotor type and was discussed in detail in Section 6.9. The resulting torque–speed characteristics are shown in Fig. 6.24. The main drawback of this method is that efficiency is reduced at lower speeds. In practice, this method is used for applications with short periods of lower-speed operation.

(c) *Rotor-Slip Energy Recovery* The input power to the rotor is given by

$$P_{\text{in},r} = \frac{3I_r^2 R_2}{s}$$

www.EngineeringEBooksPdf.com

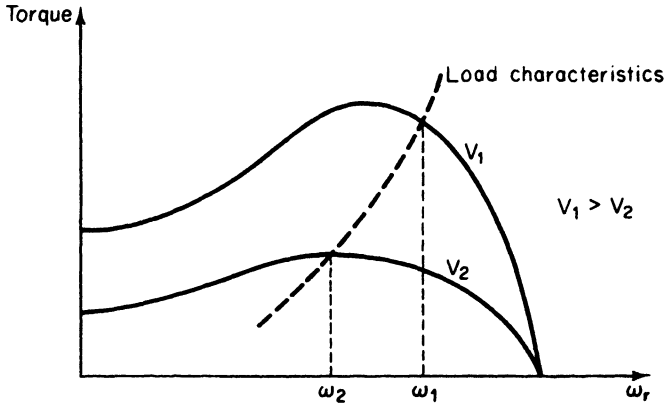


Figure 6.23 Effect of line voltage on speed of induction motor.

The rotor power output is given by

$$P_{\text{out},r} = 3I_r^2 R_2 \frac{1-s}{s}$$

As a result, the theoretical rotor efficiency is

$$\eta_r = 1 - s$$

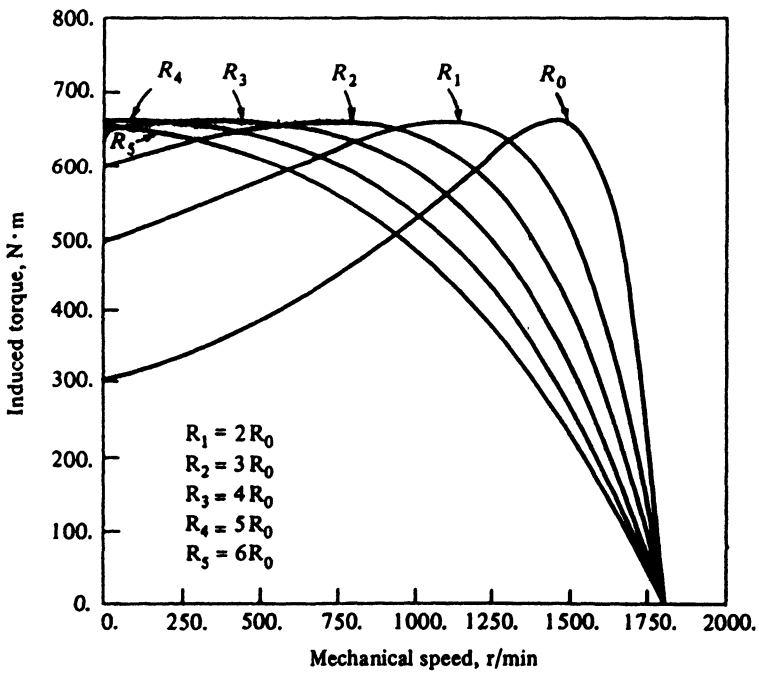


Figure 6.24 Speed control by varying the rotor resistance of a wound-rotor induction motor.

www.EngineeringEBooksPdf.com

It is thus clear that speed control by increasing s results in an increase in rotor I^2R losses, which results in decreased efficiency. There exist many methods for recovering this energy from the rotor (at rotor frequency $f_r = sf_s$), converting it to supply frequency, and subsequently returning it to the source. The devices used to achieve this are solid-state power devices, and are discussed later in this chapter.

6.13 ADJUSTABLE-SPEED DRIVES: GENERAL CONSIDERATIONS

In chapters 3 and 4 we discussed the foundations and operational principles of power semiconductor (power electronic) devices and systems. The following sections highlight the application of power semiconductor systems in static control of electric motors. The combination of a power electronic system such as a voltage controller and an electric motor with the associated control mechanisms is referred to as an *adjustable-speed drive.*

Adjustable-speed drives can be either of the ac or the dc type. In the ac type, the supply to an induction and/or a synchronous motor is controlled by an ac voltage controller, a cycloconverter, or an inverter to achieve the prescribed speed for the given load conditions. In the dc type a separately excited or series dc motor is controlled using a chopper or a rectifier circuit to achieve the desired speed characteristic. The choice of the power semiconductor driving system depends on the type of available power supply and load characteristic.

Techniques of adjustable-speed drives for an induction motor can be broadly classified into three main categories:

1. *Variable-Voltage Constant Frequency* This is also known as stator voltage control. In this technique the voltage applied to the stator is varied using ac voltage controllers while maintaining a constant frequency.
2. *Variable-Frequency Control* In this technique, the stator frequency is varied while varying either the applied voltage or current.
3. *Slip-Power Recovery* The equivalent rotor resistance can be varied electronically by use of a semiconductor power circuit connected to the rotor terminals to recover power at slip frequency and convert it to the supply line.

The variable-frequency category can be further classified into the classes of dc-link-conversion schemes and that of cycloconverters. The dc-link schemes involve rectification of the ac supply, which is followed by inversion to provide the required power drive. The inverters can be either voltage fed or current fed. In the former case, the controlled variable is the voltage applied to the stator along with the frequency. The current-fed inverter scheme provides control through the stator current and frequency. Voltage-fed inverters can be either square-wave inverters or PWM inverters. Figure 6.25 shows the classification of induction motor drive systems indicated earlier.

www.EngineeringEBooksPdf.com

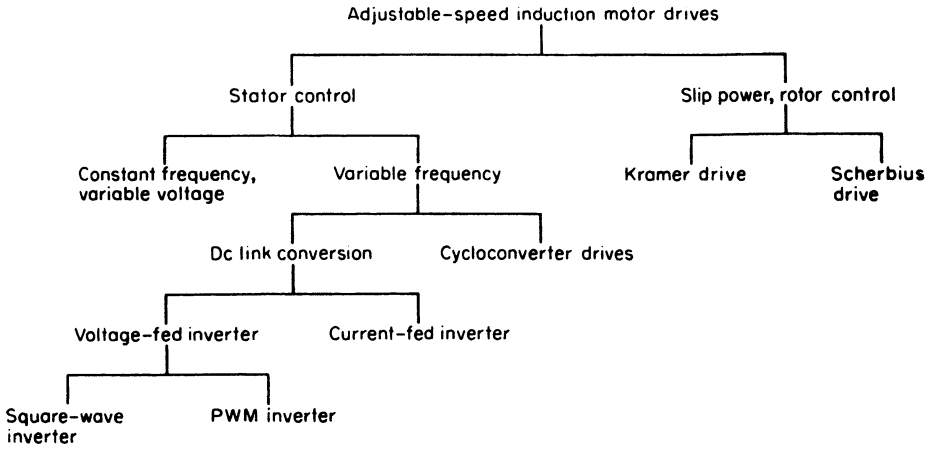


Figure 6.25 Classification of adjustable-speed induction-motor drives.

6.13.1 Three-Quadrant Operation

A three-phase induction machine operates normally in the motoring mode, where the developed torque and rotor speed are in the first quadrant of the T/ω diagram, as shown in Fig. 6.26. In this case, the developed torque is such that the rotor attempts to align itself with the rotating magnetic field set up by the three-phase supply in the three-phase stator windings. Operation in the second quadrant is commonly referred to as plugging, and in this case the motor has a direction of rotation opposite to that which would be produced by its own developed torque. In the fourth quadrant, commonly referred to as overhauling, the load tends to drive the motor in a positive direction to more than synchronous speed. Adjustable-speed drives are designed to recognize the possibility of operation in the plugging and overhauling modes.

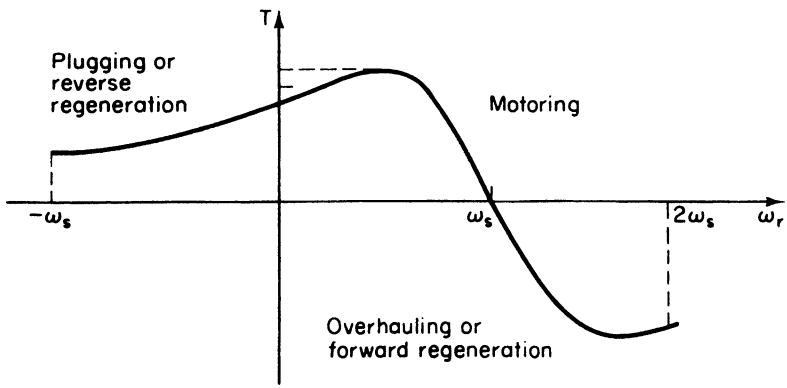


Figure 6.26 Complete torque–speed characteristics of an induction motor.

www.EngineeringEBooksPdf.com

It should be noted that plugging involves transfer of energy from the mechanical load to the rotor as well as electrical energy from the stator circuit. As a result, large motor currents can be expected, and these are accompanied by large ohmic losses that are dissipated as heat. When it is antizipated that, a motor will experience plugging conditions, it is preferable to use a wound-rotor induction motor with external resistances connected to the rotor circuit to dissipate the plugging energy.

Note that fourth-quadrant operation is simply reverse motoring. Common terminology refers to second-quadrant operation as reverse regeneration (plugging) and that in the fourth quadrant as forward regeneration (overhauling).

6.14 VARIABLE-VOLTAGE–CONSTANT-FREQUENCY DRIVES

In this method the voltages applied to the stator windings are controlled using an ac voltage controller while maintaining the frequency of the supply unchanged. The drive shown in Fig. 6.27 employs a three-phase Y-connected ac voltage controller. A typical application of this drive is at the low to medium power levels, such as pumps and blower-type loads. The same circuit is used as a solid-state starter for medium- to high-horsepower induction motors.

The stator voltage can be varied in this method between zero and full value within the trigger angle range $0 < \alpha < 120$ deg, and as a result a variac-like performance is obtained. This method is simple and economical for control of squirrel-cage class D induction motors with high slip (typically 10 to 15%). Performance of the drive is poor, since line currents carry rich harmonics and the drive has a poor power factor.

The torque output of a three-phase induction motor is given by

$$T = \frac{3|V_1|^2}{\omega_s} \frac{R_s/s}{(R_1 + R_2/s)^2 + X_T^2} \tag{6.86}$$

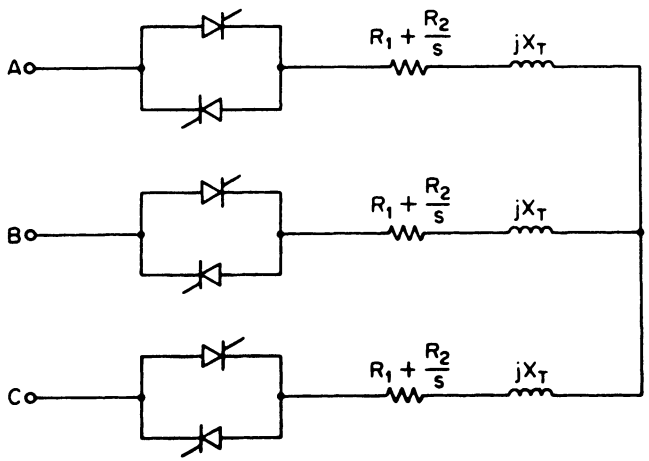


Figure 6.27 Induction-motor speed control with a three-phase ac voltage controller.

www.EngineeringEBooksPdf.com

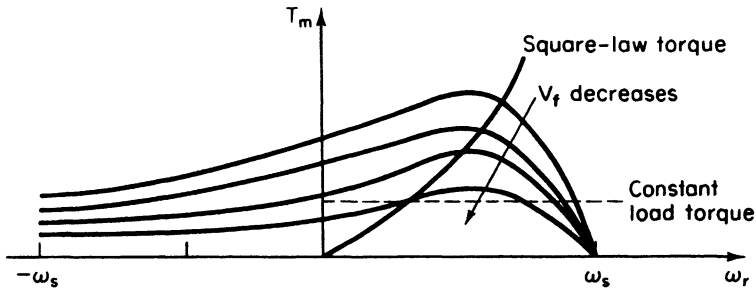


Figure 6.28 Torque–speed curves of induction motor with variable stator voltage.

It is therefore clear that the output torque varies with the square of the applied voltage at a fixed slip. Figure 6.28 shows the torque–speed characteristic of an induction motor with variable stator voltage.

To determine the speed of the motor with a given voltage value, we need the load torque–speed characteristic. Two important types of load characteristics are the constant torque load and the square-law torque typical of blowers and pumps, given by

$$T_l = k_l \omega_r^2 \tag{6.87}$$

where k_l is a constant, T_l is the load torque, and ω_r is the rotor angular speed. Recall that

$$\omega_r = \omega_s(1 - s)$$

We conclude that s, and hence ω_r, can be obtained as the solution of

$$\omega_s^2 k_l (1 - s)^2 = \frac{3|V_1|^2}{\omega_s} \frac{R_2/s}{(R_1 + R_2/s)^2 + X_T^2} \tag{6.88}$$

Figure 6.28 shows typical operating points for a three-phase induction motor with a square-law load torque. For a constant-torque load, Eq. (6.86) is solved for s simply by substituting the specified load torque, T_l, for the torque on the left-hand side.

The motor torque is related to the stator current I_s by Eq. (6.35), where the substitution $I_s \cong I_r$ is made, rewritten as

$$T = \frac{3|I_s|^2 R_2}{s\omega_s} \tag{6.89}$$

It is clear for a square-law load torque that we get

$$|I_s| = K_s \sqrt{s}(1 - s) \tag{6.90}$$

www.EngineeringEBooksPdf.com

where

$$K_s = \left(\frac{k_l \omega_s^3}{3R_2}\right)^{1/2} \tag{6.91}$$

The stator current is a maximum for $s = 0.333$, as can be verified from differentiating the expression for $|I_s|$ with respect to s and setting the result to zero. In this case, we have

$$|I_s|_{\max} = \frac{2}{3\sqrt{3}} K_s \tag{6.92}$$

The ratio of maximum stator current to its value at a given slip is therefore given by

$$\frac{|I_s|_{\max}}{|I_s|} = \frac{2}{3\sqrt{3s}(1-s)} \tag{6.93}$$

For a motor with 12% slip at full load, we find that the maximum value of stator current is only 26.3% higher than its rated value.

For a load with constant torque, we have, by Eq. (6.89),

$$|I_s| = K_c \sqrt{s} \tag{6.94}$$

where

$$K_c^2 = \frac{T_l \omega_s}{3R_2} \tag{6.95}$$

The maximum value of stator current occurs for $s = 1$ (i.e., at standstill). In this case

$$\frac{|I_s|_{\max}}{|I_s|} = \frac{1}{\sqrt{s}} \tag{6.96}$$

For a motor with 12% slip at full load, the maximum value of stator current is close to three times that at full load.

Example 6.11 A three-phase eight-pole 60-Hz induction motor has the following parameters:

$$R_2 = 0.12\ \Omega \qquad X_2 = 0.7\ \Omega$$

Neglect stator resistance and reactance, magnetizing circuit, and rotational losses.

(a) Find the slip of the motor when driving a load with characteristics as given by Eq. (6.87) with $k_l = 0.0136$, with applied phase voltages of 254 V and 200 V, respectively.

(b) Repeat part (a) for $k_l = 0.136$ and phase voltages of 300 V and 254 V.

www.EngineeringEBooksPdf.com

Solution Using Eqs. (6.88) and (6.91) and rearranging, we obtain a fourth-order equation in s given by

$$s^4 - 2s^3 + \left(1 + \frac{R_2^2}{X_2^2}\right)s^2 - \left(2\frac{R_2^2}{X_2^2} + \frac{|V_1|^2}{X_2^2 K_s^2}\right)s + \frac{R_2^2}{X_2^2} = 0$$

We have

$$R_2 = 0.12\ \Omega \qquad X_2 = 0.7\ \Omega$$

$$\omega_s = \frac{4\pi f}{P} = 30\pi \text{ rad/s}$$

$$\frac{1}{K_s^2} = \frac{3R_2}{k_l \omega_s^3} = \frac{3 \times 0.12}{k_l (30\pi)^3}$$

(a) For $k_l = 0.0136$, we obtain

$$s^4 - 2s^3 + 1.03s^2 - \left(0.0588 + \frac{|V_1|^2}{15.5 \times 10^3}\right)s + 0.0294 = 0$$

With $|V_1| = 254$ V, we solve to obtain

$$s = 6.97 \times 10^{-3}$$

With $|V_1| = 200$ V, we obtain

$$s = 1.12 \times 10^{-2}$$

Note that, as expected, a reduction in voltage results in reduced speed (increased slip).

(b) For $k_l = 0.136$, we obtain

$$s^4 - 2s^3 + 1.03s^2 - \left(0.0588 + \frac{|V_1|^2}{15.5 \times 10^4}\right)s + 0.0294 = 0$$

With $|V_1| = 300$ V, we obtain

$$s = 4.95 \times 10^{-2}$$

With $|V_1| = 254$ V, we obtain

$$s = 7.15 \times 10^{-2}$$

Note that this load results in slower speed with the same applied voltage as the load of part (a).

www.EngineeringEBooksPdf.com

6.15 VARIABLE-VOLTAGE–VARIABLE-FREQUENCY DRIVES

Improved performance of adjustable-speed drives is associated with a variable-frequency stator supply. The air-gap flux is directly proportional to the stator applied voltage and inversely proportional to the frequency. A reduction in the supply frequency to achieve speed control below rated synchronous speed will be associated with an increase in the air-gap flux if the applied voltage is maintained at rated value. To avoid saturation due to the increased flux, variable-frequency drives employ a variable voltage as well, with the object of maintaining an acceptable air-gap flux level. This concept is generally referred to as constant (V/f) control and is used in drives employing squirrel-cage induction motors of all classifications. We discuss the theory of variable-frequency operation of the induction motor.

6.15.1 Variable-Frequency Operation

Analysis of the operation of a three-phase induction motor with variable frequency requires replacing the fixed reactance X_T used earlier by a frequency-dependent term. Let us denote the frequency of the source voltages by f_i; then we have

$$X_T = \omega_i L_T \tag{6.97}$$

where L_T is the combined stator and rotor (referred) inductances, and

$$\omega_i = 2\pi f_i \tag{6.98}$$

Equation 6.18 is written as

$$n_s = \frac{120 f_i}{P} \tag{6.99}$$

As a result, the angular synchronous speed ω_s given by Eq. (6.34) can be written in the alternative form

$$\omega_s = \frac{2}{P}\omega_i \tag{6.100}$$

The torque output (neglecting rotational losses) is given by Eq. (6.38) as

$$T = \frac{3|V_1|^2}{\omega_s}\frac{R_2}{s}\frac{1}{(R_1 + R_2/s)^2 + X_T^2} \tag{6.101}$$

We can therefore conclude that an expression for the output torque that recognizes frequency variations is given by

$$T = \frac{3|V_1|^2 P R_2}{2\omega_i s[(R_1 + R_2/s)^2 + \omega_i^2 L_T^2]} \tag{6.102}$$

www.EngineeringEBooksPdf.com

The torque–speed characteristics of a three-phase induction motor with variable-frequency input can thus be developed on the basis of Eq. (6.102).

The starting (or standstill) torque is obtained by letting $s = 1$ in Eq. (6.102), to obtain

$$T_{st} = \frac{3|V_1|^2 PR_2}{2\omega_i s[(R_1 + R_2)^2 + \omega_i^2 L_T^2]} \tag{6.103}$$

Let us assume that the motor operation is such that the source-voltage-to-source-frequency ratio is maintained constant. We thus have

$$T_{st} = \frac{K_{st}\omega_i}{(R_1 + R_2)^2 + \omega_i^2 L_T^2} \tag{6.104}$$

where

$$K_{st} = \frac{3|V_1|^2 PR_2}{2\omega_i^2} \tag{6.105}$$

For large values of ω_i such that $(R_1 + R_2)^2$ is negligible in comparison with $(\omega_i L_T)^2$, we have

$$T_{st} \cong \frac{K_{st}}{\omega_i L_T^2} \qquad \text{for} \quad \omega_i \gg \frac{R_1 + R_2}{L_T} \tag{6.106}$$

In this case, the starting torque decreases as the input frequency is increased. For small values of ω_i such that $\omega_i^2 L_T^2$ is negligible in comparison with $(R_1 + R_2)^2$, we have

$$T_{st} \cong \frac{K_{st}\omega_i}{(R_1 + R_2)^2} \qquad \text{for} \quad \omega_i \ll \frac{R_1 + R_2}{L_T} \tag{6.107}$$

In this case, the starting torque increases as the input frequency is increased.

We can conclude from the preceding discussion that there is an input frequency $\omega_{i_{max}}^{T_{(st)}}$ for which the starting torque attains a maximum value. This condition is obtained by setting the derivative of T_{st} given by Eq. (6.104) with respect to ω_i to zero. The result is

$$[(R_1 + R_2)^2 + \omega_i^2 L_T^2] - 2\omega_i^2 L_T^2 = 0$$

We thus have

$$\omega_{i_{max}}^{T_{(st)}} = \frac{R_1 + R_2}{L_T} \tag{6.108}$$

www.EngineeringEBooksPdf.com

The value of maximum starting torque is therefore given by

$$T_{st_{max}} = \frac{K_{st}}{2(R_1 + R_2)L_T} \tag{6.109}$$

Equation (6.108) determines the lowest possible value of ω_i for proper operation.

The maximum (or breakdown) torque developed by the motor takes place at a slip defined by Eq. (6.41) as

$$s_{max_{T_m}} = \frac{R_2}{\sqrt{R_1^2 + \omega_i^2 L_T^2}} \tag{6.110}$$

The corresponding maximum torque is given by Eq. (6.42) as

$$T_{max_m} = \frac{3|V_1|^2 P}{4\omega_i(R_1 + \sqrt{R_1^2 + \omega_i^2 L_T^2})} \tag{6.111}$$

If the machine is operating with negative slip in the regenerative braking mode, then

$$s_{max_{T_g}} = \frac{-R_2}{\sqrt{R_1^2 + \omega_i^2 L_T^2}} \tag{6.112}$$

The corresponding maximum regenerative braking torque is given by

$$T_{max_g} = \frac{-3|V_1|^2 P}{4\omega_i(\sqrt{R_1^2 + \omega_i^2 L_T^2} - R_1)} \tag{6.113}$$

Note that if the stator resistance is negligible,

$$|T_{max_m}| = |T_{max_g}| \cong \frac{3|V_1|^2 P}{4\omega_i^2 L_T} \tag{6.114}$$

As a result, if the ratio V_1/ω_i is held constant, the breakdown torque developed by the motor will not change significantly with speed.

In Fig. 6.29, a family of torque–speed characteristics of a three-phase induction motor is shown. The angular speed, ω_{s_0}, corresponds to rated frequency operation. The speed at maximum torque for rated voltage and frequency, $\omega_{m_{T_r}}$, defines the division of the speed range into the constant-volts/Hz region to the left and the constant-voltage–variable-frequency region to the right. The envelope of the torque–speed characteristic is shown in the figure as constant up to $\omega_{m_{T_r}}$, and then follows the curve $T_{max} \alpha (1/\omega_r)$ in the higher-speed range. An example is appropriate now.

Example 6.12 A four-pole 60-Hz 440-V three-phase induction motor is supplied by a variable-voltage–variable-frequency source. The motor has negligible stator resistance and a rotor resistance of 0.1 Ω. The total inductance is 2×10^{-3} H.

www.EngineeringEBooksPdf.com

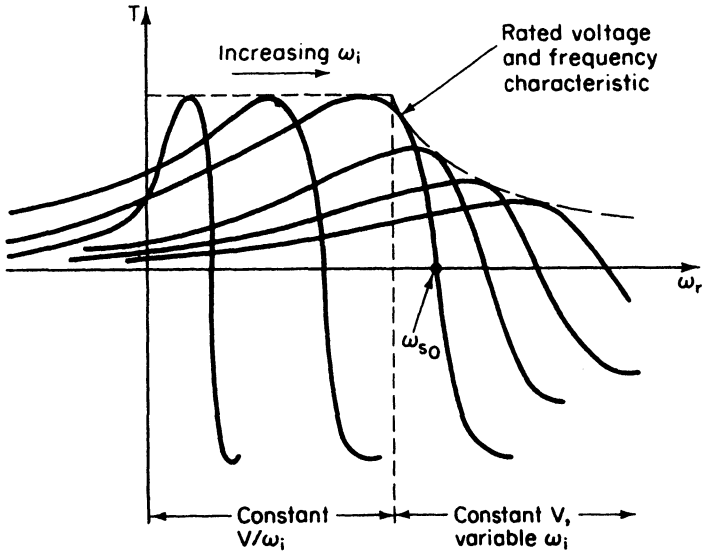


Figure 6.29 Torque–speed characteristics with variable-frequency conditions for an induction motor.

Find the lowest possible frequency and voltage of proper operation. Determine the starting torque, the speed at maximum torque, the maximum torque, and the stator's applied voltage when the supply frequency is 8 Hz, 40 Hz, and 60 Hz.

Solution The base voltage and frequency are clearly 440 V (line to line) and 60 Hz. From Eq. (6.108), we get

$$\omega_{i_{\max}}^{T_{st}} = \frac{0.1}{2 \times 10^{-3}} = 50 \text{ rad/s}$$

Thus the lowest possible frequency of operation is

$$f_{i_{\min}} = \frac{50}{2\pi} = 8 \text{ Hz}$$

The corresponding voltage is obtained by assuming the constant-volts/Hz operation as

$$V_{i_{\min}} = 8\left(\frac{440}{60}\right) = 58.67 \text{ V} \qquad \text{(line to line)}$$

We use Eq. (6.105), to obtain

$$K_{st} = \frac{3(440/\sqrt{3})^2(4)(0.1)}{2[2\pi(60)]^2} = 0.2724$$

www.EngineeringEBooksPdf.com

We then use Eq. (6.104) to obtain

$$T_{st} = \frac{0.2724(2\pi f_i)}{(0.1)^2 + (2\pi f_i)^2(2 \times 10^{-3})^2}$$

As a result,

$$T_{st} = \frac{1.7118 f_i}{0.01 + 1.58 \times 10^{-4} f_i^2}$$

From this relation we get the following starting torques:

$$f_i = 8 \text{ Hz} \qquad T_{st} = 681.1 \text{ N} \cdot \text{m}$$
$$f_i = 40 \text{ Hz} \qquad T_{st} = 260.7 \text{ N} \cdot \text{m}$$
$$f_i = 60 \text{ Hz} \qquad T_{st} = 177.55 \text{ N} \cdot \text{m}$$

The slip at maximum torque is given by

$$s_{\max T} = \frac{R_2}{\omega_i L_T} = \frac{25}{\pi f_i}$$

Recall that

$$\omega_{s_i} = \frac{4\pi f_i}{P}$$

Thus we obtain

$$\omega_{r_{\max T}} = \pi f_i - 25$$

As a result, the following angular speeds corresponding to maximum torque are obtained:

$$f_i = 8 \text{ Hz} \qquad \omega_{r_{\max T}} = 0$$
$$f_i = 40 \text{ Hz} \qquad \omega_{r_{\max T}} = 100.66 \text{ rad/s}$$
$$f_i = 60 \text{ Hz} \qquad \omega_{r_{\max T}} = 163.5 \text{ rad/s}$$

According to Eq. (6.114) the maximum torque remains invariant at

$$T_{\max} = \frac{3(440/\sqrt{3})^2(4)}{4(120\pi)^2(2 \times 10^{-3})} = 681.1 \text{ N} \cdot \text{m}$$

www.EngineeringEBooksPdf.com

The last result is the same as the maximum starting torque. The applied voltage is obtained from

$$V_i = f_i\left(\frac{440}{60}\right)$$

As a result, we obtain

$$f_i = 8 \text{ Hz} \qquad V_i = 58.67 \text{ V}$$
$$f_i = 40 \text{ Hz} \qquad V_i = 293.33 \text{ V}$$
$$f_i = 60 \text{ Hz} \qquad V_i = 440 \text{ V}$$

This concludes this example

6.16 dc-LINK-CONVERTER DRIVES

Adjustable-speed drives of ac motors requiring variable-voltage–variable-frequency from a fixed-voltage–fixed-frequency supply can be designed using an intermediate dc link. Here, ac power is converted to dc using a three-phase rectifier bridge. The dc output of the rectifier is fed through the dc link to a three-phase inverter connected to the motor's stator terminals to provide the required variable-frequency supply.

A number of dc-link-converter schemes are available, as indicated in Fig. 6.30. In schemes (a) and (b), three-phase diode rectifiers are employed. In scheme (a), fixed ac is fed to a transformer whose ratio is controlled as a function of the desired frequency output. The variable-voltage ac is then fed to the rectifier. The rectifier's variable-dc-voltage output is injected into the inverter. The inverter's output is of the required variable-voltage–variable-frequency form. Scheme (b) differs from that of (a) in that the output of the inverter is of variable frequency but fixed voltage. The desired variable-voltage feature is achieved by the use of an intermediate transformer between the inverter's output terminals and the motor's stator terminals. These two schemes are not truly static drives, as the variable transformers involve moving parts.

In scheme (c), a phase-controlled thyristor bridge rectifies the incoming ac voltage to variable dc voltage while maintaining the desired voltage-to-frequency ratio. No transformers are involved in this scheme. In scheme (d) the thyristor bridge rectifier of scheme (c) is replaced by a cascade of a diode rectifier bridge and a chopper to provide the variable dc input to the inverter.

In schemes (a) to (d) of Fig. 6.30, the inverter provides the required adjustable-frequency feature while adjusting the voltage level is done externally to the inverter. The voltage supply to the ac motor's stator terminals is a series of square voltage waves of adjustable voltage and frequency. A more attractive arrangement uses a PWM inverter, which provides both frequency and voltage control with the same

www.EngineeringEBooksPdf.com

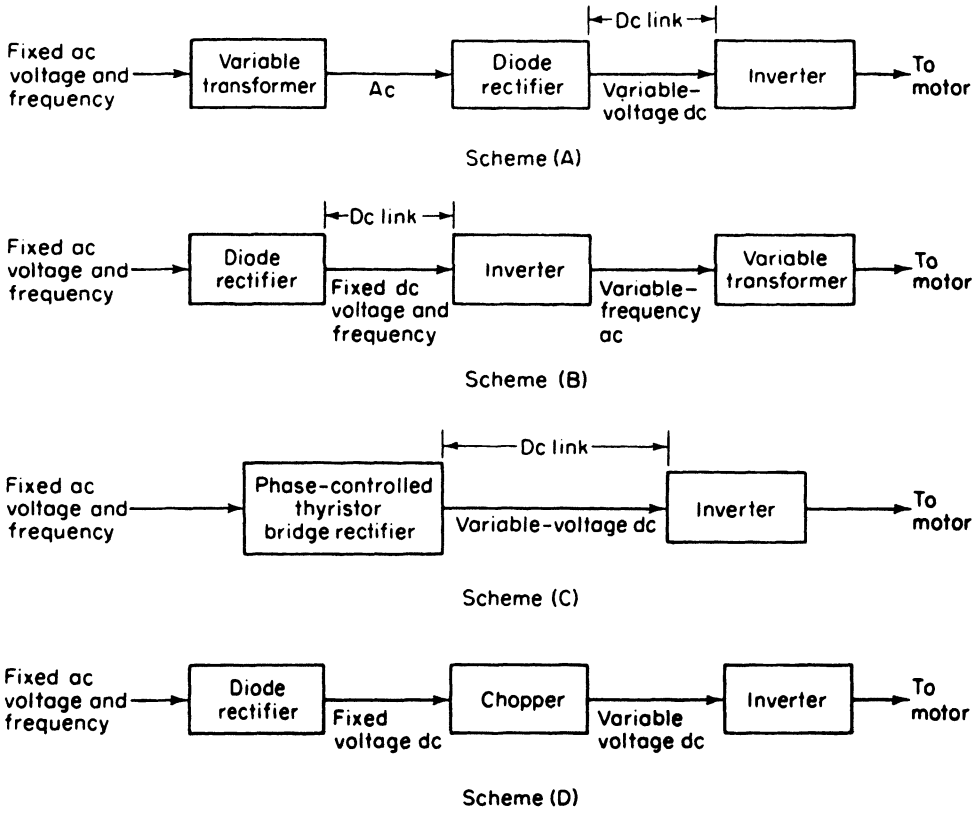


Figure 6.30 Square-wave dc-link-converter drives.

set of thyristors. The output of the PWM inverter is a series of adjustable-width pulses, which provides for an adjustable rms voltage supply. The dc supply to the inverter is furnished by a diode rectifier bridge, as shown in Fig. 6.31.

6.16.1 Voltage-Fed versus Current-Fed Inverters

In conventional dc-link-converter drive schemes, the inverter is fed with a dc voltage whose magnitude is independent of the load connected to the inverter terminals. In this case, the scheme is referred to as a voltage-fed inverter drive. A more recent development is the introduction of current-fed inverter drives where the current rather than the voltage is the independent variable. The major distinction between

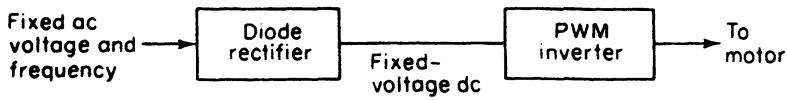


Figure 6.31 PWM-inverter dc-link-converter drive.

www.EngineeringEBooksPdf.com

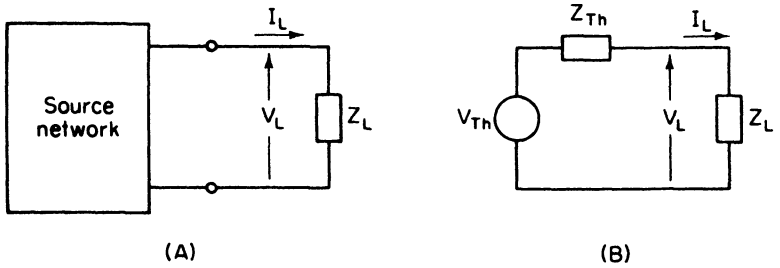


Figure 6.32 Thévenin's equivalents to distinguish between current-fed and voltage-fed inverters.

the two types lies in the Thévenin's impedance seen at the inverter terminals, as discussed next.

Consider an electric system made of a supply network connected to a load Z_L, as shown in Fig. 6.32(a). It is clear that the supply network can be reduced to the simple Thévenin's equivalent voltage source, V_{Th}, and an impedance, Z_{Th}, connected in series with the source, as shown in Fig. 6.32(b). It is clear that the load current I_L is given by

$$I_L = \frac{V_{Th}}{Z_{Th} + Z_L}$$

If Z_L is variable, such as is the case with an induction machine, then I_L will vary even though V_{Th} is fixed. If the Thévenin's impedance Z_{Th} is large enough, then I_L will remain relatively constant even though Z_L varies. The voltage applied to the load denoted by V_L is given by

$$V_L = \frac{V_{Th} Z_L}{Z_{Th} + Z_L}$$

If the Thévenin's impedance Z_{Th} is small relative to Z_L, the voltage applied to the load remains invariant even though the load impedance changes.

We therefore can conclude that if the Thévenin's impedance is relatively high, the source network appears as an independent current source to the load circuit. On the other hand, if the Thévenin's impedance is relatively low, the source network appears as an independent voltage source to the load circuit. The discussion involves impedances when the input variables to the inverter are referred to as dc, because the rectifier output is still time varying and harmonics (sinusoids) exist at the rectifier output.

6.17 VOLTAGE-FED INVERTER DRIVES

The theory of variable-voltage–variable-frequency speed control was discussed in Section 6.15. Motors used in this type are low-slip motors resulting in improved

www.EngineeringEBooksPdf.com

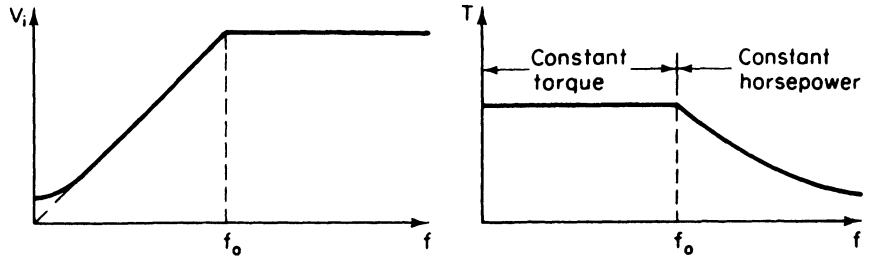


Figure 6.33 Desired voltage-frequency and torque-frequency relations for an induction motor.

efficiencies. The desired voltage-frequency and torque-frequency characteristics are shown in Fig. 6.33. In the subsynchronous region, the voltage/frequency ratio is constant, resulting in constant-torque output. For the frequency range above rated frequency, the voltage is maintained constant, resulting in constant-horsepower operation. It should be pointed out that at low frequency, the resistance effect dominates that of the leakage reactance, and additional voltage is impressed to compensate for this effect. Note that the *T-f* characteristic of Fig. 6.33 is the envelope of the torque–speed characteristics of Fig. 6.29.

As discussed earlier, there are two main classes of the voltage-fed inverter drives employing the dc-link-conversion idea. These are the square-wave inverter drives and the PWM inverter drives discussed now.

6.17.1 Square-Wave Inverter Drive

A typical arrangement of a voltage-fed square-wave inverter ac motor drive is shown in Fig. 6.34. This is essentially a detail of scheme (c) in Fig. 6.30. The inverter is called voltage fed since the capacitor *C* provides a low Thévenin's impedance to the inverter. The inverter voltage waves are not affected by the load.

Voltage-fed square-wave drives are employed in low- to medium-power applications with the speed ratio limited to 10 : 1. This type of drive has been replaced by PWM drives, which are discussed next.

6.17.2 PWM Inverter Drives

The controlled rectifier in Fig. 6.34 can be replaced by an uncontrolled diode rectifier, resulting in an uncontrolled dc-link voltage. At the same time, the inverter is controlled using a PWM strategy to provide for variable-frequency–variable-voltage output. Common practice calls for the use of sinusoidal PWM. PWM voltage control is applicable in the constant-torque region of Fig. 6.33, whereas in the constant-power region the inverter operation is identical to a square-wave drive.

An important advantage of PWM inverter drives is that a number of inverter drives can be supplied through a dc bus at the output of a single uncontrolled rectifier. The drive system can be made uninterruptible for possible ac line failure by switching in the standby battery in the dc link.

www.EngineeringEBooksPdf.com

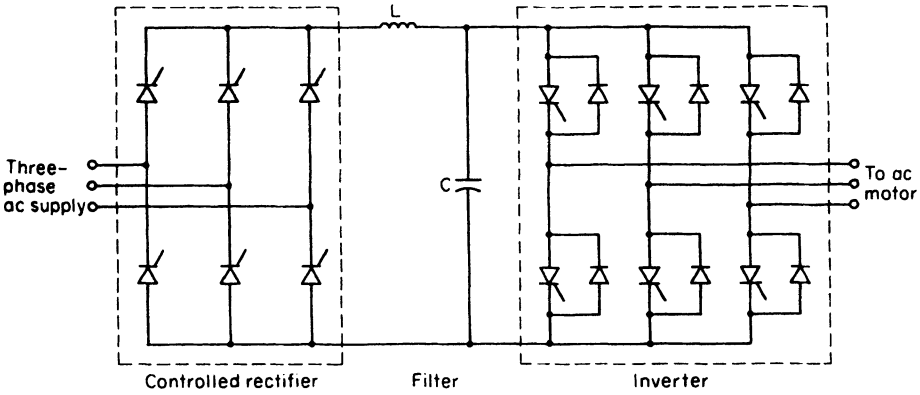


Figure 6.34 Voltage-fed square-wave inverter ac motor drive.

6.18 CURRENT-FED INVERTER DRIVES

The current-fed inverter ac motor drive shown in Fig. 6.35 consists of a controlled rectifier bridge, a dc-link filter inductor L, a three-phase inverter, and the controlled ac motor. It is thus clear that this drive is a dc-link-converter drive. The differences between a voltage-fed inverter drive and the current-fed inverter drive are that in the latter, the capacitor C of Fig. 6.34 is absent and the inductor is large enough so that the dc link presents a constant regulated dc current to the inverter. The inverter output current consists of six-stepped waves that present a stiff regulated current source with adjustable frequency to the ac motor terminals. This type of drive is used with individual motors in the medium- to high-horsepower range that have some minimum load present at all times.

The impedance of the motor is low at starting and at low speeds, so that with fixed stator current the terminal and air-gap voltages are relatively small, resulting in low air-gap flux. As the motor speed approaches synchronous speed, the impedance increases, and as a result the flux increases to saturation levels. Two torque–speed curves for the motor operating with fixed dc-link current corresponding to stator rated current and frequency are shown in Fig. 6.36. The dashed curve A corresponds to values computed neglecting saturation. This is characterized by a low starting torque and a high maximum torque occurring close to synchronous speed, with a steep decline to zero as the rotor's speed approaches synchronous speed. For

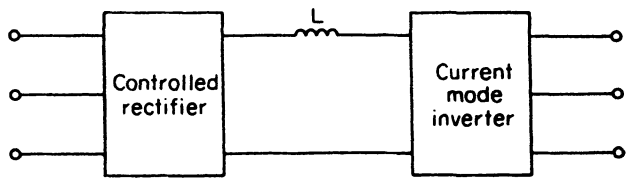


Figure 6.35 Variable-current–variable-frequency induction motor drive.

www.EngineeringEBooksPdf.com

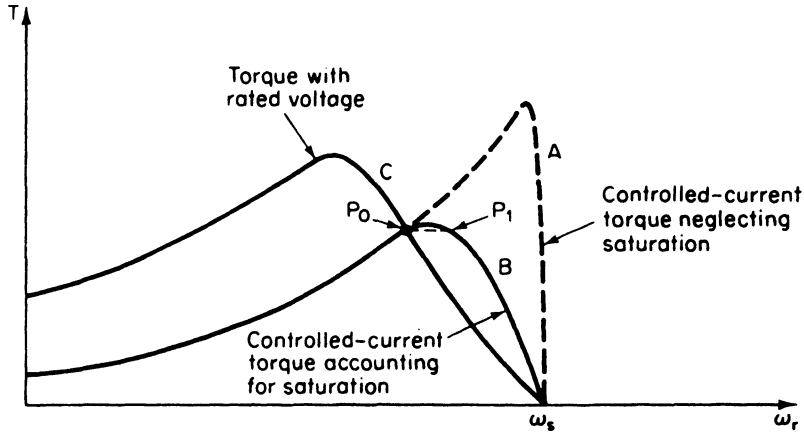


Figure 6.36 Torque–speed curves for voltage and current control.

comparison purposes, the torque–speed characteristic of the motor with controlled stator voltage and frequency at rated values marked *C* in the figure features a higher starting torque and a lower maximum torque.

It may be assumed that controlled-current operation provides greater torque than controlled voltage operation for low slip values. This is not true, since curve *A* is based on a fixed magnetizing reactance, and therefore neglects saturation. In the low speed range, the flux is below its rated value and the torque due to current control is lower than the corresponding torque obtained by rated voltage control. At point P_0, the intersection of curves *A* and *C*, the flux in the current-controlled case corresponds to its rated value. Beyond P_0, saturation effects should be accounted for, and the actual torque–speed characteristic with current control is obtained as the curve *B*, showing a lower maximum torque.

We observe that for the same output torque, the current-fed inverter drive can operate at one of two speeds corresponding to points P_0 and P_1 in Fig. 6.36. Operation at point P_0 is preferred, since at P_1, higher core losses exist. Closed-loop control to ensure that operation is at P_0 is necessary, since P_0 is on the unstable side of the characteristic.

6.19 CYCLOCONVERTER DRIVES

A cycloconverter is a direct frequency changer that converts ac power directly from one frequency level to another frequency level. No dc link is required for a cycloconverter. Normally, cycloconverters have an output frequency range of zero to one-third of the input frequency. A cycloconverter is capable of producing variable-voltage–variable-frequency output suitable for induction-motor drives using the principles of Section 6.15. Cycloconverter drives are used in large-horsepower applications, up to 20,000 hp. The system can provide reverse operation and regeneration.

www.EngineeringEBooksPdf.com

6.20 REGULATION OF SLIP POWER

We have seen that speed control can be achieved in a wound-rotor induction motor by inserting passive circuit elements such as external resistors (or capacitors) in the rotor circuit. Speed control using external resistors involves channeling a portion of the air-gap power at slip frequency into the resistors, where it is dissipated as heat. In this speed-control technology, efficiency is sacrificed to attain the required goal. The idea of regulating the slip power by inserting auxiliary, but active devices in the rotor circuit has been around for quite some time. The conventional Kramer and Scherbius drives employed rotating machines connected to the rotor circuit to channel portions of slip power back to the supply. With the introduction of the new power semiconductor-device and system technology, it became clear that these elegant speed-control schemes can be realized reliably and at considerably less cost and size than the old technology's implementation.

6.20.1 Static Kramer Drives

A conventional Kramer drive used auxiliary machines connected to the rotor circuit of a wound-rotor induction motor to convert a portion of the power of the rotor circuit from slip frequency to supply frequency, and then fed this power back to the mains. A static Kramer drive employs a diode rectifier connected to the rotor circuit

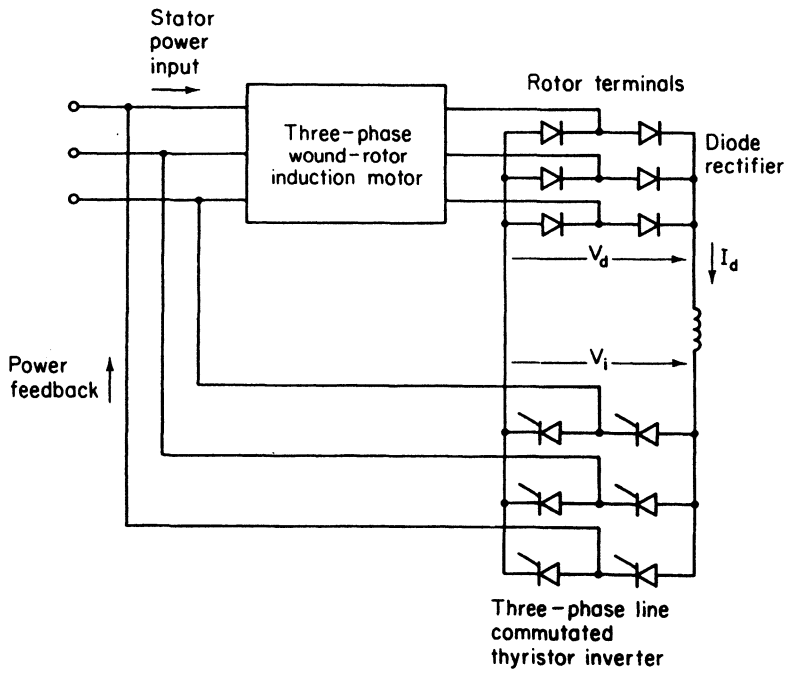


Figure 6.37 Static Kramer drive system.

www.EngineeringEBooksPdf.com

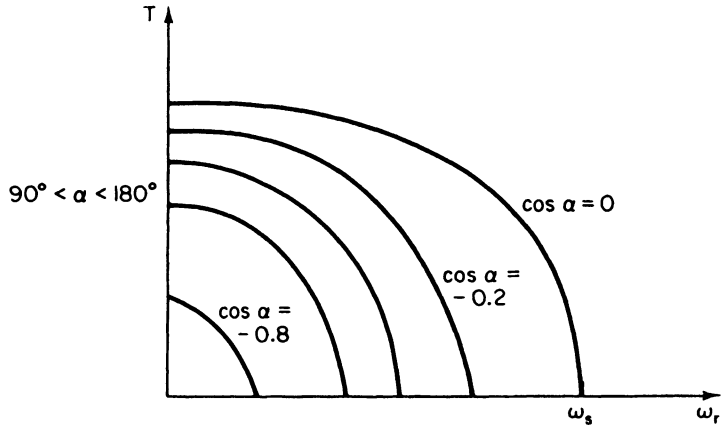


Figure 6.38 Torque–speed curves of a static Kramer drive system with different firing angles of inverter.

to convert a portion of slip frequency power to dc, which is then converted to ac at supply frequency using a line-commutated inverter, as shown in Fig. 6.37. Speed control is achieved through control of the angle of firing, α, of the inverter (90 deg $< \alpha <$ 180 deg).

The torque is proportional to the dc-link current under practical simplifying assumptions, and the torque–speed characteristics of the system for different values of α are shown in Fig. 6.38. Operating at synchronous speed corresponds to $\alpha =$ 90 deg, and the torque is zero at that point, with the result that both V_d and I_d are zero. Application of the load results in the motor slowing down, thus increasing the slip, and consequently increasing V_d and I_d until the motor's developed torque balances the load torque. For a constant-load torque, I_d is constant and the speed can be decreased by increasing $\cos\alpha$ such that V_d increases to match V_i.

The static Kramer drive system is used in large-horsepower pump and blower applications requiring a limited range of speed control in the subsynchronous (below ω_s) range.

6.20.2 Static Scherbius Drives

The static Kramer drive permits flow of slip power only from the rotor circuit to the supply lines, so operation is therefore restricted to speeds in the subsynchronous range. In the Scherbius drive, the diode rectifier is replaced by a thyristor bridge, allowing slip power to flow in either direction. The speed of the Scherbius drive can therefore be controlled in both the subsynchronous region and the supersynchronous region. In the latter case, power at slip frequency is injected in the rotor circuit. A line-commutated phase-controlled cycloconverter can be used in place of the dc-link converter in sophisticated static Scherbius drives.

www.EngineeringEBooksPdf.com

PROBLEMS

Problem 6.1 Determine the number of poles, the slip, and the frequency of the rotor currents at the rated load for three-phase induction motors rated at:

(a) 2200 V, 60 Hz, 588 rpm.
(b) 120 V, 600 Hz, 873 rpm.

Problem 6.2 The full-load speed of a 25-Hz induction motor is 720 rpm, while its no-load speed is 745 rpm. Find the slip at full load.

Problem 6.3 The full-load slip of a 60-Hz 10-pole induction motor is 0.075. Find the speed of the rotor relative to the rotating field and that of the rotating field relative to the stator.

Problem 6.4 The full-load slip of a four-pole 60-Hz induction motor is 0.05. Find the speed of the rotating field relative to the stator structure and the frequency of the rotor current.

Problem 6.5 The rotor-induced EMF per phase at standstill for a three-phase induction motor is 100 V rms. The rotor circuit resistance and leakage reactance per phase are 0.3 Ω and 1 Ω, respectively.

(a) Find the rotor current and power factor at standstill.
(b) Find the rotor current and power factor at a slip of 0.06. Compute the rotor-developed power.

Problem 6.6 A 15-hp 220-V three-phase 60-Hz six-pole Y-connected induction motor has the following parameters per phase:

$$R_1 = 0.128\ \Omega \qquad G_c = 5.4645 \times 10^{-3}$$
$$R_2 = 0.0935\ \Omega \qquad B_m = 0.125\ \text{S}$$
$$X_T = 0.496\ \Omega$$

The rotational losses are equal to the stator hysteresis and eddy-current losses. For a slip of 3%, find the following.

(a) The line current and power factor.
(b) The horsepower output.
(c) The starting torque.

Problem 6.7 A three-phase 100-hp 440-V four-pole, 60-Hz induction motor has a no-load input power of 3420 W and a no-load current of 45 A. The stator resistance is 0.06 Ω and that of the rotor is 0.08 Ω. The total reactance is 0.6 Ω. Find the line current, output torque, and horsepower for a motor speed of 1764 rpm.

www.EngineeringEBooksPdf.com

Problem 6.8 A 60-Hz four-pole 208-V three-phase induction motor has the following parameters:

$$R_1 = 0.3\ \Omega \qquad X_1 = 1\ \Omega$$
$$R_2 = 0.2\ \Omega \qquad X_2 = 1\ \Omega$$
$$G_c = 20 \times 10^{-3}\ \text{S} \qquad B_m = 60 \times 10^{-3}\ \text{S}$$

Find the speed and stator current for a slip of 2%. For a load slip of 5%, find the motor power factor and output power. Use the approximate equivalent circuit.

Problem 6.9 The horsepower output of a three-phase induction motor is 100 hp at a speed of 1732 rpm. The motor has four poles and operates on a 60-Hz supply. The friction loss is 900 W and the iron loss is 4200 W. Find the power input to the motor assuming stator ohmic loss to be 2700 W.

Problem 6.10 The efficiency of a three-phase induction motor at a full load of 15 hp is 0.89. The corresponding power factor is 0.9 for operation on 440-V supply. Neglect stator impedance and the exciting circuit. Find the slip at full load and the starting current.

Problem 6.11 The rotor resistance and reactance of a four-pole 230-V 60-Hz three-phase induction motor are 0.15 Ω and 0.5 Ω, respectively. Find the output power and torque for a slip of 5%.

Problem 6.12 The no-load input to a three-phase induction motor is 10,100 W and the current is 15.3 A for a stator voltage of 2000 V. Friction loss is estimated at 2000 W and the stator resistance is 0.22 Ω. From a blocked rotor test with 440 V, the input power is 36.4 kW and the current is 170 A. Find the parameters of the equivalent circuit.

Problem 6.13 The no-load power input to a three-phase induction motor is 2300 W and the current is 21.3 A at a rated voltage of 440 V. On full load, the motor takes 35 kW and 51 A at a speed of 1152 rpm. Assume that stator resistance is 0.125 Ω and that the motor has six poles and operates on a 60-Hz supply. Assume that stator core losses are equal to rotational losses. Find (a) the power factor, and (b) the motor efficiency at full load.

Problem 6.14 The rotor resistance and reactance of a squirrel-cage induction motor at standstill are 0.1 Ω per phase and 0.8 Ω per phase, respectively. Assuming a transformer ratio of unity, from the eight-pole stator having a phase voltage of 120 V at 60 Hz to the rotor secondary, calculate the following.

(a) Rotor starting current per phase.
(b) The value of slip-producing maximum torque.

Problem 6.15 A three-phase 50-Hz four-pole induction motor has a blocked rotor reactance that is four times the rotor resistance per phase. Find the speed at maximum torque.

www.EngineeringEBooksPdf.com

Problem 6.16 A 15-hp 440-V three-phase induction motor has a starting current of 132 A using rated voltage. Find the required starting voltage if the starting current is limited to 60 A.

Problem 6.17 An induction motor develops a starting torque of 80 N·m when 50% of the rated voltage is applied. Determine the starting torque when 65% of the rated voltage is applied.

Problem 6.18 The full-load slip of a squirrel-cage induction motor is 0.05, and the starting current is five times the full-load current. Neglecting the stator core and copper losses as well as the rotational losses, obtain:

(a) The ratio of starting torque to the full-load torque.
(b) The ratio of maximum to full-load torque and the corresponding slip.

Problem 6.19 A three-phase six-pole 60-hz induction motor develops a torque of 144 N·m at a speed of 1000 rpm. Assume that the rotor resistance is 0.2 Ω. Neglect stator impedance and the exciting circuit. Given that the maximum torque is 180 N·m, find the slip at maximum torque and the applied voltage.

Problem 6.20 The following data pertain to a 500-hp three-phase 2200-V 25-Hz 12-pole wound-rotor induction motor:

$$R_1 = 0.225\ \Omega \qquad R_2 = 0.235\ \Omega$$
$$X_T = 1.43\ \Omega \qquad G_c = 1.2821 \times 10^{-3}$$
$$B_m = 31.447 \times 10^{-3}\ \text{S}$$

(a) Find the no-load line current and input power with rated applied voltage. Assume that rotational losses are equal to the iron losses.
(b) Find the applied voltage and input power for a blocked rotor condition such that the line current is 228 A.
(c) Find the maximum torque and the corresponding slip, line current, and power factor.
(d) Find the required additional rotor resistance so that maximum torque is developed at starting, and hence find the value of the maximum torque.

Problem 6.21 The slip at maximum torque for an induction motor is 0.18. Find the power factor of the motor under these conditions, neglecting stator impedance. Suppose that it is desired to obtain maximum torque at a slip of 0.26. Find the ratio of the required additional rotor resistance to the original rotor resistance.

Problem 6.22 A three-phase induction motor has the following parameters:

$$R_1 = 0.09\,\Omega \qquad X_1 = 0.12\,\Omega$$
$$R_2 = 0.033\,\Omega \qquad X_2 = 0.11\,\Omega$$

www.EngineeringEBooksPdf.com

Find the slip at maximum torque. If it is desired to have maximum torque developed at standstill, find the required rotor resistance.

Problem 6.23 The rotor resistance is 4 Ω and the total reactance is 10 Ω for a four-pole 60-Hz induction motor. Find the applied stator voltage if the starting torque is 95 N·m. Find the starting torque if the rotor resistance is increased to 6 Ω.

Problem 6.24 The ratio of starting torque to full-load torque of a three-phase induction motor is 0.3, while the ratio of starting current to full-load current is 2.5. Find the slip at full load, neglecting stator impedance and exciting circuit.

Problem 6.25 The rotor resistance and reactance of a wound-rotor induction motor at standstill are 0.12 Ω and 0.7 Ω per phase, respectively. Assuming a transformer ratio of unity, from the eight-pole stator having a phase voltage of 254 V at 60 Hz to the rotor secondary, find the additional rotor resistance required to produce maximum torque at:

(a) Starting $s = 1$.
(b) A speed of 450 rpm.

Problem 6.26 Find the required additional rotor resistance to limit starting current to 45 A for a three-phase 600-V induction motor. Assume that

$$R_T = 1.66\ \Omega \qquad X_T = 4.1\ \Omega$$

Neglect the no-load circuit.

Problem 6.27 The rotor ohmic losses at maximum torque are 6.25 times that at full load with 0.032 slip for a three-phase induction motor. Find the slip at maximum torque and the ratio of maximum to full-load torque.

Problem 6.28 The rotor ohmic losses at starting are 6.25 times that at full load with slip of 0.035 for a three-phase induction motor. Find the slip at maximum torque, and the ratio of starting to full-load torques.

Problem 6.29 For the motor of Problem 6.7, find the slip at maximum mechanical power and the value of the maximum horsepower. Compare the rated horsepower to the theoretical maximum.

Problem 6.30 Repeat Problem 6.29, neglecting stator resistance, and compare the results.

Problem 6.31 Find the maximum power and the slip at which it occurs for the motor of Problem 6.11.

Problem 6.32 The slip at maximum torque of an induction motor is 0.125. Find the slip for maximum power.

Problem 6.33 The slip for maximum power of an induction motor is 0.11, and the rotor impedance is 0.9 Ω. Find the rotor resistance and reactance. Neglect stator impedance.

www.EngineeringEBooksPdf.com

Problem 6.34 A three-phase 50-Hz four-pole induction motor has a blocked rotor reactance that is four times the rotor resistance per phase. Find the speed at maximum power. What would be the speed at maximum power if the rotor resistance were increased by 50%?

Problem 6.35 The ratio of starting to full-load current for an induction motor is 5. The full-load slip is 0.05. Find the slip at maximum power.

Problem 6.36 A four-pole 60-Hz three-phase induction motor has a maximum power of 220 hp and a maximum torque of 1140 N·m. Find the rotor parameters, neglecting stator impedance and exciting circuit.

Problem 6.37 The maximum mechanical power output of a three-phase induction motor is 33 kW when operating on a 220-V 60-Hz supply. With 200 V and 50 Hz, the maximum mechanical power output is 31.54 kW. Find the rotor resistance and the reactance at 50 Hz and 60 Hz. Neglect stator impedance.

Problem 6.38 A 230-V three-phase four-pole 60-Hz double-cage motor has the following parameters:

Upper case: $R_u = 2.2\ \Omega$, $X_u = 0.8\ \Omega$
Lower case: $R_l = 0.24\ \Omega$, $X_l = 4.2\ \Omega$

Find the currents and torques at starting and a full-load slip at 0.04.

Problem 6.39 The lower cage resistance is 0.22 Ω and the upper cage reactance at 60 Hz is 1 Ω for a double-cage motor. The ratio of current in the upper cage to that in the lower cage is 2 and the corresponding torque ratio is 25. Find the resistance of the upper cage and reactance of the lower cage.

Problem 6.40 The ratio of torque developed by the upper cage to that developed by the lower cage at a slip of 0.04 is 0.24. The corresponding current ratio is 0.2. Assume that the lower cage impedance is given by

$$Z_l = 0.24 + j4$$

Find the impedance of the upper cage.

Problem 6.41 The resistance of the upper and lower cages of a double-cage motor are 1.44 Ω and 0.24 Ω, respectively. The ratio of upper cage torque to lower cage torque is 0.24 at a slip of 0.04, while this ratio is 0.21 at a slip of 0.03. Find the reactances of the upper and lower cages.

Problem 6.42 Find the slip at which the upper cage torque is 0.22 times that of the lower cage for the motor of Problem 6.41.

Problem 6.43 A three-phase 60-Hz eight-pole induction motor drives a load with torque–speed characteristic given by

$$T = 0.11\omega^2$$

www.EngineeringEBooksPdf.com

where ω is in rad/s and T is in N·m. The stator applied voltage is 440 V (line to line). The rotor resistance is 0.1 Ω and its reactance is 0.8 Ω. Neglect stator impedance and the magnetizing circuit. Find the rotor slip, output torque, output power, and stator current.

Problem 6.44 Repeat Problem 6.43 if the stator applied voltage is reduced to 330 V (line to line).

Problem 6.45 A three-phase four-pole 60-Hz squirrel-cage induction motor drives a load with the torque–speed characteristic given by

$$T_l = 7.2 \times 10^{-3}\omega^2$$

The motor parameters are

$$R_1 = 0.06\ \Omega \qquad R_2 = 0.08\ \Omega \qquad X_T = 0.6\ \Omega$$

(a) Obtain a formula that enables us to find the motor's slip for a given stator voltage in terms of motor and load parameters.

(b) Find the rotor slip, current, torque, and output horsepower for a line-to-line voltage of 440 V.

(c) Repeat part (b) for a line-to-line voltage of 330 V.

(d) Repeat part (c) for a line-to-line voltage of 220 V.

Problem 6.46 Assume that the motor of Problem 6.45 drives a load with the torque–speed characteristic

$$T_l = 36 \times 10^{-3}\omega^2$$

where ω is in rad/s. The supply voltage is 440 V. Find the rotor slip, speed, stator current, output torque, and power. Find the input power and losses, and comment on the results in relation to values obtained in Problem 6.45.

Problem 6.47 Repeat Problem 6.46 with the supply voltage decreased to 330 V.

Problem 6.48 A four-pole 60-Hz three-phase induction motor has a rotor resistance of 0.1 Ω. The motor drives a load with a torque–speed characteristic given by

$$T_l = 12 \times 10^{-3}\omega^2$$

where ω is in rad/s.

(a) If the motor runs at a slip of 3%, find the stator current and the developed torque.

(b) If the stator current is 100 A, find the slip and the developed torque.

www.EngineeringEBooksPdf.com

Problem 6.49 A four-pole 60-Hz three-phase induction motor drives a load with the torque–speed characteristic given by

$$T_l = 8 \times 10^{-3}\omega^2$$

(a) If the torque is 260 N·m, find the motor's slip and rotor resistance given that the stator current is 80 A.

(b) If the slip is 0.05, find the output torque and the armature current.

Problem 6.50 A four-pole 60-Hz three-phase induction motor runs at a slip of 8% and draws a stator current of 130 A when driving a square-law load. Assume that the rotor resistance is 0.08 Ω. Find the parameter k_l of the load's torque–speed characteristic. Find the motor's speed, slip, and stator current for a torque output of 280 N·m.

Problem 6.51 An eight-pole 60-Hz 440-V three-phase induction motor has a negligible stator resistance and a rotor resistance of 0.12 Ω and a total leakage inductance of 2.2×10^{-3} H. The motor's supply is of the constant-volts/Hz category. Find the minimum supply frequency and the corresponding voltage. Find the maximum torque corresponding to constant-volts/Hz operation. Find the supply voltage and rotor speed corresponding to operation at 50 Hz.

Problem 6.52 Repeat Problem 6.51 for $P = 6$, $R_2 = 0.08\ \Omega$, and $L_T = 2 \times 10^{-3}$ H. All other information is unchanged.

Problem 6.53 A three-phase induction motor has a rotor resistance of 0.1 Ω. The minimum frequency for operation in the constant-volts/Hz region is 10 Hz. Find the total leakage inductance of the motor.

Problem 6.54 An eight-pole 440-V 60-Hz three-phase induction motor is controlled so that its maximum torque is 1200 N·m under rated conditions. Find the leakage inductance of the motor's equivalent circuit. Find the rotor resistance if the minimum frequency for proper operation in the constant-volts/Hz region is 9 Hz.

Problem 6.55 A three-phase four-pole induction motor has the parameters

$$R_2 = 0.1\ \Omega \qquad L_T = 1.8 \times 10^{-3}\ \text{H}$$

Neglect stator resistance. The motor's supply provides a constant-volts/Hz input to the stator with a line-to-line voltage of 220 V. When driving a load with $k_l = 6.5 \times 10^{-3}$, the speed is 1600 rpm. Find the input frequency and rotor slip, assuming that the output torque is the maximum for the frequency chosen.

Problem 6.56 A three-phase eight-pole induction motor has the following parameters

$$R_2 = 0.09\ \Omega \qquad L_T = 1.7 \times 10^{-3}\ \text{H}$$

Neglect stator resistance. The line-to-line voltage is 220 V in a constant-volts/Hz supply. The load has a $k_l = 5 \times 10^{-3}$ and is driven at a speed of 1400 rpm. Find the input frequency and rotor slip assuming that the output torque is the maximum for the frequency chosen.

www.EngineeringEBooksPdf.com

CHAPTER 7

SYNCHRONOUS MACHINES

7.1 INTRODUCTION

Almost every daily function of today's civilization depends on electric power produced by electric utility systems. The backbone of a utility system consists of a number of generating stations that are interconnected in a grid and operate in parallel. The largest single-unit electric machine for electric-energy production is the synchronous machine. Generators with power ratings of several hundred to over a thousand megavoltamperes (MVA) are fairly common in many utility systems. A synchronous machine provides a reliable and efficient means for energy conversion.

The operation of a synchronous generator is, like all other electromechanical energy conversion devices, based on Faraday's law of electromagnetic induction. The term *synchronous* refers to the fact that this type of machine operates at a speed proportional to the system frequency under normal conditions. Synchronous machines are capable of operating as motors, in which case the electric energy supplied at the armature terminals of the unit is converted into mechanical form. Another important function of this versatile machine is as a synchronous condenser where the unit is operated as a motor running without mechanical load and supplying reactive power in much the same manner as a capacitor.

In rotating machinery the term *armature* refers to the machine part in which an alternating voltage is generated as a result of relative motion with respect to a magnetic flux field. In a synchronous machine, the armature winding is on the stator and the field winding is on the rotor, as shown in Fig. 7.1. The field is excited by direct current that is conducted through carbon brushes bearing on slip (or collector) rings. The dc source is called the exciter and is mounted on the same shaft as the synchronous machine. Various excitation systems with ac exciters and solid-state rectifiers

www.EngineeringEBooksPdf.com

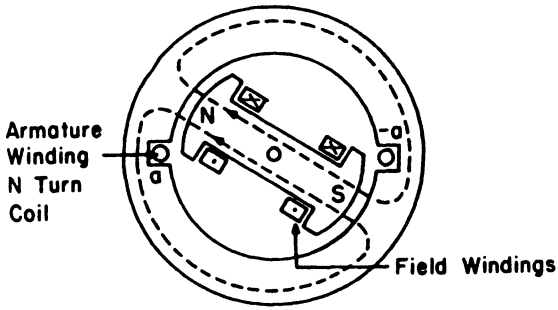


Figure 7.1 Simplified sketch of a synchronous machine.

are used with large turbine generators. The main advantages of these systems include the elimination of the cooling and maintenance problems associated with slip rings, commutators, and brushes. The pole faces are shaped such that the radial distribution of the air-gap flux density B is approximately sinusoidal.

The armature winding includes many coils. One coil is shown in Fig. 7.1 and has two coil sides (a and $-a$) placed in diametrically opposite slots on the inner periphery of the stator with conductors parallel to the shaft of the machine. The rotor is turned at a constant speed by a mechanical power source connected to its shaft. As a result, the flux waveform sweeps by coil sides a and $-a$. The induced voltage in the coil is a sinusoidal time function. It is evident that for each revolution of the two poles, the coil voltage passes through a complete cycle of values. The frequency of the voltage in cycles per second (hertz) is the same as the rotor speed in revolutions per second (rps). Thus a two-pole synchronous machine must revolve at 3600 rpm to produce a 60-Hz voltage, common in North America. In systems requiring 50-Hz voltage, the two-pole machine runs at 3000 rpm.

7.1.1 *P*-Pole Machines

Many synchronous machines have more than two poles. A P-pole machine satisfies the following relation derived in Chapter 2 and used repeatedly in Chapter 6:

$$f = \frac{Pn}{120} \tag{7.1}$$

The frequency f is proportional to the speed n in rpm. Note that P is the number of poles of the machine.

In treating P-pole synchronous machines, it is more convenient to express angles in electrical degrees rather than in the more familiar mechanical units. Here, we conceptually concentrate on a single pair of poles and recognize that the conditions associated with any other pair are simple repetitions of those of the pair under consideration. As discussed in Chapter 2, we have

$$\theta_e = \frac{P}{2}\theta_m \tag{7.2}$$

where θ_e and θ_m denote angles in electrical and mechanical degrees, respectively.

www.EngineeringEBooksPdf.com

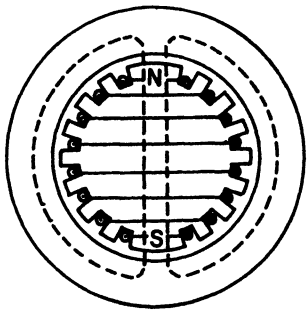


Figure 7.2 Cylindrical-rotor two-pole machine.

7.1.2 Cylindrical versus Salient-Pole Construction

Machines like the ones illustrated in Fig. 7.1 have rotors with salient poles There is another type of rotor, which is shown in Fig. 7.2. The machine with such a rotor is called a *cylindrical rotor* or *nonsalient-pole machine*. The choice between the two designs (salient or nonsalient) for a specific application depends on the proposed prime mover. For hydroelectric generation, a salient-pole construction is employed. This is because hydraulic turbines run at relatively low speeds, and in this case, a large number of poles are required to produce the desired frequency, as indicated by Eq. (7.1). On the other hand, steam and gas turbines perform better at relatively high speeds, and two- or four-pole cylindrical rotor turboalternators are used in this case. This avoids the use of protruding parts on the rotor, which at high speeds give rise to dangerous mechanical stresses.

7.1.3 Three-Phase Machines

With very few exceptions, synchronous generators (commonly referred to as alternators) are three-phase machines. For the production of a set of three voltages, phase displaced by 120 electrical degrees in time, it follows that a minimum of three coils phase displaced 120 electrical degrees in space must be used. An elementary three-phase two-pole machine with one coil per phase is shown in Fig. 7.3.

For clarity of presentation, we represent each coil as a separate generator. An immediate extension of single-phase circuits would be to carry the power from the three generators along six wires. However, for the sake of economy, instead of having a return wire from each load to each generator, a single wire is used for the return of all three. The current in the return wire will be $I_a+I_b+I_c$; and for a balanced load, these will cancel out, as may be seen by inspecting the phasor diagram in Fig. 7.4. If the load is unbalanced, the return current will still be small compared to either I_a, I_b, or I_c. Thus the return wire could be made smaller than the other three. This connection is known as a four-wire three-phase system. It is desirable for safety and system protection to have a connection from the electrical system to ground. A logical point for grounding is the generator neutral point, the junction of the Y.

www.EngineeringEBooksPdf.com

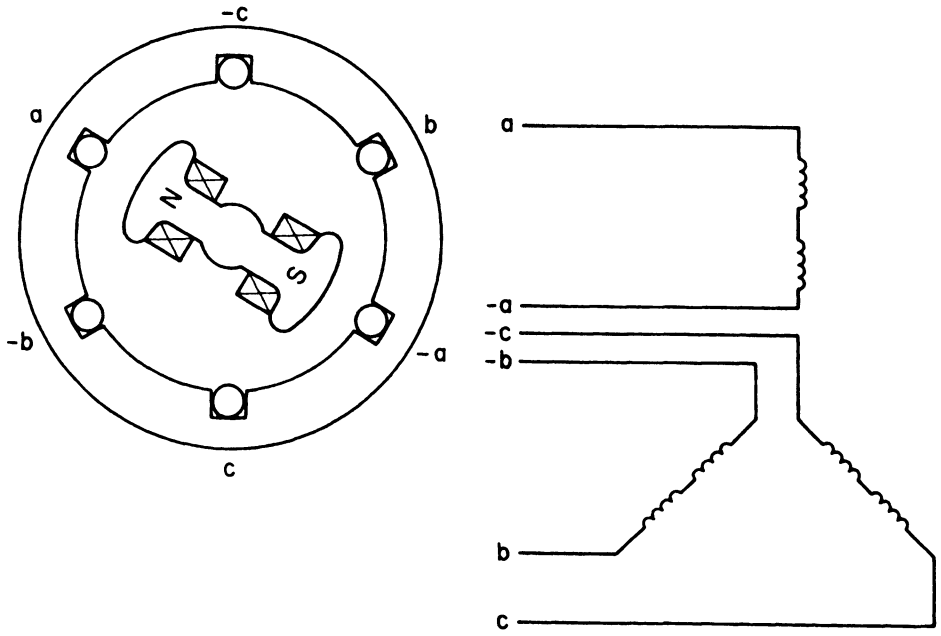


Figure 7.3 Elementary three-phase two-pole machine.

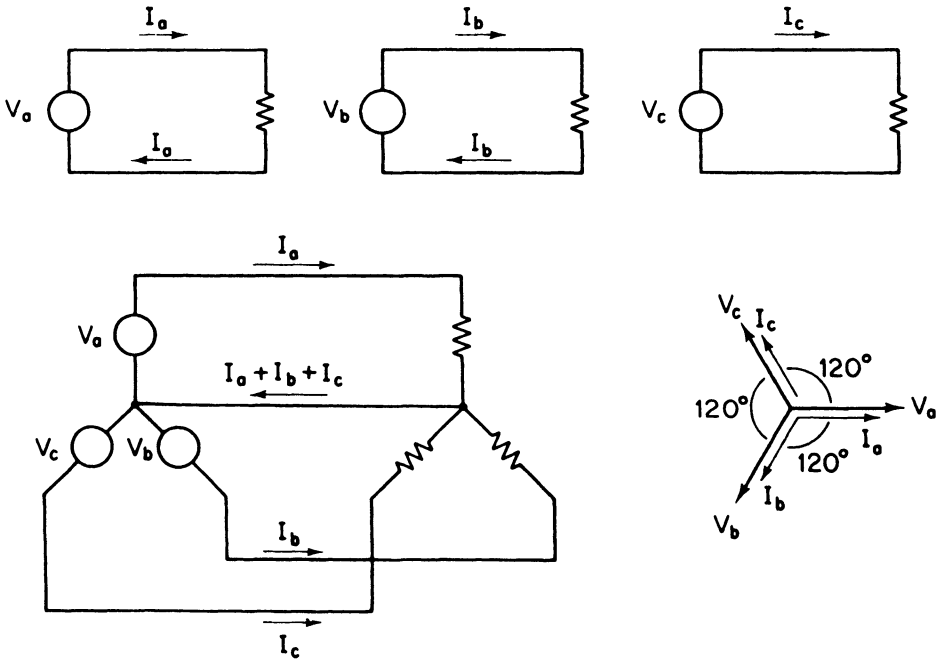


Figure 7.4 Three-phase system.

www.EngineeringEBooksPdf.com

7.2 ROUND-ROTOR MACHINES: EQUIVALENT CIRCUIT

Consider a three-phase synchronous machine with a round rotor operating in the steady state. The flux linkages, λ_a, for phase a windings are written as

$$\lambda_a = L_{aa} i_a + L_{ab} i_b + L_{ac} i_c + L_{af} I_f \tag{7.3}$$

The subscript f refers to the field windings, which are placed on the rotor and carry a direct current I_f. For the present modeling purposes, the inductances required for our equation are given by

$$L_{aa} = L_0 + L_1 \tag{7.4}$$

$$L_{ab} = L_{ac} = \frac{-L_0}{2} \tag{7.5}$$

$$L_{af} = M \cos\theta \tag{7.6}$$

The angle θ is that between the stator and rotor magnetic axes. The self-inductance L_{aa} is the sum of a component L_0 due to main air-gap flux and L_1 due to the armature leakage flux. The mutual inductances L_{ab} and L_{ac} are assumed to be due only to the main air-gap flux. The factor $-\frac{1}{2}$ is due to the 120-deg spatial displacement between phases ($\cos \pm 120 \text{ deg} = -\frac{1}{2}$). The mutual inductance between phase a and the field varies as $\cos\theta$, as discussed in Chapter 2.

Let us assume balanced three-phase operation, and hence

$$i_a + i_b + i_c = 0 \tag{7.7}$$

Combining Eq. (7.3) with Eq. (7.7), we get

$$\lambda_a = (L_1 + L_\phi) i_a + M I_f \cos\theta \tag{7.8}$$

where L_ϕ is given by

$$L_\phi = \frac{3}{2} L_0 \tag{7.9}$$

The rotor is assumed to be running at constant synchronous speed, and thus the angular displacement is

$$\theta(t) = \omega_s t + \theta_0 \tag{7.10}$$

As a result, the rate of change of the phase a flux linkages is given by

$$\frac{d\lambda_a}{dt} = (L_1 + L_\phi)\frac{di_a}{dt} + \omega_s M I_f \cos\left(\omega_s t + \theta_0 + \frac{\pi}{2}\right) \tag{7.11}$$

www.EngineeringEBooksPdf.com

The terminal voltage of phase a is therefore given by

$$v_t = R_a i_a + \frac{d\lambda_a}{dt} \tag{7.12}$$

The resistance of phase a is denoted by R_a. Equation (7.12) relates to the machine operating as a motor. For the machine operating as a generator, we have

$$\frac{d\lambda_a}{dt} = v_t + R_a i_a \tag{7.13}$$

In this case, we have

$$\lambda_a = -(L_l + L_\phi) i_a + M I_f \cos\theta \tag{7.14}$$

Let us define the field excitation voltage magnitude in effective (rms) value by

$$E_f = \frac{\omega_s M I_f}{\sqrt{2}} \tag{7.15}$$

We also define the synchronous inductance L_s by

$$L_s = L_l + L_\phi \tag{7.16}$$

As a result for the motor case, Eqs. (7.11) and (7.12) reduce to

$$v_t = R_a i_a + L_s \frac{di_a}{dt} + \sqrt{2} E_f \cos\left(\omega_s t + \theta_0 + \frac{\pi}{2}\right) \tag{7.17}$$

For the generator case, we find that Eqs. (7.13) and (7.14) reduce to

$$v_t = \sqrt{2} E_f \cos\left(\omega_s t + \theta_0 + \frac{\pi}{2}\right) - \left(R_a i_a + L_s \frac{di_a}{dt}\right) \tag{7.18}$$

Equations (7.17) and (7.18) provide the basis for equivalent circuits and phasor diagrams for the round-rotor synchronous machine operating in the steady state as either motor or generator.

Let the phase a current be a sinusoidal described by the steady-state expression

$$i_a(t) = \sqrt{2} I_a \cos\omega_s t \tag{7.19}$$

As a result, Eq. (7.17) for the motor case yields

$$v_t = \sqrt{2} I_a \left[R_a \cos\omega_s t + \omega_s L_s \cos\left(\omega_s t + \frac{\pi}{2}\right)\right] + \sqrt{2} E_f \cos\left(\omega_s t + \theta_0 + \frac{\pi}{2}\right) \tag{7.20}$$

www.EngineeringEBooksPdf.com

It is evident that v_t is sinusoidal as well. We can therefore write the following complex equivalent of Eq. (7.20) with I_a as reference:

$$\mathbf{V}_t = (R_a + jX_s)\mathbf{I}_a + \mathbf{E}_f \tag{7.20a}$$

The phasor $\mathbf{E}_f$ is given by the polar form

$$\mathbf{E}_f = E_f\left(\theta_0 + \frac{\pi}{2}\right) \text{ deg} \tag{7.21}$$

The reference current is

$$\mathbf{I}_a = I_a \angle 0 \text{ deg} \tag{7.22}$$

In Eq. (7.20), X_s denotes the *synchronous reactance* given by

$$X_s = \omega_s L_s \tag{7.23}$$

Recalling Eq. (7.16), it is clear that X_s can be expressed as the sum of the leakage reactance X_l and the reactance X_ϕ, commonly known as the armature reaction reactance:

$$X_s = X_l + X_\phi \tag{7.24}$$

with

$$X_l = \omega_s L_l \tag{7.25}$$

$$X_\phi = \omega_s L_\phi \tag{7.26}$$

At this point, we also define the synchronous impedance Z_s by

$$Z_s = R_a + jX_s \tag{7.27}$$

We are now ready to detail equivalent circuits and phasor diagrams of the round-rotor machine.

The excitation voltage E_f is represented as an independent sinusoidal source, as shown in Fig. 7.5(a). The synchronous impedance Z_s is in series with the source. It is clear that Eq. (7.20) is satisfied by this equivalent circuit. The phasor diagram of Fig. 7.5(b) is drawn with I_a as the reference phasor. We assume θ_0 to be negative in this construction. Voltage E_f leads I_a by the angle $(\theta_0 + \pi/2)$. The terminal voltage V_t is obtained by adding the voltage drop $I_a Z_s$ to E_f, as shown in the phasor diagram.

The equivalent circuit for the case of the machine operating as a generator is shown in Fig. 7.6(a) and can be seen to satisfy Eq. (7.18), written in the phasor form

$$E_f = V_t + I_a Z_s \tag{7.28}$$

www.EngineeringEBooksPdf.com

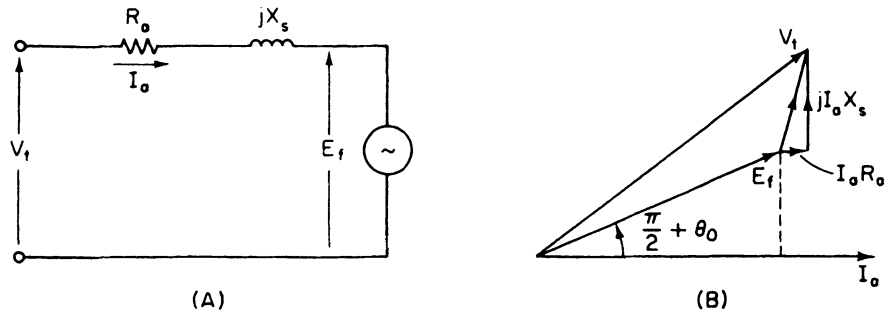


Figure 7.5 Round-rotor synchronous machine as a motor: (a) equivalent circuit; (b) phasor diagram.

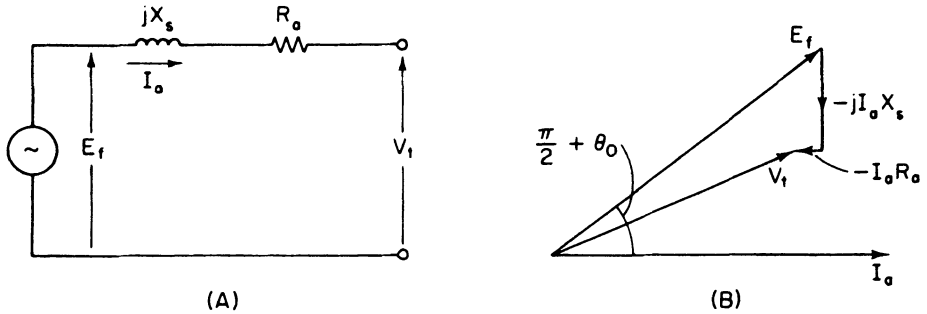


Figure 7.6 Round-rotor synchronous machine as a generator: (a) equivalent circuit; (b) phasor diagram.

The phasor diagram shown in Fig. 7.6(b) is similar in construction to that of Fig. 7.5(b), except that I_aZ_s is subtracted from E_f to obtain V_t.

The choice of I_a as reference was dictated by the simplicity of the resulting trignometric manipulations in the foregoing analysis. It is more practical, however, to take the terminal voltage V_t as reference and proceed given the terminal power factor (cosine of angle between V_t and I_a) to find E_f, as shown in Fig. 7.7(a) for the motor case and Fig. 7.7(b) for the generator case. The angle between E_f and

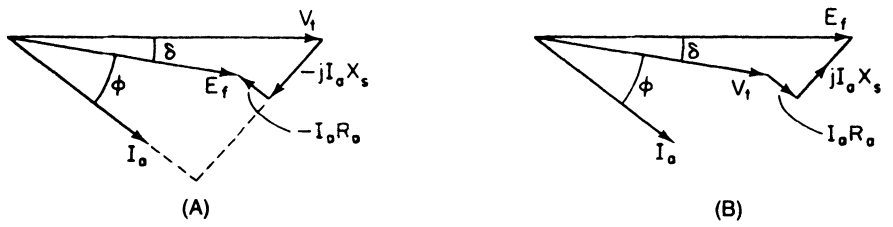


Figure 7.7 Round-rotor machine phasor diagrams with V_t as reference: (a) motor case; (b) generator case.

www.EngineeringEBooksPdf.com

V_t is commonly known as the torque or power angle δ. An example is presented at this point.

Example 7.1 A 1250-kVA three-phase Y-connected 4160-V 10-pole 60-Hz synchronous generator has an armature resistance of 0.126 Ω per phase and a synchronous reactance of 3 Ω per phase. Find the full-load generated voltage per phase at 0.8 PF lagging.

Solution We have

$$I_a = \frac{1250 \times 10^3}{\sqrt{3}(4160)} = 173.48 \text{ A}$$

Thus in polar form

$$I_a = 173.48\angle -36.87 \text{ deg A}$$

Given that

$$\begin{aligned} Z_s &= 0.123 + j3 \\ &= 3.0026\angle 87.595 \text{ deg } \Omega \end{aligned}$$

we apply Eq. (7.28) to obtain

$$E_f = \frac{4160}{\sqrt{3}} + (173.48\angle -36.87 \text{ deg})(3.00264\angle 87.595 \text{ deg}) = 2761.137\angle 8.397 \text{ deg V}$$

At this point we present another example, but here we deal with a motor.

Example 7.2 The rotational losses for a 1000-hp synchronous motor are found to be 18 kW. The motor operates from a 2300-V three-phase supply at 0.8 PF lagging. Find the excitation voltage at full load assuming that the machine's synchronous reactance is 1.9 Ω and that the armature resistance is negligible.

Solution The total input power is the sum of the output power and losses. As a result,

$$P_{\text{in}} = 746 \times 10^3 + 18 \times 10^3 = 764 \times 10^3 \text{ W}$$

The current is thus obtained as

$$I_a = \frac{764 \times 10^3}{\sqrt{3}(2300)(0.8)} = 239.726\angle -36.87 \text{ deg A}$$

www.EngineeringEBooksPdf.com

We now have

$$\begin{aligned} E_f &= V_t - jI_aX_s \\ &= \frac{2300}{\sqrt{3}} - j(239.726\angle -36.87 \text{ deg})(1.9) \\ &= 1115.793\angle -19.061 \text{ deg V} \end{aligned}$$

This is the required excitation voltage per phase.

7.3 ARMATURE REACTION

We have seen in Chapter 6 that a rotating magnetic field results from a three-phase balanced current in a set of three-phase windings that are placed 120 deg apart spatially. It is therefore clear that the armature currents in a three-phase synchronous machine create a rotating MMF. This MMF wave is commonly called *armature reaction MMF*. This MMF wave rotates at synchronous speed and is directly opposite to phase a at the instant when phase a has its maximum current ($t = 0$). The dc field winding produces a sinusoid F with an axis 90 deg ahead of the axis of phase a, in accordance with Faraday's law.

The resultant magnetic field in the machine is the sum of the two contributions from the field and armature reaction. Figure 7.8 shows a sketch of the armature and field windings of a cylindrical rotor generator.

The space MMF produced by the field winding is shown by the sinusoid F. This is shown for the specific instant when the force EMF of phase a, due to excitation, has its maximum value. The time rate of change of flux linkages with phase a is a maximum under these conditions, and thus the axis of the field is 90 deg ahead of phase a. The armature-reaction wave is shown as the sinusoid A in the figure. This is drawn opposite phase a because at this instant both I_a and the EMF of the field E_f (also

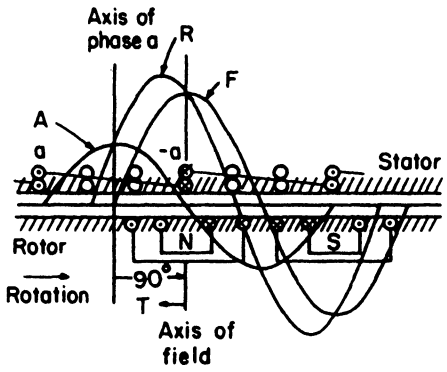


Figure 7.8 Spatial MMF waves in a cylindrical-rotor synchronous generator.

www.EngineeringEBooksPdf.com

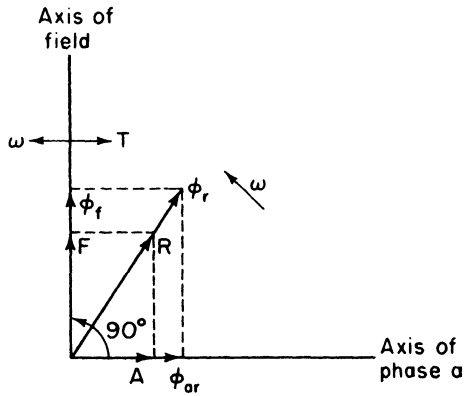


Figure 7.9 Space phasor diagram for armature current in phase with excitation voltage.

called excitation voltage) have their maximum value. The resultant magnetic field in the machine is denoted by R and is obtained by graphically adding the F and A waves.

Sinusoids can conveniently be handled using phasor methods. We can thus perform the addition of the A and F waves using phasor notation. Figure 7.9 shows a space phasor diagram where the fluxes ϕ_f (due to the field), ϕ_{ar} (due to the armature reaction), and ϕ_r (the resultant flux) are represented. It is clear that under the assumption of a uniform air gap and no saturation these are proportional to the MMF waves F, A, and R, respectively. The figure is drawn for the case when the armature current is in phase with the excitation voltage. The situation for the case when the armature current lags the excitation voltage, E_f, is shown in Fig. 7.10.

The effect of the armature-reaction flux is represented by an inductive reactance. The basis for this is shown in Fig. 7.11, where the phasor diagram of the component fluxes and corresponding voltages is given. The field flux ϕ_f is added to the

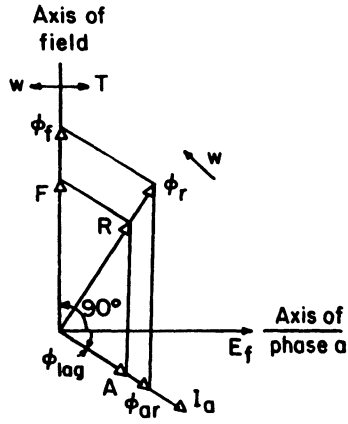


Figure 7.10 Space phasor diagram for armature current lagging the excitation voltage.

www.EngineeringEBooksPdf.com

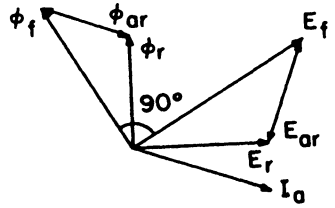


Figure 7.11 Phasor diagram for fluxes and resulting voltages in a synchronous machine.

armature-reaction flux ϕ_{ar} to yield the resultant air-gap flux ϕ_r. The armature-reaction flux ϕ_{ar} is in phase with the armature current, I_a. The excitation voltage, E_f, is generated by the field flux, and E_f lags ϕ_f by 90 deg. Similarly, E_{ar} and E_r are generated by ϕ_{ar} and ϕ_r, respectively, with each of the voltages lagging the flux causing it by 90 deg.

If we introduce the constant of proportionality, x_ϕ, that relates the rms values of E_{ar} and I_a, we can write

$$E_{ar} = -jx_\phi I_a \tag{7.29}$$

where the $-j$ emphasizes the 90 deg lagging effect. We therefore have for the generator case

$$E_r = E_f - jx_\phi I_a \tag{7.30}$$

The equivalent circuit of Fig. 7.6(a) is modified to show the armature reaction effects as shown in Fig. 7.12. The inductive reactance x_ϕ, known as the magnetizing reactance of the machine, accounts for the armature-reaction effects and is the same as the reactance x_ϕ defined in Eq. (7.26).

Example 7.3 A 10-MVA 13.8-kV 60-Hz two-pole Y-connected three-phase alternator has an armature-winding resistance of 0.07 Ω per phase and a leakage reactance of 1.9 Ω per phase. The armature-reaction EMF for the machine is related to the armature current by

$$E_{ar} = -j19.91 I_a$$

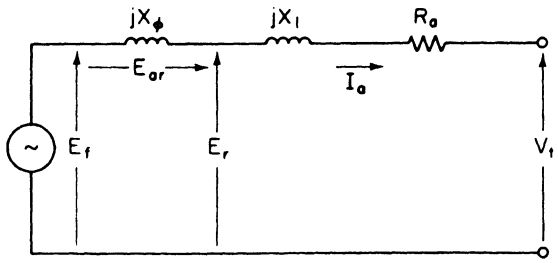


Figure 7.12 Equivalent circuit of a round-rotor synchronous generator showing armature-reaction effects.

www.EngineeringEBooksPdf.com

Assume that the generated EMF is related to the field current by

$$E_f = 60I_f$$

(a) Compute the field current required to establish the rated voltage across the terminals of a load when the rated armature current is delivered at 0.8 PF lagging.

(b) Compute the field current needed to provide the rated terminal voltage to a load that draws 100% of the rated current at 0.85 PF lagging.

Solution The terminal voltage (line to neutral) is given by

$$V_t = \frac{13{,}800}{\sqrt{3}} = 7967.43 \text{ V}$$

(a) The rated armature current is obtained as

$$I_a = \frac{10 \times 10^6}{\sqrt{3}(13{,}800)} = 418.37 \text{ A}$$

From the equivalent circuit of Fig. 7.12,

$$\begin{aligned} E_r &= V_t + I_a(R_a + jX_1) \\ &= 7967.43 + (418.37\angle -\cos^{-1}0.8)(0.07 + j1.9) \end{aligned}$$

Thus

$$E_f = 8490.35\angle 4.18 \text{ deg V}$$

From the specifications,

$$E_{ar} = -j(19.91)(418.37\angle -\cos^{-1}0.8 \text{ deg})$$

Thus

$$E_{ar} = -8329.75\angle 53.13 \text{ deg V}$$

Now, the field excitation is

$$E_f = E_r - E_{ar}$$

Thus we obtain

$$\begin{aligned} E_f &= 8490.35\angle 4.18 \text{ deg} + 8329.75\angle 53.13 \text{ deg} \\ &= 15{,}308.61\angle 28.40 \text{ deg V} \end{aligned}$$

www.EngineeringEBooksPdf.com

From the given relation, we obtain the required field current:

$$|I_f| = \frac{15{,}308.61}{60} = 255.14 \text{ A}$$

(b) In this case we have

$$\begin{aligned} I_a &= (418.37)(1.0)\angle -\cos^{-1}0.85 \text{ deg} \\ &= 418.37\angle -31.79 \text{ deg A} \end{aligned}$$

As a result,

$$\begin{aligned} E_r &= 7967.43 + (418.37\angle -31.79 \text{ deg})(0.07 + j1.9) \\ &= 8436.94\angle 4.49 \text{ deg V} \end{aligned}$$

We now calculate

$$\begin{aligned} E_{ar} &= -j(19.91)(418.37\angle -31.79 \text{ deg}) \\ &= -8329.74\angle 58.21 \text{ deg V} \end{aligned}$$

As a result,

$$\begin{aligned} E_f &= E_r - E_{ar} \\ &= 8436.94\angle 4.48 \text{ deg} + 8329.74\angle 58.21 \text{ deg} \\ &= 14{,}957.72\angle 31.16 \text{ deg V} \end{aligned}$$

The field current is thus obtained as

$$|I_f| = \frac{E_f}{60} = 249.30 \text{ A}$$

7.4 PRINCIPAL STEADY-STATE CHARACTERISTICS

The model of a round-rotor synchronous machine obtained in the form of the equivalent circuit of Section 7.2 is now used to obtain performance characteristics of the machine operating in the steady state as a generator. These describe the interrelations among terminal voltage, field current, armature current, and power factor.

We begin by considering a synchronous generator delivering power to a constant-power-factor load at a constant frequency. A compounding curve shows the variation of the field current required to maintain the rated terminal voltage with the load, as represented by armature current. Since excitation voltage, E_f, is assumed to be

www.EngineeringEBooksPdf.com

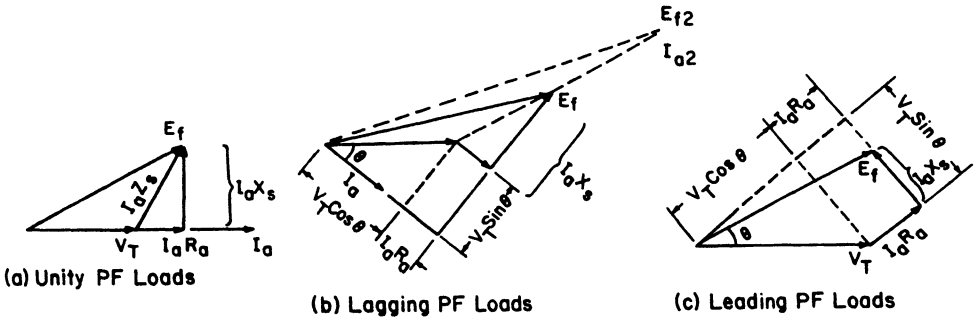


Figure 7.13 Phasor diagrams for a synchronous machine operating at different power factors are: (a) unity PF loads; (b) lagging PF loads; (c) leading PF loads.

proportional to the field current, I_f, it is then only necessary to examine the variation of $|E_f|$ with I_a to obtain the compounding curve for a given power factor. This can be done on the basis of Eq. (7.28) with V_t fixed at its rated value and varying I_a and computing $|E_f|$.

The nature of the compounding curves can be determined form the following equation derived from Eq. (7.28):

$$|E_f|^2 = V_t^2 + 2|Z_s||I_a|V_t\cos(\psi + \phi) + |Z_s|^2|I_a|^2 \tag{7.28a}$$

where it is assumed that ψ is the angle of Z_s and that ϕ is the phase angle between I_a and V_t.

For no load, $I_a = 0$, the excitation voltage $|E_f|$ is equal to terminal rated voltage. As the load (I_a) is increased, we see that $|E_f|$ increases provided that ψ is negative (lagging power factor) or zero, as $\cos(\psi + \phi)$ will be positive in that case. For leading power factors $\phi > 0$, and since ψ is close to 90 deg, we find that $\cos(\psi + \phi)$ can be negative. In this case, an increase in I_a can result in a decrease in the excitation voltage. The phasor diagrams shown in Fig. 7.13 help illustrate the points made here. Typical compounding curves for a round-rotor generator are shown in Fig. 7.14. An example is given now to illustrate the various points on a compounding curve.

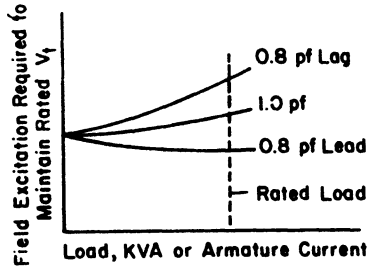


Figure 7.14 Synchronous-machine compounding curves.

www.EngineeringEBooksPdf.com

Example 7.4 A 10-MVA three-phase Y-connected 13,800-V two-pole 60-Hz turbogenerator has an armature resistance of 0.06 Ω per phase and a synchronous reactance of 1.8 Ω per phase. Find the excitation voltage at no load, half load, and full load for power factors of (a) 0.8 leading, (b) unity, and (c) 0.8 lagging with rated terminal voltage.

Solution We have

$$Z_s = 0.06 + j1.8 = 1.801\angle 88.09 \text{ deg}$$

The full-load current is obtained as

$$I_{af} = \frac{10 \times 10^6}{\sqrt{3}(13{,}800)} = 418.37 \text{ A}$$

The terminal voltage per phase is

$$V_t = \frac{13{,}800}{\sqrt{3}} = 7967.434 \text{ V}$$

We thus have

$$E_f = 7967.434 + \sigma(418.37)(1.801)\angle(88.09 \text{ deg} + \phi)$$

where σ is the fraction of the full load considered and ϕ is the phase angle.

(a) For a power factor of 0.8 leading,

$$\phi = 36.87 \text{ deg}$$

At no load, $\sigma = 0$,

$$E_f = 7967.434 \text{ V}$$

At half load, $\sigma = 0.5$,

$$\begin{aligned} E_f &= 7967.434 + 0.5(418.37)(1.801)\angle 124.961 \text{ deg} \\ &= 7757.702\angle 2.281 \text{ deg V} \end{aligned}$$

At full load, $\sigma = 1$, and we calculate

$$E_f = 7560.935\angle 4.685 \text{ deg V}$$

Note that $|E_f|$ is decreased as loading is increased.

www.EngineeringEBooksPdf.com

(b) For a unity power-factor load, $\phi = 0$: at no load, $\sigma = 0$, $E_f = 7967.434$ V. At half load, $\sigma = 0.5$,

$$E_f = 7967.434 + 0.5(418.37)(1.801)\angle 88.09 \text{ deg}$$
$$= 7988.863\angle 2.701 \text{ deg V}$$

At full load, we get

$$E_f = 8027.935\angle 5.383 \text{ deg V}$$

Note that $|E_f|$ is increased as loading is increased.

(c) For a power factor of 0.8 lagging, $\phi = -36.87$ deg. At half load, we have

$$E_f = 7967.434 + 0.5(418.37)(1.801)\angle 51.221 \text{ deg}$$
$$= 8208.65\angle 2.05 \text{ deg V}$$

At full load, we have

$$E_f = 8459.772\angle 3.981 \text{ deg V}$$

Again, we note the increase in $|E_f|$ as loading is increased.

The second characteristic of the round-rotor synchronous machine considered here is the variation of the machine terminal voltage as the armature current is varied for fixed-field current corresponding to producing full-load armature current at rated terminal voltage. Each characteristic curve is obtained for a given power factor. The nature of the characteristic can be examined by rewriting Eq. (7.28a):

$$V_t^2 + [2|Z_s||I_a|\cos(\psi + \phi)]V_t + |Z_s|^2|I_a|^2 - |E_f|^2 = 0 \tag{7.28b}$$

Clearly, at no load, the value of V_t is equal to $|E_f|$. Note, however, that the value of $|E_f|$ used in establishing this characteristic depends on the power factor chosen, and is picked from the corresponding compounding curve. The general trend from Eq. (7.28b) is that of a parabolic variation, as shown in Fig. 7.15. Note that for a leading power factor for currents above rated value, the curve yields two values for the resulting terminal voltage. An example will illustrate how this characteristic is constructed.

Example 7.5 Consider the machine of Example 7.4 operating at 0.8 PF leading. Construct the V_t versus I_a curve by computing selected points on the curve.

Solution From Example 7.4 at 0.8 PF leading, we found that for the rated terminal voltage, we need an excitation voltage of

$$E_f = 7560.935 \text{ V}$$

www.EngineeringEBooksPdf.com

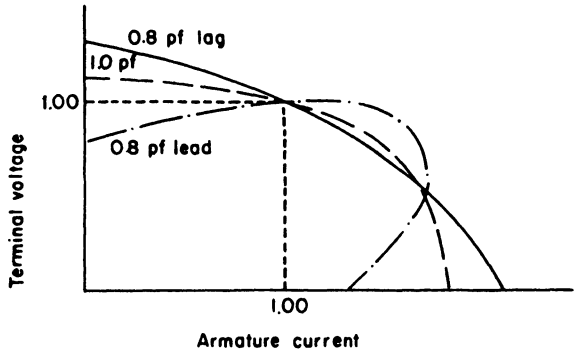


Figure 7.15 Constant-field-current volt-ampere characteristic of synchronous machine.

Substituting in Eq. (7.28b), the characteristic is described by

$$V_t^2 - 2.064 V_t I_a + (3.244 I_a^2 - 5.7168 \times 10^7) = 0$$

The first point to find is at no load, $I_a = 0$, where we find that

$$V_t = E_f = 7560.935 \text{ V}$$

The full-load current is 418.37 A, and we now compute V_t for half load as

$$V_{t_{1/2}} = 7770.5 \text{ V}$$

The other root of the equation is negative. At full load, we get

$$V_{t_f} = 7967.434 \text{ V}$$

For two times full load, we get

$$V_{t_2} = 8322.9 \text{ V}$$

Note that the terminal voltage increases with an increase in load.

The voltage, V_t, will be single-valued when the quadratic has two equal roots, and this takes place at

$$(2.064 I_a)^2 - 4(3.244 I_a^2 - 5.7168 \times 10^7) = 0$$

As a result, the current at the knee (k) of the curve is

$$I_{a_k} = 5122.3 \text{ A}$$

www.EngineeringEBooksPdf.com

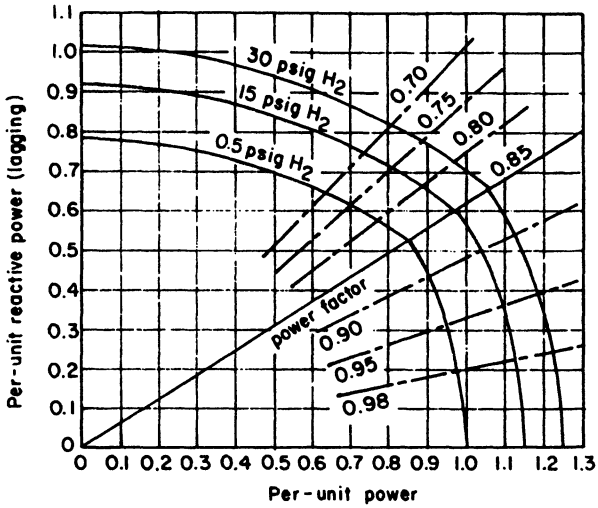


Figure 7.16 Generator reactive-capability curves.

This is almost 12 times full load. The corresponding value of V_t is obtained as

$$V_{t_k} = 5286.5 \text{ V}$$

The final point to obtain is that for which $V_t = 0$, and is found to be at

$$I_a = 4198.2 \text{ A}$$

That is about 10 times full-load current.

Important characteristics of the synchronous machine are given by the reactive-capability curves. These give the maximum reactive power loadings corresponding to various active power loadings for the rated voltage operation. Armature heating constraints govern the machine for power factors from rated to unity. Field heating represents the constraints for lower power factors. Figure 7.16 shows a typical set of curves for a large turbine generator.

7.5 POWER ANGLE CHARACTERISTICS AND THE INFINITE-BUS CONCEPT

Consider the simple circuit shown in Fig. 7.17. The impedance Z connects the sending end, whose voltage is E, and the receiving end, with voltage V. Let us assume that in polar form, we have

$$E = E\angle\delta$$
$$V = V\angle 0$$
$$Z = Z\angle\psi$$

www.EngineeringEBooksPdf.com

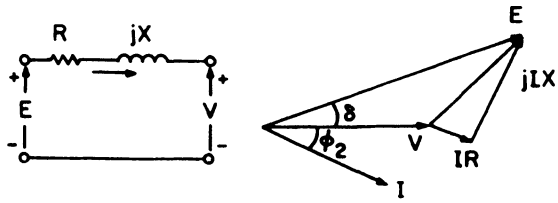


Figure 7.17 Equivalent circuit and phasor diagram for a simple link.

We therefore conclude that the current I is given by

$$I = \frac{E - V}{Z}$$

This reduces to

$$I = \frac{E}{Z}\angle\delta - \psi - \frac{V}{Z}\angle -\psi \tag{7.31}$$

The complex power S_1 at the receiving end is

$$S_1^* = E^* I$$

Similarly, the complex power S_2 at the receiving end is

$$S_2^* = V^* I$$

Using Eq. (7.31), we thus have

$$S_1^2 = \frac{E^2}{Z}\angle -\psi - \frac{EV}{Z}\angle -\psi - \delta \tag{7.32}$$

$$S_2^* = \frac{EV}{Z}\angle\delta - \psi - \frac{V^2}{Z}\angle -\psi \tag{7.33}$$

Recall that

$$S^* = P - jQ$$

We thus have the power equations:

$$P_1 = \frac{E^2}{Z}\cos(-\psi) - \frac{EV}{Z}\cos(\psi + \delta) \tag{7.34}$$

$$Q_1 = \frac{E^2}{Z}\sin\psi - \frac{EV}{Z}\sin(\psi + \delta) \tag{7.35}$$

$$P_2 = \frac{EV}{Z}\cos(\delta - \psi) - \frac{V^2}{Z}\cos\psi \tag{7.36}$$

$$Q_2 = \frac{EV}{Z}\sin(\psi - \delta) - \frac{V^2}{Z}\sin\psi \tag{7.37}$$

www.EngineeringEBooksPdf.com

An important case is when the resistance is negligible; then

$$\psi = 90 \text{ deg} \tag{7.38}$$

$$Z = X \tag{7.39}$$

Here we have Eqs. (7.34) to (7.37) reducing to

$$P_1 = P_2 = \frac{EV}{X}\sin\delta \tag{7.40}$$

$$Q_1 = \frac{E^2 - EV\cos\delta}{X} \tag{7.41}$$

$$Q_2 = \frac{EV\cos\delta - V^2}{X} \tag{7.42}$$

In large-scale power systems, a three-phase synchronous machine is paralleled through an equivalent system reactance (X_e) to the network, which has a high generating capacity relative to any single unit. We often refer to the network or system as an infinite bus when a change in input mechanical power or in field excitation to the unit does not cause an appreciable change in system frequency or terminal voltage. Fig. 7.18 shows such a situation, where V is the infinite-bus voltage.

The foregoing analysis shows that in the present case, we have for power transfer,

$$P = P_{\max}\sin\delta \tag{7.43}$$

with

$$P_{\max} = \frac{EV}{X_t} \tag{7.44}$$

and

$$X_t = X_s + X_e \tag{7.45}$$

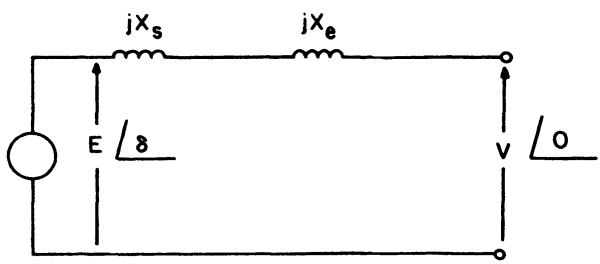


Figure 7.18 Synchronous machine connected to an infinite bus.

www.EngineeringEBooksPdf.com

It is clear that if an attempt were made to advance δ further than 90 deg (corresponding to maximum power transfer) by increasing the mechanical power input, the electrical power output would decrease from the P_{max} point. Therefore, the angle δ increases further as the machine accelerates. This drives the machine and system apart electrically. The value P_{max} is called the steady-state stability limit or pull-out power. We consider the following example, which illustrates the utility of the foregoing discussion.

Example 7.6 The synchronous reactance of a cylindrical-rotor machine is 1.2 per unit (p.u.). The machine is connected to an infinite bus whose voltage is 1 p.u. through an equivalent reactance of 0.3 p.u. For a power output of 0.7 p.u., the power angle is found to be 30 deg.

(a) Find the excitation voltage, E_f, and the pull-out power.

(b) For the same power output, the power angle is to be reduced to 25 deg. Find the value of the reduced equivalent reactance connecting the machine to the bus to achieve this. What would be the new pull-out power?

Solution

(a) We are given

$$X_t = 1.5 \text{ p.u.}$$
$$P = P_{max} \sin\delta$$
$$0.7 = P_{max} \sin 30\,\text{deg}$$

Hence

$$P_{max} = 1.4 \text{ p.u.}$$

Thus we calculate

$$1.4 = \frac{E_f(1)}{1.5}$$
$$E_f = 2.1$$

(b) We use the power relation

$$0.7 = P_{max} \sin 25\,\text{deg}$$
$$P_{max} = 1.66$$
$$1.66 = \frac{E_f V}{X_{new}} = \frac{2.1(1)}{X_{new}}$$
$$X_{new} = \frac{2.1}{1.66} = 1.27 \text{ p.u.}$$
$$x_e = 1.27 - 1.2 = 0.07 \text{ p.u.}$$

www.EngineeringEBooksPdf.com

7.5.1 Reactive Power Generation

Inspection of Eq. (7.42) reveals that the generator produces reactive power ($Q_2 > 0$) if

$$E\cos\delta > V$$

In this case, the generator appears to the network as a capacitor. This condition applies for high magnitude, E, and the machine is said to be overexcited. On the other hand, the machine is underexcited if it consumes reactive power ($Q_2 < 0$). Here we have

$$E\cos\delta < V$$

Figure 7.19 shows phasor diagrams for both cases. The overexcited synchronous machine is normally employed to provide synchronous condenser action, where usually no real load is carried by the machine ($\delta = 0$). In this case, we have

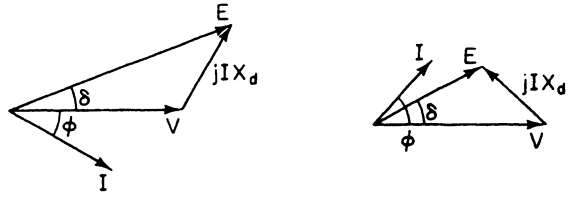
$$Q_2 = \frac{V(E - V)}{X}$$

Control of reactive power generation is carried out by simply changing E, by varying the dc excitation. An example will help demonstrate the use of these concepts.

Example 7.7 A cylindrical-rotor machine is supplying a load of 0.8 PF lagging at an infinite bus. The ratio of the excitation voltage to the infinite-bus voltage is found to be 1.25. Compute the power angle δ.

Solution For a power factor of 0.8, we have

$$\frac{Q}{P} = \tan\phi = 0.75$$



$0 < \delta < 90°$	$0 < \delta < 90°$
$0 < \phi < 90°$	$-90° < \phi < 0$
Overexcited generator	Underexcited generator
$P_G > 0$	$P_G > 0$
$Q_G > 0$	$Q_G < 0$

Figure 7.19 Phasor diagrams for overexcited and underexcited synchronous machines.

www.EngineeringEBooksPdf.com

Using the active and reactive power formulas, Eqs. (7.40) and (7.42), we have

$$\frac{Q}{P} = \frac{\cos\delta - \dfrac{V}{E}}{\sin\delta}$$

$$0.75 = \frac{\cos\delta - 0.8}{\sin\delta}$$

Cross multiplying, we have

$$0.8 + 0.75\sin\delta = \cos\delta$$

Using

$$\cos^2\delta = 1 - \sin^2\delta$$

We get

$$[(0.75)^2 + 1]\sin^2\delta + 2(0.8)(0.75)\sin\delta + [(0.8)^2 - 1] = 0$$

Consequently,

$$\sin\delta = 0.23$$

$$\delta = 13.34 \text{ deg}$$

7.5.2 Static-Stability Limit Curves

Let us consider a machine with synchronous reactance, X_s, connected to an infinite bus of voltage V through the reactance X_e, as shown in Fig. 7.20. We wish to determine the relationship between P, Q, V_t, and δ, as V and E are obtained on the

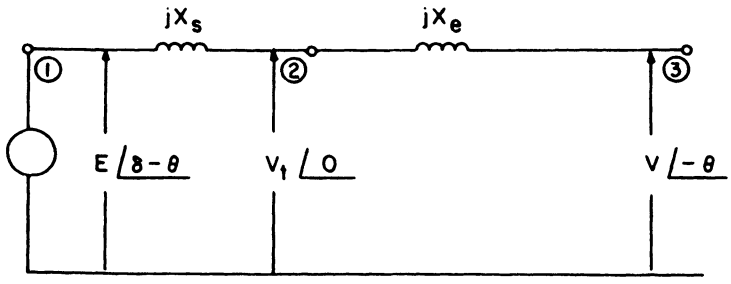


Figure 7.20 Equivalent circuit for a synchronous machine connected through an external network to an infinite bus.

www.EngineeringEBooksPdf.com

basis of Eqs. (7.40) and (7.42):

$$P = \frac{E V_t \sin(\delta - \theta)}{X_s} \tag{7.46}$$

$$Q = \frac{E V_t \cos(\delta - \theta) - V_t^2}{X_s} \tag{7.47}$$

To eliminate E from the preceding relationships, we note that two additional expressions for P can be obtained, since active power losses are not present. The first is based on the transfer from node 1 to node 3 across the total reactance X_t. The second is based on the transfer between nodes 2 and 3 across the reactance X_e. We therefore have

$$P = \frac{EV \sin\delta}{X_t} = \frac{V_t V \sin\theta}{X_e} \tag{7.48}$$

where X_t is given by Eq. (7.45).

Eliminating E and θ, we obtain

$$\left[P + \frac{V_t^2 X_t}{2X_s X_e \tan\delta}\right]^2 + \left[Q - \frac{V_t^2(X_s - X_e)}{2X_s X_e}\right]^2 = \left[\frac{V_t^2 X_t}{2X_s X_e \sin\delta}\right]^2 \tag{7.49}$$

Equation (7.49) indicates that the locus of P and Q delivered by the machine is a circle with its center at (P_0, Q_0) and radius R_0, where

$$P_0 = \frac{-V_t^2 X_t}{2X_s X_e \tan\delta} \tag{7.50}$$

$$Q_0 = \frac{V_t^2}{2}\left(\frac{1}{X_e} - \frac{1}{X_s}\right) \tag{7.51}$$

$$R_0 = \frac{V_t^2}{2\sin\delta}\left(\frac{1}{X_s} + \frac{1}{X_e}\right) \tag{7.52}$$

The static-stability limit curve for the machine is obtained from Eq. (7.49) by setting δ to 90 deg. Hence we have

$$P^2 + \left[Q - \frac{V_t^2}{2}\left(\frac{1}{X_e} - \frac{1}{X_s}\right)\right]^2 = \left[\frac{V_t^2}{2}\left(\frac{1}{X_s} + \frac{1}{X_e}\right)\right]^2 \tag{7.53}$$

The static-stability limit curve is commonly referred to as the pull-out curve of P and Q, and will determine the minimum permissible output var for output watts and terminal voltage specifications. Figure 7.21 shows such a curve.

www.EngineeringEBooksPdf.com

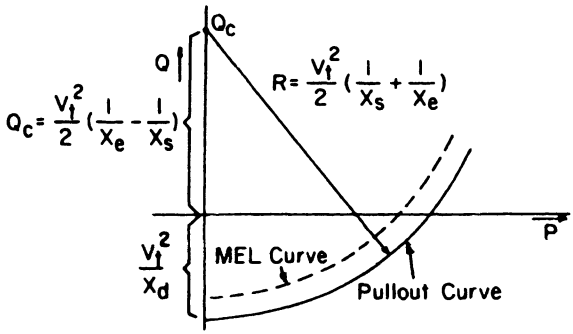


Figure 7.21 Static-stability limit curve for a synchronous machine.

Example 7.8 Given a generator and a system with reactances of $X_s = 1.2$ and $X_e = 0.2$, both on a 100-MVA base, assume a generator terminal voltage of 0.95 p.u. The infinite-bus voltage is unknown. Find the minimum permissible output var for the p.u. output watts varying from zero to 1 in steps of 0.25.

Solution The given parameters inserted in the static-stability limit curve equation [Eq. (7.53)] yield

$$P^2 + (Q - 1.88)^2 = 6.93$$

For $P = 0$, we have by simple substitution:

$$Q = -0.752$$

Similarly, we get

For $P = 0.25$: $Q = -0.740$.
For $P = 0.5$: $Q = -0.704$.
For $P = 0.75$: $Q = -0.643$.
For $P = 1.00$: $Q = -0.555$.

7.5.3 Power Angle Characteristics

The discussion of the present section shows that the active power of a round-rotor synchronous machine with negligible armature resistance is given by Eq. (7.43), written as

$$P = \frac{EV}{X_s} \sin\delta \tag{7.54}$$

It is clear, therefore, that for fixed-field excitation and terminal voltage, the active power variation with the power angle δ is as shown in Fig. 7.22. For positive δ, the

www.EngineeringEBooksPdf.com

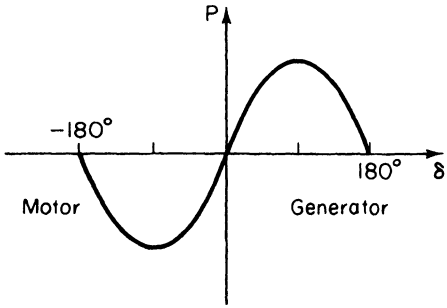


Figure 7.22 Synchronous-machine power angle characteristic for round-rotor type.

excitation voltage leads the terminal voltage and the machine acts as a generator. For negative δ, the excitation voltage lags the terminal voltage and the machine acts as a motor, as discussed in the next section.

7.6 SYNCHRONOUS-MOTOR OPERATION

A synchronous machine can be operated as a motor by supplying three-phase voltage to the armature terminals and direct current to the rotor (field windings). It should be noted, however, that unlike an induction machine, a synchronous machine is not self-starting. Arrangements for starting a stationary synchronous motor must be made as discussed later in this section. Once the machine is running at synchronous speed, it will continue to do so. We discuss presently an important performance characteristic of the synchronous motor, the V curves.

The V curves of a synchronous motor for a given terminal voltage relate the armature current, I_a, to the field excitation voltage, E_f. Each curve is constructed for a constant active power output. Assuming that armature resistance is negligible, we write

$$V_t = E_f + jI_a X_s \tag{7.55}$$

Therefore,

$$|E_f|\angle\delta = V_t - j|I_a|X_s\angle\phi$$

As a result, separating real and imaginary parts yields

$$E_f \cos\delta = V_t + I_a X_s \sin\phi \tag{7.56}$$

$$E_f \sin\delta = -I_a X_s \cos\phi \tag{7.57}$$

Note that δ is negative for motor operation. The phasor diagrams for leading and lagging power factors are shown in Fig. 7.23. The drop, $I_a X_s$, is at right angles to I_a.

www.EngineeringEBooksPdf.com

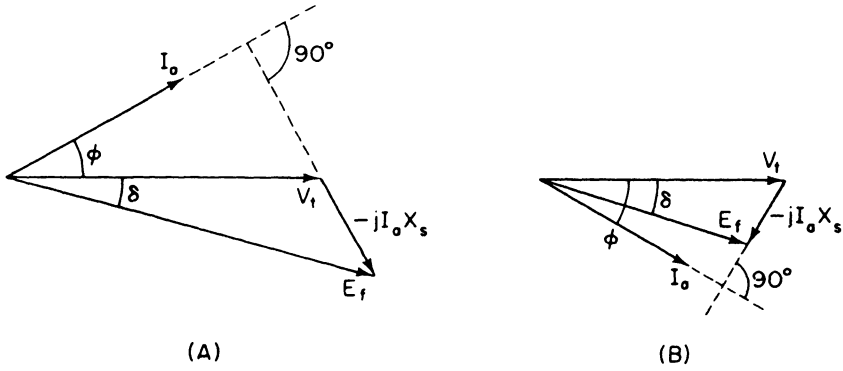


Figure 7.23 Phasor diagrams of round-rotor synchronous machine as motor: (a) leading power factor; (b) lagging power factor.

The condition of constant power operation can be seen on the basis of Eq. (7.54) or Eq. (7.57) to require that

$$E_f \sin\delta = \text{constant}$$

As a result, we conclude that for constant power, the tip of the phasor, E_f, is on the horizontal line *abcd* in the phasor diagrams of Fig. 7.24.

Point *a* on the phasor diagram corresponds to E_f lagging V_t by 90 deg, the maximum permissible power angle. For this condition, $\delta = -90$ deg and the value of $|I_a|$ is maximum, as can be seen from Fig. 7.25. Point *b* corresponds to a lagging-power-factor mode of operation, where it is clear that $|I_a|$ is decreased while $|E_f|$ is increased.

Point *c* corresponds to unity-power-factor operation (V_t and I_a are in phase) and $|I_a|$ is seen to have a minimum value.

Point *d* corresponds to a leading power factor. A representative set of V curves is shown in Fig. 7.25.

An analytical procedure for establishing a V curve can be followed from a study of the following example.

Example 7.9 Consider the motor of Fig. 7.2. Establish the following points ($|I_a|$ and $|E_f|$) on the V curve corresponding to full-load power output:

(a) Stability limit, $\delta = -90$ deg.
(b) Power factor of 0.8 lgging.
(c) Unity power factor.
(d) Power factor of 0.8 leading.

www.EngineeringEBooksPdf.com

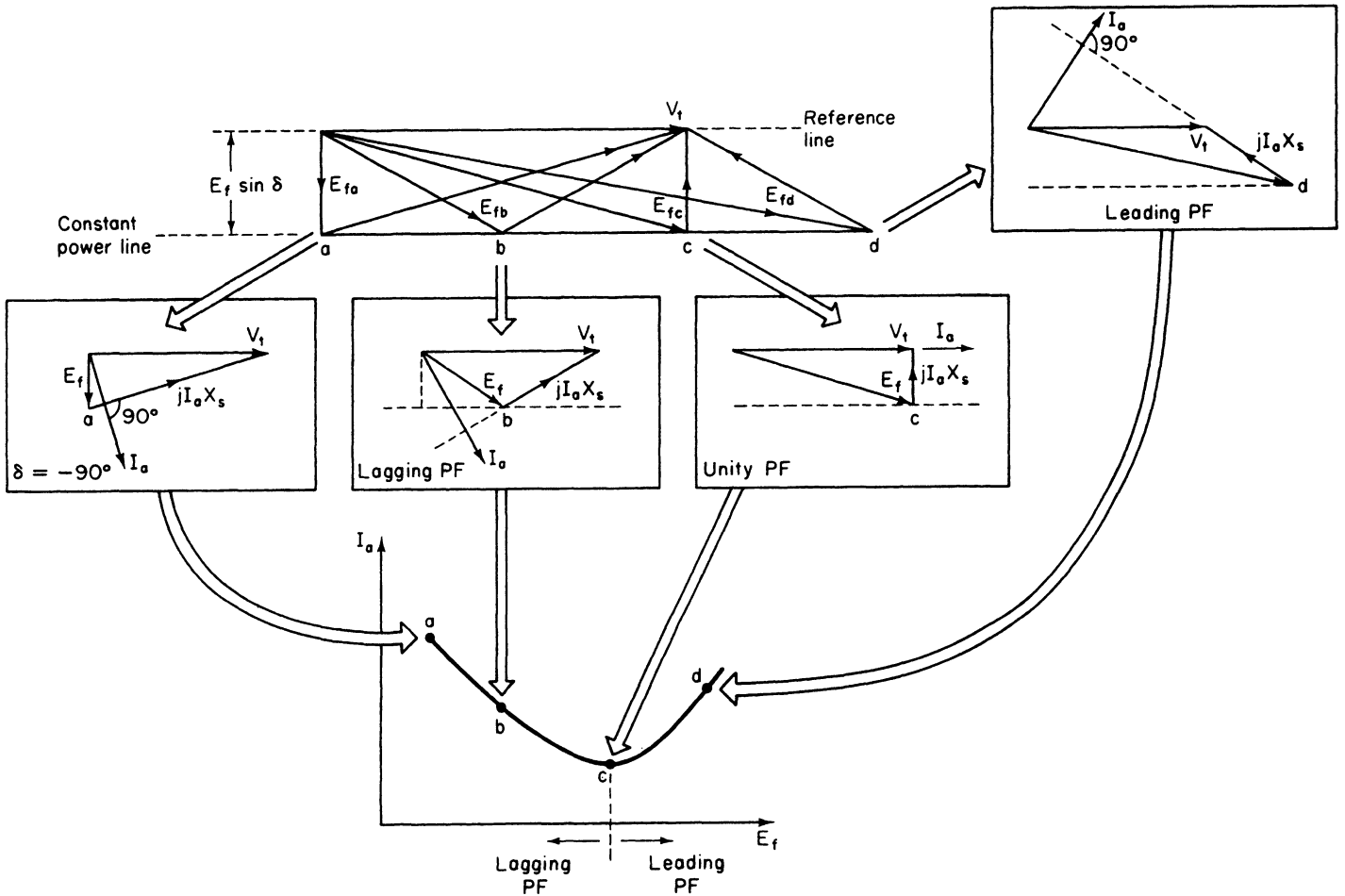


Figure 7.24 Establishing a V curve for a synchronous motor.

www.EngineeringEBooksPdf.com

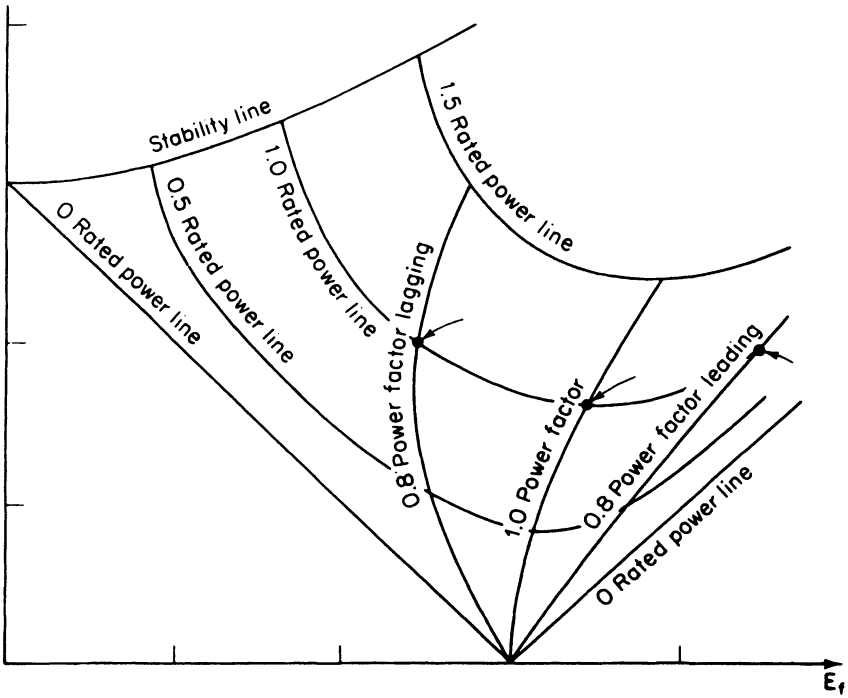


Figure 7.25 V curve of a round-rotor synchronous motor.

Solution We recall the following specifications from Example (7.2) on a per-phase basis:

$$V_t = \frac{2300}{\sqrt{3}} = 1327.91 \text{ V}$$

$$P = \frac{764 \times 10^3}{3} \text{ W}$$

$$X_s = 1.9 \ \Omega$$

As a result, we have

$$\frac{764 \times 10^3}{3} = \frac{-1327.91}{1.9} |E_f| \sin \delta$$

Thus

$$|E_f| \sin \delta = -364.38 \text{ V}$$

(a) For $\delta = -90$ deg, we get

$$|E_f| = 364.38 \text{ V}$$

www.EngineeringEBooksPdf.com

We find I_a by using

$$I_a = \frac{V_t - E_f}{jX_s} = \frac{1327.91 - 364.38\angle -90 \text{ deg}}{j1.9}$$
$$= 724.73\angle -74.66 \text{ deg A}$$

(b) For $\phi = -\cos^{-1}0.8 = -36.87$ deg,

$$I_a = \frac{764 \times 10^3}{\sqrt{3}(2300)(0.8)} = 239.73\angle -36.87 \text{ deg A}$$

We find E_f from

$$E_f = V_t - jI_a X_s$$
$$= 1327.91 - (239.73\angle -36.87 \text{ deg})(1.9\angle 90 \text{ deg})$$
$$= 1115.793\angle -19.061 \text{ deg V}$$

(c) For unity power factor

$$I_a = \frac{764 \times 10^3}{2300\sqrt{3}} = 191.78\angle 0 \text{ A}$$

We can get the same result from

$$-|I_a|X_s = |E_f| \sin\delta = -364.38 \text{ V}$$

The value of E_f is obtained from

$$E_f = 1327.91 - 191.78(1.9)\angle 90 \text{ deg}$$
$$= 1377\angle -15.34 \text{ deg V}$$

(d) For a power factor of 0.8 leading, we have

$$I_a = 239.73\angle 36.87 \text{ deg A}$$
$$E_f = 1327.91 - (239.73\angle 36.87 \text{ deg})(1.9\angle 90 \text{ deg})$$
$$= 1642.17\angle -12.82 \text{ deg V}$$

This concludes this example. We now discuss methods for starting a synchronous motor.

www.EngineeringEBooksPdf.com

7.6.1 Starting

A synchronous motor must be brought up to a speed close to synchronous speed so that the rotor locks into synchronism with the rotating field. There is more than one method to carry this out. The most common method is running the machine as an induction motor by using amortisseur or damper windings on the rotor of the machine. The dc field winding is not energized at starting, and the damper windings act as a squirrel cage to provide starting torque. The rotor is brought to a speed close to synchronous speed (small slip value) due to induction-motor action. Subsequent to this, the dc field winding is energized and the magnetic fluxes lock into synchronism. It is clear that an induction-motor starting mechanism, such as that discussed in Chapter 6, must be employed.

For synchronous machines without a damper winding, a dc motor coupled to the synchronous-motor shaft can be used. It is often practical to use the field-exciter generator as a dc motor for starting. An alternative method of starting involves using a small induction motor with at least one pair of poles less than the synchronous motor's poles to compensate for the loss in induction-motor speed due to slip.

7.6.2 Synchronous Capacitors

An important application of a synchronous motor is its use for power factor improvement as a synchronous capacitor (or condenser). The motor is manufactured without a shaft extension, as it is operated without a mechanical load. The motor is overexcited without load, and the armature current leads the terminal voltage by close to 90 deg and hence appears to the network as a capacitor. The synchronous capacitor is connected in parallel with loads characterized by a low power factor, such as induction motors. The result is an increase in the power factor at the network terminals. The following example illustrates a number of relevant points.

Example 7.10 An 800-hp three-phase induction motor operated at 0.7 PF lagging from a 2300-V supply.

(a) Find the line current.

(b) The synchronous motor of Example 7.2 is connected in parallel with the induction motor and is operated as a capacitor (zero power factor). Find the necessary excitation voltage to improve the line power factor to 0.9 lagging.

(c) Repeat part (b) for an improved power factor of 0.95 lagging.

Solution

(a) The line current with the induction motor operating alone is

$$I_{L_0} = \frac{800 \times 746}{\sqrt{3}(2300)(0.7)}$$

$$= 214.01 \angle -45.57 \text{ deg A}$$

www.EngineeringEBooksPdf.com

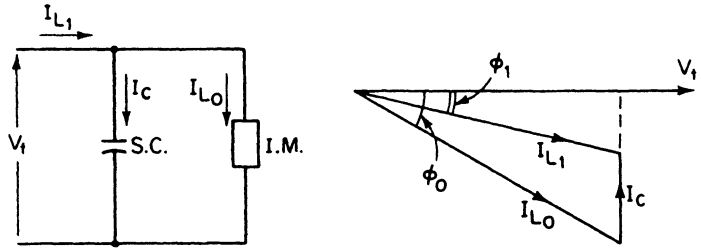


Figure 7.26 Equivalent circuit and phasor diagram for Example 7.10.

(b) To improve the line power factor to 0.9 PF lagging, we have the phasor diagram of Fig. 7.26. The armature current of the synchronous motor is denoted by I_c and the line current is I_{L_1}. Thus

$$I_{L_1} = I_{L_0} + I_c$$

As a result,

$$|I_{L_1}| \angle -\cos^{-1} 0.9 = 214.01 \angle -45.57 \text{ deg} + j|I_c|$$

The real part of the foregoing yields

$$0.9|I_{L_1}| = 149.81$$

Thus

$$|I_{L_1}| = 166.46 \text{ A}$$

The imaginary part yields

$$0.44|I_{L_1}| = 152.84 - |I_c|$$

Thus

$$|I_c| = 80.28 \text{ A}$$

To obtain the required excitation voltage, we use

$$\begin{aligned} E_f &= V_t - jIX_s \\ &= \frac{2300}{\sqrt{3}} - j(80.28 \angle 90 \text{ deg})(1.9) \\ &= 1480.44 \text{ V} \end{aligned}$$

www.EngineeringEBooksPdf.com

(c) To improve the power factor to 0.95 lagging, we repeat the foregoing to obtain

$$|I_{L_2}| = 157.69\,\text{A}$$
$$|I_c| = 103.6\,\text{A}$$

and

$$E_f = 1524.74\,\text{V}$$

We note that the magnitude of the line current is reduced by inserting the synchronous capacitor. A higher improvement in power factor requires a larger field excitation.

7.7 SALIENT-POLE MACHINES

The magnetic reluctance of the air gap in a machine with salient poles is not uniform due to the presence of protruding field poles. The reluctance along the polar axis is appreciably less than that along the interpolar axis. We often refer to the polar axis as the direct axis and the interpolar as the quadrature axis. This effect can be taken into account by resolving the armature current, I_a, into two components, one in time phase and the other in time quadrature with the excitation voltage, as shown in Fig. 7.27. The component I_d of the armature current is along the direct axis (the axis of the field poles), and the component I_q is along the quadrature axis.

Let us consider the effect of the direct-axis component alone. With I_d lagging the excitation EMF, E_f, by 90 deg, the resulting armature-reaction flux ϕ_{ad} is directly opposite the field poles, as shown in Fig. 7.28. The effect of the quadrature-axis component is to produce an armature-reaction flux ϕ_{aq}, which is in the quadrature-axis direction, as shown in Fig. 7.28. The phasor diagram with both components present is shown in Fig. 7.29.

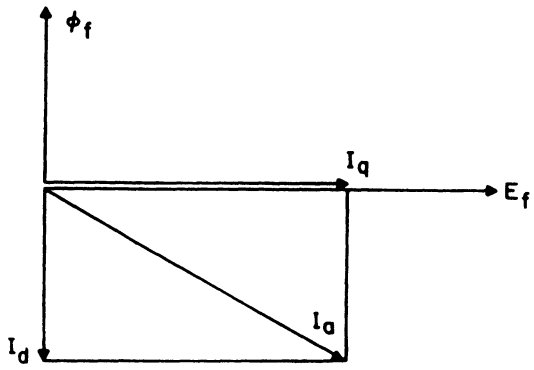


Figure 7.27 Resolution of armature current in two components.

www.EngineeringEBooksPdf.com

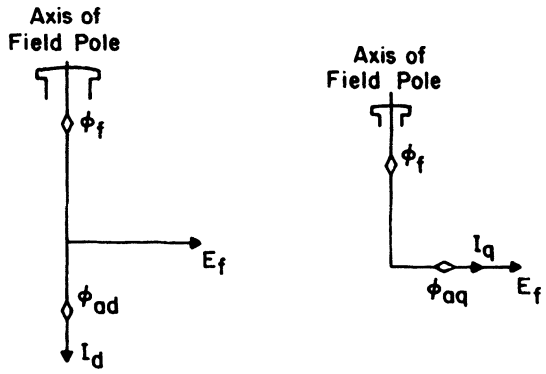


Figure 7.28 Direct-axis and quadrature-axis air-gap fluxes in a salient-pole synchronous machine.

We recall that in the cylindrical-rotor machine case, we employed the synchronous reactance, X_s, to account for the armature-reaction EMF in an equivalent circuit. The same argument can be extended to the salient-pole case. With each of the components currents I_d and I_q, we associate component synchronous-reactance voltage drops, jI_dx_d and jI_qx_q, respectively. The direct-axis synchronous reactance, x_d, and the quadrature-axis synchronous reactance, x_q, are given by

$$x_d = x_l + x_{\phi d}$$
$$x_q = x_l + x_{\phi q}$$

where x_l is the armature leakage reactance and is assumed to be the same for direct-axis and quadrature-axis currents. The direct-axis and quadrature-axis magnetizing reactances, $x_{\phi d}$ and $x_{\phi q}$, account for the inductive effects of the respective armature-reaction flux. Figure 7.30 shows a phasor diagram implementing the result.

$$E_f = V_t + I_a r_a + jI_a x_d + jI_q x_q \tag{7.58}$$

In many instances, the power factor angle Φ at the machine terminals is explicitly known rather than the internal power factor angle $(\phi + \delta)$, which is required for the

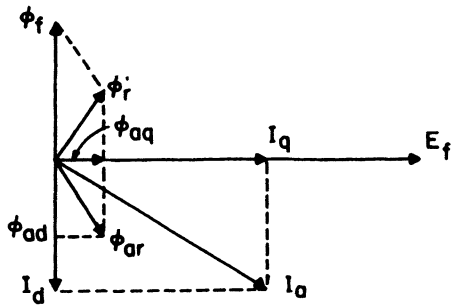


Figure 7.29 Phasor diagram for a salient-pole synchronous machine.

www.EngineeringEBooksPdf.com

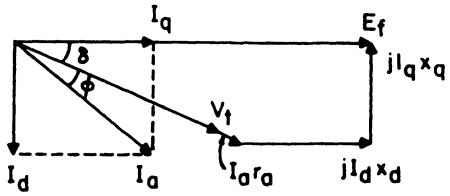


Figure 7.30 Phasor diagram for a synchronous machine.

decomposition of I_a into its direct-axis and quadrature-axis components. We can circumvent this difficulty by recalling that in phasor notation,

$$I_a = I_q + I_d \tag{7.59}$$

Substituting Eq. (7.58) into Eq. (7.59) for I_q and rearranging, we obtain

$$E_f = V_t + I_a(r_a + jx_q) + jI_d(x_d - x_q) \tag{7.60}$$

Let us define

$$E'_f = V_t + I_a(r_a + jx_q) \tag{7.61}$$

where E'_f as defined is in the same direction as E_f, since jI_d is also along the same direction. Our procedure, then, is to obtain E'_f as given by Eq. (7.61) and then obtain the component I_d based on the phase angle of E'_f. Finally, we find E_f as a result of

$$E_f = E'_f + jI_d(x_d - x_q) \tag{7.62}$$

This is shown in Fig. 7.31.

Table 7.1 gives typical ranges for values of x_d and x_q for synchronous machines. Note that x_q is less than x_d because of the greater reluctance of the air gap in the quadrature axis. We give an example at this point.

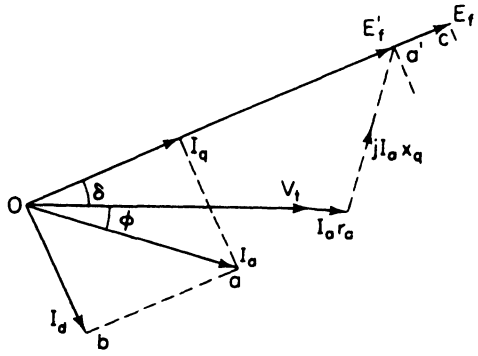


Figure 7.31 Modified phasor diagram for a salient-pole synchronous machine.

www.EngineeringEBooksPdf.com

TABLE 7.1 Typical Per-Unit Values of Machine Reactances

	Two-Pole Turbine Generators	Four-Pole Turbine Generators	Salient-Pole Generators	Condensers (Air-Cooled)
x_d	0.85–1.45	1.00–1.45	0.6–1.5	1.25–2.20
x_q	0.92–1.42	0.92–1.42	0.4–0.8	0.95–1.3

Note: Machine kVA rating as base.

Example 7.11 The reactances x_d and x_q of a salient-pole synchronous generator are 0.95 and 0.7 p.u., respectively. The armature resistance is negligible. The generator delivers rated kVA at unity PF and rated terminal voltage. Calculate the excitation voltage.

Solution We apply

$$E_f' = V_t + jI_a x_q$$

As a result,

$$E_f' = 1 + j(1)(0.7) = 1.22\angle 34.99 \text{ deg}$$

We now have

$$\begin{aligned} I_d &= I_a \sin 34.99 \text{ deg} \\ &= 0.57 \text{ p.u.} \end{aligned}$$

We can thus compute

$$\begin{aligned} |E_f| &= |E_f'| + |I_d(x_d - x_q)| \\ &= 1.22 + 0.57(0.25) \\ &= 1.36 \\ \delta &= 34.99 \text{ deg} \end{aligned}$$

Figure 7.32 pertains to this example.

7.7.1 Power Angle Characteristics

The power angle characteristics for a salient-pole machine connected to an infinite bus of voltage V through a series reactance of x_e can be arrived at by considering the

www.EngineeringEBooksPdf.com

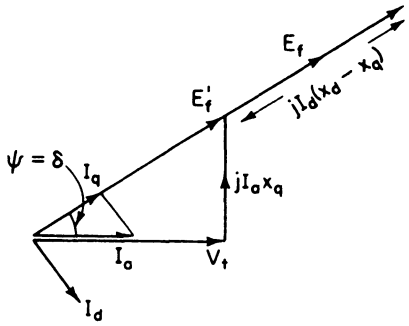


Figure 7.32 Phasor diagram for Example 7.11.

phasor diagram shown in Fig. 7.33. The active power delivered to the bus per phase is

$$P = (I_d \sin\delta + I_q \cos\delta)V \tag{7.63}$$

Similarly, the delivered reactive power, Q, is

$$Q = (I_d \cos\delta - I_q \sin\delta)\, V \tag{7.64}$$

To eliminate I_d and I_q, we need the following identities obtained from inspection of the phasor diagram:

$$I_d = \frac{E_f - V\cos\delta}{X_d} \tag{7.65}$$

$$I_q = \frac{V\sin\delta}{X_q} \tag{7.66}$$

where

$$X_d = x_d + x_e \tag{7.67}$$

$$X_q = x_q + x_e \tag{7.68}$$

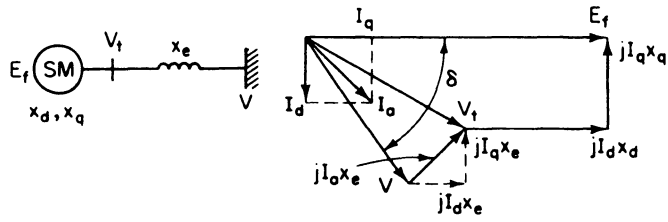


Figure 7.33 Salient-pole machine connected to an infinite bus through an external impedance.

www.EngineeringEBooksPdf.com

Substitution of Eqs. (7.65) and (7.66) into (7.63) and (7.64) yields

$$P = \frac{VE_f}{X_d} \sin \delta + \frac{V^2}{2}\left(\frac{1}{X_q} - \frac{1}{X_d}\right) \sin 2\delta \tag{7.69}$$

$$Q = \frac{VE_f}{X_d} \cos \delta - V^2\left(\frac{\cos^2 \delta}{X_d} + \frac{\sin^2 \delta}{X_q}\right) \tag{7.70}$$

Equations (7.69) and (7.70) contain six quantities—the two variables P and δ and the four parameters E_f, V, X_d, and X_q—and can be written in many different ways. The following form illustrates the effect of saliency. Define P_d and Q_d as

$$P_d = \frac{VE_f}{X_d} \sin \delta \tag{7.71}$$

and

$$Q_d = \frac{VE_f}{X_d} \cos \delta - \frac{V^2}{X_d} \tag{7.72}$$

The preceding equations give the active and reactive power generated by a round-rotor machine with synchronous reactance, X_d. We thus have

$$P = P_d + \frac{V^2}{2}\left(\frac{1}{X_q} - \frac{1}{X_d}\right) \sin 2\delta \tag{7.73}$$

$$Q = Q_d - V^2\left(\frac{1}{X_q} - \frac{1}{X_d}\right) \sin^2 \delta \tag{7.74}$$

The second term in the two preceding equations introduces the effect of salient poles, and in the power equation, the term corresponds to the reluctance torque. Note that if $X_d = X_q$, as in a uniform-air-gap machine, the second terms in both equations are zero. Figure 7.34 shows the power angle characteristics of a typical salient-pole machine.

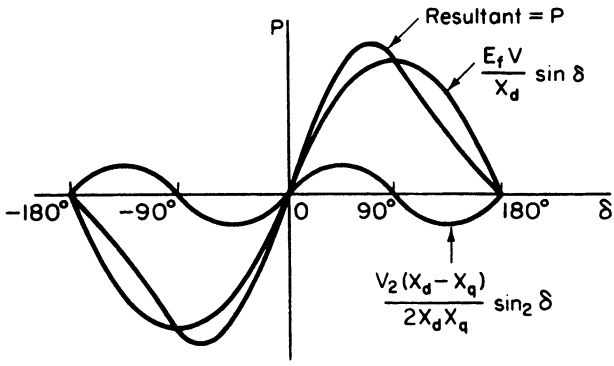


Figure 7.34 Power angle characteristics of a salient-pole synchronous machine.

www.EngineeringEBooksPdf.com

The pull-out power and power angle for the salient-pole machine can be obtained by solving Eq. (7.75), requiring that the partial derivative of P with respect to δ be equal to zero:

$$\frac{\partial P}{\partial \delta} = 0 \tag{7.75}$$

The actual value of pull-out power can be shown to be higher than that obtained assuming nonsaliency.

Example 7.12 The machine of Example 7.11 is connected to an infinite bus through a link with reactance of 0.2 p.u. The excitation voltage is 1.3 p.u. and the infinite-bus voltage is maintained at 1 p.u. For a power angle of 25 deg, compute the active and reactive power supplied to the bus.

Solution We have

$$X_d = 0.95 + 0.2 = 1.15\,\text{p.u.}$$
$$X_q = 0.7 + 0.2 = 0.9\,\text{p.u.}$$
$$E_f = 1.3 \qquad \delta = 25\ \text{deg} \qquad V_t = 1$$

As a result, we use Eq. (7.69) to obtain

$$\begin{aligned} P &= \frac{E_f V}{X_d}\sin\delta + \frac{V^2}{2}\left(\frac{1}{X_q} - \frac{1}{X_d}\right)\sin 2\delta \\ &= \frac{1.3(1)}{1.15}\sin 25\,\text{deg} + \frac{1}{2}\left(\frac{1}{0.9} - \frac{1}{1.15}\right)\sin 50\,\text{deg} \\ &= 0.57\,\text{p.u.} \end{aligned}$$

Equation (7.70) yields

$$\begin{aligned} Q &= \frac{E_f V}{X_d}\cos\delta - V^2\left(\frac{\cos^2\delta}{X_d} + \frac{\sin^2\delta}{X_q}\right) \\ &= \frac{1.3(1)}{1.15}\cos 25\,\text{deg} - \left(\frac{\cos^2 25}{1.15} + \frac{\sin^2 25}{0.9}\right) \\ &= 0.11 \end{aligned}$$

which are the required answers.

Example 7.13 A synchronous machine is supplied from a constant-voltage source. At no load, the motor armature current is found to be negligible when the excitation is 1.0 p.u. The p.u. motor constants are $x_d = 1.0$ and $x_q = 0.6$.

www.EngineeringEBooksPdf.com

(a) If the machine loses synchronism when the angle between the quadrature axis and the terminal voltage phasor direction is 60 electrical degrees, what is the p.u. excitation at pull-out?

(b) What is the load on the machine at pull-out? Assume the same excitations as in part (a).

Solution

(a)

$$P = \frac{VE_f}{X_d}\sin\delta + \frac{V^2}{2X_dX_q}(X_d - X_q)\sin 2\delta$$
$$= \frac{E_f(1)}{1}\sin\delta + \frac{1}{2\times 0.6}(1-0.6)\sin 2\delta$$
$$= E_f\sin\delta + \frac{1}{3}\sin 2\delta$$

For pull-out power, we have

$$\frac{\partial P}{\partial \delta} = E_f\cos\delta + \frac{2}{3}\cos^2\delta = 0$$

The pull-out angle is

$$\delta_m = 60 \text{ deg}$$

Hence we obtain

$$E_f = \frac{2}{3}\text{ p.u.}$$

(b) Consequently, the pull-out load is found to be

$$P = \frac{2}{3}\sin 60 \text{ deg} + \frac{1}{3}\sin 120 \text{ deg} = 0.866\text{ p.u.}$$

PROBLEMS

Problem 7.1 A 180-kVA three-phase Y-connected 440-V 60-Hz synchronous generator has a synchronous reactance of 1.6 Ω and a negligible armature resistance. Find the full-load generated voltage per phase at 0.8 PF lagging.

Problem 7.2 A 9375-kVA 13,800-kV 60-Hz two-pole Y-connected synchronous generator is delivering rated current at rated voltage and unity PF. Find the armature resistance and synchronous reactance given that the field excitation voltage is 11,935.44 V and leads the terminal voltage by an angle 47.96 deg.

www.EngineeringEBooksPdf.com

Problem 7.3 The magnitude of the field excitation voltage for the generator of Problem 7.2 is maintained constant at the value specified earlier. Find the terminal voltage when the generator is delivering rated current at 0.8 PF lagging.

Problem 7.4 The armature resistance and synchronous reactance of a three-phase synchronous motor are 0.8 and 6 Ω, respectively. The terminal voltage is 400 V (line to line). Find the excitation voltage when the motor draws a line current of 18 A at 0.8 PF leading.

Problem 7.5 The excitation voltage of a synchronous motor is 6370.5 V per phase and lags the terminal voltage by 4.5 deg. Assume that the terminal voltage is 11,000 V (line to line). The synchronous reactance is 10 Ω and armature resistance is negligible. Find the armature current and power factor for this condition of operation.

Problem 7.6 The power input to a three-phase synchronous motor is 400 kW. The excitation voltage is $5200\angle -9$ deg (line to line) with terminal voltage taken as reference. Assume that the armature resistance is negligible and that the synchronous reactance is 8 Ω. Find the terminal voltage and the power factor of the motor.

Problem 7.7 A 9375-kVA three-phase Y-connected 13,800-V (line to line) two-pole 60-Hz turbine generator has an armature resistance of 0.064 Ω per phase and a synchronous reactance of 1.79 Ω per phase. Find the full-load generated voltage per phase at:

(a) Unity power factor.
(b) A power factor of 0.8 lagging.
(c) A power factor of 0.8 leading.

Problem 7.8 A 5-kVA 220-V 60-Hz six-pole Y-connected synchronous generator has a leakage reactance per phase of 0.78 Ω and negligible armature resistance. The armature-reaction EMF for this machine is related to the armature current by

$$E_{ar} = -j16.88(I_a)$$

Assume that the generated EMF is related to field current by

$$E_f = 25I_f$$

(a) Compute the field current required to establish the rated voltage across the terminals of a unity power factor load that draws rated generator armature current.
(b) Determine the field current needed to provide rated terminal voltage to a load that draws 125% of rated current at 0.8 PF lagging.

Problem 7.9 For the machine of Example 7.3, the field current is adjusted to 250 A and the armature current is 400 A. Find the power factor at the machine's terminals.

www.EngineeringEBooksPdf.com

Problem 7.10 For the machine of Example 7.3, the field current is adjusted to 250 A and the machine's terminal power factor is 0.85 lagging. Find the armature current.

Problem 7.11 Repeat Example 7.5 for a power factor of 0.8 lagging.

Problem 7.12 The synchronous reactance of a cylindrical-rotor synchronous generator is 0.9 p.u. If the machine is delivering active power of 1 p.u. to an infinite bus whose voltage is 1 p.u. at unity PF, calculate the excitation voltage and power angle.

Problem 7.13 A synchronous generator with a synchronous reactance of 1.3 p.u is connected to an infinite bus whose voltage is 1 p.u. through an equivalent reactance of 0.2 p.u. The maximum permissible output is 1.2 p.u.

(a) Compute the excitation voltage E.

(b) The power output is gradually reduced to 0.7 p.u. with fixed-field excitation. Find the new current and power angle δ.

Problem 7.14 Compute the reactive power generated by the machine of Problem 7.13 under the conditions in part (b). If the machine is required to generate a reactive power of 0.4 p.u. while supplying the same active power by changing the field excitation, find the new excitation voltage and power angle δ.

Problem 7.15 The apparent power delivered by a cylindrical-rotor synchronous machine to an infinite bus is 1.2 p.u. The excitation voltage is 1.3 p.u. and the power angle is 20 deg. Compute the synchronous reactance of the machine given that the infinite-bus voltage is 1 p.u.

Problem 7.16 The synchronous reactance of a cylindrical rotor generator is 1 p.u. and its terminal voltage is 1 p.u. when connected to an infinite bus through a reactance of 0.4 p.u. Find the minimum permissible output vars for zero-output active power and unity-output active power.

Problem 7.17 A cylindrical-rotor machine is delivering active power of 0.8 p.u. and reactive power of 0.6 p.u. when the excitation voltage is 1.2 p.u. and the power angle is 25 deg. Find the terminal voltage and synchronous reactance of the machine.

Problem 7.18 A cylindrical-rotor machine is delivering active power of 0.8 and reactive power of 0.6 p.u. at a terminal voltage of 1 p.u. If the power angle is 20 deg, compute the excitation voltage and the machine's synchronous reactance.

Problem 7.19 The synchronous reactance of a cylindrical rotor machines is 0.8 p.u. The machine is connected to an infinite bus through two identical parallel transmission links with a reactance of 0.4 p.u. each. The excitation voltage is 1.4 p.u. and the machine is supplying a load of 0.8 p.u.

(a) Compute the power angle δ for the outlined conditions.

(b) If one link is opened with the excitation voltage maintained at 1.4 p.u., find the new power angle to supply the same load as in part (a).

www.EngineeringEBooksPdf.com

Problem 7.20 The synchronous reactance of a cylindrical rotor machine is 0.9 p.u. The machine is connected to an infinite bus through two identical parallel transmission links with a reactance of 0.6 p.u. each. The excitation voltage is 1.5 p.u., and the machine is supplying a load of 0.8 p.u.

(a) Compute the power angle δ for the given conditions.

(b) If one link is opened with the excitation voltage maintained at 1.5 p.u., find the new power angle to supply the same load as in part (a).

Problem 7.21 A round-rotor synchronous machine has a synchronous reactance of 1 p.u. The machine is connected to an infinite bus whose voltage is maintained at a voltage V. The following table lists information available about two conditions of operation. Complete the table and find V.

Condition	P	Q	E	δ (deg)
A	0.63	−0.1	?	35
B	?	−0.08	1.2	?

Problem 7.22 A round-rotor synchronous machine is connected to an infinite bus whose voltage is maintained at 1.05 p.u. Find the synchronous reactance of the machine and complete the following table.

Condition	P	Q	E	δ (deg)
A	1.07	−0.31	1.15	?
B	0.95	?	?	40

Problem 7.23 A round-rotor synchronous machine has a synchronous reactance of 0.9 p.u. The machine is connected to an infinite bus whose voltage is maintained at a value of 1.1 p.u. Complete the following table for two conditions of operation.

Condition	P	Q	E	δ (deg)
A	?	0.04	?	25
B	?	?	1.2	30

Problem 7.24 Repeat Example 7.9 for 80% of full-load power.

Problem 7.25 The synchronous reactance of a round-rotor synchronous motor is 2 Ω. The motor draws 240 A at a lagging PF for an excitation voltage of $1120\angle -20$ deg, phase value. The terminal voltage is taken as reference. Find the PF of the motor and the terminal voltage.

Problem 7.26 A round-rotor synchronous machine has a synchronous reactance of 1.8 Ω. The machine is operated as a synchronous condenser on a 2000-V bus and

www.EngineeringEBooksPdf.com

draws a current of 250 A. Find the excitation voltage and reactive power of the motor.

Problem 7.27 A 200-hp induction motor operates at 0.75 PF lagging. Find the reactive power required to improve the PF to 0.9 lagging.

Problem 7.28 An induction motor delivers 150 hp to a mechanical load. The power factor is 0.7 lagging. A synchronous condenser is connected in parallel with the motor and supplies a leading reactive power of 800 kvar. Find the PF of the combination. Neglect losses in the induction motor.

Problem 7.29 An induction motor delivers 100 hp to a load. Losses are neglected in the motor. A synchronous condenser in parallel with the motor delivers 45 kvar at a leading PF of 0.05. Find the power factor of the combination.

Problem 7.30 For the synchronous condenser of Problem 7.27, assume that the line voltage is 2300 V. Find the required field excitation assuming that the synchronous reactance is 2 Ω.

Problem 7.31 A 5-kVA 220-V Y-connected three-phase salient-pole synchronous generator is used to supply power to a unity power factor load. The direct-axis synchronous reactance is 12 Ω and the quadrature-axis synchronous reactance is 7 Ω. Assume that the rated current is delivered to the load at rated voltage and that armature resistance is negligible. Compute the excitation voltage and the power angle.

Problem 7.32 A three-phase synchronous machine has the following parameters:

$$r_a = 0 \quad X_d = 9.13\ \Omega$$
$$X_d = 7.03\ \Omega$$

The machine delivers 5 kW at unity power factor at 220. Find the excitation voltage and power angle δ.

Problem 7.33 The excitation voltage (line to line) in a 5-kVW 220-V Y-connected three-phase salient-pole synchronous generator is found to be 300 V when delivering rated current at unity power factor. The power angle δ is found to be 36 deg. Find the direct-axis and quadrature-axis synchronous reactance. Neglect armature resistance.

Problem 7.34 A salient-pole synchronous machine is connected to an infinite bus through a link with reactance of 0.2 p.u. The direct-axis and quadrature-axis reactances of the machine are 0.9 and 0.65 p.u., respectively. The excitation voltage 1.3 p.u., and the voltage of the infinite bus is maintained at 1 p.u. For a power angle of 30 deg, compute the active and reactive power supplied to the bus.

Problem 7.35 A salient-pole synchronous machine is connected to an infinite bus through a link with reactance of 0.2 p.u. The direct-axis reactance of the machine is 0.95 p.u.; the quadrature-axis reactance is yet to be determined. The excitation voltage is 1.35 and the voltage of the infinite bus is maintained at 1 p.u. For a power angle of 35 deg and active power of 0.79 p.u., find the quadrature-axis reactance of the machine and the reactive power delivered.

www.EngineeringEBooksPdf.com

Problem 7.36 A salient-pole machine supplies a load of 1.2 p.u. at unity power factor to an infinite bus whose voltage is maintained at 1.05 p.u. The machine excitation voltage is computed to be 1.4 p.u. when the power angle is 25 deg. Evaluate the direct-axis and quadrature-axis synchronous reactances.

Problem 7.37 A salient-pole machine is connected to an infinite bus whose voltage is kept constant at 1 p.u. The direct-axis and quadrature-axis reactances of the machine are $X_d = 1.2$ and $X_q = 0.8$. The following table details two operating conditions. Complete the table, neglecting armature resistance.

Condition	P	Q	E	δ (deg)
1	1.0	?	?	36
2	?	0.3	1.7	?

Problem 7.38 A salient-pole synchronous machine supplies a load at unity power factor to an infinite bus whose voltage is maintained at 1.05 p.u. Excitation voltage is given by 1.4 for a certain power angle. The direct axis reactance is 0.93 p.u. and that of the quadrature axis is 0.43 p.u. Find the active power delivered, P, and the power angle, δ, for the specified operating conditions.

Problem 7.39 A 5-kVA 220-V Y-connected three-phase salient-pole synchronous generator supplies rated current at rated voltage at 0.8 PF lagging to a local load. The direct-axis synchronous reactance is 12 Ω and the quadrature-axis synchronous reactance of the machine is 7 Ω. Compute the excitation voltage and the power angle, neglecting armature resistance.

Problem 7.40 The reactances x_d and x_q of a salient-pole synchronous generator are 1.00 and 0.6 p.u., respectively. The excitation voltage is 1.77 p.u. and the infinite-bus voltage is maintained at 1 p.u. For a power angle of 19.4 deg, compute the active and reactive power supplied to the bus.

Problem 7.41 For the machine of Problem 7.40, assume that the active power supplied to the bus is 0.8 p.u. Compute the power angle and the reactive power supplied to the bus. (*Hint*: Assume that $\cos \delta \cong 1$ for an approximation.)

Problem 7.42 For the machine of Problem 7.40, assume that the reactive power supplied to the bus is 0.6 p.u. Compute the power angle and the active power supplied to the bus.

Problem 7.43 A salient-pole machine supplies a load of 1.2 p.u. at unity PF to an infinite bus. The direct-axis and quadrature-axis synchronous reactances are

$$x_d = 0.9283 \qquad x_q = 0.4284$$

The power angle δ is 25 deg. Evaluate the excitation and terminal voltages.

www.EngineeringEBooksPdf.com

CHAPTER 8

FRACTIONAL-HORSEPOWER ALTERNATING CURRENT MOTORS

8.1 INTRODUCTION

We discuss the class of fractional-horsepower motors used for low power output, small size, and reliability applications. Standard ratings for this class range from 1/20 to 1 hp. Motors rated for less than 1/20 hp are called *subfractional-horsepower motors* and are rated in millihorsepower and range from1 to 35 mhp. These motors provide power for all types of equipment in the home, office, and commercial installations. The majority are of the induction-motor type and operate from a single-phase supply. Our discussion begins with an examination of rotating magnetic fields in single-phase induction motors.

8.2 ROTATING MAGNETIC FIELDS IN SINGLE-PHASE INDUCTION MOTORS

In studying the polyphase induction motor, we discussed the production of a rotating magnetic field due to three-phase stator windings that are displaced by 120 deg in space as well as in time. To understand the operation of common single-phase induction motors, it is necessary to start by discussing two-phase induction machines. In a true two-phase machine two stator windings, labeled AA' and BB', are placed at 90-deg spatial displacement, as shown in Fig. 8.1. The voltages v_A and v_B form a set of balanced two-phase voltages with a 90-deg time (or phase) displacement. Assuming that the two windings are identical, then the resulting flux ϕ_A and ϕ_B

www.EngineeringEBooksPdf.com

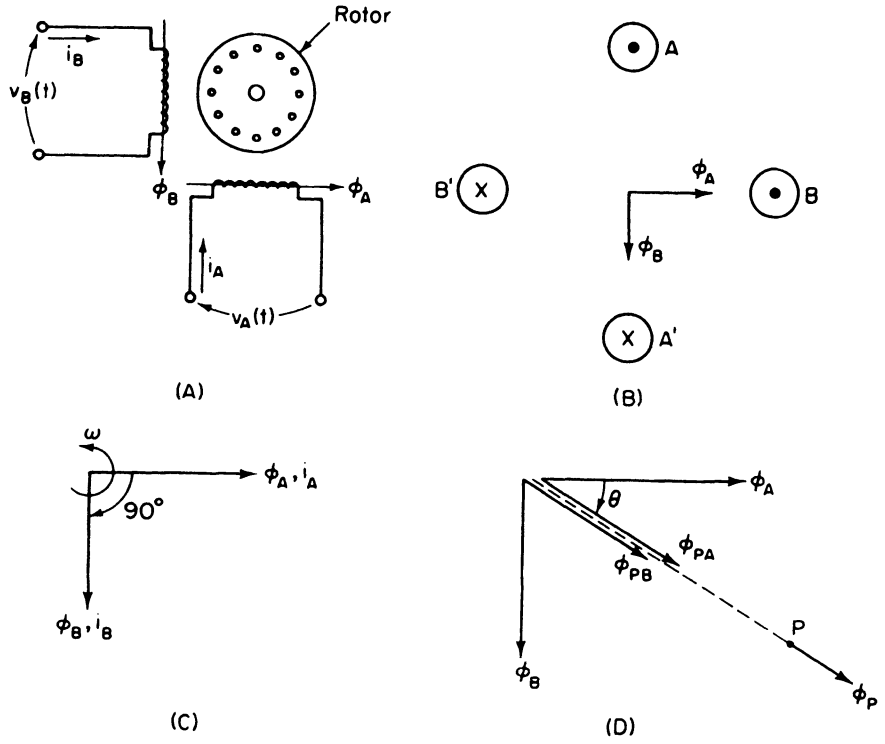


Figure 8.1 Rotating magnetic field in a balanced two-phase stator: (a) winding schematic; (b) flux orientation; (c) phasor diagram; (d) space phasor diagram.

are given by

$$\phi_A = \phi_M \cos \omega t \tag{8.1}$$

$$\phi_A = \phi_M \cos (\omega t - 90 \text{ deg}) = \phi_M \sin \omega t \tag{8.2}$$

where ϕ_M is the peak value of the flux. In Fig. 8.1(b) the flux ϕ_A is shown to be at right angles to ϕ_B in space. It is clear that because of Eqs. (8.1) and (8.2), the phasor relation between ϕ_A and ϕ_B is shown in Fig. 8.1(c), with ϕ_A taken as the reference phasor.

The resultant flux ϕ_P at a point P displaced by a spatial angle θ from the reference is given by

$$\phi_P = \phi_{PA} + \phi_{PB}$$

where ϕ_{PA} is the component of ϕ_A along the OP axis and ϕ_{PB} is the component of ϕ_B along the OP axis, as shown in Fig. 8.1(d). Here we have

$$\phi_{PA} = \phi_A \cos\theta$$

$$\phi_{PB} = \phi_B \sin\theta$$

www.EngineeringEBooksPdf.com

As a result, we have

$$\phi_P = \phi_M(\cos\omega t\cos\theta + \sin\omega t\sin\theta)$$

The preceding relationship can be written alternatively as

$$\phi_P = \phi_M\cos(\theta - \omega t) \tag{8.3}$$

The flux at point P is a function of time and the spatial angle θ, and has a constant amplitude ϕ_M. This result is similar to that obtained earlier for the balanced three-phase induction motor.

The flux ϕ_P can be represented by a phasor ϕ_M that is coincident with the axis of phase a at $t = 0$. The value of ϕ_P is $\phi_M \cos\theta$ at that instant, as shown in Fig. 8.2(a). At the instant $t = t_1$, the phasor ϕ_M has rotated an angle ωt_1 in the positive direction of θ, as shown in Fig. 8.2(b). The value of ϕ_P is seen to be $\phi_M\cos(\theta - \omega t_1)$ at that instant. It is thus clear that the flux waveform is a rotating field that travels at an angular velocity ω in the forward direction of an increase in θ.

The result obtained here for a two-phase stator winding set and for a three-phase stator winding set can be extended to an N-phase system. In this case, the N windings are placed at spatial angles of $2\pi/N$ and excited by sinusoidal voltages of time displacement $2\pi/N$.

The resultant flux at a point P is given by the sum

$$\phi_P = \sum_{i=1}^{N} \phi_{Pi}$$

Each of the individual components is given by

$$\phi_{Pi} = \phi_i\cos\left[\theta - (i-1)\frac{2\pi}{N}\right]$$

Thus we have

$$\phi_{Pi} = \phi_M\cos\left[\theta - (i-1)\frac{2\pi}{N}\right]\cos\left[\omega t - (i-1)\frac{2\pi}{N}\right]$$

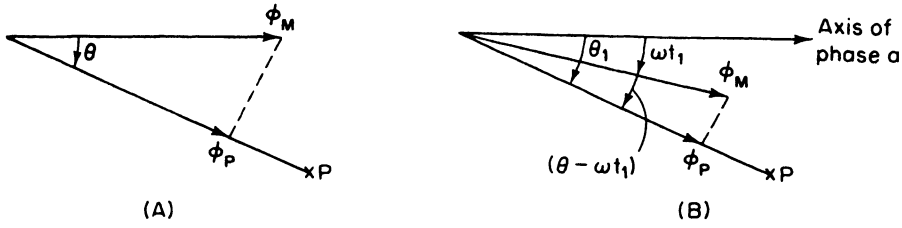


Figure 8.2 Illustrating the forward-rotating magnetic field: (a) $t = 0$; (b) $t = t_1$.

www.EngineeringEBooksPdf.com

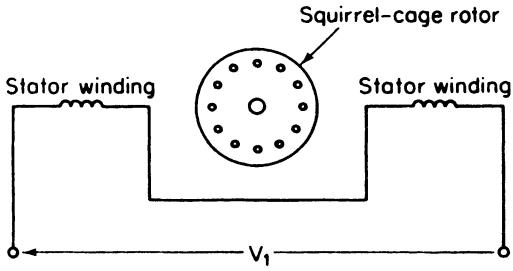


Figure 8.3 Schematic of a single-phase induction motor.

This reduces to

$$\phi_{pi} = \frac{\phi_M}{2}[\cos(\omega t - \theta) - \cos(\omega t + \theta - 2\alpha_i)]$$

where we define

$$\alpha_i = (i - 1)\frac{2\pi}{N}$$

The resultant flux is then given by

$$\phi_P = \frac{\phi_M}{2}\left[\sum_{i=1}^{N} \cos(\omega t - \theta) - \sum_{i=1}^{N} \cos(\omega t + \theta - 2\alpha_i)\right]$$

The second sum is zero, and therefore

$$\phi_P = \frac{N\phi_M}{2}\cos(\theta - \omega t) \tag{8.4}$$

A rotating magnetic field of constant magnitude will be produced by an N-phase winding excited by balanced N-phase currents when each phase is displaced $2\pi/N$ electrical degrees from the next phase in space.

To understand the operation of a single-phase induction motor, we consider the configuration shown in Fig. 8.3. The stator carries a single-phase winding and the rotor is of the squirrel-cage type. This configuration corresponds to a motor that has been brought up to speed, as is discussed presently.

Consider a single-phase stator winding as shown in Fig. 8.4(a). The flux ϕ_A is given by

$$\phi_A = \phi_M \cos\omega t \tag{8.5}$$

The flux at point P displaced by angle θ from the axis of phase a is clearly given by

$$\phi_P = \phi_A \cos\theta$$

www.EngineeringEBooksPdf.com

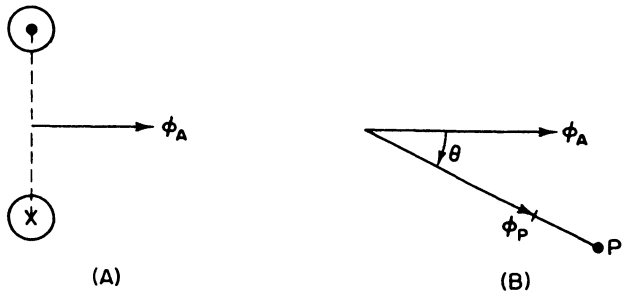


Figure 8.4 (a) Single-phase winding; (b) the flux at a point *P*.

Using Eq. (8.5), we obtain

$$\phi_P = \phi_M \cos\theta \cos\omega t \tag{8.6}$$

An alternative form of Eq. (8.6) is given by

$$\phi_P = \frac{\phi_M}{2}[\cos(\theta - \omega t) + \cos(\theta + \omega t)] \tag{8.7}$$

The flux at point *P* can therefore be seen to be the sum of two waveforms ϕ_f and ϕ_b given by

$$\phi_f = \frac{\phi_M}{2}\cos(\theta - \omega t) \tag{8.8}$$

$$\phi_b = \frac{\phi_M}{2}\cos(\theta + \omega t) \tag{8.9}$$

The waveform ϕ_f is of the same form as that obtained in Eq. (8.3), which was shown to be rotating in the forward direction (increase in θ from the axis of phase *a*). The only difference between Eqs. (8.8) and (8.3) is that the amplitude of ϕ_f is half of that of *P* in Eq. (8.3). The subscript *f* in Eq. (8.8) signifies the fact that $\cos(\theta - \omega t)$ is a forward-rotating wave.

Consider now the waveform ϕ_b of Eq. (8.9). At $t = 0$, the value of ϕ_b is $(\phi_M/2)$ $\cos\theta$ and is represented by the phasor $(\phi_M/2)$, which is coincident with the axis of phase *a*, as shown in Fig. 8.5(a). Note that at $t = 0$, both ϕ_f and ϕ_b are equal in value.

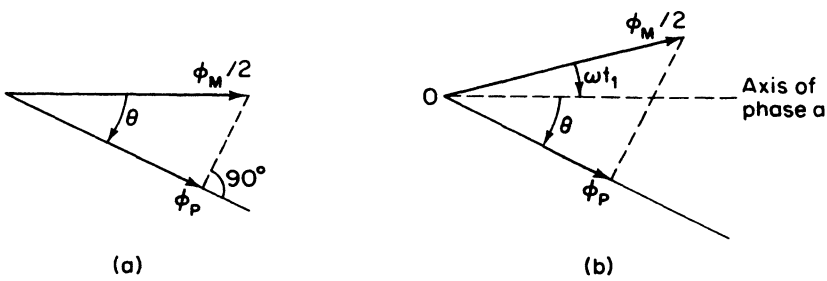


Figure 8.5 Showing that ϕ_b is a backward-rotating wave: (a) $t = 0$; (b) $t = t_1$.

www.EngineeringEBooksPdf.com

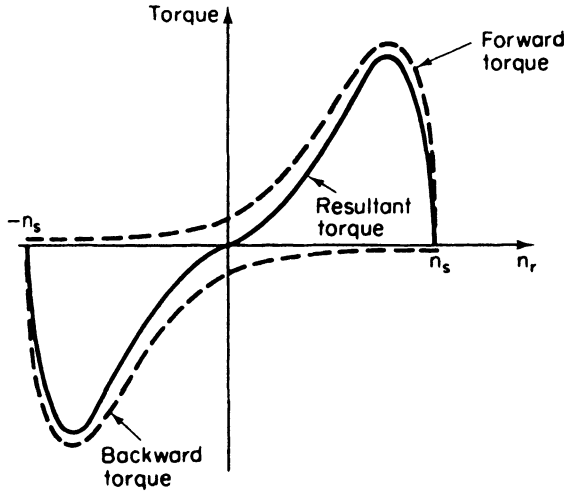


Figure 8.6 Torque–speed characteristics of a single-phase induction motor.

At a instant $t = t_1$, the phasor $(\phi_M/2)$ is seen to be at angle ωt_1 with the axis of phase a, as shown in Fig. 8.4(b). The waveform ϕ_b can therefore be seen to be rotating at an angular velocity ω in a direction opposite to that of ϕ_f and we refer to ϕ_b as a backward-rotating magnetic field. The subscript b in Eq. (8.9) signifies the fact that $\cos(\theta + \omega t)$ is a backward-rotating wave.

The result of our discussion is that in a single-phase induction machine there are two magnetic fields rotating in opposite directions. Each field produces an induction-motor torque in a direction opposite to the other. If the rotor is at rest, the forward torque is equal and opposite to the backward torque and the resulting torque is zero. What we have just discovered is that a single-phase induction motor is incapable of producing a torque at rest and is therefore not a self-starting machine. If the rotor is made to rotate by an external means, each of the two fields would produce a torque–speed characteristic similar to a balanced three-phase (or two-phase) induction motor, as shown by the dashed curves in Fig. 8.6. The resultant torque–speed characteristic is shown in a solid line. The foregoing argument will be confirmed once we develop an equivalent circuit for the single-phase induction motor.

8.3 EQUIVALENT CIRCUITS FOR SINGLE-PHASE INDUCTION MOTORS

In Section 8.2 we have seen that in a single-phase induction motor, the pulsating flux wave resulting from the single-winding stator MMF is equal to the sum of two rotating flux components. The first component is referred to as the forward field and has a constant amplitude equal to half of that of the stator waveform. The forward field rotates at synchronous speed. The second component, referred to as the backward

www.EngineeringEBooksPdf.com

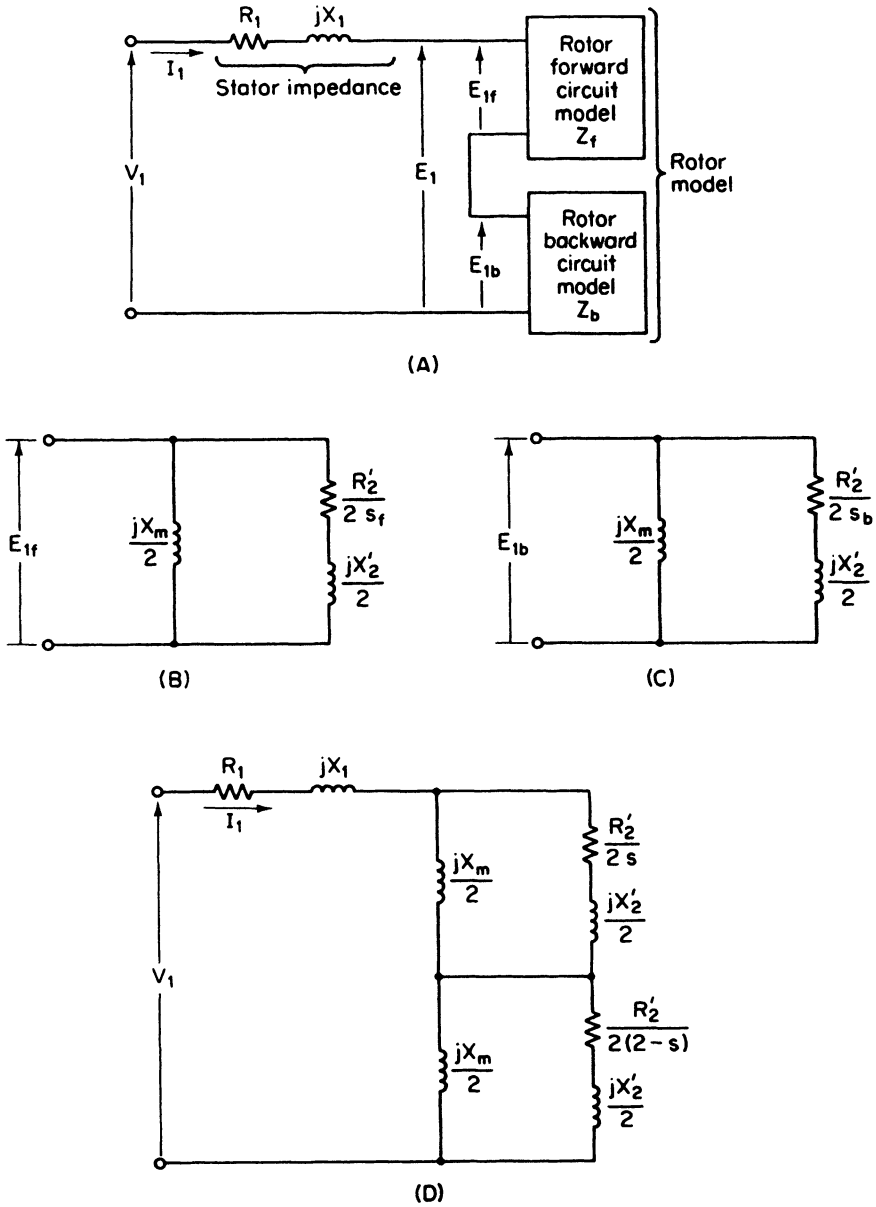


Figure 8.7 Developing an equivalent circuit for single-phase induction motors: (a) basic concept; (b) forward model; (c) backward model; (d) complete equivalent circuit.

field, is of the same constant amplitude, but rotates in the opposite (or backward) direction at synchronous speed. Each component induces its own rotor current and creates induction-motor action in the same manner as in a balanced three-phase induction motor. It is on this basis that we conceive the circuit model of Fig. 8.7(a).

www.EngineeringEBooksPdf.com

Note that R_1 and X_1 are the stator resistance and leakage reactance, respectively, and V_1 is the stator input voltage. The EMF E_1 is assumed to be the sum of two components, E_{1_f} and E_{1_b}, corresponding to the forward- and backward-field waves, respectively. Note that since the two waves have the same amplitude, we have

$$E_{1_f} = E_{1_b} = \frac{E_1}{2} \tag{8.10}$$

The rotor circuit is modeled as the two blocks shown in Fig. 8.7(a), representing the rotor forward-circuit model Z_f and the rotor backward-circuit model Z_b, respectively.

The model of the rotor circuit for the forward-rotating wave, Z_f, is simple, since we are essentially dealing with induction-motor action, and the rotor is set in motion in the same direction as the stator synchronous speed. The model of Z_f is shown in Fig. 8.7(b) and is similar to that of the rotor of a balanced three-phase induction motor. The impedances dealt with are half of the actual values, to account for the division of E_1 into two equal voltages. In this model X_m is the magnetizing reactance, and R_2' and X_2' are rotor resistance and leakage reactance, both referred to the stator side. The slip s_f is given by

$$s_f = \frac{n_s - n_r}{n_s} \tag{8.11}$$

This is the standard definition of slip as the rotor is revolving in the same direction as that of the forward-flux wave.

The model of the rotor circuit for the backward-rotating wave, Z_b, is shown in Fig. 8.7(c) and is similar to that of Z_f, with the exception of the backward slip, denoted by s_b. The backward wave is rotating at a speed of $-n_s$, and the rotor is rotating at n_r. We thus have

$$s_b = \frac{(-n_s) - n_r}{-n_s} = 1 + \frac{n_r}{n_s} \tag{8.12}$$

Using Eq. (8.11), we have

$$s_f = 1 - \frac{n_r}{n_s} \tag{8.13}$$

As a result, we conclude that the slip of the rotor with respect to the backward wave is related to its slip with respect to the forward wave by

$$s_b = 2 - s_f \tag{8.14}$$

We now let s be the forward slip,

$$s_f = s \tag{8.15}$$

www.EngineeringEBooksPdf.com

and thus

$$s_b = 2 - s \tag{8.16}$$

On the basis of Eqs. (8.15) and (8.16), a complete equivalent circuit as shown in Fig. 8.7(d) is now available. The core losses in the present model are treated separately in the same manner as the rotational losses.

The forward impedance Z_f is obtained as the parallel combination of $(jX_m/2)$ and $[(R_2'/2s) + j(X_2'/2)]$, given by

$$Z_f = \frac{j(X_m/2)[(R_2'/2s) + j(X_2'/2)]}{(R_2'/2s) + j[(X_m + X_2')/2]} \tag{8.17}$$

Similarly, for the backward impedance, we get

$$Z_b = \frac{j(X_m/2)\{[(R_2'/2(2-s)) + j(X_2'/2)]\}}{[R_2'/2(2-s)] + j[(X_m + X_2')/2]} \tag{8.18}$$

Note that with the rotor at rest, $n_r = 0$, and thus with $s = 1$, we get $Z_f = Z_b$. An example is appropriate now.

Example 8.1 The following parameters are available for a 60-Hz four-pole single-phase 110-V 1/2-hp induction motor.

$$R_1 = 1.5\ \Omega \qquad R_2' = 3\ \Omega$$
$$X_1 = 2.4\ \Omega \qquad X_2' = 2.4\ \Omega$$
$$X_m = 73.4\ \Omega$$

Calculate Z_f, Z_b, and the input impedance of the motor at a slip of 0.05.

Solution

$$Z_f = \frac{j36.7(30 + j1.2)}{30 + j37.9} = 22.796\angle 40.654 \text{ deg } \Omega$$
$$= 17.294 + j14.851\ \Omega$$

The result obtained above is a direct application of Eq. (8.17). Similarly, using Eq. (8.18), we get

$$Z_b = \frac{j36.7[(1.5/1.95) + j1.2]}{(1.5/1.95) + j37.9} = 1.38\angle 58.502 \text{ deg } \Omega$$
$$= 0.721 + j1.1766\ \Omega$$

www.EngineeringEBooksPdf.com

We observe here that $|Z_f|$ is much larger than $|Z_b|$ at this slip, in contrast to the situation at starting ($s = 1$), for which $Z_f = Z_b$.

The input impedance Z_i is obtained as

$$\begin{aligned} Z_i &= Z_1 + Z_f + Z_b = 19.515 + j18.428 \\ &= 26.841 \angle 43.36 \text{ deg } \Omega \end{aligned}$$

Equations (8.17) and (8.18) yield the forward and backward impedances on the basis of complex number arithmetic. The results can be written in the rectangular forms

$$Z_f = R_f + jX_f \tag{8.19}$$

and

$$Z_b = R_b + jX_b \tag{8.20}$$

Using Eq. (8.17), we can write

$$2R_f = \frac{a_f X_m^2}{a_f^2 + X_t^2} \tag{8.21}$$

and

$$X_f = \frac{R_f}{a_f X_m}(a_f^2 + X_t X_2') \tag{8.22}$$

where

$$a_f = \frac{R_2'}{s} \tag{8.23}$$

$$X_t = X_2' + X_m \tag{8.24}$$

In a similar manner, using Eq. (8.18), we have

$$2R_b = \frac{a_b X_m^2}{a_b^2 + X_t^2} \tag{8.25}$$

$$X_b = \frac{R_b}{a_b X_m}(a_b^2 + X_t X_2') \tag{8.26}$$

where

$$a_b = \frac{R_2'}{2 - s} \tag{8.27}$$

www.EngineeringEBooksPdf.com

It is often desirable to introduce some approximations in the formulas just derived. As is the usual case, for $X_t > 10\,a_b$, we can write an approximation to Eq. (8.25) as

$$2R_b \cong a_b\left(\frac{X_m}{X_t}\right)^2 \tag{8.28}$$

As a result, by substitution in Eq. (8.26), we get

$$X_b \cong \frac{X_2' X_m}{2X_t} + \frac{a_b R_b}{X_m} \tag{8.29}$$

We can introduce further simplifications by assuming that $X_m/X_t \cong 1$, to obtain from Eq. (8.28)

$$2R_b \cong a_b = \frac{R_2'}{2 - s} \tag{8.30}$$

Equation (8.29) reduces to the approximate form

$$X_b \cong \frac{X_2'}{2} + \frac{a_b^2}{2X_m} \tag{8.31}$$

Of course, if we neglect the second term in Eq. (8.31), we obtain the most simplified representation of the backward impedance as

$$R_b = \frac{R_2'}{2(2 - s)} \tag{8.32}$$

$$X_b = \frac{X_2'}{2} \tag{8.33}$$

Equations (8.32) and (8.33) imply that $X_m/2$ is considered an open circuit in the backward-field circuit, as shown in Fig. 8.8.

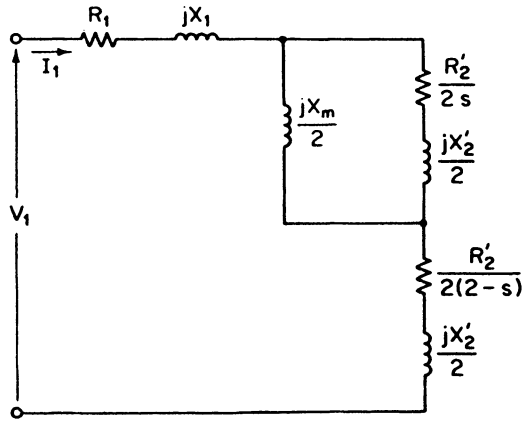


Figure 8.8 Approximate equivalent circuit of a single-phase induction motor.

www.EngineeringEBooksPdf.com

8.4 POWER AND TORQUE RELATIONS

The development of an equivalent-circuit model of a running single-phase induction motor enables us to quantify power and torque relations in a simple way. The power input to the stator P_i is given by

$$P_i = V_1 I_1 \cos\phi_1 \tag{8.34}$$

where ϕ_1 is the phase angle between V_1 and I_1. Part of this power will be dissipated in stator ohmic losses, P_{l_s}, given by

$$P_{l_s} = I_1^2 R_1 \tag{8.35}$$

The core losses will be accounted for as a fixed loss and are treated in the same manner as the rotational losses at the end of the analysis. The air-gap power, P_g, is thus given by

$$P_g = P_i - P_{l_s} \tag{8.36}$$

The air-gap power is the power input to the rotor circuit and can be visualized to be made up of two components. The first component is the power taken up by the forward field and is denoted by P_{gf}, and the second is the backward field power denoted by P_{gb}. Thus we have

$$P_g = P_{gf} + P_{gb} \tag{8.37}$$

Since we have modeled the forward-field circuit by an impedance Z_f, it is natural to write

$$P_{gf} = |I_1|^2 R_b \tag{8.38}$$

Similarly, we write

$$P_{gb} = |I_1|^2 R_b \tag{8.39}$$

The ohmic losses in the rotor circuit are treated in a similar manner. The losses in the rotor circuit due to the forward field, $P_{l_{rf}}$, can be written as

$$P_{l_{rf}} = s_f P_{gf} \tag{8.40}$$

Similarly, the losses in the rotor circuit due to the backward field $P_{l_{rb}}$ are written as

$$P_{l_{rb}} = s_b P_{gb} \tag{8.41}$$

www.EngineeringEBooksPdf.com

Equations (8.40) and (8.41) are based on arguments similar to those used with the balanced three-phase induction motor. Specifically, the total rotor equivalent resistance in the forward circuit is given by

$$R_{rf} = \frac{R_2'}{2s_f} \tag{8.42}$$

This is written as

$$R_{rf} = \frac{R_2'}{2} + \frac{R_2'(1 - s_f)}{2s_f} \tag{8.43}$$

The first term corresponds to the rotor ohmic loss due to the forward field, and the second represents the power to mechanical load and fixed losses. It is clear from Fig. 8.9 that

$$P_{l_{rf}} = |I_{rf}|^2 \frac{R_2'}{2} \tag{8.44}$$

and

$$P_{gf} = |I_{rf}|^2 \frac{R_2'}{2s_f} \tag{8.45}$$

Combining Eqs. (8.44) and (8.45), we get (8.40). A similar argument leads to Eq. (8.41). It is noted here that Eqs. (8.38) and (8.45) are equivalent, since the active power to the rotor circuit is consumed only in the right-hand branch, with $jX_m/2$ being a reactive element.

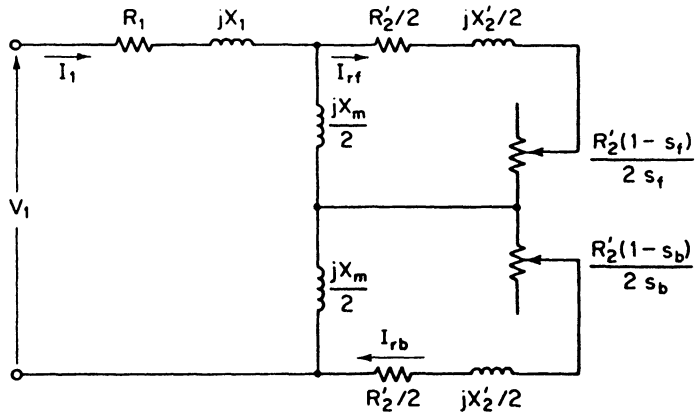


Figure 8.9 Equivalent circuit of single-phase induction motor showing rotor-loss components in the forward and backward circuits.

www.EngineeringEBooksPdf.com

The net power from the rotor circuit is denoted by P_m and is given by

$$P_m = P_{mf} + P_{mb} \tag{8.46}$$

The component P_{mf} is due to the forward circuit and is given by

$$P_{mf} = P_{gf} - P_{l_f} \tag{8.47}$$

Using Eq. (8.40), we get

$$P_{mf} = (1 - s_f)P_{gf} \tag{8.48}$$

Similarly, P_{mb} is due to the backward circuit and is given by

$$P_{mb} = P_{gb} - P_{l_b} \tag{8.49}$$

Using Eq. (8.41), we get

$$P_{mb} = (1 - s_b)P_{gb} \tag{8.50}$$

Recall that

$$s_f = s$$
$$s_b = 2 - s$$

As a result,

$$P_{mf} = (1 - s)P_{gf} \tag{8.51}$$
$$P_{mb} = (s - 1)P_{gf} \tag{8.52}$$

We now substitute Eqs. (8.51) and (8.52) into (8.46), to obtain

$$P_m = (1 - s)(P_{gf} - P_{gb}) \tag{8.53}$$

The shaft power output, P_o, can now be written as

$$P_o = P_m - P_{rot} - P_{core} \tag{8.54}$$

The rotational losses are denoted by P_{rot} and the core losses are denoted by P_{core}.

The output torque, T_o, is obtained as

$$T_o = \frac{P_o}{\omega_r} \tag{8.55}$$

www.EngineeringEBooksPdf.com

If fixed losses are neglected, then

$$T_m = \frac{P_m}{\omega_s(1-s)} \tag{8.56}$$

As a result, using Eq. (8.53), we get

$$T_m = \frac{1}{\omega_s}(P_{gf} - P_{gb}) \tag{8.57}$$

The torque due to the forward field is

$$T_{mf} = \frac{P_{mf}}{\omega_r} = \frac{P_{gf}}{\omega_s} \tag{8.58}$$

The torque due to the backward field is

$$T_{mb} = \frac{P_{mb}}{\omega_r} = \frac{P_{gb}}{\omega_s} \tag{8.59}$$

It is thus clear that the net mechanical torque is the algebraic sum of a forward torque T_{mf} (positive) and a backward torque T_{mb} (negative). Note that at starting, $s = 1$ and $R_f = R_b$, and as a result $P_{gf} = P_{gb}$, giving zero output torque. This confirms our earlier statements about the need for starting mechanisms for a single-phase induction motor. This is treated in Section 8.5. We now look at an example.

Example 8.2 For the single-phase induction motor of Example 8.1, it is required that the power and torque output, and the efficiency when running at a slip of 5%, be found. Neglect core and rotational losses.

Solution In Example 8.1, we obtained

$$Z_i = 26.841\angle 43.36 \text{ deg}$$

As a result, with $V_1 = 110\angle 0$, we obtain

$$I_1 = \frac{110\angle 0}{26.841\angle 43.36 \text{ deg}} = 4.098\angle -43.36 \text{ deg A}$$

The power factor is thus

$$\cos\phi_1 = \cos 43.36 \text{ deg} = 0.727$$

The power input is

$$P_1 = V_1 I_1 \cos\phi_1 = 327.76 \text{ W}$$

www.EngineeringEBooksPdf.com

We have from Example 8.1 for $s = 0.05$,

$$R_f = 17.294\ \Omega \qquad R_b = 0.721\ \Omega$$

Thus we have

$$P_{gf} = |I_1|^2 R_f = (4.098)^2(17.294) = 290.46\,\text{W}$$
$$P_{gb} = |I_1|^2 R_b = (4.098)^2(0.721) = 12.109\,\text{W}$$

The output power is thus obtained as

$$P_m = (1 - s)(P_{gf} - P_{gb})$$
$$= 0.95(290.46 - 12.109) = 264.43\,\text{W}$$

As we have a four-pole machine, we get

$$n_s = \frac{120(60)}{4} = 1800\,\text{rpm}$$
$$\omega_s = \frac{2\pi n_s}{60} = 188.5\,\text{rad/s}$$

The output torque is therefore obtained as

$$T_m = \frac{1}{\omega_s}(P_{gf} - P_{gb})$$
$$= \frac{290.46 - 12.109}{188.5} = 1.4767\,\text{N} \cdot \text{m}$$

The efficiency is now calculated as

$$\eta = \frac{P_m}{P_1} = \frac{264.43}{327.76} = 0.8068$$

It is instructive to account for the losses in the motor. Here we have the static ohmic losses obtained as

$$P_{l_s} = |I_1|^2 R_1 = (4.098)^2(1.5) = 25.193\,\text{W}$$

The forward rotor losses are

$$P_{l_\eta} = sP_{gf} = 0.05(290.46) = 14.523\,\text{W}$$

www.EngineeringEBooksPdf.com

The backward rotor losses are

$$P_{l_{rb}} = (2 - s)P_{gb} = 1.95(12.109) = 23.613\,\text{W}$$

The sum of the losses is

$$P_l = 25.193 + 14.523 + 23.613 = 63.329\,\text{W}$$

The power output and losses should match the power input:

$$P_m + P_l = 264.46 + 63.33 = 327.76\,\text{W}$$

which is indeed the case.

8.5 STARTING SINGLE-PHASE INDUCTION MOTORS

Earlier we showed that a single-phase induction motor with one stator winding is not capable of producing a torque at starting [see, for example, Eq. (8.53) with $s = 1$]. Once the motor is running, it will continue to do so, since the forward-field torque dominates that of the backward-field component. We have also seen that with two stator windings that are displaced by 90 deg in space and with two-phase excitation, a purely forward-rotating field is produced, and therefore this form of a motor (like the balanced three-phase motor) is self-starting.

Methods of starting a single-phase induction motor rely on the fact that given two stator windings displaced by 90 deg in space, a starting torque will result if the flux in one of the windings lags that of the other by a certain phase angle ψ. To verify this, we consider the situation shown in Fig. 8.10. Assume that

$$\phi_A = \phi_M \cos \omega t \tag{8.60}$$

$$\phi_B = \phi_M \cos(\omega t - \psi) \tag{8.61}$$

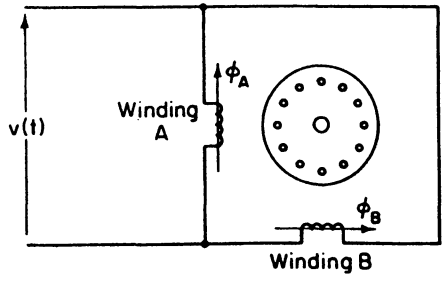


Figure 8.10 Two stator windings to explain the starting mechanism of single-phase induction motors.

www.EngineeringEBooksPdf.com

Clearly, the flux at P is given by the sum of ϕ_{P_A} and ϕ_{P_B}, where

$$\phi_{P_A} = \phi_A \cos\theta \tag{8.62}$$
$$\phi_{P_B} = \phi_B \sin\theta \tag{8.63}$$

As a result, we have

$$\phi_{P_A} = \frac{\phi_M}{2}[\cos(\theta - \omega t) + \cos(\theta + \omega t)] \tag{8.64}$$
$$\phi_{P_B} = \frac{\phi_M}{2}\{\cos\psi[\sin(\theta + \omega t) + \sin(\theta - \omega t)] + \sin\psi[\cos(\theta - \omega t) - \cos(\theta + \omega t)]\} \tag{8.65}$$

The flux at P is therefore obtained as

$$\phi_P = \frac{\phi_M}{2}[a_{f_r}\cos(\theta - \omega t) + a_{f_i}\sin(\theta - \omega t) + a_{b_r}\cos(\theta + \omega t) + a_{b_i}\sin(\theta + \omega t)] \tag{8.66}$$

where we have

$$a_{fr} = 1 + \sin\psi \tag{8.67}$$
$$a_{fi} = \cos\psi \tag{8.68}$$
$$a_{b_r} = 1 - \sin\psi \tag{8.69}$$
$$a_{b_i} = \cos\psi \tag{8.70}$$

Note that we can also define the magnitudes a_f and a_b by

$$a_f^2 = a_{f_r}^2 + a_{f_i}^2 = 2(1 + \sin\psi) \tag{8.71}$$
$$a_b^2 = a_{b_r}^2 + a_{b_i}^2 = 2(1 - \sin\psi) \tag{8.72}$$

The angles α_f and α_b are defined next by

$$\cos\alpha_f = \frac{a_{f_r}}{a_f} = \sqrt{\frac{1 + \sin\psi}{2}} \tag{8.73}$$
$$\cos\alpha_b = \frac{a_{b_r}}{a_b} = \sqrt{\frac{1 - \sin\psi}{2}} \tag{8.74}$$
$$\sin\alpha_f = \frac{a_{f_i}}{a_f} = \frac{\cos\psi}{\sqrt{2(1 + \sin\psi)}} \tag{8.75}$$
$$\sin\alpha_b = \frac{a_{b_i}}{a_b} = \frac{\cos\psi}{\sqrt{2(1 - \sin\psi)}} \tag{8.76}$$

www.EngineeringEBooksPdf.com

We can now write the flux ϕ_P as

$$\phi_P = \frac{\phi_M}{2}[a_f \cos(\theta - \omega t + \alpha_f) + a_b \cos(\theta + \omega t - \alpha_b)] \tag{8.77}$$

It is clear that ϕ_P is the sum of a forward-rotating component ϕ_f and a backward-rotating component ϕ_b given by

$$\phi_P = \phi_f(t) + \phi_b(t) \tag{8.78}$$

where

$$\phi_f(t) = \frac{a_f \phi_M}{2} \cos(\theta - \omega t + \alpha_f) \tag{8.79}$$

$$\phi_b(t) = \frac{a_b \phi_M}{2} \cos(\theta + \omega t - \alpha_b) \tag{8.80}$$

Let us note here that from Eqs. (8.71) and (8.72), we can see that

$$a_f > a_b \tag{8.81}$$

As a result, the magnitude of the forward-rotating wave is larger than that of the backward-rotating wave. Equation (8.3) for a two-phase machine is a special case of Eq. (8.77), with $\psi = 90$ deg, and hence, $a_b = 0$, as can be seen from Eq. (8.72). It is now clear that for the arrangement of Fig. 8.10, a starting torque should result. This is the basis of the starting mechanisms for the single-phase induction motors discussed in this section.

Single-phase induction motors are referred to by names that describe the method of starting. A number of types of single-phase induction motors are now discussed.

8.5.1 Split-Phase Motors

A single-phase induction motor with two distinct windings on the stator that are displaced in space by 90 electrical degrees is called a split-phase motor. The main (or running) winding has a lower R/X ratio than the auxiliary (or starting) winding. A

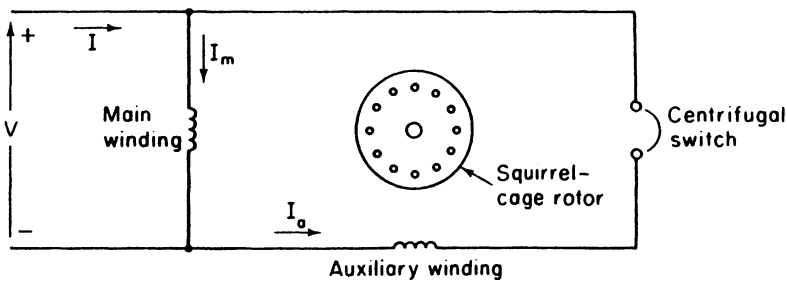


Figure 8.11 Schematic diagram of a split-phase induction motor.

www.EngineeringEBooksPdf.com

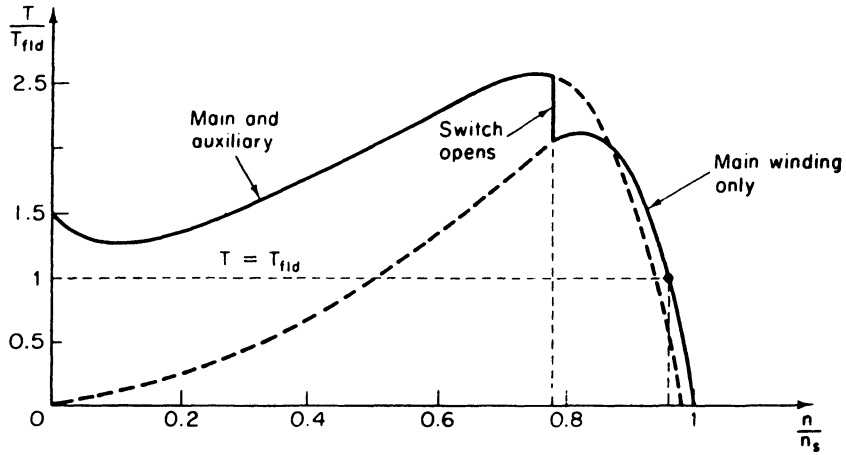


Figure 8.12 Torque–speed characteristic of a split-phase induction motor.

starting switch disconnects the auxiliary winding when the motor is running at approximately 75 or 80% of synchronous speed. The switch is centrifugally operated. The rotor of a split-phase motor is of the squirrel-cage type. At starting, the two windings are connected in parallel across the line, as shown in Fig. 8.11.

The split-phase design is one of the oldest single-phase motors, and is most widely used in the ratings of 0.05 and 0.33 hp. A split-phase motor is used in machine tools, washing machines, oil burners, and blowers, to name just a few of its applications.

The torque–speed characteristic of a typical split-phase induction motor is shown in Fig. 8.12. At starting the torque is about 150% of its full-load value. As the motor speed picks up, the torque is increased (except for a slight decrease at low speed) and may reach higher than 250% of full-load value. The switch is opened and the motor runs on its main winding alone and the motor reaches its equilibrium speed when the torque developed is matched by the load.

8.5.2 Capacitor-Start Motors

The class of single-phase induction motors in which the auxiliary winding is connected in series with a capacitor is referred to as that of capacitor motors. The auxiliary winding is placed 90 electrical degrees from the main winding. There are three distinct types of capacitor motors in common practice. The first type, which we discuss presently, employs the auxiliary winding and capacitor only during starting and is thus called a capacitor-start motor. It is therefore evident that a centrifugal switch that opens at 75 to 80% of synchronous speed is used in the auxiliary winding circuit (sometimes called the capacitor phase). A sketch of the capacitor-start motor connection is shown in Fig. 8.13. A commercial capacitor-start motor is not simply a split-phase motor with a capacitor inserted in the auxiliary circuit, but is a specially designed motor that produces higher torque than the corresponding split-phase version.

Capacitor-start motors are extremely popular and are available in all ratings from 0.125 hp and up. For ratings at one-third hp and above, capacitor-start motors are

www.EngineeringEBooksPdf.com

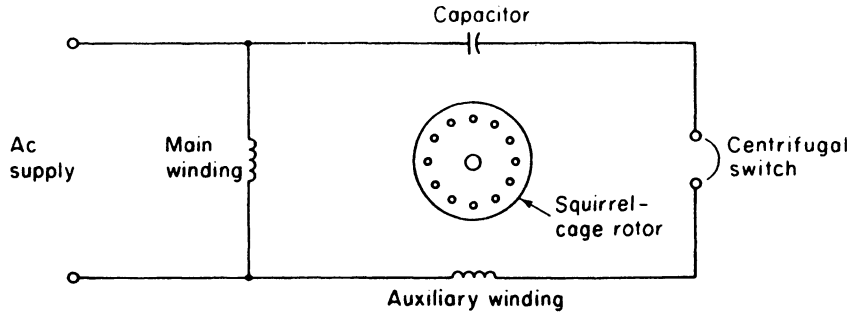


Figure 8.13 Capacitor-start motor.

wound as dual-voltage so that they can be operated on either a 115- or a 230-V supply. In this case, the main winding is made of two sections that are connected in series for 230-V operation or in parallel for 115-V operation. The auxiliary winding in a dual-voltage motor is made of one section that is connected in parallel with one section of the main winding for 230-V operation.

It is important to realize that the capacitor voltage increases rapidly above the switch-open speed and the capacitor can be damaged if the centrifugal switch fails to open at the designated speed. It is also important that switches not flutter, as this causes a dangerous rise in the voltage across the capacitor.

A typical torque–speed characteristic for a capacitor-start single-phase induction motor is shown in Fig. 8.14. The starting torque is very high, which is a desirable feature of this type of motor.

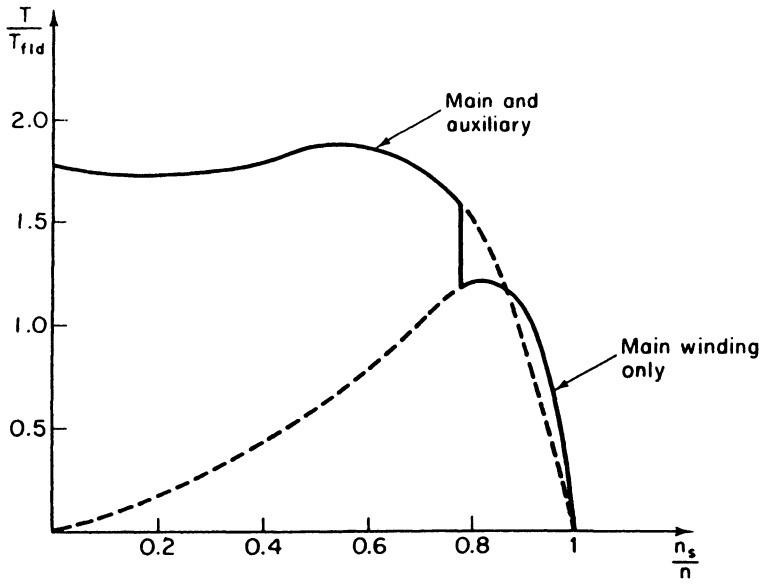


Figure 8.14 Torque–speed characteristic of a capacitor-start motor.

www.EngineeringEBooksPdf.com

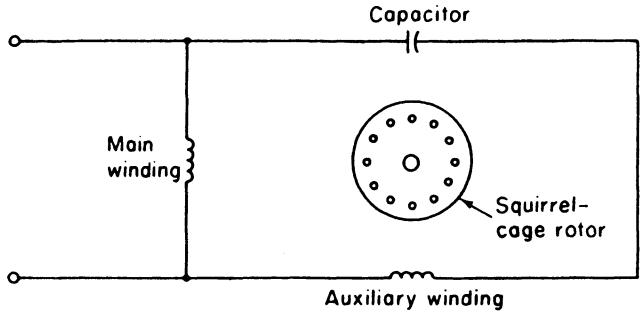


Figure 8.15 Permanent-split capacitor motor.

8.5.3 Permanent-Split Capacitor Motors

The second type of capacitor motor is referred to as the permanent-split capacitor motor, where the auxiliary winding and the capacitor are retained at normal running speed. This motor is used for special-purpose applications requiring high torque and is available in ratings from 10^{-3} hp to 1/3–3/4 hp. A schematic of the permanent-split capacitor motor is shown in Fig. 8.15.

A typical torque–speed characteristic for a permanent-split capacitor motor is shown in Fig. 8.16. The starting torque is noticeably low, since the capacitance is a compromise between best running and starting conditions. The next type of motor overcomes this difficulty.

8.5.4 Two-Value Capacitor Motors

A two-value capacitor motor is the third type of the class of capacitor motors and starts with one value of capacitors in series with the auxiliary winding and runs with a different capacitance value. This change can be done either using two

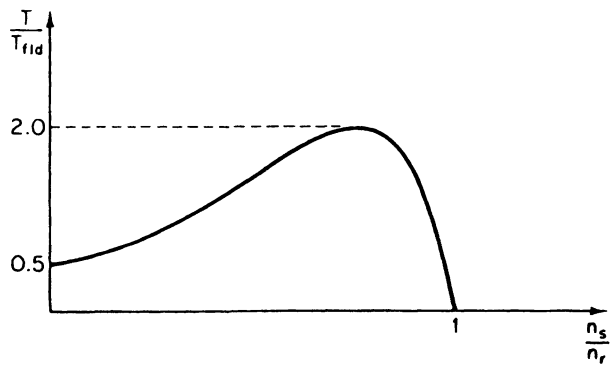


Figure 8.16 Torque–speed characteristic of a permanent-split single-phase induction motor.

www.EngineeringEBooksPdf.com

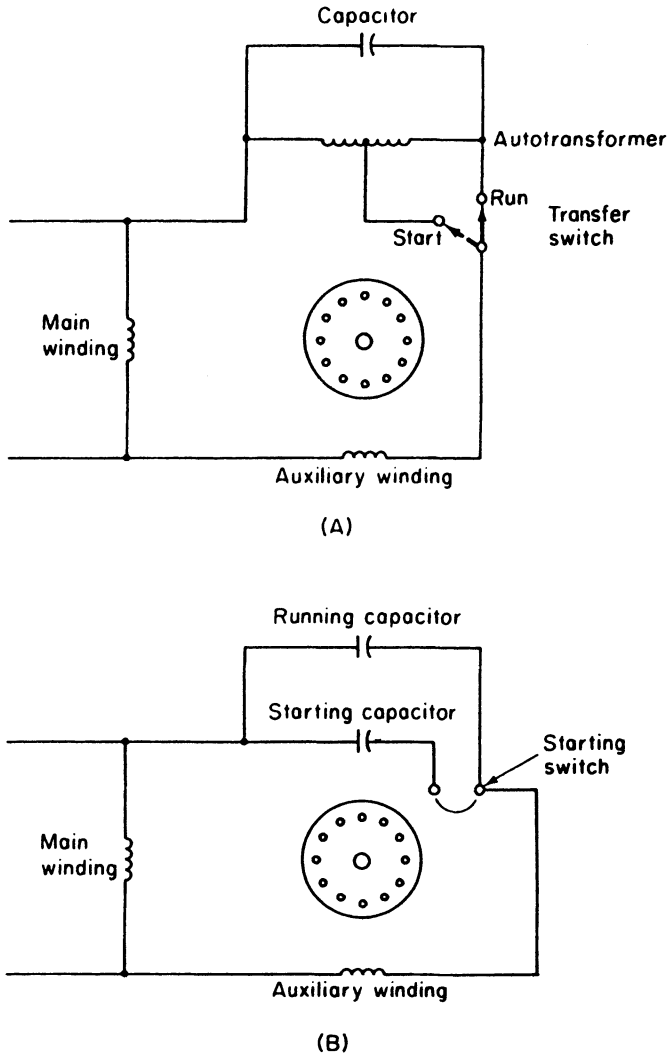


Figure 8.17 Two-value capacitor motor: (a) autotransformer type; (b) two-capacitor type.

separate capacitors or through the use of an autotransformer. This motor has been replaced by the capacitor-start motor for applications such as refrigerators and compressors.

For the motor using an autotransformer, a transfer switch is used to change the tap on the autotransformer, as shown in Fig. 8.17(a). This arrangement appears to be obsolete now and the two-capacitor mechanism illustrated in Fig. 8.17(b) is used.

A typical torque–speed characteristic for a two-value capacitor motor is shown in Fig. 8.18. Note that optimum starting and running conditions can be accomplished in this type of motor.

www.EngineeringEBooksPdf.com

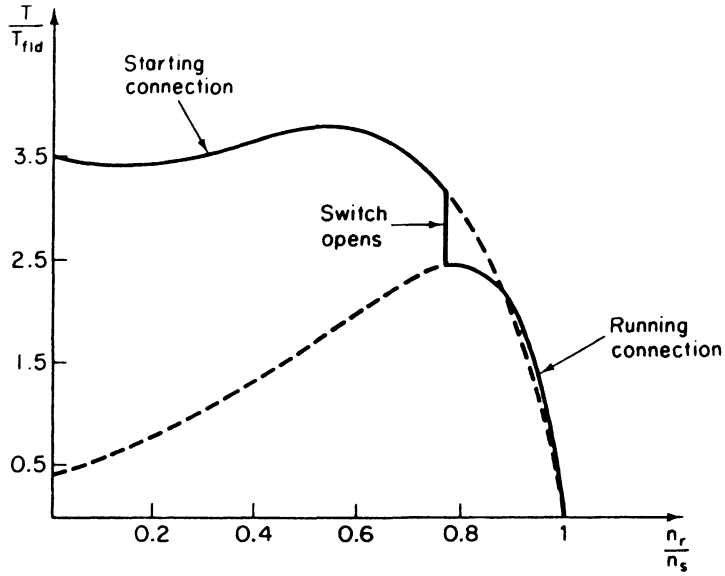


Figure 8.18 Torque–speed characteristic of a two-value capacitor motor.

8.5.5 Repulsion-Type Motors

A repulsion motor is a single-phase motor with power connected to the stator winding and a rotor whose winding is connected to a commutator. The brushes on the commutator are short-circuited and are positioned such that there is an angle of 20 to 30 between the magnetic axis of the stator winding and the magnetic axis of the rotor winding. A representative torque–speed characteristic for a repulsion motor is shown in Fig. 8.19. A repulsion motor is a variable-speed motor.

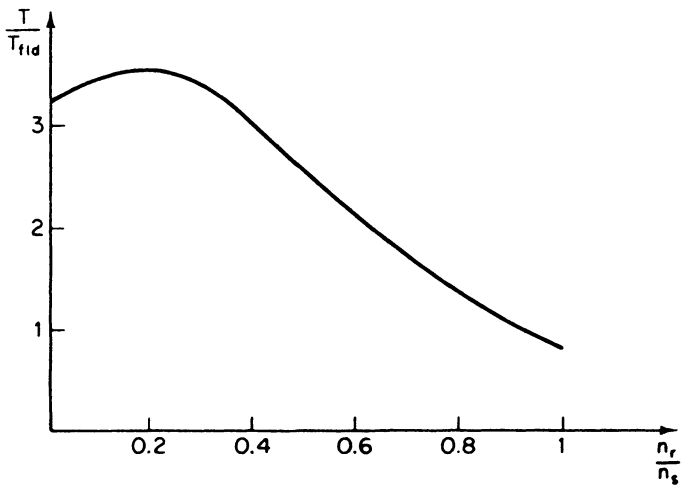


Figure 8.19 Torque–speed characteristic of a repulsion motor.

www.EngineeringEBooksPdf.com

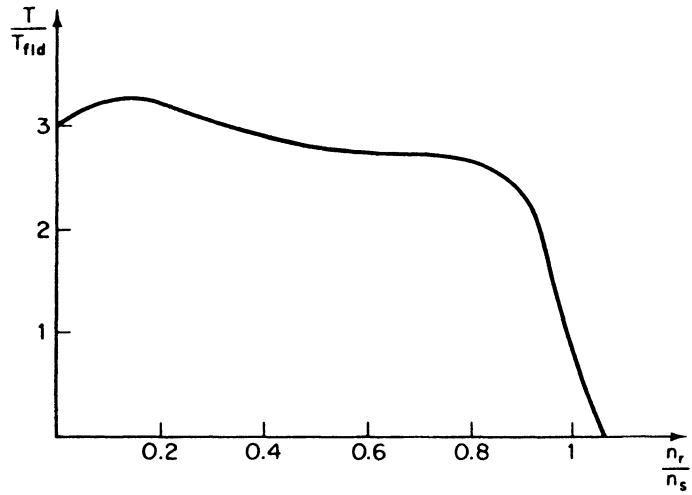


Figure 8.20 Torque–speed characteristic of a repulsion–induction motor.

If in addition to the repulsion winding, a squirrel-cage type of winding is embedded in the rotor, we have a repulsion–induction motor. The torque–speed characteristic for a repulsion–induction motor is shown in Fig. 8.20 and can be thought of as a combination of the characteristics of a single-phase induction motor and that of a straight repulsion motor.

A repulsion-start induction motor is a single-phase motor with the same windings as a repulsion motor, but at a certain speed the rotor winding is short-circuited to give the equivalent of a squirrel-cage winding. The repulsion-start motor is the first type of single-phase motor that gained wide acceptance. In recent years, however, it has been replaced by capacitor-type motors. A typical torque–speed characteristic of a repulsion-start induction motor is shown in Fig. 8.21.

8.5.6 Shaded-Pole Induction Motors

For applications requiring low power of 1/4 hp or less, a shaded-pole induction motor is the standard general-purpose device for constant-speed applications. The torque characteristics of a shaded-pole motor are similar to those of a permanent-split capacitor motor as shown in Figure 8.22. It is important to understand the action of pole shading, which is discussed next.

8.5.6.1 Shaded-Pole Action Consider the magnetic structure shown in Fig. 8.23(a). If we neglect the reluctance of the iron path, an equivalent circuit is obtained, as shown in Fig. 8.23(b). The flux ϕ_s is seen to be equal to the flux ϕ_m if the two air gaps are identical. The MMF of the main coil $F_1 = N_1 I_1$ is sinusoidal if the coil is connected to an ac source, and thus ϕ_s and ϕ_m are also sinusoidal of equal magnitude and phase.

www.EngineeringEBooksPdf.com

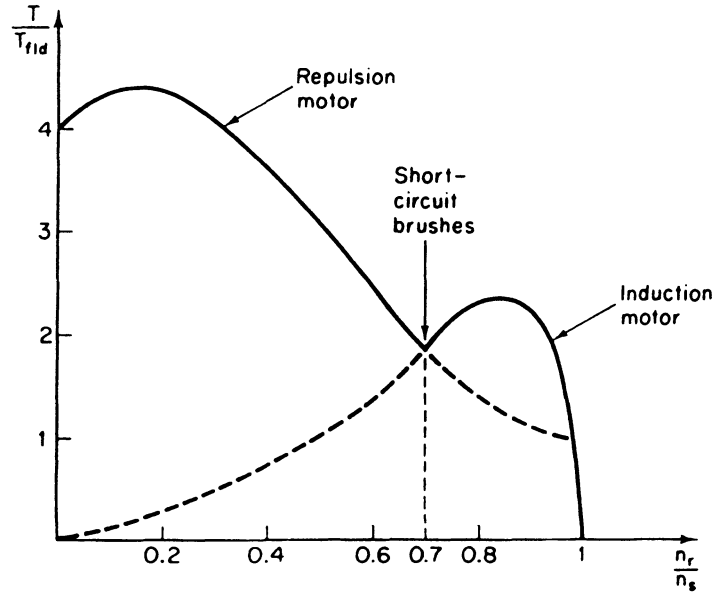


Figure 8.21 Torque–speed characteristic of a repulsion-start single-phase induction motor.

The magnetic structure of Fig. 8.23(c) is similar to that of Fig. 8.23(a), except that a coil of N_s turns is placed on the rightmost portion. The coil is called a *shading coil*, and its two terminals are short-circuited. As a result of the sinusoidal variations of ϕ_s, an induced EMF E_s is produced in the shading and it lags ϕ_s by 90 deg. A current, I_s, is set up in the shading coil and lags E_s by the angle $\theta_s = \arctan(\omega L_s/R_s)$, where ω is due to the supply and L_s and R_s are the inductance and resistance of the shading-coil winding, respectively. A phasor diagram showing ϕ_s, E_s, and I_s is given in Fig. 8.23(d).

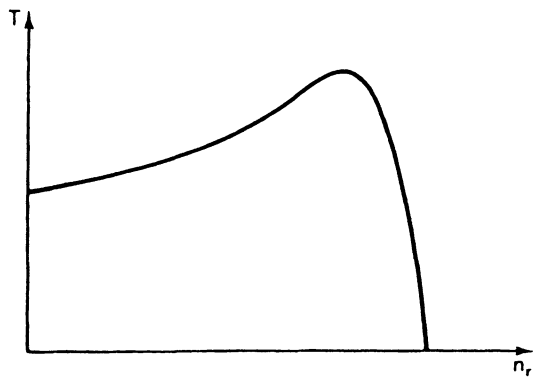


Figure 8.22 Torque–speed characteristic of a shaded-pole induction motor.

www.EngineeringEBooksPdf.com

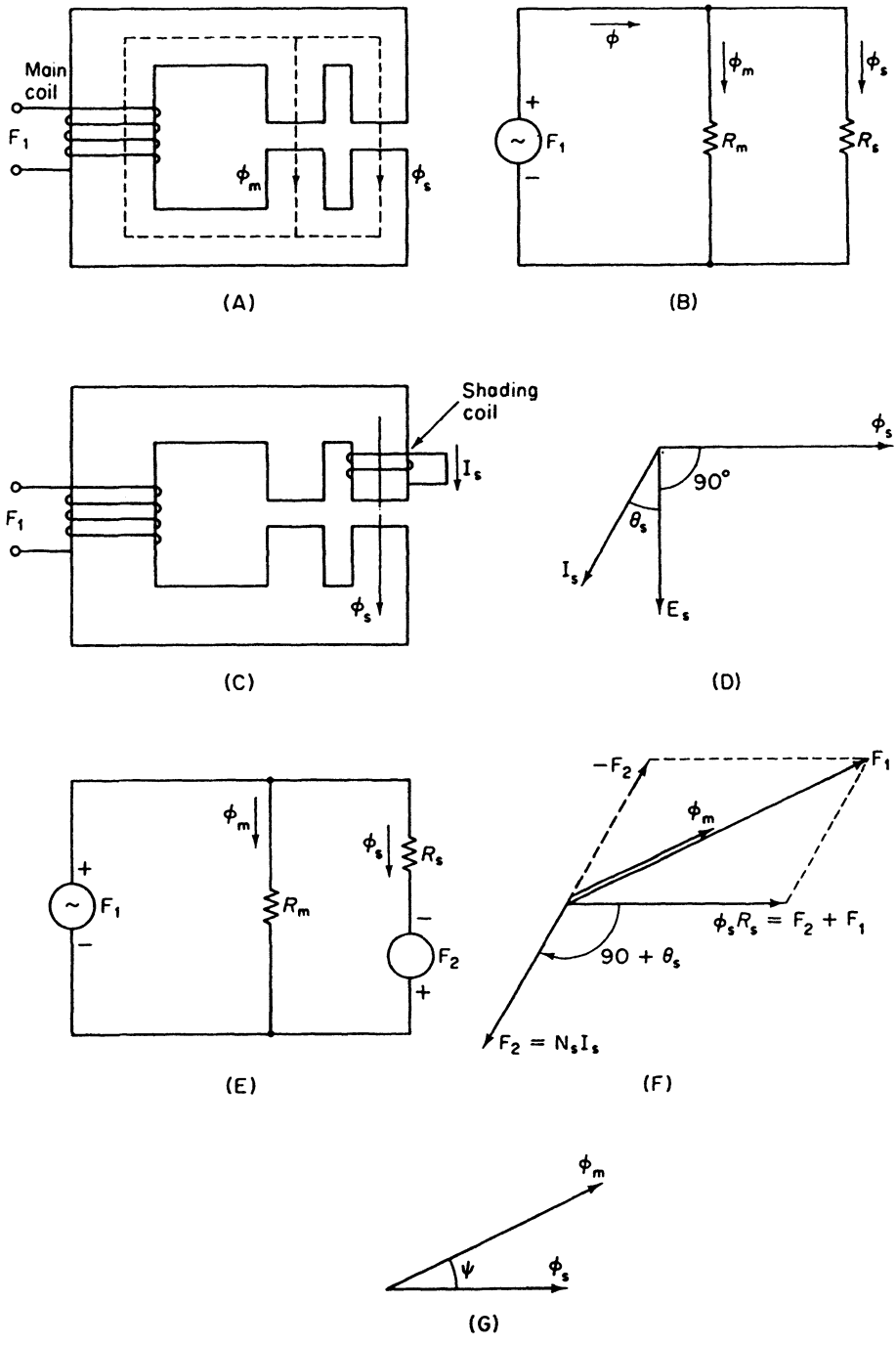


Figure 8.23 Shaded-pole action.

www.EngineeringEBooksPdf.com

The shading coil is thus seen to produce an MMF $F_2 = N_s I_s$, which is proportional to and in phase with I_s. The magnetic equivalent circuit of Fig. 8.23(e) shows the effect of the shading pole. The MMF of the right-hand reluctance is $\Re_s$, and is given by

$$\phi_s \Re_s = F_1 + F_2$$

It is clear by inspection of Fig. 8.23(f) that F_1 is obtained by subtracting F_2 from $\phi_s \Re_s$. Observing that F_1 impressed on $\Re_m$ leads us to conclude that ϕ_m is in phase with F_1. It is clear now that the effect of the shading coil is to cause the flux, ϕ_s, to lag ϕ_m by a certain angle, ψ. This is shown in Fig. 8.23(g) and is the basis of explaining the operation of shaded-pole motors.

Some Solved Problems

Problem 8.A.1 A single-phase induction motor takes an input power of 490 W at a power factor of 0.57 lagging from a 110-V supply when running at a slip of 5%. Assume that the rotor resistance and reactance are 1.78 Ω and 1.28 Ω, respectively, and that the magnetizing reactance is 25 Ω. Find the resistance and reactance of the stator.

Solution The equivalent circuit of the motor yields

$$Z_f = \frac{\{[1.78/2(0.05)] + j0.64\}(j12.5)}{[1.78/2(0.05)] + j(0.64 + 12.5)} = 5.6818 + j8.3057$$

$$Z_b = \frac{\{[1.78/2(1.95)] + j0.64\}(j12.5)}{[1.78/2(1.95)] + j(0.64 + 12.5)} = 0.4125 + j0.6232$$

As a result of the problem specifications:

$$P_i = 490\,\text{W} \qquad \cos\phi = 0.57 \qquad V = 110$$

$$I_i = \frac{P_i}{V\cos\phi} = \frac{590}{110(0.57)} = 7.815\angle -55.2488 \text{ deg}$$

Thus the input impedance is

$$Z_i = \frac{V}{I_i} = \frac{110}{7.815}\angle 55.2498 \text{ deg} = 8.023 + j11.5651$$

The stator impedance is obtained as

$$Z_1 = Z_i - (Z_f + Z_b) = 1.9287 + j2.636\,\Omega$$

Problem 8.A.2 The forward-field impedance of a one-quarter-hp four-pole 110-V 60-Hz single-phase induction motor for a slip of 0.05 is given by

$$Z_f = 12.4 + j16.98\ \Omega$$

www.EngineeringEBooksPdf.com

Assume that

$$X_m = 53.5\ \Omega$$

Find the values of the rotor resistance and reactance.

Solution We have

$$Z_f = \frac{j0.5X_m[0.5(R_2'/s) + j0.5X_2']}{0.5(R_2'/s) + j0.5(X_2' + X_m)}$$

Thus

$$12.4 + j16.98 = \frac{j26.75[(R_2'/s) + jX_2']}{(R_2'/2) + j(X_2' + 53.5)}$$

As a result, cross multiplying and separating real and imaginary parts, we obtain

$$0.3652\frac{R_2'}{s} - 0.4636X_s' = 24.8$$
$$0.4636\frac{R_2'}{s} - 0.3652X_s' = 33.96$$

Solving the two equations, we get

$$X_2' = 2.605\ \Omega$$
$$\frac{R_2'}{s} = 71.208$$

Thus

$$R_2' = 3.5604\ \Omega$$

Problem 8.A.3 For the motor of Problem 8.A.2, assume that the stator impedance is given by

$$Z_1 = 1.86 + j2.56\ \Omega$$

Find the internal mechanical power, output power, power factor, input power, developed torque, and efficiency, assuming that friction losses are 15 W.

Solution We need the backward-field impedance

$$Z_b = \frac{j0.5X_m'[0.5(R_2'/(2-s)) + j0.5X_2']}{0.5(R_2'/(2-s)) + j0.5(X_2' + X_m')}$$
$$= \frac{j26.75[(1.78/1.95) + j1.3]}{(1.78/1.95) + j(1.3 + 26.75)}$$
$$= 0.8293 + j1.2667\ \Omega$$

www.EngineeringEBooksPdf.com

As a result,

$$\begin{aligned} Z_i &= Z_1 + Z_f + Z_b \\ &= 15.089 + j20.8067 = 25.7023\angle 54.05 \text{ deg}\,\Omega \end{aligned}$$

The input current is thus

$$I_1 = \frac{V}{Z_i} = \frac{110\angle 0}{25.7023\angle 54.05} = 4.2798\angle -54.05 \text{ deg A}$$

The forward-gap power is

$$P_{gf} = |I_1|^2 R_f = 227.125 \text{ W}$$

The backward-gap power is

$$P_{gb} = |I_1|^2 R_b = 15.1899 \text{ W}$$

As a result, the internal mechanical power is

$$\begin{aligned} P_m &= (1 - s)(P_{gf} - P_{gb}) \\ &= 201.338 \text{ W} \end{aligned}$$

The output power is thus

$$P_o = 201.338 - 15 = 186.338 \text{ W}$$

The power factor is given by

$$\text{PF} = \cos 54.05 \text{ deg} = 0.5871$$

The input power is calculated as

$$P_{in} = 110(4.2798)(0.5871) = 276.383 \text{ W}$$

As a result, the efficiency is

$$\eta = \frac{P_o}{P_{in}} = \frac{186.338}{276.383} = 0.6742$$

The synchronous speed is

$$n_s = \frac{120f}{P} = 1800 \text{ rpm}$$

www.EngineeringEBooksPdf.com

The rotor speed in rad/s is thus

$$\omega_r = \frac{2\pi n_s}{60}(1 - s) = 57\pi$$

The torque output is given by

$$T_o = \frac{P_o}{\omega_r} = \frac{186.338}{57\pi} = 1.0406\,\text{N} \cdot \text{m}$$

PROBLEMS

Problem 8.B.1 The following parameters are available for a single-phase induction motor

$$R_1 = 1.4\ \Omega \qquad R_2' = 3.34\ \Omega$$
$$X_1 = X_2' = 3.2\ \Omega \qquad X_m = 98\ \Omega$$

Calculate Z_f, Z_b, and the input impedance of the motor for a slip of 0.06.

Problem 8.B.2 The induction motor of Problem 8.B.1 is a 60-Hz 110-V four-pole machine. Find the output power and torque under the conditions of Problem 8.B.1, assuming that the core losses are 66 W. Neglect rotational losses.

Problem 8.B.3 A four-pole 110-V 60-Hz single-phase induction motor has the following parameters:

$$R_1 = 0.83\ \Omega \qquad R_2' = 0.94\ \Omega$$
$$X_1 = X_2' = 1.92\ \Omega \qquad X_m = 42\ \Omega$$

The core losses are equal to the rotational losses, which are given by 40 W. Find the output power and efficiency at a slip of 0.05.

Problem 8.B.4 The following parameters are available for a single-phase 110-V induction motor:

$$R_1 = R_2' = 2.65\ \Omega$$
$$X_1 = X_2' = 2.7\ \Omega$$
$$X_m = 70.8\ \Omega$$

The core losses are 18.5 W and rotational losses are 17 W. Assume that the machine has four poles and operates on a 60-Hz supply. Find the rotor ohmic losses, output power, and torque for a slip of 5%.

www.EngineeringEBooksPdf.com

Problem 8.B.5 The stator resistance of a single-phase induction motor is 1.95 Ω and the rotor resistance referred to the stator is 3.4 Ω. The motor takes a current of 4.2 A from the 110-V supply at a power factor of 0.624 when running at a slip of 0.05. Assume that the core loss is 36 W and that the approximation of Eq. (8.32) is applicable. Find the motor's output power and efficiency, neglecting rotational losses.

Problem 8.B.6 A single-phase induction motor takes an input power of 280 W at a power factor of 0.6 lagging from a 110-V supply when running at a slip of 5%. Assume that the rotor resistance and reactance are 3.38 and 2.6 Ω, respectively, and that the magnetizing reactance is 60 Ω. Find the resistance and the reactance of the stator.

Problem 8.B.7 For the motor of Problem 8.B.6, assume that the core losses are 35 W and the rotational losses are 14 W. Find the output power and efficiency when running at a slip of 5%.

Problem 8.B.8 The output torque of a single-phase induction motor is 0.82 N · m at a speed of 1710 rpm. The efficiency is 60% and the fixed losses are 37 W. Assume that the motor operates on a 110-V supply and that the stator resistance is 2 Ω. Find the input power factor and input impedance. Assume that the rotor ohmic losses are 35.26 W. Find the forward- and backward-gap power and the values of R_f and R_b. Assume a four-pole machine.

www.EngineeringEBooksPdf.com

BIBLIOGRAPHY

Adler, M. S., Owyang, K. W., Baliga, B. J., and Kokosa, R. A., "The Evolution of Power Device Technology," *IEEE Trans. Electron Devices*, Nov. 1984, pp. 1570–1591.

Bird, B. M., King, K. G., and D. A. G. Pedder, *An Introduction to Power Electronics*, 2nd ed., Wiley, New York, 1993.

Bose, B. K. *Power Electronics & AC Drives*, Prentice Hall, Englewood Cliffs, NJ, 1986.

Bose, B. K., "Introduction to Power Electronics," in *Modern Power Electronics: Evolution, Technology, and Applications*, B. K. Bose, Editor, IEEE Press, 1992, pp. 3–40.

Datta, S. K., *Power Electronics and Controls*, Reston Publishing, Reston, VA, 1985.

Dewan, S. B. and Straughen, A., *Power Semiconductor Circuits*, Wiley, New York, 1975.

Dubey, G. K., *Power Semiconductor Controlled Drives*, Prentice Hall, Englewood Cliffs, NJ, 1989.

El-Hawary, M. E., *Principles of Electric Machines with Power Electronic Applications*, Reston Publishing, Reston, VA, 1986.

Fisher, M. J., *Power Electronics*, PWS-Kent, Boston, MA, 1991.

Ghandi, S. K., *Semiconductor Power Devices*, Wiley-Interscience, New York, 1977.

Grant, D. A. and Gover, J., *Power MOSFETS: Theory and Application*, Wile-Interscience, New York, 1989.

Kassakia, J. G., Schlecht, M. F., and Vergriese, G. C., *Principles of Power Electronics*, Addison-Wesley, Reading, MA, 1991.

Lander, C. W., *Power Electronics*, 2nd ed., McGraw-Hill, New York, 1987.

Mohan, N., Undeland, T. M., and Robbins, W. P., *Power Electronics: Converters, Applications, and Design*, Wiley, New York, 1989.

Pearman, R. A., *Power Electronics: Solid State Motor Control*, Reston Publishing, Reston, VA, 1980.

www.EngineeringEBooksPdf.com

Ramshaw, R. S., *Power Electronics: Thyristor Controlled Power for Electric Power Motors*, Chapman & Hall, London, 1973.

Rashid, M. H., *Power Electronics: Circuits, Devices, and Applications*, Prentice Hall, Englewood Cliffs, NJ, 1988.

Rice, L. R., *Westinghouse Silicon Controlled Rectifier Designers Handbook*, Westinghouse, Youngwood, PA, 1970.

Sen, P. C., *Thyristor DC Drives*, Wiley, New York, 1981.

Steimer, P. K., Gruning, H. E., Werniger, J., Carroll, E., Klaka, S., and Linder, S., "IGCT—A New Emerging Technology for High Power, Low Cost Inverters," *IEEE Industry Applications Magazine*, July/Aug. 1999, pp. 12–18.

Tarter, R. E., *Principles of Solid State Power Conversion*, SAMS, Indianapolis, IN, 1985.

Vithayathil, J., *Power Electronics: Principles and Applications*, McGraw-Hill, New York, 1995.

www.EngineeringEBooksPdf.com

INDEX

A

ac to ac converter, 178
ac voltage controller, 175
ac-dc drives for dc motor, 255
adjustable-speed dc motor drive, 251
air gap, smooth, 80
air gaps, 48
Alexanderson, E.F.W., 14
Ampère, André Marie, 6
Ampère's bonne homme, 61
Ampère's circuital law, 23, 29, 33, 35
Arago, François, 6
armature, 397
armature-circuit model, 186
armature reaction, 406
  reactance, 403
armature shunt resistance curent control, 226
arrangement, double-cage, 357
asymmetrical SCR, 17
autotransformer, 313, 314
  starting, 356
  three-winding, 315

B

backward field, 454
Bailey, Walter, 12
Bell Laboratories, 16
B-H characteristic, 33
bi-directional ac switch (TRIAC), 17
bi-directional current capability, 108
bi-directional triode thyristor, 145
Biot-Savart law, 23, 26
bipolar junction transistor, 116
bipolar transistors, 117
bipolar voltage-withstanding capability, 108
BJT, 104, 116
  NPN, 105
  PNP, 105
breakdown voltage, 125

C

Capability:
  bi-directional current, 108
  bipolar voltage-withstanding, 108
capacitor, synchronous, 428
capacitor-start motor, 462
changing line frequency, 365
chopper, 177
chopper circuit, 114
circuit:
  chopper, 114
  high-voltage integrated, 18
  Jones, 173
  Morgan, circuit, power integrated, 178
CMOS-technology, 179

www.EngineeringEBooksPdf.com

collector-base saturation voltage, 124
collector-emitter saturation voltage, 124
combined modulation, 177
commutation, 159
  circuitry, 104
  external pulse, 174
  line, 161
  parallel-capacitor, 168
  series capacitor, 161
commutator, 184
composite, 20
compound, differential, 215
compound motor, 212
compound-motor speed control, 238
connection, Δ, 302
consequent pole, 363
constant power load, 220
constant torque load, 219
constant-volts/Hz, 378
control:
  compound-motor speed, 238
  field resistance, 232
  line-voltage, 232, 368
  one-quadrant chopper, 261
  on-off, 176
  phase, 176
  rotor-resistance, 368
  series armature resistance, 230, 235, 236, 239, 240
  series motor speed, 224
  series resistance voltage, 25
  shunt armature resistance, 230, 236, 240
  shunt-field armature resistance, 235, 239
  shunt-field series resistance, 238
  variable-frequency, 370
controlled rectifier, 176
controller, ac voltage, 175
control-type transformer, 273
conventional speed control of dc motor, 224
conversion, electromechanical energy, 23
conversion, high-voltage dc, 139
converter, ac to ac, 178
converter, dc to dc, 177
core loss, 59, 60
critical rate of rise of forward voltage, 157
cross product, 24
crossover time, 125
cumulative compound machine, 213
current, high-voltage direct, 103
current, maximum:
  average forward, 111
  peak leakage, 112
  peak one-cycle nonrepetitive forward, 111
  peak repetitive forward current, 111
  peak reverse, 112
  rms forward, 111
current-fed inverter, 382
  drive, 385
cycloconverter drive, 386
cylindrical construction, 399
cylindrical-rotor, 19, 431

D

Darlington transistor, 17
Davenport, Thomas, 10
dc gain, 124
dc series motor, 190
dc shunt motor, 203
dc to dc converter, 177
dc-dc drives for dc motor, 261
dc-link-converter drive, 381
deep-bar rotor, 356
DeForest, Lee, 14
Δ-connection, 302
depletion MOSFET, 126
Design class:
  A, 351
  B, 352
  C, 353
  D, 353
differential compound, 215
  motor, 214
diode, 105
  characteristic, 108
  general-purpose, 110
  power, 108
diodes, fast-recovery, 110
direct-axis synchronous reactance, 431
direct-current motor, 183
distributed winding, 325
distribution system, 20
double-cage arrangement, 357
double-squirrel-cage rotor, 356
doubly excited system, 75
drive:
  adjustable-speed dc motor, 251
  current-fed inverter, 385
  cycloconverter, 386
  dc-link converter, 381
  static Kramer, 387
  static Scherbius, 288
  voltage-fed inverter, 383

www.EngineeringEBooksPdf.com

E

ECC, 20
eddy-current, 59, 60, 273
Edison, Thomas Alva, 11
efficiency, 199
  transformer, 288
electric power input, 62
electrical degrees, 89
electromechanical energy conversion, 23
energy, 50
  control center (ECC), 20
  flow, 60
  relations, 23
enhancement MOSFET, 126
equivalent circuits of transformer, 283
excitation system, 397
external pulse commutation, 174
external-resistance starting, 355

F

Faraday, Michael, 7, 8
Faraday's law, 23, 62
fast-recovery diodes, 110
ferromagnetic, 57
  material, 32
FET-controlled thyristor, 147
field-circuit model, 187
field control using controlled rectifier, 259
field energy, 64
field resistance control, 232
field weakening, 252
flux (Φ), 37
flux density, 24
  B, 37
flux linkages, 50
forward bias, 104
forward field, 454
forward slope resistance, 112
forward voltage drop, 111
forward-biased safe operating area, 125
fractional-horsepower alternating current motor, 443
frequency modulation, 177
frequency, changing line, 365
frequency, variable-voltage constant, 370
fringing effects, 49

G

Galvani, Luigi, 4
gate turn-off thyristor (GTO), 17, 144
gate-assisted turn-off thyristor, 104, 143
GATT, 104
Gaulard, Lucien, 12
general-purpose diode, 110
generator reactive-capability curves, 415
generator, synchronous, 18
Gibbs, John D., 12
Grey, Stephen, 3
GTO, 17, 105, 144

H

hard ferromagnetic material, 32
hard magnetic material, 58
Henry, Joseph, 6
high-voltage dc conversion (HVDCC), 139
high-voltage direct current (HVDC), 103
high-voltage integrated circuit (HVIC), 18
high-voltage substation, 19
high-voltage transmission line, 19
hoisting motoring, 243
Holmes, Frederick Hale, 9
HVDC, 103, 139
HVIC, 18
hysteresis, 58
  loop, 54, 56, 57
  loss, 273

I

ideal transformer, 274
ignitron, 16
IGT, 18
induced voltage, 50
inductance, 23, 50
induction machine, 84, 323
induction motor, 323
inductive susceptance, 331
industrial, 20
infinite-bus concept, 415
input, electric power, 62
insulated gate bipolar transistor, 136
insulated gate transistor (IGT), 18
inverter, 178
  current-fed, 382
  thyristor, 141
  voltage-fed, 382

J

Jones circuit, 173
junction temperature, 154
junction transistor, 16

www.EngineeringEBooksPdf.com

L

LASCR, 105
Lenz, Heinrich, 11
light-activated silicon-controlled rectifier, 143
light-triggered thyristor, 143
line commutation, 161
line-voltage control, 232, 368
load:
  constant power, 220
  constant torque, 219
  matching, 219
  torque-speed characteristic, 220
Logan, Frank G., 15
Lorentz force law, 23, 25

M

machine:
  cumulative compound, 213
  induction, 84, 323
  p-pole, 85, 89, 398
  round air-gap, 80
  salient-pole, 77, 430
  smooth air-gap, 80
  synchronous, 84, 397
  three-phase, 299
  two-phase, 81
magnetic circuit, 23, 35
magnetic field, 24
  intensity, 31, 32
magnetomotive force, 37
material, hard ferromagnetic, 32
material, hard magnetic, 58
material, soft ferromagnetic, 32
material, soft magnetic, 58
maximum average forward current, 111
maximum peak:
  forward voltage, 112
  leakage current, 112
  nonrepetitive reverse voltage, 111
  one-cycle nonrepetitive forward current, 111
  repetitive forward current, 111
  peak reverse current, 112
maximum power transfer, 418
maximum repetitive peak reverse voltage, 111
maximum rms forward current, 111
mechanical speed, 89
metal-oxide-semiconductor:
  field-effect transistor, 116
  insulated-gate transistor, 116
mmf wave, 324
model, field circuit, 187
model, transformer, 278
modulation:
  combined, 177
  pulse-width, 177
Moll, 17
Morgan circuit, 172
MOSFET, 18, 116
  depletion, 126
  enhancement, 126
  N-Channel, 105
  P-Channel, 105
  power, 104, 106, 126
MOS-gated thyristor, 18
MOSIGT, 132
motor matching, 219
motor:
  ac-dc drives for dc, 255
  capacitor-start, 462
  compound, 212
  conventional speed control of dc, 224
  dc series, 190
  dc shunt, 203
  dc-dc drives for dc, 261
  differential compound, 214
  direct-current, 183
  fractional-horsepower alternating current, 443
  induction, 323
  permanent-split capacitor, 464
  reluctance, 72
  repulsion-type, 466
  separately excited dc, 251
  shaded-pole induction, 467
  single-phase induction, 448
  split-phase, 461
  starting dc, 241
  starting induction, 354
  starting single-phase induction, 459
  two-value, 464
motoring, hoisting, 243
multiple stator winding, 363
multiply excited, 69

N

N-Channel MOSFET, 105
nonrecurrent SCR current rating, 156
NPN BJT, 105

O

Oersted, Hans Christian, 5
Ohm, Georg Simon, 6

www.EngineeringEBooksPdf.com

one-quadrant chopper control, 261
on-off control, 176
overdrive factor, 120
overexcited, 419
overhauling, 371
overhauling generating, 243
overload protection, 359, 361

P

Page, C.G., 12
Page, Charles G., 10
PAM, 363
parallel connection, 294
parallel-capacitor commutation, 168
parallel-series connection, 293
P-Channel MOSFET, 105
percentage voltage regulation, 286
permanent-split capacitor motor, 464
permeability, 31, 38
phase control, 176
  thyristor, 140
  thyristor bridge, 381
phase rotation, 300
phase sequence, 300
plugging, 371
PNP BJT, 105
P-N-P-N transistor, 17
pole, consequent, 363
pole-amplitude modulation, 363
power:
  angle characteristic, 415, 422, 433
  bipolar junction transistor, 104
  diode, 108
  dissipation, 154
  electronics, 13
  integrated circuit, 178
  MOSFET, 104, 106, 126
  systems load, 20
  transistor, 115
  pull-out, 436
  regulation of slip, 387
p-pole machine, 85, 89, 398
Prins Eugen, 16
pull-out power, 436
pulse gate requirement, 108
pulse-width modulation, 177
PVR, 286
PWM, 177
PWM inverter drive, 384

Q

quadrature-axis synchronous reactance, 431

R

RCT, 17
reactance:
  armature reaction, 403
  direct-axis synchronous, 431
  quadrature-axis synchronous, 431
  synchronous, 403
reaction, armature, 406
reactive power generation, 419
rectifier, 16
  controlled, 176
  field control using controlled, 259
  light-activated silicon-controlled, 143
  silicon-controlled (SCR), 17
recurrent SCR current rating, 156
reduced-voltage starting, 355
regulation of slip power, 387
regulation, percentage voltage, 286
reluctance, 38
reluctance motor, 72
repulsion-type motor, 466
residential, 20
resistance, forward slope, 112
reversal of direction of rotation, 241
reverse biased, 108
  safe operating area, 125
reverse conducting thyristor (RCT), 17, 142
reverse recovery:
  characteristic, 109
  charge, 112
  time, 109, 112, 113
rotating magnetic field, 324, 327, 443
rotor:
  deep-bar, rotor, double-squirrel cage, 356
  squirrel-cage, 323
  impedance, 348
  resistance control, 368
  slip energy recovery, 368
round air-gap machine, 80
round-rotor, 401

S

salient-pole construction, 399
salient-pole machine, 77, 430
SCADA, 20

www.EngineeringEBooksPdf.com

Scherbius drive, 387
Schottky diodes, 110
Schweigger, Johann, 6
Scott, C.F., 13
SCR, 17, 103
SCR dynamic characteristics, 152
separately excited dc motor, 251
series armature resistance control, 230, 235, 236, 239, 240
series capacitor commutation, 161
series motor speed control, 224
series resistance voltage control, 25
series-parallel connection, 292
series-series connection, 292
shaded-pole action, 467
shaded-pole induction motor, 467
short-circuit protection, 359, 360
shunt armature resistance control, 230, 236, 240
shunt conductance, 331
shunt diverter, 230
shunt-field armature resistance control, 235, 239
shunt-field series resistance control, 238
silicon-controlled rectifier (SCR), 17
single-phase:
  ac supply, 255
  connection, 292
  induction motor, 448
SIT, 137
SITH, 146
Slip, 329
slip frequency, 329
slip-power recovery, 370
smart power, 178
smooth air gap, 80
smooth air-gap machine, 80
soft ferromagnetic material, 32
soft magnetic material, 58
solid-state circuit breaker, 139
speed, synchronous, 18, 329
speed-firing-angle relation, 260
split-phase motor, 461
Sprague, Frank Julian, 11
square-law torque, 373
square-wave inverter drive, 384
squirrel-cage rotor, 323
St. Elmo's fire, 2
stacking factor, 60
starting:
  autotransformer, 356
  code letter, 354
  dc motor, 241
  external-resistance, 355
  induction motor, 354
  single-phase induction motor, 459
static:
  induction thyristor, 146
  Kramer drive, 387
  stability limit curve, 420
  Scherbius drive, 388
  var compensation, 139
step-down transformer, 275
step-up autotransformer, 314
step-up transformer, 19, 275
Sturgeon, William, 6
subfractional-horsepower, 443
supervisory control and data acquisition, 20
synchronous:
  capacitor, 428
  generator, 18
  machine, 84, 397
  motor operation, 423
  reactance, 403
  speed, 18, 329
system:
  distribution, 20
  doubly excited, 75
  excitation, 397

T

tesla, 24
Tesla, Nikola, 13
third-harmonic current, 280
three-phase ac supply, 257
three-phase machine, 399
three-winding autotransformer, 315
three-winding transformer, 296
threshold voltage, 112
thyratron, 16
thyristor, 103, 105, 138
  bi-directional triode, 145
  FET-controlled, 147
  gate turn-off (GTO), 17, 144
  gate-assisted turn-off, 104, 143
  inverter, 141
  light-triggered, 143
  MOS-gated, 18
  phase-control, 140
  reverse conducting (RCT), 17, 142
  static induction, 146
toroid, 39
torque-slip characteristic, 339
transformer, 273
  control-type, 273
  equivalent circuits, 283

www.EngineeringEBooksPdf.com

ideal, 274
model, 278
step-down, 275
step-up, 19, 275
performance measure, 286
three-winding, 296
transistor:
bipolar, 117
bipolar junction, 116
Darlington, 17
insulated gate, 18
insulated gate, bipolar, 136
junction, 16
metal-oxide semiconductor field-effect, 116
metal-oxide-semiconductor insulated-gate, 116
P-N-P-N, 17
power, 115
power bipolar junction, 104
TRIAC, 17, 105
turn-off, 159
turn-off time, 104, 124
turn-on time, 124
two-phase machine, 81
two-value capacitor motor, 464

U

Underexcited, 419
undervoltage protection, 359
unidirectional current capability, 108
unipolar voltage-withstanding capability, 108

V

V curves, 423
variable-frequency control, 370
variable-frequency operation, 376
variable-resistance starting, 355
variable-voltage constant frequency, 370
Varley, C.F., 12
vector product, 24
Volta, Alesandro, 4
Voltage:
breakdown, 125
collector-base saturation, 124
collector-emitter saturation, 124
critical rate of rise of forward, 157
induced, 50
maximum peak:
forward, 112
nonrepetitive reverse, 111
reverse, 111
threshold, 112
voltage-fed inverter, 382
drive, 383

W

weber turn, 51
Westinghouse, George, 12
Wilde, Henry, 10
winding, distributed, 325
wound-rotor construction, 323

Y

y-connection, 301

www.EngineeringEBooksPdf.com